Université Paris Cité

École doctorale Bio Sorbonne Paris Cité (BioSPC, ED 562)

Institut Cochin – INSERM U1016 – CNRS UMR8104
Equipe Bactéries et Périnatalité
22 rue Méchain 75014 PARIS

FabT, régulateur transcriptionnel de la voie de biosynthèse des acides gras, impliqué dans la virulence de *Streptococcus pyogenes*

Par Clara LAMBERT

Thèse de doctorat de Microbiologie

Dirigée par Dr. Agnès FOUET

Présentée et soutenue publiquement le lundi 12 décembre 2022

Devant le JURY composé de :

Dr. Agnès FOUET, Directrice de recherche, Université Paris Cité	Directrice de thèse
Dr. Florence DUBOIS-BRISSONNET, Professeur HDR, Université Paris Saclay	Rapporteur
Dr. Christophe GRANGEASSE, Directeur de recherche, Université de Lyon	Rapporteur
Dr. Claire MORVAN, Maître de conférences, Université Paris Cité	Examinateur
Dr. Pascale SERROR, Directrice de recherche, Université Paris Saclay	Examinateur
Dr. Ivo GOMPERTS BONECA, Directeur de recherche, Université Paris Cité	Examinateur
Dr. Alexandra GRUSS, Directrice de recherche, Université Paris Saclay	Membre invité

Institut Cochin

FabT, régulateur transcriptionnel de la voie de biosynthèse des acides gras, impliqué dans la virulence de *Streptococcus pyogenes*.

Résumé

Streptococcus pyogenes ou Streptocoque du groupe A (SGA) est une bactérie pathogène strictement humaine, responsable d'environ 517 000 décès par an dans le monde. Son spectre d'infection est large, allant d'infections superficielles à des infections sévères, dites invasives. Les premières étapes des infections à SGA correspondent à l'adhésion des bactéries au tissu et à leur multiplication à sa surface. Les mécanismes mis en jeu lors de ces étapes n'ont pas encore été élucidés. Différentes études les ont analysés, dont une utilisant un modèle *in vivo* de fasciite nécrosante chez le primate non humain. Plus de 11,8 % des souches prélevées au point d'inoculation possèdent des mutations ponctuelles dans le gène *fabT*, alors que les isolats cliniques d'infections invasives n'en présentent pas. Ceci met en évidence une contre-sélection des souches mutées dans *fabT* dans les maladies sévères. De plus, l'inoculation de souches de SGA mutées dans *fabT* révèle que ces souches ont une virulence fortement atténuée. Le but de la thèse est de comprendre le lien entre la perte de fonction de FabT et ce défaut de virulence. FabT est le répresseur transcriptionnel des gènes impliqués dans la voie de biosynthèse des acides gras, FASII, chez les Streptocoques, les Entérocoques et les Lactocoques. FabT contrôle ainsi la composition en acides gras de la membrane bactérienne. L'hypothèse est que ces modifications, affectant l'homéostasie membranaire, peuvent impacter les capacités d'adaptation de la bactérie à son environnement et ainsi rendre compte du défaut de virulence.

Après construction d'une souche mutante *fabT* chez SGA, le rôle de FabT a été étudié, dans une situation mimant les conditions physiologiques *in vivo* par ajout, dans le milieu de culture, d'acides gras qui couplés, à une « acyl carrier protein », ACP, sont les corépresseurs de FabT. En utilisant un éventail de techniques allant de la bactériologie classique aux techniques dites « omiques », nous avons défini que FabT contrôle probablement directement la régulation des gènes FASII et d'un unique autre gène *degV*. La dérégulation des gènes FASII au sein de la souche mutante *fabT* influence la composition en acides gras et en lipides de la

membrane de SGA pouvant rendre compte d'un défaut d'adaptation de la bactérie à son environnement. Afin de mieux caractériser la relation entre FabT et la virulence, nous avons comparé le comportement des souches sauvage et mutante *fabT* lors des premières étapes d'infection à SGA. La souche sauvage se multiplie en présence de cellules humaines en utilisant des lipides sécrétés par ces cellules. Cependant, la souche mutante *fabT* présente un défaut d'adhésion et de croissance en présence de ces cellules, ce qui limite la colonisation lors de l'infection. De fait, dans un modèle d'infection de tissu humain *ex vivo,* la souche mutante *fabT* présente un défaut de colonisation de la surface de celui-ci dû au défaut de multiplication. Le défaut de croissance résulte en partie d'une plus forte mortalité de la souche mutante *fabT*, mais également d'une plus grande consommation d'énergie, conséquence de l'absence de répression de FASII.

Par ailleurs, SGA possédant deux ACPs, AcpA et AcpB, nous avons étudié l'implication de ces protéines dans la régulation des gènes contrôlés directement par FabT. Nous avons observé par qRT-PCR que le niveau de répression des gènes FASII d'une souche délétée de *acpB* est similaire à celui de la souche mutante *fabT*. Ainsi, la protéine AcpB, couplée à un acide gras, forme le complexe de corépression de FabT assurant la répression des gènes FASII chez SGA. Enfin, *degV*, qui est corégulé par ce complexe, code une protéine intervenant dans le contrôle de l'excès d'acides gras endogènes.

Ainsi, le défaut de répression de FASII dans une souche mutée dans *fabT* mène à un cycle inutile de synthèse des acides gras qui limite la capacité de la bactérie à se multiplier et donc restreint la virulence de SGA.

Mots-clés

- *Streptococcus pyogenes*
- Métabolisme
- Acide gras
- Régulation
- Virulence

FabT, a transcriptional regulator of the fatty acid biosynthesis pathway, involved in *Streptococcus pyogenes* virulence.

Summary

Streptococcus pyogenes or Group A Streptococcus (GAS) is a strictly human pathogenic bacterium, responsible for approximately 517,000 deaths per year worldwide. Its spectrum of infection is wide, ranging from superficial infections to severe, invasive infections. The first stages of severe GAS infections correspond to the bacterial adhesion to the tissue and their multiplication on its surface. The mechanisms involved in the early stages of infection have not yet been elucidated. Different studies have analyzed them, including one using an *in vivo* model of necrotizing fasciitis in non-human primates. More than 11.8 % of the strains collected at the point of inoculation have point mutations in the *fabT* gene, whereas clinical isolates from invasive infections do not. This highlights a counter-selection of *fabT* mutant strains in severe infections. Furthermore, inoculation of *fabT*-mutant GAS strains reveals that these strains have a strongly attenuated virulence. The goal of this thesis is to understand the link between FabT loss of function and this virulence defect. FabT is the transcriptional repressor of the genes involved in the fatty acid biosynthetic pathway, FASII, in Streptococci, Enterococci and Lactococci. FabT thus controls the fatty acid composition of the bacterial membrane. Our hypothesis is that these modifications, affecting membrane homeostasis, may impact the bacterial ability to adapt to its environment and thus account for the virulence defect.

After construction of a *fabT* mutant strain in GAS, the role of FabT was studied in a situation mimicking physiological conditions *in vivo* by adding, in the culture medium, fatty acids, which coupled to an acyl carrier protein, ACP, are FabT corepressors. Using a wide range of techniques from classical bacteriology to “omics”, we defined that a mutation in FabT controls, probably directly, the expression regulation of the FASII genes and of a single other gene, *degV*. The deregulation of the FASII genes in the *fabT* mutant strain then influences the fatty acid and lipid composition of the GAS membrane, which may account for a lack of adaptation of the bacterium to its environment. To better characterize the relationship between FabT and virulence, we compared the behavior of wild-type and *fabT* mutant strains

during the first stages of GAS infection. The wild-type strain multiplies in the presence of human cells, using lipids secreted by these cells. However, the *fabT* mutant strain exhibits defects in adhesion and in growth in the presence of these cells, and this limits colonization during infection. In fact, in an *ex vivo* human tissue infection model, the *fabT* mutant strain shows a colonization defect on the surface of this tissue due to the multiplication defect. The growth defect results in part from a higher mortality of the *fabT* mutant strain, but also from a higher energy consumption because of the absence of FASII repression.

In addition, since GAS produces two ACPs, AcpA and AcpB, we studied the involvement of these proteins in the regulation of genes directly controlled by FabT. We observed by qRT-PCR that the level of gene repression of an *acpB*-deleted strain is like that in the *fabT* mutant strain. Thus, the AcpB protein, coupled to a fatty acid, forms the FabT corepression complex ensuring FASII gene repression in GAS. Finally, *degV*, which is coregulated by this complex, encodes a protein involved in the control of endogenous fatty acid excess.

Thus, the lack of FASII repression in a *fabT*-mutant strain leads to an unnecessary cycle of fatty acid synthesis that limits the bacterium's ability to multiply and thus restricts the virulence of GAS.

Keywords

- *Streptococcus pyogenes*
- Metabolism
- Fatty acid
- Regulation
- Virulence

Remerciements

Ce mémoire signe la fin de quatre années de thèse durant lesquelles j'ai eu la chance de rencontrer et de travailler avec de nombreuses personnes. Je vais faire tout mon possible, pour n'en oublier aucune.

Je voudrais, tout d'abord, remercier Mme Florence Dubois-Brissonnet et M Christophe Grangeasse qui ont accepté d'être les rapporteurs de ma thèse, ainsi que Mme Claire Morvan, Mme Pascale Serror et M Ivo Gomperts Boneca d'avoir accepté de faire partie de mon jury en tant qu'examinateurs.

Je tiens à remercier Mesdames Claire Poyart et Agnès Fouet pour m'avoir accueillie au sein de leur équipe, écoutée et conseillée. Je remercie plus particulièrement Agnès Fouet, ma directrice de stage puis de thèse qui m'a encadrée pendant ces 58 mois. Ce fût un honneur de travailler et de grandir scientifiquement à tes côtés. Je ne te remercierai jamais assez pour la richesse de nos échanges, ta pédagogie et ta rigueur. J'espère rester à la hauteur de ton enseignement et le transmettre aux générations futures. Au-delà du côté scientifique, je tiens à te remercier pour ton écoute, ta compréhension et ton soutien. Je souhaite aussi remercier ton mari Claude, notre « UberPasteur ». Merci Claude d'avoir « vidé » les stocks de poudre de l'Institut Pasteur pour mon projet. Je vous souhaite à tous les deux, une heureuse retraite pleine de belles randonnées !

Merci à Antonin Weckel et Antoine Hautcoeur d'avoir commencé ce projet et éveillé ma curiosité sur ce sujet, il y a maintenant cinq ans. Je remercie également mes acolytes Caroline Bachmann et Marine Gaillard pour leur aide, leur bonne humeur et leurs suggestions culinaires ! De nombreux stagiaires ont aussi participé à ce projet. Je pense particulièrement à Thiphaine, Margaux, Alice, Imane, Maëva, Lauryn et Élisabeth. J'ai beaucoup apprécié de travailler avec vous, de partager mes désillusions et surtout de vous transmettre ma passion. Merci à toutes pour votre aide !

Pour leurs conseils, leur bonne ou mauvaise humeur, les coups de gueule et surtout les souvenirs heureux, je remercie chaleureusement les membres actuels, Julie Guignot, Asmaa Tazi, Céline Plainvert, Cécile Guyonnet, Éva Aznar, Sébastien Le Huu Nghia et passés, Anne-Sophie Bourrel, Constantin Hays, Amandine Picart, Lionel Costa, Gérald Touak, de l'équipe « Bactéries et Périnatalité ».

Au cours de ma thèse, j'ai eu la chance de collaborer avec Alexandra Gruss et son équipe. Merci à Jamila Anba-Mondoloni, Jasmina Vidic et Vincent Leguillier pour leur accueil et leurs discussions. For Paprapach Wongdontree: « Yok », I will never forget our travel in Boston. Good luck for the end of your thesis. Je souhaite remercier tout particulièrement Karine Gloux pour ses conseils sur les acides gras, nos échanges autour de la CpG et sa patience avec les nombreux problèmes de cette machine. Il m'est bien évidemment impossible d'oublier de remercier Sandy ! Un énorme merci de m'avoir transmis une partie de tes connaissances sur les acides gras et la membrane des bactéries. Depuis le Master 2, tu as su stimuler ma curiosité et me pousser dans mes retranchements pour rendre le projet meilleur. A ce titre, tu es pour moi ma deuxième directrice de thèse. Je suis honorée d'avoir travaillé avec toi et j'espère pouvoir continuer de le faire dans le futur. Thank you Sandy!

J'ai aussi pu échanger et collaborer avec des équipes de l'Institut Cochin. Je remercie Frédéric Bouillaud pour avoir pris le temps de discuter et avoir suggéré l'hypothèse du cycle futile. Je remercie tout spécialement Céline Méhats et Léa Chicoisne nos collaboratrices « tissu » de l'équipe de Daniel Vaiman, sans qui nous n'aurions pu étudier la colonisation de *S. pyogenes* sur tissus humains et avoir « la cerise sur le gâteau » dixit Agnès. Je remercie David Espié de l'équipe de Emmanuel Donnadieu pour son aide technique lors des expériences sur tissu au L2 de Roussy. Je remercie également l'équipe de Ivan Matic, notamment Arnaud Guiterrez pour nos discussions et ses conseils.

J'ai, également, travaillé avec de nombreuses plateformes de l'Institut Cochin, Genom'IC, Proteom'IC, Imag'IC, Cybio et PIME. Je remercie l'ensemble de leur personnel pour leur implication et leurs conseils, notamment Benjamin Saint-Pierre, Cédric Broussard, François Guillonneau, Muriel Audrieu, Jean-Marc Masse, Alain Schmitt et surtout, un grand merci à Thomas Guilbert pour ses séances de « psy » qui m'ont permis de prendre confiance en moi face au microscope et pour son aide lors des analyses d'images. Je tiens aussi à remercier Audrey Solgadi et Bastien Prost de la plateforme SAMM de l'Université Paris Saclay qui ont ranimé la flamme familiale de chimiste qui sommeillait en moi.

Je souhaite remercier les membres de mon Comité de Suivi Individuel (CSI), Mesdames Sandra Guilmeau et Florence Dubois-Brissonnet qui ont pris le temps de m'écouter, de discuter avec moi et de me conseiller. Je souhaite également remercier Mme. Clarisse Berlioz pour ses conseils et son soutien dans ma demande d'aide individuelle « Fin de thèse » à la Fondation pour la Recherche Médicale (FRM).

Je tiens aussi à remercier toutes les personnes avec qui j'ai partagé mes études et notamment ces années de thèse, Amandine Piedvache, Isabel Souza, Roy Matkovic et tous les collègues du bâtiment Méchain. Je remercie aussi les personnes de l'ombre qui sont indispensables, Maryline Bajolle au secrétariat, Khemwantee Harah à la laverie et le « monsieur du ménage » qui a toujours eu un petit mot pour moi.

Je n'aurais pas pu finir cette thèse sans le soutien et les encouragements de mon compagnon Alexis. Merci d'avoir, toujours, été là pour moi durant ces années. Merci d'avoir accepté que ma thèse prenne autant de place dans notre couple. Je te remercie pour tous les sacrifices que tu as faits et pour tous ceux que nous nous apprêtons à prendre, ensemble ! Je souhaite aussi remercier tes parents qui m'ont accueillie et m'ont supportée pendant les périodes de télétravail à La Rochelle. Merci pour votre soutien ! Je remercie aussi ton couple d'amis inséparables, Maxence et Cloé, de m'avoir adoptée et pour les moments passés ensemble à discuter, à rire ou à angoisser. Merci pour votre soutien.

Mes remerciements vont également à ma famille, mes oncles, tantes, cousins et cousines qui ont toujours cru en moi et m'ont soutenue durant ces années d'études. Merci à Émilie pour m'avoir fait découvrir le monde de la recherche ! Je remercie aussi ma sœur pour ses encouragements, nos querelles et nos réconciliations. Je suis fière de toi. Enfin, mes plus profonds remerciements vont à mes parents. Je vous remercie pour tous les sacrifices que vous avez faits, pour l'amour et le soutien que vous m'avez apportés durant toutes ces années. Je vous suis reconnaissante pour tout ce que vous avez pu faire pour moi et je vous en remercie du fond du cœur.

Listes des principales abréviations

ACP	« Acyl Carrier Protein »
CE	Ester de Cholestérol
Cfa	« Cyclopropane Fatty Acid »
CL	Cardiolipine
DGDG	Digalactosyldiacylglycérol
eFAs	Acides gras exogènes
Fak	« Fatty Acid Kinase »
FASII	Synthèse des acides gras
FCT	« Fibronectin and Collagen binding protein and T-antigen »
FnBP	« Fibronectin-Binding-Protein »
LPA	Acide lysophosphatidique
LTA	Acide lipoteichoique
MarR	« Multiple antibiotic resistance Regulator »
MEC	Matrice Extracellulaire
MGDG	Monogalactosyldiacylglycérol
NET	« Neutrophil extracellular traps »
PA	Acide phosphatidique
PG	Phosphatidylglycérol
PMN	Neutrophyle polymorphonucléaire
PTS	« Phosphotransferase system »
ROS	« Reactive Oxygen Species »
SAgs	Super-Antigènes
SGA	Streptocoque du groupe A
SI	Système Immunitaire
SLO	Streptolysine O
SLS	Streptolysine S
SOF	« Serum Opacity Factor »
STSS	Syndrôme de choc toxique streptococcique
TCS	« Two-Component signal transduction Systems »
UPR	« Unfolded Protein Response »

Table des illustrations

Figure 1. Morphologie de *S. pyogenes* 18
Figure 2. Spectre d'infections de *S. pyogenes* 20
Figure 3. Classification des *emm*-patterns. 27
Figure 4. Organisation des gènes au sein des neuf régions FCT différentes chez *S. pyogenes*. 28
Figure 5. Mécanisme général d'infection de *S. pyogenes* 38
Figure 6. Mécanismes d'invasion de *S. pyogenes* 40
Figure 7. Principales voies composant le métabolisme des sucres chez *S. pyogenes* 44
Figure 8. Métabolisme des acides aminés chez *S. pyogenes* 46
Figure 9. Régulation du métabolisme des sucres par CcpA lors de croissance dans un environnement riche en glucose de *S. pyogenes* 49
Figure 10. Régulation transcriptionnelle par CovR/S, gènes régulés et fonctions associés 50
Figure 11. Inter-régulation des régulateurs transcriptionnels Mga, RALPs et Rgg/RopB dépendant de la phase de croissance de *S. pyogenes* 51
Figure 12. Régulon du régulateur transcriptionnel Mga. 51
Figure 13. Réseau de régulation du régulateur transcriptionnel Rgg ou RopB 53
Figure 14. Exemple de familles lipidiques présentes au sein des membranes des bactéries. 55
Figure 15. Les différents types de phospholipides. 57
Figure 16. Synthèse des lipides. 59
Figure 17. La synthèse des acides gras, FASII 63
Figure 18. Les locus FASII communs aux Streptocoques (*S. pneumoniae*, *S. pyogenes*, *S. agalactiae*), à *E. faecalis* et à *L. lactis* 64
Figure 19. Caractérisation des protéines AcpA et AcpB 65
Figure 20. Le système d'incorporation FakA/B décrit chez *S. pneumoniae* 68
Figure 21. Caractéristiques structurales des protéines MarR. 72
Figure 22. Régulations transcriptionnelles dépendant du ligand au sein de la famille MarR. 73
Figure 23. Comparaison des séquences de FabT chez *S. pyogenes, S. pneumoniae, E. faecalis* et *L. lactis* 74
Figure 24. Sites de fixation décrits au sein de FASII 76
Figure 25. Séquence consensus du site de fixation de l'ADN de FabT. 76
Figure 26. Modèle du mécanisme de répression de FabT proposé chez *S. pneumoniae* 82
Figure 27. Conservation des acides aminés constituant le site de fixation des protéines FakB1 et $DegV_{1638}$ 192
Figure 28. Mécanisme de répression de FabT chez *S. pyogenes* (A) en absence d'acides gras et (B) conditions physiologiques dites « *in vivo* », en présence d'acides gras exogènes. 194
Figure 29. Différentes hypothèses *concernant* le défaut d'incorporation des acides gras exogènes dans la membrane de la souche mutante mFabT chez *S. pyogenes* 196
Figure 30. Modèle d'étude illustrant le défaut de virulence des souches *S. pyogenes* mutées dans *fabT* 202
Figure 31. Proposition de rôle de la protéine $DegV_{1638}$ dans le métabolisme des acides gras endogènes chez *S. pyogenes* 205

Sommaire

Introduction 17

1. Aspects microbiologiques de *Streptococcus pyogenes* 17

1.1. Classification phylogénétique de *S. pyogenes* 17

1.2. Epidémiologie des infections à *S. pyogenes* 18

1.3. Caractéristiques génétiques de *S. pyogenes* 26

1.4. Le répertoire de facteurs de virulence de *S. pyogenes* 30

1.5. Les premières étapes du mécanisme d'invasion de *S. pyogenes* 37

1.6. L'adaptation de *S. pyogenes* à son environnement 42

2. La synthèse de la membrane cytoplasmique 54

2.1. La synthèse des lipides membranaires 54

2.2. La synthèse des acides gras, FASII 61

2.3. Le maintien de l'équilibre membranaire 66

3. FabT, le régulateur transcriptionnel de FASII 71

3.1. Les régulateurs de la famille MarR 71

3.2. La régulation transcriptionnelle de FASII par FabT 74

3.3. FabT : une nouvelle cible thérapeutique ? 87

Contexte et objectifs des travaux 91

Résultats 93

Partie 1 : Rôle de FabT dans la virulence de *S. pyogenes.* 95

Partie 2 : AcpB, corépresseur de FabT chez *S. pyogenes.* 147

Partie 3 : Rôle de la protéine $DegV_{1638}$ chez *S. pyogenes.* 167

Discussion et Perspectives 193

Références bibliographiques 209

Annexes 235

Introduction

1. Aspects microbiologiques de *Streptococcus pyogenes*

1.1. Classification phylogénétique de *S. pyogenes*

S. pyogenes, aussi appelé Streptocoque du Groupe A (SGA), appartient à l'ordre des *Lactobacillales*, autrement connu sous le nom de bactéries lactiques, faisant partie de la classe des *Bacilli*, phylum des *Firmicutes*. Cet ordre regroupe six familles dont les *Streptococcaceae,* à laquelle appartient le genre *Streptococcus* (1).

Le genre *Streptococcus* regroupe 130 espèces et sous-espèces commensales ou pathogènes. Il s'agit de bactéries Gram-positives à faible teneur en G + C dans l'ADN (34 à 46 %) (2). Ces bactéries forment des colonies dont le diamètre est supérieur à 0,5 millimètre et de surface lisse et blanc-grisâtre. Elles se présentent en paires ou chaînes de coques, non mobiles et non-sporulantes. Toutes les espèces de ce genre sont anaérobies facultatives, catalases négatives, mésophiles et chimiohétérotrophes (1).

L'identification des différentes espèces de streptocoques est principalement basée sur leur culture. Une de leurs caractéristiques est leur propriété à lyser les érythrocytes lorsque les bactéries se développent sur une gélose contenant 5 % de sang de cheval, permettant ainsi d'étudier le type d'hémolyse : beta (β) ou complète avec une zone de lyse claire ; alpha (α) ou complète autour de la colonie ; incomplète avec une coloration verdâtre d'un à trois millimètres autour de la colonie et enfin absence d'hémolyse. Basés sur cette caractéristique et sur leur morphologie, trois groupes de streptocoques ont été définis :

- Les streptocoques pyogènes, pathogènes associés à la formation de pus, β-hémolytiques, sous forme de chaînes de coques, par exemple *S. pyogenes et Streptococcus agalactiae* ;
- Les streptocoques oraux, α-hémolytiques, pathogènes tels que *Streptococcus pneumonaie* et *Streptococcus mutans* ou commensales, sous forme de diplocoques, par exemple *Streptococcus salivarius* et *Streptococcus mitis*.
- Les autres streptocoques, ne pouvant être définis dans les deux autres groupes.

Afin de distinguer les différents streptocoques pyogènes, d'autres techniques ont été développées, basées sur des études de sérologie, telle que la classification de Lancefield, sur

la présence d'une enzyme telle que le test colorimétrique L-pyrrolidonyl-β-naphthylamide (PYR) ou sur leur résistance à certaines molécules telle que la bacitracine. La classification de Lancefield basée sur la sérologie de sucres présents à la surface des bactéries permet de les classer en 24 groupes allant du streptocoque du groupe A aux streptocoque du groupe X (3). Le streptocoque du groupe A ou *S. pyogenes* est β-hémolytique, PYR positive et résistant à la bacitracine. Il se présente sous forme de chainettes de coques (Figure 1).

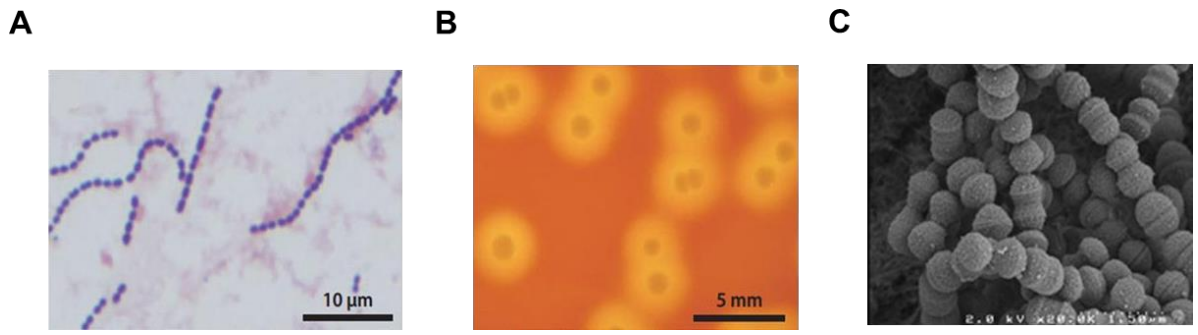

Figure 1. Morphologie de *S. pyogenes*. (A) Coloration de Gram de *S. pyogenes* isolés de sang humain. (B) Isolement sur gélose Columbia additionnée de 5 % de sang de cheval. (C) Chaînettes de *S. pyogenes* par microscopie électronique à balayage. D'après Thèse de Microbiologie, Antonin Weckel, BioSPC, 2018.

1.2. Epidémiologie des infections à *S. pyogenes*

Malgré les prises de conscience concernant l'hygiène, l'incidence de cas d'infection à *S. pyogenes*, notamment la scarlatine et les fièvres puerpérales, a fortement augmenté au 19ème siècle, permettant à Louis Pasteur de définir les infections à *S. pyogenes* comme la première maladie contagieuse.

1.2.1. *S. pyogenes*, un véritable problème de santé publique

S. pyogenes est un pathogène strictement humain, responsable de plus 517 000 morts par an dans le monde (4). En 2005, une étude épidémiologique a recensé plus de 18,1 millions de personnes souffrant d'infection invasive à *S. pyogenes* dont plus de 1,78 millions de nouveaux cas par an, faisant ainsi de *S. pyogenes* un véritable problème de santé publique.

Ces données épidémiologiques sont néanmoins sous-estimées du fait de l'indisponibilité des chiffres de l'ensemble des pays du monde (Asie, Europe de l'est, Amérique latine).

Ce pathogène est présent sous forme de portage principalement au niveau du pharynx et de la peau (5 à 30 % de la population) et plus rarement au niveau du vagin et du rectum (0,03 %) (5,6). Il est responsable d'infections communautaires mais aussi d'infections nosocomiales invasives ou non. À ce jour, il est compliqué de distinguer les cas d'infections asymptomatiques, des portages. La seule indication est la réponse du système immunitaire qui sera différente : dans le cas d'une infection, la réponse immunitaire se déclare au bout de sept à dix jours contre plusieurs semaines voire plusieurs mois pour le portage (7).

Les modes de transmission de *S. pyogenes* se font par contacts directs ou *via* l'environnement (8). Cependant, le mode le plus fréquent reste *via* les voies respiratoires, en particulier les microgouttelettes. De plus, *S. pyogenes* étant présente sous forme de portage, il peut y avoir transmission de personne à personne ou auto-contamination par transfert d'une zone à une autre, de la sphère oto-rhino-laryngée (ORL) vers la peau et inversement, d'où l'importance des mesures d'hygiène dans ce cas de transmission.

1.2.2. Les facteurs de risques d'infection à *S. pyogenes*

En 2008, une étude épidémiologique a essayé de comprendre et de dresser une liste potentielle des corrélations entre les risques et les infections à *S. pyogenes* (9). Il a été mis en évidence une corrélation entre le sexe et le risque d'infection, les hommes étant plus susceptibles que les femmes. Les catégories de patients majoritaires sont les personnes âgées suivies des enfants. De plus, des facteurs environnementaux peuvent également intervenir. En effet, le taux d'infection chez l'enfant augmente de 20 % durant la saison hivernale correspondant à l'augmentation de cas d'angine dans les pays développés. D'autre part, suivant les zones géographiques, l'incidence de certaines infections à *S. pyogenes* varie. En effet, les infections de la sphère ORL sont plus spécifiques aux pays ayant un climat tempéré contrairement aux infections cutanées spécifiques aux pays ayant un climat tropical ou subtropical.

Les facteurs de types socio-économiques reflètent les disparités entre les pays. En effet, liés au manque d'hygiène et de prise en charge, les cas d'infection dans les pays dit en

développement sont plus nombreux et conduisent majoritairement à des complications post-infectieuses voire la mort du patient.

Des corrélations avec des facteurs de risque à titre individuel comme les risques liés à la grossesse et l'accouchement ont été mis en évidence pour les femmes. De plus, des risques de co-infection ont également été décrits notamment à la suite d'infection de type varicelle ou gale, les lésions cutanées observées offrent une porte d'entrée pour *S. pyogenes* et lors de diabète ou d'infection à influenza ou de type varicelle, la réponse immunitaire est particulièrement modifiée favorisant les infections à *S. pyogenes* (10–12).

1.2.3. Le spectre d'infections à *S. pyogenes*

Le spectre d'infections à *S. pyogenes* est large allant des infections non invasives aux infections invasives traduisant la capacité de *S. pyogenes* à coloniser les tissus normalement stériles (Figure 2). De plus, l'ensemble des maladies à *S. pyogenes* peuvent induire à long terme de lourdes séquelles post-infectieuses qui sont responsables de la grande majorité des décès à l'échelle mondiale. Cette diversité de pathologies est liée à la grande variété des répertoires des facteurs de virulence de *S. pyogenes* dépendant de sa grande variabilité génétique.

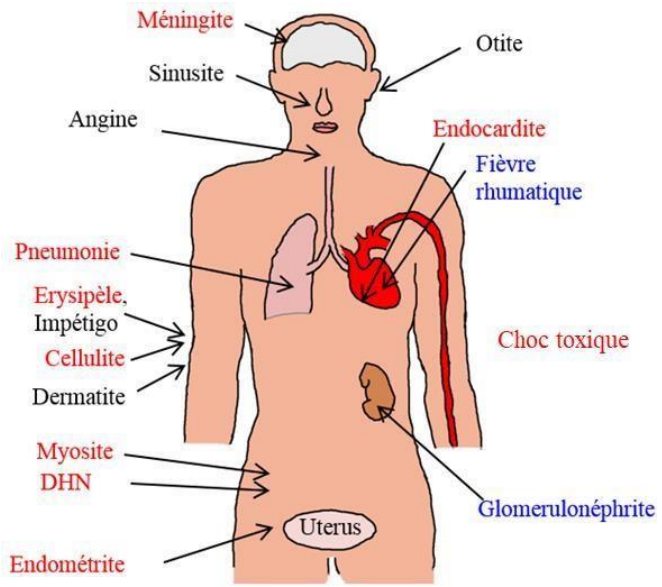

Figure 2. Spectre d'infections de *S. pyogenes*. Les infections non invasives à *S. pyogenes* sont représentées en noir, les infections invasives en rouge et les séquelles post-streptococciques en bleu. Adaptée de http://textbookofbacteriology.net/streptococcus_2.html.

1.2.3.1. Les infections non invasives à *S. pyogenes*

Les infections non invasives, ou superficielles, à *S. pyogenes*, telles que l'angine et l'impétigo, sont majoritairement des maladies bénignes, pouvant se traiter par antibiothérapie. La tranche d'âge concernée dans le monde est majoritairement les enfants de 2 à 15 ans. Ces infections ont été largement étudiées en prenant comme exemples principalement les cas d'impétigo et d'angine.

L'angine est la manifestation clinique d'infection à *S. pyogenes* la plus répandue dans le monde. En 2005, le rapport de l'Organisation Mondiale de la Santé (OMS) a recensé plus de 616 millions de cas par an dans le monde, et plus particulièrement dans les pays au climat tempéré. Les enfants sont les personnes les plus atteintes (15-30 % contre 5-10 % pour les adultes) (13). Cette infection va être caractérisée par les manifestations cliniques suivantes : un début de fièvre brutal, des malaises, des maux de gorge, des douleurs à la déglutition et le gonflement des ganglions lymphatiques. La présence de l'ensemble de ces symptômes ne signe pas directement une infection par *S. pyogenes*. En effet, d'autres pathogènes peuvent être responsables de ces symptômes tels que certains virus. Le diagnostic se fait à partir des signes cliniques et des outils tels que des tests antigéniques rapides (exemple du BDveritor™system) (14). L'angine étant une maladie légère, les patients peuvent être traités ou non par antibiotique (pénicilline). Sans traitement, la guérison est généralement observée dans les trois à six jours après infection (15).

L'impétigo ou le pyoderme sont des termes utilisés pour définir les lésions purulentes discrètes produites par une forte réponse immunitaire face à la présence de *S. pyogenes*. Suivant les couches de la peau atteintes, *S. pyogenes* provoque des infections cutanées plus ou moins sévères (16). L'impétigo est l'infection cutanée à *S. pyogenes* la plus prévalente dans le monde. En 2010, une étude a référencé plus de 140 millions de cas par an, faisant rentrer *S. pyogenes* dans le classement des 50 premières maladies cutanées mondiales (17). Cette maladie touche principalement les enfants de 2 à 15 ans vivant majoritairement dans les pays dont le climat est humide et chaud à savoir tropical ou subtropical. Contrairement à l'angine, aucune incidence en fonction des saisons n'est observée. L'atteinte de la couche de kératinocytes superficielles se manifeste généralement par des papules évoluant en pustules qui en éclatant, au bout de quatre à six jours, forment des croûtes épaisses, caractéristiques

de l'impétigo. La guérison est plutôt lente et laisse souvent des zones de dépigmentation sur les surfaces exposées telles que le visage et les extrémités du corps. Le traitement par antibiotique est ici un problème qui est lié notamment à la probabilité de co-infection avec *Staphylococcus aureus*, également responsable d'infections cutanées, et résistant à de nombreux antibiotiques (18).

1.2.3.2. Les infections invasives à *S. pyogenes*

Les facteurs de virulence de *S. pyogenes* tels que l'exotoxine SpeB et les super-antigènes (SAgs) lui confèrent la capacité de rompre les épithéliums pour envahir les tissus plus profonds (19). Une étude épidémiologique de 2005 met en évidence la forte incidence de ces maladies dans le monde avec plus de 663 000 nouveaux cas par an dont 163 000 cas mortels (4). Elles touchent principalement les adultes. Il s'agit d'infections brutales entrainant dans 20 % des cas la mort du patient dans les sept jours suivant le début de l'infection. La mortalité dépend du site d'infection et des conditions physiques du patient. Les infections invasives les plus communes et étudiées sont la fasciite nécrosante et le syndrome de choc toxique streptococcique (« Streptococcal toxic Shock Syndrome », STSS). Les infections de type fièvre puerpérale ou endométrite et méningite sont moins fréquentes.

La fasciite nécrosante est une infection des tissus sous-cutanés par *S. pyogenes*, caractérisée par une rapide nécrose de la peau et des structures sous-jacentes, fréquemment associée à une bactériémie. Elle a une évolution très rapide, 24 à 72 heures après inoculation, la peau devient sombre et violacée et des bulles de liquide jaunâtre ou hémorragiques se forment. Cette infection est le plus souvent liée à un trauma formant une porte d'entrée pour la bactérie au sein des tissus cutanés ou des muqueuses. Les principaux signes cliniques sont une fièvre élevée et des douleurs extrêmes. Le taux de mortalité est important même avec traitement, 70 à 80 % de morts en 2013. Ce taux peut être expliqué par le diagnostic tardif, basé sur les signes cliniques. Au cours des dernières années, une augmentation de l'incidence des fasciites nécrosantes à *S. pyogenes* a été observée liée notamment à l'atteinte des muscles de plus en plus commune. De plus, cette augmentation peut également être rattachée au fait que 50 % des patients ne présentent pas de porte d'entrée liée à un trauma mais une cause interne, par exemple à la suite d'hématome ou de déchirement musculaire, remettant en cause l'origine de cette infection à *S. pyogenes* et retardant le diagnostic (19).

Le syndrome de choc toxique streptococcique (STSS) est une infection aigüe liée à la présence de toxines bactériennes telles que les super-antigènes (SAgs) qui induisent une forte sécrétion de molécules d'inflammation dans le corps provoquant alors la destruction des tissus (cf. L'échappement au système immunitaire de l'hôte). Les symptômes caractéristiques du STSS sont une forte fièvre, une hypotension, la défaillance de plusieurs organes et une éruption cutanée diffuse avec desquamation des tissus. Le STSS est le plus souvent associé à une complication, survenant à la suite d'infections virales (varicelle, grippe), d'une angine ou encore d'un traumatisme local des tissus mous à la suite d'une fasciite nécrosante par exemple. Cette maladie touche les enfants de moins de 5 ans et les adultes de plus de 45 ans. Son incidence en corrélation avec les saisons est plus importante au cours de l'hiver et du printemps. Le STSS est associé à un fort taux de mortalité, variant de 3 à 10 % chez les enfants et de 30 à 80 % chez les adultes. Malgré la difficulté des médecins à établir un diagnostic rapide, le STSS est généralement traitable par antibiothérapie (20).

Le laboratoire étudie les mécanismes moléculaires impliqués dans les étapes précoces des infections invasives à *S. pyogenes*, avec comme modèle d'étude la fièvre puerpérale, plus précisément la première étape caractéristique, l'endométrite, c'est-à-dire l'infection de l'endomètre, muqueuse interne de l'utérus. La fièvre puerpérale est une infection invasive à *S. pyogenes* connue bien avant le 19ème siècle, où Louis Pasteur a désigné *S. pyogenes* comme agent responsable de cette infection. En 2017-2018, à partir des données du Centre National de référence des Streptocoques (CNR) de France, le laboratoire a mis en évidence qu'en moyenne 60 % des infections invasives à *S. pyogenes* sont survenues dans la sphère gynéco-obstétricale chez les femmes de 18 à 40 ans (21). Cette infection est considérée comme une maladie spécifique de la femme enceinte qui a 20 fois plus de risque de contracter l'infection notamment lors de l'accouchement (22). Elle est également décrite à la suite d'examen gynécologique invasif tel que la pause d'un stérilet ou la fécondation in *vitro*. Le diagnostic de l'endométrite est très difficile du fait de la non-spécificité des symptômes (fièvre, douleurs abdominales, hypotension, malaises, nausées). De manière générale, l'infection se déclare quatre jours après l'accouchement et seulement 13,9 % des cas sont d'origine nosocomiale (23). Lors de l'apparition des symptômes, un traitement antibiotique adapté est prescrit pour diminuer de 42 % les risques d'infection (24). Une minorité de femmes développe des complications telles que le STSS.

1.2.3.3. Les séquelles post-streptococciques

Les séquelles post-streptococciques sont responsables de la grande majorité des décès liée à une infection à *S. pyogenes.* Ils résultent d'une réaction auto-immune basée sur un mécanisme moléculaire mimétique. En effet, *S. pyogenes* possède des antigènes à réaction croisée avec les molécules de l'hôte et qui, lors d'une infection, induisent une réponse auto-immune contre les tissus de l'hôte (25). Deux types de séquelles sont référencés, la glomérulonéphrite et les fièvres rhumatiques.

La glomérulonéphrite aiguë post-streptococcique est liée à une réponse immunitaire complexe au niveau des glomérules, à la suite d'une infection cutanée ou de la sphère ORL. Elle se caractérise par la production d'urine foncée et peu abondante après un temps de latence suivant l'infection. De plus, le temps de latence varie également en fonction du site d'infection, de sept à dix jours pour une infection de la sphère ORL et de deux à quatre semaines pour une infection cutanée. Des études épidémiologiques ont montré que la glomérulonéphrite touchait les enfants de 2 à 18 ans et les hommes plus que les femmes (26). De plus, une disparité entre les pays a également été mise en évidence avec une diminution de l'incidence dans les pays développés par rapport aux pays en développement, surement liée aux progrès du diagnostic, aux mesures de préventions en question d'hygiène et aux traitements antibiotiques (27).

La fièvre rhumatique aiguë est la maladie cardiaque la plus commune chez les enfants de 5 à 15 ans, de sexe féminin, dans les pays en voie de développement (28). L'environnement a un rôle important dans le développement de cette maladie comme l'hygiène et la nutrition. De plus, les patients ayant une susceptibilité génétique sont également plus aptes à contracter cette maladie (29). En 2005, une étude a référencé plus de 471 000 cas par an (4). Les manifestations cliniques associées à cette maladie sont principalement de la fièvre (90 %), l'arthrite (75 %) et la plus sévère, l'endocardite (50 %), menant au développement de la maladie chronique cardiaque (30). Contrairement à la glomérulonéphrite aiguë, cette maladie résulte d'une infection de la gorge et nécessite une hospitalisation du patient d'au moins deux à trois semaines. Les symptômes liés y seront traités mais les problèmes cardiaques tels que les dommages aux valves du cœur persisteront. Les conséquences cardiaques des fièvres rhumatiques sont asymptomatiques et rendent donc le diagnostic très compliqué. Cependant,

les progrès de la médecine avec le développement de l'échocardiographie et l'évolution des critères de diagnostic ont permis de déceler un grand nombre de malades (31,32).

1.2.4. Les traitements des infections à *S. pyogenes*

Le traitement curatif commun au cas d'infection non-invasive ou invasive à *S. pyogenes* est l'antibiothérapie. La classe d'antibiotique de référence administrée est celles des β-lactamines. De plus, *S. pyogenes* est également sensible aux antibiotiques de la famille des macrolides tels que l'érythromycine et la clindamycine. L'érythromycine peut être utilisée lorsque le patient présente une allergie aux β-lactamines. De plus, dans le cas d'infection invasive sévère telle que la fasciite nécrosante ou le STSS, les β-lactamines sont couplées avec la clindamycine ou les immunoglobulines intraveineuses humaines poly-spécifiques (IVIG) afin d'inhiber respectivement la synthèse ou l'activité de toxines et des facteurs de virulence de *S. pyogenes* (33).

L'apparition de résistances aux antibiotiques couplée à la problématique des séquelles post-infectieuses constitue un argument fort pour le développement d'un vaccin contre *S. pyogenes* (34). L'établissement d'une stratégie vaccinale efficace et abordable représente un défi pour la communauté scientifique, du fait de la grande variabilité génétique des souches, des nombreuses molécules qui leur sont spécifiques et des réactions croisées avec le système de l'hôte (35). Depuis 1909, de nombreux facteurs de virulence ont été ciblés par les stratégies vaccinales tels que la protéine M, l'antigène T, la protéine ScpA, les protéines se liant à la fibronectine et les sucres présents à la surface de la bactérie (36). L'efficacité de ces vaccins candidats a été approuvée dans des modèles *in vivo* d'infection d'animaux à *S. pyogenes*. Néanmoins, la mise sur le marché de ces derniers présente un autre enjeu mondial. En effet, afin d'obtenir un impact positif sur le nombre de décès associés à une infection à *S. pyogenes*, il faudrait dès à présent développer des vaccins qui répondent aux besoins mondiaux et qui restent efficaces pour prévenir d'éventuelles séquelles et maladies sévères (37).

Dans l'attente de ces derniers, la prévention est un atout considérable pour limiter le nombre de cas d'infection. Celle-ci consiste à mieux comprendre les schémas de transmission et identifier les cibles des mesures de prévention par des analyses épidémiologiques en

prenant en compte l'intégralité des facteurs de risques. Les mesures de préventions peuvent inclure la décontamination de l'environnement, l'amélioration de l'hygiène et l'antibioprophylaxie pour éliminer le portage (38).

1.3. Caractéristiques génétiques de *S. pyogenes*

1.3.1. Le génome de *S. pyogenes*

Suite aux progrès en biologie moléculaire et en génétique des années 1980 et 1990, le premier séquençage de génome entier de *S. pyogenes* a été publié en 2001 (39). Par la suite, les génomes de 2 073 souches de *S. pyogenes* ont été séquencés et annotés entièrement et sont disponibles sur le site du « National Center for Biotechnology Information » (NCBI). Le génome de *S. pyogenes* est circulaire. Il code plus de 1 689 protéines réparties sur 1,7 à 1,8 mégabases (40).

1.3.2. Identification de la diversité des souches de *S. pyogenes*

Afin de mieux comprendre les bases des épidémies à *S. pyogenes*, des méthodes d'identification ont été développées, basées initialement sur les caractéristiques biochimiques et physiologiques de la bactérie. Puis des techniques de sérotypage ont été développées reposant sur les propriétés antigéniques de différents composants présents dans la paroi.

En 1928, Rebecca Lancefield a entrepris de classer les souches de *S. pyogenes* en fonction de la protéine M, protéine de surface (41). Il s'agit d'une protéine dimérique constituée de deux chaînes polypeptidiques enroulées en hélice α qui est impliquée dans la virulence de *S. pyogenes*, notamment dans l'étape d'adhésion (Figure 3B) (42). Elle est ancrée à la paroi *via* la sortase A, par le motif LPxTG présent à son extrémité C-terminale. Son extrémité N-terminale est hypervariable, du fait de la présence ou non de régions répétées. La protéine M est codée par le gène *emm* présent chez toutes les souches de *S. pyogenes*. Ainsi la première technique de sérotypage, *emm*-typing, est basée sur le séquençage de l'extrémité 5' du gène *emm,* correspondant à la partie variable de cette protéine. A ce jour, plus de 250 *emm*-types sont répertoriés (42). En 2019, les *emm*-types prédominants en France

sont *emm1* (20,3 %), *emm89* (13,2 %), *emm87* (8,2 %) et *emm28* (7,4 %) (43). Malgré les mesures d'hygiène prises en 2020, liées à la pandémie de coronavirus, les *emm*-types prédominants restent, avec une légère diminution par rapport à 2019, l'*emm1* (18.3 %), *emm89* (9.5 %), *emm87* (7.7 %) et *emm28* (5.7 %) (44).

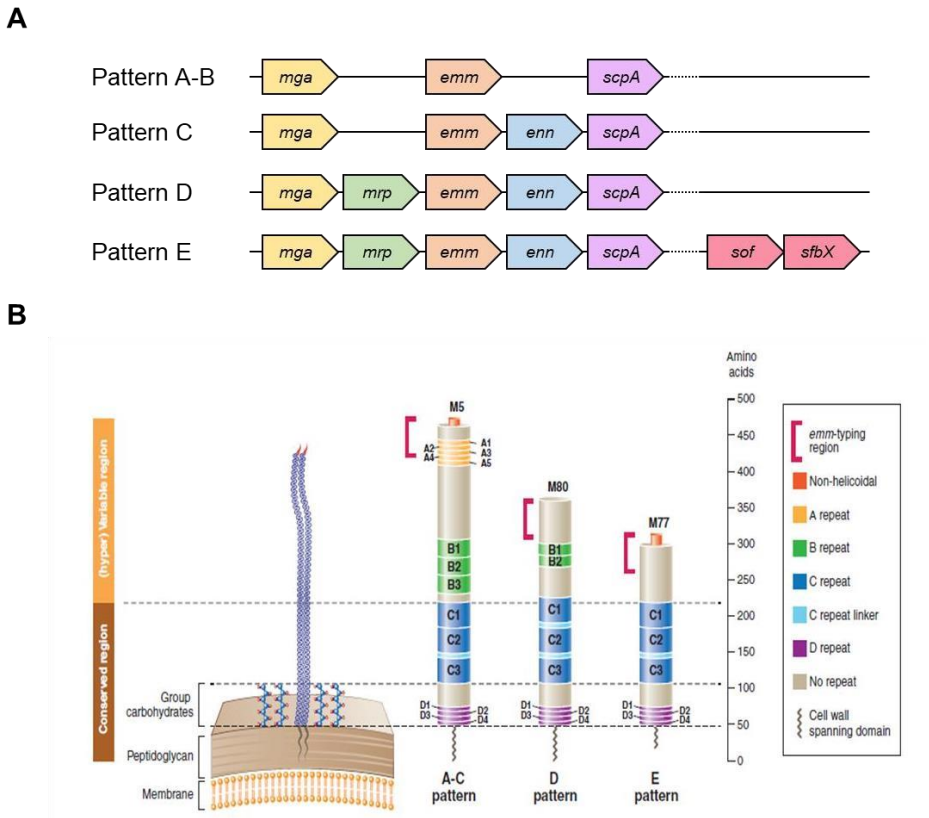

Figure 3. Classification des *emm*-patterns. (A) Composition de la région Mga. Arrangement des gènes codés dans la région Mga permettant de distinguer les trois patterns (A-C, D et E). Le régulateur transcriptionnel contrôle l'expression de 10% du génome de *S. pyogenes* dont les gènes codés dans cette région, de manière positive. D'après (45). (B) Représentation des trois types de protéines M de *S. pyogenes* (M5, M80 et M77). Ces représentations de la structure des différentes protéines M mettent en évidence la région N-terminale hypervariable utilisée pour le sérotypage des souches *S. pyogenes* (crochet rouge). La longueur de la protéine M et la taille des régions répétées et non répétées sont dessinées à l'échelle. D'après (42) et Thèse de Microbiologie, Antonin Weckel, BioSPC, 2018.

Le gène *emm* est situé au sein de la région Mga (« Multiple virulence gene regulator of Group A *Streptococcus* »). Cette région, très conservée (74,3 %) correspond au régulon du régulateur transcriptionnel Mga, allant du gène codant le régulateur Mga à celui codant ScpA, une C5a peptidase (Figure 3A). Elle comprend également, ou non, des gènes codant des protéines M-like (Mrp et Enn), conservées à 93,9 % entre les souches de *S. pyogenes*. La différence de répartition de ces gènes ainsi que la structure de la protéine M ont permis de déterminer des *emm*-patterns A-C, D et E (Figure 3B). Les protéines de pattern A-C

comprennent les protéines M les plus longues possédant les séquences répétées A, B et C. Celles de pattern D et E possèdent la protéine Mrp, présente dans 88,9 % des génomes de *S. pyogenes*, et se distinguent par la présence des séquences répétées B et C, B étant absent du pattern E. Le nombre de répétitions de la région C varie entre un et cinq. La grande majorité des protéines (90 %) possède trois régions répétées C.

D'autres techniques de sérotypage ont été développées en complément de celle dépendant de la protéine M. En 1934, le typage en fonction de l'antigène T a été entrepris par Fred Griffith (47). Il s'agit du deuxième sérotypage majeur, qui a permis de mettre en évidence plus de 22 « T-typing ». L'antigène T (« Trypsin resistant T antigen ») est une protéine de surface constituant du squelette du pilus de *S. pyogenes* (45). Le gène codant l'antigène T est présent sur une région FCT, « Fibronectin and Collagen binding protein and T-antigen » (Figure 4). *S. pyogenes* possède neuf versions de la région FCT. Ces régions possèdent cinq à dix ORFs codant des protéines de fixation à la fibronectine et au collagène, des éléments du pilus, des enzymes participant à la formation du pilus et des régulateurs transcriptionnels. Malgré l'éloignement d'environ 250 kb du gène *emm*, une forte association avec le *emm*-type a été montrée. Les FCT les plus couramment retrouvées en Europe sont FCT 1 (*emm6*), FCT 2 (*emm1* et *emm28*), FCT 3 (*emm3* et *emm12*), FCT 4 *(emm12, emm28* et *emm89*) et FCT 5 (*emm4*) (48).

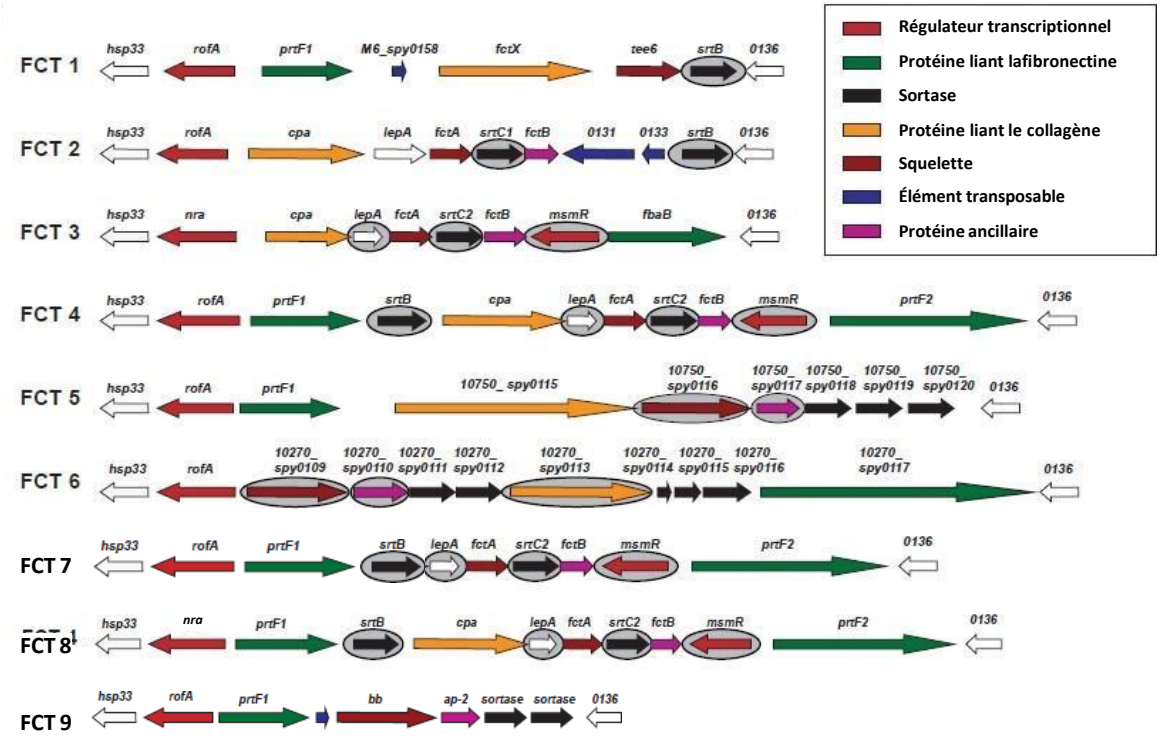

Figure 4. Organisation des gènes au sein des neuf régions FCT différentes chez *S. pyogenes*. D'après Thèse de Microbiologie, Céline Plainvert, BioSPC, 2013.

Aux vues de la recrudescence des cas d'infection à *S. pyogenes* dans les années 1980, les progrès scientifiques ont permis de mettre en œuvre de nouvelles techniques d'identification des souches de *S. pyogenes* tels que le « Pulsed Field Gel Electrophoresis » (PFGE), le « Multi Locus Sequence Typing » (MLST) et le « fluorescent amplified fragment length polymorphisms » (FAFLP). La technique alors utilisée était le MLST, basée sur l'amplification et le séquençage de sept gènes de ménage. Une corrélation a été établie entre le *emm*-type et le MLST (50). Ces techniques sont décrites comme étant peu discriminantes pour distinguer des souches clonales.

1.3.3. La variabilité génétique de *S. pyogenes*

La variabilité génétique de *S. pyogenes* repose sur l'évolution génétique de ces souches et l'acquisition au cours des générations d'éléments spécifiques tels que des facteurs de virulence et des toxines. L'acquisition d'information génétique s'effectue *via* différents mécanismes soit des recombinaisons homologues soit encore des transferts horizontaux à partir de différentes espèces. L'information peut également être modifiée par des mutations génomiques. Les pattern A-C sont plus sujets aux mutations contrairement aux pattern D et E faisant plus de recombinaison homologue (45). Ces évènements conduisent à la présence d'éléments mobiles tels que les prophages, les « Integrative Conjugative Elements » (ICE) et les « Mobile genetic element » (MGE), représentant 15 % du génome bactérien. Chaque souche contient huit à dix régions prophagiques et celles-ci sont différentes d'un *emm*-type à un autre, impliquant la grande diversité des répertoires de facteur de virulence et par conséquent expliquant l'adaptation de *S. pyogenes* à différents environnements (2). A ce jour, il est décrit deux catégories de phages. La première correspond aux phages pouvant altérer l'expression des gènes par insertion dans des régions promotrices. La seconde confère des régions codant des facteurs de virulence renforçant ainsi la virulence de la bactérie. Par exemple, en plus des modifications de régulation de l'expression des gènes *slo-nga*, les souches *emm1* ont acquis leur caractère hypervirulent par transfert d'une région prophagique de souches *emm12* codant le superantigène SpeA1 (51,52). De plus, ces mécanismes peuvent donner un avantage sélectif à la bactérie en lui permettant de s'adapter à son environnement, et par ailleurs être aussi à l'origine du tropisme tissulaire de la souche. En effet, la souche

emm28 est associée aux infections gynéco-obstétriques où elle y est retrouvée dans 25% des cas. Cette spécificité est liée au transfert d'un élément mobile de souches de *Streptococcus agalactiae*, composant de la flore vaginale. Il s'agit de la région RD2, codant des régulateurs transcriptionnels, des protéines extracellulaires exprimées pendant l'infection, notamment l'adhésine R28 (53–55).

Ainsi, cette grande variabilité génétique est responsable du tropisme tissulaire de *S. pyogenes*, qui est à l'origine de la diversité de ses répertoires de facteurs de virulence, la définissant alors comme un véritable pathogène majeur de santé publique.

1.4. Le répertoire de facteurs de virulence de *S. pyogenes*

S. pyogenes a longtemps été considéré comme étant un pathogène extracellulaire. Cependant, son observation lors d'infection *in vivo*, a conduit à le reconsidérer comme un pathogène également intracellulaire. Son large spectre d'infections résulte de sa diversité génétique qui lui confère une multiplicité de facteurs de virulence.

1.4.1. Les adhésines

La diversité d'infection de *S. pyogenes* peut être liée notamment à son répertoire divers et complexe d'adhésines qui lui permet de coloniser différents tissus (Tableau 1). Par conséquent, le tropisme tissulaire dépend des adhésines présentes à la surface de *S. pyogenes*. De plus, l'expression des gènes les codant dépend de l'environnement et de la régulation de certaines régulateurs transcriptionnels tels que CovR/CovS, Mga, RALPS et Rgg (56). Les principaux récepteurs des adhésines sont les protéines constituant de la matrice extracellulaire telles que la fibronectine, le fibrinogène et la laminine. La plus commune est la fibronectine, homodimère de 460 kDa. Elle présente des domaines rigides permettant les interactions avec d'autres composants de la matrice extracellulaire. Elle intervient dans différentes fonctions cellulaires comme la migration et la prolifération.

Les adhésines sont classées en 4 familles suivant leur ancrage à la paroi bactérienne : (i) celles-ci peuvent être liées de manière covalente au peptidoglycane par l'extrémité C-terminale avec un motif LPxTG *via* la sortase A ; (ii) liée de manière covalente par l'extrémité

Tableau 1. Les adhésines impliquées dans la virulence de *S. pyogenes.*

Adhésine	Déterminant génétique	Nature biochimique	Rôle(s)	Référence(s)
AspA	*aspA*	Protéine de la famille AgI/II liant des glycoprotéines d'agglutinine salivaires (SAG)	Adhésion cellulaire Formation des biofilms Echappement au SI* : protection contre la phagocytose	(75–77)
cpa	*cpa*	Protéine liant le collagène	Adhésion cellulaire	(60)
Fba	*fba*	Protéine liant la fibronectine	Adhésion cellulaire Echappement au SI : inhibition de l'opsonisation	(78,79)
Fbp54		Protéine liant la fibronectine et le fibrinogène	Adhésion cellulaire	(80)
GAPDH/SDH	*plr*	Protéine liant le plasminogène	Adhésion cellulaire Diffusion tissulaire Echappement au SI : inhibition de la phagocytose	(81–84)
Lbp	*lbp*	Protéine liant la laminine	Adhésion cellulaire	(83,85)
PAM	*pam*	Protéine liant le plasminogène	Diffusion tissulaire	(86–89)
Pilus	Région FCT		Adhésion cellulaire Formation du biofilm	(61,63, 64,90)
Protéine M et M-like	*emm, enn, mrp*	Protéine liant les protéines composant la matrice extracellulaire	Adhésion cellulaire Colonisation de l'oropharynx Internalisation Echappement au SI : inhibition de l'opsonisation, multiplication dans les PMNs** et macrophages	(91–103)
Prp		Protéine liant le plasminogène	Diffusion tissulaire	(104)
PrtF1/SfbI	*prfF1/sfbI*	Protéine liant la fibronectine	Adhésion cellulaire Internalisation Echappement au SI : inhibition de l'opsonisation	(59,105,106)
PrtF2	*prtF2*	Protéine liant la fibronectine	Adhésion cellulaire Internalisation	(107–109)
R28	*spy1336*	Protéine liant les intégrines	Adhésion cellulaire	(54)
SclA/Scl1	*scl1*	Protéine liant le collagène et la fibronectine	Adhésion cellulaire Formation du biofilm Internalisation	(72–74, 110,111)
SEN	*eno*	α-énolase liant le plasminogène	Adhésion cellulaire Invasion tissulaire	(112–114)
SfbX	*sfbx*	Protéine liant la fibronectine	Adhésion cellulaire Echappement au SI : inhibition de la phagocytose	(71,115)
Shr	*shr*	Protéine liant la fibronectine et la laminine	Adhésion cellulaire	(116,117)
SOF/SfbII	*sof/sfbII*	Protéine liant la fibronectine	Adhésion cellulaire Invasion tissulaire Echappement au SI : résistance à la phagocytose, inhibition de la réponse inflammatoire	(68–70, 115,118, 119)

*SI : Système Immunitaire.

**PMNs : Neutrophyles Polymorphonucléaires.

N-terminale avec des lipides (lipoprotéines) ; (iii) liée par des interactions non covalentes avec des composants de la surface bactérienne tels que les polysaccharides ; (iv) liée par un mécanisme encore non défini, « anchorless adhesin ». A ce jour, plus de dix-sept adhésines ont été décrites comme ayant un rôle dans l'adhésion cellulaire de *S. pyogenes* (57).

Les « fibronectin-binding-protein » (FnBP) sont les protéines les plus abondantes à la surface, ancrées par un motif LPxTG. Elles sont majoritairement codées au sein des régions FCT et MSCRAMM (« Microbial Surface Components Recognizing Adhesine Matrix Molecules »). Il est important de définir la fonction de ces protéines en prenant en compte la sérologie et le tropisme. *S. pyogenes* possède plus de dix FnBP caractéristiques dont les protéines M, M-like, SOF, SfbX, SclA, SfbI ou PrtF1. Ces protéines lui permettent alors d'adhérer à différents types cellulaires (58).

Les protéines M et M-like (Enn et Mrp) sont des adhésines se liant aux différentes protéines de la matrice extracellulaire de l'hôte. La protéine M est l'un des facteurs de virulence majeure de *S. pyogenes*. Elle est présente chez toutes les souches de *S. pyogenes* (cf. Identification de la diversité des souches de *S. pyogenes*). Il existe un large nombre de protéine M, ayant des rôles communs et spécifiques. A ce jour, la protéine M la plus étudiée est la protéine M1. Elle présente une forte spécificité pour l'adhésion aux protéines de la matrice extracellulaire, telle que la fibronectine et la laminine. Elle participe également à l'invasion tissulaire par le mécanisme « zipper-like » (cf. 1.5.3. L'invasion du tissu).

Les protéines de la région FCT sont des protéines se liant à la fibronectine et au collagène de la matrice extracellulaire. Cette région contient notamment les gènes codant pour la protéine SfbI, Cpa et le pilus. La protéine SfbI, ou PrtF1, est présente dans plus de 70 % des souches isolées de *S. pyogenes* (59). Tout comme la protéine M, son mécanisme d'adhésion est majeur pour la bactérie et participe à l'invasion tissulaire et la survie bactérienne au sein du tissu (cf. 1.5.3. L'invasion du tissu). La protéine Cpa est présente dans environ 10 % des souches de *S. pyogenes*. Elle est impliquée dans l'adhésion au collagène de type I contribuant notamment à l'infection des os et des articulations (60). Le pilus est composé principalement de pilines et protéines auxiliaires constituant un filament long, flexible, de 3 µm de diamètre (61). Il est ancré à la paroi bactérienne par la sortase A. L'ensemble des sous-unités participant à sa mise en place est codé au sein de la région FCT (Figure 4) (62). Il joue un rôle important dans la virulence de *S. pyogenes*, intervenant notamment dans l'adhésion aux cellules, la colonisation (63,64). L'adhésion par le pilus est médiée par les protéines auxiliaires, AP-1 et

AP-2. La protéine AP-2 permet la première étape réversible de l'adhésion et la protéine AP-1, possédant des régions de fixation au collagène, permet la deuxième étape irréversible, consolidant l'adhésion (65).

Les protéines SOF et SfbX sont des protéines de surface ancrées à la membrane par un motif LPxTG. Elles sont codées sur un même opéron régulé positivement par le régulateur transcriptionnel Mga (66). La protéine SOF (« Serum Opacity Factor ») est présente dans 40 à 50 % des souches de *S. pyogenes* (67). Il s'agit d'une protéine bifonctionnelle. *Via* son domaine C-terminal, elle participe à l'adhésion aux protéines de la matrice extracellulaire telles que la fibronectine, le fibrinogène et la fibuline (68,69). Il s'agit également d'une lipoprotéinase participant *via* son domaine N-terminal à l'opacification du sérum (70). La protéine SfbX est toujours associée au facteur SOF. Elle comprend un domaine C-terminal impliqué dans l'adhésion à la fibronectine et un domaine N-terminal de fonction inconnue (71).

La protéine SclA est une protéine de surface homodimérique ancrée à la membrane par un motif LPxTG situé en partie C-terminal. Cette protéine interagit avec le collagène et la fibronectine. Elle permet également l'internalisation de la bactérie et la formation de biofilm (72–74).

La protéine R28 est une protéine de surface ancrée à la membrane par un motif LPxTG. Elle est codée au sein de la région RD2, spécifique aux souches *emm28*. Cette région est à l'origine du tropisme tissulaire des souches *emm28* (cf. 1.3.3. La variabilité génétique de *S. pyogenes*). Cette protéine est impliquée dans l'adhésion aux cellules de l'hôte, en se liant aux intégrines *via* son domaine N-terminal (54).

1.4.2. Autres composés de la surface bactérienne

Outre les adhésines, d'autres composés de la surface bactérienne interviennent dans la virulence de *S. pyogenes* que ce soit au niveau de l'adhésion (les acides lipotéichoïques) mais aussi dans l'invasion et l'échappement au système immunitaire tel que la capsule (Tableau 2).

Les acides lipotéichoïques (LTA) sont des molécules amphiphiles ancrées à la membrane par une partie lipidique et comportant une partie constituée d'une chaine de sucres à la surface de la bactérie. L'ancrage lipidique est relativement constant suivant les espèces bactériennes contrairement à la partie sucre permettant ainsi de les classer en cinq familles.

Les LTA de *S. pyogenes* sont des LTA de type IV composés d'unités de pseudo-pentasaccharides répétés (2-acétamido-4-amino-2,4,6-trideoxy-D-galactose (AATGal), Glc, RboP) et de deux résidus glucose N-acétylglucosamine (120). Les LTA sont synthétisés par une succession de réactions enzymatiques et nécessitent le passage de la membrane cytoplasmique qui se produit *via* un mécanisme de « flip-flop » tout comme la synthèse du peptidoglycane (121). Les LTA sont des molécules chargées impliquées notamment dans l'interaction avec les cellules de l'hôte et la résistance aux peptides cationiques (122).

Tableau 2. Composés de surface bactérienne impliqués dans la virulence de *S. pyogenes*.

Composés bactériens	Déterminant génétique	Nature biochimique	Rôle(s)	Référence(s)
Capsule	Opéron *has*	Polymère d'acide hyaluronique	Colonisation nasopharyngée Invasion tissulaire Echappement au SI* : inhibition de l'opsonisation	(126–133)
C5a peptidase	*scpA*	Endopeptidase de surface	Invasion tissulaire Echappement au SI : inhibition du complément, du recrutement des PMNs**	(140,101, 130,131)
Isp2	*isp2*	Protéine de surface	Colonisation du tractus uro-génital Modification de la paroi bactérienne : hydrolysation du peptidoglycane (domaine CHAP)	(135,136)
LTA	Multiples	Polymère de glycérophosphate	Adhésion cellulaire Formation du biofilm Internalisation Réaction inflammatoire	(122, 137–141)
SpyA	*spyA*	Protéine de surface	Invasion tissulaire : dégradation de la vimentine	(142,143)
SpyAD	*spyAD*	Protéine de surface	Division bactérienne Adhésion cellulaire Colonisation du tractus uro-génital	(135,144)
SpyCEP	*spyCEP*/*cepA*	Protéase de surface	Echappement au SI : dégrade IL8 impliquée dans le recrutement des PMNs, résistance à la phagocytose des PMNs et aux NETs***	(145–151)

*SI : Système Immunitaire.
**PMNs : Neutrophyles Polymorphonucléaires.
***NETs : Pièges extracellulaires des neutrophiles.

La capsule est principalement composée d'acide hyaluronique, appartenant à la famille des glycosaminoglycanes, polymères linaires de monosaccharides, unités de N-acétylglucosamine et d'acide glucuronique. Elle constitue une barrière de protection pour la bactérie face aux réponses de l'hôte et permet ainsi la survie et l'invasion du tissu. Son implication dans la dissémination est décrite comme étant un mécanisme important dans l'invasion des tissus. En effet, en se fixant au récepteur CD44 des cellules, elle induit des

réarrangements du cytosquelette cellulaire et ainsi la rupture des jonctions intercellulaires telles que les jonctions serrées, permettant ainsi la dissémination bactérienne par la voie paracellulaire (123).

La protéine ScpA, ou C5a peptidase, est une protéine de surface ancrée dans la membrane par le motif LPxTG *via* son domaine C-terminal. Elle est codée au sein du locus Mga et est commune à toutes les souches de *S. pyogenes* tout comme les protéines M et M-like (cf. 1.3.2. Identification de la diversité des souches de *S. pyogenes*). Il s'agit d'une protéase de la famille des sérine-protéases de type subtilisine. ScpA est une protéine multifonctionnelle participant à l'invasion tissulaire indépendamment de la fibronectine et à l'échappement au système immunitaire en inhibant le complément (124,125).

1.4.3. Les facteurs de virulence sécrétés : les toxines

S. pyogenes possède un large répertoire de facteurs de virulence sécrétés intervenant principalement dans la colonisation et l'invasion. Ces éléments ne possèdent pas de séquences d'ancrage à la paroi mais des peptides signaux de sécrétion. Il existe différentes familles dont les hémolysines, les protéases et les super-antigènes (Tableau 3).

La cystéine protéase SpeB est le « couteau suisse » de *S. pyogenes*, en raison de ses multiples rôles dans les infections, démontrés *in vitro* et *in vivo*. Il s'agit d'une protéine d'environ 28 kDa. Elle est produite en fin de phase exponentielle et début de phase stationnaire, puis maturée par clivage et sécrétée *via* le complexe de l'Exportal (152). SpeB interagit avec les intégrines *via* le motif RGD (153). Ainsi, SpeB intervient principalement dans l'invasion en dégradant la matrice extracellulaire par clivage de la fibronectine, dégradation de la vimentine et activation des métalloprotéase (154,155), et aussi à l'échappement au système immunitaire en inhibant l'opsonisation (cf. L'échappement au système immunitaire de l'hôte) et dans la mort cellulaire (156,157).

Les Streptolysines O (SLO) et S (SLS) sont des hémolysines capables de lyser les érythrocytes. Elles interviennent dans l'invasion tissulaire en formant des trous dans la membrane des cellules et en induisant ainsi la mort cellulaire en créant un stress du réticulum endoplasmique. Les pores formés par SLS et SLO sont différents par leur taille. Les pores formés par SLS sont moins importants. De plus, SLO est une protéine codée par un seul gène

Tableau 3. Composés sécrétés impliqués dans la virulence de *S. pyogenes*.

Composés sécrétés	Déterminant génétique	Nature biochimique	Rôle(s)	Référence(s)
cAMP factor	*cfa*	Enzyme	Adhésion cellulaire Echappement au SI* : résistance à la phagocytose	(162–164)
CIP	*cip*	Protéine	Échappement au SI : inhibition du complément	(165)
EndoS	*ndoS*	Endoglycosidase	Echappement au SI : clive les IgG	(156,166, 167)
GRAB	*grab*	Protéine de surface	Facteur de virulence régulant la protéolyse	(168,169)
Hly	*hylA*	Hyaluronidase	Invasion tissulaire	(170)
IdeS/Mac	*mac*	IgG-degrading enzyme	Echappement au SI : clive les IgG, liaison au récepteur CD11b des PMNs** entravant la phagocytose	(171–175)
NADase	*nga*	NAD-glycohydrolase	Facteur agissant en synergie avec SLO Déplétion de l'énergie de la cellule de l'hôte Echappement au SI : inhibition de la maturation du phagosome	(158, 176–182)
Sda1	*sda1*	Streptodornase ou DNAse	Echappement au SI : résistance à la phagocytose des PMNs et aux NETs***	(183–185)
SIC	*sic*	Protéine extracellulaire	Inhibition de l'adhésion cellulaire Multiplication dans la salive Colonisation du nasopharynx Echappement au SI : inhibitrice du complément, inhibition de l'opsonisation, inhibition de la phagocytose, dégradation des peptides antimicrobiens Réaction inflammatoire	(186–196)
Ska	*ska*	Streptokinase	Invasion tissulaire : dégrade le plasminogène en plasmine	(197,198)
Sla	*sla*	Phospholipase A2	Adhésion cellulaire Initiation de la colonisation	(191,199)
SLO	*slo*	Streptolysine O	Echappement au SI : lyse des PMNs, inhibition de la maturation du phagosome Invasion tissulaire Réaction inflammatoire	(158,180, 200–208)
SLS	Opéron *sag*	Streptolysine S	Formation de biofilm Invasion tissulaire Echappement au SI : inhibition du recrutement des neutrophiles, lyse des PMNs	(182, 189–195)
SpeA, SpeC, SpeG, SpeH, SpeI, **SpeJ, SpeK, SpeL, SpeM, Ssa et SmeZ**	*speA, speC, speG, speH, speI, speJ, speK, speL, speM, ssa* et *smeZ*	Super-antigènes	Stimulation du SI, Réaction inflammatoire	(154, 216–227)
SpeB	*speB*	Cystéine protéinase	Echappement au SI : inhibition de l'opsonisation par clivage des IgG, dégradation des peptides antimicrobiens de l'immunité innée, clivage des IgA Invasion tissulaire : dégrade la matrice extracellulaire Réaction inflammatoire	(156,167, 228,229)
Sse	*sse*	Estérase	Echappement au SI : inhibition du recrutement des PMNs	(212, 230,231)

*SI : Système Immunitaire.

**PMNs : Neutrophyles Polymorphonucléaires.

***NETs : Pièges extracellulaires des neutrophiles

slo contrairement à SLS qui a une synthèse non ribosomale, *via* un opéron composé de huit gènes. SLO agit en synergie avec la toxine NAD-glycohydrolase (NADase), codés sur le même opéron. Initialement, le mécanisme suggérait que SLO formait des pores permettant à la NADase de pénétrer dans la cellule. Une fois à l'intérieur, celle-ci provoque une perte de l'énergie de l'hôte, ayant ainsi pour conséquence la mort cellulaire (158). Cependant, la NADase ne passe pas par les pores formés par SLO mais entre dans la cellule *via* un autre mécanisme également dépendant de cette hémolysine (159).

Les super-antigènes (SAgs) sont des petites molécules non glycosylées de 22 à 29 kDa. Chez *S. pyogenes*, dix SAgs ont été décrits. Ces répertoires sont conservés au sein des *emm*-types. Ils sont capables de se lier à la fois au récepteur des cellules T et au complexe majeur d'histocompatibilité, activant alors les lymphocytes T et la surproduction de molécules inflammatoires, telles que les cytokines. Ceci a pour conséquences une forte inflammation et la destruction des tissus (154). Ce mécanisme est à l'origine du choc toxique.

La Streptokinase, Ska, est une protéine de 45,54 kDa sécrétée par la bactérie. Cette protéine intervient dans l'activation du plasminogène en plasmine en induisant un changement de conformation après fixation démarrant la protéolyse (160,161). Le plasminogène est une glycoprotéine à chaîne unique qui fait partie du plasma et des fluides extracellulaires. Il s'agit d'un élément clé dans le processus de fibrinolyse, indispensable à la coagulation sanguine. En effet, sa conversion en plasmine permet la lyse des caillots de fibrine, protéine filamenteuse issue du fibrinogène. Ska entraîne alors une augmentation de la production de plasmine et par conséquent une augmentation de la dégradation des tissus.

1.5. Les premières étapes du mécanisme d'invasion de *S. pyogenes*

Le mécanisme général d'infection invasive de *S. pyogenes* a été étudié *in vitro* par interaction avec des cellules épithéliales, *ex vivo* sur biopsie ou *in vivo* dans des modèles animaux. Au laboratoire, nous divisons ce mécanisme en quatre étapes : l'adhésion et la colonisation de la surface du tissu, suivi de l'invasion du tissu et de l'échappement au système immunitaire de l'hôte (Figure 5).

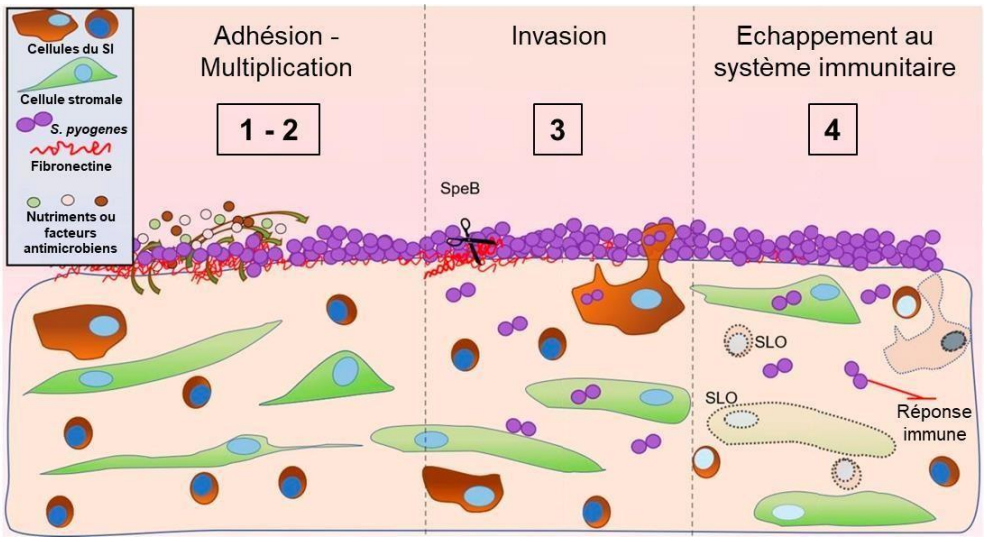

Figure 5. Mécanisme général d'infection de *S. pyogenes*. Ce schéma représente l'hypothèse de travail concernant le mécanisme général d'infection de *S. pyogenes*. Celui-ci peut être décomposé en plusieurs phases : l'adhésion, la multiplication, l'invasion et l'échappement au système immunitaire. D'après (21).

1.5.1. L'adhésion au tissu

L'adhésion au tissu par *S. pyogenes* est la première étape du mécanisme d'infection mettant en jeu des stratégies complexes, multiples et variables. En effet, cette étape dépend du répertoire d'adhésines et des capacités d'adaptation à l'environnement de la souche de *S. pyogenes* (65). L'interaction avec le tissu n'est pas directe avec les cellules mais indirecte via la matrice extracellulaire (MEC) qui représente alors un « pont » entre la bactérie et les cellules du tissu. Ainsi, l'adhésion est découplée en deux sous-étapes comprenant un contact à distance avec la MEC puis un contact rapproché. La première étape de l'adhésion à longue distance est majoritairement réalisée par des composants de la surface bactérienne tels que les LTA et le pilus, permettant de faire face à la répulsion des charges électrostatiques entre la surface bactérienne et les éléments de la MEC. Cette étape est réversible et ne dépend pas du type cellulaire. Afin de rendre l'adhésion irréversible, les adhésines ancrées à la surface de la bactérie vont alors renforcer la fixation à la MEC, ou directement aux cellules. Cette étape dépend alors d'adhésines et donc de leur cible, elle participe ainsi à définir le tropisme tissulaire (57,232).

1.5.2. La colonisation de la surface du tissu

L'étape d'adhésion est suivie par la colonisation de la surface du tissu caractérisée par la formation de micro-colonies de type « biofilm-like ». Cette étape est complexe et multifactorielle (57). Du fait des répertoires variés des protéines sécrétées et de surface, elle dépend essentiellement du *emm*-type de la souche (233). Le processus de formation du biofilm est complexe et encore peu étudié. Sa mise en place dépend de certaines adhésines telles que les protéines M et M-like, le pilus et la capsule et de l'environnement tel qu'un environnement ayant un pH acide (63,234,235). Le biofilm est aussi décrit comme structure de défense face à la réponse de l'hôte. Dans le cas d'infection des muqueuses, aucune formation de biofilm n'est observée, l'adhésion sera suivie de l'internalisation de la bactérie au sein des cellules (65).

1.5.3. L'invasion du tissu

L'invasion du tissu est caractérisée par la dégradation de la MEC. Les progrès en microscopie notamment en « Field Emission Scanning Electron Microscopy » (FESEM) ont permis de mettre en évidence différents mécanismes d'internalisation (65).

L'invasion du tissu par *S. pyogenes* est dépendante des caractéristiques de celui-ci. En effet, la décidue ne possédant pas de jonction, après colonisation de sa surface, l'invasion de ce tissu s'effectue par dégradation de la MEC *via* la cystéine protéase SpeB (21). De plus, *S. pyogenes* a la capacité d'envahir le tissu de l'hôte par translocation paracellulaire médiée, ou dégradation des jonctions cellulaires par interaction de la capsule avec les cellules immunitaires CD44 (123).

S. pyogenes est également capable d'envahir les cellules de l'hôte via deux mécanismes clairement décrits. Le premier est dépendant de la protéine M, interagissant avec différentes protéines de la MEC puis adhérant aux intégrines *via* ces dernières (236). Cela induit la polymérisation des filaments d'actine au niveau des points d'adhésion et ainsi permet l'internalisation par un mécanisme de type « zipper-like » (Figure 6A). Le deuxième mécanisme est médié par la protéine de surface SfbI (237,238). Il est similaire au premier mais n'induit pas de réarrangement du cytosquelette cellulaire. En effet, l'interaction

SfbI/fibronectine suffit pour permettre l'agrégation de cavéoles, qui fusionnant entre elles forment une invagination dans la membrane et ainsi la bactérie pénètre dans la cellule dans une grande vacuole, le cavéosome (Figure 6B). Cette structure ne peut fusionner avec le lysosome protégeant ainsi *S. pyogenes* de la dégradation via cette voie.

Les mécanismes d'internalisation mis en place sont dépendants de l'environnement de la bactérie. En absence d'oxygène et donc en forte teneur en CO_2, l'expression du gène codant la protéine SfbI est diminuée à l'inverse de l'expression du gène codant la protéine M. Dans ces conditions, la protéine SfbI serait requise pour l'invasion des cellules aux sites d'infection contrairement à la protéine M qui contribuerait à l'invasion des cellules plus profondes dans les tissus (233).

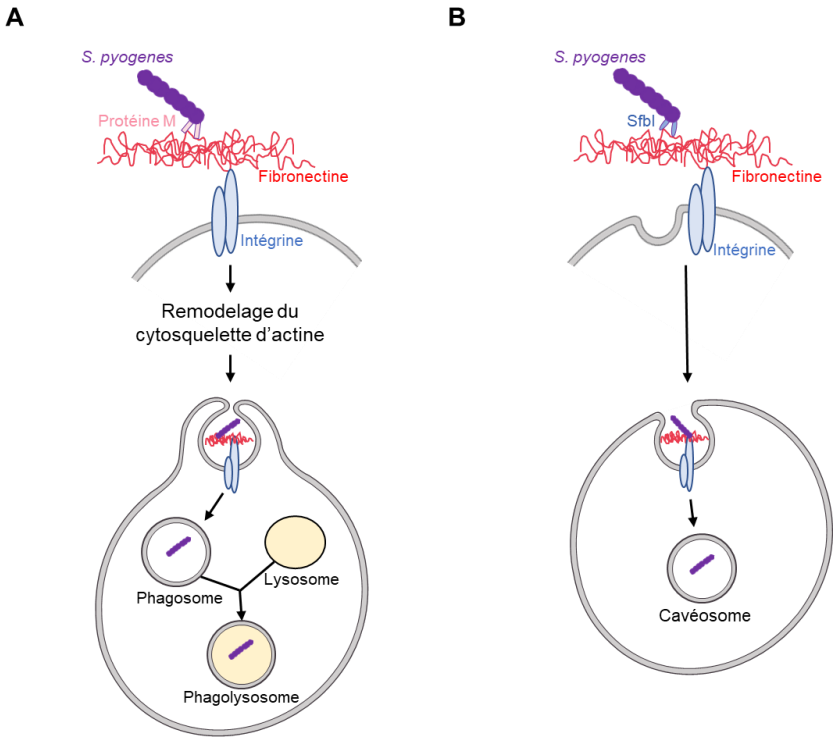

Figure 6. Mécanismes d'invasion de *S. pyogenes*. (A) Mécanisme dépendant de la protéine M. (B) Mécanisme dépendant de la protéine SfbI. Figure adaptée de (233).

1.5.4. L'échappement au système immunitaire de l'hôte

Pour contrer l'infection, l'hôte met en place des réponses immunitaires telles que la sécrétion de peptides antimicrobiens, de molécules inflammatoires comme les cytokines permettant l'activation de nombreuses cellules immunitaires et le système du complément permettant l'opsonisation et la clairance bactérienne. Néanmoins, *S. pyogenes* a dû

développer et sélectionner, au cours de l'évolution, des mécanismes de résistance lui permettant d'échapper à son sort.

La résistance au complément est un des mécanismes d'échappement de *S. pyogenes*. Celui-ci peut empêcher la formation et le recrutement du complément par l'intermédiaire de différents facteurs. En effet, la protéine SpeB clive les protéines impliquées dans la formation du complexe (C6, C7, C8, C9) et la protéine EndoS clive les immunoglobulines permettant la reconnaissance des bactéries (156). De plus, la peptidase ScpA empêche le recrutement de cellules immunitaires en clivant les protéines C5a (239).

La résistance à la phagocytose implique de nombreux procédés tels que le détournement de cellules immunitaires et le camouflage. *S. pyogenes* a la faculté de détourner les mécanismes des cellules immunitaires notamment l'apoptose des leucocytes polymorphonucléaires (PMNs), en agissant sur la production d'espèces dérivées réactifs de l'oxygène (ROS) et de peptides antimicrobiens. En effet, en réponse à l'interaction avec des PMNs, une modulation de l'expression des gènes de virulence et de résistance aux produits de lyse est observée (240). En exploitant ce mécanisme, *S. pyogenes* diminue son exposition aux ROS et peptides antimicrobiens favorisant sa survie (241). De plus, des composés de surface de *S. pyogenes*, tels que sa capsule et les FnBPs, représentent des barrières physiques face aux cellules immunitaires permettant ainsi la survie et l'invasion des tissus. En effet, les adhésines FnBPs, telles que SfbI ont la capacité de fixer la fibronectine qui interagit alors avec le collagène. Cette interaction fibronectine-collagène va induire la formation d'agrégats bactériens. Ce mécanisme permet à *S. pyogenes* de camoufler les épitopes présents à sa surface et ainsi le protège de la phagocytose (242). Un autre mécanisme d'échappement est l'aptitude de *S. pyogenes* à contourner sa lyse par des mimiques moléculaires. En effet, *S. pyogenes* sécrète des protéines Mac qui présentent une homologie avec la sous-unité α de la protéine Mac-1 (CD11b). Cette protéine immunitaire intervient dans la régulation des fonctions des PMNs (adhésion, migration, phagocytose, etc.). De cette manière, *S. pyogenes* empêche le recrutement d'anticorps et bloque la phagocytose et donc la destruction de *S. pyogenes* par les PMNs (171). *S. pyogenes* peut également échapper à la phagocytose en utilisant des structures telles que le cavéosome ou encore survivre au sein du lysosome en empêchant sa maturation en phagolysosome.

S. pyogenes a la capacité d'échapper aux pièges extracellulaires des neutrophiles, les NETs. Il s'agit d'un mécanisme bactéricide par lequel les neutrophiles libèrent leurs granules

microbicides pour capturer et lyser les bactéries (243). En plus de pouvoir contourner la lyse par les NETs, *S. pyogenes* induit la mort cellulaire en dégradant ces derniers (244).

1.6. L'adaptation de *S. pyogenes* à son environnement

S. pyogenes est très exigeant pour sa croissance. Ses capacités biosynthétiques étant limitées, il faut lui fournir un environnement favorable, supplémenté avec diverses sources de vitamines et d'acides aminés et une température optimale de croissance comprise entre 35 et 37 °C. L'altération de ces conditions de culture peut entraîner des modifications du métabolisme bactérien. Du fait de son large spectre d'infection, les environnements de *S. pyogenes* sont très divers. Ces derniers se distinguent notamment au niveau de la quantité et la qualité des nutriments, des sources de sucre, d'acide aminé, d'oxygène, de l'osmolarité et de leur pH. *S. pyogenes* doit donc continuellement moduler son métabolisme afin de s'adapter à celui-ci et y survivre. Le métabolisme et le niveau de régulation des gènes de virulence de ce pathogène sont étroitement liés chez ce pathogène, favorisant cette adaptation.

1.6.1. Les principales voies métaboliques de *S. pyogenes*

S. pyogenes est une bactérie lactique qui produit son énergie à partir de la fermentation de source carbonée dont la principale est le glucose. Cette fermentation induit une diminution de la concentration de glucose et l'accumulation d'acide lactique dans le milieu conduisant alors à son acidification. Ainsi les sources carbonées permettent la croissance de la bactérie. Le métabolisme de *S. pyogenes* est principalement étudié au sein des souches *emm*1. Il est composé d'un complexe réseau de voies métaboliques qui sont actives suivant les conditions de croissance de la bactérie. Nous pouvons ainsi citer les principales voies connues à ce jour (245) :

- Le métabolisme des sucres (décrit ci-dessous).
- Le métabolisme des acides aminés (décrit ci-dessous).
- Le métabolisme de l'acétate qui est actif dans les milieux riches en nutriments et utilisé comme source d'énergie pendant la croissance en présence de glucose.

- Le métabolisme des lipides et la synthèse des acides gras (décrit dans le chapitre d'introduction 2. La synthèse de la membrane cytoplasmique).
- Le métabolisme aérobie avec l'activation de la synthèse du NAD^+ qui est un facteur de croissance essentiel impliqué dans de nombreuses réactions biochimiques.
- La synthèse des nucléotides *via* deux classes de composés azotés, les purines et les pyrimidines, qui est encore mal connue chez *S. pyogenes*.
- Le métabolisme des métaux tels que le fer, le cuivre et le manganèse est important pour la physiologie et la pathogénicité de *S. pyogenes*.

Le métabolisme des sucres est le réseau métabolique central de la bactérie. La voie principale de ce métabolisme est la glycolyse aussi nommée voie de Embden-Meyerhof-Parnas (EMP) (Figure 7) (245). Après transport du glucose par un système de phosphotransférase (PTS), elle permet sa conversion en pyruvate, à partir de deux molécules d'ATP et de deux $NADH_2$, par l'intervention de douze enzymes cytoplasmiques. Le pyruvate ainsi produit est normalement transformé en acétyl-CoA. Contrairement aux autres bactéries Gram-positives, *S. pyogenes* possède un cycle de Krebs incomplet et donc non fonctionnel. Par la suite, l'acétyl-CoA est alors utilisé par d'autres voies métaboliques telles que le métabolisme de l'acétate et des lipides. De la même manière, *S. pyogenes* possède une voie Entner-Doudoroff (ED), alternative à la glycolyse, responsable de la transformation de glucose en pyruvate par des étapes de non-phosphorylation, incomplète. Le fait que ces deux voies soient incomplètes renforce l'importance de la glycolyse pour la croissance de ce pathogène. La régulation de cette voie dépend de la concentration de glucose présent dans l'environnement. Le plasma, le sérum et le sang sont des environnements riches en glucose. En revanche, la sphère ORL et la peau, par exemple, sont des environnements faibles en glucose pourtant *S. pyogenes* y prolifère. En effet, lorsque la concentration en glucose est insuffisante, *S. pyogenes* utilise d'autres sources de carbone telles que des sucres complexes (246), du lactose ou encore du maltose, comme source d'énergie alternative. L'utilisation des différentes voies de conversion des sucres est contrôlée par la voie de répression catabolique du carbone (CCR, « carbon catabolite repression »), permettant à la bactérie de répondre rapidement à ces besoins énergétiques et nutritifs.

Le métabolisme du lactose permet la conversion du lactose ou du galactose en pyruvate. Les enzymes participant à son transport et à son métabolisme sont codées au sein de deux

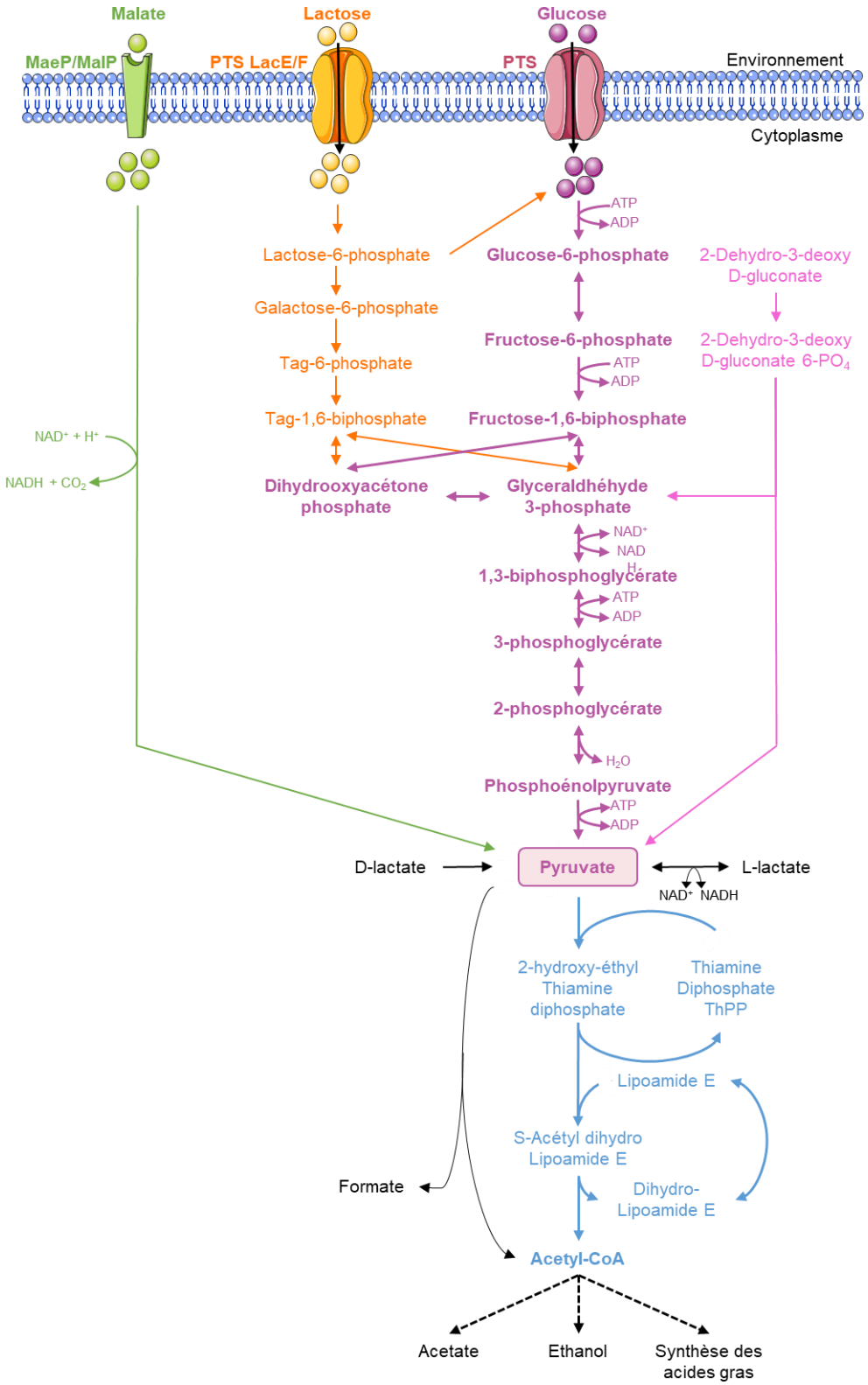

Figure 7. Principales voies composant le métabolisme des sucres chez *S. pyogenes*. La glycolyse (violet) est la principale voie métabolique permettant la formation de molécule de pyruvate à partir de glucose. Par la suite le pyruvate est transformé en acétyl-CoA *via* un cycle de Krebs incomplet (bleu), précurseur pour la synthèse des acides gras. Lorsque *S. pyogenes* se trouve dans un environnement faible en glucose, d'autres voies énergétiques sont activées, telles que la voie incomplète Entner-Doudoroff (rose claire), le métabolisme du malate (vert) et celui du lactose (orange). Ces voies ont pour but commun de fournir de l'énergie à la bactérie à partir de source carbonée et ainsi lui permettre de survivre dans son environnement. Figure adaptée de (245).

opérons, *lac.1* et *lac.2*, dans le génome de *S. pyogenes* (247). Ces deux opérons, différents par leur composition génique, n'ont pas la même fonction. L'opéron Lac.1 contenant les gènes de régulation, LacD.1 et LacR.1, est impliqué dans la régulation transcriptionnelle répondant aux modifications des conditions environnementales tels que le pH et l'osmolarité (248). En revanche, l'opéron Lac.2 possède l'ensemble des gènes codant les enzymes permettant le transport et la conversion du lactose en glucose. Le glucose ainsi produit sera alors pris en charge par la glycolyse et convertie en pyruvate.

Le métabolisme du malate permet la conversion du malate en pyruvate grâce à l'enzyme malique, MaeE (245). Le malate, abondant dans les tissus et dans l'environnement, est transporté au sein de la bactérie par une malate permease, MalP/MaeP. L'activation de cette voie dépend de plusieurs critères. Le premier est bien évidemment la concentration en malate dans l'environnement, contrôlé directement par un système à deux composants, MaeK/MaeR. Le deuxième dépend de la concentration de glucose et de la production en acide lactique et donc de l'acidification du milieu, qui stimule alors l'expression des gènes de cette voie (249).

S. pyogenes, possédant un cycle de Krebs non fonctionnel, n'est pas en mesure de fournir les précurseurs nécessaires à la formation des acides aminés. Ce pathogène est donc auxotrophe pour quinze acides aminés requis pour sa croissance et sa persistance. Afin de coloniser son environnement, *S. pyogenes* va donc utiliser les acides aminés présents dans celui-ci. Deux types d'ABC transporteurs ont été décrits, Opp et Dpp, respectivement utilisé pour le transport des oligopeptides et des dipeptides. *S. pyogenes* module son métabolisme en fonction de la concentration en acides aminés présent dans son milieu. Lorsque le milieu est pauvre en acide aminé, deux voies de réponses sont présentes chez *S. pyogenes* (Figure 8). La première est dépendante de l'activation de la protéine RelA qui induit alors une réponse au stress par l'activation de l'alarmone (p)ppGpp. La deuxième, RelA-indépendante, induit la production d'acides aminés *via* la dégradation de protéines et ainsi permet la croissance de la bactérie dans son environnement, sans déclenchement de la réponse stringente au stress observée dans la réponse RelA-dépendante (250).

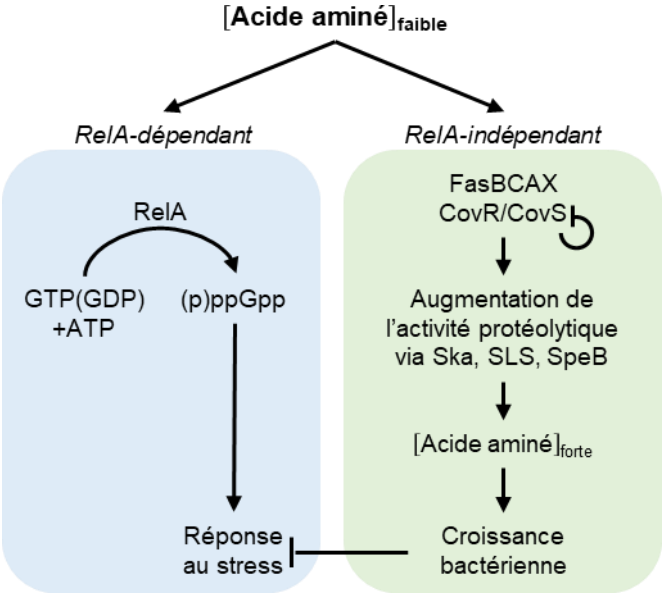

Figure 8. Métabolisme des acides aminés chez *S. pyogenes*. Ce métabolisme dépend de la concentration en acides aminés présents dans l'environnement. Lorsque la concentration en acides aminés est faible voire nulle, deux réponses peuvent être induites. La première réponse, RelA dépendante, induit l'activation de l'alarmone, (p)ppGpp, conduisant à une réponse stringente pour résister au stress rencontrer et survivre. La deuxième réponse, RelA-indépendante, permet l'augmentation de la concentration d'acides aminés par l'activation d'enzyme protéolytique. Cet enrichissement lui permettra d'utiliser ces acides aminés en source d'énergie alternative et ainsi de croître au sein de son environnement. Figure adaptée de (251).

De plus, *S. pyogenes* peut utiliser les acides aminés présents dans l'environnement comme source d'énergie alternative. En effet, il a été montré que dans un environnement à faible teneur en glucose, *S. pyogenes* utilise l'arginine de l'hôte afin de le coloniser (252). Ce pathogène a également développé des mécanismes lui permettant de détourner la cellule hôte afin de mieux utiliser ces acides aminés. *S. pyogenes*, *via* ses hémolysines, induit un stress oxydatif dans le cytoplasme de la cellule hôte permettant ainsi une augmentation de la production d'asparagine par la cellule (253). De la même manière, il a également été décrit que *S. pyogenes* utilise le glutathion, tripeptide composé de glutamate, de cystéine et de glycine, des cellules hôtes (254). L'import de ces différents acides aminés permet alors à la bactérie de se multiplier et de survivre au sein de la cellule hôte.

S. pyogenes utilise donc ses facteurs de virulence comme une boîte à outils pour trouver des conditions optimales de croissance en enrichissant son environnement en nutriments et ainsi croitre au sein des tissus de l'hôte. Ainsi il existe un lien entre le métabolisme et la virulence chez *S. pyogenes*.

1.6.2. Lien entre métabolisme et virulence chez *S. pyogenes* : la régulation

Afin de permettre son adaptation, *S. pyogenes* régule fortement l'expression des gènes codant les enzymes des voies métaboliques et les facteurs de virulence suivant la composition de son environnement. Les régulateurs transcriptionnels sont décrits comme agissant spécifiquement sur un régulon et également en interconnexion entre eux (Tableau 4). On ne peut les restreindre à deux familles de régulateurs, régulateurs du métabolisme ou de la virulence, du fait de la relation entre ces deux permettant l'adaptation de *S. pyogenes* à son environnement. Néanmoins, en raison de leur importance, certains régulateurs ont été classés dans ces catégories tels que CcpA en tant que régulateur du métabolisme et Mga régulateur de la virulence chez *S. pyogenes*.

Le métabolisme des sucres est un élément central dans la croissance de *S. pyogenes*. Il est donc extrêmement contrôlé par la bactérie notamment par la voie de répression catabolique du carbone, CCR dont fait partie le répresseur transcriptionnel CcpA (« Catabolite Control Protein A »). CcpA réprime environ 6 % du génome de *S. pyogenes*, dont la voie métabolique des sucres, des gènes de virulence et d'autres régulateurs transcriptionnels (255). L'activité de ce régulateur dépend de la concentration en glucose présent dans l'environnement (Figure 9). En effet, il est actif lorsque la bactérie se trouve dans un milieu riche en glucose afin d'activer la transcription des gènes pour la croissance en présence de glucose et d'inhiber les voies énergétiques alternatives (256). CcpA réprime également l'expression de gènes de virulence directement (SLS) ou indirectement *via* la répression d'autres régulateurs transcriptionnels tel que Mga en se fixant sur des sites de fixation spécifiques, les régions CRE (« Catabolic-Responsive Element ») dans les régions promotrices de ces gènes (255,257).

L'expression des gènes de virulence est contrôlée par trois types de régulateurs : les systèmes de régulation à deux composants (TCS, « Two-Component signal transduction Systems »), les régulateurs transcriptionnels dits autonomes (activateurs et/ou répresseurs) et les ARN non codants. A ce jour, 13 TCS et au moins 30 régulateurs transcriptionnels ont été décrits comme participant, entre autres, à la virulence de *S. pyogenes* (259).

Tableau 4. Principaux mécanismes de régulation des gènes de virulence et des voies métaboliques chez *S. pyogenes*.

Stimuli	[Sucres]	[Acides aminés]	[Métal]	Quorum sensing	Peptides antimicrobiens	Stress oxydatif	pH acide	Régulateur
Régulateurs transcriptionnels*								
CcpA	X		X	X				X
CodY		X		X	X			
LacD.1	X			X				
Mga	X			X	X			X
MtsR	X		X			X	X	X
PerR	X	X	X		X	X		X
RALPs				X	X			X
Rgg/RopB	X			X		X	X	X
Sil		X		X				X
Srv		X						X
Systèmes à deux composants (TCS)								
CiaH/CiaR	X					X		
CovR/CovS		X	X	X	X			X
Ihk/Irr	X	X	X		X	X	X	X
TrxS/TrxR		X		X	X			X
VicR/VicK					X			X
ARN non codants								
FasBCAX				X	X			
Fonction régulée	**Métabolisme des sucres**	**Métabolisme des acides aminés**	**Métabolisme des acides gras**	**Métabolisme de certains métaux**	**Quorum sensing**	**Résistance au stress**	**Virulence**	**Régulation**

* Tableau adapté de (245).

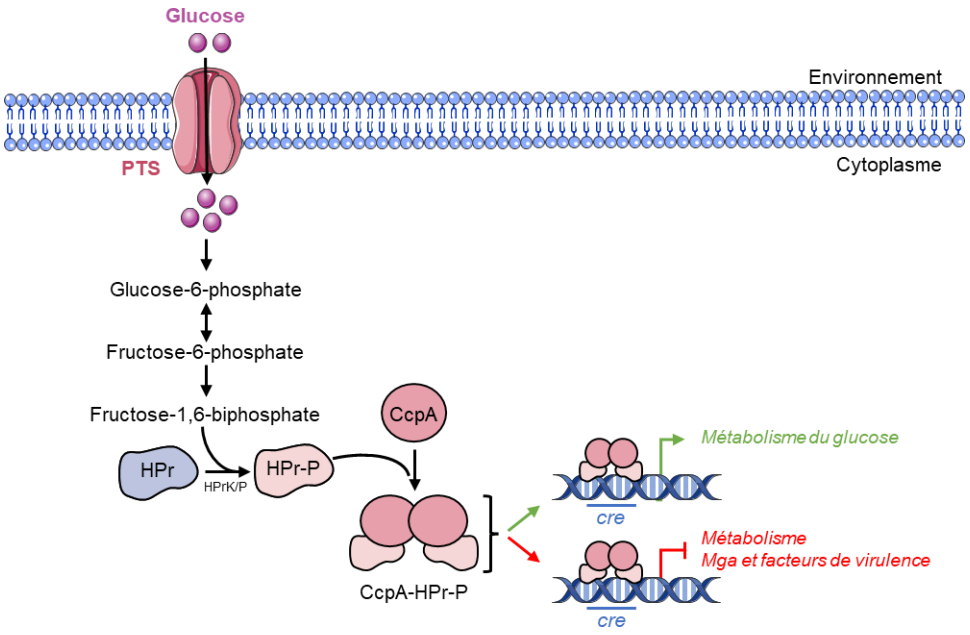

Figure 9. Régulation du métabolisme des sucres par CcpA lors de croissance dans un environnement riche en glucose de *S. pyogenes*. Figure adaptée de (245,258).

Les TCS sont des éléments qui répondent à un stimulus extérieur *via* une histidine kinase. La kinase s'autophosphoryle puis phosphoryle la protéine régulatrice permettant ainsi le contrôle de l'expression des gènes de son régulon et par conséquent l'adaptation de la bactérie à son environnement. Le TCS le plus étudié chez *S. pyogenes* est le système de régulation CovR/CovS (« Control Of Virulence »), aussi nommé CsrR/CsrS (« Capsule Synthesis Regulator »). Il s'agit du régulateur majeur de *S. pyogenes*, régulant de manière directe ou indirecte 10 à 15 % de son génome (Figure 10). Ce TCS est constitué d'une histidine kinase CovS et d'un régulateur CovR. En réponse à différents stimuli environnementaux tels qu'une augmentation de la température, un pH acide, une forte osmolarité, une modification de la concentration en Mg^{2+} et la présence du peptide antimicrobien LL-37, CovS est présente sous forme active, CovS-P, dans la bactérie et peut alors activer CovR en le phosphorylant, CovR-P. En revanche, l'addition de LL-37 entraîne la déphosphorylation de CovR, contrairement aux autres stimuli. CovR-P va alors réprimer l'expression d'un certain nombre de gènes impliqués notamment dans le métabolisme (adaptation au stress), la virulence (sécrétion de protéines, protéines de surface) et la régulation *via* le contrôle d'autres régulateurs transcriptionnels. Ainsi ce système permet à la bactérie de répondre de manière directe ou indirecte aux variationx de l'environnement et de proliférer dans celui-ci (256,260).

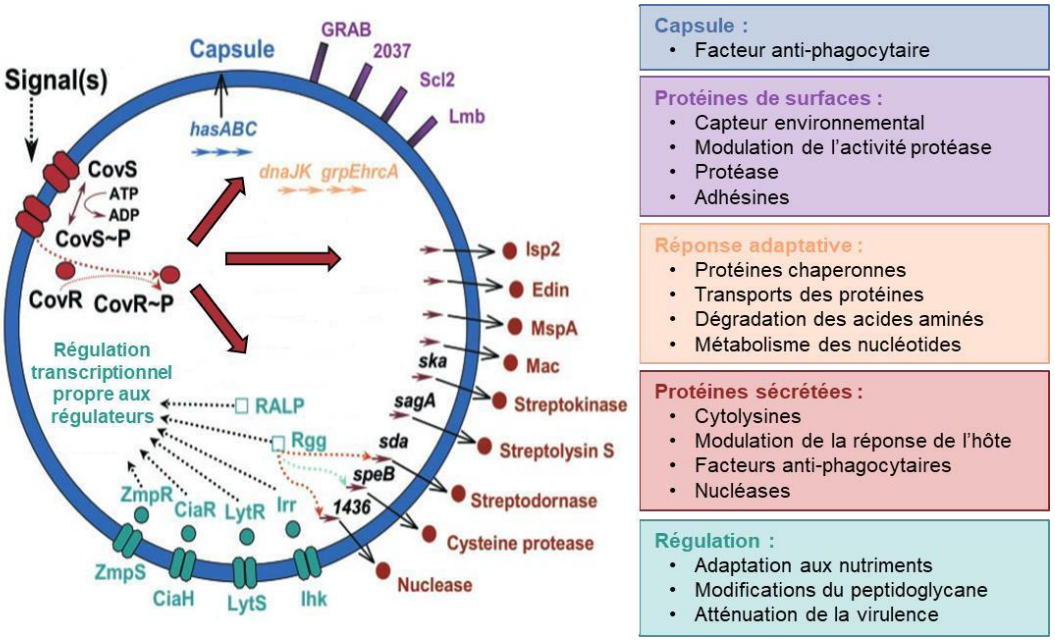

Figure 10. Régulation transcriptionnelle par CovR/S, gènes régulés et fonctions associés. Les différents gènes régulés par CovR/S sont indiqués à gauche et les fonctions associées à ces régulations à droite. D'après (260) et Thèse de Microbiologie, Antonin Weckel, BioSPC, 2018.

Les régulateurs transcriptionnels dit autonomes, répondent également au changement de l'environnement. Contrairement aux TCS, ces derniers répondent de manière indirecte à un signal externe. La détection de ces signaux reste encore mal connue tout comme leur lien avec la physiologie bactérienne. A ce jour, seul trois de ces régulateurs ont été clairement identifiés comme jouant un rôle dans la pathogénicité et la physiologie de *S. pyogenes* : Mga, RALPs et Rgg/RopB (Figure 11). L'activité de ces trois régulateurs dépend de l'état physiologique de la bactérie et par conséquent des conditions nutritives de son environnement. De plus, leur expression est interconnectée facilitant ainsi la transition entre chaque phase de croissance.

Mga est le premier régulateur de gènes multiples décrit chez *S. pyogenes*. Il est commun à tous les sérotypes de *S. pyogenes*. Il s'agit d'une protéine de 62 kDa codée au sein de la région Mga (262). En se liant à un site de fixation spécifique dans la région promotrice, Mga régule l'expression de gènes codant des protéines de surface et sécrétées essentielles aux premières étapes d'infection de *S. pyogenes*, telles que l'adhésion et la colonisation des tissus de l'hôte, et à l'échappement au système immunitaire (262). De plus, contrôlant l'expression des gènes de la région Mga, Mga s'auto-régule conduisant alors à l'amplification de l'expression de gènes de son régulon (Figure 12). L'activation de cette régulation est

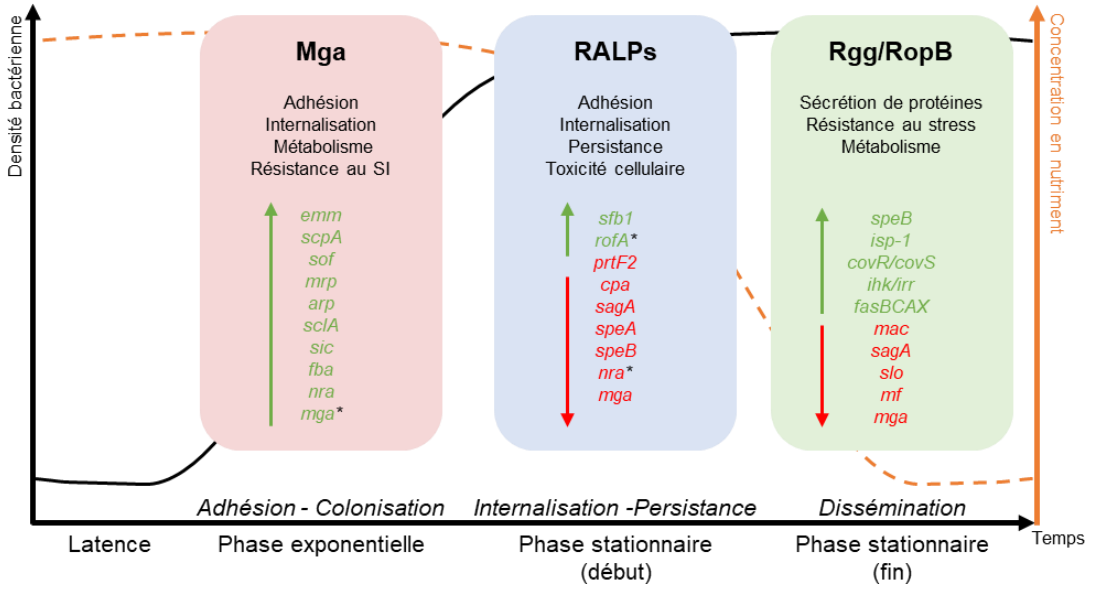

Figure 11. Inter-régulation des régulateurs transcriptionnels Mga, RALPs et Rgg/RopB dépendant de la phase de croissance de *S. pyogenes*. Les trois cases représentent chacune un régulateur, Mga (rose), RAPLs (bleu) et Rgg/RopB (vert) et contiennent les gènes dont l'expression est régulée de manière positive (vert, flèche verte vers le haut) et négative (rouge, flèche rouge vers le bas). Les autorégulations sont représentées par un astérisque noir. En arrière-plan, une courbe pleine noire représente la croissance de *S. pyogenes* et une courbe pointillée orange permet de suivre la qualité nutritionnelle de son environnement en fonction du temps. Figure adaptée de (261) et Thèse de Microbiologie, Antonin Weckel, BioSPC, 2018.

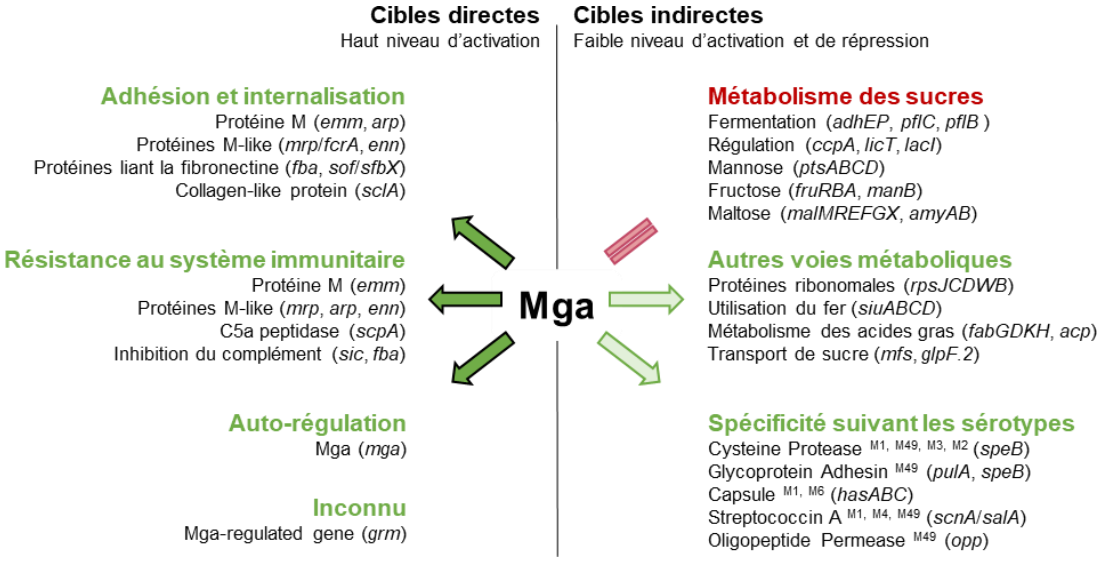

Figure 12. Régulon du régulateur transcriptionnel Mga. Vert, Gènes dont l'expression est activée par Mga. Rouge, Gènes dont l'expression est réprimée par Mga. D'après (262) et Thèse de Microbiologie, Antonin Weckel, BioSPC, 2018.

dépendante des conditions de croissance de la bactérie. En effet, l'expression de *mga* est maximale en phase exponentielle, où le milieu est riche en nutriments et est également liée au niveau de CO_2, à la concentration en fer présent dans l'environnement et à sa température (261). Cette activation a longtemps suggéré qu'il pourrait s'agir d'un TCS mais aucune kinase et aucune forme phosphorylée n'ont été associées à Mga.

Les régulateurs de la famille RofA-like protéine, RALPs, sont impliqués dans l'interaction avec les cellules de l'hôte et la résistance au système immunitaire. Quatre RALPs, RofA, Nra, Ralp3 et RivR ou Ralp4, ont été identifiés chez *S. pyogenes*. Toutes les souches possèdent des RALPs mais la combinaison et le régulon de ces régulateurs sont différents suivant le sérotype de la souche (263). L'expression des RALPs dépend des premières étapes d'infection et de la persistance de la bactérie au sein des cellules hôtes, suggérant alors l'importance de ces régulateurs dans la transition entre la colonisation et la dissémination. Pour marquer cette transition, durant le début de la phase stationnaire, il réprime le régulateur Mga ainsi que les gènes codant les facteurs de virulence qui ont permis l'entrée dans la cellule hôte telles que les adhésines (MSCRAMMs, les protéines liant la fibronectine et le collagène), les hémolysines et les protéases (261). Les deux régulateurs les plus décrits sont RofA et Nra, respectivement étudiés dans les souches *emm*6 et *emm*49.

RofA est à la fois un répresseur (*sagA*, *speB* et *mga*) et un activateur transcriptionnel (*sfbI* et la région FCT) dont l'activité varie en fonction du niveau d'oxygène présent dans l'environnement (264). Le gène codant RofA est situé de manière anti-sens avec le gène *prtF* (région FCT) qu'il régule (265). Les deux gènes partagent donc la même région promotrice, où se situe un site de fixation de RofA. Par conséquent, tout comme Mga, RofA a la capacité de s'autoréguler.

Nra est principalement décrit comme étant un répresseur transcriptionnel (266). Il présente 62 % d'identité avec le régulateur RofA, lui permettant alors de se fixer sur les mêmes sites de fixation. Son régulon comprend donc les gènes contrôlés par les RALPs mais également *rofA*. L'expression du gène codant Nra est activée par Mga entre la phase exponentielle et stationnaire où son activité de répresseur est la plus importante. Contrairement à RofA, l'activité de Nra ne dépend pas des conditions atmosphériques de culture.

Rgg, aussi nommé RopB, a principalement été étudié chez les souches *emm*49, où il régule plus de 30 % du génome. La taille et la composition du régulon de Rgg varie en fonction des souches de *S. pyogenes*. L'activité de ce régulateur transcriptionnel est requise durant la phase stationnaire tardive de croissance bactérienne. Lors de cette phase, l'environnement de la bactérie est pauvre en nutriments. La bactérie doit alors trouver une source d'énergie alternative, les acides aminés. Rgg agit de manière positive sur le métabolisme des acides aminés. L'expression de ce régulateur est donc activée en réponse à un stress nutritif. De plus, Rgg réprime l'expression de gènes de virulence tels que SLO, NADase, GRAB, intervenant dans l'entrée dans la cellule hôte et est important pour l'expression de certains facteurs de virulence sécrétés durant la phase stationnaire tels que les exoprotéines, et notamment SpeB, participant à l'invasion de l'hôte (267,268). Ces éléments confirment l'importance de ce régulateur lors de l'étape de dissémination et d'invasion lors d'infection à *S. pyogenes*. À ce jour, le mécanisme d'action de ce régulateur reste mal connu. En effet, aucun site de fixation spécifique n'a été décrit dans les régions promotrices de ses gènes cibles. Cela suggère une action indirecte de celui-ci *via* l'interaction avec d'autres régulateurs transcriptionnels (Figure 13) (269). En effet, Rgg réprime Mga et active CovR/CovS, Ihk/Irr et FasBCA. D'où une influence de ce dernier sur la sécrétion de protéines majoritairement contrôlée par le système CovR/CovS.

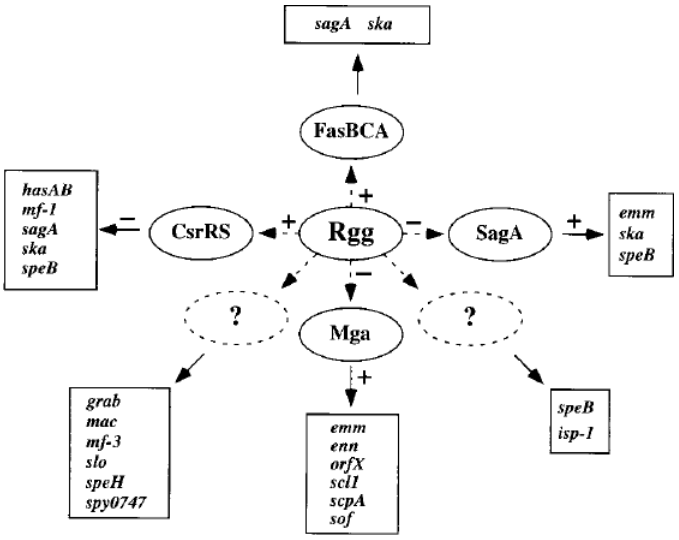

Figure 13. Réseau de régulation du régulateur transcriptionnel Rgg ou RopB. D'après (269).

2. La synthèse de la membrane cytoplasmique

La membrane bactérienne, constituée d'une bicouche lipidique, représente une barrière perméable sélective permettant le transport des éléments nutritifs et des déchets. Elle est aussi le lieu de détection de signaux de l'environnement et de processus métaboliques comme les mécanismes impliqués dans la respiration anaérobie. Du fait de ces différents rôles, il est essentiel pour la bactérie de maintenir l'homéostasie de sa membrane, dépendante de sa composition en lipide, afin de permettre son adaptation et par conséquent sa survie dans divers environnements (270).

2.1. La synthèse des lipides membranaires

Les lipides sont des molécules amphipathiques composées d'un corps apolaire constitué d'au moins deux chaines d'acide gras et d'une tête polaire spécifique à chaque famille lipidique mais ayant en commun un groupement glycérol. A partir de cette structure, deux types de lipides sont distingués, les lipides simples tels que l'acylglycérol et les lipides complexes tels que les glycosyldiacylglycérols et les phospholipides (Figure 14). La tête polaire de ces derniers est associée à un autre groupement, respectivement ici un sucre et un phosphate. Leur propriété amphiphile est essentielle pour la formation de la bicouche lipidique. Leur répartition au sein de la bicouche est hétérogène et dépendante de l'espèce bactérienne. A partir d'une étude décrivant la diversité des lipides membranaires et leur synthèse au sein de bactéries, nous pouvons remarquer une distinction entre les bactéries à Gram-positive et celles à Gram-négative. Les membranes des bactéries à Gram-positive se différencient de celles à Gram-négative par la présence de glycosyldiacylglycérols et l'absence de phosphatidyléthanolamine, à l'exception de *Bacillus subtilis* (271).

Les acylglycérols sont des lipides simples composés d'un glycérol sur lequel est réparti une à trois chaines d'acides gras (Figure 14). On distingue les mono-, les di- et les tri-acylglycérols. Les monoacylglycérols n'ont pas la capacité de former des bicouches lipidiques contrairement au di- et tri-acylglycérols. Ils sont principalement issus de la dégradation de différents intermédiaires de la synthèse lipidique tels que le diacylglycérol et le 1-acyl-glycerol-phosphate (272,273). Le diacylglycérol est un lipide neutre impliqué dans la

synthèse des lipides et la mise en place des LTA (121,274). Il peut également être toxique pour la bactérie. En effet, son accumulation peut entrainer une disruption de la membrane. Le triacylglycérol est très peu connu, mais il semblerait qu'il soit impliqué dans la régulation de la fluidité membranaire et dans le transport des électrons.

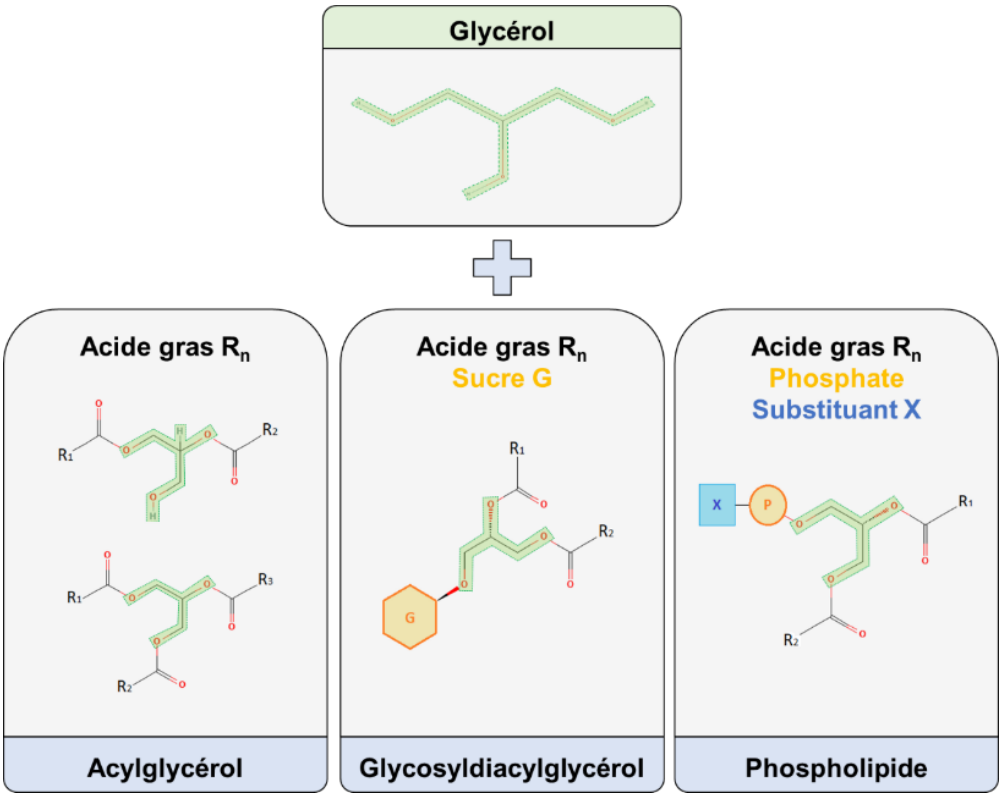

Figure 14. Exemple de familles lipidiques présentes au sein des membranes des bactéries. Les lipides membranaires possèdent en commun un groupement glycérol (en vert) composant la partie polaire de la molécule et d'acides gras lui conférant son caractère apolaire. Les acides gras sont représentés par « R », les groupements sucre et phosphate sont en jaune et les substituants des phospholipides en bleu. Structure adaptée de https://pubchem.ncbi.nlm.nih.gov/.

Les glycosyldiacylglycérols sont des lipides complexes dérivés du diacylglycérol. Ils se distinguent par la présence d'un ou deux sucre(s) lié(s) au glycérol, monogalactosyldiacylglycerol (MGDG) et digalactosyldiacylglycerol (DGDG). Chez *S. pneumoniae*, les principaux DGDG présents au sein de la membrane sont composés d'un groupement galactose et glucose, α-Gal (1➔2) α-GlcD (275). La fonction de ces lipides est partiellement connue. Mais ils sembleraient être impliqués dans le maintien de l'homéostasie membranaire. En effet, chez *Acholeplasma laidlawii*, une augmentation de la température et une modification de la composition en acide gras membranaire en faveur des acides gras insaturés a pour conséquence d'augmenter le pourcentage de MGDG dans la membrane au

détriment des DGDG (276). Chez *A. laidlawii*, ces lipides semblent donc être impliqués dans l'adaptation de la bactérie à son environnement.

Les phospholipides sont les lipides anioniques les plus abondants au sein de la membrane, représentant environ 10 % du poids sec bactérien (245). Ils se caractérisent par une tête hydrophile constituée d'un acide phosphatidique et de deux chaines d'acides gras formant la partie hydrophobe. La famille des phospholipides est vaste (Figure 15). Ils se distinguent par le groupement lié à l'acide phosphatidique *via* une liaison phosphodiester avec un groupement alcool. Ainsi les liaisons avec un groupement glycérol et phosphatidylglycérol permet respectivement la formation de phosphatidylglycérol (PG) et de cardiolipine (CL), espèces prédominantes chez les bactéries Gram-positive (271,277).

Les phosphatidylglycérols sont des phospholipides caractérisés par une tête polaire composée de deux groupements glycérol. Ils sont impliqués dans l'ancrage de certaines structures de surface comme les LTA. En effet, chez *S. pneumoniae*, les LTA sont ancrés aux phosphatidylglycérols par la ligase TacL (278).

Les cardiolipines sont des phospholipides portant deux charges négatives. Ils sont essentiels dans l'organisation dynamique des membranes bactériennes. Répartis de manière locale au sein de la membrane, ils forment ainsi des microdomaines spécifiques, participant à de nombreuses fonctions bactériennes, telles que la division et le transport de molécules. Chez *S. pyogenes*, ces microdomaines associés à des protéines forment le complexe nommé ExPortal (279). Celui-ci est impliqué dans la sécrétion de protéines telles que la cystéine protéase SpeB, facteur de virulence majeur de cette bactérie (280). De plus, une colocalisation du site de démarrage de la synthèse du peptidoglycane et de l'ExPortal a été mise en évidence au niveau du septum, suggérant son implication dans la division bactérienne de *S. pyogenes.* L'implication des cardiolipines dans la division et le transport de protéines a également été décrit chez *B. subtilis* et *E. coli*, participant respectivement dans la mise en place de la « Z-ring » et du transporteur ProP (281–284). D'autre part, les cardiolipines jouent aussi un rôle dans l'adaptation de *S. pyogenes* à son environnement. En effet, la modification de son intégrité perturbe la sensibilité de la bactérie aux peptides anti-microbiens tels que la polymyxine B (284).

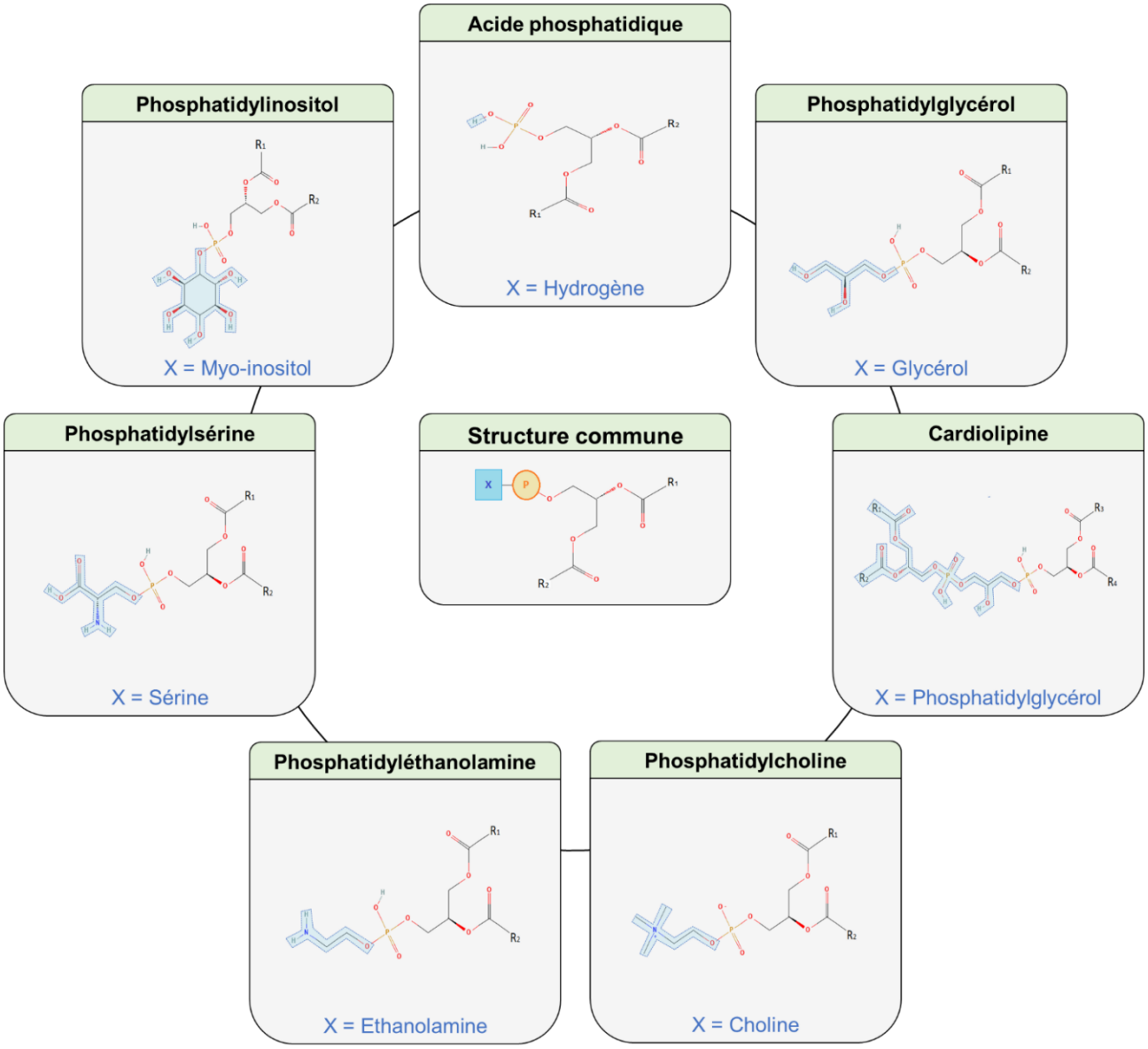

Figure 15. Les différents types de phospholipides. La structure commune des phospholipides est représentée au milieu. Les substituants « X » sont en bleu, le groupement phosphate « P » en orange et les acides gras par « R ». Les structures sont adaptées de https://pubchem.ncbi.nlm.nih.gov/.

La synthèse des lipides, un mécanisme indispensable pour le développement de la bactérie, nécessite énormément d'énergie, 32 moles d'ATP pour la formation d'une mole de lipide (245). Elle dépend de deux systèmes non exclusifs PlsB/PlsC et PlsX/PlsY/PlsC. L'analyse des génomes de plus de 600 bactéries, représentant 30 classes, a permis de définir la distribution génétique de ces deux systèmes au sein des différentes familles bactériennes (285). Ainsi sur les 30 classes analysées, une possède uniquement le système PlsB/PlsC, il s'agit des Xanthomonadales, 17 possèdent uniquement le système PlsX/PlsY/PlsC et 12 possèdent les deux systèmes. Il est intéressant de noter que la majorité des protéobactéries possède les deux systèmes alors que les firmicutes, dont font partie les Streptococcaceae, ont uniquement le système PlsX/PlsY/PlsC. Ainsi le réseau protéique PlsX/PlsY/PlsC est commun à la grande majorité des bactéries. Chez les bactéries firmicutes, ce système a principalement été étudié chez *B. subtilis* et *S. pneumoniae.* A partir des analyses des séquences des protéines PlsX, PlsY, et PlsC de *B. subtilis, Enterococcus faecalis, S. pneumoniae* et *S. pyogenes,* nous avons construit un arbre phylogénétique qui montre la forte conservation des séquences protéiques entre ces espèces de firmicutes (Figure 16A-B). Le précurseur des lipides, l'acide phosphatidique (PA), est produit par une succession d'acylation (Figure 16C). La protéine PlsX convertit l'acyl-ACP, issu de la synthèse des acides gras, en acyl-phosphate. Puis la protéine PlsY réalise la première étape d'acylation pour former l'acide lysophosphatidique (LPA). Enfin, la protéine PlsC, commune à toutes les bactéries, acyle le LPA pour former l'acide phosphatidique.

La protéine PlsX est la protéine majeure dans le démarrage de la synthèse des lipides (273). Son gène est le plus souvent présent au sein ou à proximité de régions regroupant des protéines participant à la synthèse des acides gras. Chez *E. faecalis* et les Streptocoques, elle est en opéron avec un gène codant une « Acyl Carrier Protein » (Figure 18). PlsX est une phosphotransacétylase qui catalyse de manière réversible le transfert d'un acyle de l'acyl-ACP ou de l'acyl-CoA à un acyl-phosphate. Chez *B. subtilis*, PlsX peut utiliser l'acyl-ACP et l'acyl-CoA alors que chez *S. pneumoniae,* l'acyl-ACP est l'unique substrat de PlsX (286). L'étude cristallographique de PlsX chez *B. subtilis* a permis de déterminer sa localisation et son comportement au sein de la bactérie (288). PlsX est présente sous forme de dimère. Sa dimérisation est indispensable pour son interaction avec la membrane et son activité catalytique. Ne possédant pas de segment transmembranaire, PlsX interagit avec la membrane *via* un domaine composé de résidus hydrophobes et chargés positivement.

A

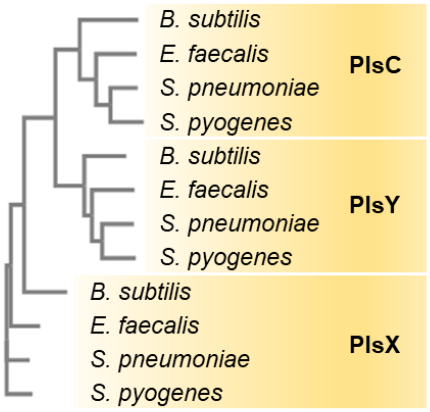

B

Pourcentage d'identité de séquence par rapport aux protéines de *S. pneumoniae*

	PlsC	PlsY	PlsX
B. subtilis	32,7 %	49,8 %	53,4 %
E. feacalis	55,3 %	53,9 %	70,8 %
S. pyogenes	67,1 %	64,3 %	73,3 %

C

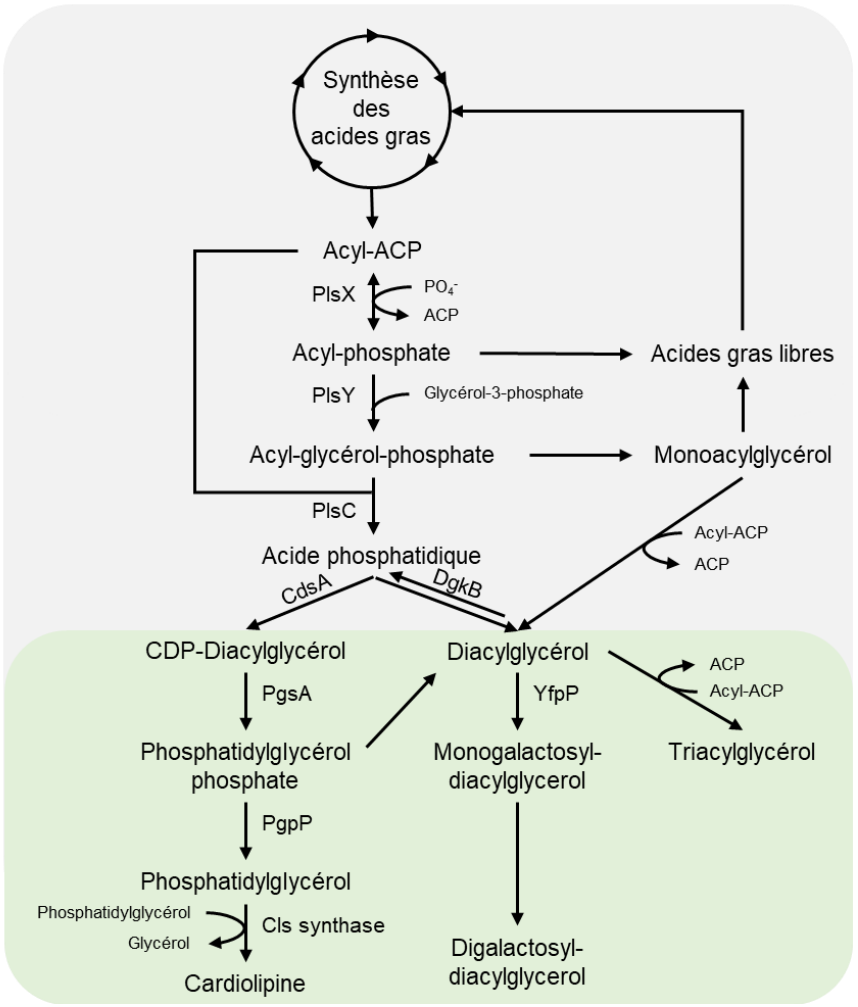

Figure 16. Synthèse des lipides. (A) Arbre phylogénétique obtenu à partir d'un alignement de séquences multiples réalisé à l'aide de Clustal W (1.83). (B) Tableau regroupant les pourcentages d'identité de séquence des protéines PlsX, PlsY et PlsC de *B. subtilis*, *E. faecalis* et *S. pyogenes* par rapport à celles de *S. pneumoniae*. (C) Le système PlsX/PlsY/PlsC. Ce système, commun aux bactéries Gram-positives, permet la formation de l'acide phosphatidique, précurseur de la synthèse des phospholipides membranaires. D'après (273,286). (D) La synthèse des lipides présents dans la membrane des Streptocoques, phosphatidylglycérol, cardiolipine, monogalactosyldiacylglycérol et digalactosyldiacylglycérol. D'après (272,287).

Cette interaction est dépendante de la composition en lipide de la membrane, PlsX de *B. subtilis* interagissant préférentiellement dans les régions membranaires fluides (289). Son rôle dans la synthèse des lipides dépend de cette interaction avec la membrane. En effet, une mutation au sein du domaine d'interaction induit une diminution de sa capacité à transférer l'acyl-phosphate à PlsY, ce qui se traduit par une accumulation d'acyl-ACP et d'acide gras libre (288). L'association de PlsX avec la membrane est donc cruciale dans la première étape d'acylation. De plus, l'analyse de la capacité de PlsX à former de l'acyl-ACP à partir de l'acyl-phosphate et de holo-ACP montre qu'une mutation dans le site d'interaction avec la membrane n'a aucune conséquence sur l'activité catalytique de PlsX contrairement à une mutation dans le site de dimérisation. Son activité acyltransférase dépend donc de sa dimérisation et non de sa localisation. Par conséquent, nous supposons ainsi que la présence cytoplasmique de PlsX active permet la réaction catalytique inverse.

La protéine PlsY est une acyl-phosphate acyltransférase glycérol-phosphate dépendante. Elle catalyse la formation d'acyl-glycérol-phosphate ou LPA à partir d'un acyl-phosphate et d'un glycérol-3-phosphate (273,286). La structure de PlsY a été analysée chez *S. pneumoniae* (290). Il s'agit d'une protéine membranaire composée de cinq segments transmembranaires. Trois motifs conservés et impliqués dans son activité ont été identifiés. Les deux premiers motifs, situés dans les boucles cytoplasmiques, comprennent respectivement le site de fixation du phosphate et celui du glycérol-3-phosphate. Le troisième motif, situé dans le domaine cytoplasmique C-terminal, joue un rôle dans la conformation de la protéine.

La protéine PlsC est une acyl-glycérol-3-phosphate acyltransférase. Il s'agit d'une protéine universelle partagée par l'ensemble des bactéries. Son substrat est dépendant de l'espèce bactérienne. Chez *B. subtilis* et *S. pneumoniae,* elle finalise la synthèse du précurseur des lipides, l'acide phosphatidique, en transférant l'acyle d'un acyl-ACP sur la molécule d'acyl-glycérol-phosphate (273,286). Elle possède un motif conservé contenant le site de fixation au phosphate de l'acyl-glycérol-phosphate (285).

La synthèse des différentes familles lipidiques dépend d'une succession de réaction enzymatique à partir de l'acide phosphatidique (Figure 16D) (287,272). Elle est très peu connue chez les Streptococcaceae et peu de gènes ont été identifiés comme impliqués dans celle-ci. Les glycosyldiacylglycérols sont formés à partir de la transformation de l'acide

phosphatidique en diacylglycérol puis de deux réactions de glycosylation. Cette réaction est réversible médiée par une diacylglycérol kinase (DgkB). Elle permet ainsi le recyclage du diacylglycérol et d'éviter son effet toxique. Les phosphatidylglycérols sont formés à partir de la transformation de l'acide phosphatidique et de cytosine triphosphate en diphosphate cytosine-diacylglycérol (CDP-Diacylglycérol) par l'enzyme CdsA. Par la suite, deux étapes ont lieu, l'une, permettant la formation de phosphatidylglycérol-phosphate *via* l'acquisition de glycérol-3-phosphate par PgsA et, l'autre, permettant la déphosphorylation du phosphatidylglycérol-phosphate par PgpP. Pour finir, la synthèse des cardiolipines dépend de la formation de phosphatidylglycérol. En effet, ils sont synthétisés par la condensation de deux molécules de phosphatidylglycérol grâce aux enzymes Cls synthase.

2.2. La synthèse des acides gras, FASII

Les acides gras, principaux composants de tous les lipides, sont des molécules amphiphiles composées d'un groupement carboxyle et d'une chaine linéaire hydrocarbonée, comportant un nombre pair de carbones. Il existe principalement deux types d'acides gras,

Tableau 5. Exemple de différents types d'acides gras présents chez les bactéries.

Acide gras saturé *		
	Acide stéarique Nomenclature : 18:0 Formule chimique : $C_{18}H_{36}O_2$	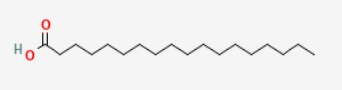
Acide gras insaturé		
Trans	**Acide *trans*-oléique** Nomenclature : 18:1Δ9 Formule chimique : $C_{18}H_{34}O_2$	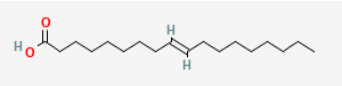
Cis	**Acide *cis*-oléique** Nomenclature : 18:1Δ9 Formule chimique : $C_{18}H_{34}O_2$	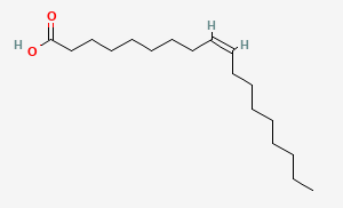
Acide gras « cyclique »		
	Acide dihydrosterculique ou acide oléique cyclopropane Nomenclature : 19Δ9 Formule chimique : $C_{19}H_{36}O_2$	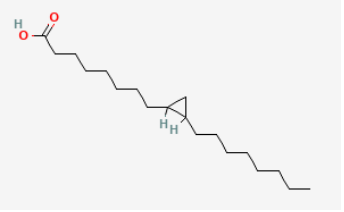

* Structure d'après https://pubchem.ncbi.nlm.nih.gov/.

les acides gras saturés et les acides insaturés se distinguant respectivement par la présence ou non d'au moins une double liaison carbonée au sein de leur chaine apolaire (Tableau 5). Les acides gras insaturés se distinguent en plusieurs classes en fonction du nombre d'insaturation, mono- ou poly-insaturés, et de leur conformation, « *trans* » ou « *cis* ». Cette dernière correspond à la position des chaines en fonction de la double liaison, soit de part et d'autre du plan horizontal, mimant ainsi un acide gras saturé pour la conformation « *trans* » ou soit du même côté pour la conformation « *cis* ». Contrairement à *S. pyogenes*, certaines espèces bactériennes, comme *E. faecalis* et *Lactococcus lactis*, synthétisent également des acides gras avec des cycles à trois carbones, dits « cycliques », comportant un cycle cyclopropane à la place de la double liaison de la chaîne carbonée (291). Ces acides gras ont des propriétés similaires aux acides gras insaturés de conformation « *trans* ».

La voie de biosynthèse bactérienne des acides gras, nommée FASII, est très répandue. Elle est décomposée en deux phases, la phase d'amorçage suivie de la phase d'élongation (Figure 17A). La phase d'amorçage est la première étape de FASII générant le malonyl-ACP, précurseur pour la phase d'élongation, à partir de l'acétyl-CoA issu du métabolisme (292). La phase d'élongation représente la machinerie centrale du système FASII (287). Elle fait intervenir quatre enzymes permettant la succession de quatre réactions répétées : la condensation, la réduction, la déshydratation et une nouvelle réduction (293). Ces étapes permettent donc la conversion du malonyl-ACP en acyl-ACP. L'allongement de l'acyl-ACP, ainsi produit, est de deux carbones à chaque cycle. Ces produits sont nommés acides gras ou acyles.

La synthèse des acides gras insaturés dépend d'une dérivation par rapport au cycle FASII (Figure 17A). Les enzymes intervenants sont spécifiques pour l'ajout de la double liaison et sont dépendant du genre bactérien. En effet, chez les γ-protéobactéries comme *E. coli*, deux enzymes participent, FabA et FabB, contre une seule, FabM chez les Streptocoques et FabN chez *E. faecalis* (295). Chez les Streptocoques, la compétition entre les enzymes FabK et FabM maintient l'équilibre de la membrane en acide gras saturés et insaturés. Chez les Entérocoques, la formation d'acide gras « cyclique » est réalisée par l'enzyme Cfa synthase (« Cyclopropane Fatty Acid synthase ») qui catalyse le transfert d'un groupement méthyle à la double liaison d'une chaîne carbonée (Figure 17B) (291).

A

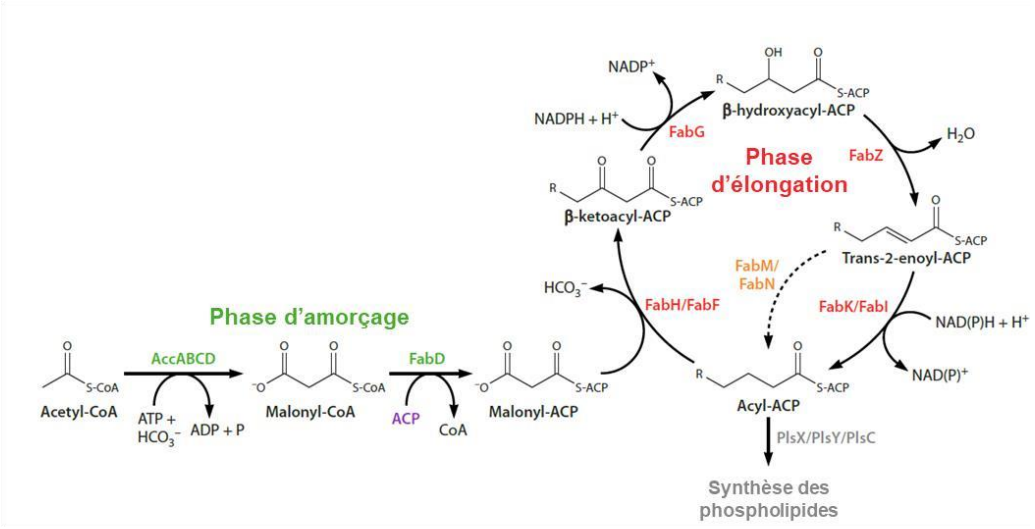

B

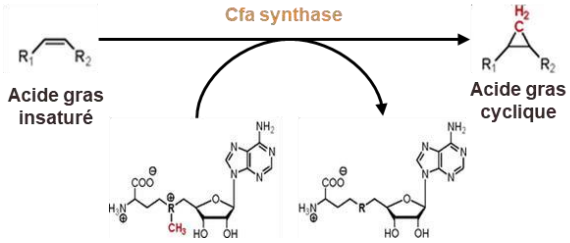

Figure 17. La synthèse des acides gras, FASII. (A) FASII est composé de deux phases, la phase d'amorçage suivi de la phase d'élongation, respectivement en vert et rouge. D'après (294). (B) La synthèse des acides gras dits « cycliques » chez E. *faecalis*, *L. lactis* et certains Streptocoques. Dans (A) et (B), les substrats et les produits sont indiqués en noir ; les protéines de la phase d'amorçage sont en vert, les enzymes de l'élongation sont en rouge, et celles participant à la synthèse d'acide gras insaturé et cyclique en orange quant aux enzymes de synthèse des phospholipides, ils sont en noir.

Les enzymes intervenant dans la phase d'amorçage sont communes à tous les genres bactériens contrairement à celles de la phase d'élongation (287). Les gènes codant l'ensemble de ces enzymes sont présents en cluster dans le génome. Le cluster FASII est composé de trois à quatre unités transcriptomiques (296). Leur organisation au sein du génome est dépendante du genre bactérien mais leur régulation est commune (Figure 18). Le principal locus FASII est composé des opérons *fabT* à *acpA* et *fabK* à *accA*, présents simultanément au même endroit sur le chromosome bactérien des trois genres. Chez *E. faecalis* et *L. lactis*, deux autres unités FASII sont présentes ailleurs dans le génome. Ces unités codent les enzymes permettant la synthèse des acides gras insaturés. De plus, un deuxième gène, *fabG2* codant une β-Ketoacyl-ACP réductase, a été identifié dans le génome de *E. faecalis,* mais son rôle est encore inconnu (297).

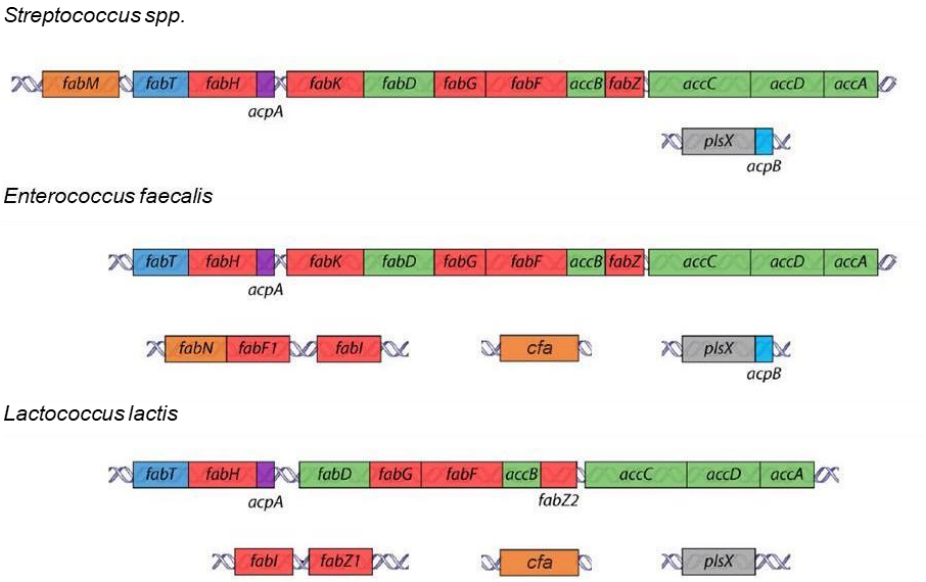

Figure 18. Les locus FASII communs aux Streptocoques (*S. pneumoniae*, *S. pyogenes*, *S. agalactiae*), à *E. faecalis* et à *L. lactis*. Les gènes codant les protéines intervenant dans la phase d'amorçage sont en vert, dans la phase d'élongation en rouge et pour la formation d'acide gras insaturé en orange. Le gène codant le régulateur transcriptionel FabT est en bleu et ceux codant les ACPs sont respectivement en violet et bleu clair pour AcpA et AcpB. Chez *E. faecalis*, *fabF1* est aussi appelé *fabO*. Figure adaptée de (294).

Dans la bactérie, les acides gras sont liés à des protéines nommées ACP, « Acyl Carrier Protein ». Il s'agit de petites protéines d'environ 9 kDa ayant un rôle central dans leur synthèse et dans l'incorporation des acides gras au sein de la membrane (298,299). *S. pneumoniae*, *S. pyogenes* et *E. faecalis* possèdent deux ACPs, à l'exception notamment de *L. lactis*. AcpA est codée au sein du locus FASII, et AcpB est codée en aval de PlsX (Figure 18). Par comparaison de séquence, nous avons pu établir que ces protéines présentent une identité de séquence entre elles d'environ 43,7 % chez *S. pneumoniae*, 25,7 % chez *S. pyogenes* et de 35,6 % chez *E. faecalis.* A partir de ces analyses, nous avons construit un arbre phylogénétique qui permet de mettre en évidence le regroupement des protéines AcpA mais pas des protéines AcpB (Figure 19C). En effet, AcpA de *S. pneumoniae* présente respectivement 67,1 %, 91,9 % et 65,8 % d'identité de séquence avec AcpA de *E. faecalis, S. pyogenes* et *L. lactis, contrairement à AcpB* qui a 43,4 % et 39,5 % d'identité avec AcpB de *E. faecalis* et *S. pyogenes*. Ces analyses suggèrent que AcpA peut avoir plus de contraintes fonctionnelles que AcpB. Le rôle de ces protéines dans la synthèse des acides gras et des lipides a été défini chez *E. faecalis* après étude *in vitro* des phénotypes de souches délétées des gènes les codant (299). Alors que AcpA est essentiel à la croissance bactérienne en absence d'acide gras, AcpB ne l'ai pas, la souche délété de *acpB* poussant en présence ou en

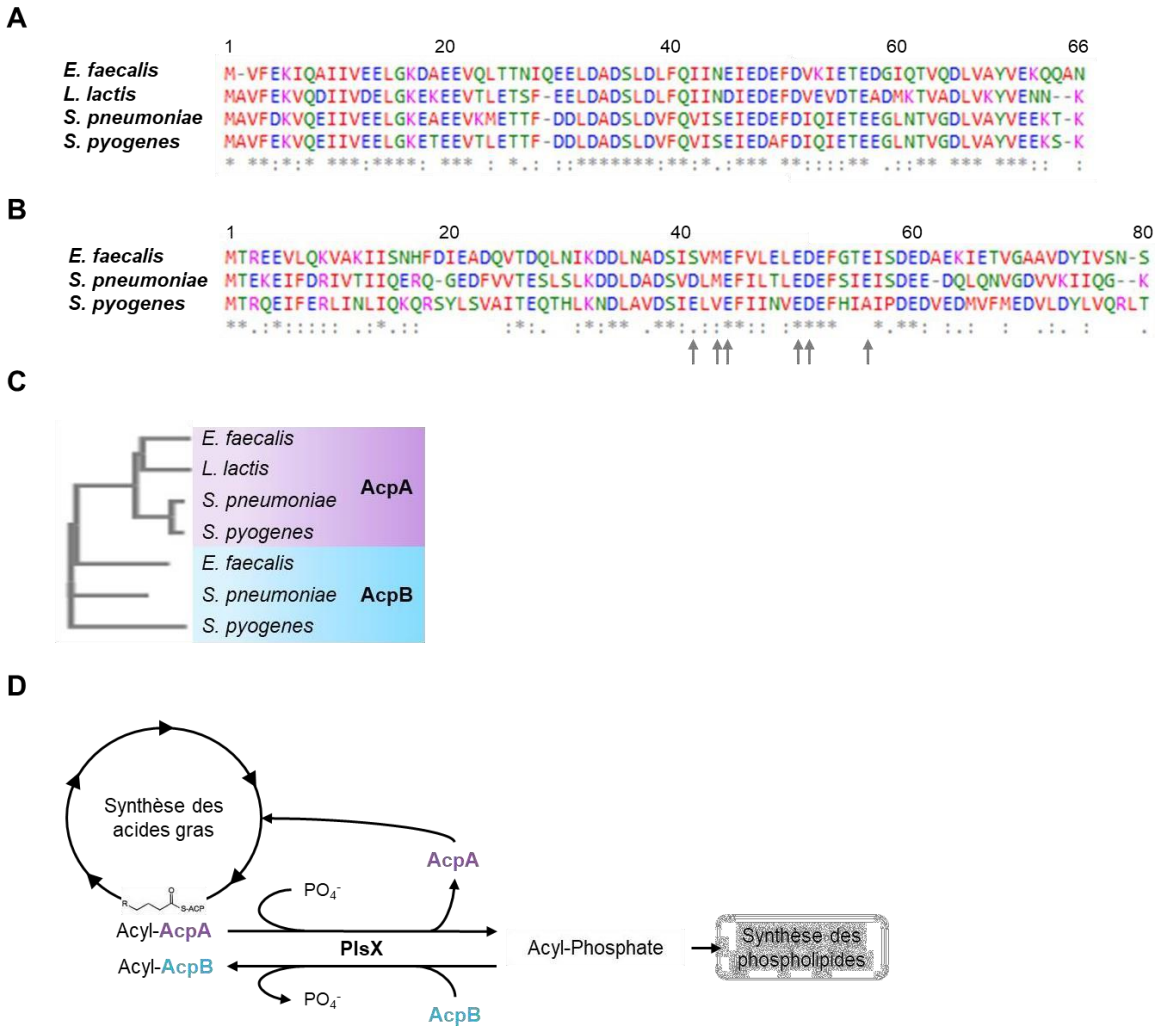

Figure 19. Caractérisation des protéines AcpA et AcpB. (A) Alignement de AcpA et (B) alignement de AcpB ; l'alignement des séquences a été effectué à l'aide de Clustal W (1.83), le code couleur suit la classification fonctionnelle ; *, identique chez les espèces ; : même classe structurelle ; les flèches grises verticales indiquent les résidus d'acides aminés, qui sont impliqués dans l'interaction FabT-AcpB (301). (C) Arbre phylogénétique obtenu à partir d'un alignement de séquences multiples réalisé à l'aide de Clustal W (1.83). (D) Rôle des protéines AcpA et AcpB dans la synthèse des acides gras et des phospholipides. D'après (299,302).

absence d'acides gras exogènes. L'implication d'AcpA et d'AcpB dans FASII a été définie en analysant leurs interactions avec FabI et FabK, qui catalysent la dernière étape de FASII pour produire l'acyl-ACP (Figure 17) (300). FabI est plus efficace que FabK pour réduire le précurseur acyl-AcpA ; inversement, FabK réduit le précurseur acyl-AcpB plus efficacement que FabI (299). Ces résultats suggèrent que AcpA participe à la synthèse *de novo* des acides gras, contrairement à AcpB dont le rôle dans FASII reste encore mal connu chez *E. faecalis*. Néanmoins, il est important de remarquer que ces interactions n'ont pas été étudiées chez les streptocoques, qui ne possèdent que FabK. Afin de définir le rôle de AcpA et AcpB dans la

synthèse des phospholipides, la réaction catalytique réversible de PlsX a été étudiée (cf. 2.1. La synthèse des lipides membranaires). Dans un premier temps, le transfert par PlsX d'acyle entre l'acyl-ACP et un groupement phosphate pour former l'acyl-phosphate a été évalué. Les deux acyl-ACP donnent leur acyle au phosphate, mais le transfert à partir de l'acyl-AcpA est beaucoup plus efficace que celui à partir de l'acyl-AcpB. Dans un second temps, l'analyse de la réaction inverse *via* PlsX démontre un meilleur transfert de l'acyle vers AcpB que vers AcpA. Par conséquent, l'acyl-AcpA est le substrat privilégié de PlsX pour synthétiser l'acyl-phosphate, amorçant la synthèse des lipides. Cependant, la protéine libre AcpB est utilisée par PlsX pour produire de l'acyl-AcpB, dans la réaction inverse, en présence d'acides gras exogènes. Ainsi, l'ensemble de ces résultats suggèrent que la protéine AcpA est nécessaire à la synthèse *de novo* des acides gras et que la protéine AcpB, codée sur le même opéron que *plsX*, joue un rôle dans l'utilisation des acides gras exogènes pour la synthèse des phospholipides (Figure 19D) (299).

2.3. Le maintien de l'équilibre membranaire

Les types d'acides gras synthétisés et leur concentration au sein des lipides membranaires contribuent à l'homéostasie de la membrane. Cette dernière dépend de certaines propriétés telles que la fluidité. La fluidité membranaire correspond à la viscosité de la bicouche lipidique, dépendant du ratio d'acide gras saturés et insaturés « *cis* » *versus* acides gras insaturés « *trans* » ainsi que de la longueur de la chaîne carbonée. En effet, l'augmentation du nombre d'acides gras saturés a tendance à rigidifier la membrane, autrement dit à diminuer sa fluidité. Cette modification est accentuée avec l'augmentation du nombre de carbones présents par chaîne. Cela aurait pour conséquence de réduire la perméabilité de la membrane, c'est-à-dire la capacité de la membrane à transporter de manière passive certaines molécules, et donc les échanges de la bactérie avec son environnement (270,287).

La température, la phase de croissance et l'environnement nutritionnel affectent la composition en acide gras de la membrane bactérienne et ont ainsi un impact sur sa fluidité (303–305). La bactérie contrôle la quantité et la structure des acides gras *via* différents mécanismes lui permettant de s'adapter rapidement à son environnement. En effet, chez *B. subtilis,* en réponse à une diminution de la température, l'expression du gène codant la

désaturase DesA est induite *via* le système à deux composants, DesR/DesK (306,307). DesA introduit alors une double liaison au niveau des carbones situés en position 5 ou 9 d'une chaîne d'acide gras saturé. La fluidité de la membrane de *B. subtilis* est ainsi augmentée, lui permettant de résister aux variations de température. De plus, lorsque *E. coli* est cultivé dans un milieu à pH acide, l'expression du gène codant la protéine Cfa est plus important qu'en condition normale de croissance. Ainsi le pourcentage d'acides gras cycliques est augmenté dans la membrane d'*E. coli*, la rendant plus stable et lui permettant de survivre à pH acide (308).

Dans un environnement riche en acide gras, les bactéries ont la capacité de les incorporer dans leur membrane. Ils peuvent être incorporés *via* trois mécanismes :
i) l'acyl-CoA synthétase principalement présent chez les γ-protéobactéries, ii) l'acyl-ACP synthétase présent chez les bactéries Gram-négatives et iii) les « Fatty Acid Kinases » (Fak), présents chez des bactéries Gram-positives (309). Le système Fak a été décrit chez *S. aureus* et *S. pneumoniae* (Figure 20). Il dépend d'au moins deux protéines de la famille DegV, FakA et FakB. De manière générale, après que l'acyle soit entré dans la bactérie, il est pris en charge par FakB qui interagit alors avec FakA permettant la phosphorylation de l'acyle. Deux destins s'offrent alors à l'acyl-phosphate. Il est confié soit à PlsY pour amorcer la synthèse des lipides, soit à PlsX pour être converti en acyl-ACP (310). La protéine FakA est une protéine kinase, présente sous forme de dimère au sein de la bactérie. Récemment, l'étude de sa structure chez *Streptococcus suis* a permis de mieux caractériser le système Fak. Un monomère de FakA possède trois domaines, FakA-N, FakA-M et FakA-C ou DegV, impliqués respectivement dans la fixation de l'ATP, la dimérisation et la fixation de l'acyle (311). A partir de cette analyse, il a été suggéré que la dimérisation de FakA permet la formation d'un canal formant le site de fixation de l'acyl-FakB. Les protéines FakB transportent les acides gras exogènes ou les acyl-phosphate vers ces différents partenaires. La nature des acides gras étant diverse, il existe différentes protéines FakB suivant le type d'acides gras, FakB1 exclusivement pour les acides gras saturés et FakB2 pour les acides gras saturés et monoinsaturés. Une troisième protéine FakB3 a été décrite chez *S. pneumoniae* permettant la prise en charge des acides gras polyinsaturés (312). Après analyses de séquences, nous avons constaté que ces protéines sont conservées chez *S. pyogenes*, FakB1 ayant 57,4 % d'identité de séquence, FakB2 63,9 % et FakB3 61,7 %. L'étude cristallographique de FakB2 de *S. aureus* couplée à l'analyse de l'alignement de 288 séquences de protéines FakB provenant de différents organismes a mis

en évidence la conservation de 6 % des résidus (313). Cinq acides aminés fortement conservés ont été décrits comme participant à la fixation de l'acyle, Thr-61, Ser-93 et His-266, au transfert du phosphate ou à l'interaction avec l'acyl-phosphate, Arg-170 et intervenant dans les interactions protéines-protéines, Arg-202. Néanmoins, l'analyse comparative des différentes structures des FakBs de *S. pneumoniae* a permis de définir la spécificité de chacune des protéines à fixer différents acides gras (312). L'acyle est ancré par des liaisons hydrogène dans une poche hydrophe au sein de la protéine. Dans la majorité des cas, les FakB1 et FakB2 interagissent *via* les liaisons hydrogène Ser-Thr-carboxyle-His entre le groupement carboxyle de l'acyle et la protéine. Par contre, FakB3 se distingue par une interaction de type Ser-carboxyle-Ser-Tyr qui lui est propre, favorisant l'interaction avec les acides gras polyinsaturés.

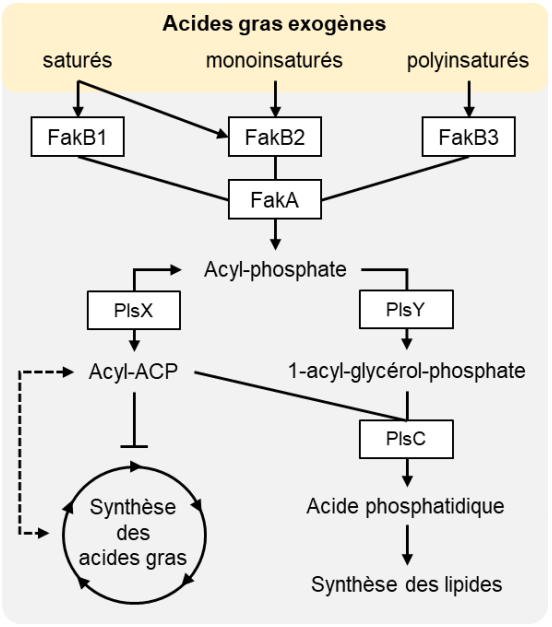

Figure 20. Le système d'incorporation FakA/B décrit chez *S. pneumoniae*. D'après (312).

Le contrôle de la concentration d'acyl-ACP au sein de la bactérie est crucial pour son développement. En effet, chez *S. aureus* et *E. faecalis*, des études basées sur les capacités d'incorporation des acides gras exogènes confirment que l'augmentation du taux d'acides gras dans la bactérie impacte l'équilibre de la membrane et a des conséquences sur sa fluidité, la morphologie, les capacités de croissance et la résistance à certains antibiotiques de la bactérie comme la daptomycine (314–316). Les différentes possibilités de devenir de l'acide gras au sein de la bactérie soulignent l'existence d'un couplage entre la synthèse des acides gras et celle des lipides dans lequel les acyl-ACP à chaînes longues jouent un rôle important. Chez

B. subtilis, le rôle des enzymes Pls dans ce couplage a été montré en étudiant l'impact de leur inhibtion sur FASII et la synthèse de l'acide phosphatidique (273). La délétion de PlsX impacte les deux synthèses alors que celles de PlsY et PlsC ont des conséquences uniquement sur la synthèse du précurseur des lipides. De plus, dans la souche mutante pour PlsY, l'absence d'accumulation d'acyl-phosphate mais l'accumulation d'acyl-ACP montre l'importance de PlsX dans la régulation du taux d'acyl-ACP au sein de la bactérie. Ces acyl-ACP ainsi produits sont ensuite utilisés par PlsC pour la formation d'acide phosphatidique contournant l'inhibition de PlsY. Cependant, l'accumulation d'acyl-ACP au sein de la souche délétée PlsC suggère que cette réaction est lente et dépendante de la concentration du substrat. Ainsi, ces résultats indiquent que PlsX est la seule protéine a avoir un rôle crutial dans le couplage des deux synthèses en contrôlant le taux d'acyl-ACP et régulant ainsi l'équilibre membranaire. Néanmoins, dans la souche mutée pour PlsX, aucune augmentation de la concentration en produits intermédiaires n'a été observée, suggérant l'action d'autres enzymes. Chez *S. pneumoniae* et *B. subtilis,* la thioestérase TesS hydrolyse les acyl-ACP endogènes accumulés contournant le besoin en acide gras exogènes dans une souche mutée pour PlsX (317,318).

Les bactéries ont développé différents mécanismes pour contrer l'excès d'acides gras. Chez *B. subtilis* et *E. coli*, les acides gras sont dégradés par β-oxydation *via* un système qui est contrôlé par FadR (319). En revanche, *S. aureus* ne possède pas ce système mais une pompe à efflux, FarE, l'expression de son gène étant contrôlée par un régulateur, FarR, répondant aux acyl-ACP à chaines longues (320,321). Ces mécanismes ne sont pas communs à toutes les espèces bactériennes. En effet, ils n'ont pas été décrits chez les Streptocoques et chez les Lactocoques. Par ailleurs, après avoir effectué une recherche *in silico*, nous n'avons trouvé aucun système de β-oxydation, ni de pompe à efflux FarE chez les Streptocoques. Toutefois, *S. pyogenes* possède un mécanisme de détoxification de la bactérie répondant à l'accumulation d'acides oléiques (18:1Δ9), une hydratase, la « Myosin Cross-reactive Antigen » (322), également mise en évidence par des analyses *in silico* au sein de souches *S. pyogenes* de génotype *emm1* (M5005_Spy0385) et *emm28* (M28_Spy0371). En revanche, ce mécanisme ne semble pas être suffisant, chez les Streptocoques, les Lactocoques et les Entérocoques. La régulation transcriptionnelle de FASII, en fonction de la quantité de produit final et non issu de la phase d'amorçage, semble être privilégiée pour la survie bactérienne en réponse à un excès d'acides gras.

La régulation de l'expression des gènes FASII est dépendante du type bactérien (Tableau 6) (323). En effet, les bactéries Gram-négatives contrôlent l'expression de ces gènes *via* deux régulateurs, essentiellement étudiés chez *E. coli*, FabR, régulant la synthèse FASII et FadR contrôlant la dégradation des acides gras. Au contraire, les bactéries Gram-positives ont un unique régulateur, mais différent selon les espèces, soit FapR soit FabT, à l'exception de *B. subtilis* qui posséde FapR et FadR. Ces régulateurs, à l'exception de FabT, ont pour ligand un des produits issus de la phase d'amorçage de FASII, l'acyl-CoA, le malonyl-CoA ou encore le malonyl-ACP. Le régulateur transcriptionnel FapR est le premier système de régulation de FASII mis en évidence chez les bactéries Gram-positives (324). Très conservé, il est principalement étudié chez *S. aureus* et *B. subtilis*. Il réprime à la fois la synthèse des acides gras et la synthèse des phospholipides, faisant de lui un régulateur global de la synthèse membranaire de ces bactéries. Son mécanisme de répression est assez simple. Après dimérisation, il se fixe à l'ADN sur des sites spécifiques au sein de la région promotrice de ses gènes cibles. Cette régulation est dépendante de la concentration intracellulaire en malonyl-CoA, intermédiaire de la phase d'amorçage. En effet, le malonyl-CoA a le rôle

Tableau 6. Régulateurs transcriptionnels impliqués dans les modifications des acides gras.

Régulateur	Genre bactérien	Rôle(s)		Ligand(s)	Référence(s)
		Activateur	Répresseur		
Gram-négative					
FabR	*Escherichia, Salmonella, Vibrio, Shigella, Haemophilus*	Aucun	*fabA, fabB*	Acyl-CoA, Acyl-ACP	(327,328)
FadR [1]	*Escherichia, Salmonella, Vibrio, Shigella, Yersinia, Haemophilus, Klebsiella*	*fabA, fabB, iclR*	*fadI, fadD, fadBA, fadE, fadF, fadIJ, plsB*	Acyl-CoA	(329–332)
DesT	*Pseudomonas*	Aucun	*desCB, fabAB*	Acyl-CoA	(333,334)
Gram-positive					
FapR	*Bacillus, Staphylococcus, Clostridium, Desulfitobacterium, Carboxidothermus*	Aucun	*fabH, fabF, fabI, fabD, fabG, ydhO, fapR, plsX,plsC*	Malonyl-CoA [2]	(326)
FabT	*Streptococcus, Enterococcus, Lactococcus*	Aucun	*fabT, fabH, fabK, fabD, fabZ, fabG, fabF, accABCD, fabM*	Acyl-ACP	(301,335)
FarR	*Staphylococcus*	*farE*	Aucun	Acyl-ACP	(321,322)

Bleu : gènes de FASII.
Vert : système de détoxification lié à un excès d'acides gras.
iclR : Régulateur de l'opéron de dérivation glyoxylate *aceBAK.*
desCB : Opéron d'acyl-CoA désaturase.
ydhO : Peptidoglycane hydrolase.
[1] Exception : présence de FadR chez *Bacillus subtilis*, bactérie Gram-positive.
[2] Chez *B. subtilis*, FapR possède deux ligands, le malonyl-CoA et le malonyl-ACP (335).

d'inducteur de FASII en se fixant à FapR, il induit un changement de conformation conduisant à la perte d'affinité pour la séquence cible (325).

3. FabT, le régulateur transcriptionnel de FASII

3.1. Les régulateurs de la famille MarR

Le régulateur transcriptionnel FabT est membre de la famille des régulateurs MarR, « Multiple antibiotic resistance Regulator », commun aux archées et aux bactéries (336,337). Les bactéries possèdent, suivant les espèces, de trois à 20 gènes codant des protéines MarR par génome. Les séquences de ces gènes présentent moins de 30 % d'identité, reflétant les différences de mécanismes de régulation (338). Les régulateurs MarR sont principalement des répresseurs de l'expression génique et plus de la moitié s'autorégulent (339). Ils sont principalement impliqués dans la résistance aux antibiotiques, (MarR chez *E.coli* et MexR chez *Pseudomonas aeruginosa*) (340,341) et la réponse aux stress (MexR chez *P. aeruginosa* et OhrR chez *Bacillus*) (342,343) ainsi que dans la virulence (MarR chez *E.coli,* MgrA chez *S. aureus* et SlyA chez *Salmonella typhimurium*) (344–346) et la production ou la dégradation de produits du métabolisme (HpaR chez *E.coli*, HucR chez *Deinococcus radiodurans*) (347,348). Cette famille de régulateurs a été découverte et caractérisée pour la première fois chez *E. coli,* avec son régulateur MarR. MarR, dont le gène est présent au sein de l'opéron *marRAB*, est une protéine présente sous forme d'homodimère libre ou lié à l'ADN. Elle est impliquée dans la réponse à l'environnement de *E. coli* notamment dans la résistance à différentes molécules telles que des antibiotiques (tétracycline, chloramphénicol, β-lactamine, et fluoroquinolone), des composés phénoliques, des solvants organiques et des détergents (340,349).

La structure de cette famille de régulateurs transcriptionnels est très conservée (339). Elle est composée de six hélices alpha et de trois feuillets béta : α1-α2-β1-α3-α4-β2-β3-α5-α6 (Figure 21). Des études de cristallographie ont mis en évidence la participation des deux sous-unités de l'homodimère dans la fixation à l'ADN. De plus, la comparaison des séquences de membres de la famille MarR révèle la conservation de certains résidus, tels que les acides

aminés hydrophobes de certaines hélices potentiellement impliquées dans l'assemblage et la stabilisation du dimère.

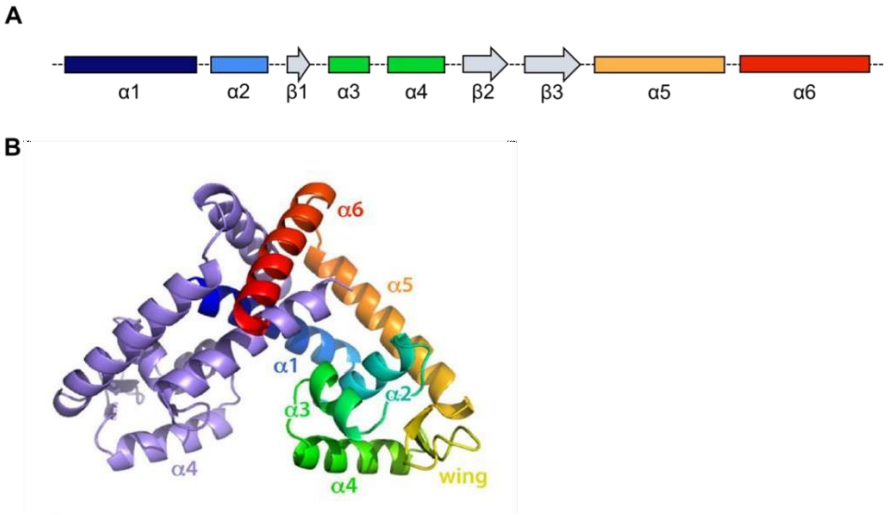

Figure 21. Caractéristiques structurales des protéines MarR. (A) Structure secondaire linéaire des protéines MarR. (B) Structure secondaire de l'homodimère de MarR. Un monomère est représenté en multicolore et l'autre en violet. Les couleurs de (A) sont équivalentes à celle en (B). D'après (294).

La dimérisation est une des étapes importantes pour la fixation à l'ADN des MarR. Les cristallographies de différents MarR révèlent un site de dimérisation pauvre en boucle favorisant les changements conformationnels des hélices. Le site de dimérisation comprend trois hélices alpha, α1, α5 et α6, interagissant *via* leur face hydrophobe. Un problème de dimérisation peut affecter la fidélité et la force de fixation à l'ADN des MarR. Ainsi L'interface de dimérisation influence la fixation à l'ADN (350,351). En effet, il existe une interaction entre le domaine de dimérisation et celui de fixation à l'ADN de la protéine, les hélices α1 et α5 connectant les deux sites. Ces données indiquent que la flexibilité de la protéine est indispensable à l'optimisation de sa fixation à l'ADN.

Le site de fixation à l'ADN est différent suivant le régulateur MarR. Il s'agit de sa signature. Il comprend généralement deux hélices alpha et trois feuillets bêta, β1-α3-α4-β2-β3 (Figure 21). Chaque site de fixation est stabilisé par des interactions hydrophobes impliquant 14 résidus se trouvant sur les hélices alpha et constituant un motif Hélice-Tour-Hélice (HTH). Ce site de fixation correspond à une séquence spécifique pseudo-palindromique de 16 à 20 pb chevauchant principalement les sites de reconnaissance de l'ARN polymérase, suggérant un rôle inhibiteur par encombrement stérique (339,352). L'affinité et le mode de fixation sont

dépendants du régulateur ou des potentielles interactions protéines/protéines consolidant le complexe à l'ADN.

Le mécanisme de régulation des MarR principalement décrit est caractérisé par un changement de conformation médié par l'interaction d'au moins un ligand. Cette fixation a pour conséquence de modifier son interaction avec l'ADN et donc de modifier l'expression des gènes sous son contrôle. Cette régulation dite allostérique permet au ligand de consolider ou d'atténuer la fixation à l'ADN du régulateur. Cette régulation dépend alors de la concentration intracellulaire du ligand. Le ligand peut se fixer sur un ou plusieurs sites sur le régulateur (339). Chez *E. coli*, le régulateur MarR, qui a deux ligands connus pour inhiber son activité à une concentration de l'ordre du milli-molaire, possède deux sites de fixation, dont l'un a été décrit au niveau de l'hélice α4 de fixation à l'ADN. Les deux sites de fixation proches de la fixation à l'ADN n'y participent pas mais l'influencent (353). La régulation de l'expression des gènes observée peut être donc due à la nature du ligand qui peut être soit inducteur, soit corépresseur (Figure 22). Ainsi, le ligand peut bloquer l'action du répresseur, empêchant la répression, comme chez *E. coli* où la fixation de molécule de salicylate abroge la répression de MarR permettant ainsi l'expression du gène MarA, il s'agit alors d'un inducteur (354,349). Au contraire, le ligand peut activer l'action du répresseur, corépresseur, déclenchant la

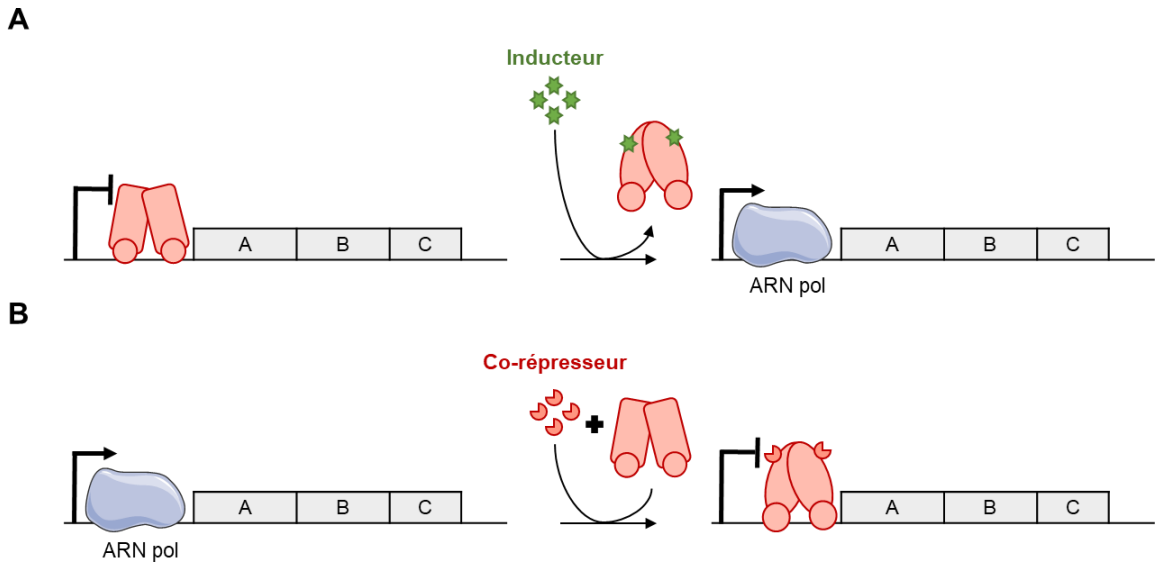

Figure 22. Régulations transcriptionnelles dépendant du ligand au sein de la famille MarR. (A) Ligand inducteur. La fixation du ligand sur le répresseur induit l'expression des gènes. (B) Ligand corépresseur. La fixation du ligand permet la fixation à l'ADN du répresseur et ainsi la répression de l'expression des gènes.

répression, comme chez *S. pneumoniae* où FabT lié à son ligand réprime l'expression des gènes empêchant le recrutement de l'ARN polymérase (334).

L'importance de cette famille de régulateur au sein de la bactérie et leur diversité mécanistique offrent de nouvelles perspectives sur l'identification à titre individuel des effecteurs et de leur mécanisme de contrôle de ces régulateurs. Dans cet objectif et prenant en compte l'importance des acides gras dans la survie bactérienne, nous avons décidé d'étudier le rôle et les conséquences de la régulation médiée par FabT.

3.2. La régulation transcriptionnelle de FASII par FabT

3.2.1. Le régulateur FabT

FabT est une protéine régulatrice de 144 acides aminés, présente chez les trois genres bactériens *Enterococcus*, *Lactococcus* et *Streptococcus*. Cependant, elle a été principalement étudiée chez les Streptocoques, plus particulièrement chez *S. pneumoniae*. La séquence protéique de FabT est conservée au sein de ces différents genres bactériens. En effet, FabT de *S. pneumoniae* présente respectivement 64 %, 62 %, 51 %, et 59 % d'identité de séquence avec FabT de *S. pyogenes, S. agalactiae, E. faecalis,* et *L. lactis*. De plus, les acides aminés les plus conservés sont ceux impliqués dans les sites de fixation du ligand et à l'ADN de la protéine (Figure 23).

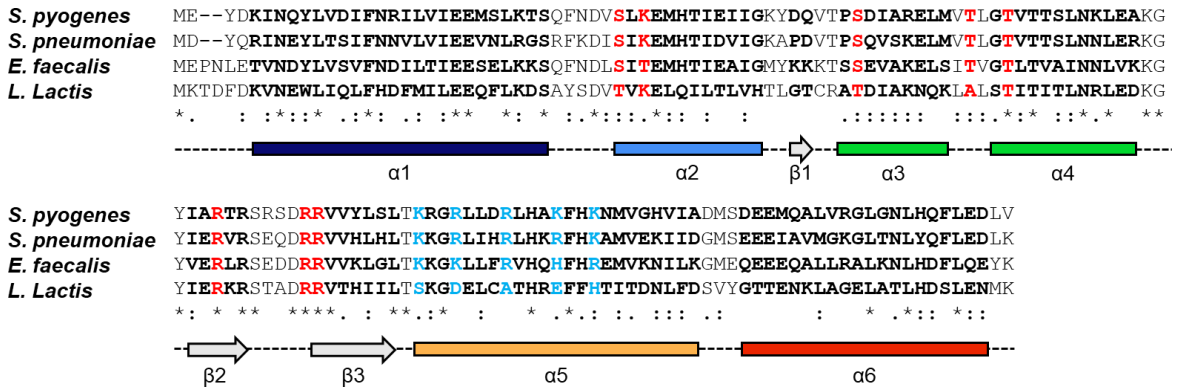

Figure 23. Comparaison des séquences de FabT chez *S. pyogenes, S. pneumoniae, E. faecalis* et *L. lactis*. Rouge, acides aminés impliqués dans l'interaction avec l'ADN. Bleu, acides aminés impliqués dans l'interaction avec l'ACP. *, identique entre les quatre espèces ; : la même classe structurelle. D'après (355,301).

La structure du régulateur FabT a été définie à partir d'une étude cristallographique chez *S. pneumoniae*. Cette dernière est similaire à celle des régulateurs de la famille MarR (Figure 21) (301). En effet, la région de dimérisation de FabT est formée par l'entrelacement de l'hélice α1 de la première sous-unité avec les hélices α5 et α6 de la deuxième sous-unité, formant ainsi un dimère stable et compact (Figure 21). Les hélices α2, α3 et α4 avec les feuillets β1 et β2 constituent le domaine de liaison à l'ADN. La fixation de FabT à l'ADN est non spécifique et nécessite la présence d'un corépresseur, l'acyl-ACP, pour augmenter son affinité avec l'ADN. En effet, il existe une seule interaction entre un résidu d'acide aminé (arginine 89) de FabT et un nucléotide (thymine). Contrairement à la majorité des ligands inducteurs des membres de la famille MarR, le ligand de FabT est utilisé comme corépresseur. Ainsi, une molécule d'acyl-ACP se fixe à chaque sous-unité du dimère de FabT. La formation du complexe FabT-(acyl-ACP) provoque un changement de conformation de FabT favorisant sa fixation aux sites spécifiques de l'ADN (301). D'autres analyses structurelles seront nécessaires pour déterminer la pertinence biologique et les interactions moléculaires impliquées dans une liaison efficace FabT-(acyl-ACP)-ADN.

Les sites spécifiques de fixation de l'ADN ont tout d'abord été définis chez *S. pneumoniae* par des analyses de retard sur gel, indiquant ainsi la présence de deux sites de fixation dans les régions promotrices, à respectivement 10 et 30 pb des sites de liaisons au ribosome des opérons *fabT* et *fabK* (334). Puis par comparaison des séquences, un site de fixation, très controversé, a été proposé en amont de *fabM* chez *S. pneumoniae* et *S. pyogenes* (Figure 24) (295,355). Ainsi, FabT inhiberait le recrutement de l'ARN polymérase ou empêcherait l'élongation d'un ARN. À partir des données obtenues chez *S. pneumoniae*, quatre sites spécifiques de FabT chez *L. lactis* ont été définis par comparaison des séquences puis confirmés par retard sur gel et empreinte à la DNAse I (296). De même, après analyse *in silico* des séquences, quatre sites ont été proposé chez *E. faecalis* (356).

La séquence nucléotidique de ces sites spécifiques a été établie par des analyses de biologie moléculaire et bio-informatique, chez *S. pneumoniae* 5'-GTTTTGATTGTAAAAGT-3', chez *E. faecalis* 5'-AGTTTGATAATCAAATT-3' et chez *L. lactis* 5'-TTTGAWAWAGAAA-3' (356,334,296). Une séquence consensus a été proposée après alignement *in silico* de 56 séquences prédites ou confirmées (Figure 25). Elle est dite pseudo-palindromique,

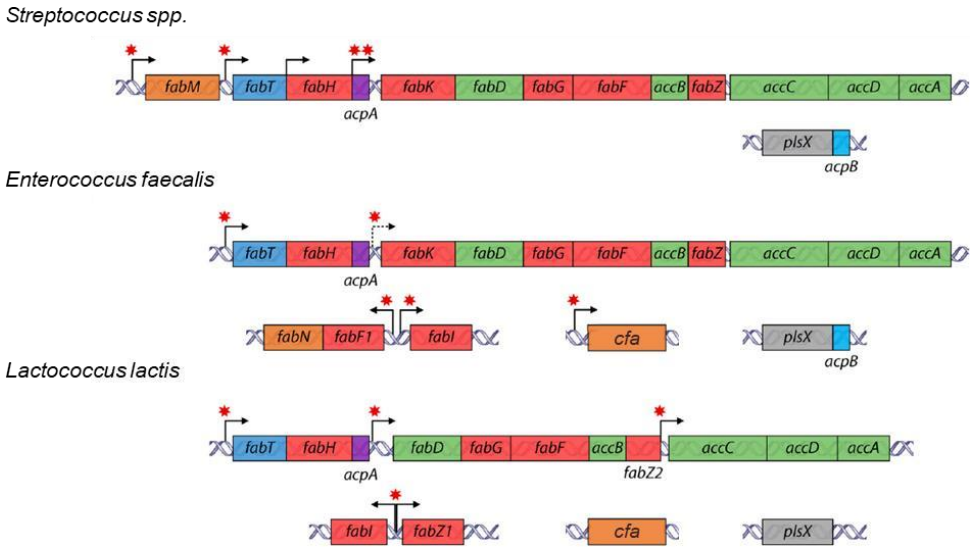

Figure 24. Sites de fixation décrits au sein de FASII. Les flèches coudées représentent les sites de démarrage de la transcription (334,357) ; la flèche coudée en pointillé, un site de réinitialisation de la transcription suggéré chez *E. faecalis* ; les étoiles rouges, les sites de fixation de FabT correspondant à une ou deux séquences consensus étroitement localisées. D'après (294).

confortant l'interaction avec FabT en tant qu'homodimère. Elle est caractérisée par la présence de résidus « TTTGA » en 5' et du triple adénosine en 3'.



Figure 25. Séquence consensus du site de fixation de l'ADN de FabT. Le motif a été calculé à partir de 56 séquences de liaison à l'ADN de FabT (https://regprecise.lbl.gov/regulog.jsp?regulog_id=3571). La taille relative des lettres correspond à la fréquence relative à laquelle chaque nucléotide est présent. D'après (294).

3.2.2. Les régulons de FabT

Afin de définir le rôle de FabT en tant que régulateur transcriptionnel, des mutants perte de fonction, mutation non sens en début de gène ou délétion, et gain de fonction, surexpression, ont été construits chez *S. pneumoniae*, *S. mutans*, *S. pyogenes*, *E. faecalis* et *L. lactis* (334,296,358,355,359,360,302). Puis l'étendue du régulon FabT a été défini par analyse transcriptionnelle en comparant l'expression de l'ensemble des gènes des souches

sauvages et mutantes, après croissance dans différentes conditions, impliquant ou non des modifications de l'homéostasie membranaire.

L'analyse transcriptomique à 37 °C met en évidence une légère augmentation de l'expression des gènes FASII chez les souches délétées. En effet, chez *S. pneumoniae* et *S. pyogenes*, l'expression des gènes FASII des souches mutantes augmente 2 à 9 fois par rapport à celle des souches sauvages (284,334,355). FabT réprime donc l'expression des gènes FASII au sein de ces organismes. Néanmoins, chez *S. pneumoniae*, l'expression du gène *fabM* ne semble pas être contrôlée par FabT. Chez *L. lactis*, seules les expressions de trois gènes du locus principal, *fabD*, *fabG1* et *accB* et de deux gènes présents sur un autre locus, *fabZ1* et *fabI*, augmentent, de 2,1 à 6,5, au sein de la souche délétée par rapport à la souche sauvage. Ces résultats suggèrent que la répression de ces gènes est faible, c'est-à-dire en dessous du seuil de détection fixé dans les conditions testées (296). En effet, dans une souche *L. lactis* surexprimant *fabT*, 135 fois, tous les gènes FASII sauf *fabH* sont réprimés d'un facteur 2,5 à 5,3, indiquant que ces gènes sont contrôlés par FabT (296). Les effets modérés de FabT sur l'expression des gènes FASII dans ces conditions, évoquent la possibilité que l'activité de FabT soit modulée par un cofacteur et/ou en fonction de l'état de la membrane. En effet, chez *S. mutans* et *S. pyogenes*, des variations de transcription des gènes FASII ont été observées en fonction des conditions de culture, respectivement en fonction du pH, neutre ou acide, et à différentes températures et phases de croissance (358,355). Ainsi chez *S. pyogenes*, les auteurs ont conclu que FabT contrôle tous les gènes de la voie FASII, bien que l'expression de *fabM* soit moins modifiée à 35 °C que celle des autres gènes. Le contrôle plus faible de *fabM* rappelle les résultats obtenus chez *S. pneumoniae*, où il n'est pas réprimé par FabT (334). Les conditions de culture imposées, à savoir la modification du pH et de la température de croissance, sont suffisantes pour induire un stress membranaire qui est compensé par la modification de la composition en acides gras de la membrane. Ces études transcriptomiques suggèrent donc que le rôle du régulateur FabT est plus important en réponse à un stress membranaire que lors de culture en condition non stressante, où son rôle est mineur. Cela suggère que FabT participe au maintien de l'homéostasie membranaire. En conclusion, FabT réprime les gènes FASII d'une manière coordonnée mais non identique. La régulation différentielle de l'élongation et de l'insaturation des acides gras pourrait être importante pour l'adaptation aux conditions de stress membranaire. D'autre part, en tant que régulateur de la famille MarR, FabT possède un ligand agissant comme corépresseur (cf. 3.2.1 Le régulateur

FabT). Ainsi, il serait plus intéressant de définir le régulon de FabT dans des conditions optimales de répression, c'est-à-dire en présence de son corépesseur.

La comparaison des profils transcriptomiques de souches sauvages et délétées de *fabT* cultivées à 37 °C en milieu de culture de laboratoire fait également ressortir de nombreux gènes autres que FASII dont l'expression dépend directement ou indirectement de FabT. Chez *S. pneumoniae*, la délétion de *fabT* a entraîné des changements d'expression mineurs (jusqu'à 5 fois) et majeurs (12 à 50 fois) pour 85 gènes régulés à la hausse et mineurs pour 4 gènes régulés à la baisse, impliqués dans le transport, le métabolisme des lipides, de l'ADN et la synthèse des protéines, ainsi que des protéines de fonction inconnue (334). Les variations transcriptionnelles observées sont probablement des effets indirects de la délétion de *fabT* qui sont requis pour l'adaptation de la bactérie aux modifications du rapport entre les acides gras saturés et insaturés (cf. 3.2.5. Conséquences physiologiques de mutation dans FabT). De plus, chez *L. lactis*, la comparaison des transcriptomes des souches sauvage et délétée *fabT* a révélé des changements dans l'expression de seulement 10 gènes autres que FASII contre 125 gènes lors de la surexpression de *fabT* (296). Ces gènes appartiennent aux mêmes catégories fonctionnelles que celles identifiées chez *S. pneumoniae*.

De manière intéressante, chez *S. pneumoniae,* FabT réprime l'expression de deux gènes impliqués, l'un dans le transport des acides gras, *fakB3*, et, l'autre dans le métabolisme des phospholipides, *plsC*. Le gène *fakB3* code la protéine DegV, FakB3, qui permet l'incorporation des acides gras poly-insaturés (361,312). Le gène *plsC* code la protéine PlsC, enzyme de la voie de biosynthèse des phospholipides (cf. 2.1. La synthèse des lipides membranaires) (334). Il existerait donc un couplage de la régulation de la synthèse des phospholipides et des acides gras chez *S. pneumoniae* comme décrit chez *B. subtilis* mais par un mécanisme différent (273).

Chez *S. mutans*, la comparaison des profils transcriptomiques des souches sauvage et délétée de *fabT* après une croissance à pH 7 ou pH 5 met en évidence la modification de l'expression de 25 % des gènes de *S. mutans* à pH 7 et de 7 % à pH 5 (358). Ces gènes font partie des mêmes catégories fonctionnelles que celles décrites chez *S. pneumoniae*. La délétion de *fabT* pourrait donc avoir plus de conséquences à un pH neutre, comme celui trouvé normalement dans la cavité buccale, qu'à un pH acide, comme celui produit lors de la croissance de *S. mutans*. Notons également qu'un pH acide crée des perturbations

membranaires, pouvant être similaires à celles générées par la délétion de *fabT*, de sorte que les changements seraient déjà en place.

Des analyses transcriptionnelles de souches sauvage et délétée de *fabT* ont également été réalisées chez *S. pyogenes*, dans lesquelles la phase de croissance (exponentielle ou stationnaire) et la température (35 ou 40 °C) ont été modifiées. La majorité des gènes modifiés, soit environ 28,5 %, ont une expression plus importante en phase de croissance stationnaire et à 40 °C. La plupart des gènes sont moins exprimés dans la souche délétée (355). Les gènes, dont l'expression est modifiée, codent principalement des protéines impliquées dans le métabolisme des sucres et des voies de synthèse des purines et des pyrimidines. Ces résultats suggèrent que la délétion de FabT peut conduire à un déséquilibre du métabolisme de *S. pyogenes*.

La régulation directe de ces gènes par FabT reste encore à être démontrée. Cependant, l'absence de séquence de fixation de FabT dans leurs régions promotrices couplée pour certains à l'activation de leur expression et non la répression suggèrent fortement que la plupart des changements d'expression observés soient des conséquences indirectes. De plus, l'analyse *in silico* des sites de fixation à l'ADN de FabT chez *S. pyogenes* révèle la présence de quatre autres sites autres que ceux de FASII (355). Par ailleurs, la séquence consensus choisie dans cette analyse est basée sur le motif « TTTnnTnnnnAAA » dans une bactérie dont le génome est riche en « AT ». Cette constatation remet en cause la spécificité de cette séquence et la présence des sites dans cette étude. L'ensemble de ces observations soutient donc le fait que la majorité des variations soient indirectes. Les conditions de culture et l'environnement de la bactérie sont connus pour affecter la composition de la membrane et ses propriétés (cf. 2.3. Le maintien de l'équilibre membranaire). Ainsi, FabT assurerait le maintien de l'homéostasie membranaire en réponse à un stress, chez les bactéries l'ayant comme régulateur transcriptionnel de FASII.

3.2.3. Le mécanisme de répression de FabT

Le mécanisme de répression de FabT, membre de la famille MarR, est dépendant de la présence d'un ligand. L'identification de ce dernier a été réalisée dans un premier temps chez *S. pneumoniae* puis dans un second temps chez *E. faecalis*. Afin de définir la nature du ligand,

un criblage de différentes molécules intracellulaires a été réalisé *via* des analyses biochimiques basées sur le principe du retard sur gel, « electrophoretic mobility shift », après purification de la protéine FabT de *S. pneumoniae* (362). Préalablement, les composés candidats ont été sélectionnés en fonction de leur implication chez les régulateurs MarR, leur nature biochimique et de leur rôle au sein de la synthèse des acides gras. Cette première analyse a permis de définir que les effecteurs connus régulant les MarR tels que le salicylate et les produits issus de la phase d'initiation de FASII tels que le malonyl-CoA n'interviennent pas dans cette interaction. Cela conforte le fait que la régulation de FASII par FabT est différente de celles de FapR chez *B. subtilis* et *S. aureus*. En revanche, les produits issus de la phase d'élongation, les acyl-ACP, favorisent l'interaction de FabT avec l'ADN. L'intensité de cette interaction augmente avec la longueur de la chaine carbonée de l'acyle et est optimale à partir de 18 carbones. De plus, à l'issue de la comparaison des analyses transcriptomiques, nous avons constaté une faible répression, *in vitro*, des gènes de FASII suggérant alors un effet limitant de la concentration du ligand (cf. 3.2.2. Les régulons de FabT). L'effet dose-réponse a été testé par retard sur gel en utilisant une concentration fixe de protéine FabT mais en variant les concentration d'acyl-ACP (362). Une corrélation est ainsi observée entre l'augmentation de la quantité d'acyl-ACP et l'affinité de FabT à l'ADN. D'autre part, ces expériences ont été réalisées en présence d'acyl-ACP insaturé, 18:1Δ11-ACP et saturé 16:0-ACP. La fixation à l'ADN du répresseur est plus importante en présence de 18:1Δ11-ACP qu'avec le 16:0-ACP. Bien qu'il ait été montré que la longueur de la chaîne de l'acyl-ACP est essentielle à la consolidation de la fixation de FabT à l'ADN, la différence d'affinité entre l'ajout de 18:1Δ11-ACP et de 16:0-ACP suggère également une implication du niveau d'insaturation dans la stabilisation du complexe à l'ADN. Pour répondre à cette question, chez *E. faecalis*, le niveau de répression de FASII a été analysé en fonction de l'ajout de différents acides gras dans le milieu de culture (302). La répression de FASII par FabT est plus importante en présence d'acides gras insaturés de conformation « *cis »* (16:1, 18:1Δ9, 18:1Δ11 et 18:2) qu'en présence d'acides gras insaturés de conformation « *trans »* (18:1Δ11) ou « cyclique » (c19:0) et encore moins en présence d'acides gras saturés (16:0 et 18:0). Par conséquent, la présence d'insaturation et la conformation de l'acyle interagissant avec FabT sont impliquées dans la fixation de ce répresseur à l'ADN, chez *E. faecalis*. Ainsi, l'ensemble de ces résultats suggère fortement que l'interaction d'un acyle insaturé à chaîne longue maximise la fixation du complexe de

répression FabT-(acyl-ACP) à l'ADN. Les acyl-ACP à chaines longues étant les produits finaux de FASII, il existerait donc un rétrocontrôle de FASII chez les bactéries possédant FabT.

Après avoir défini la nature de l'acyle, les auteurs se sont questionnés sur le rôle des deux protéines ACP, AcpA et AcpB, dans la corépression de FASII chez *S. pneumoniae* et *E. faecalis* (cf. 2.2. La synthèse des acides gras, FASII) (299,301,302). L'interaction avec FabT de l'acyl-AcpA et de l'acyl-AcpB semble être dépendante de l'espèce bactérienne. Du fait que les protéines de *S. pneumoniae* et *S. pyogenes* sont plus proches entre elles (91,9 % d'identité de séquence pour AcpA et 39,5 % pour AcpB) que de celle de *E. faecalis* (67,1 % d'identité de séquence avec AcpA de *S. pneumoniae* et *S. pyogenes* ; 43.4 % avec AcpB de *S. pneumoniae* et 34,2 % avec AcpB de *S. pyogenes*) (Figure 19C), nous avons décidé de focaliser notre attention sur l'analyse réalisée chez *S. pneumoniae* (301). En combinant des approches cristallographique, biochimique et génétique (301), les auteurs ont analysé la fixation à l'ADN du complexe FabT-(acyl-ACP) en fonction des protéines AcpA et AcpB, après purification et couplage de ces protéines à un acyle. Il s'avère que seul le complexe FabT-(acyl-AcpB) augmente la fixation du répresseur à l'ADN. Afin de caractériser les régions d'interaction de FabT avec l'acyl-AcpB, les auteurs ont établi un modèle de fixation à l'ADN du complexe FabT-(acyl-AcpB). L'implication des acides aminés des protéines FabT et AcpB mis en évidence a ensuite été confirmée par mutagénèse (Figure 19B et Figure 23). Ainsi, FabT interagit avec l'acyl-AcpB *via* la fixation directe de l'acyle au sein d'une poche hydrophobe, favorisant alors l'interaction de l'AcpB sur l'hélice α5 de FabT, conduisant à la formation du complexe FabT-(acyl-AcpB). Ces résultats suggèrent donc que la protéine AcpB serait également impliquée dans la régulation de FASII et que l'acyl-AcpB serait le ligand physiologique de FabT chez *S. pneumoniae*. Après comparaison *in silico* des séquences d'AcpB, les acides aminés décrits comme étant impliqués dans l'interaction avec FabT chez *S. pneumoniae* sont conservés chez *E. faecalis*. Cependant, chez *E. faecalis,* la composition en acides gras et le niveau de régulation de FabT au sein de la souche délétée de *acpB* sont identiques à ceux de la souche sauvage. Par conséquent, l'acyl-AcpB ne serait pas le seul corepresseur de FabT en présence ou absence d'acide gras exogènes chez *E. faecalis* (302). Les protéines AcpB n'auraient donc pas les mêmes rôles en fonction du genre bactérien. De plus, certaines espèces, dont FASII est contrôlé par FabT, telles que *L. lactis* et certaines souches de
S. agalactiae, ne possèdent pas AcpB. Le mécanisme de régulation mis en jeu serait donc également différent d'une espèce à une autre. Les hypothèses les plus simples que nous

pouvons formuler, expliquant alors les différences de régulation, sont i) que l'acyl-AcpA serait le corépresseur de FabT chez ces espèces ou ii) que les deux ACPs participeraient à différents degrés à la répression.

S'appuyant sur l'ensemble de ces données, un modèle de régulation a été proposé chez *S. pneumoniae* (Figure 26) (301). En condition *in vitro*, en absence d'acides gras exogènes, FabT forme un complexe avec l'acyl-AcpA, FabT-(acyl-AcpA). Ce complexe se lie de manière lâche aux sites spécifiques de fixation de l'ADN et par conséquent, une faible répression est observée (niveau basal). En revanche, en condition *in vivo*, c'est-à-dire en présence d'acides gras exogènes, *S. pneumoniae* incorpore les acides gras exogènes qui sont ensuite pris en charge par FakB, et phosphorylés par FakA. L'acyl-phosphate ainsi formé est pris en charge soit dans la synthèse des lipides, soit par PlsX qui va catalyser la formation de l'acyl-AcpB. Par

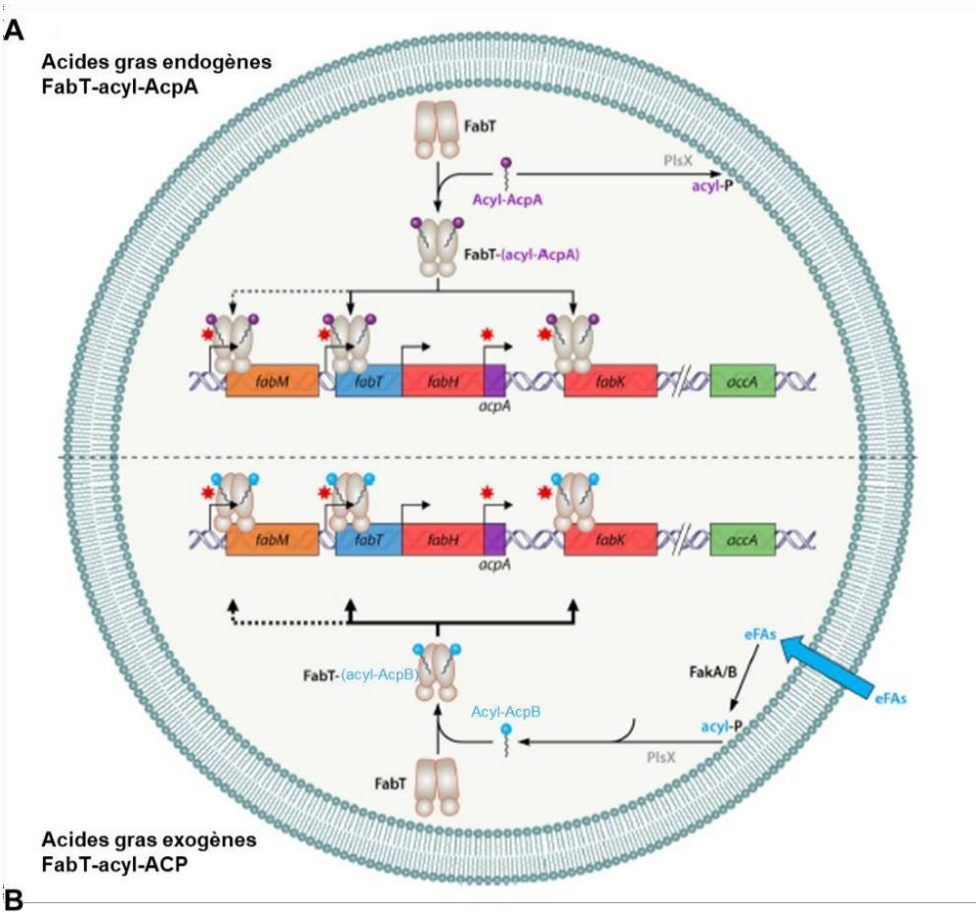

Figure 26. Modèle du mécanisme de répression de FabT proposé chez *S. pneumoniae*. (A) Synthèse des acides gras endogènes contrôlées par le complexe FabT-(acyl-AcpA). (B) Utilisation des acides gras exogènes et régulation de FASII par le complexe FabT-(acyl-AcpB). eFAs : Acides gras ou acyles

exogènes ; Trait en pointillé, régulation controversée ; Trait fin, répression faible ; Trait épais, répression forte ; Etoile rouge : site de fixation à l'ADN de FabT. D'après (294).

la suite, les acyl-AcpB se lient à FabT, formant ainsi un complexe stable, FabT-(acyl-AcpB), favorisant la répression de FASII. Il est important de noter que, contrairement à celle d'*acpA* et de *fabT*, l'expression du gène codant AcpB est constitutive lors de la croissance en présence ou en absence d'acides gras exogènes (334,363,355). La concentration d'acyl-AcpB dépend donc de la quantité d'acides gras exogènes. Par conséquent, l'efficacité de la répression repose sur la quantité et la composition en acides gras de l'acyl-AcpB.

3.2.4. Régulation de l'expression de *fabT* ou de l'activité de FabT

Chez *S. pneumoniae*, l'expression du gène codant FabT est régulé par un système à deux composants nommé VicKR, WalKR, MicAB, ou TCS02, répondant à un stress membranaire (364). La kinase VicK phosphoryle le régulateur VicR en réponse à un stress de membrane ayant pour conséquence la répression de l'ensemble des gènes du régulon VicRK (365). Sous sa forme non-phosphorylée, donc en absence de stress membranaire, le régulateur VicR contrôle de manière indirecte l'expression des gènes du cluster FASII en se fixant sur une séquence spécifique dans la région promotrice de l'opéron *fabT*. Des expériences de retard sur gels et des analyses transcriptomiques avec le régulateur purifié et la région promotrice de l'opéron *fabT* ont permis de définir une répression directe de l'expression de ces gènes (366). Par conséquent, la répression de *fabT* par VicR entraine l'absence de répression de l'opéron *fabK* et par conséquent une augmentation de l'expression de ces gènes et de la quantité d'acides gras à longues chaines (364). Cette altération de FASII participe à modifier les propriétés membranaires comme la fluidité, importante pour la mise en place du septum, et ainsi affecte la division bactérienne (367). La modification de la composition des membranes en réponse à un stress démontre le rôle de cette régulation dans l'adaptation bactérienne à son environnement.

Chez *S. pyogenes*, Stk est la kinase d'un système à deux composants de type histidine kinase/régulateur (368). L'analyse transcriptomique de la souche délétée *stk* suggère que Stk active indirectement l'expression des gènes de la voie FASII. Deux hypothèses ont été proposées. La plus simple est que Stk phosphoryle FabT, l'empêchant d'exercer son rôle de

répresseur transcriptionnel. La seconde postule que Stk phosphoryle les enzymes FASII et qu'une perte de fonction entraîne une activation en retour de l'expression du gène FASII. Ainsi, le rôle de Stk dans la régulation de l'activité de FabT reste encore à être établi.

Ainsi les régulations au niveau transcriptionnel et post-traductionnel de FabT observées permettent de le contrôler et de maintenir l'homéostasie membranaire. Celles-ci soulignent l'importance du régulateur transcriptionnel FabT au sein de la bactérie.

3.2.5. Conséquences physiologiques de mutation dans FabT

FabT régule donc l'expression des gènes impliqués dans la voie FASII. Un dérèglement de cette synthèse peut avoir des conséquences directes sur la composition des acides gras membranaires (cf. 2.3. Le maintien de l'équilibre membranaire). Chez *S. pneumoniae* et chez *L. lactis*, les compositions en acides gras membranaires ont été comparées entre une souche sauvage et une souche mutée pour FabT (296,334). Le pourcentage d'acides gras à chaines longues est plus important dans la souche mutée que dans la souche sauvage, confirmant la dérégulation des gènes FASII et donc la moindre inhibition de l'élongation des acides gras. L'équilibre entre les taux d'acides gras saturés et insaturés membranaires est également perturbé, en faveur des acides gras saturés. Ces résultats reflètent la différence de régulation de l'expression des gènes FASII. Partageant le même substrat, *fabM*, dont le produit est impliqué dans la formation des acides gras insaturés, semble être moins contrôlé que *fabK* (Figure 17). Ainsi, la modification membranaire peut aussi être liée au niveau de répression exercé par FabT sur les différentes unités transcriptionnelles. FabT n'exerce pas une même répression sur les différentes unités transcriptionnelles, voire n'en exerce pas sur l'une. D'autre part, ces données suggèrent également une modification de la composition des phospholipides membranaires dans les souches mutées, les acides gras étant les composés principaux des phospholipides. Cette hypothèse est confortée par le fait que FabT régule l'expression du gène codant PlsC chez *S. pneumoniae*. Par ailleurs, les premiers mutants *fabT chez S. pyogenes* ont été observés lors de l'étude d'un complexe de lipides anioniques membranaires, l'ExPortal. Pour mieux comprendre l'organisation de ce complexe, les auteurs ont sélectionné des souches en fonction de leur résistance à la polymyxine B, antibiotique ciblant les lipides anioniques. Après séquençage entier de leur génome, une à quatre

mutations ont été révélés dans 7 gènes centraux dont *fabT* (284). Les conséquences de mutations dans *fabT* sur la résistance à cet antibiotique ont été confirmées par analyse phénotypique d'une souche délétée *fabT* (355). Ces données suggèrent que ce phénotype est une conséquence indirecte de la perte de fonction de FabT. En effet, la résistance de ces souches peut être liée aux modifications de la composition lipidique membranaire. La composition lipidique de la membrane n'ayant pas encore été définie, nous supposons que la souche mutée possède moins de complexes lipidiques anioniques.

La nature des acides gras présents dans la membrane contribue à maintenir son homéostasie dépendant de certaines propriétés (cf. 2.3. Le maintien de l'équilibre membranaire). Afin de définir les conséquences de l'altération de l'équilibre d'acides gras, la perméabilité membranaire a été étudiée en mesurant les capacités d'incorporation de bromure d'éthidium chez *L. lactis*. La membrane de la souche mutée est plus perméable que celle de la souche sauvage (296). La perméabilité dépendant de la fluidité membranaire, nous supposons que celle-ci est également modifiée dans la souche mutée : le taux d'acides gras saturés étant plus important chez le mutant, la membrane serait moins fluide. Ainsi, le déséquilibre du taux d'acides gras membranaire en faveur des acides gras saturés lié à une mutation dans *fabT* a pour conséquence de modifier les propriétés membranaires.

Les modifications membranaires peuvent affecter la composition en protéines de la membrane, de la paroi et celles qui sont sécrétées. En effet, certaines protéines membranaires, telles que SecA et la sortase A sont respectivement impliquées dans la sécrétion de facteur de virulence et la mise en place de protéines de surface (369). De ce fait, les capacités d'adaptation de la bactérie à son environnement, par réception d'un signal, importation ou efflux de molécules, adhésion à des substrats, peuvent être modifiées. Néanmoins, les conséquences sur la composition protéique restent encore à être démontrées.

La perturbation de l'équilibre membranaire peut aussi modifier la résistance de la bactérie à différents stress (cf. 2.3. Le maintien de l'équilibre membranaire). Chez *S. pneumoniae*, afin d'étudier l'impact de la délétion de *fabT* dans l'adaptation bactérienne, la résistance de la souche mutée à différents stress connus (température, pH, ROS, détergents) a été défini par étude de croissance bactérienne (334). De fait, la souche mutée est plus sensible à un pH acide, mais plus résistante aux détergents tels que le déoxycholate. En revanche, la souche mutée ne présente pas de différence de résistance aux ROS, ni aux différentes températures, suggérant que FabT n'influence pas ces sensibilités.

L'ensemble de ces observations souligne le rôle de FabT dans la physiologie et l'adaptation à l'environnement de la bactérie. De ce fait, le mécanisme d'infection peut également être impacté par une mutation dans *fabT*. Deux équipes indépendantes ont étudié l'implication de FabT dans la virulence de *S. pyogenes* (355,359). Dans la première étude, 74 isolats cliniques de *S. pyogenes* provenant soit d'infections invasives (principalement STSS), soit d'infections non invasives, ont été analysés (359). Des mutations ponctuelles dans *fabT* ont été détectées uniquement dans les souches issues d'infections non invasives (2 isolats sur 38). La deuxième étude a observé neuf « Single Nucleotide Polymorphism » (SNP) ou insertions/délétions non synonymes dans *fabT* en comparant les séquences de plus de 3615 isolats cliniques de de *S. pyogenes* issus d'infections invasives et non invasives (52,355). Malheureusement, la distribution des mutants *fabT* entre les infections invasives et non invasives n'a pas été prise en compte (355). Dans un contraste frappant avec la faible incidence des polymorphismes *fabT* parmi les isolats invasifs, leur occurrence est passée à 12 % parmi les isolats récupérés au site d'infection de primates non humains dans des expériences de fasciite nécrosante. En effet, 44 remplacements d'acides aminés ont été identifiés à 30 positions différentes dans FabT. Le mécanisme d'infection de *S. pyogenes* lors de fasciite nécrosante débute par l'entrée de la bactérie dans le tissu *via* un trauma, ici une brèche, suivie de sa dissémination au sein du tissu (cf. 1.2.3.2. Les infections invasives à *S. pyogenes*). Les souches sélectionnées au point d'inoculation n'ont donc pas envahi le tissu. Par conséquent, elles sont considérées comme non invasives. Les observations faites lors de ces deux études suggèrent que les mutations spontanées dans *fabT* sont contre-sélectionnées dans les infections invasives et peu fréquentes dans les infections non invasives. Puis le caractère infectieux des souches mutantes *fabT* a été étudié dans deux modèles d'infection *in vivo* de fasciite nécrosante, murins et primates non humains (355,359). Dans le modèle murin, les souris ont été infectées avec la souche sauvage et les souches cliniques mutées dans *fabT*. La mortalité des souris du groupe infecté avec la souche clinique (0 à 2 sur 12 souris) est minime en comparaison de celle du groupe sauvage (7 à 10 sur 12 souris), suggérant l'implication de FabT dans la virulence de *S. pyogenes*. Dans le modèle d'infection de primates non humains, la souche délétée de *fabT* a provoqué une dissémination significativement moindre, des lésions plus petites et moins de destruction tissulaire que la souche sauvage. Ainsi, malgré la

différence de démarches expérimentales, l'ensemble de ces résultats suggère fortement l'implication de FabT dans la virulence de *S. pyogenes*.

En conclusion, des mutants *fabT* apparaissent spontanément parmi les isolats cliniques issus d'infections très probablement non invasives et, ils présentent une virulence fortement atténuée. Ainsi, la dérégulation de FabT induit des conséquences directes au niveau de la composition membranaire induisant des conséquences indirectes sur les capacités d'adaptation de la bactérie et sur sa virulence. De plus, la pression de sélection de FabT et les différents types de régulation présents dans la bactérie confortent l'importance du maintien de l'équilibre membranaire dans la survie bactérienne. Ainsi, l'ensemble de ces éléments permet d'envisager cet équilibre comme une cible thérapeutique.

3.3. FabT : une nouvelle cible thérapeutique ?

Avec l'émergence de bactéries multi-résistantes aux antibiotiques et la prise de conscience de l'existence des différents microbiotes, le choix des cibles thérapeutiques se veut plus spécifique à l'espèce bactérienne considérée. La voie de synthèse des acides gras est indispensable pour la survie bactérienne ce qui, en apparence, en fait une très bonne cible thérapeutique. Les inhibiteurs de FASII ont principalement un effet bactériostatique. Les enzymes participant à FASII sont majoritairement communes à l'ensemble des genres bactériens tels que les enzymes de la phase de démarrage, en revanche, d'autres sont plus spécifiques telles que les enzymes de la phase d'élongation. De nombreux inhibiteurs de FASII ont ainsi été décrits dans différentes espèces. Des différences d'efficacité de certains composés ont été observées en fonction des genres bactériens malgré la présence de cible commune. En effet, le triclosan est l'inhibiteur ciblant les enoyl-ACP réductases. Des différences de sensibilités ont été observées entre *S. aureus*, *B. subtilis* et *S. pneumoniae*, allant de la bactérie la plus sensible à la moins sensible (370–372). Une analyse de comparaison de séquences révèle que ces trois espèces bactériennes possèdent différentes enoyl-ACP réductase, respectivement FabI, FabL et FabK. Ces différences de sensibilité peuvent être expliquées par à une différence soit d'affinité du triclosan pour ces trois enzymes, soit de séquences des enzymes. Par ailleurs, *S. aureus* est aussi plus résistant à la cérulénine que *S. pneumoniae*, la concentration minimale inhibitrice observée est respectivement de 64 $\mu g.ml^{-1}$ contre moins de 2 $\mu g.ml^{-1}$ (373,374). La cérulénine ciblant la

cystéine du site actif de FabF, la différence observée semble être liée aux caractéristiques particulières des sites actifs entre les deux genres bactériens. Ces observations confortent alors la spécificité d'utiliser FASII en tant que cible thérapeutique. Ainsi pour l'ensemble de ces raisons, FASII a semblé être une excellente cible antibactérienne.

Cependant, en condition *in* vivo, c'est-à-dire en présence de source d'acides gras, l'utilisation des anti-FASII est inefficace. En effet, les bactéries ont la capacité d'incorporer les acides gras exogènes (cf. 2.3. Le maintien de l'équilibre membranaire). Chez *S. agalactiae*, les capacités de croissance et la composition en acides gras membranaires de différentes souches mutées dans des enzymes de FASII ont été testées en présence ou non de source d'acides gras exogènes (373). Alors que les souches mutantes ne poussent pas en absence d'acides gras exogène, elles ne présentent pas de différence de croissance par rapport à la souche sauvage en présence de sérum humain, source d'acides gras exogènes. Ainsi l'ajout de sérum permet à la bactérie de contourner le rôle de FASII. D'autre part, en étudiant la composition en acides gras membranaires après 3 et 12 heures de culture en présence d'acides gras exogènes, il s'avère que plus le temps d'adaptation est important, plus la composition en acides gras des souches est proche de celle du sérum. Donc l'adaptation de la bactérie à son environnement est graduelle. Par conséquent, ces études ont permis de mettre en évidence que les acides gras exogènes ont la capacité d'effacer les différences de composition membranaire de *S. agalactiae* lors de perte de fonction de FASII. De même, en condition mimant la situation *in vivo,* en présence de sérum humain, la bactérie contourne l'action de l'inhibiteur en incorporant les acides gras de son environnement, restaurant ainsi l'équilibre de sa membrane. L'impact de mutation FASII et de l'ajout d'anti-FASII a ensuite été analysé *in vivo* en utilisant un modèle de septicémie chez le rat. Aucune différence n'a été observée entre l'infection avec les souches sauvage ou mutées et le traitement anti-FASII. *S. agalactiae* contourne donc l'inhibition de FASII en incorporant des acides gras exogènes. L'inactivation de FASII a également été étudiée chez *E. faecalis*, bactérie présentant des acides gras « cycliques » dans sa membrane (297). L'analyse de la composition en acides gras des mutants FASII et des capacités *in vivo* d'infection confirment les résultats obtenus chez *S. agalactiae*. Par ailleurs, chez *S. aureus,* dont la membrane possède des acides gras spécifiques non présents dans l'environnement, l'inefficacité des anti-FASII a également été confirmée *in vivo* en utilisant un modèle murin de septicémie (375). Seize heures après l'infection, les souris ont été traitées avec un anti-FASII. Soixante-douze heures après le traitement, les bactéries

persistent au sein des différents organes, en modifiant progressivement leur composition membranaire *via* l'incorporation des acides gras exogènes.

En conclusion, l'ensemble des études réalisées souligne l'importance du maintien de l'équilibre membranaire crucial pour la survie des bactéries. L'inefficacité des anti-FASII couplée à la capacité d'incorporer les acides gras exogènes ne permet plus de considérer FASII comme une cible thérapeutique. En revanche, les données obtenues sur le répresseur FabT chez *S. pneumoniae* et *E. faecalis* permettent d'envisager la surexpression de FASII *via* l'inactivation de FabT comme une nouvelle stratégie thérapeutique. Ainsi, le développement d'inhibiteurs de FabT tels que des acyles formant des analogues toxiques d'acyl-ACP, pourrait ouvrir la voie à de nouveaux outils antibactériens plus spécifiques.

Contexte et objectifs des travaux

Streptococcus pyogenes est une bactérie Gram-positive, pathogène strictement humain, responsable d'environ 517 000 décès par an dans le monde (4). Son spectre d'infection est large, allant d'infections superficielles à des infections invasives. Les premières étapes des infections à *S. pyogenes* correspondent à l'adhésion des bactéries au tissu et à leur multiplication à sa surface. Le projet de recherche du laboratoire vise à mieux comprendre les mécanismes moléculaires mis en jeu lors de ces étapes avec, comme modèle d'étude, l'endométrite. A partir des données du CNR des Streptocoques (https://cnr-strep.fr/), le laboratoire a mis en évidence que les souches *S. pyogenes* de génotype *emm28* sont associées aux infections gynéco-obstétricales qui représentent 60 % des infections invasives chez les femmes en âge de procréer (21). Dans une étude récente, nous avons analysé l'interaction d'un isolat clinique *emm28* issu d'une endométrite avec la membrane de l'utérus pendant la grossesse, la décidue, en mettant en place un modèle d'infection *ex vivo* de ce tissu humain (21). *S. pyogenes* adhère au tissu, se multiplie à sa surface puis l'envahit. La multiplication de *S. pyogenes* à la surface du tissu dépend de la sécrétion de produits cellulaires. Une fois dans le tissu, *S. pyogenes* induit la mort des cellules et altère la réponse immunitaire de l'hôte, grâce notamment à l'intervention de deux facteurs de virulence, SpeB et SLO. Le laboratoire souhaite désormais décortiquer les mécanismes impliqués dans ces premières étapes, et plus particulièrement dans la multiplication bactérienne à la surface du tissu, afin de définir les éléments engagés dans la virulence de *S. pyogenes*.

Récemment, différentes études ont analysé les processus potentiellement impliqués dans la virulence de *S. pyogenes*. Deux études comparant les génomes d'isolats cliniques de *S. pyogenes* provenant d'infections invasives ou non invasives ont mis en évidence l'absence de mutation dans le gène *fabT* au sein de souches invasives (52,359). De plus, une autre étude utilisant un modèle primate non humain d'infection *in vivo* de fasciite nécrosante, révèle que plus de 54,5 % des souches prélevées au point d'inoculation, c'est-à-dire n'ayant pas envahi le tissu, présentent des mutations ponctuelles dans *fabT* (355). L'ensemble de ces résultats démontre une contre-sélection des souches mutées dans *fabT* dans les maladies invasives. Par la suite, le rôle de FabT dans la virulence de *S. pyogenes* a été analysé en utilisant des modèles d'infection *in vivo* de fasciite nécrosante. Les souches mutées dans *fabT* présentent un défaut de virulence (355,359). Ainsi FabT est impliqué dans la virulence de *S. pyogenes*. FabT est le

répresseur transcriptionnel des gènes de la voie de biosynthèse des acides gras, FASII, chez les streptocoques, *E. faecalis* et *L. lactis* (296,302,334). Au sein des souches mutées *fabT*, la dérégulation des gènes FASII a des conséquences sur la composition en acides gras de la membrane bactérienne. Les acides gras étant les gardiens de l'homéostasie membranaire, ces modifications rendent également compte des variations de perméabilité observées chez *L. lactis* (296). Ainsi, FabT contrôle la composition en acides gras de la membrane et de cette manière participerait au maintien de son homéostasie.

L'objectif de la thèse est de comprendre le lien entre la perte de fonction de FabT et le défaut de virulence observé. L'hypothèse est que les modifications, affectant l'homéostasie membranaire, peuvent impacter les capacités d'adaptation de la bactérie à son environnement et ainsi rendre compte du défaut de virulence.

Pour répondre à cette question, nous avons étudié, dans un premier temps, les conséquences physiologiques d'une mutation dans *fabT,* dans une situation mimant les conditions physiologiques *in vivo* par ajout, dans le milieu de culture, d'acides gras qui couplés, à une « acyl carrier protein », ACP, sont les corépresseurs de FabT. A partir de cette analyse, nous avons obtenu une vue holistique du rôle de FabT chez *S. pyogenes.*

S. pyogenes possèdent deux ACPs, AcpA et AcpB. Leur rôle dans la synthèse des acides gras et des lipides a été défini chez *E. faecalis* (299). Néanmoins, leur implication respective en tant que corépresseur de FabT est controversée (302). Nous avons donc étudié, dans un second temps, le rôle de AcpB dans la régulation des gènes contrôlés par FabT et les conséquences physiologiques de sa délétion chez *S. pyogenes*.

Lors de l'analyse du rôle de FabT et de son corepresseur, le gène, $degV_{1636}$, est ressorti comme étant le seul gène parfaitement corégulé avec les gènes FASII. Ce gène code une protéine de la famille DegV, possédant un domaine de fixation des acides gras, dont le rôle n'a pas encore été précisé (376). Nous avons analysé, dans un dernier temps, le rôle de cette protéine dans le transport et le métabolisme des acides gras et des lipides chez *S. pyogenes.*

Résultats

Partie 1 Rôle de FabT dans la virulence de *S. pyogenes.*

Article ***Streptococcus pyogenes* FASII regulator FabT avoids unnecessary energy expenditure and is required for human tissue infection.**

Clara Lambert, Caroline Bachmann, Marine Gaillard, Antoine Hautcoeur, Karine Gloux, Thomas Guilbert, Celine Méhats, Bastien Prost, Audrey Solgadi, Sonia Abreu, Muriel Andrieu, Claire Poyart, Alexandra Gruss and Agnes Fouet.

En cours de soumission.

Partie 2 AcpB, corépresseur de FabT chez *S. pyogenes.*

Article **Acyl-AcpB, a FabT co-repressor in *Streptococcus pyogenes.***

Clara Lambert, Alice d'Orfani, Qiufen Zhang, Karine Gloux, Claire Poyart and Agnès Fouet.

En cours de soumission.

Partie 3 Rôle de la protéine $DegV_{1638}$ chez *S. pyogenes.*

Article **A novel mechanism of endogenous fatty acid excess control in *Streptococcus pyogenes.***

Clara Lambert, Thifaine Pouillon, Qiufen Zhang, Alain Schmitt, Jean-Marc Masse, Karine Gloux, Claire Poyart and Agnès Fouet.

En cours de soumission.

Partie 1 : Rôle de FabT dans la virulence de *S. pyogenes.*

Streptococcus pyogenes FASII regulator FabT avoids unnecessary energy expenditure and is required for human tissue infection.

Clara Lambert[1], Caroline Bachmann[1], Marine Gaillard[1], Antoine Hautcoeur[1], Karine Gloux[2], Thomas Guilbert[1], Celine Méhats[1], Bastien Prost[3], Audrey Solgadi[3], Sonia Abreu[4], Muriel Andrieu[1], Claire Poyart[1,5], Alexandra Gruss[2] and Agnes Fouet[1]✉.

[1] Université Paris Cité, Institut Cochin, INSERM, U1016, CNRS, UMR8104, Paris, France;
[2] Micalis Institute, INRAE, AgroParisTech, Université Paris-Saclay, Jouy en Josas, France;
[3] UMS-IPSIT - Plateforme SAMM, Université Paris Saclay, France ;
[4] Lipides, Systèmes Analytiques et Biologiques, Université Paris-Saclay, Châtenay-Malabry, France;
[5] AP-HP Centre–Université Paris Cité, Paris, France.

✉ email: agnes.fouet@inserm.fr

Orcid numbers: A. Fouet, 0000-0001-7715-9157; A. Gruss, 0000-0001-7426-5229; C. Lambert, 0000-0003-2740-1755; T. Guilbert, 0000-0001-5069-0730.

Abstract

Membranes are a universal barrier to all cells. In most known bacteria, a phospholipid membrane structure comprises a polar head and apolar fatty acid (FA) chains. In streptococcaceae and enterococci the FA synthesis pathway (FASII) is controlled by the FabT repressor. *Streptococcus pyogenes fabT* mutants arise and are associated with virulence defects in *in vivo* animal models. We conducted an in-depth study to elucidate the consequences of *fabT* mutation on virulence. Our results confirm that FabT adjusts membrane FA composition in response to environmental FAs by modulating FA chain length and composition. Moreover, a *fabT* mutant led to a specific downshift in the proportion of cardiolipin. *fabT* deregulation of fatty acid synthesis further led to defects in adhesion and growth in the presence of eucaryotic cells, growth during which wild-type and a *fabT* mutant strains use cholesterol esters. The *fabT* growth defect is linked to an increased energy consumption due to futile FASII activity and causes an infection defect. This establishes the link between the FabT repressor status and virulence.

Introduction

Bacterial membranes form a mutable permeable barrier that modulates the transport of nutrients and responds to signals to facilitate adaptation to a changing environment. They usually comprise a phospholipid bilayer composed of a polar head and apolar fatty acid (FA) chains. The FAs, which may be saturated or unsaturated, are synthesized by the FA synthesis pathway (FASII) that is widespread among bacteria. It consists of an initiation phase followed by a recursive elongation cycle, whose product is acyl-acyl carrier protein (acyl-ACP). Unsaturated FAs are produced *via* a shunt of this cycle that is catalyzed by FabM in streptococci. While the FASII pathway is conserved (although enzymes may vary), regulation of the FASII genes is not. In streptococcaceae, a unique feedback mechanism controls expression of the FASII genes, involving a repressor, FabT, encoded in the FASII main locus. FabT, a member of the MarR family of regulators, possesses an unconventional corepressor, acyl-ACP [[1], for review [2]]. Notably, the affinity of FabT-(acyl-ACP) binding to DNA, on a specific palindromic sequence, increases with the length of the acyl carbon chain and the presence of an unsaturation [3]. FabT regulons have been mapped in various streptococcaceae species and in different conditions that predictably affect membrane FA composition, such as growth temperature, pH or growth phase [4-8]. The regulons all comprise the FASII genes; yet, the expression of *fabT*, *fabH*, *acpA* and *fabM* show little or no variation. The differential control of the genes encoding elongation steps, mainly the *trans*-2-Enoyl-ACP reductase II FabK, and of *fabM*, encoding an ACP-isomerase, correlate with longer and more saturated FAs observed in *fabT* mutant strains [5]. The regulons also comprise non-FASII genes that vary according to reports and species under study, involved in transport, DNA and carbohydrate metabolism, protein, purine and pyrimidine synthesis. FabT likely has similar but not identical roles in different streptococcaceae. However, the FabT regulons have not been established in the presence of exogeneous FAs (eFAs), which enhance FabT transcriptional repression [3].

Streptococcus pyogenes, also known as Group A *Streptococcus*, GAS, is an important human pathogen responsible for a large variety of clinical manifestations ranging from mild superficial infections to more life-threatening invasive infections including necrotizing fasciitis, streptococcal toxic shock syndrome and postpartum infections, as well as post-streptococcal sequelae, leading altogether to over 500,000 deaths annually worldwide;
S. pyogenes is still among the top ten causes of death due to bacterial infections worldwide [9].

No vaccine exists, so antibiotics are essential for effective treatment. Treatment failure remains a major apprehension. FASII pathway enzymes have been considered as potential antimicrobial targets. However, based on the streptococcaceae ability to incorporate host derived extracellular FAs to synthesize membrane phospholipids, FASII can no longer be considered a suitable target in these and other Firmicute bacteria [10,11]. In contrast, FASII gene regulators may constitute an interesting target in streptococcaceae. This is supported by the fact that *S. pyogenes fabT* mutant strains displayed virulence defects in two *in vivo* necrotizing fasciitis models [4,12]. In a murine model, strains harboring *fabT* point mutations display smaller size lesions, no loss of body weight and a lower mortality than their wild-type counterparts [12]. In a non-human primate model, the *fabT* deleted strain decreases in dissemination capacity [4]. Finally, survival of the *fabT* deleted strain decreases in human blood or in the presence of human polymorphonuclear leukocytes [4].

This study aims to understand the precise link between FabT and virulence. Integrated transcriptomic, lipidomic, proteomic, metabolomic, cell culture and *ex vivo* approaches led us to narrow down the role of FabT in limiting futile FASII synthesis and promoting advantageous interaction of *S. pyogenes* with the host.

Results

Construction and characterization of *fabT* mutant strains.

A *fabT* deleted strain, ΔFabT, was constructed in the wild-type (WT) reference strain, M28PF1 [13]. Growth of ΔFabT and WT strains was compared in laboratory THY medium and in THY supplemented with Tween 80 as a source of FAs. Exogenous FAs (eFAs) are incorporated by Streptococcaceae and acyl-ACP act as FabT corepressors (Fig. 1a, b) [1,10]. The ΔFabT strain latency phase was longer than that of the WT, 60 *versus* 10 min in THY and 30 *versus* 10 min in THY-Tween, as described previously [4]. However, in contrast to that previous report, the ΔFabT strain displayed a growth defect compared to the WT strain, 126 *vs* 39 min per doubling in THY, respectively, and 113 *vs* 55 min in THY-Tween, hampering further analyses. We decided to construct a strain with a point mutation, mFabT. We chose to replace the Histidine 105 residue by a Tyrosine for two reasons. The replacement of this Histidine residue by other residues, including Tyrosine, has been observed in multiple independent clones harvested from the site infection of nonhuman primates [4]. The 105th residue is in the middle of the α5 helix that is involved in FabT dimerization and acyl-ACP binding [14]. The mFabT strain grew like the WT in both THY and THY-Tween media (Fig. 1a, b). We performed "omics" approaches to obtain an overall view of the consequences of FabT^{H105Y} mutation on global bacterial physiology by comparing transcriptomic, FA, lipidome and envelope proteome, profiles of mFabT and the WT strain without and with environmental fatty acid.

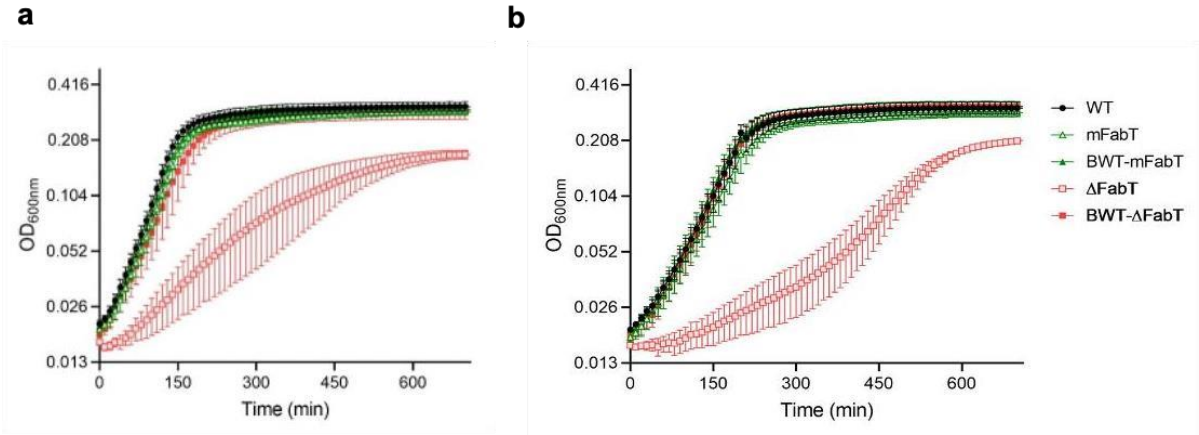

Fig. 1 | Impact of FabT mutations on *S. pyogenes* growth. a-b, Growth curves of WT, mFabT, BWT-mFabT, ΔFabT and BWT-ΔFabT strains in laboratory media, **a**, THY, **b**, THY-Tween.

FabT regulon in the presence of exogenous FAs and expression effects of *fabT* mutation.

To evaluate the breadth of the FabT regulon when bacteria are grown in the presence of eFAs, transcriptomic profiles were determined in four conditions, WT cultivated in THY and THY-Tween, and mFabT in THY and THY-Tween. Data were then analyzed by comparing results pairwise between WT and mFabT grown in THY, then comparing each strain in THY and THY-Tween, and, finally, WT and mFabT, both grown in THY-Tween; the results were confirmed by qRT-PCR (Fig. 2a, b; Extended Data Table 1; Fig. S1, Table S1). Our main observations are that 1- the FASII genes, except *fabK*, are not differentially expressed in the WT and mFabT strain in THY (Fig. S1a). 2- in the WT strain, addition of eFAs led to the repression of expression of the FASII genes (Fig. 2a, b; Extended Data Table 1). 3- in the mFabT strain, addition of eFAs did not lead to the repression of expression of the FASII genes (Fig. S1b). 4- in the presence of eFAs, the FASII genes are, as well as a single other gene, $degV_{1638}$, overexpressed in the mFabT strain (Fig. S1b).

In THY, about 2% of the genome, were differentially expressed: 17 genes showed decreases, and 21 increases of expression in the mFabT strain compared to the WT strain (Fig. 2a, Extended Data Table 1). Down-regulated genes included those encoding virulence factors such as adhesins, carbohydrate transport, and stress response proteins. The up-regulated genes encoded proteins involved in purine and lipid metabolism, potassium transport, and virulence factors such as other adhesins, and cell-wall synthesis enzymes. Thus, FabT mutation has a modest impact on *S. pyogenes* gene expression in the absence of the co-repressor.

FabT-mediated repression is activated by exogenous FAs joined to ACP (see [2] for Review). Transcriptomic profiles were thus determined on WT and mFabT strains in the presence of an FA source, here Tween. Results were confirmed by qRT-PCR on chosen genes (Fig. 2b, Table 1, Extended Data Table 1, Fig. S1). Adding Tween to the growth medium led to modified expression of 46 genes in the WT strain (Fig. 2b, Table 1, Extended Data Table 1, Fig. S1). As expected, Tween addition leads to repression of FASII gene expression and 14 other genes, for which the effect could be direct or indirect. In contrast, up-regulation of 20 genes is likely due to indirect effects linked either to secondary regulators or as a consequence of membrane changes following the incorporation of eFAs and arrest of FA synthesis.

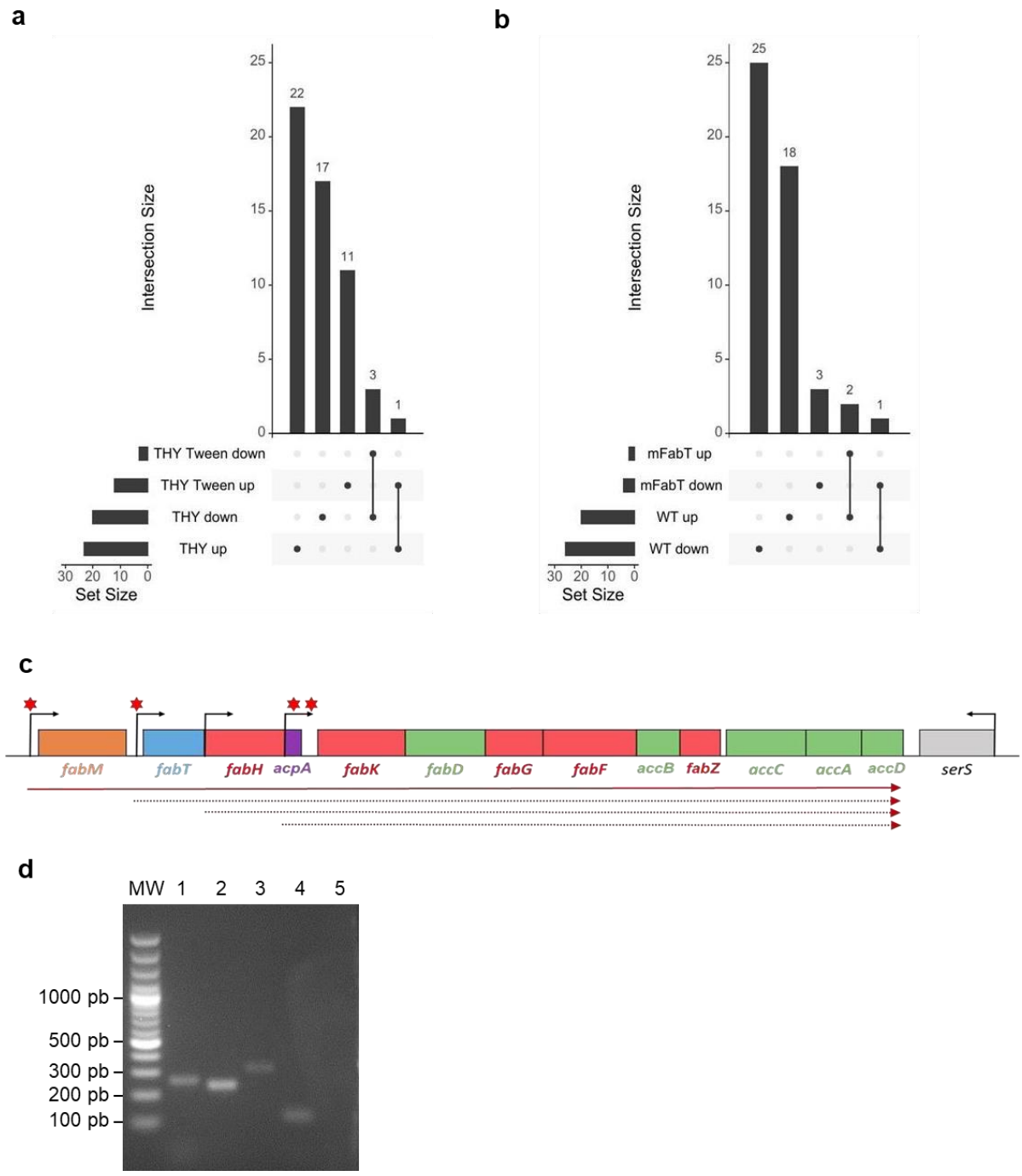

Fig. 2 | FabT regulon in the presence of eFAs and genetic organization of the *S. pyogenes* FASII genes. a-b, Upset plots of differentially expressed genes, **a**, in the mFabT *versus* the WT strain in THY and in THY-Tween; **b**, in THY-Tween *versus* THY in the WT and the mFabT strains. **c**, Schematic representation of *S. pyogenes* FASII locus. Gene positions with names below are represented. Above, asterisks, putative FabT binding sites; bent arrows, transcription start sites; below, solid arrow, transcript defined by RT- PCRs, dotted arrows transcripts identified by transcription start sites. The transcripts may end before the *accD* gene. **d**, Analysis of the mRNA transcripts of FASII locus: agarose gel of PCR amplification products on cDNA using primer pairs from neighboring genes; MW, Generuler 100 bp ThermoFischer Sientific (Ref. SM0321); Lane 1, *fabM-fabT* (234 bp); 2, *fabH-acpA* (221 bp); 3, *acpA-fabK* (302 bp); 4, *fabZ-accC* (105 bp); 5, *accD-serS* (288 bp).

In contrast, addition of Tween to the mFabT strain growth medium left the FASII gene expression unchanged. Only 6 genes were differentially expressed, including 3 shared with the WT strain. Hence, the FabT^{H105Y} protein is unable to repress the expression of many genes controlled by FabT, including the FASII genes.

To further characterize the gene expression difference between both strains we compared the transcriptomic profiles of both strains grown in THY-Tween (Fig. 2a, Table 1, Extended Data Table 1, Fig. S1b, c). Fifteen genes were differently impacted by the addition of Tween depending on the state of the FabT protein. Nine FASII and 3 other genes were upregulated in the mFabT strain compared to the WT strain. Two genes, *norA* and *uspA*, organized in an operon were downregulated. These results confirm that the eFA-dependent control on gene expression exerted by the FabT^{H105Y} protein differs from that of the WT FabT protein.

Of note, neither *acpA* nor *fabT* were highlighted in the RNA-seq experiments, although addition of Tween led to a repression of *fabT* expression in the WT strain as found in the more sensitive qRT-PCR experiments (Fig. S1b). Twelve genes, the 11 FabT-controlled genes of the FASII locus, from *fabM* to *accD*, and *degV$_{1638}$*, are the only fully co-regulated genes, suggesting they are the only genes, whose expression is directly controlled by FabT. Consensus FabT binding sequences are found along the FASII locus (Fig. 2c) [[2] and references herein]. We sought whether there were other such sequences on the WT strain genome using ANTTTGATTATCAAATT as a probe and 100 % identity on 15 out of 17 nucleotides criterion. A single sequence was highlighted; it is located between the previously described *degV$_{1638}$* transcription start site and its translation start site [15]. This indicates that *degV$_{1638}$* and only this gene, in addition to the FASII genes, is directly controlled by FabT.

In a previous study, we had determined the transcription landscape in an *emm1* strain grown in THY [15]. We have shown in *Enterococcus faecalis* that transcripts can overlap genes located before and after a FabT-controlled transcription start site. We consequently assessed, by overlapping reverse transcription (RT-PCR) whether *fabM* and *fabT*, on one hand, and *acpA* and *fabK*, on the other hand, could be co-transcribed (Fig. 2c, d). Each of these gene couples, as well as, as expected, *fabH* and *acpA*, and *fabZ* and *accC*, belonged to same transcripts. This indicates that there is one transcript covering from *fabM* to *accD* with controlled or non-controlled transcription restarting sites.

Table 1. Metabolism and virulence genes differently expressed under all conditions tested.

Locus	Gene	Gene product	THY mFabT *vs* WT	WT THY-Tween *vs* THY	mFabT THY-Tween *vs* THY	THY-Tween mFabT *vs* WT	Function
Metabolism							
M28_Spy0022	*purC*	Phosphoribosylaminoimidazole-succinocarboxamide synthase, PurC	1.327				Purine synthesis
M28_Spy0023	*purL*	Phosphoribosylformylglycinamidine synthase, PurL	1.245				Purine synthesis
M28_Spy0024	*purF*	Amidophosphoribosyltransferase, PurF	1.102				Purine synthesis
M28_Spy0025	*purM*	Phosphoribosylformylglycinamidine cyclo-ligase, PurM	1.313				Purine synthesis
M28_Spy0026	*purN*	Phosphoribosylglycinamide formyltransferase, PurN	1.469				Purine synthesis
M28_Spy0371**	*M28_Spy0371*	67 kDa myosin-crossreactive antigen	1.534	1.941	*0.588*		Fatty acid degradation
M28_Spy0853**	*M28_Spy0853*	Diacylglycerol kinase family lipid kinase	*0.877*		-1.102		Lipid metabolism
M28_Spy1112**	*gapN*	NADP-dependent glyceraldehyde-3-phosphate dehydrogenase, GapN	-1.220	*-0.740*			Glycolysis
M28_Spy1136	*M28_Spy1136*	D-alanyl-D-alanine carboxypeptidase	1.633	*0.917*			Peptidoglycan biosynthesis
M28_Spy1434	*M28_Spy1434*	DegV family protein, FakB3		-1.491	-1.409		Lipid metabolism
M28_Spy1473**	*accD*	Acetyl-coenzyme A carboxylase carboxyl transferase subunit alpha, AccD		-2.343		2.567	Fatty acid biosynthesis
M28_Spy1474**	*accA*	Acetyl-coenzyme A carboxylase carboxyl transferase subunit beta, AccA		-2.357		2.589	Fatty acid biosynthesis
M28_Spy1475**	*accC*	Biotin carboxylase, AccC		-2.431		2.666	Fatty acid biosynthesis
M28_Spy1476**	*fabZ*	3-hydroxyacyl-[acyl-carrier-protein] dehydratase, FabZ		-2.335		2.559	Fatty acid biosynthesis
M28_Spy1477**	*accB*	Biotin carboxyl carrier protein of acetyl-CoA carboxylase, AccB		-2.535		2.534	Fatty acid biosynthesis
M28_Spy1478**	*fabF*	3-oxoacyl-[acyl-carrier-protein] synthase 2, FabF		-2.524		2.601	Fatty acid biosynthesis
M28_Spy1479**	*fabG*	3-oxoacyl-[acyl-carrier-protein] reductase, FabG		-2.486		2.676	Fatty acid biosynthesis
M28_Spy1480**	*fabD*	Malonyl CoA-acyl carrier protein transacylase, FabD		-2.430		2.434	Fatty acid biosynthesis
M28_Spy1481**	*fabK*	Enoyl-[acyl-carrier protein] reductase (NADH), FabK		-2.397		2.351	Fatty acid biosynthesis
M28_Spy1483	*fabH*	3-oxoacyl-[acyl-carrier-protein] synthase 3, FabH		-1.176		*0.679*	Fatty acid biosynthesis
M28_Spy1484	*fabT*	Transcriptional regulator, FabT		*-0.921*			Fatty acid biosynthesis
M28_Spy1485*	*fabM*	Enoyl-CoA hydratase, FabM		-1.160			Fatty acid biosynthesis
M28_Spy1638**	*M28_Spy1638*	DegV family protein		-1.083		*0.835*	Lipid metabolism
Virulence							
M28_Spy0107	*cpa*	Collagen-binding protein, Cpa	1.937				Adhesin
M28_Spy0108	*sipA*	Signal peptidase I, SipA	2.081				Signal peptidase
M28_Spy0109	*M28_Spy0109*	T28 T-antigen	2.195				Adhesin
M28_Spy0110	*srtB*	Class B sortase protein, SrtB	1.734				Sortase
M28_Spy0111	*fctB*	Pilin minor structural protein, FctB	1.949				Adhesin
M28_Spy0137*	*nga*	NAD glycohydrolase, Nga	-1.350				Virulence factor
M28_Spy0138*	*ifs*	Immunity factor for SPN/NAD glycohydrolase protein, Ifs	-1.540				Resistance factor
M28_Spy0139*	*slo*	Thiol-activated cytolysin, SLO	-1.357				Virulence factor
M28_Spy1098**	*grab*	Protein G-related alpha 2M-binding protein, Grab	1.647				Virulence factor
M28_Spy1336	*M28_Spy1336*	R28 protein	1.041	1.412			Adhesin
M28_Spy1672*	*ska*	Streptokinase, Ska	*0.929*	1.069			Tissue invasion
M28_Spy1675	*sclA/scl1*	Collagen-like surface protein A, SclA/Scl1	-1.823	-0.996			Adhesin
M28_Spy1699**	*M28_Spy1699*	Cell surface protein	*-0.923*	-1.822			Adhesin
M28_Spy1700**	*scpA*	C5a peptidase, ScpA	-1.162	-2.073			Adhesin
M28_Spy1701	*M28_Spy1701*	Enn protein	*-0.871*	-1.026			Adhesin
M28_Spy1702	*M28_Spy1702*	Emm28 protein	-1.985				Adhesin
M28_Spy1715	*sfbX*	Fibronectin-binding protein, SfbX	*-0.889*	-1.359			Adhesin
M28_Spy1716	*sof*	Serum opacity factor	-1.093	-1.375			Adhesin

A gene is considered modified when log2-Foldchange (FC) is below -1 or above +1 and the adjusted p-value is less than 0.05. The asterisk highlighted gene expressions that are shared with a previous transcriptomic analysis of *S. pyogenes fabT* deleted mutant versus WT strain cultivated under different temperatures, 35°C (blue asterisk) and 40°C (red asterisk), in the exponential phase. In italic, log2 Fold change that are outside our chosen threshold but have a p-value below 0.05 and are significantly modified in others comparisons.

fabM expression control depends on a single FabT binding site, whereas a second FabT binding site is present upstream from *fabT*. This may explain the weaker control of *fabM* than of other FASII genes. A transcription start site was defined, upstream *fabH*, that is not closely followed by consensus FabT binding sequences (Fig. 2c). This uncontrolled transcription is probably the cause of a weaker expression ratio for *fabH* than for the other genes between the WT and mFabT strains. Finally, there are two further consensus FabT binding sequences upstream from *fabK.* This may account for *fabK* being the gene whose expression ratio is the highest in the various conditions compared and is even controlled by FabT in the absence of Tween (Fig. S1a).

Altogether, these results reveal the breadth of the FabT regulon in rich medium laboratory conditions and in the presence of the acyl co-repressor and prove that FabT^{H105Y} has lost its repressor activity.

The FabT-H105Y mutation modifies membrane fatty acid and lipid composition of *S. pyogenes*.

Since the FabT^{H105Y} mutation leads to a deregulation of FASII gene expression, we tested its consequences on FA and lipid composition when bacteria were grown in the absence or presence of Tween (Fig. 3a-c, Extended Data Table 2, Fig. S2, Table S2). In the absence of added Tween, the relative amount of 14:0 was one third (0.67 % *vs* 2.2 %), of 16:0, 8 % less 16:0 (21.63 % *vs* 29.03 %) and of and 16.1 twice less 16:1 (8.77 % *vs* 17.53 %) in the mFabT strain membrane than in the WT strain. Conversely that of 18:0 was four time more important (25.68 % *vs* 6.72 %) in the mFabT strain membrane than in the WT strain, correlating with a loss of FASII repression. Altogether this led to an increased C18:C16 ratio and a decreased unsaturated/saturated FAs ratio in mFabT strain indicating that compared to the WT membrane, the mFabT mutant membrane may be more rigid.

In the presence of Tween, WT *S. pyogenes* efficiently incorporates 18:1Δ9, together with other minor FAs (Tween 80 comprises 70-80 % 18:1Δ9). 18:1Δ9 appeared to be less incorporated in the mFabT strain. To test the possibility that the mFabT strain was defective for eFA incorporation, we compared incorporation of 17:1, a FA normally absent from *S. pyogenes* membrane and whose presence is dependent on its incorporation (Fig. 3d, e).

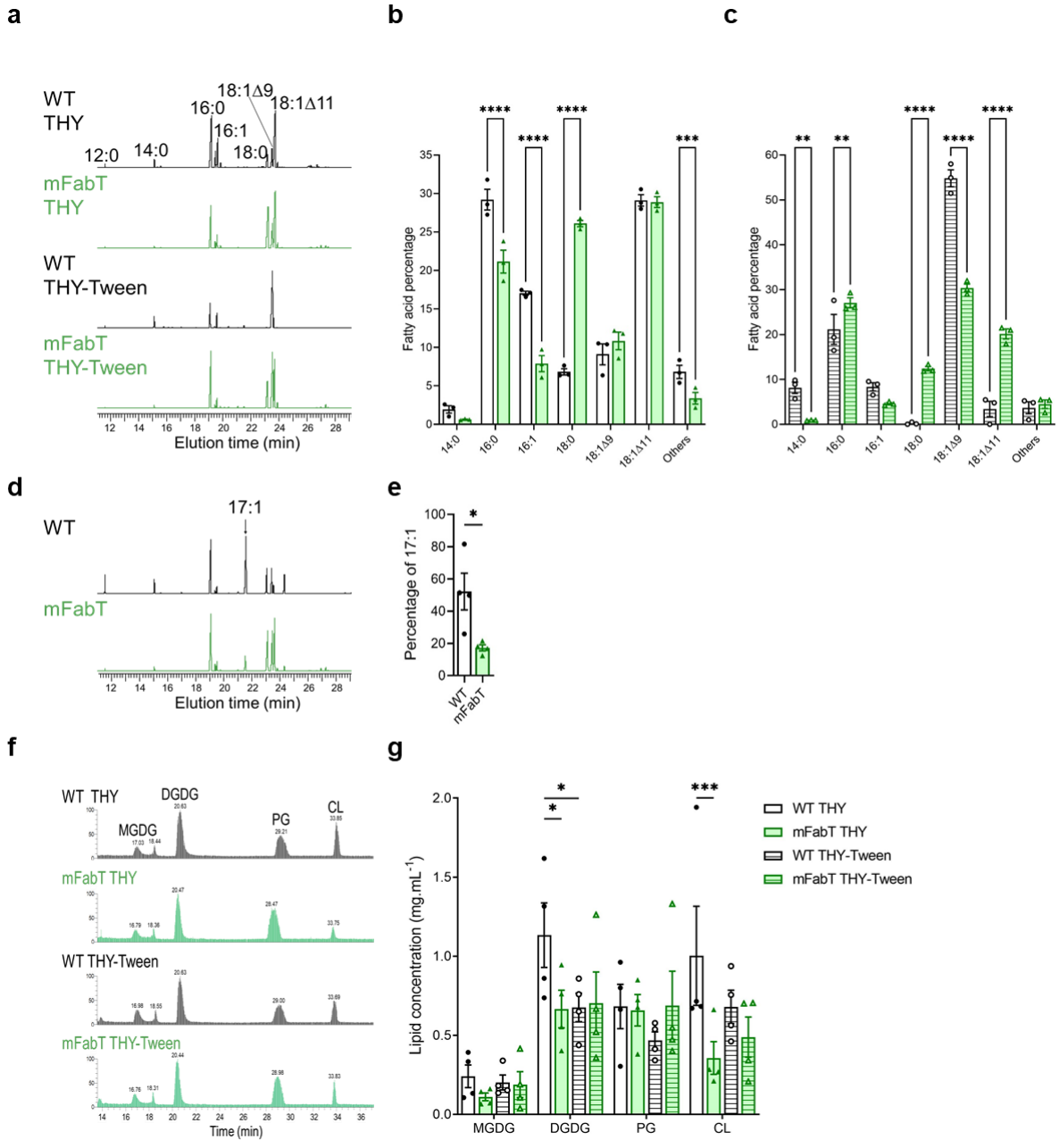

Fig. 3 | Fatty acid and lipid membrane composition of the mFabT strain differs from those of the WT strain. a-b, WT and mFabT strains were grown in THY medium supplemented or not with Tween. **a**, profiles of the membrane fatty acids of the WT or mFabT strains, grown in THY or THY-Tween; **b, c**, fatty acid percentage. N=3 (Extended Data Table 2, Statistical values, including for the comparison between growth in THY and THY-Tween for each strain, are indicated in the Extended Table 2). **d-e**, 17:1 Incorporation, **d**, fatty acid profiles of the WT or mFabT strains grown in THY medium supplemented with 17:1, **e**, percentage of 17:1 in the membranes. **f-g,** Lipid composition or concentration in the WT and mFabT strains grown in THY or THY-Tween medium, **f**, HPLC-MS profile representing the main lipid classes, **g**, lipid concentration by class of lipids: MGDG, monogalactosyldiacylglycerol; DGDG, digalactosyldiacylglycerol; PG, phosphatidylglycerol; CL, cardiolipin. Bars and symbols, white, WT strain; green, mFabT strain. N=4 (Extended Data Table 3). **b**, **c**, **g**, 2-way ANOVA, Bonferroni post-test, **e**, t-test, *p<0.05; **p<0.01; ***p<0.001; ****p<0.0001.

The relative proportion of 17:1 was 52.16 % in the WT, compared to only 17.23 % in the mFabT strain, demonstrating an FA incorporation defect in the mFabT strain. The other major change was an increase of 14:0 in, and only in, the WT membrane; this correlates well with the eFA-elicited repression of FASII expression in the WT strain and its absence in the mFabT strain. In conclusion, the $FabT^{H105Y}$ mutation yields a strain with an FA composition different from that of the WT both in the absence and the presence of exogenous FA, and to an eFA incorporation defect.

The WT and mFabT strain harboring different FA composition led us to assess the consequences on their lipid content (Fig. 3f, g, Extended Data Table 3). Significant differences were observed for two lipid species, particularly in the absence of exogenous FA, DGDG, and cardiolipins were notably lower in the mFabT strain. The observed differences were less evident when strains were grown with Tween. Importantly, while equivalent cell weights were used for analyses, the total amounts of lipids were higher in the WT strain grown in THY. Thus, in *S. pyogenes*, changes in FA composition appears to alter the lipid balance.

Differences in membrane FA and lipid composition yield minor differences in related properties and in cell-envelope protein composition.

The differences in membrane lipid composition between WT and mFabT strains led us to determine whether known membrane-related features, including membrane properties, bacterial morphology and temperature-related growth properties also differ (Fig. S3). Surprisingly, the strains behaved similarly, regardless of the presence or not of eFA (Fig. S3a-d). Also, electron microcopy analysis showed no marked differences in bacterial size or morphology between the two strains (Fig. S3e, f). This could be explained by the fact that FabT regulation maintains a functional membrane homeostasis and when FASII repression occurs the WT membrane composition gets closer to that of the mFabT strain. Also, FA contents influence growth temperature and response to temperature shock [5]. The mFabT strain grew slightly slower than the WT strain at 30 °C (47 +/- 4 min *vs* 51 +/- 5 min, respectively) (Fig. 1a, S3g, h). The growth rates were similar at 37 °C and, as previously reported, at 40 °C [4]. Also, the growth variations following temperature shocks were the same for both strains (Fig. S3i). The FA composition differences had therefore minor consequences on these properties.

As cationic antimicrobial peptides reportedly target anionic lipids such as cardiolipins we asked whether the decreased cardiolipin levels in the mFabT strain could elicit polymyxin B resistance. (Fig. 4a) [4,16]. The mFabT strain is more resistant than the WT strain, as previously reported [4,16]. Also, cardiolipin quantities are similar in both strains in Tween medium and both strains were polymyxin B resistant in this medium. Cardiolipins are implicated in microdomain formation, the Exportal [17]. We asked whether the number of Exportal domains are affected by the FabT^{H105Y} mutation. Exportals were visualized by the 10-Nonylacridine orange bromide (NAO) fluorescent probe, highlighting clusters of cardiolipins, as described [17] (Fig. 4b, c). NAO clusters in the two strains were comparable; nevertheless, there were significantly lower numbers in both strains grown in THY-Tween. Hence the nearly 2-fold lower amounts of cardiolipin in the mFabT mutant were insufficient to impact the number of Exportals.

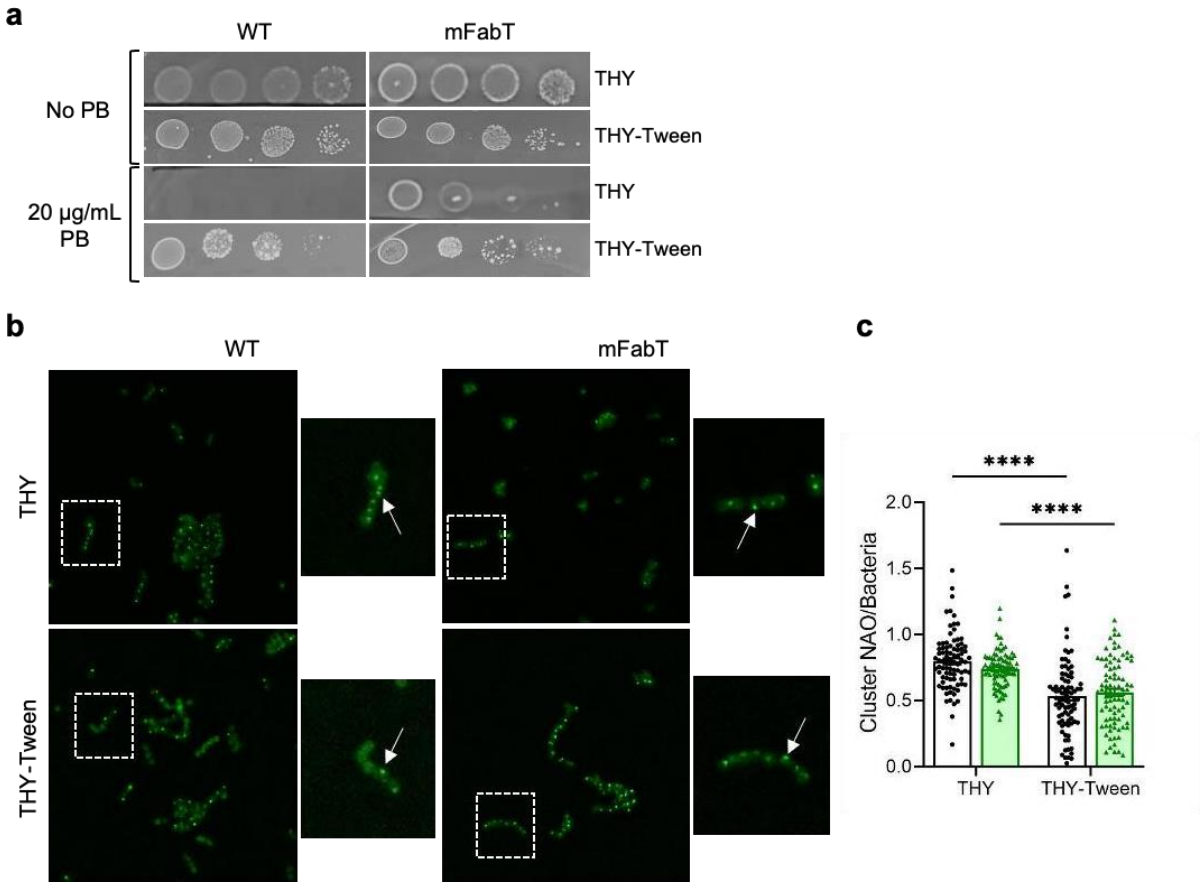

Fig. 4 | Lipid composition modification induces few changes in bacterial surface properties. a, Polymyxin B sensitivity, WT and mFabT were precultured to OD_{600} = 0.05 in THY or THY-Tween 80 and dilution were spread on plates of the same medium supplemented or not with polymyxin B (PB); **b-c,** Exportal visualized by **b,** NAO-highlighted clusters (100X), **c,** quantification of these clusters; Bars and symbols, white, WT strain; green, mFabT strain. **c**, 2-way ANOVA, Bonferroni post-test, ****p<0.0001.

The variation in membrane FA and lipid composition could give rise to changes in membrane and cell-wall protein composition, in addition to the protein variations due to that of gene expression. The expression differences between WT and mFabT envelopes were assessed by proteomics (Extended Data Table 4, 5). Regarding the cell-wall proteins, only two proteins, FtsL and a siderophore (M28_Spy1520) displayed different levels between strains, with ~2-fold greater abundance in the WT (Extended Data Table 4). The other variations were consequences of growth in the presence of Tween, including two virulence factors that were less abundant in the WT strain grown in the presence of Tween than in its absence. Regarding the membrane proteins, the quantity of only one protein, an uncharacterized one, was affected, decreased, in the mFabT strain when both strains were grown in THY (Extended Data Table 5). Adding Tween to the growth medium led, in the WT strain, to an increased quantity of nine proteins and decreased quantity of two proteins, mainly transporters, and, in the mFabT strain, the increase of two and decrease of five proteins, also mainly transporters. These changes are due to the presence of Tween. The comparison of the proteomic profiles when both strains were grown in the presence of Tween, and disregarding the changes induced by the Tween and transcriptomic variation, indicated that only one protein was differently expressed, TcyB. TcyB is a cystine transport system permease protein that was less abundant in the mFabT strain. Although subtle, these differences, in addition to those linked to the transcription differences, may have physiological consequences.

The mFabT strain displays an adhesion defect and a growth defect in the presence of eukaryotic cells or in their supernatants

The comparisons of the transcriptomic profiles and the proteomics of the strains indicated that the mFabT strain displays less adhesins to its surface than the WT strain; this may lead to an adhesion defect. The adhesion capacity of WT and mFabT strains was thus assessed on various human cell lines, endometrial cells and keratinocytes, differentiated or undifferentiated (Fig. 5a-c, and Fig. S4a-b). Both strains adhered to all cell-types. The mFabT strain displayed an adhesion defect on all these cells except the differentiated keratinocytes. We then assayed whether cultivating the bacteria in the presence of Tween, prior the adhesion step, would modify the adhesion capacity of either bacterial strain (Fig. S4a-b). The WT adhesion capacity was diminished and became similar to that of the mFabT strain,

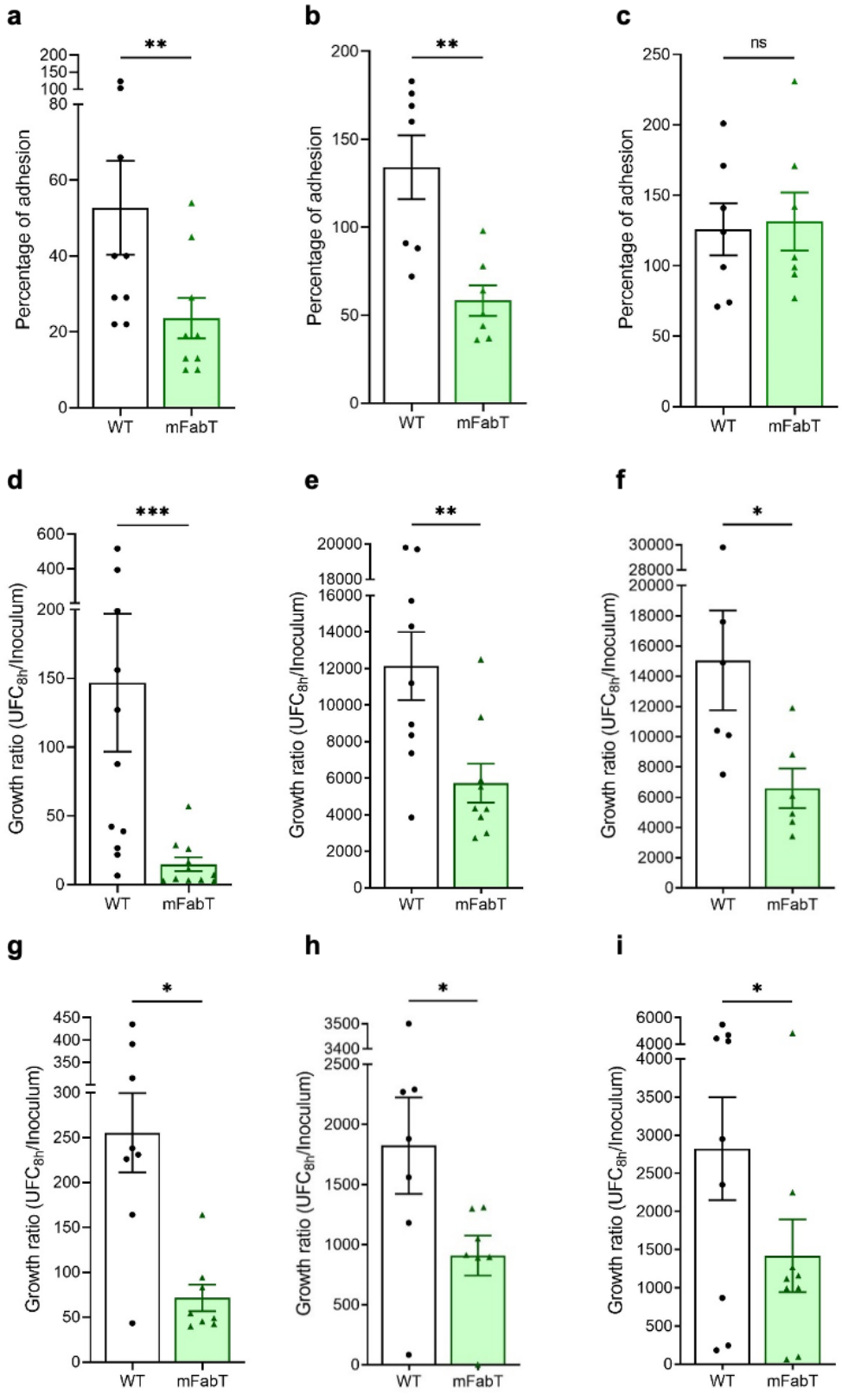

Fig. 5 | The mFabT mutant strain has adhesion and growth defects in the presence of human cells or in conditioned cell supernatant. Comparison of WT and mFabT strain **a-c**, adhesion capacity, and **d-i**, strain growth capacity in **d-f**, the presence of cells, **g-i**, conditioned supernatants, **a**, **d**, **g**, endometrial cells, **b**, **e**, **h**, undifferentiated and **c**, **f**, **i**, differentiated keratinocytes. Growth experiments were started with 10^3 bacteria per ml. Bars and symbols, white, WT strain; green, mFabT strain. **a**, **e**, **i** N=9, **b**, **c**, **h** N=7, **d** N=11, **f** N=6, **g** N=8, **a**, **d**, **g**, **h**, Wilcoxon test, **b**, **c**, **e**, **f**, **i**, t test; *p<0.05; **p<0.01; ***p<0.001.

reminiscent of the changes observed in lipid amounts. Hence, the FabT^{H105Y} mutation consequences hamper the bacterial adhesion capacity.

The *fabT* mutant strains display attenuated virulence [4,12]; we wondered whether, in addition to the adhesion defect, they could have a growth defect in the presence of eucaryotic cells. We first cultivated both strains in a cell culture medium, RPMI (Fig. S4c). The growth ratio was 0.4 for both strains, indicating that they did not grow in that medium and, moreover, that they died in eight hours. We then infected endometrial cells, undifferentiated and differentiated keratinocytes (Fig. 5d-f) for eight hours. Both strains grew in the presence of all human epithelial cell-lines. However, in all cases, the growth of the mFabT strain was lower than that of the WT strain, 90 %, 53 % and 56 %, in the presence of endometrial cells, undifferentiated and differentiated keratinocytes, respectively. The FabT^{H105Y} mutation induced a growth defect in the presence of eucaryotic cells. The mFabT growth defect could be linked its adhesion defect, either because adhesion is necessary for growth, or because cells secrete nutrients or toxic products only if they are infected and the mFabT strain responds differently than the WT strain to any of these compounds. To test these possibilities, we assayed the bacterial growth in uninfected cell supernatant, termed conditioned supernatant (Fig. 5g-i). Both strains grew in conditioned supernatant. This indicates that adhesion is not required for *S. pyogenes* growth in this experimental set-up. The growth defect of the mFabT strain was conserved, 72 %, 50 % and 50 %, in the presence of endometrial, undifferentiated and differentiated keratinocyte conditioned supernatants, respectively. This indicates that the mFabT strain growth defect is not due to the adhesion defect. The growth ratios were of the same magnitude in the presence of endometrial cells and in endometrial conditioned supernatants. This suggests that endometrial cells may secrete the same compounds independently of the infection or that an enhanced nutriment secretion is compensated by an increased toxicity. In contrast, the growth ratios were lower in the supernatants of keratinocytes than in the presence of these cells. This may be due to a lesser nutriment secretion or an enhanced toxicity. These data support the hypothesis that these cells secrete nutrient compounds and/or toxic products and that the mFabT strain is less adapted to use the nutriments, either a sensing or/and a transport deficiency, or to resist cell-elicited toxicity. Another non-exclusive possibility is that the mFabT strain wastes its

energy synthesizing its FAs, and the growth difference that results from it is not seen in laboratory rich medium (THY), but has a toll in poorer media, such as RPMI.

The mFabT strain growth defect is multifactorial, a higher susceptibility to toxic compounds and an unnecessary energy expenditure.

The mFabT strain growth defect could reflect a different time to reach exponential phase or a slower growth. To discriminate between these hypotheses, we monitored in real-time the growth of both strains in non-infected endometrial cells supernatant (Fig. 6a, b). The latency period was similar for both strains. In contrast, the doubling time was longer for the mFabT strain (65 +/- 15 min) than for the WT strain (31 +/- 3 min). These results were confirmed by determining the CFU counts also at 4h (Fig. 6c). The growth ratios were indeed similar for both strains at 4 h, and higher for the WT strain at 8h, correlating with this result (Fig. 6c). This slower doubling accounts for the growth defect. It could result from a slower division but also, and in addition, to a higher death rate throughout growth. To assess a potential higher mFabT strain fragility, we followed the growth ratio of both strains at longer time period (Fig. 6c). Whereas the WT strain CFU counts slowly decreased after eight hours, those of the mFabT strain dropped sharply. Cell death was also compared 8 h after supernatant inoculation (Fig. 6d). The mFabT strain dies 1.5-fold more than the WT strain. Due to its membrane differences, the mFabT strain could be more susceptible to various cell secreted products toxic to *S. pyogenes* (Fig. S5). The mFabT strain had the same resistance than the WT strain to the antimicrobial peptide LL-37 and to H_2O_2 (Fig. S5a, b). Regarding the acidic pH, there was a tendency for the mFabT strain to be more sensitive to pH 6 but not to pH 5.5 (doubling time and maximum OD_{600nm}) (Fig. 5c, d). This does not exclude that the mFabT is badly adapted to other toxic compounds accounting for part of the growth defect. Altogether, these results account for a weaker growth of the mFabT strain in the presence of cells and cell secreted products.

To assess whether the mFabT strain has also a *stricto sensu* growth defect, *i.e.* an incapacity to use cell-secreted products to grow, we determined the metabolites enabling *S. pyogenes* to grow in conditioned supernatant by comparing metabolites present in higher concentrations in conditioned supernatant than in the cell culture medium (RPMI), as well as

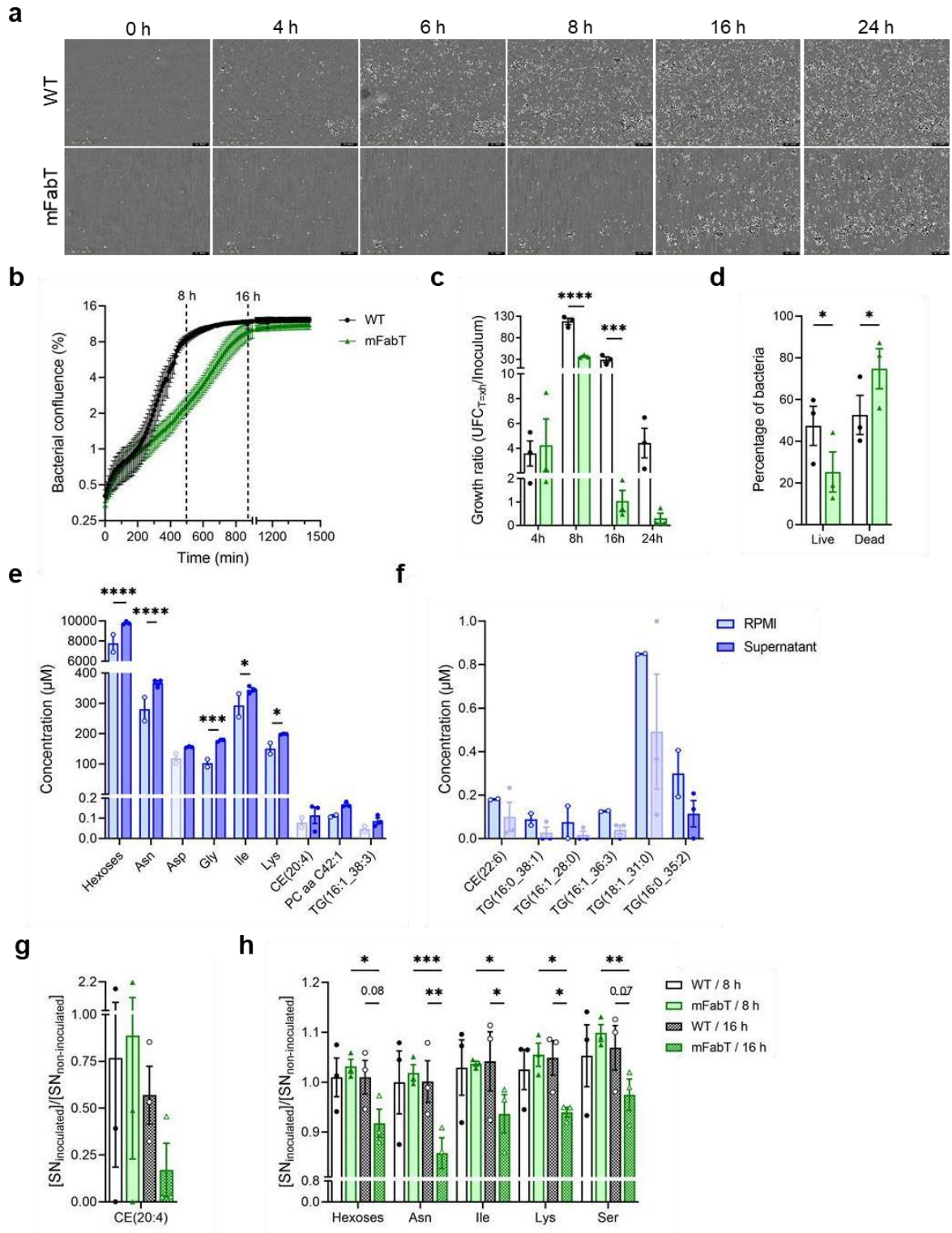

Fig. 6 | Characterization of the mFabT strain growth defect. a, Real-time monitoring of growth in conditioned supernatants with Incucyte® (20X). **b**, Confluence curves corresponding to the Incucyte® experiments. **c**, Bacterial growth kinetic in conditioned supernatants (CFU.mL^{-1}). **d**, Live & Dead bacteria after 8 hours of growth in conditioned supernatants. **e-h**, Metabolomic analysis of RPMI, conditioned supernatants, supernatants inoculated with WT or mFabT strain during 8 or 16 hours. **e**, Metabolites produced by the cells. **f**, Metabolites used by cells. **g**, CE(20:4) consumption by both bacterial strains. **h**, Amino acids and carbohydrate consumption by the mFabT strain. Blurred colors, below the detection threshold. **c-d**, bars and symbols, white, WT strain; green, mFabT strain. **b-h** N=3, **c-h**, 2-way ANOVA, Bonferroni post-test; *p<0.05; **p<0.01; ***p<0.005; ****p<0.001.

those that were still present after 8 or 16 hours of growth in either the WT- or the mFabT-inoculated conditioned supernatant (Fig. 6e-i, Extended Data Table 6). The main metabolites produced by the uninfected cells were hexoses, amino-acid residues, Asn, Asp, Gly, Ile and Lys, one cholesterol ester, CE(20:4), one phosphatidylcholine diacyl, PC aa C42:1 and a triglyceride (TG), TG(16:1_38:3) (Fig. 6e, Extended Data Table 6).

Some metabolites were consumed by the cells, *i.e.*, the cholesterol ester CE 22:6 and five triglycerides (Fig. 6f, Extended Data Table 6). One metabolite produced by the cells, CE(20:4), was consumed by WT and mFabT strains as soon as 8 h, suggesting that it is, at least in part, responsible for *S. pyogenes* growth in conditioned supernatant (Fig. 6g, Extended Data Table 6). We then compared metabolites that would be differentially consumed by both strains, irrespective of their production by cells. Indeed, a metabolite can be used by bacteria when growth is supported by another indispensable metabolite, absent from RPMI. The TGs were such metabolites (Extended Data Table 6). Their consumption analysis was further complicated by the fact that for all but TG(16:0_35:2) and TG(16:0_31:0) their concentration increases after 8 or even 16 h in one or both strains. This could be due to TG being produced by the degradation of other lipids or released by bacterial lysis. This is supported for the TG(16:0_38:1), TG(16:0_38:2), TG(18:2_33:1) that are more abundant in the mFabT than the WT supernatants. Finally, two classes of metabolites that were produced by the cells, hexoses and amino acid residues were, except for aspartate and glycine, as well as serine, which was not more abundant in conditioned supernatant, were significantly more consumed by the mFabT than by the WT strain (Fig. 6h, Extended Data Table 6). This overconsumption is not linked to a higher bacterial yield, and in fact the reverse. This indicates that the mFabT strain wastes its energy to grow; it wastes it producing unnecessarily FAs; this is known as a futile synthesis cycle.

The mFabT growth defect in the presence of eucaryotic cells, due to a higher sensitivity to cell secreted toxic compounds and to a synthetic futile cycle, accounts for its virulence defect.

The mFabT strain grows poorly on human decidua.

To further link the *in vitro* growth defect and the attenuated virulence, and the *emm28* strains being associated to puerperal fever [4,12,18,19], we assessed the *ex vivo* growth of the mFabT strain on human decidua [20]. Human decidual explants were infected within hours of delivery with the WT or the mFabT strains. We first tested whether the mFabT strain had a growth defect in the presence of human decidua (Fig. 7a). Importantly, the growth ratio was always smaller (63 %-fold less) for the mFabT strain than the WT strain. Hence, the mFabT displays a growth defect in the presence of human decidua.

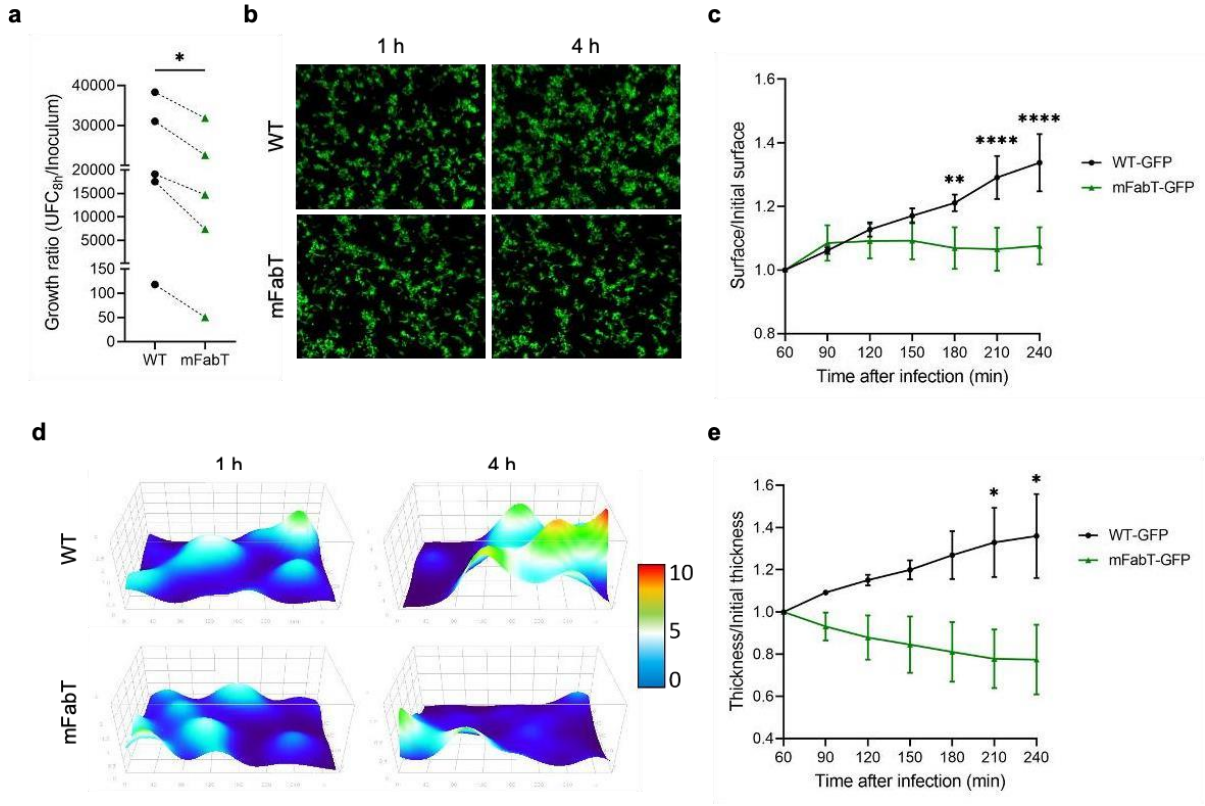

Fig. 7 | The mFabT strain grew poorly on human tissue *ex vivo*. a, Growth in the presence of decidua tissue N=5. **b-e**, Bacterial multiplication at the tissue surface; **b,** bacterial multiplication in 2D. **c,** Ratio over time of the area covered by the GFP-WT or GFP-mFabT strains. **d,** 3D surface heatmap of the bacterial layer thickness at two time points (hr) (live imaging). The x, y, and z axes are scaled, color code in µm. **e,** Ratio over time of the thickness of the WT-GFP or mFabT-GFP strains. **b-e**, N=3; **a**, T-test, **c**, **e**, 2-way ANOVA, Bonferroni post-test; *p<0.05; **p<0.01; ****p<0.0001.

We then followed growth in a time-lapse approach. We precisely quantified *S. pyogenes* multiplication at the tissue surface during the first four hours after infection in flow conditions (Fig. 7b, c). Whereas the surface colonized by the WT strain increased throughout the experiment, that by the mFabT strain only increased during the first half-hour after image

acquisition started. Determination of the thickness of bacterial microcolonies further showed that the mean value increased for the WT strain while it decreased for the mFabT strain (Fig. 7d, e). Altogether, the WT strain grew with a doubling time of roughly 200 min whereas the mFabT strain did not grow. This demonstrates that the mFabT strain has a major growth defect in the presence of human decidua. The existence of a futile cycle and differences in nutrient use and capacity to resist tissue toxicity would be responsible for this effect that accounts for mutant *fabT* strains attenuated virulence.

Discussion

This study deciphers the link between the inactivation of the FASII repression *via* FabT and *S. pyogenes* virulence attenuation. Although some hints were known, *e.g.* loss of membrane homeostasis, differential metabolic gene expression, no clear cause was demonstrated. Our approach was to discover the consequences of a *fabT* mutation on many aspects of the bacterial physiology and to establish a causal link with virulence.

In the absence of eFAs, the FASII gene transcription was barely modified by the mutation in FabT. The situation is similar in other streptococcaceae, with the exception of *S. pneumoniae*, variations of FASII gene expression being reported when either imposing a membrane stress, temperature, pH, growth phase, or by overexpressing FabT [4-8]. This suggests that FabT activity is not required in the laboratory rich medium, but is important during the infection process, where the bacteria encounter varying ecological niches.

When eFAs were added, conditions that drove FASII gene derepression, the difference in the expression between WT and mFabT strain was not the same for all FASII genes. *fabM* expression was less modified than that of most other FASII genes and particularly *fabK* that encodes the final elongation reaction that is shunted by FabM. This indicates that a role of FabT is to maintain a balance between saturation ratio and chain length; this favors a limited variation of membrane permeability and fluidity. Thus, FabT ensures the maintenance of membrane homeostasis in response to membrane stress.

To further decipher this fine tuning of the FASII gene expression at the molecular level, we analyzed the genetic organization of the FASII genes. In contrast to current models, *fabM* is cotranscribed with the other FASII genes [2]. The many transcription start sites that we previously highlighted are therefore transcription reinitiation sites [15]. The FabT binding sites enable FabT to repress the expression of downstream genes. This leads to a modulation of the expression of genes or group of genes depending on the number and location of FabT binding sequences and transcription start sites. Whereas *fabM* is preceded by a single repression site, *fabK* is preceded by two, accounting for the different ratio of FabT-elicited repression. In addition, *fabH*, whose product catalyzes the entry into the elongation cycle of the malonyl-ACP, is preceded by a transcription start site without colocalized FabT binding site, ensuring a certain constitutive level of expression.

Among the non-FASII genes whose expression is modified in the *fabT* mutant strain, a single gene is coregulated with the FASII genes, indicating a direct control by FabT. It encodes a DegV protein, predicted to bind FA, suggesting a role with endogenous FAs [our study, [4,21]]. The expression of the gene encoding an oleic acid hydratase, coined the myosin-cross reactive antigen, that participates in FA detoxification [22], was higher in the mFabT strain in the absence of eFAs and enhanced by their addition in both strains. Very little is known regarding lipid detoxification in *S. pyogenes*, hence $DegV_{1638}$ warrants further studies.

Addition of eFAs modified the expression of more genes in the WT than in the mFabT strain, indicating that the membrane perturbation created a stress to which the WT strain responded by modifying its metabolic pathways. In the presence of eFAs, where the membrane of both strains shared C18:C16 and UFA:SFA ratios, the number of genes differentially controlled in the mFabT *versus* the WT strains is lower than in the absence of eFAs. This suggests most genes of the FabT regulon are indirectly controlled by FabT. It also further supports that the expression modulation is in response to the membrane state.

The difference of FA composition of WT and mFabT strains prompted us to compare their lipidic composition which, to our knowledge, had never been compared. The chain lengths of the lipid constituting FAs were, as expected different, following the differences highlighted in the FA composition analysis. The most striking difference resided in the amount of the different lipid classes with digalactosyldiacylglycerols and cardiolipins being more abundant in the WT than the mFabT strain. These differences were cancelled when bacteria were grown in the presence of eFAs, mainly because, in contrast to that of the WT strain, the mFabT strain lipid composition barely changed. To note the mFabT strain, as described previously, incorporated less FAs than the WT strain and its FA composition varied but less than that of the WT strain [3]. These data suggest that lipid composition changes correlate with membrane FA composition changes, whether they arise from an overproduction, a *fabT* mutation, or an incorporation of eFAs. The first *S. pyogenes fabT* mutant strain described was obtained by selecting spontaneous polymyxin B resistant mutants that still bound polymyxin B like the wild-type strain [16]. However, the exact cause of the polymyxin B resistance was not determined. Our data indicated that the *fabT* mutant strain resistance may be due to the variation in cardiolopin amount. Yet the unchanged number of NAO-binding foci, indicative of

the presence of Exportal, supports the Exportal integrity, that was a further criterion during the selection applied by Port *et al.* [16].

We previously described the initial infection steps where following tissue adhesion, *S. pyogenes* multiplies using decidua secreted nutriments [20]. The mFabT strain displayed an adhesion defect to different cell types, as was described for *S. pneumoniae* [8]. *S. pyogenes* harbors more than fifty adhesins, although not all are shared by all *S. pyogenes* strains [23]. Our transcriptomic and proteomic analysis indicated that pilus components and R28 were more abundant in the mFabT strain than in the WT strain, whereas seven other adhesins, including the M protein, were more abundant in the WT strain. We have previously shown that R28 promotes adhesion to endometrial cells, and changes *S. pyogenes* capacity to adhere to primary decidual cells [24]; yet, its overproduction did not counter the diminished quantity of many other adhesins in causing an mFabT strain adhesion defect on endometrial cells and undifferentiated keratinocytes. This defect is most probably a cause of the mFabT strain attenuated virulence.

S. pyogenes has many growth requirements; it is auxotrophic for fifteen amino acids, has incomplete Entner-Doudoroff and tricarboxylic acid, known as Krebs cycle, pathways and relies extensively on the glycolysis for its energy [25,26]. Both WT and mFabT strains were uncapable of growing in RPMI, a classical cell culture medium, that contains glucose and the amino-acid residues to which *S. pyogenes* is auxotroph. However, it grew in the presence of endometrial cells and keratinocytes as well as in these cell conditioned supernatants. This indicates that these cells secrete compounds that are used as nutriments by *S. pyogenes*. Importantly, the mFabT strain grew less than the WT strain. An enhanced bacterial death is in part responsible for the mFabT strain apparent growth defect, which is the resultant from growth *stricto sensu* and bacterial death. Yet, that both strains grew indicates that both strains used cell-derived nutriments. In fact, both strains consumed cholesterol ester, CE(20:4) (Fig. 8a). Cholesterol ester was secreted by the endometrial cells which is in agreement with current knowledge; cholesterol is produced by the endoplasmic reticulum, this production is enhanced during endoplasmic reticulum stress, and cholesterol ester is exported by eucaryotic cells [27-29]. Cholesterol ester is consumed by many bacteria, including *Mycobacterium tuberculosis* and *Helicobacter pylori* [30-32; for review, 33,34]. *Via* different

pathways, cholesterol that can be incorporated in the bacterial membrane, is a source of lipids as well as of carbon and energy. *S. pyogenes* incorporates host lipids in its membrane when grown in human serum [35]. Also, *S. pyogenes* hemolysins SLO and SLS induce endoplasmic reticulum stress which leads to cholesterol overproduction favoring the CE(20:4) presence in the conditioned supernatants [29,36,37]. Moreover, some *S. pyogenes* strains, including M28PF1, are well equipped to use cholesterol ester *via* the secreted serum opacity factor (SOF) that disrupts high density lipoprotein structures, creating cholesterol ester-rich emulsion [38,39]. Altogether, our data demonstrate that *S. pyogenes* uses cholesterol to grow and this most probably occurs *in vivo*.

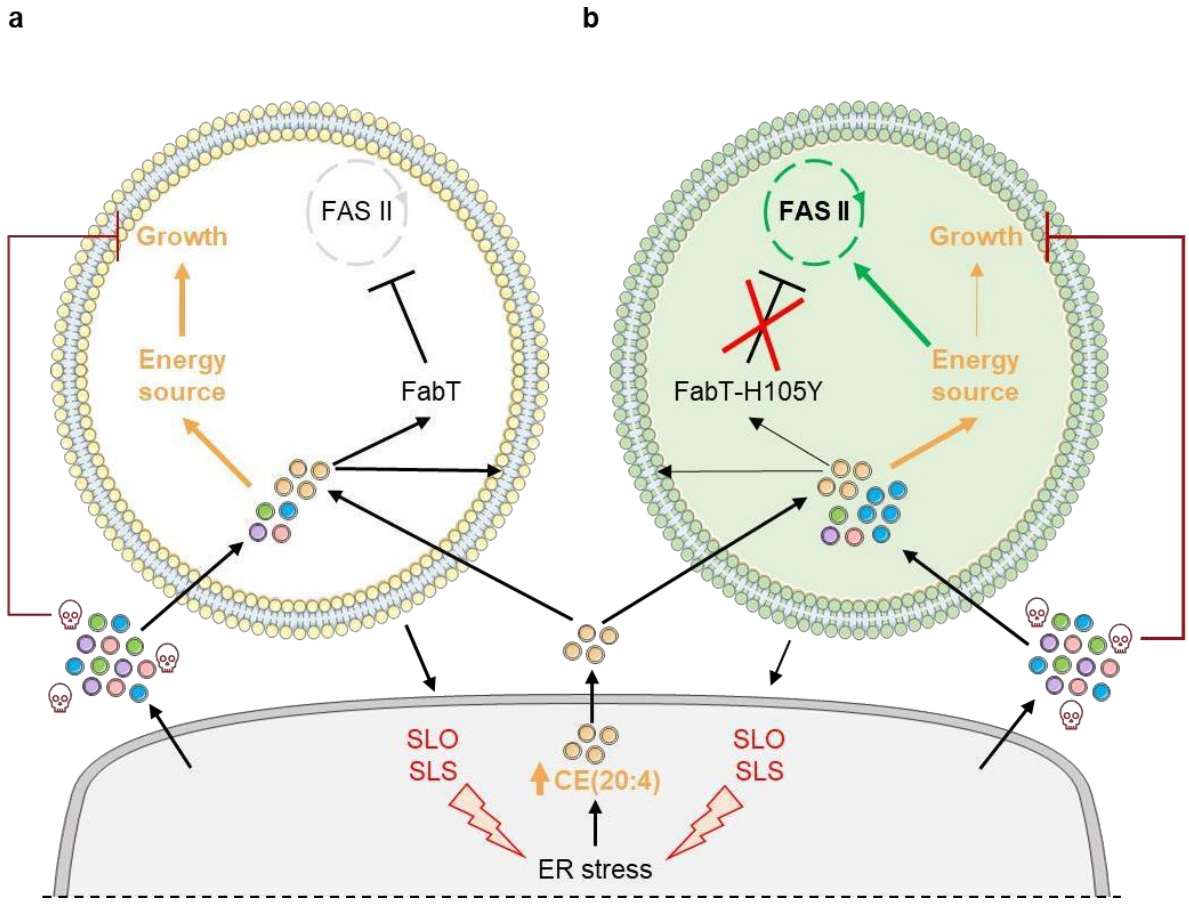

Fig. 8 | Current model of *fabT S. pyogenes* strains virulence defect. a, Wild-type *S. pyogenes* strains use cells secreted products (colored circles) notably the cholesterol ester CE(20:4) (yellow circle) as source of FAs and energy; **b**, the *fabT* mutant strain spends its energy synthesizing FAs, green arrow, and consequently consumes more cell secreted products than the WT strain especially amino acids and hexoses (blue circles). Skulls, antimicrobial compounds, red broken line, antimicrobial activities, the thickness symbolizes the strain susceptibility. This is the cause for a growth defect in the host, causing, at least in part, the virulence defect. FabT represses FASII, T bar, light grey cycle, whereas FabT^{H105Y} does not, red cross, green cycle. SLO and SLS, *S. pyogenes* hemolysins, enhance cholesterol ester production.

In addition to the CE(20:4) consumption, the mFabT strain, whose yield was lower than that of the WT strain, consumed more hexoses (Fig. 8b). This signs more energy expense. The unnecessary FA synthesis, consequence of the FabT^{H1O5Y} mutation and absence of FASII gene repression, perfectly accounts for this expenditure since each mole of lipid requires approximately 32 moles of ATP for biosynthesis [26]. This futile synthesis cycle could in turn limit mFabT growth.

Our current model linking FabT loss of function and hampered virulence is that the energy unnecessary spent by *fabT* mutant strains participates in the growth defect (Fig. 8). This in turn gives a great advantage to the host enhancing the importance of its defense mechanisms. This model is supported by our *ex vivo* experiments, where the mFabT strain, in contrast to the WT strain, did not grow on the decidua. By determining a causal link between FabT loss of function and strongly diminished virulence, we confirm that FabT is an interesting target for new therapeutics.

Methods

Bacterial strains and culture conditions. The strains used in this study are described in Table S3. *S. pyogenes* strains were grown under static condition at 37 °C in Todd Hewitt broth supplemented with 0.2 % Yeast Extract (THY) or on THY agar (THYA) plates. To study, the role of eFA addition, the medium was supplemented with 0.1 % Tween 80 (THY-Tween) (Sigma-Aldrich, P1754), essentially composed of 18:1Δ9. For GFP strains, the medium was supplemented with 10 µg.ml^{-1} of erythromycin. For all experiments, strains were prepared as follows. Overnight cultures were diluted to an OD_{600nm} = 0.05 and grown in THY to the exponential phase (OD_{600nm} comprised between 0.4 and 0.5). For GFP expression, exponential-phase bacteria were further diluted to OD = 0.1 in THY supplemented with 10 µg.ml^{-1} erythromycin and 20 ng.ml^{-1} anhydrotetracycline, grown for 90 min at 37 °C, and diluted in RPMI.

Strain construction. The primers used for the generation of the plasmids and verifying the different strains are described in Table S4. The ΔFabT and mFabT strains correspond to a *fabT* deleted mutant and a *fabT* mutant with a point mutation, respectively. They were obtained by homologous recombination of the plasmid pG1-ΔFabT and pG1-mFabT following the same protocol as described previously [24,40].

The DNA fragments encompassing *fabT* were cloned in BamHI – EcoRI digested pG1 using the In Fusion cloning kit® (Clonetech). This led to the deletion of *fabT* from nucleotides 49 to 389. The plasmid pG1-mFabT was obtained by amplifying nucleotides -222 to +805, relative to the translation start site from the chromosome of a spontaneous mutant, CCH1963, where the C in position 313 was replaced by a T, leading to the replacement of the histidine in position 105 by a tyrosine, from our collection. The back-to-the-WT (BWT-mFabT and BWT-ΔFabT) strains were obtained during the second cross-over, which leads to the mutant or back to the WT strain. The mFabT-GFP strain, harboring an integrated inducible *gfp* gene, was constructed as previously described for the WT-GFP strain [20]. The whole genomes of the constructed strains were sequenced, no surreptitious mutations were found.

Growth curves. *S. pyogenes* stationary precultures were diluted in THY or THY-Tween to an OD_{600nm} = 0.05 and transferred to 96-well plates. These were incubated at 37 °C in a Thermo Scientific Multiskan GO (ThermoFischer Scientific) and growth was determined by measuring absorbance at 600 nm every 10 min after shaking the plates.

RNA isolation and Illumina RNA-seq sequencing. *S. pyogenes* strains were cultured at 37°C in THY or THY-Tween, and cells were harvested at exponential growth phase (OD comprised between 0.4 and 0.5). After adding 2 volumes of RNA protect* (Qiagen) Total RNA was extracted from three independent cultures for each condition after lysing the bacteria by a 30 min 15 $mg.ml^{-1}$ lysozyme, 300 $U.ml^{-1}$ mutanolysine treatment at 20°C followed by two cycles of Fast-prep (power 6, 30 s) at 4 °C, using the Macherey-Nagel RNA extraction kit, as indicated. RNA integrity was analyzed using an Agilent Bioanalyzer (Agilent Biotechnologies) and a PCR. Absence of DNA was further confirmed by PCR. 23S and 16S rRNA were depleted from the samples using the MICROBExpress Bacterial mRNA enrichment kit (InVitrogen) and depletion was controlled on Agilent Bioanalyzer (Agilent Biotechnologies). Libraries were prepared using an Illumina TS kit. Libraries were sequenced generating 10,000,000 to 20,000,000 75-bp-long reads per sample.

RNA-Seq data analysis. The MGAS6180 strain sequence (NCBI), that is nearly identical to M28PF1[13], was used as a reference sequence to map sequencing reads using the STAR software (2.5.2b). RNA-seq data were analyzed using the *hclust* function and a principal component analysis in R 3.5.1 (version 2018-07-02). For differential expression analysis, normalization and statistical analyses were performed by using the SARTools package and DESeq2 [41,42] *p* values were calculated and adjusted for multiple testing using the false discovery rate controlling procedure [43]. We used UpsetR to visualize set intersections in a matrix layout comprising the mFabT *versus* the WT strain grown in THY and in THY-Tween, and growth in THY-Tween *versus* THY in both strains. [44,45]

First-strand cDNA synthesis, quantitative PCR (qPCR) and PCR Five hundred nanograms of total RNA was used for first-strand cDNA synthesis using SuperScriptTM II reverse transcriptase and random primers according to the manufacturer's instructions (Invitrogen, Life technologies).

Quantitative PCR was carried out with SYBR Green PCR kits (Applied Biosystems, Life technologies) using six pairs of primers (Table 2). *gyrA* and *rpoB* were used as the housekeeping reference genes. Relative quantification of specific gene expression was calculated with the $2-\Delta\Delta Ct$ method using *gyrA* as the reference gene and expressed in log2-fold change. Each assay was performed in triplicate on each sample.

PCRs were carried out on cDNA using primer pairs flanking neighboring FASII genes (Table S4) and the GoTaq® green master mix (Promega). PCR amplicons were examined on a 2 % agarose gel. The 100 bp ruler was used to estimate the length of the fragments (SM0321 ThermoFischer Scientific).

In silico analysis. The presence of putative FabT binding sequences on the M28PF1 genome was sought with the ANTTTGATTATCAAATT sequence as a probe, accepting up to 2 mismatches using Geneious prime Biomatters development, www.geneious.com.

Fatty acid analysis. Strains were grown in THY or THY-Tween until OD_{600nm} = 0.4 - 0.5. Fatty acids were extracted and analyzed as previously described [46].

Lipids analysis. Strains were grown in THY or THY-Tween until OD_{600nm} = 0.4 - 0.5. Lipid extractions were performed as previously described [47]. Lipids were identified following the method previously described [48]. The lipid separation was realized by normal phase HPLC (U3000 ThermoFisher Scientific) using a Inertsil Si 5µm column (150 x 2.1 mm I.D.) from GL Sciences Inc (Tokyo, Japan). Lipids were quantified using a Corona-CAD Ultra and identified by mass-spectrometry negative ionization and MS^2/MS^3 fragmentations (LTQ-Orbitrap Velos Pro). The concentration of each lipid class was determined as previously described using as standards DGDG, 840524P-5MG; MGDG, 840523P-5MG; CL (heart CA), 840012P-25MG; PG (egg), 841138P-25MG [49]. Lipids spectra were analyzed on Xcalibur™ software (ThermoFisher Scientific, version 4.2.47).

Polymyxin B assay. Polymyxine B sensitivity was assayed as previously described with modifications [4]. Bacteria were grown to an OD_{600nm} of 0.4 to 0.5 in THY or THY-Tween. Serial dilutions were made in PBS, and 2.5 µl of each dilution was inoculated onto THY or THY-Tween plates containing or not 20 $\mu g.ml^{-1}$ polymyxin B (Sigma-Aldrich, Ref. 81271). The plates were incubated at 37 °C for 24 h to 48 h.

Cardiolipins microdomains analysis. The cardiolipins microdomains were observed as described using 10-Nonylacridine orange bromide (NAO) coloration (Sigma-Aldrich, Ref. A7847) [50]. Images were captured using an inverted microscope Nikon eclipse TI (objectif apofluor 100X; Camera orca flash). The number of NAO-labeled microdomains were quantified in ImageJ using MicrobeJ plugging. The ratio of cluster number per bacteria present in each image was calculated.

Proteomic analysis. Bacteria were grown to an OD_{600nm} of 0.4 to 0.5 in THY or THY-Tween. After centrifugation, the pellets were resuspended in TSMg solution (20 mM Tris-HCl pH8.0, 1 mM EDTA, 20 % sucrose and 50 mM NaCl) supplemented with 300 $U.ml^{-1}$ mutanolysine and 2 $mg.ml^{-1}$ lysozyme and incubated 45 min at 4 °C. The suspension was centrifugated at 8000 *g* 10 min at 4 °C and the supernatant, *i.e.* the cell-wall fraction, was conserved. The pellet was washed with one volume of lysis buffer, MBP (20 mM Tris-HCl, 200 mM NaCl and 1 mM EDTA) and bacteria were lyzed with a FastPrep treatment, (4 cycles at power 6.5, 20 sec,). After 30 min of centrifugation at 13500 *g* at 4 °C, the supernatant was incubated with 10 $\mu g.ml^{-1}$ ribonuclease A during 15 minutes at room temperature and centrifugated, 55000 *g* 30 min 4°C. The supernatant, *i.e.* the cytoplasmic fraction, was conserved and the pellet, *i.e.* the membrane fraction, was washed twice with 0.5 $mol.L^{-1}$ TrisHCl pH7.5 and then resuspended with 250 µl of TES buffer (20 mM Tris-HCl pH8, 1 mM EDTA and 20% sucrose). The protein concentration was determined by BCA assay (QPBCA-1KT, Sigma-Aldrich) and protein purity was verified by SDS-PAGE gel migration of 100 $\mu g.ml^{-1}$ of each fraction. Finally, proteins were digested in peptides using the S-Trap technique according to the manufacturer's protocol (Protifi, NY, USA). Briefly, 30 µg of protein from the above lysates was diluted to 100 µL in lysis buffer. Proteins were digested for 14 h at 37°C with 1 µg sequencing grade trypsin (Promega, Charbonnières-les-Bains, France). After speed-vacuum drying, eluted peptides were solubilized in 10µL of 10% acetonitrile and 0.1% trifluoroacetic acid (TFA).

LC-MS analyses were performed on a Dionex U3000 HPLC nanoflow chromatographic system coupled to a Q-Exactive Orbitrap mass spectrometer (both from Thermo Fisher Scientific, Les Ulis, France). Briefly: 1 µl of each sample was concentrated and washed on a C_{18} reverse-phase precolumn (3 µm particle size, 100 Å pore size, 75 µm inner diameter, 2 cm length, Thermo Fischer Scientific), then separated using a C_{18} reverse-phase analytical column (2 µm particle size, 100 Å pore size, 75 µm inner diameter, 25 cm length from Thermo Fischer Scientific) with a 3 h gradient starting from 99% of solvent A (0.1% formic acid) to 55% of solvent B (80% ACN and 0.085% formic acid). The mass spectrometer acquired data throughout the elution process and operated in a data-dependent scheme with full MS scans acquired, followed by up to 10 successive MS/MS HCD-fragmentations on the most abundant ions detected. Settings for Q-Exactive were: full MS automated gain control (AGC) target 1.10^6 with 60 ms maximum ion injection time (MIIT) and resolution of 70 000. The MS scans spanned

from 350 to 1500 Th. Precursor selection window was set at 2 Th. HCD normalized collision energy (NCE) was set at 27% and MS/MS scan resolution was set at 17 500 with AGC target 1.10^5 within 60ms MIIT. Dynamic exclusion time was set to 30 s and spectra were recorded in profile mode.

The mass spectrometry data were analyzed using Maxquant version 1.6.4.0 [51]. The database used was a concatenation of *Streptococcus pyogenes* M28PF1 sequences from the Uniprot-Swissprot database (Uniprot, release 2019-12) and an incremented list of contaminants. The enzyme specificity was trypsin. The precursor mass tolerance was set to 4.5 ppm and the fragment mass tolerance to 20 ppm. Carbamidomethylation of cysteins was set as constant modification and acetylation of protein N-terminus and oxidation of methionines were set as variable modifications. Second peptide search was allowed and minimal length of peptides was set at seven amino acids. False discovery rate (FDR) was kept below 1% on both peptides and proteins. Label-free protein quantification (LFQ) was done using both unique and razor peptides. At least two ratio counts were required for LFQ. All experiments were analyzed simultaneously using normalization and with the 'match between runs' option with a match time window of 0.7 min and an alignment time window of 20 min.

Data were statistically challenged using Perseus 1.6.2.3 software [52]. Selection of protein concentration amount modification was realized by steps using the T-test difference with absolute value of (logA-logB) >1 and the p-value < 0.05 and taking the protein localization into account.

Cell culture. HEC-1-A (ATCC_ HTB-112TM) endometrial epithelial cells were cultured as recommended, in McCoy's 5A medium (Gibco, Ref. 26600080) supplemented with 10 % fetal bovine serum at 37 °C, 5 % of CO_2. HaCaT (Addex-Bio T0020001) keratinocytes were cultivated as recommended, in DMEM high glucose medium (Gibco, Ref. 31966) supplemented with 10 % fetal bovine at 37 °C, 5 % of CO_2. To maintain undifferentiated HaCaT, cells were cultivated in a poor DMEM medium (Gibco, Ref. 21068-028) supplemented with 1X glutaMax (Gibco, Ref. 35050-038), 1X sodium pyruvate (Gibco, Ref. 11360-039), 2 % fetal bovine serum and 8 % chelated fetal bovine serum using Chelex® 100 Resin (BioRad, Ref. 142-1253). To differentiate HaCaT cells, 2.8 mM $CaCl_2$ (Sigma-Aldrich, Ref. 21115) was added to the medium. Cells were differentiated after seven days.

Bacterial adhesion capacity. *S. pyogenes* adhesion capacity was realized as described previously after growing the bacteria in THY or THY-Tween to an OD_{600nm} of 0.4 to 0.5 [24]. The values were normalized to the inoculum for each experiment.

Bacterial growth capacity in the presence of eukaryotic cells or their culture supernatant. *S. pyogenes* bacteria were grown in THY or THY-Tween to an OD_{600nm} of 0.4 to 0.5, the culture was washed twice in PBS and diluted in RPMI medium without glutamine (Gibco, Ref. 32404-014) to infect cell cultures or inoculate filtered cell culture supernatants (conditioned supernatants) at a final concentration of 10^3 and 10^4 bacteria per ml, respectively. Confluent cells in 24-well plates were starved 24 h before the experiment, *i.e.* incubated in RPMI medium without glutamine, and washed twice in PBS. Cells were infected with 1 ml of bacteria and incubated at 37 °C + 5 % CO_2. After 8 h, the supernatant was recovered and cells were lysed with 1 ml distilled water. The fractions were pooled and serial dilutions plated on THY agar plates. Conditioned supernatant were prepared by incubating cells were in 1 ml RPMI at 37°C + 5 % CO_2 for 8 h. The conditioned supernatant was recovered and inoculated with 10^3 bacteria and incubated for another 4, 8, 16 or 24 h. Serial dilutions were plated on THYA plates. The number of CFUs was determined after 24 h of growth at 37 °C and normalized to the inoculum for each experiment.

Real-time bacterial growth: strains were diluted at 10^3 bacteria per ml in endometrial conditioned supernatant and incubated at 37 °C + 5 % CO_2 for 24 h. Bacterial growth was followed by imaging every 10 min using IncuCyte® Live-Cell Analysis Systems (Sartorius) (20X). Bacterial covered surface was determined using Basic analyzer.

Live & Dead analysis. After bacterial growth in the HEC-1-A conditioned supernatant during 8 h, bacterial mortality was determined using the LIVE/DEAD® BacLight™ Bacterial Viability Kit (ThermoFischer Scientific, Ref. L7012) as described for flow cytometry utilization using an ACCURI C6 cytometer (BD Biosciences, Le pont de Claix,France) from the CYBIO Core Facility. Results of three independent experiments were analyzed using the BD Accuri C6 software. To simplify the analysis, two populations were defined, live bacteria (propidium iodure negative and SYTO 9 dye positive bacteria) and dead bacteria (propidium iodure positive or/and SYTO 9 dye positive bacteria).

Metabolomic analysis. HEC-1-A conditioned supernatants were inoculated or not with the WT or mFabT strains during 8 or 16 h and prepared as previously described in “Bacterial growth

capacity". The metabolite composition of these supernatants were analyzed using MxP® Quant 500 kit (Biocrates) by two analytical methods, LC-MS/MS for small molecules and FIA-MS/MS for lipids. This analysis was repeated on three independent series of supernatants and on RPMI. These analyses have a defined detection threshold (LOD) for each family of metabolite. A metabolite was defined to be present in the medium when its concentration was higher than LOD for at least two replicates.

***Ex vivo S. pyogenes* growth capacity analysis.** Human placenta with attached maternal-fetal membranes were collected and processed as previously described with the following modifications [20]. The tissues were obtained after vaginal delivery, and the samples used were from regions located far from the cervix, known as zone of intact morphology [53].

Ex vivo bacterial growth capacity in the presence of decidua human tissue: Exponentially growing GFP-expressing bacteria were washed twice in PBS and diluted in RPMI at a final concentration of 10^4 bacteria per ml. Decidua tissue were washed twice in PBS and incubated with 1 ml of bacteria at 37°C + 5 % CO_2. After 8 h, the tissues were shredded using Precellys Evolution (Bertin Technologies) (6 x 20 s at 5500 rpm with a 20 s pause between shakings). Serial dilutions of shredded material were plated on THYA plates. The number of CFUs was determined after 24 h of growth at 37 °C and normalized to the inoculum for each experiment.

Live bacterial multiplication on human tissue: infection of maternal-fetal explants, image acquisition and treatments were realized as previously described [20].

Study approval. The study of the human maternal-fetal membranes was approved by the local ethics committee (Comité de Protection des Personnes Ile de France III, no. Am5724-1-COL2991, 05/02/2013). All participants provided written informed consent prior to inclusion in the study at the Department of Obstetrics, Port Royal Maternity, Cochin University Hospital, Paris, France.

Statistical analysis. Data were analyzed with GraphPad Prism version 9.4.1. The tests used are indicated in the figure legends. Statistical significance is indicated by: ns (not significant, $p > 0.05$); *, $p < 0.05$; **, $p < 0.01$; ***, $p < 0.001$; ****, $p < 0.0001$.

References

1 Jerga, A. & Rock, C. O. Acyl-Acyl carrier protein regulates transcription of fatty acid biosynthetic genes *via* the FabT repressor in *Streptococcus pneumoniae*. *J Biol Chem* **284**, 15364-15368, doi:10.1074/jbc.C109.002410 (2009).

2 Lambert, C., Poyart, C., Gruss, A. & Fouet, A. FabT, a Bacterial Transcriptional Repressor That Limits Futile Fatty Acid Biosynthesis. *Microbiol Mol Biol Rev*, e0002922, doi:10.1128/mmbr.00029-22 (2022).

3 Zou, Q., Zhu, L. & Cronan, J. E. The *Enterococcus faecalis* FabT transcription factor regulates fatty acid synthesis in response to exogenous fatty acids. *Front Microbiol* **13**, 877582, doi:doi: 10.3389/fmicb.2022.877582 (2022).

4 Eraso, J. M. *et al.* Genomic Landscape of Intrahost Variation in Group A *Streptococcus*: Repeated and Abundant Mutational Inactivation of the fabT Gene Encoding a Regulator of Fatty Acid Synthesis. *Infect Immun* **84**, 3268-3281, doi:10.1128/IAI.00608-16 (2016).

5 Lu, Y. J. & Rock, C. O. Transcriptional regulation of fatty acid biosynthesis in *Streptococcus pneumoniae*. *Mol Microbiol* **59**, 551-566, doi:10.1111/j.1365-2958.2005.04951.x (2006).

6 Eckhardt, T. H., Skotnicka, D., Kok, J. & Kuipers, O. P. Transcriptional regulation of fatty acid biosynthesis in *Lactococcus lactis*. *J Bacteriol* **195**, 1081-1089, doi:10.1128/JB.02043-12 (2013).

7 Faustoferri, R. C. *et al.* Regulation of fatty acid biosynthesis by the global regulator CcpA and the local regulator FabT in *Streptococcus mutans*. *Mol Oral Microbiol* **30**, 128-146, doi:10.1111/omi.12076 (2015).

8 Zhang, J. *et al.* Inactivation of Transcriptional Regulator FabT Influences Colony Phase Variation of *Streptococcus pneumoniae*. *mBio* **12**, e0130421, doi:10.1128/mBio.01304-21 (2021).

9 Carapetis, J. R., Steer, A. C., Mulholland, E. K. & Weber, M. The global burden of group A streptococcal diseases. *Lancet Infect Dis* **5**, 685-694, doi:S1473-3099(05)70267-X [pii] 10.1016/S1473-3099(05)70267-X (2005).

10 Brinster, S. *et al.* Type II fatty acid synthesis is not a suitable antibiotic target for Gram-positive pathogens. *Nature* **458**, 83-86, doi:10.1038/nature07772 (2009).

11 Parsons, J. B., Frank, M. W., Subramanian, C., Saenkham, P. & Rock, C. O. Metabolic basis for the differential susceptibility of Gram-positive pathogens to fatty acid synthesis inhibitors. *Proc Natl Acad Sci U S A* **108**, 15378-15383, doi:10.1073/pnas.1109208108 (2011).

12 Tatsuno, I. *et al.* Relevance of spontaneous *fabT* mutations to a streptococcal toxic shock syndrome to non-streptococcal toxic shock syndrome transition in the novel-type *Streptococcus pyogenes* isolates that lost a salRK. *APMIS* **124**, 414-424, doi:10.1111/apm.12521 (2016).

13 Longo, M. *et al.* Complete Genome Sequence of *Streptococcus pyogenes emm28* Clinical Isolate M28PF1, Responsible for a Puerperal Fever. *Genome Announc* **3**, doi:10.1128/genomeA.00750-15 (2015).

14 Zuo, G. *et al.* Structural insights into repression of the Pneumococcal fatty acid synthesis pathway by repressor FabT and co-repressor acyl-ACP. *FEBS Lett* **593**, 2730-2741, doi:10.1002/1873-3468.13534 (2019).

15 Rosinski-Chupin, I., Sauvage, E., Fouet, A., Poyart, C. & Glaser, P. Conserved and specific features of *Streptococcus pyogenes* and *Streptococcus agalactiae* transcriptional landscapes. *BMC Genomics* **20**, 236, doi:10.1186/s12864-019-5613-5 (2019).
16 Port, G. C., Vega, L. A., Nylander, A. B. & Caparon, M. G. *Streptococcus pyogenes* polymyxin B-resistant mutants display enhanced ExPortal integrity. *J Bacteriol* **196**, 2563-2577, doi:10.1128/JB.01596-14 (2014).
17 Rosch, J. W. & Caparon, M. G. The ExPortal: an organelle dedicated to the biogenesis of secreted proteins in *Streptococcus pyogenes*. *Mol Microbiol* **58**, 959-968, doi:10.1111/j.1365-2958.2005.04887.x (2005).
18 Green, N. M. *et al.* Genome sequence of a serotype M28 strain of group a streptococcus: potential new insights into puerperal sepsis and bacterial disease specificity. *J Infect Dis* **192**, 760-770, doi:JID33878 [pii]
10.1086/430618 (2005).
19 Plainvert, C. *et al.* Invasive group A streptococcal infections in adults, France (2006-2010). *Clin Microbiol Infect* **18**, 702-710, doi:10.1111/j.1469-0691.2011.03624.x (2012).
20 Weckel, A. *et al. Streptococcus pyogenes* infects human endometrium by limiting the innate immune response. *J Clin Invest* **131**, doi:10.1172/JCI130746 (2021).
21 Gullett, J. M., Cuypers, M. G., Frank, M. W., White, S. W. & Rock, C. O. A fatty acid-binding protein of *Streptococcus pneumoniae* facilitates the acquisition of host polyunsaturated fatty acids. *J Biol Chem* **294**, 16416-16428, doi:10.1074/jbc.RA119.010659 (2019).
22 Volkov, A. *et al.* Myosin cross-reactive antigen of *Streptococcus pyogenes* M49 encodes a fatty acid double bond hydratase that plays a role in oleic acid detoxification and bacterial virulence. *J Biol Chem* **285**, 10353-10361, doi:10.1074/jbc.M109.081851 (2010).
23 Nobbs, A. H., Lamont, R. J. & Jenkinson, H. F. *Streptococcus* adherence and colonization. *Microbiol Mol Biol Rev* **73**, 407-450, Table of Contents, doi:10.1128/MMBR.00014-09 (2009).
24 Weckel, A. *et al.* The N-terminal domain of the R28 protein promotes *emm28* group A *Streptococcus* adhesion to host cells *via* direct binding to three integrins. *J Biol Chem* **293**, 16006-16018, doi:10.1074/jbc.RA118.004134 (2018).
25 Davies, H. C., Karush, F. & Rudd, J. H. Effect of Amino Acids on Steady-State Growth of a Group a Hemolytic *Streptococcus*. *J Bacteriol* **89**, 421-427, doi:10.1128/jb.89.2.421-427.1965 (1965).
26 Pancholi, V. & Caparon, M. in *Streptococcus pyogenes : Basic Biology to Clinical Manifestations* (eds J. J. Ferretti, D. L. Stevens, & V. A. Fischetti) (2016).
27 Ikonen, E. Cellular cholesterol trafficking and compartmentalization. *Nat Rev Mol Cell Biol* **9**, 125-138, doi:10.1038/nrm2336 (2008).
28 Lauressergues, E. *et al.* Does endoplasmic reticulum stress participate in APD-induced hepatic metabolic dysregulation? *Neuropharmacology* **62**, 784-796, doi:10.1016/j.neuropharm.2011.08.048 (2012).
29 Moncan, M. *et al.* Regulation of lipid metabolism by the unfolded protein response. *J Cell Mol Med* **25**, 1359-1370, doi:10.1111/jcmm.16255 (2021).
30 Testerman, T. L., McGee, D. J. & Mobley, H. L. *Helicobacter pylori* growth and urease detection in the chemically defined medium Ham's F-12 nutrient mixture. *J Clin Microbiol* **39**, 3842-3850, doi:10.1128/JCM.39.11.3842-3850.2001 (2001).

31 Pandey, A. K. & Sassetti, C. M. Mycobacterial persistence requires the utilization of host cholesterol. *Proc Natl Acad Sci U S A* **105**, 4376-4380, doi:10.1073/pnas.0711159105 (2008).
32 Lee, W., VanderVen, B. C., Fahey, R. J. & Russell, D. G. Intracellular *Mycobacterium tuberculosis* exploits host-derived fatty acids to limit metabolic stress. *J Biol Chem* **288**, 6788-6800, doi:10.1074/jbc.M112.445056 (2013).
33 Vromman, F. & Subtil, A. Exploitation of host lipids by bacteria. *Curr Opin Microbiol* **17**, 38-45, doi:10.1016/j.mib.2013.11.003 (2014).
34 Toledo, A. & Benach, J. L. Hijacking and Use of Host Lipids by Intracellular Pathogens. *Microbiol Spectr* **3**, doi:10.1128/microbiolspec.VMBF-0001-2014 (2015).
35 Joyce, L. R., Guan, Z. & Palmer, K. L. *Streptococcus pneumoniae*, *S. pyogenes* and *S. agalactiae* membrane phospholipid remodelling in response to human serum. *Microbiology (Reading)* **167**, doi:10.1099/mic.0.001048 (2021).
36 Baruch, M. *et al.* An extracellular bacterial pathogen modulates host metabolism to regulate its own sensing and proliferation. *Cell* **156**, 97-108, doi:10.1016/j.cell.2013.12.007 (2014).
37 Baruch, M. *et al.* Induction of endoplasmic reticulum stress and unfolded protein response constitutes a pathogenic strategy of group A *streptococcus*. *Front Cell Infect Microbiol* **4**, 105, doi:10.3389/fcimb.2014.00105 (2014).
38 Courtney, H. S., Zhang, Y. M., Frank, M. W. & Rock, C. O. Serum opacity factor, a streptococcal virulence factor that binds to apolipoproteins A-I and A-II and disrupts high density lipoprotein structure. *J Biol Chem* **281**, 5515-5521, doi:10.1074/jbc.M512538200 (2006).
39 Pownall, H. J., Courtney, H. S., Gillard, B. K. & Massey, J. B. Properties of the products formed by the activity of serum opacity factor against human plasma high-density lipoproteins. *Chem Phys Lipids* **156**, 45-51, doi:10.1016/j.chemphyslip.2008.09.001 (2008).
40 Six, A. *et al.* Srr2, a multifaceted adhesin expressed by ST-17 hypervirulent Group B *Streptococcus* involved in binding to both fibrinogen and plasminogen. *Mol Microbiol* **97**, 1209-1222, doi:10.1111/mmi.13097 (2015).
41 Anders, S. *et al.* Count-based differential expression analysis of RNA sequencing data using R and Bioconductor. *Nat Protoc* **8**, 1765-1786, doi:10.1038/nprot.2013.099nprot.2013.099 [pii] (2013).
42 Varet, H., Brillet-Gueguen, L., Coppee, J. Y. & Dillies, M. A. SARTools: A DESeq2- and EdgeR-Based R Pipeline for Comprehensive Differential Analysis of RNA-Seq Data. *PLoS One* **11**, e0157022, doi:10.1371/journal.pone.0157022 (2016).
43 Benjamini, Y. & Hochberg, Y. Controlling the False Discovery Rate: A Practical and Powerful Approach to Multiple Testing. *J Royal Statistical Society Series B* **57**, 289-300, doi:10.1111/j.2517-6161.1995.tb02031.x (1995).
44 Lex, A., Gehlenborg, N., Strobelt, H., Vuillemot, R. & Pfister, H. UpSet: Visualization of Intersecting Sets. *IEEE Trans Vis Comput Graph* **20**, 1983-1992, doi:10.1109/TVCG.2014.2346248 (2014).
45 Conway, J. R., Lex, A. & Gehlenborg, N. UpSetR: an R package for the visualization of intersecting sets and their properties. *Bioinformatics* **33**, 2938-2940, doi:10.1093/bioinformatics/btx364 (2017).

46 Hays, C. *et al.* Type II Fatty Acid Synthesis Pathway and Cyclopropane Ring Formation Are Dispensable during *Enterococcus faecalis* Systemic Infection. *J Bacteriol* **203**, e0022121, doi:10.1128/JB.00221-21 (2021).
47 Kenanian, G. *et al.* Permissive Fatty Acid Incorporation Promotes Staphylococcal Adaptation to FASII Antibiotics in Host Environments. *Cell Rep* **29**, 3974-3982 e3974, doi:10.1016/j.celrep.2019.11.071 (2019).
48 Abreu, S., Solgadi, A. & Chaminade, P. Optimization of normal phase chromatographic conditions for lipid analysis and comparison of associated detection techniques. *J Chromatogr A* **1514**, 54-71, doi:10.1016/j.chroma.2017.07.063 (2017).
49 Moulin, M. *et al.* Sex-specific cardiac cardiolipin remodelling after doxorubicin treatment. *Biol Sex Differ* **6**, 20, doi:10.1186/s13293-015-0039-5 (2015).
50 Rosch, J. W., Hsu, F. F. & Caparon, M. G. Anionic lipids enriched at the ExPortal of *Streptococcus pyogenes*. *J Bacteriol* **189**, 801-806, doi:10.1128/JB.01549-06 (2007).
51 Cox, J. *et al.* Accurate proteome-wide label-free quantification by delayed normalization and maximal peptide ratio extraction, termed MaxLFQ. *Mol Cell Proteomics* **13**, 2513-2526, doi:10.1074/mcp.M113.031591 (2014).
52 Tyanova, S. *et al.* The Perseus computational platform for comprehensive analysis of (prote)omics data. *Nat Methods* **13**, 731-740, doi:10.1038/nmeth.3901 (2016).
53 Marcellin, L. *et al.* Immune Modifications in Fetal Membranes Overlying the Cervix Precede Parturition in Humans. *J Immunol* **198**, 1345-1356, doi:10.4049/jimmunol.1601482 (2017).

Acknowledgments

We thank Benjamin Saint-Pierre (Genom'IC facility of the Institut Cochin) for help with the transcriptomic experiments, Cédric Broussard, Virginie Salnot and François Guillonneau (Proteom'IC facility of the Institut Cochin) for help with the proteomic analysis, the Imag'IC and Cybio core facilities of the Institut Cochin, Arnaud Gutierrez (Institut Cochin) for help with NAO analysis, Alain Schmitt et Jean-Marc Masse (PIME facility of the Institut Cochin) for the electron microcopy experiments, and Alice d'Orfani, Lauryn Moali, Iman Nasr and Laure Detheve, undergraduates in the laboratory for technical help and all the personnel of the CIC Mère-Enfant Cochin-Necker.

CL was supported by Université Paris Cité (BioSPC, n°51809666), FRM (FDT202106012831) and FEMS (FEMS Congress Attendance Grant for poster n° 7875 in 2021 and FEMS grant - LISSSD 2022 n° LISS-213065). This work was supported by DIM One Health (RPH17043DJA), Agence Nationale de la Recherche (StaphEscape project ANR-16-CE15-0013). IMAG'IC core facility is supported by the National Infrastructure France BioImaging (grant ANR-10-INBS-04).

Extented Data Tables

Extended Data Table 1. Modification of genes expressions under all conditions tested.

Locus	Gene	Gene product	THY mFabT *vs* WT	WT THY-Tween *vs* THY	mFabT THY-Tween *vs* THY	THY-Tween mFabT *vs* WT	Function
M28_Spy0022	*purC*	Phosphoribosylaminoimidazole-succinocarboxamide synthase, PurC	1.327				Purine synthesis
M28_Spy0023	*purL*	Phosphoribosylformylglycinamidine synthase, PurL	1.245				Purine synthesis
M28_Spy0024	*purF*	Amidophosphoribosyltransferase, PurF	1.102				Purine synthesis
M28_Spy0025	*purM*	Phosphoribosylformylglycinamidine cyclo-ligase, PurM	1.313				Purine synthesis
M28_Spy0026	*purN*	Phosphoribosylglycinamide formyltransferase, PurN	1.469				Purine synthesis
M28_Spy0107	*cpa*	Collagen-binding protein, Cpa	1.937				Adhesin
M28_Spy0108	*sipA*	Signal peptidase I, SipA	2.081				Signal peptidase
M28_Spy0109	*M28_Spy0109*	T28 T-antigen	2.195				Adhesin
M28_Spy0110	*srtB*	Class B sortase protein, SrtB	1.734				Sortase
M28_Spy0111	*fctB*	Pilin minor structural protein, FctB	1.949				Adhesin
M28_Spy0137*	*nga*	NAD glycohydrolase, Nga	-1.350				Virulence factor
M28_Spy0138*	*ifs*	Immunity factor for SPN/NAD glycohydrolase protein, Ifs	-1.540				Resistance factor
M28_Spy0139*	*slo*	Thiol-activated cytolysin, SLO	-1.357				Virulence factor
M28_Spy0140	*M28_Spy0140*	Uncharacterized protein	-1.578	-1.688			Unknown function
M28_Spy0184*	M28_Spy0184	RofA-related transcriptional regulator		-1.082			Transcriptional regulator
M28_Spy0249	*M28_Spy0249*	Transposase	-14.443				DNA regulation
M28_Spy0338	*M28_Spy0338*	Uncharacterized protein	-1.613	-1.207		*-0.836*	Unknown function
M28_Spy0341	*M28_Spy0341*	Uncharacterized protein	-1.689	*-0.895*			Unknown function
M28_Spy0346	*M28_Spy0346*	Uncharacterized protein	-1.475	-1.011			Unknown function
M28_Spy0371**	*M28_Spy0371*	67 kDa myosin-crossreactive antigen	1.534	1.941	*0.588*		Fatty acid degradation
M28_Spy0658	*M28_Spy0658*	5'-nucleotidase	1.187				DNA regulation
M28_Spy0757	*M28_Spy0757*	PTS system, mannose/fructose family IIA component	-0.996				Phosphotransferase system
M28_Spy0853**	*M28_Spy0853*	Diacylglycerol kinase family lipid kinase	*0.877*		-1.102		Lipid metabolism
M28_Spy0855**	*M28_Spy0855*	Uncharacterized protein	1.609		-1.969		Unknown function
M28_Spy0977	*phage protein*	Hyaluronoglucosaminidase		1.594			Phage
M28_Spy1014	*M28_Spy1014*	Phage DNA/RNA helicase	1.028				Phage
M28_Spy1098**	*grab*	Protein G-related alpha 2M-binding protein, Grab	1.647				Virulence factor
M28_Spy1112**	*gapN*	NADP-dependent glyceraldehyde-3-phosphate dehydrogenase, GapN	-1.220	*-0.740*			Glycolysis
M28_Spy1136	*M28_Spy1136*	D-alanyl-D-alanine carboxypeptidase	1.633	*0.917*			Peptidoglycan biosynthesis
M28_Spy1137	*M28_Spy1137*	Uncharacterized protein	1.596				Unknown function
M28_Spy1138	*M28_Spy1138*	Uncharacterized protein	1.767				Unknown function
M28_Spy1147*	*kup*	Probable potassium transport system protein, Kup	2.234		*-0.854*		Transporter
M28_Spy1228	*M28_Spy1228*	Phage protein		1.361			Phage
M28_Spy1229	*M28_Spy1229*	Phage protein		1.061			Phage
M28_Spy1234	*M28_Spy1234*	Phage endopeptidase		1.082			Phage
M28_Spy1236	*M28_Spy1236*	Phage protein		1.223			Phage
M28_Spy1237	*M28_Spy1237*	Phage protein		1.160			Phage
M28_Spy1238	*M28_Spy1238*	Phage protein		1.240			Phage
M28_Spy1239	*M28_Spy1239*	Major tail shaft protein		1.302			Phage
M28_Spy1244	*M28_Spy1244*	Major head protein		1.258			Phage
M28_Spy1245	*M28_Spy1245*	Phage protein		1.199			Phage
M28_Spy1249	*M28_Spy1249*	Minor capsid protein		1.126			Phage
M28_Spy1251	*M28_Spy1251*	Phage protein		1.225			Phage
M28_Spy1255	*M28_Spy1255*	ParB-like protein		1.219			Phage
M28_Spy1336	*M28_Spy1336*	R28 protein	1.041	1.412			Adhesin
M28_Spy1434	*M28_Spy1434*	DegV family protein, FakB3		-1.491	-1.409		Lipid metabolism
M28_Spy1473**	*accD*	Acetyl-coenzyme A carboxylase carboxyl transferase subunit alpha, AccD		-2.343		2.567	Fatty acid biosynthesis
M28_Spy1474**	*accA*	Acetyl-coenzyme A carboxylase carboxyl transferase subunit beta, AccA		-2.357		2.589	Fatty acid biosynthesis
M28_Spy1475**	*accC*	Biotin carboxylase, AccC		-2.431		2.666	Fatty acid biosynthesis
M28_Spy1476**	*fabZ*	3-hydroxyacyl-[acyl-carrier-protein] dehydratase, FabZ		-2.335		2.559	Fatty acid biosynthesis
M28_Spy1477**	*accB*	Biotin carboxyl carrier protein of acetyl-CoA carboxylase, AccB		-2.535		2.534	Fatty acid biosynthesis
M28_Spy1478**	*fabF*	3-oxoacyl-[acyl-carrier-protein] synthase 2, FabF		-2.524		2.601	Fatty acid biosynthesis
M28_Spy1479**	*fabG*	3-oxoacyl-[acyl-carrier-protein] reductase, FabG		-2.486		2.676	Fatty acid biosynthesis
M28_Spy1480**	*fabD*	Malonyl CoA-acyl carrier protein transacylase, FabD		-2.430		2.434	Fatty acid biosynthesis
M28_Spy1481**	*fabK*	Enoyl-[acyl-carrier protein] reductase (NADH), FabK		-2.397		2.351	Fatty acid biosynthesis
M28_Spy1483	*fabH*	3-oxoacyl-[acyl-carrier-protein] synthase 3, FabH		-1.176		*0.679*	Fatty acid biosynthesis
M28_Spy1484	*fabT*	Transcriptional regulator, FabT		*-0.921*			Fatty acid biosynthesis
M28_Spy1485*	*fabM*	Enoyl-CoA hydratase, FabM		-1.160			Fatty acid biosynthesis
M28_Spy1562**	*uspA*	Universal stress protein family, UspA	-1.740	1.843		-4.066	Stress response
M28_Spy1563**	*norA*	Quinolone resistance protein, NorA	-1.288	1.529		-3.229	Antibiotic resistance
M28_Spy1638**	M28_Spy1638	DegV family protein		-1.083		*0.835*	Lipid metabolism
M28_Spy1672*	*ska*	Streptokinase, Ska	*0.929*	1.069			Tissue invasion
M28_Spy1675	*sclA/scl1*	Collagen-like surface protein A, SclA/Scl1	-1.823	-0.996			Adhesin
M28_Spy1699**	*M28_Spy1699*	Cell surface protein	*-0.923*	-1.822			Adhesin
M28_Spy1700**	*scpA*	C5a peptidase, ScpA	-1.162	-2.073			Adhesin
M28_Spy1701	*M28_Spy1701*	Enn protein	*-0.871*	-1.026			Adhesin
M28_Spy1702	*M28_Spy1702*	Emm28 protein	-1.985				Adhesin
M28_Spy1715	*sfbX*	Fibronectin-binding protein, SfbX	*-0.889*	-1.359			Adhesin
M28_Spy1716	*sof*	Serum opacity factor	-1.093	-1.375			Adhesin
M28_Spy1813	*M28_Spy1813*	Phage protein	-1.491				Phage
M28_Spy1838**	*M28_Spy1838*	Phage protein	2.661	3.203	2.160	1.618	Phage

A gene expression was considered modified when absolute value of log2-Foldchange (FC) was greater than or equal to 1 and the adjusted p-value lower than 0.05. The asterisk highlighed genes expression that are in common with a previous transcriptomic analysis of S. pyogenes fabT deleted mutant versus WT strain cultivated at different temperatures, 35°C (blue asterisk) and 40°C (red asterisk), in the exponential phase. In italic, log2 Fold change that are outside our chosen threshold but have a p-value below 0.05 and are significantly modified in others comparisons.

Extended Data Table 2. FabT regulation of fatty acid composition.

	Cultivated in THY		Cultivated in THY-Tween		*p-value* THY-Tween *vs* THY	
Fatty acids [a]	**WT**	**mFabT**	**WT**	**mFabT**	**WT**	**mFabT**
14:0	2.20 ± 0.55	0.67 ± 0.13	9.55 ± 2.48	0.87 ± 0.07	****	ns
16:0	29.03 ± 1.39	21.63 ± 2.38	23.48 ± 5.24	27.06 ± 1.95	****	****
16:1	17.53 ± 0. 60	8.77 ± 2	7.23 ± 1.89	4.59 ± 0.44	****	*
18:0	6.72 ± 0.45	25.68 ± 1	0.12 ± 0.22	12.39 ± 0.84	****	****
18:1Δ9	8.93 ± 1.77	10.41 ± 1.78	52.38 ± 4.05	30.36 ± 1.52	****	****
18:1Δ11	28.53 ± 1.02	28.01 ± 1.61	3.70 ± 2.14	20.12 ± 1.93	****	****
others [b]	7.27 ± 3.49	3.68 ± 1.37	2.94 ± 2.03	4.47 ± 1.64	ns	ns
(C18):(C16) [c]	0.95	2.11	1.83	1.99	**	ns
UFA:SFA [d]	1.45	0.98	1.91	1.37	ns	ns

[a] Percentage of total FAs
[b] Fatty acids representing less than 2 % total FAs
[c] Ratio of length chain = (C18:0 + C18:1)/(C16:0 + C16:1)
[d] Ratio unsaturated/saturated FAs = (16:1 + 18:1Δ9 + 18:1Δ11)/(14:0 + 16:0 + 18:0)

Extended Data Table 3. Membrane lipid family composition.

	Cultivated in THY		Cultivated in THY-Tween	
Lipids	**WT**	**mFabT**	**WT**	**mFabT**
MGDG	0.242 ± 0.14	0.111 ± 0.05	0.203 ± 0.09	0.188 ± 0.16
DGDG	1.133 ± 0.41	0.666 ± 0.24	0.677 ± 0.18	0.703 ± 0.39
PG	0.683 ± 0.28	0.659 ± 0.20	0.468 ± 0.11	0.689 ± 0.43
CL	1.003 ± 0.63	0.357 ± 0.21	0.680 ± 0.21	0.489 ± 0.25

MGDG, monogalactosyldiacylglycerol; DGDG, digalactosyldiacylglycerol; PG, phosphatidylglycerol; CL, cardiolipin.

Extented Data Table 4. Impact on cell-wall protein composition.

Protein IDs	Locus	Gene	Protein name	Localisation	THY mFabT *vs* WT	WT THY-Tween *vs* THY	mFabT THY-Tween *vs* THY	THY-Tween mFabT *vs* WT	Function
AKJ91848.1	M28_Spy0107	*cpa*	Collagen-binding protein, Cpa	Cell-wall		1.676		1.013	Adhesin
AKJ91850.1	M28_Spy0109	*M28_Spy0109*	T28 T-antigen	Cell-wall		2.104			Adhesin
AKJ92838.1	M28_Spy0658	*M28_Spy0658*	5'-nucleotidase	Cell-wall		3.573			Purine, Pyrimidine, Nicotinate & nicotinamide metabolism
AKJ92212.1	M28_Spy1336	*M28_Spy1336*	R28 protein	Cell-wall		3.017	1.888		Adhesin
AKJ93470.1	M28_Spy1409	*ftsL*	Cell division protein, FtsL	Membrane	-2.267				Cell division
AKJ92048.1	M28_Spy1520	*M28_Spy1520*	Putative Fe3+-siderophore transport protein	Cell-wall	-2.000				Transporter
AKJ93280.1	M28_Spy1700	*scpA*	C5a peptidase, ScpA	Cell-wall		-4.947			Tissu invasion and escape to immune system
AKJ93282.1	M28_Spy1702	*M28_Spy1702*	Emm28 protein	Cell-wall		-2.742			Adhesin

Cell-wall proteomic analysis of WT and mFabT strains cultivated in THY supplemented or not with Tween. A protein is considered modified when -1 < T-test difference > 1 and the p-value is less than 0.05. In red, protein modification linked to a transcriptomic change.

Extended Data Table 5. Impact on membrane protein composition.

Protein IDs	Locus	Gene	Protein name	Localisation	THY mFabT *vs* WT	WT THY-Tween *vs* THY	mFabT THY-Tween *vs* THY	THY-Tween mFabT *vs* WT	Function
AKJ91775.1	M28_Spy0031	*purK*	N5-carboxyaminoimidazole ribonucleotide synthase, PurK	Membrane			1.133		Purine metabolism
AKJ91849.1	M28_Spy0108	*sipA*	Signal peptidase I, SipA	Membrane	1.889	2.257			Signal peptidase
AKJ93146.1	M28_Spy0312	*fhuD*	Ferrichrome-binding protein, FhuD	NI		1.666			Transporter
AKJ93091.1	M28_Spy0371	*M28_Spy0371*	67 kDa myosin-crossreactive antigen	Membrane		1.334			Fatty acid biosynthesis
AKJ93008.1	M28_Spy0469	*M28_Spy0469*	Uncharacterized protein	Membrane	-1.387				Unknown function
AKJ92870.1	M28_Spy0620	*pyrP*	Uracil permease, PyrP	Membrane		1.128			Pyrimidine metabolism
AKJ92865.1	M28_Spy0627	*M28_Spy0627*	ABC transporter permease protein	Membrane			-1.140		ABC transporter
AKJ92810.1	M28_Spy0687	*M28_Spy0687*	Cystine transport system permease protein, TcyB	Membrane				-1.166	Membrane transporter
AKJ92745.1	M28_Spy0758	*ptsB*	PTS system, mannose/fructose family IIB component, PtsB or GfrB	Cytoplasme		-1.349			Phosphotransferase system
AKJ92657.1	M28_Spy0855	*M28_Spy0855*	Uncharacterized protein	NI	2.595		-2.236		Unknown function
AKJ92580.1	M28_Spy0938	*M28_Spy0938*	ABC transporter permease protein, SalY	Membrane		2.342	2.266		ABC transporter
AKJ92579.1	M28_Spy0939	*M28_Spy0939*	ABC transporter ATP-binding protein	NI		1.497			ABC transporter
AKJ92375.1	M28_Spy1161	*M28_Spy1161*	Lead, cadmium, zinc and mercury transporting ATPase	Membrane			-2.538		Membrane transporter
AKJ92149.1	M28_Spy1404	*M28_Spy1404*	ABC transporter permease protein	Membrane		1.575			ABC transporter
AKJ92097.1	M28_Spy1466	*M28_Spy1466*	Guanine-hypoxanthine permease	Membrane		1.443			Transporter
AKJ92060.1	M28_Spy1506	*M28_Spy1506*	Uncharacterized protein	Membrane			-1.797		Unknown function
AKJ92059.1	M28_Spy1507	*M28_Spy1507*	Putative ATP transporter	NI			-1.236		Transporter
AKJ91986.1	M28_Spy1593	*M28_Spy1593*	Membrane protease family protein	Membrane			-1.149		Peptidase activity
AKJ93225.1	M28_Spy1638	*M28_Spy1638*	DegV domain protein	NI		-1.388		1.725	Lipid metabolism
AKJ93282.1	M28_Spy1702	*emm28*	Emm28 protein	Cell-wall	-2.746	-4.447			Adhesin
AKJ93294.1	M28_Spy1715	*sfbX*	Fibronectin-binding protein, SfbX	Cell-wall	-2.213	-4.869			Adhesin
AKJ93339.1	M28_Spy1768	*M28_Spy1768*	PTS system, trehalose-specific IIBC component, TreB	Membrane		1.176			Phosphotransferase system
AKJ93397.1	M28_Spy1836	*M28_Spy1836*	Uncharacterized protein	Membrane		1.241			Unknown function
AKJ93399.1	M28_Spy1838	*M28_Spy1838*	Phage protein	Membrane	3.779	5.449	1.543		Phage

Membrane proteomic analysis of WT and mFabT strains cultivated in THY supplemented or not with Tween. A protein concentration was considered modified when absolute value of log2-Foldchange (FC) was greater than or equal to 1 and the adjusted p-value lower than 0.05. In red, protein modification linked to a transcriptomic change. NI, Not indicated.

Extended Data Table 6. List of metabolites present in the different media tested.

Metabolites	LOD [µM]	Infection medium (RPMI)		Conditioned supernatants (SN)			SN inoculated with											
							WT strain during 8 hours			mFabT strain during 8 hours			WT strain during 16 hours			mFabT strain during 16 hours		
		1	2	1	2	3	1	2	3	1	2	3	1	2	3	1	2	3
Amino acids																		
Arg	81.3	Infinity	Infinity	Infinity	Infinity	Infinity	Infinity	Infinity	Infinity	Infinity	Infinity	Infinity	Infinity	Infinity	Infinity	Infinity	Infinity	Infinity
Asn	102	242	320	375	375	353	392	328	381	394	378	352	371	351	381	341	301	304
Asp	153	103	134	155	158	154	162	165	168	170	175	164	211	163	183	174	182	189
Gly	103	90	115	180	180	173	185	164	180	185	186	175	190	167	181	172	160	165
His	20.1	56.6	73.3	85.5	86.4	82.5	93.6	83.5	89.6	91.8	91.3	87.5	92.1	82.4	89.9	83.4	80	82.1
Ile	205	255	332	344	357	333	369	328	365	357	367	348	374	330	371	332	307	328
Lys	104	133	169	200	199	197	213	188	210	211	218	200	216	195	214	190	183	187
Met	44.6	39.5	51.1	60.2	59.5	58.6	63.6	55.7	63.9	63.8	64.7	61.4	66.6	57.5	63.5	59.2	56.4	58.7
Pro	93.8	107	136	159	161	154	169	152	165	165	173	163	169	155	173	155	148	153
Ser	156	183	228	198	210	200	226	196	217	224	229	215	223	206	220	202	192	198
Thr	116	109	140	164	167	158	172	156	173	170	172	169	177	155	173	158	151	153
Tyr	42.2	66.1	83.4	97.8	98.9	95.6	103	92.4	103	105	105	99.8	108	94	105	93.8	90.6	93.8
Kynurenine	0.285	0.87	1.21	1.4	1.5	1.44	1.53	1.44	1.52	1.55	1.63	1.42	1.59	1.45	1.61	1.36	1.43	1.39
Met-SO	27.9	24.4	31	34.1	35.2	33.7	37	34.4	36.9	36.5	37.4	36	36.8	34.4	37.4	33.4	32.5	32.9
Cholesterol esters																		
CE(20:4)	0.128	0.103	0.055	0.152	0.034	0.158	0	0.065	0.062	0.074	0.074	0	0.081	0.029	0.051	0.004	0.001	0.072
CE(22:6)	0.108	0.178	0.183	0.233	0.027	0.039	0.244	0	0	0.017	0.103	0	0	0.095	0.102	0.252	0.327	0.107
Glycerophospholipids																		
PC aa C42:1	0.037	0.106	0.117	0.182	0.161	0.16	0.206	0.197	0.202	0.211	0.183	0.175	0.167	0.172	0.151	0.204	0.156	0.206
Triacylglycerols																		
TG(14:0_34:1)	0.171	0	0.071	0	0	0.09	0.34	0	0	0	0	0	0	0.53	0.255	0	0	0
TG(16:0_30:2)	0.182	0	0	0.147	0.184	0.146	0.364	0	0.176	0.05	0.259	0.123	0.019	0.06	0.371	0.43	0.271	0
TG(16:0_32:2)	0.303	0	0	0	0	0	0	0	0	0.368	0	0.307	0	0	0.725	0.112	0.219	0
TG(16:0_34:2)	0.058	0	0	0	0	0	0	0	0.021	0	0	0.173	0	0	0	0.124	0	0.414
TG(16:0_35:2)	0.125	0.406	0.192	0	0.135	0.207	0.14	0	0.218	0	0	0.241	0.023	0	0.043	0	0.019	0.172
TG(16:0_38:1)	0.046	0.061	0.115	0.001	0	0.078	0.036	0	0.043	0.125	0	0.19	0.045	0.019	0.094	0.08	0.124	0.026
TG(16:1_28:0)	0.119	0.15	0	0.051	0	0	0.005	0.068	0.123	0	0	0	0	0	0	0	0.145	0.203
TG(16:1_34:0)	0.241	0.094	0	0.121	0.342	0	0.261	0	0.33	0.226	0	0.061	0.481	0.035	0.102	0.223	0	0
TG(16:1_36:3)	0.12	0.128	0.124	0.061	0.06	0	0.223	0.034	0.045	0.011	0.061	0.294	0.203	0.066	0.248	0.029	0.209	0
TG(16:1_38:3)	0.073	0.033	0.061	0.082	0.062	0.116	0.101	0.114	0.01	0.089	0.039	0.025	0.078	0.121	0.153	0.081	0.051	0.003
TG(18:0_30:0)	0.105	0.152	0	0	0	0.638	0	0	0	0	0	0	0.273	0.277	0.051	0	0.061	0
TG(18:1_31:0)	0.414	0.848	0.851	0.366	0.109	1	1.25	0.304	0.377	0.7	0.413	0.546	0.204	0	0.846	0	0	0.277
TG(18:2_33:1)	0.143	0	0.167	0	0.152	0	0.018	0.044	0.109	0	0.278	0.259	0.055	0.134	0.137	0	0	0.068
TG(18:3_38:5)	0.028	0.047	0.041	0.036	0.028	0.039	0.037	0.021	0.052	0.027	0.02	0.043	0.029	0.019	0.063	0.018	0.023	0.023
Vitamins & Cofactors																		
Choline	10.3	10.1	12.3	13.1	13.3	13.1	14.4	12.7	13.7									
Sugar																		
Hexoses	529	6915	8642	9672	9746	9962	10393	9172	10093									

Grey cells correspond to limit of detection.

Supplementary figures

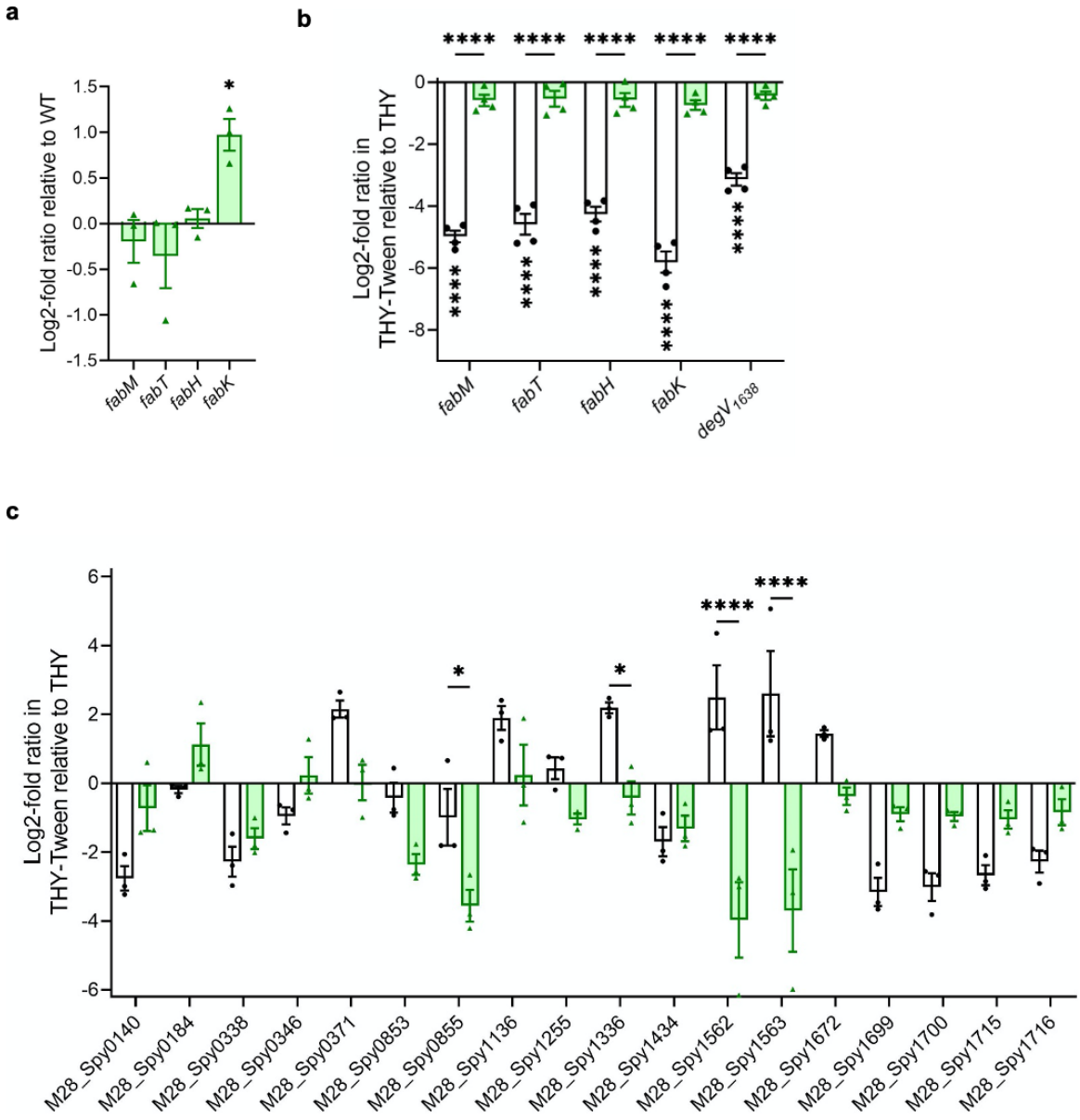

Fig. S1 | Comparison of the repression of FASII genes in *S. pyogenes* grown in the absence or presence of eFAs. Strains were grown in **a-c**) THY or **b, c**) THY-Tween medium and RNAs were quantified by qRT-PCR. Expression was normalized to that of *gyrA*, relative gene expression is expressed as the log2-fold ratio **a**) of FASII genes in mFabT *versus* WT strain; **b, c**) in THY-Tween *versus* in THY; **b)** FASII genes and the similarly regulated gene; **c)** genes regulated differently than the FASII genes. White, WT; green mFabT. The stars below the bars correspond to the difference in expression in the two media for a given strain. Those above the bars correspond to the difference in expression in the two media between the strains **a, b**, N=4; **c**, N=3. **a-c**, 2-way ANOVA, Bonferroni post-test *p<0.05; ****p<0.0001.

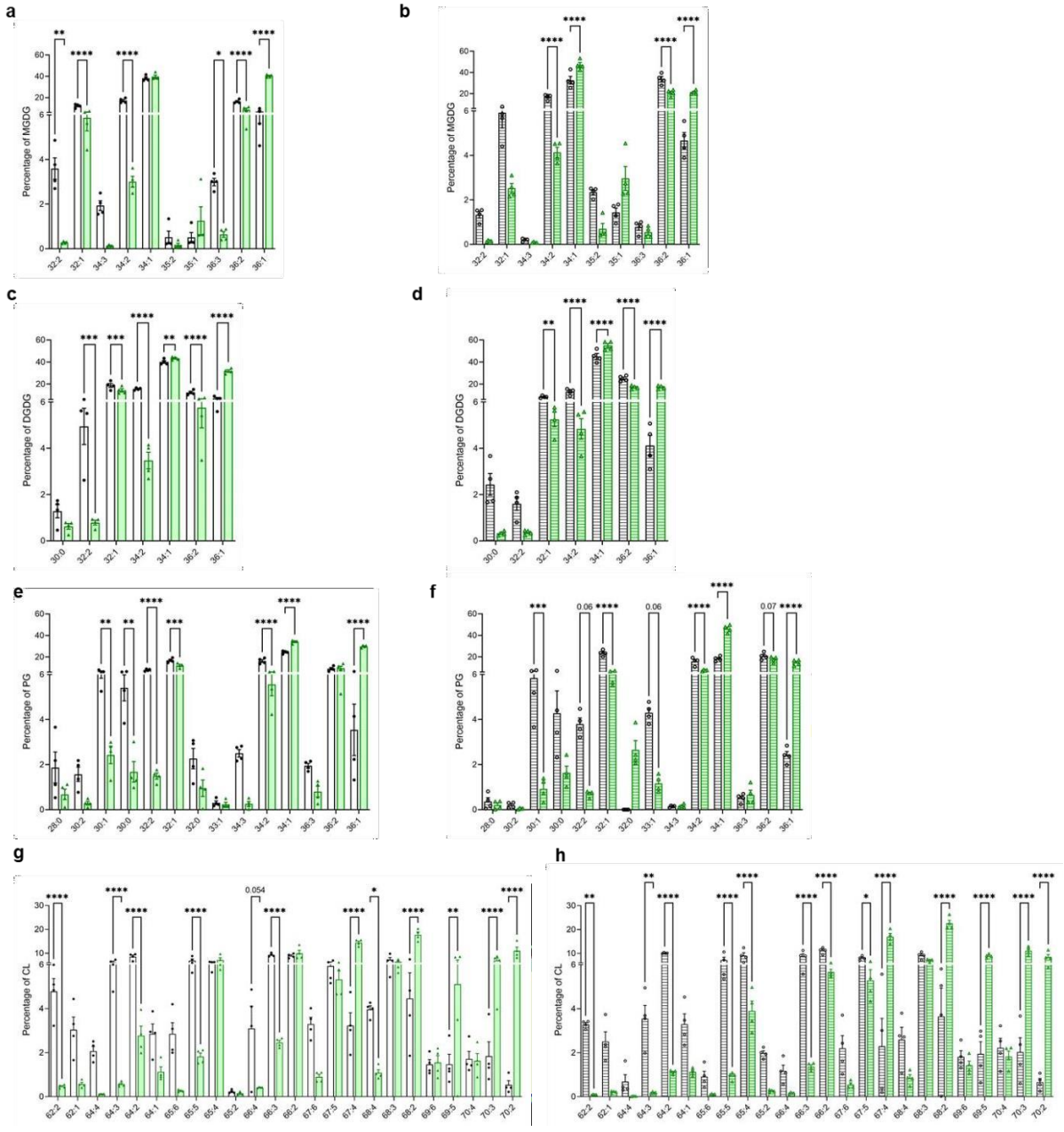

Fig. S2 | Phospholipid membrane composition. Identification of **a-b**, mono-glycolipid (MGDG), **c-d**, di-glycolipid (DGDG), **e-f**, phosphatidylglycerol (PG) and **g-h**, cardiolipin (CL) represented as the percentage of each class to the total. Strains grown in **a**, **c**, **e**, **g**, THY; **b**, **d**, **f**, **h**, THY-Tween. Statistical values, including for the comparison between growth in THY and THY-Tween for each strain, are indicated in the Table S2, 2-way ANOVA, Bonferroni post-test. *p<0.05; ** p<0.01; *** p<0.001; ****p<0.0001.

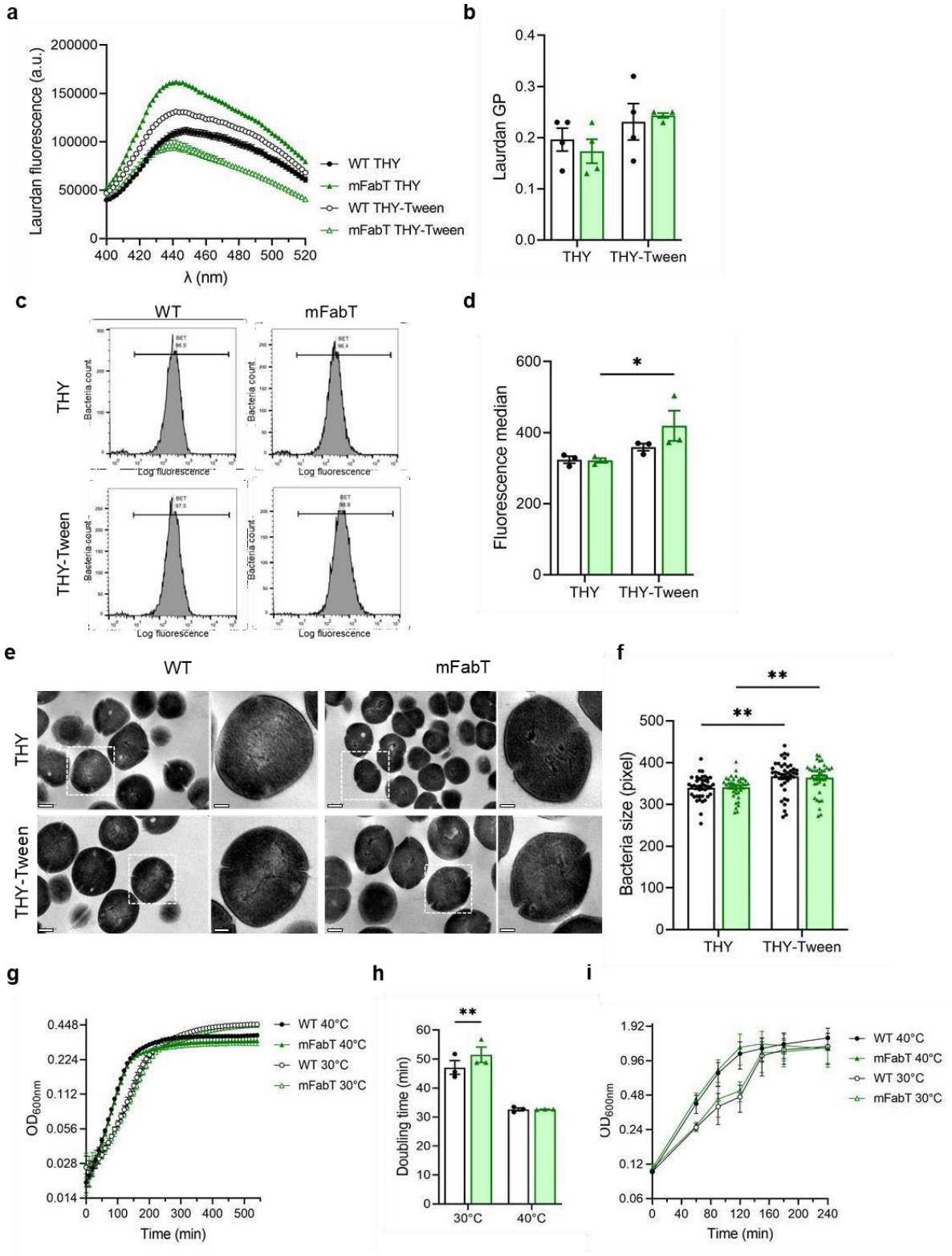

Fig. S3 | mFabT membrane properties are barely modified. a-b, membrane fluidity by laurdan incorporation; **c-d**, membrane permeability by BET incorporation analysis using flow cytometry; **e-g**, temperature impact on growth, **e-f**, growth at different temperatures, **g**, growth after temperature shock. **a-b**, N=4, **c-g**, N=3; **b-f**, 2-way ANOVA, Bonferroni post-test; *p<0.05; **p<0.01.

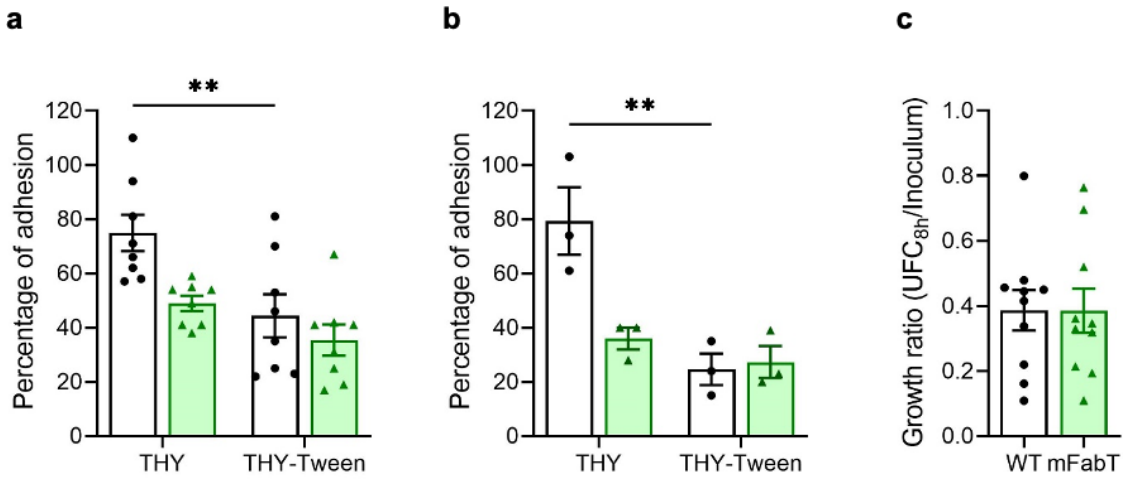

Figure S4 | Adhesion capacity of the WT and mFabT strain after growth in THY-Tween medium and growth capacity of these strains in RPMI. a-b, Comparaison of WT and mFabT strain adhesion capacity after growth in THY or THY-Tween to **a**, endometrial cells, N=8 **b**, undifferenciated keratinocytes, N=3. Only the statistic analysis of growth in the presence of Tween is shown. **c**, Comparison of the WT and mFabT strain growth in the cell culture medium, RPMI, N=10. **a-b**, 2-way ANOVA, Bonferroni post-test, **c**, t test; ** $p<0.01$.

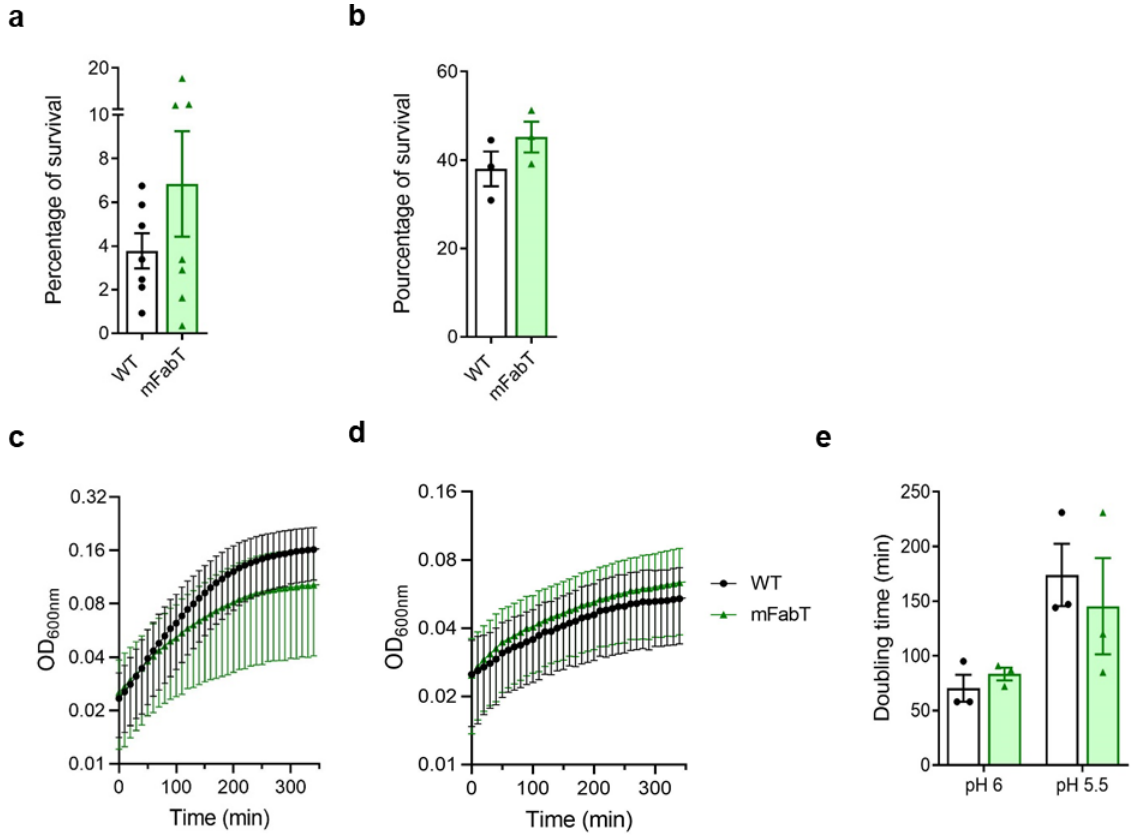

Figure S5 | Bacterial toxicity sensibility. a, Bacterial survival to LL37; **b,** H_2O_2 sensitivity at 30 min; **c-e,** Growth curves in THY buffered at different pHs. **c**, pH 6.0. **d**, pH 5.5; **e**, strain doubling time at each pH. Bars and symbols, white, WT strain; green mFabT strain. **a**, N=7, **b-e** N=3. **a, b**, t test; **c**, 2-way ANOVA, Bonferroni post-test.

Supplementary Tables

Table S1. Confirmation of gene expression variations under all conditions by qRT-PCR analysis.

Locus	Gene	Gene product	THY mFabT *vs* WT	WT THY-Tween *vs* THY	mFabT THY-Tween *vs* THY	THY-Tween mFabT *vs* WT	Function
M28_Spy0140	*M28_Spy0140*	Uncharacterized protein	-0.783	-1.550	-0.689	0.078	Unknown function
M28_Spy0184*	M28_Spy0184	RofA-related transcriptional regulator	-0.486	0.228	0.563	-0.151	Transcriptional regulator
M28_Spy0338	*M28_Spy0338*	Uncharacterized protein	-1.733	-2.043	-1.618	-1.308	Unknown function
M28_Spy0346	*M28_Spy0346*	Uncharacterized protein	-1.042	-0.343	0.228	-0.471	Unknown function
M28_Spy0371**	*M28_Spy0371*	67 kDa myosin-crossreactive antigen	0.950	2.589	0.358	-1.281	Fatty acid degradation
M28_Spy0853**	*M28_Spy0853*	Diacylglycerol kinase family lipid kinase	2.013	-0.152	-0.186	1.979	Lipid metabolism
M28_Spy0855**	*M28_Spy0855*	Uncharacterized protein	1.919	-0.668	-2.324	0.263	Unknown function
M28_Spy1136	*M28_Spy1136*	D-alanyl-D-alanine carboxypeptidase	1.074	1.746	0.407	-0.265	Peptidoglycan biosynthesis
M28_Spy1255	*M28_Spy1255*	ParB-like protein	1.226	1.183	-0.994	-0.951	Phage
M28_Spy1336	*M28_Spy1336*	R28 protein	1.044	3.022	1.095	-0.883	Adhesin
M28_Spy1434	*M28_Spy1434*	DegV family protein, FakB3	-0.267	-0.616	-0.690	-0.341	Lipid metabolism
M28_Spy1481**	*fabK*	Enoyl-[acyl-carrier protein] reductase (NADH), FabK	0.973	-5.543	-0.647	5.870	Fatty acid biosynthesis
M28_Spy1483	*fabH*	3-oxoacyl-[acyl-carrier-protein] synthase 3, FabH	0.057	-4.073	-0.490	3.640	Fatty acid biosynthesis
M28_Spy1484	*fabT*	Transcriptional regulator, FabT	-0.353	-4.410	-0.420	3.637	Fatty acid biosynthesis
M28_Spy1485*	*fabM*	Enoyl-CoA hydratase, FabM	-0.193	-4.837	-0.523	4.120	Fatty acid biosynthesis
M28_Spy1562**	*uspA*	Universal stress protein family, UspA	0.792	2.841	-0.444	-2.493	Stress response
M28_Spy1563**	*norA*	Quinolone resistance protein, NorA	0.983	2.489	-1.217	-2.723	Antibiotic resistance
M28_Spy1638**	M28_Spy1638	DegV family protein	-0.023	-3.233	-0.440	2.770	Lipid metabolism
M28_Spy1672*	*ska*	Streptokinase, Ska	-0.070	2.314	0.958	-1.426	Tissue invasion
M28_Spy1699**	*M28_Spy1699*	Cell surface protein	-1.226	-2.013	-0.188	0.599	Adhesin
M28_Spy1700**	*scpA*	C5a peptidase, ScpA	-1.633	-3.076	-0.502	0.941	Adhesin
M28_Spy1715	*sfbX*	Fibronectin-binding protein, SfbX	-1.220	-1.243	-0.572	-0.549	Adhesin
M28_Spy1716	*sof*	Serum opacity factor	-0.849	-1.083	-0.566	-0.332	Adhesin

* The asterisk highlighed genes expression that are in commun with previous transcriptomic analysis of GAS fabT mutant versus GAS WT strain cultivated under different temperatures, 35°C (blue asterisk) and 40°C (red asterisk), in the exponential phase.

Table S2. Membrane lipid composition.

	Relative abondance (%)				*p-value*	
	Cultivated in THY		Cultivated in THY-Tween		THY-Tween *vs* THY	
Lipids	**WT**	**mFabT**	**WT**	**mFabT**	**WT**	**mFabT**
MGDG species						
32:2	3.59 ± 0.95	0.28 ± 0.05	1.33 ± 0.29	0.15 ± 0.03	ns	ns
32:1	12.14 ± 1.75	5.87 ± 1.16	5.92 ± 1.36	2.52 ± 0.43	*	****
34:3	1.93 ± 0.44	0.13 ± 0.04	0.20 ± 0.07	0.08 ± 0.03	ns	ns
34:2	17.16 ± 2.20	3.01 ± 0.48	17.00 ± 2.62	4.14 ± 0.46	****	ns
34:1	38.15 ± 2.53	39.68 ± 3.00	32.62 ± 7.37	46.95 ± 4.62	****	***
35:2	0.51 ± 0.55	0.17 ± 0.15	2.35 ± 0.23	0.70 ± 0.48	ns	ns
35:1	0.51 ± 0.44	1.25 ± 1.25	1.43 ± 0.40	2.97 ± 1.07	ns	ns
36:3	2.99 ± 0.33	0.64 ± 0.26	0.78 ± 0.29	0.54 ± 0.24	ns	ns
36:2	16.31 ± 1.68	8.66 ± 2.69	33.71 ± 5.02	20.74 ± 3.14	****	****
36:1	6.71 ± 2.21	40.32 ± 1.35	4.67 ± 0.72	21.22 ± 1.79	****	ns
DGDG species						
30:0	1.28 ± 0.57	0.63 ± 0.25	2.44 ± 0.94	0.33 ± 0.09	ns	ns
32:2	4.94 ± 1.57	0.79 ± 0.21	1.60 ± 0.57	0.36 ± 0.10	ns	**
32:1	18.78 ± 3.62	14.27 ± 3.14	8.43 ± 0.95	5.25 ± 0.63	**	****
34:2	15.53 ± 1.00	3.47 ± 0.72	13.26 ± 2.70	4.84 ± 0.88	****	ns
34:1	40.05 ± 2.48	43.33 ± 1.46	45.07 ± 5.31	54.91 ± 3.90	****	****
36:2	12.31 ± 2.13	5.76 ± 1.75	25.08 ± 2.52	17.12 ± 1.47	****	****
36:1	7.10 ± 1.40	31.76 ± 2.24	4.12 ± 0.89	17.18 ± 1.50	****	*
PG species						
28:0	1.87 ± 1.38	0.68 ± 0.46	0.36 ± 0.34	0.21 ± 0.19	ns	ns
30:2	1.57 ± 0.64	0.29 ± 0.17	0.20 ± 0.12	0.04 ± 0.03	ns	ns
30:1	6.40 ± 1.13	2.43 ± 0.77	5.84 ± 1.77	0.92 ± 0.49	****	ns
30:0	5.41 ± 1.16	1.68 ± 0.91	4.28 ± 1.99	1.63 ± 0.59	*	ns
32:2	7.81 ± 1.03	1.49 ± 0.27	3.79 ± 0.54	0.69 ± 0.14	**	***
32:1	16.73 ± 2.01	12.10 ± 2.05	23.51 ± 2.73	6.19 ± 0.73	****	****
32:0	2.27 ± 0.9	0.95 ± 0.73	0.00	2.64 ± 0.83	*	ns
33:1	0.30 ± 0.16	0.24 ± 0.18	4.29 ± 0.42	1.16 ± 0.37	**	***
34:3	2.50 ± 0.34	0.26 ± 0.21	0.14 ± 0.04	0.15 ± 0.08	ns	ns
34:2	16.23 ± 2.58	5.55 ± 1.00	15.78 ± 3.58	7.35 ± 0.60	****	ns
34:1	24.39 ± 1.32	34.12 ± 1.51	18.20 ± 2.28	46.09 ± 3.47	****	****
36:3	1.95 ± 0.21	0.80 ± 0.47	0.51 ± 0.19	0.66 ± 0.41	ns	ns
36:2	9.03 ± 2.24	9.58 ± 3.78	20.69 ± 3.28	17.63 ± 2.52	**	****
36:1	3.54 ± 2.28	29.83 ± 1.11	2.40 ± 0.36	14.62 ± 2.63	****	ns
CL species						
62:2	4.79 ± 1.16	0.47 ± 0.08	3.28 ± 0.17	0.09 ± 0.01	***	ns
62:1	3.04 ± 1.16	0.57 ± 0.16	2.51 ± 0.88	0.22 ± 0.05	*	ns
64:4	2.06 ± 0.43	0.12 ± 0.01	0.68 ± 0.64	0.02 ± 0.01	ns	ns
64:3	6.14 ± 1.05	0.57 ± 0.11	3.55 ± 1.21	0.18 ± 0.04	***	**
64:2	8.53 ± 1.35	2.77 ± 0.87	10.09 ± 0.23	1.12 ± 0.09	****	ns
64:1	2.85 ± 0.90	1.13 ± 0.45	3.29 ± 0.95	1.13 ± 0.17	*	ns
65:6	2.86 ± 1.02	0.26 ± 0.05	0.91 ± 0.49	0.11 ± 0.03	ns	ns
65:5	6.90 ± 1.43	1.82 ± 0.32	7.20 ± 2.43	0.94 ± 0.18	****	ns
65:4	6.16 ± 0.34	7.18 ± 1.80	9.00 ± 2.55	3.90 ± 0.90	****	**
65:2	0.23 ± 0.08	0.14 ± 0.06	1.98 ± 0.22	0.27 ± 0.05	ns	ns
66:4	3.10 ± 2.04	0.42 ± 0.02	1.17 ± 0.53	0.16 ± 0.03	ns	ns
66:3	9.28 ± 0.70	2.45 ± 0.20	8.70 ± 2.34	1.37 ± 0.17	****	ns
66:2	8.89 ± 0.87	9.94 ± 2.54	11.14 ± 1.27	5.66 ± 0.26	****	*
67:6	3.29 ± 0.63	0.90 ± 0.23	2.20 ± 1.16	0.55 ± 0.16	ns	ns
67:5	5.94 ± 0.82	5.32 ± 0.78	8.01 ± 0.80	5.29 ± 0.98	**	*
67:4	3.23 ± 1.17	14.46 ± 1.29	2.29 ± 2.54	16.97 ± 2.76	****	ns
68:4	3.96 ± 0.34	1.08 ± 0.28	2.59 ± 1.13	0.85 ± 0.31	ns	ns
68:3	7.28 ± 1.82	6.40 ± 0.83	9.09 ± 1.44	7.04 ± 0.60	*	ns
68:2	4.46 ± 2.34	17.72 ± 2.35	3.65 ± 2.57	22.59 ± 2.59	****	ns
69:6	1.46 ± 0.45	1.55 ± 0.64	1.81 ± 0.55	1.42 ± 0.40	ns	ns
69:5	1.47 ± 0.91	5.11 ± 4.11	1.95 ± 1.11	8.89 ± 0.75	****	ns
70:4	1.71 ± 0.69	1.63 ± 0.66	2.22 ± 0.87	1.82 ± 0.50	ns	ns
70:3	1.84 ± 1.31	6.97 ± 2.10	2.03 ± 1.31	11.07 ± 1.74	****	ns
70:2	0.54 ± 0.38	11.01 ± 3.13	0.66 ± 0.34	8.36 ± 2.27	****	ns

MGDG, monogalactosyldiacylglycerol; DGDG, digalactosyldiacylglycerol; PG, phosphatidylglycerol; CL, cardiolipin.

Table S3. Strains and plasmids used in this study.

Strains or plasmids	Relevant properties	Source or reference
Streptococcus pyogenes		
WT	Wild-type representative *emm28* clinical isolate, M28PF1	1
CCH1718	M28PF1 deivative harboring multiple mutations including the replacement in *fabT* of C313 by T	Laboratory collection
Δ*fabT*	M28PF1 deleted for *fabT*	This study
mFabT	M28PF1 mutated in *fabT* C313T (H105Y)	This study
BWT-ΔFabT	Back-to-the-wild-type, the reverting strain of the ΔFabT construction	This study
BWT-mFabT	Back-to-the-wild-type, the reverting strain of the mFabT construction	This study
WT-GFP	M28PF1 with the integrated pG1-lacA-PTetO-gfp	2
mFabT-GFP	mFabT with the integrated pG1-lacA-PTetO-gfp	This study
Escherichia coli		
Stellar™	F-, *endA1*, supE44, *thi-1*, *recA1*, *gyrA96*, *phoA*, *Φ80d lacZ* Δ M15, Δ(*lacZYA – argF*) U169, Δ(*mrr – hsdRMS –mcrBC*), Δ*mcrA*, *λ*-	Clontech
Plasmids		
pG1	thermosensitive broad-host-range vector	3
pG1-ΔFabT	pG1-ΔFabT construct for *fabT* deletion in *S. pyogenes*	This study
pG1-mFabT	pG1-mFabT construct for the introduction of a punctual mutation in *fabT* in *S. pyogenes*	This study
pG1-lacAPTetO-gfp	pG1-lacA-Perm-gfp with the Erm promoter replaced by the tetO tetR Pxyl promoter of pTCV_TetO. Can be integrated in *S. pyogenes* genome for anhydrotetracycline inducible *gfp* expression	2

1. Longo M, De Jode M, Plainvert C, Weckel A, Hua A, Chateau A, Glaser P, Poyart C, Fouet A. 2015. Complete Genome Sequence of Streptococcus pyogenes emm28 Clinical Isolate M28PF1, Responsible for a Puerperal Fever. Genome Announc 3.
2. Weckel A, Guilbert T, Lambert C, Plainvert C, Goffinet F, Poyart C, Mehats C, Fouet A. 2021. Streptococcus pyogenes infects human endometrium by limiting the innate immune response. J Clin Invest 131.
3. Biswas I, Gruss A, Ehrlich SD, Maguin E. 1993. High-efficiency gene inactivation and replacement system for gram-positive bacteria. J Bacteriol 175:3628-35.

Table S4. Primers used in this study for cloning, checking cloning and PCR and PCR experiments.

Primer name	Sequence	Used for
P47	CGCCAGGGTTTTCCCAGTCACGAC	Plasmid construction for mFabT and ΔFabT strains
RP48	AGCGGATAACAATTTCACACAGGA	Plasmid construction for mFabT and ΔFabT strains
ermB-F	GAGTGTGTTGATAGTGCAGT	Plasmid construction for mFabT and ΔFabT strains
ermB-R	TAGGCGCTAGGGACCTCTTTA	Plasmid construction for mFabT and ΔFabT strains
FabT-222_am	GACTCTAGAGGATCCGGTCTGGCAAAGCTTTTTCA	Plasmid construction for mFabT strain
Fabt+805_av	CATGATTACGAATTCGGCACCTGATGCAATAAGCT	Plasmid construction for mFabT strain
FabT-ext-am	CCGGTTGAAAATATCAACTAAGTATT	Plasmid construction for mFabT strain
FabT-ext-av	CCCCATGTCAAACCTCCA	Plasmid construction for mFabT strain
FabTavF	GATATTTTCAACCGGGCGTGGACTAGGGAATCTAC	Plasmid construction for ΔFabT strain
FabTavR2	CCATGATTACGAATTCGCACCATCTGTGTGTAAT	Plasmid construction for ΔFabT strain
FabTamR	CCGGTTGAAAATATCAACTAAGTATT	Plasmid construction for ΔFabT strain
FabTamF2	CGACTCTAGAGGATCCGCCAAAACCAGTCATCCTT	Plasmid construction for ΔFabT strain
PFabTamEco	ATATAGAATTCGGCAGAGCTTGCTATTCAAGA	PCR overlapping *fabM* and *fabT*
PFabTavBam	ATAGGATCCGCAAGATCATCTACAACATCA	PCR overlapping *fabM* and *fabT*
fabH_acpP_Am	GGGACAGATTAGGTTAGATGGT	PCR overlapping *fabH* and *acpA*
fabH_acpP_Av	GCGTTACTTCTTCTGTCTCCTT	PCR overlapping *fabH* and *acpA*
acpP_fabK_Am	GGTGACCTTGTTGCTTA	PCR overlapping *acpA* and *fabK*
acpP_fabK_Av	CCATTCCTCCTTGAAAA	PCR overlapping *acpA* and *fabK*
fabZ_accC_Am	GCAGCAAGTGGAACATTAA	PCR overlapping *fabZ* and *accC*
fabZ_accC_Av	CACCACGATTAGCAATTAA	PCR overlapping *fabZ* and *accC*
accD-end	GCGTTACCAACGCTTTCGTAAA	PCR overlapping *accD* and *serS*
serS-end	GGCGAAACCGTCATTTCACCT	PCR overlapping *accD* and *serS*
gyrA1	CTGCTCGTATTACGGGTGATGT	qRT-PCR of *gyrA*
gyrA2	GGCGATAACTCCACCACTGA	qRT-PCR of *gyrA*
rpoB1	CCGTACACGTCGTAGCTTTT	qRT-PCR of *rpoB*
rpoB2	GCATCGTGGATACGAGCTTC	qRT-PCR of rpoB
FabM am	CTGTAGCTGGAGCGGCTTTTA	qRT-PCR of *fabM*
FabM av	CCGGTGCTAGTCCAACATTTAC	qRT-PCR of *fabM*
FabT-3'	CCCTAGTCCACGCACCAATGCCT	qRT-PCR of *fabT*
FabT-5'	GGGACAGTAACGACTAGCTTAAATA	qRT-PCR of *fabT*
FabH am	GGTGCCTACCAAAACGGAATG	qRT-PCR of *fabH*
FabH av	CACCAGCTCCGTCTCCAAAA	qRT-PCR of *fabH*
FabK am	CCAGGCGGGTATAATCGTTGT	qRT-PCR of *fabK*
FabKav	GCCAATATGTCCTCCAGCTTC	qRT-PCR of *fabK*
0140-Am	CGCCTCGTCTACCTCTTGGT	qRT-PCR of M28_*Spy0140*
0140-Av	CCCCTTTGTTAAACCTTGGTTATA	qRT-PCR of M28_*Spy0140*
rofA-Am	GGCGTTAAATTGTCGAAGATACTGC	qRT-PCR of M28_*Spy0184* coding for RofA
rofA-Av	CCTACTGGCTATTTTGTTGACAGAA	qRT-PCR of M28_*Spy0184* coding for RofA
0338-Am	GGGGGTTCAGACTCATTCCAAC	qRT-PCR of M28_*Spy0338*
0338-Av	GGGCACGATCACGTAACAATCA	qRT-PCR of M28_*Spy0338*
0346-Am	GGAGGCTCTTCAGAGATTCCCT	qRT-PCR of M28_*Spy0346*
0346-Av	GCGCGTAGACCAAAGAATAGAA	qRT-PCR of M28_*Spy0346*
0371-Am	GCCGATTTCTGATCTACCCCTT	qRT-PCR of M28_*Spy0371*
0371-Av	GCCCTTACCTTTGGAGTGATGA	qRT-PCR of M28_*Spy0371*
0853_Am	GCCAACATGGTTTTTCCGAA	qRT-PCR of M28_*Spy0853*
0853_Av	GGGATAACCAAGTCAATCTT	qRT-PCR of M28_*Spy0853*
0855_Am	CCTCCCTGATTTAGACTTA	qRT-PCR of M28_*Spy0855*
0855_AV	CCCATGCTTGACGTAATTA	qRT-PCR of M28_*Spy0855*
1136-Am	CCGGATATGCAAGAATATTCCTT	qRT-PCR of M28_*Spy1136*
1136-Av	CCCGTAGCGGTCAAATAATTGGT	qRT-PCR of M28_*Spy1136*
ParB-Am	GGCTGTTGGACCAGTTGCTGAA	qRT-PCR of M28_*Spy1255* coding for ParB
ParB-Av	GGGCTGCTTTATAACGAGTGT	qRT-PCR of M28_*Spy1255* coding for ParB
R28-Am	GGGCGCAATTACCTTTACTGCAAA	qRT-PCR of M28_*Spy1336* coding for R28
R28-Av	CCGTTTGGTCCTTACCTTTTGGTT	qRT-PCR of M28_*Spy1336* coding for R28
1434-Am	CCCTACAGATTGGCACAGAAAT	qRT-PCR of M28_*Spy1434* coding for FakB3
1434-Av	GGGCTTGGACAGCTAGATGT	qRT-PCR of M28_*Spy1434* coding for FakB3
1562-Am	GCACGTTTAGATACATGACAATTGG	qRT-PCR of M28_*Spy1562* coding for UspA
1562-Av	GCTCTCACGATCAACAGATCAAT	qRT-PCR of M28_*Spy1562* coding for UspA
1638-Am	GCCAGCTTTCATCTTTTTCAAAAGG	qRT-PCR of M28_*Spy1638* coding for $DegV_{1638}$
1638-Av	GGGCAGAAGATCATGATATTGTC	qRT-PCR of M28_*Spy1638* coding for $DegV_{1638}$
norA-Am	GTGGCCATCACAGTAATAAACTTT	qRT-PCR of M28_*Spy1563* coding for NorA
norA-Av	CCCTGTTGCCAATCCTGCCT	qRT-PCR of M28_*Spy1563* coding for NorA
ska-Am	CCGTCCATCTGTCAACAACAGCCA	qRT-PCR of M28_*Spy1672* coding for Ska
ska-Av	CCTCCATGAGCAGGTTGTGATGTT	qRT-PCR of M28_*Spy1672* coding for Ska
csp-Am	GGCTGCATGCTATCTACGGCA	qRT-PCR of M28_*Spy1699* coding for Cell Surface protein
csp-Av	GCCGCTATTCCATTCGCAAACT	qRT-PCR of M28_*Spy1699* coding for Cell Surface protein
scpA-Am	GGGGGTTCTACGGCTTGTTC	qRT-PCR of M28_*Spy1700* coding for ScpA
scpA-Av	GCGCTCATGTCTACGAGCAT	qRT-PCR of M28_*Spy1700* coding for ScpA
sfbX-Am	GGGGCTTGAAACTCGGTGTT	qRT-PCR of M28_*Spy1715* coding for SfbX
sfbX-Av	GGCCAAGTCTGGGACCCACT	qRT-PCR of M28_*Spy1715* coding for SfbX
sof-Am	GGGGTGAGGCTGGAGTAGTG	qRT-PCR of M28_*Spy1716* coding for SOF
sof-Av	GCAGCTGGGAGCGGAGCTA	qRT-PCR of M28_*Spy1716* coding for SOF

Supplementary Methods

Membrane fluidity analysis. *S. pyogenes* membrane fluidity was defined as previously with modifications [1]. THY and THY-Tween exponential cultures ($0.4 < OD_{600nm} < 0.5$) were centrifuged and the pellets resuspended in 1ml PBS. Bacteria were incubated with 0.1 mM of Laurdan (6-Dodecanoyl-N,N-dimethyl-2-naphthylamine) (Sigma-Aldrich, Ref. 40227) at 30 °C. After 10 min, bacteria were washed four times in pre-warmed (30°C) Laurdan buffer and resuspended by vortexing shortly. Laurdan fluorescence was analyzed using a Tecan SPARK (Ref. 30086376) and the Laurdan GP was calculated comparing (λ_{440nm} - λ_{500nm}) to (λ_{440nm} + λ_{500nm}).

Membrane permeability analysis. *S. pyogenes* membrane permeability was determined as previously with modifications [2]. THY and THY-Tween exponential phase cultures ($0.4 < OD_{600nm} < 0.5$) were centrifuged and the pellets resuspended in 1ml PBS twice and then resuspended in 100 µL PBS. Bacteria were incubated with 1 $\mu g.ml^{-1}$ ethidium bromide at 37 °C during 15 min and washed twice in PBS. Ethidium bromide fluorescence was analyzed by flow cytometry using FORTESSA (BD Biosciences).

Temperature sensitivity analysis. Temperature sensitivity of strains were analyzed with two methods. The first one was as described in "Methods, Growth curves", following the bacterial growth in THY and THY-Tween at 30 and 40 °C. For the second one, consisting in a temperature shock treatment, exponential phase cultures ($0.4 < OD_{600nm} < 0.5$) obtained at 37 °C, were diluted in appropriately prewarmed THY and THY-Tween at $OD_{600nm} = 0.05$ and immediately transferred to 30 °C and 40 °C water baths and OD_{600nm} was followed every 30 min during 4 h.

LL37 cytotoxicity assay. Bacteria sensitivity to LL37 were defined as previously described with modifications [3]. THY and THY-Tween exponential phase cultures ($0.4 < OD_{600nm} < 0.5$) were centrifuged and the pellets resuspended in 1ml PBS twice and incubated with LL37 2.5µM at 37 °C during 45 min. Then, serial dilutions were plated on THYA plates. The number of CFUs was determined after 24 h of growth at 37 °C.

H_2O_2 sensitivity assay. Bacteria sensitivity to H_2O_2 were defined as previously described with modifications [4]. THY and THY-Tween exponential phase cultures ($0.4 < OD_{600nm} < 0.5$) were divided in two, $H_2O_2$10 mM was added to one culture. After 30 min of culture at 37 °C, serial

dilutions were plated on THYA plates. The number of CFUs was determined after 24 h of growth at 37 °C.

pH sensitivity analysis. Strains pH sensitivity was determined by following the bacterial growth in THY or THY-Tween pH 5.5 and pH 6.0 as described previously in "Methods, Growth curves". pH was adjusted by adding citrate-phosphate buffer at pH and 5.5 and 6.0.

Bacterial morphology and size analysis. THY and THY-Tween exponential phase cultures ($0.4 < OD_{600nm} < 0.5$) were centrifuged and the pellets resuspended in 1ml PBS twice and incubated at 4°C with a fixative solution (4 % paraformaldehyde and 2.5 % glutaraldehyde). After 30 minutes, bacteria were washed three times in PBS then treated as previously described, with slight modifications [5]. Secondary fixation was performed with 1% osmium tetroxide in phosphate buffer saline for 1 h at room temperature, then bacteria were centrifuged, the pellets washed 3 times in H_2O and further dehydrated with increasing concentrations of ethanol (70%, 90%, and 100% twice). After dehydration, pellets were infiltrated with sequential 3:1, 1:1, and 1:3 solutions of resin (Embed 812 kit; Electron Microscopy Sciences, Hatfield, PA) and 100% ethanol for 1 h separately at room temperature. Finally, the samples were incubated with propylene oxide for 2 m and placed in the embedding molds with resin. The embedding resin blocks were polymerized in an oven at 60 °C for 24 h. Ultrathin sections (90 nm) were cut from the block surface using an ultramicrotome (Reichert Ultracut S ultramicrotome, Leica Microsystems) then stained with uranyl acetate and lead citrate (LFG, France) and observed by TEM (JEOL 1011, JEOL, Japan)) at 80 kV of acceleration voltage. Acquisitions were performed by an Orius 1000 CCD Camera (GATAN, USA) using Digital Micrograph software (GATAN, USA).

To determine the bacterial size, on each independent image, the larger bacteria were selected as representative of those sliced through the sphere diameter. The pixels along the diameter were then quantified.

References for supplementary material

1 Wenzel, M., Vischer, N. O. E., Strahl, H. & Hamoen, L. W. Assessing Membrane Fluidity and Visualizing Fluid Membrane Domains in Bacteria Using Fluorescent Membrane Dyes. *Bio Protoc* **8**, e3063, doi:10.21769/BioProtoc.3063 (2018).

2 Eckhardt, T. H., Skotnicka, D., Kok, J. & Kuipers, O. P. Transcriptional regulation of fatty acid biosynthesis in *Lactococcus lactis*. *J Bacteriol* **195**, 1081-1089, doi:10.1128/JB.02043-12 (2013).

3 Makthal, N. *et al.* Signaling by a Conserved Quorum Sensing Pathway Contributes to Growth Ex Vivo and Oropharyngeal Colonization of Human Pathogen Group A *Streptococcus*. *Infect Immun* **86**, doi:10.1128/IAI.00169-18 (2018).

4 Yamamoto, Y. *et al.* The Group B *Streptococcus* NADH oxidase Nox-2 is involved in fatty acid biosynthesis during aerobic growth and contributes to virulence. *Mol Microbiol* **62**, 772-785, doi:10.1111/j.1365-2958.2006.05406.x (2006).

5 Vadia, S. *et al.* Fatty Acid Availability Sets Cell Envelope Capacity and Dictates Microbial Cell Size. *Curr Biol* **27**, 1757-1767 e1755, doi:10.1016/j.cub.2017.05.076 (2017).

Partie 2 : AcpB, corépresseur de FabT chez *S. pyogenes.*

Acyl-AcpB, a FabT co-repressor in *Streptococcus pyogenes.*

Clara Lambert[a], Alice d'Orfani[a], Qiufen Zhang[a]*, Karine Gloux[b], Claire Poyart[a,c], and Agnès Fouet[a].

[a] Université Paris Cité, Institut Cochin, INSERM U1016, CNRS UMR8104, Paris, France;
[b] Micalis Institute, INRAE, AgroParisTech, Université Paris-Saclay, Jouy en Josas, France;
[c] AP-HP Centre-Université Paris Cité, Paris France.

Orcid numbers: A. Fouet, 0000-0001-7715-9157; C. Lambert, 0000-0003-2740-1755.

Address correspondence to Agnes Fouet, agnes.fouet@inserm.fr.

* Present address: Medicinal Chemistry and Bioinformatics Center, Shanghai Jiao Tong University School of Medicine, Shanghai China.

Abstract

Membranes are a universal barrier to all cells. Phospholipids, essential bacterial membrane components, are composed of a polar head and apolar fatty acid (FA) chains. Most bacterial FA are synthesized by the FA synthesis pathway (FASII). In streptococcaceae, enterococci and *Lactococcus lactis*, a unique feedback mechanism controls the FASII gene expression. FabT, encoded in the FASII main locus, is the repressor and it is activated by acyl-ACP. Many Streptococci, *Enterococcus faecalis*, but not *L. lactis*, possess two ACPs. AcpA encoding gene is within the FASII locus and is, to a certain extent, coregulated with the FASII genes. Acyl-AcpA is the end product of FASII. AcpB encoding gene is in operon with *plsX*, PlsX is involved in the phospholipid biosynthetic pathway. The role of AcpB as FabT corepressor is controversial. *Streptococcus pyogenes*, which causes a wide variety of diseases ranging from mild non-invasive to severe invasive infections, possesses AcpB. In this study, we show by comparing gene repression of FASII genes in wild-type, *fabT* mutant and *acpB* mutant strains grown in the presence and absence of exogenous FAs, that AcpB is FabT main co-repressor. *acpB* deletion impacts the membrane FA composition. Furthermore, the *acpB* deleted strain displays defects in adhesion and growth in the presence of eucaryotic cells.

Importance

Membranes contain phospholipids that are composed of fatty acids (FA) and a polar head. Membrane FA composition is crucial for bacterial growth or interaction with the environment. Bacteria synthesize FAs *via* the FASII pathway. Streptococci control the expression of the FASII genes *via* a transcriptional repressor, FabT, with acyl-ACP as a co-repressor. Many streptococci possess two ACPs. AcpA, but not AcpB, is a FASII gene. The role of AcpB as FabT corepressor is controversial. *Streptococcus pyogenes* causes a wide variety of diseases ranging from mild non-invasive to severe invasive infections. Here we show that *S. pyogenes* AcpB is FabT main corepressor. Also, its deletion has consequences on the membrane FA composition and bacterial interaction with host cells.

Keywords

Streptococcus pyogenes, fatty acid synthesis, regulation, Acyl-ACP, co-repressor

Introduction

Cell membranes commonly comprise a phospholipid bilayer composed of a polar head and an apolar body constituted of fatty acids (FA). FA structure and length are decisive for membrane topology and properties such as fluidity, permeability and integrity. These features are crucial for the adaptation of bacteria to various environments (1). The FAs are synthesized by the FA synthesis pathway (FASII) that is widespread among bacteria. It consists of an initiation phase followed by a recursive elongation cycle, which produces acyl-acyl carrier protein (acyl-ACP). Unsaturated FAs are produced *via* a shunt of this cycle that is catalyzed by FabM in streptococci. In contrast to the FASII pathway, the regulation of the FASII genes is not conserved. In streptococci, enterococci and *Lactococcus lactis*, a unique feedback mechanism controls the expression of the FASII genes, involving a repressor, FabT, encoded in the FASII main locus. Depending on the *Streptococcus* species, the *fabM* gene is either not controlled or less repressed by FabT than the *fabK* gene, inducing a shift in the proportion of saturated - unsaturated FAs in *fabT* mutant strains (2, 3).

FabT, a member of the MarR family of regulators, possesses an unconventional corepressor, acyl-ACP [(4) for review (5)]. FabT – acyl-ACP binding to its DNA target varies according to the acyl length, increasing with long chain acyls (4). It also depends on the saturation state of the FA, the *cis* unsaturated FA maximizing FabT-DNA affinity (6). The role of FabT as a FASII repressor in the presence of exogenous FAs (eFAs) can readily be observed by the repression of the FASII genes in the wild-type strain grown in the presence of eFA and the loss of this repression in *fabT* mutant strains grown similarly (6)(Lambert *et al.*, FabT manuscript).

In addition to acyl moiety variation, the ACP may differ. Indeed, in many streptococci, as well as in *E. faecalis*, but not in *L. lactis*, there are two ACPs. AcpA is encoded within the FASII locus; the AcpB encoding gene is found in the same operon as *plsX* (7-9). Whereas *acpA* expression is controlled by FabT, although with repression folds weaker than those of other genes, that of *acpB* is not (6)(Lambert *et al.*, FabT manuscript). The role of AcpB in FASII gene control is controversial. FabT – acyl-ACP DNA binding affinity tests using *S. pneumoniae* purified FabT and acyl-AcpA or acyl-AcpB indicated that only AcpB increased it (7). In contrast, in *E.* faecalis, no difference was observed in the *fabT* gene expression between wild-type and *acpB* mutant strains, grown either in the presence or absence of eFAs (6).

In addition to investigating the gene repression level when *E. faecalis* strains were grown in the presence or absence of eFAs, their incorporation in the membrane was compared in wild-type and mutant strains. Whereas the *fabT* mutant strain displays a strong incorporation defect, down to one fourth, the *acpB* mutant strain displays a mild one, of five percent (6).

In *Streptococcus pyogenes* the expression of the FASII genes is controlled by FabT and this species possesses an AcpB. *S. pyogenes* is a Gram positive strictly human pathogen that yields a wide range of clinical manifestations from mild superficial infections to more life-threatening invasive infections including necrotizing fasciitis (NF), streptococcal toxic shock syndrome (STSS). GAS infections are also responsible for post-infectious complications (10). Altogether, GAS infections are responsible for 517,000 deaths annually worldwide (11).

To determine whether, and to what extent, AcpB is a FabT co-repressor in *S. pyogenes*, we studied the effects of deleting *acpB* on FASII gene expression in bacteria grown in the presence or absence of eFAs. We also determined the membrane FA composition in these bacteria as well as the consequences of *acpB* deletion on bacterial host cells interaction.

Results and discussion

***S. pyogenes* AcpB is a FabT corepressor**. An *acpB* deleted strain, ΔAcpB, was constructed in the wild-type (WT) reference strain, M28PF1 (Table S1) (9). Growths of WT, mFabT (Lambert *et al*., FabT manuscript), ΔAcpB and BWT strains, the latter two sharing the same surreptitious mutation, were compared in the laboratory media THY and in THY-Tween 80, as a source of FAs (Fig. S1). All strains grew similarly.

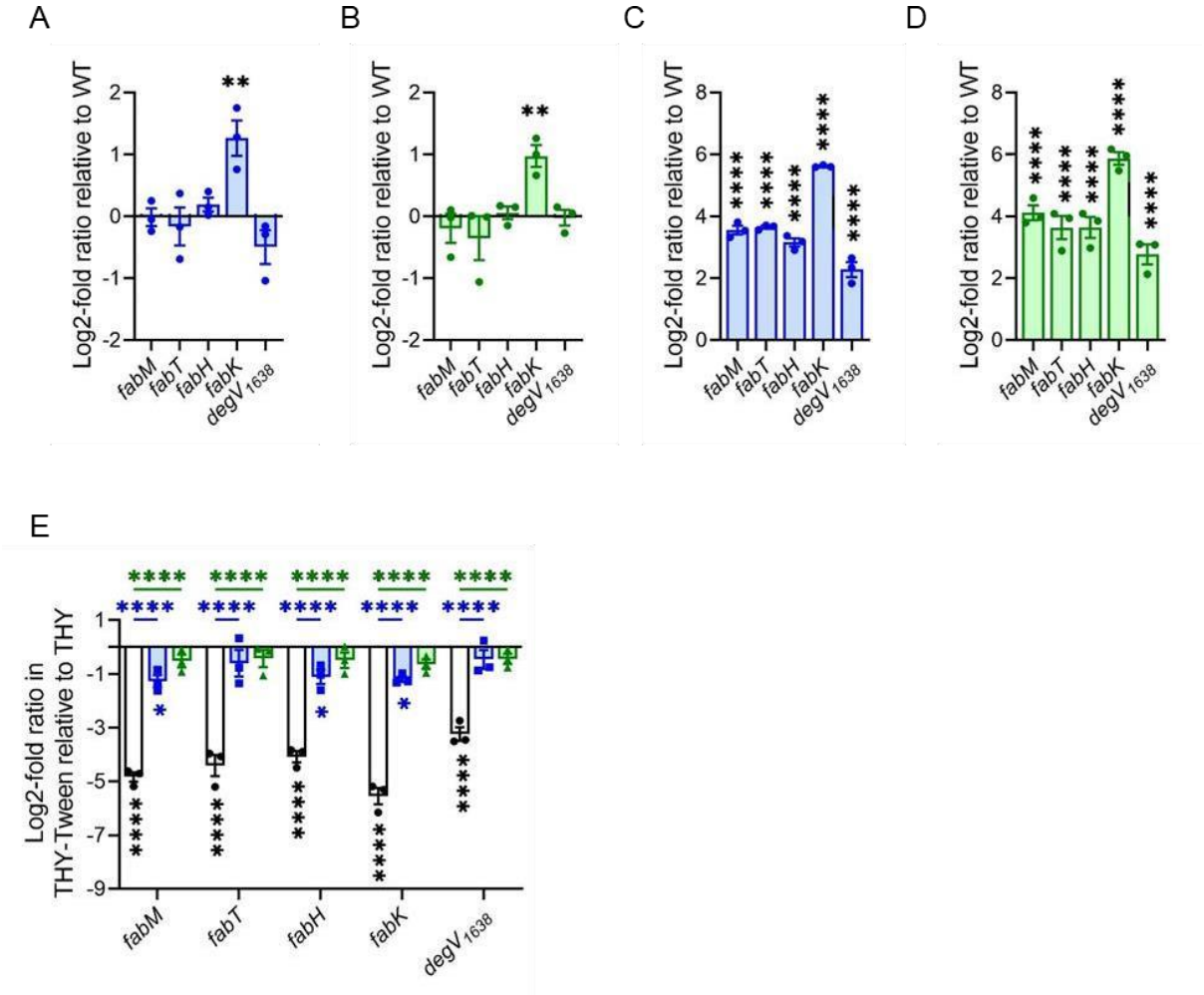

Figure 1. Comparison of the repression of FASII genes in *S. pyogenes* WT, ΔAcpB and mFabT strains grown in the absence or presence of eFAs. Strains were grown in THY (A, B, E) or THY-Tween 80 (C, D, E) and RNAs were quantified by qRT-PCR. Expression was normalized to that of *gyrA*; relative gene expression is expressed as the log2-fold ratio in ΔAcpB *versus* WT strain (A, C) and mFabT *versus* WT strain (B, D). E) The relative gene expression is expressed as the log2-fold ratio in a given strain grown in THY-Tween 80 *versus* in THY. White, WT; blue, ΔAcpB, green mFabT. The stars below the bars correspond to the difference in expression in the two media for a given strain. Those above the bars correspond to the difference in expression in the two media between two strains. n =3. 2-way ANOVA, Bonferroni post-test, * $p < 0.05$; **, $p < 0.01$; ****$p<0.001$.

To analyze the role of AcpB as a FabT co-repressor, the effects of AcpB on the expression of a set of genes, containing FASII genes and the coregulated *degV*$_{1638}$ gene, were determined either in the absence or in the presence of Tween 80 and compared to those of the WT and the mFabT strains (Fig. 1). qRT-PCR were performed on RNA extracted from six conditions: WT, ΔAcpB and mFabT strains, each grown in THY and THY-Tween 80. As a control, the expression of the set of genes was compared in the BWT and the WT strains and found to be unchanged (Fig. S2). Data were then analyzed by comparing results pairwise between ΔAcpB and WT or mFabT and WT strains in each medium (Fig. 1 A-D). In THY, the expression of *fabK* is differentially expressed, in fact overexpressed, in both mutant strains (Fig. 1A, 1B). In THY-Tween 80, all genes were more expressed in both mutant strains than in the WT strain. (Fig. 1C, 1D). These data suggested that AcpB is involved in the FASII gene repression in the absence and in the presence of exogenous FAs.

To compare the repression defect in the presence of exogenous eFAs in the mFabT and ΔAcpB strains, we analyzed the repression exerted in each strain in the presence of Tween 80 (Fig. 1E). Whereas this addition led to a repression fold between 12 and 25 in the WT strain, it was just above 2 for three out of the five genes in the ΔAcpB strain, and below 2 for all genes in the mFabT strain. We then compared whether the repression exerted in each strain was different from that in the other strains (Fig. 1E). That in the WT strain is different from that of both mutant strains. The variation of the expression ratio between the ΔAcpB and the mFabT was not statistically different. Altogether, these results confirm that *S. pyogenes* AcpB is involved in the transcriptional repression of the FASII genes.

Our data are in sharp contrast with those obtained in *E. faecalis*, when FASII gene expression was assessed in an *acpB* mutant strain, but in agreement with the conclusion drawn from results obtained by a biochemical approach in *S. pneumoniae* (6, 7). Hence, our data strongly suggest that in *S. pyogenes* AcpB is FabT main corepressor and that this may be the case in many *Streptococcus* species. Furthermore, AcpB would exert its role both in the absence and the presence of eFAs. Altogether this indicates that AcpB role may be different in various species and warrants further analysis in other organisms.

AcpB deletion modifies the *S. pyogenes* membrane FA composition. Since the AcpB deletion leads to a deregulation of FASII gene expression, we tested its consequences on FA composition when bacteria were grown in the absence or presence of Tween 80 (Fig. 2A-D). As a control, the membrane FA composition of the BWT and the WT strains was compared and found to be unchanged (Fig. S3, Table S2). The striking differences, in the absence of Tween 80, were that the ΔAcpB membrane contained less 16:1 and 18:1Δ11 and more 18:0 than the WT strain. In the presence of Tween 80, the ΔAcpB membrane contained less 14:0 but more 16:0 and somewhat less 18:1Δ9 and more 18:1Δ11 The weaker 18:1Δ9 percentage suggested an incorporation defect. However, this was not the case; the percentage of 17:1, that is not synthesized by bacteria, was similar in both strains grown in 17:1 supplemented medium, as already described in *E. faecalis* (Fig. 2E, F)(6). The shifts toward saturated and longer FAs correlate well with an increased elongation due to an unchanged *fabM* expression and slight *fabK* derepression in the absence of Tween 80 and more important derepression of *fabK* than *fabM* in the presence of Tween 80.

The membrane composition of the mFabT strain was also determined and compared pairwise with those of the WT and ΔAcpB strains. As previously described, the mFabT membrane is different from that of the WT strain, particularly in the presence of Tween 80 (6)(Lambert *et al.*, FabT manuscript). Importantly, the 16:0 decrease and 18:0 increase in the absence of Tween 80 and the 18:1Δ9 decrease and 18:1Δ11 increase in the presence of Tween 80 were more important in the mFabT than in the ΔAcpB strains. This latter shift is due to the mFabT strain eFA incorporation defect (Fig. 2E, 2F) (6)(Lambert *et al.*, FabT manuscript). The difference in the saturated FA shift between the ΔAcpB and the mFabT strains is probably due, although it did not appear statistically significant, to a repression difference (Fig. 1E). This may correspond to a threshold between not fully and fully derepressed FASII genes that is amplified at the level of FA synthesis.

Our data indicate that AcpB, as a FabT co-repressor, controls the membrane FA composition. They also suggest that AcpB is the main but not the sole FabT co-repressor. This further suggests that in the absence of AcpB, acyl-AcpA is also a corepressor. Moreover, since the mFabT and AcpB membrane FA composition is different both in the presence and absence

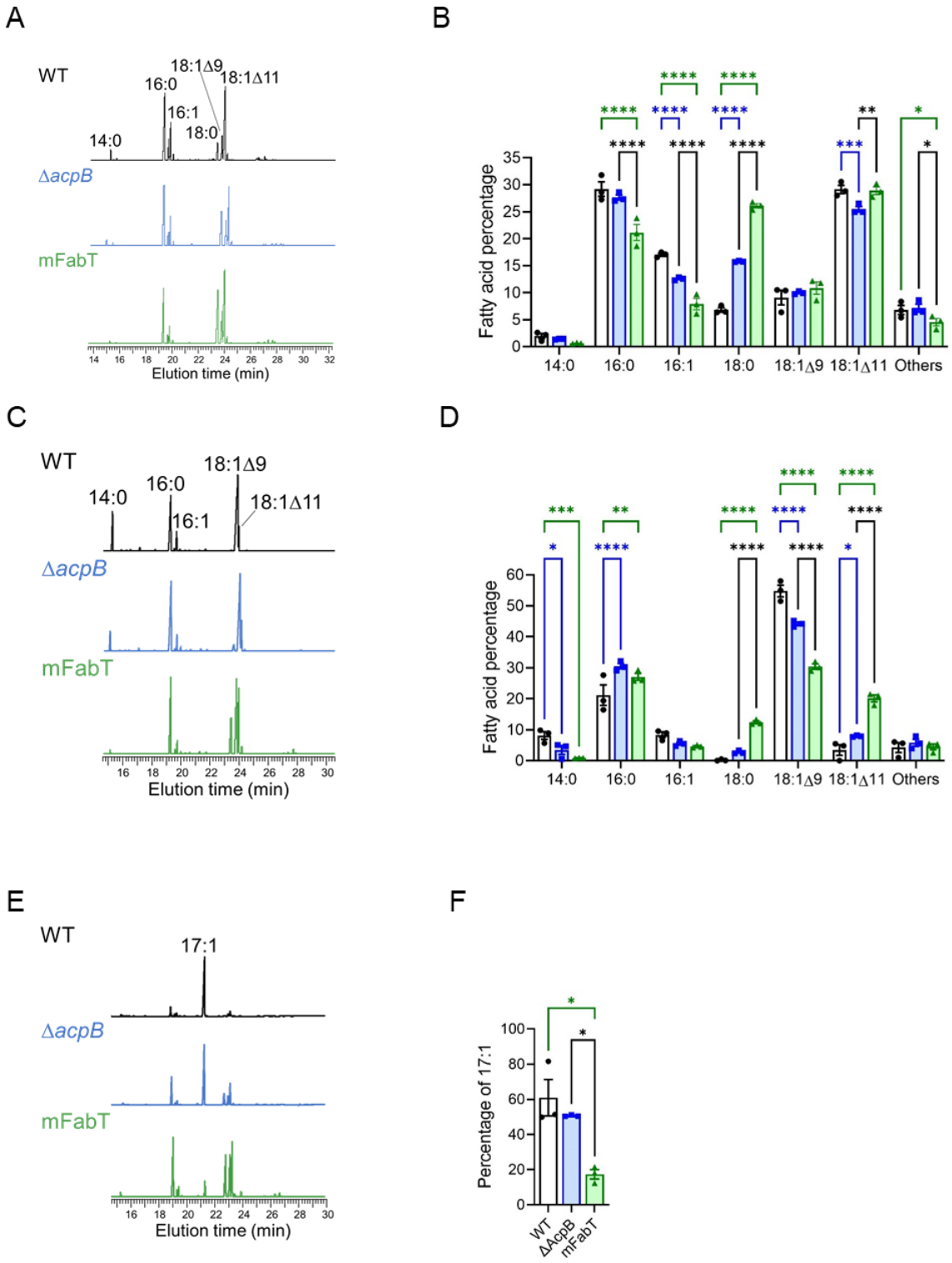

Figure 2. Fatty acid membrane composition of WT, ΔAcpB and mFabT strains. A-D) WT, ΔAcpB and mFabT strains were grown in A, B) THY medium C, D) THY-Tween 80. A, C, profiles of the membrane fatty acids of the WT, ΔAcpB or mFabT strains; B, D) FA percentage. N=3 (Table S2). E, F) 17:1 FA incorporation, E) FA profiles of the WT, ΔAcpB and mFabT strains grown in THY medium supplemented with 17:1, E) profiles, F) percentage of 17:1 in the membranes. -B, D, F) 2way ANOVA, Bonferroni post-test, *, $p < 0.05$; **, $p < 0.01$; ***, $p < 0.001$; ****$p<0.0001$.

of eFAs, acyl-AcpA may operate in both conditions, acyl-AcpA thus resulting from the interaction of *de novo* synthesized acyls but also from eFAs. The latter are produced by the reverse PlsX reaction that catalyzes the production of Acyl-ACP from acyl-phosphate.

The AcpB strain displays an adhesion defect to eucaryotic cells and a growth defect in their supernatants. The mFabT strain displays defects in its adhesion capacity to eucaryotic cells and its growth capacity in cell supernatant conditioned supernatant (Lambert *et al.*, FabT manuscript). The ΔAcpB strain membrane FA composition was in-between that of the WT and the mFabT strains. We thus wondered whether the ΔAcpB strain would display such defects (Fig3A, 3B). Whereas the mFabT strain has an adhesion defect, there is a tendency for a defect in the adhesion of the ΔAcpB strain. A similar trend was observed regarding the growth defect.

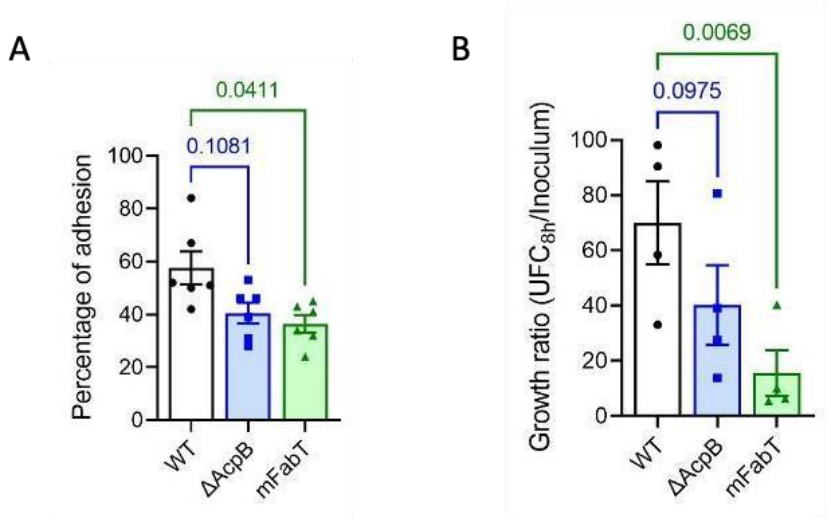

Figure 3. The ΔAcpB mutant strain has adhesion and growth defects in the presence of human cells or in cell supernatant. Comparison of WT, ΔAcpB and mFabT strains A) adhesion capacity, B) growth capacity in conditioned supernatants. Growth experiments were started with 10^3 bacteria per ml. Bars and symbols, white, WT strain; blue, ΔAcpB strain; green, mFabT strain. A) N= 6 and B) N= 4, One-way ANOVA ; the p values are indicated.

Our results thus suggest that the variation in the membrane FA composition of the ΔAcpB strain, although not as strong as that of the mFabT strain, modifies the *S. pyogenes* interaction with eucaryotic cells. This supports that even a smaller membrane FA composition variation leads to a modified capacity of interaction with host cells. This is yet another strong evidence for the importance of membrane homeostasis for bacterial interaction with its

environment and particularly for virulence in the case of a pathogen. It further supports that the FASII gene expression is a promising antimicrobial target.

In conclusion, AcpB is FabT main co-repressor in *S. pyogenes* and most probably other streptococci. In the presence of eFAs, FASII gene expression is repressed and, although *acpA* repression is not as strong as that of other FASII genes, this leads to a weaker AcpA concentration than in their absence (3). In contrast, *acpB* expression is unaffected by the presence of eFAs (3)(Lambert *et al.*, FabT manuscript). This implies that the role of AcpB as FabT corepressor is enhanced when *S. pyogenes* encounters eFAs, which is the case *in vivo*, supporting that it becomes FASII main transcriptional co-repressor. In fact, *S. pyogenes* AcpB is in involved in the interaction with the host cells.

Material and Methods

Bacterial strains and culture conditions. The strains used in this study are described in Table S1. *S. pyogenes* strains were grown under static condition at 37 °C in Todd Hewitt broth supplemented with 0.2 % Yeast Extract (THY) or on THY agar plates. To study, the role of eFA addition or eFA incorporation, the medium was supplemented with 0.1 % Tween 80 (THY-Tween 80) (Sigma-Aldrich, P1754), essentially composed of 18:1Δ9 or 100 μM 17:1 (Larodan, Sweden). Overnight cultures were diluted to an OD_{600nm} = 0.05 and grown in the indicated medium to the exponential phase (OD_{600nm} comprised between 0.4 and 0.5).

Strain construction. The primers used for the generation of the plasmids and verifying the different strains are described in Table S3. The ΔAcpB were obtained by homologous recombination of the plasmid pG1AcpB following the same protocol as described previously (12, 13). The DNA fragments encompassing *fabT* were cloned in BamHI – EcoRI digested pG1 using the In Fusion cloning kit® (Clonetech) (14). This led to the deletion of *acpB* from nucleotides 14 to 203, relative to the translation initiation site. The back-to-the wild-type (BWT), *i.e.* reversion of the single cross-over and restauration of a wild-type *acpB*, was carried out as previously described. The whole genomes of the constructed strains were sequenced; one identical surreptitious mutation was found in both the ΔAcpB and the BWT strains in *priA*, the G in position 1073 was replaced by a T leading to the replacement of the 358th amino acid residue, a tryptophane by a leucine.

RNA isolation and First-strand cDNA synthesis, quantitative PCR (qPCR). *S. pyogenes* strains were cultured at 37°C in THY or THY-Tween 80, and cells were harvested at exponential growth phase (OD comprised between 0.4 and 0.5). RNA isolation, cDNA synthesis and quantitative PCR were carried out as previously described (Lambert et al, FabT manuscript).

Fatty acid analysis. Strains were grown in THY, THY-Tween 80, or THY-17:1 until OD_{600nm} = 0.4 - 0.5. FAs were extracted and analyzed as previously described (15).

Cell culture. HEC-1-A (ATCC_ HTB-112TM) endometrial epithelial cells were cultured as recommended, in McCoy's 5A medium (Gibco, Ref. 26600080) supplemented with 10 % fetal bovine serum at 37 °C, 5 % of CO_2.

Bacterial adhesion capacity. *S. pyogenes* adhesion capacity was realized as described previously after growing the bacteria in THY to an OD_{600nm} of 0.4 to 0.5; bacteria were added

at a multiplicity of infection of 1 (12). The values were normalized to the inoculum for each experiment.

Bacterial growth capacity in the presence of eukaryotic cells or their culture supernatant. *S. pyogenes* bacteria were grown in THY to an OD_{600nm} of 0.4 to 0.5, the culture was washed twice in PBS and diluted in RPMI medium without glutamine (Gibco, Ref. 32404-014) to inoculate filtered cell culture supernatants (conditioned supernatants) at a final concentration of 10^3 bacteria per ml as previously described (Lambert et al, FabT manuscript). After 8 h incubation, serial dilutions were plated on THY-agar plates. The number of CFUs was determined after 24 h of growth at 37 °C and normalized to the inoculum for each experiment.

Statistical analysis. Data were analyzed with GraphPad Prism version 9.4.1. The tests used are indicated in the figure legends. Statistical significance is indicated by: ns (not significant, $p > 0.05$); *, $p < 0.05$; **, $p < 0.01$; ***, $p < 0.001$; ****, $p < 0.0001$.

Acknowledgements

We thank A. Gruss for her constant interest and support. We thank Audrey Solgadi and Bastien Prost (UMS-IPSIT-Plateforme SAMM) for help with the lipid analysis Tiphaine Pouillon, Maëva Gauduin undergraduates, and Marine Gaillard engineer in the laboratory for technical help.

CL was supported by Université Paris Cité (BioSPC, n°51809666), FRM (FDT202106012831) and FEMS (FEMS Congress Attendance Grant for poster n° 7875 in 2021 and FEMS grant - LISSSD 2022 n° LISS-213065). QZ was supported by bourse SSHN jeune chercheur and innovative research team of high-level local universities in Shanghai (SHSMU-ZDCX20212700). This work was supported by DIM One Health (RPH17043DJA).

References

1. Zhang YM, Rock CO. 2008. Membrane lipid homeostasis in bacteria. Nat Rev Microbiol 6:222-33.
2. Lu YJ, Rock CO. 2006. Transcriptional regulation of fatty acid biosynthesis in *Streptococcus pneumoniae*. Mol Microbiol 59:551-66.
3. Eraso JM, Olsen RJ, Beres SB, Kachroo P, Porter AR, Nasser W, Bernard PE, DeLeo FR, Musser JM. 2016. Genomic Landscape of Intrahost Variation in Group A *Streptococcus*: Repeated and Abundant Mutational Inactivation of the fabT Gene Encoding a Regulator of Fatty Acid Synthesis. Infect Immun 84:3268-3281.
4. Jerga A, Rock CO. 2009. Acyl-Acyl carrier protein regulates transcription of fatty acid biosynthetic genes *via* the FabT repressor in *Streptococcus pneumoniae*. J Biol Chem 284:15364-8.
5. Lambert C, Poyart C, Gruss A, Fouet A. 2022. FabT, a Bacterial Transcriptional Repressor That Limits Futile Fatty Acid Biosynthesis. Microbiol Mol Biol Rev 86:e0002922.
6. Zou Q, Zhu L, Cronan JE. 2022. The *Enterococcus faecalis* FabT transcription factor regulates fatty acid synthesis in response to exogenous fatty acids. Front Microbiol 13:877582.
7. Zuo G, Chen ZP, Jiang YL, Zhu Z, Ding C, Zhang Z, Chen Y, Zhou CZ, Li Q. 2019. Structural insights into repression of the Pneumococcal fatty acid synthesis pathway by repressor FabT and co-repressor acyl-ACP. FEBS Lett 593:2730-2741.
8. Zhu L, Zou Q, Cao X, Cronan JE. 2019. *Enterococcus faecalis* Encodes an Atypical Auxiliary Acyl Carrier Protein Required for Efficient Regulation of Fatty Acid Synthesis by Exogenous Fatty Acids. mBio 10:e00577-19.
9. Longo M, De Jode M, Plainvert C, Weckel A, Hua A, Chateau A, Glaser P, Poyart C, Fouet A. 2015. Complete Genome Sequence of *Streptococcus pyogenes emm28* Clinical Isolate M28PF1, Responsible for a Puerperal Fever. Genome Announc 3.
10. Cunningham MW. 2008. Pathogenesis of group A streptococcal infections and their sequelae. Adv Exp Med Biol 609:29-42.
11. Carapetis JR, Steer AC, Mulholland EK, Weber M. 2005. The global burden of group A streptococcal diseases. Lancet Infect Dis 5:685-94.
12. Weckel A, Ahamada D, Bellais S, Mehats C, Plainvert C, Longo M, Poyart C, Fouet A. 2018. The N-terminal domain of the R28 protein promotes emm28 group A *Streptococcus* adhesion to host cells *via* direct binding to three integrins. J Biol Chem 293:16006-16018.
13. Six A, Bellais S, Bouaboud A, Fouet A, Gabriel C, Tazi A, Dramsi S, Trieu-Cuot P, Poyart C. 2015. Srr2, a multifaceted adhesin expressed by ST-17 hypervirulent Group B *Streptococcus* involved in binding to both fibrinogen and plasminogen. Mol Microbiol 97:1209-22.
14. Biswas I, Gruss A, Ehrlich SD, Maguin E. 1993. High-efficiency gene inactivation and replacement system for gram-positive bacteria. J Bacteriol 175:3628-35.
15. Hays C, Lambert C, Brinster S, Lamberet G, du Merle L, Gloux K, Gruss A, Poyart C, Fouet A. 2021. Type II Fatty Acid Synthesis Pathway and Cyclopropane Ring Formation Are Dispensable during *Enterococcus faecalis* Systemic Infection. J Bacteriol 203:e0022121.

Supplementary figures

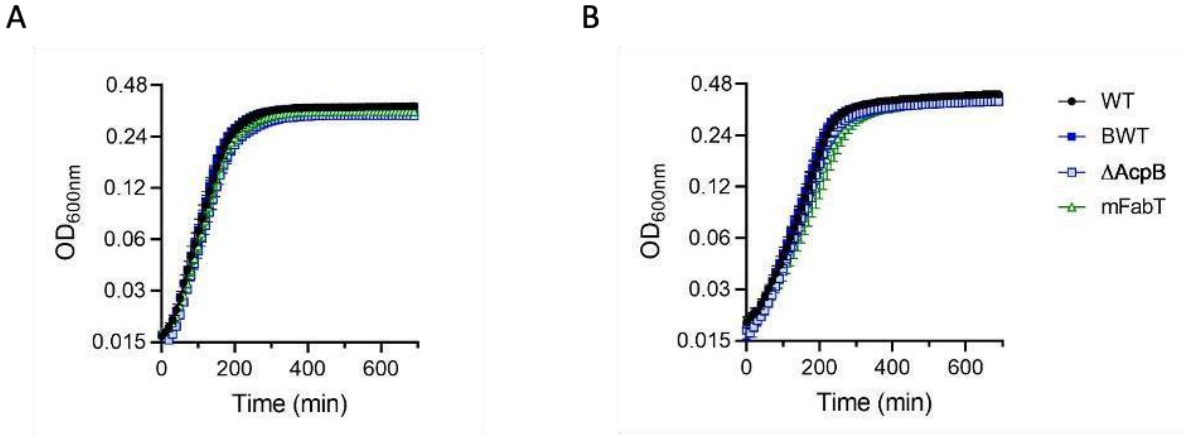

Figure S1. Influence of *acpB* mutation on bacterial growth capacity in rich media. Bacterial growth in A) THY, B) THY-Tween 80.

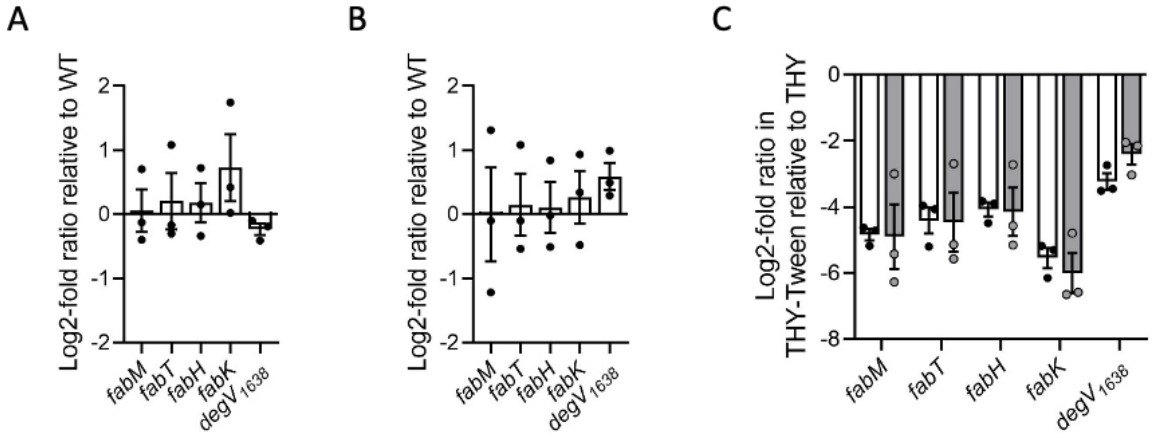

Figure S2. Comparison of the repression of FASII genes in *S. pyogenes* WT and BWT strains. Strains were grown in (A, C) THY or (B, C) THY-Tween 80 and RNAs were quantified by qRT-PCR. Expression was normalized to that of *gyrA*; (A, B) relative gene expression is expressed as the log2-fold ratio in BWT *versus* WT strain. C) The relative gene expression is expressed as the log2-fold ratio between a given strain grown in THY Tween 80 versus THY. Bars, white, WT; grey, BWT.

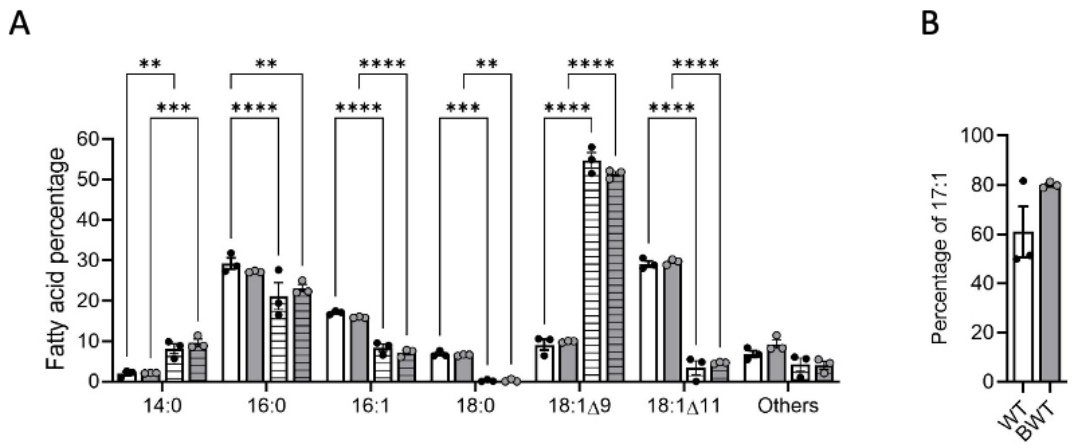

Figure S3. Membrane FA composition of WT and BWT strains. A) Fatty acid percentages in the membrane of WT and BWT strains grown in THY or THY-Tween 80. B) percentage of 17:1 in the membranes of WT and BWT strains grown in THY-17:1. Bars, white, WT; grey, BWT., empty THY, hatched THY-Tween 80. 2way ANOVA, Bonferroni post-test, **, $p < 0.01$; ***, $p < 0.001$; ****$p<0.0001$.

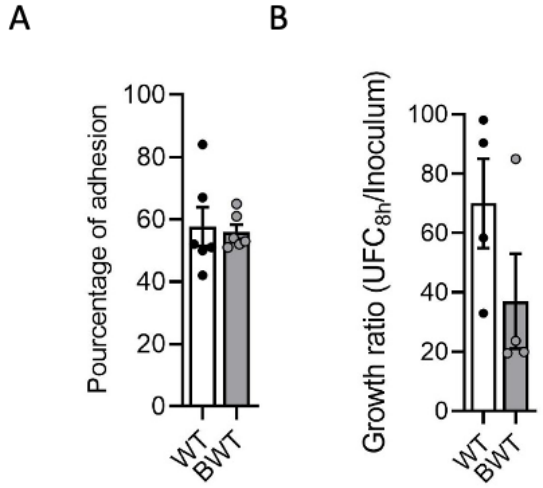

Figure S4. Adhesion and growth capacity of WT and BWT strains. Comparison of WT and BWT strains A) adhesion capacity, B) growth capacity in conditioned supernatants.

Supplementary Tables

Table S1. Strains and plasmids used in this study.

Strains or plasmids	Relevant properties	Source or reference
Streptococcus pyogenes		
WT	Wild-type representative *emm28* clinical isolate, M28PF1	1
mFabT	M28PF1 mutated in *fabT* C313T (H105Y)	Lambert *et al.* FabT manuscript
ΔAcpB	M28PF1 deleted in *acpB*	This study
BWT	Back-to-the-wild-type, the reverting strain of the ΔAcpB construction	This study
Escherichia coli		
Stellar™	F-, endA1, supE44, thi-1, recA1, gyrA96, phoA, Φ80d lacZΔ M15, Δ(lacZYA – argF) U169, Δ(mrr – hsdRMS –mcrBC), ΔmcrA, λ-	Clontech
Plasmids		
pG1	Thermosensitive broad-host-range vector	2
pG1-AcpB	pG1-AcpB construct for *acpB* deletion in *S. pyogenes*	This study

1. Longo M, De Jode M, Plainvert C, Weckel A, Hua A, Chateau A, Glaser P, Poyart C, Fouet A. 2015. Complete Genome Sequence of *Streptococcus pyogenes emm28* Clinical Isolate M28PF1, Responsible for a Puerperal Fever. Genome Announc 3
2. Biswas I, Gruss A, Ehrlich SD, Maguin E. 1993. High-efficiency gene inactivation and replacement system for gram-positive bacteria. J Bacteriol 175:3628-35.

Table S2. Consequences of a *acpB* deletion on fatty acid membrane composition in different media.

	THY			THY-Tween			*p-value* THY *vs* THY-Tween		
Strain	WT	ΔAcpB	mFabT	WT	ΔAcpB	mFabT	WT	ΔAcpB	mFabT
14:0 [a]	1.93 ± 0.82	1.42 ± 0.08	0.63 ± 0.09	8.13 ± 2.16	3.42 ± 2.48	0.87 ± 0.07	**	ns	ns
16:0	29.20 ± 2.34	27.64 ± 0.83	21.15 ± 2.58	21.15 ± 5.79	30.50 ± 1.52	27.06 ± 1.95	***	*	***
16:1	17.04 ± 0.46	12.55 ± 0.27	7.88 ± 1.82	8.34 ± 1.59	5.52 ± 0.80	4.59 ± 0.44	***	****	*
18:0	6.82 ± 0.71	15.78 ± 0.13	26.08 ± 0.71	0.20 ± 0.27	2.72 ± 0.49	12.39 ± 0.84	**	****	****
18:1Δ9	9.09 ± 2.37	9.99 ± 0.27	10.84 ± 1.98	54.80 ± 3.27	44.18 ± 0.99	30.36 ± 1.52	****	****	****
18:1Δ11	29.11 ± 1.30	25.46 ± 0.90	28.88 ± 1.21	3.41 ± 2.97	7.88 ± 0.24	20.12 ± 1.93	****	****	****
Others [b]	6.81 ± 1.48	7.15 ± 1.27	4.54 ± 1.21	4.22 ± 2.79	5.80 ± 2.00	4.47 ± 1.64	ns	ns	ns

[a] Percentage of total FAs.
[b] Fatty acids representing less than 2 % total FAs.

Table S3. Primers used in this study for cloning, checking cloning and PCR and PCR experiments.

Primer name	Sequence	Used for
P47	CGCCAGGGTTTTCCCAGTCACGAC	Plasmid for the ΔAcpB strain construction
RP48	AGCGGATAACAATTTCACACAGGA	Plasmid for the ΔAcpB strain construction
ermB-F	GAGTGTGTTGATAGTGCAGT	Plasmid for the ΔAcpB strain construction
ermB-R	TAGGCGCTAGGGACCTCTTTA	Plasmid for the ΔAcpB strain construction
AcpBamF	AAAGGATCCGGGATTGCTAATCCACGTGTTGGTCTA	Plasmid for the ΔAcpB strain construction
AcpBamR	CCTGTCTAGTCATTTACTTGAGTCTCCTTA	Plasmid for the ΔAcpB strain construction
AcpBavF	GGGAGACGTTTTAGATTATTTAGTTCAGCG	Plasmid for the ΔAcpB strain construction
AcpBavR	AAAGAATTCGCCTGCTATCACATTCCGTAACACC	Plasmid for the ΔAcpB strain construction
AcpBextam	GGAGCTAATGCTGAAAATACGGCAA	Plasmid for the ΔAcpB strain construction
AcpBavext	GGCGTTTCAAGAACACGTCCTTC	Plasmid for the ΔAcpB strain construction
gyrA1	CTGCTCGTATTACGGGTGATGT	qRT-PCR of *gyrA*
gyrA2	GGCGATAACTCCACCACTGA	qRT-PCR of *gyrA*
rpoB1	CCGTACACGTCGTAGCTTTT	qRT-PCR of *rpoB*
rpoB2	GCATCGTGGATACGAGCTTC	qRT-PCR of *rpoB*
FabM am	CTGTAGCTGGAGCGGCTTTTA	qRT-PCR of *fabM*
FabM av	CCGGTGCTAGTCCAACATTTAC	qRT-PCR of *fabM*
FabT-3’	CCCTAGTCCACGCACCAATGCCT	qRT-PCR of *fabT*
FabT-5’	GGGACAGTAACGACTAGCTTAAATA	qRT-PCR of *fabT*
FabH am	GGTGCCTACCAAAACGGAATG	qRT-PCR of *fabH*
FabH av	CACCAGCTCCGTCTCCAAAA	qRT-PCR of *fabH*
FabK am	CCAGGCGGGTATAATCGTTGT	qRT-PCR of *fabK*
FabKav	GCCAATATGTCCTCCAGCTTC	qRT-PCR of *fabK*
1638-Am	GCCAGCTTTCATCTTTTTCAAAAGG	qRT-PCR of $degV_{1638}$
1638-Av	GGGCAGAAGATCATGATATTGTC	qRT-PCR of $degV_{1638}$

* in bold, added restriction enzyme sites, EcoRI or BamH1.

Supplementary Material and Methods

Growth curves. *S. pyogenes* stationary precultures were diluted in THY or THY-Tween 80 to an OD_{600nm} = 0.05 and transferred to 96-well plates. These were incubated at 37 °C in a Thermo Scientific Multiskan GO (ThermoFischer Scientific) and growth was determined by measuring absorbance at 600 nm every 10 min after shaking the plates.

Partie 3 : Rôle de la protéine DegV$_{1638}$ chez *S. pyogenes.*

A novel mechanism of endogenous fatty acid excess control in *Streptococcus pyogenes.*

Clara Lambert[a], Thifaine Pouillon[a*], Qiufen Zhang[a‡], Alain Schmitt[a], Jean-Marc Masse[a], Karine Gloux[b], Claire Poyart[a,c] and Agnès Fouet[a].

[a] Université Paris Cité, Institut Cochin, INSERM U1016, CNRS UMR8104, Paris, France ;
[b] Micalis Institute, INRAE, AgroParisTech, Université Paris-Saclay, Jouy en Josas, France;
[c] AP-HP Centre-Université Paris Cité, Paris, France.

Orcid numbers: A. Fouet, 0000-0001-7715-9157; C. Lambert, 0000-0003-2740-1755.

Address correspondence to Agnes Fouet, agnes.fouet@inserm.fr.

[*] Present address: I-stem, Génopole, Corbeil-Essonnes, France

[‡] Present address: Medicinal Chemistry and Bioinformatics Center, Shanghai Jiao Tong University School of Medicine, Shanghai China.

Abstract

Membranes contain phospholipids that are composed of fatty acids (FA) and a polar head. Membrane homeostasis is crucial for bacterial growth and interaction with the environment. Streptococci control their FA synthetic pathway, FASII, *via* a transcriptional repressor that is active in the presence of long chain FAs. Furthermore, Gram-positive bacteria incorporate exogenous fatty acids which need to be phosphorylated to become substrate of the phospholipid biosynthetic pathway. This is carried out by the Fak complex which is composed of two subunits, FakA and FakB. FakA is the kinase. FakB proteins are members of the DegV family, known to bind fatty acids. FakB are of two or three types depending on the bacterial species and they bind, respectively, saturated and unsaturated, or saturated, mono-unsaturated and poly-unsaturated fatty acids. In some species, a fourth DegV protein is present whose role has not been determined. *Streptococcus pyogenes*, which causes a wide variety of diseases ranging from mild non-invasive to severe invasive infections, possesses four DegV family proteins. The *degV$_{1638}$* gene was co-regulated with the FASII genes. The

membrane fatty acid and lipid compositions of the *degV* mutant and the wild-type strains were identical. However, the *degV* mutant strain produced more phospholipids than the wild-type strain. Excess phospholipids were found as extracellular membrane vesicles. Altogether, our data suggested that DegV stocks supernumerary endogenous fatty acid molecules. As such DegV would constitute a new mechanism involved in the detoxification of endogenous fatty acid excess.

IMPORTANCE

Membrane fatty acid (FA) composition is crucial for bacterial growth or interaction with the environment. Bacteria can synthesize and incorporate FAs. The incorporation is dependent on FA phosphorylation, which involves a kinase, FakA, and a FA binding protein, FakB; FakBs are members of the DegV family of proteins. *Streptococcus pneumoniae* possesses three FakB proteins, binding saturated, mono-unsaturated and poly-unsaturated FAs. *Streptococcus pyogenes* that causes a wide variety of diseases ranging from mild non-invasive to severe invasive infections possesses a fourth DegV protein. A *degV* mutant strain produces more phospholipids than the wild-type strain, indicating that DegV binds supernumerary endogenous FAs. The phospholipid excess present in the mutant strain is found as extracellular membrane vesicles. Hence, DegV participates in FA detoxification.

Key words

Streptococcus pyogenes, fatty acids, DegV family proteins, detoxification, extracellular membrane vesicles

Introduction

Cell membranes commonly comprise a phospholipid bilayer composed of a polar head and an apolar body constituted of fatty acids (FA). FA structure and length are decisive for membrane topology and properties such as fluidity, permeability and integrity. These features are crucial for the adaptation of bacteria to various environments (1). Most bacteria synthesize FA *via* the FASII pathway. The FASII gene expression is, depending on the species, controlled by feed-forward or feedback mechanism. In streptococci, *Enterococcus faecalis* and *Lactococcus lactis*, a feedback mechanism involves the FabT repressor, a member of the MarR family (2). The FabT corepressor is an acyl-Acyl Carrier Protein (ACP), the affinity of the FabT-acyl-ACP interaction with DNA increasing with the length of the acyl carbon chain and the presence of unsaturation (3, 4). The FASII pathway is not essential in Firmicutes that use exogenous FAs (eFAs) to synthesize their phospholipids (5-8). Incorporation of eFAs into the phospholipids of Gram-positive pathogens involves a FA kinase (Fak) complex that phosphorylates eFAs, yielding a substrate for the phospholipid synthesis. The acyl-PO_4 is used by PlsY or transformed in an acyl-ACP that is either used by PlsC or elongated *via* FASII (9). The Fak complex is composed of two proteins; FakA provides the kinase activity and it interacts with proteins of the DegV family (10, 11). DegV proteins bind FA with high affinity indicating that DegV proteins may take part in lipid transport and, in complex with other proteins, in FA metabolic processes (12). DegV proteins interacting with FakA have been named FakB (10). Single *fakA* genes are found in bacteria belonging to the Firmicutes, whereas, *degV* genes are multiple; two, three and four have been respectively identified in *Staphylococcus aureus*, *Streptococcus pneumoniae*, and *Enterococcus faecalis* and *S. suis* (4, 10, 13, 14). In *S. aureus*, FakB1 and FakB2 bind exclusively saturated and preferentially unsaturated FAs, respectively. In *S. pneumoniae* FakB1, FakB2 and FakB3 bind saturated, mono-unsaturated and poly-unsaturated FAs, respectively. In *E. faecalis* FakB1 binds preferentially saturated FAs, whereas the three others bind unselectively FAs. The role of FakB4 could not be studied in *S. suis* by the biochemical approach used because it appeared as inclusion bodies *in vitro* (14). Four DegV family protein are found in S*. pyogenes* (15, 16).

S. pyogenes (group A *Streptococcus*, GAS), a Gram-positive bacterium, is an important human pathogen responsible for a large variety of clinical manifestations ranging from mild superficial infections to more life-threatening invasive infections including necrotizing fasciitis

(NF), streptococcal toxic shock syndrome (STSS). GAS infections are also responsible for post-infectious complications such as rheumatic arthritis and glomerulonephritis (17). Altogether, GAS infections are responsible for 517,000 deaths annually worldwide (18).

The phylogenetic proximity of *S. pyogenes* and *S. pneumoniae* and *S. suis* suggests they all possess three *sensu stricto* FakB proteins, and questions the role of the fourth DegV protein. To address this question, we determined whether $degV_{1638}$ is coregulated with the FASII genes. We also constructed a $degV_{1638}$ mutant strain and compared the FA and lipid compositions of its membrane to that of the wild-type strain. We also characterized the becoming of the FAs not taken care of by DegV in the mutant strain.

Results

DegV is shared by various Gram-positive species. The *degV*$_{1638}$ product, coined DegV, belongs to the DegV protein family. We wondered whether it could be a fourth FakB protein. We extracted the three *S. pyogenes* WT FakB sequences (M28_Spy0652, FakB1; M28_Spy1165, FakB2; M28_Spy1434, FakB3) and the three *S. pneumoniae* TIGR4 FakB sequences and compared them (13) (Table 1). The identity percentage was around 60 % for the homologous proteins and covered the entire length of the proteins, A DegV protein was then sought in *S. pneumoniae* TIGR4 strain and none was found. The closest protein highlighted in the Blastp search was FakB1, with 40.46 % identity with only 58 % of the protein length covered. However, when tBlastn searches were carried out on all the *S. pneumoniae* available genomes, genomes encoding four DegV family members were recovered, displaying, for example, 56.29 % identity, for one and 27.30 % to 24.09 % identity for the three others, on 100 % to 94 % of the length. This indicates that these strains possess a DegV protein in addition the three FakB proteins. When the *S. agalactiae* database was similarly screened, genomes with only three DegV family proteins were recovered. This indicated that DegV is not a streptococci ubiquitous protein, but is not restricted to *S. pyogenes*. The search was also carried out on *Enterococcus faecalis* genomes and strains with four DegV family members, sharing 36.33 % identity for one, and 23 to 25 % identity for the three others, on 100 % to 95 % of the protein lengths were recovered. Hence, a fourth DegV family protein is present also outside the streptococci. The physiological role of this protein remained undetermined.

Table 1. Sequence comparison between *S. pyogenes and* S. *pneumoniae* FakB and DegV proteins.

S. pyogenes	*S. pneumoniae*	Identity (%)	Length coverage (%)
FakB1	FakB1	57.39	98
FakB2	FakB2	63.89	100
FakB3	FakB3	61.72	100
DegV	FakB1	40.46	58

The *degV*$_{1638}$ gene is controlled by FabT. DegV proteins have been characterized as FA binding proteins, so we wondered whether *degV*$_{1638}$ could be coregulated with the FASII genes. We compared by qRT-PCR, the relative expressions of *fabT*, A FASII gene that is repressed by FabT, and *degV*$_{1638}$ in a *fabT* mutant strain (mFabT, Table S3) versus WT strain grown in THY and

THY-Tween 80 (Fig. 1A). The expression of both genes was unchanged in THY but strongly derepressed in the mFabT strain grown in THY-Tween. This confirmed that *degV*$_{1638}$ is coregulated with the FASII genes. Consensus FabT binding sequences are found along the FASII locus [(2), and references herein]. We sought whether one was also present downstream from the *degV*$_{1638}$ transcription start site previously described (19). Using ANTTTGATTATCAAATT as a probe, we found the sequence, ATTTTGATTATCAAA, that shows 100 % identity on 15 out of 17 nucleotides (Fig. 1B). This suggests that *degV*$_{1638}$ is directly controlled by FabT.

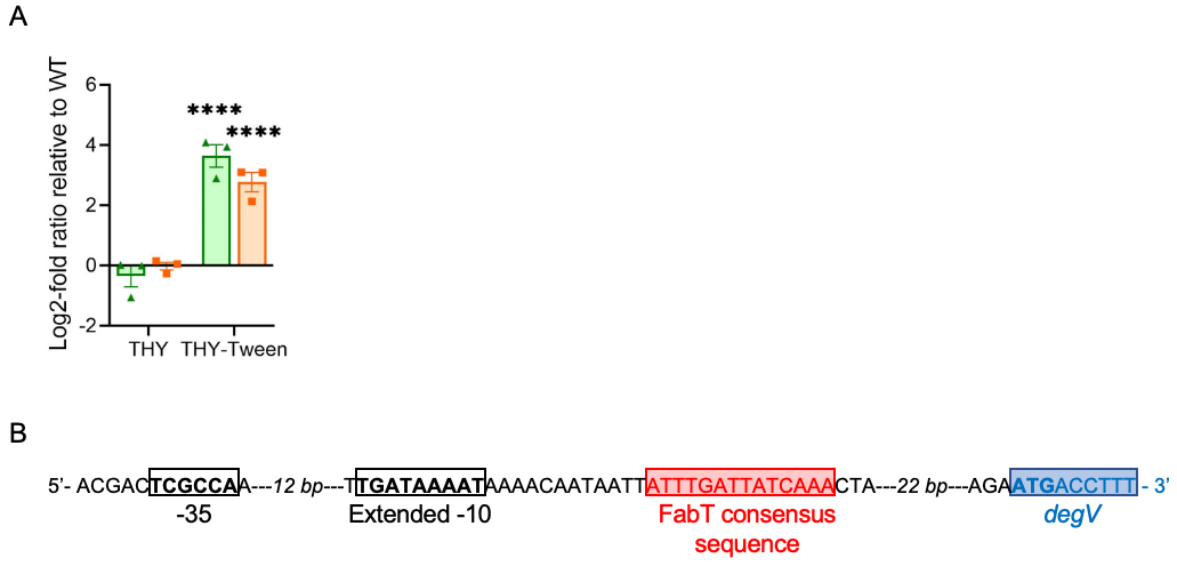

Figure 1. The *degV*$_{1638}$ gene belongs to the FabT regulon. A) Relative expression of *fabT*, green, and *degV*$_{1638}$, orange, in the mFabT versus the WT strain. Strains were grown in THY or THY-Tween medium and RNAs were quantified by qRT-PCR. Expression was normalized to that of *gyrA*; relative gene expression is expressed as the log2-fold ratio in the mFabT versus the WT strain. 2-way ANOVA, Bonferroni post-test, ****p<0.0001. B) Cartoon representing the regulatory region of the *degV*$_{1638}$ gene with -35 and extended -10 boxes, previously published (19), FabT consensus sequence and *degV*$_{1638}$ translation initiation site indicated in black, red and blue, respectively.

Construction and growth characteristic of the mDegV mutant strain. To further characterize the role of DegV, we constructed an isogenic mutant strain in which *degV* is interrupted by the insertion of a plasmid containing a *degV*$_{1638}$ internal fragment. We hypothesized that the growth characteristics of the WT and mDegV strain would be identical in rich laboratory medium, but may differ in unsaturated or in a mix of saturated and unsaturated FA-containing medium, if DegV was involved in specific FA uptake (Fig. S1). However, both strains had exactly the same growth characteristics at 37 °C in THY, THY-Tween or THY-FBS.

***S. pyogenes* WT and mDegV strains contain different lipid quantities.** The Fak complexes, containing the kinase FakA interacting with various FakB isoforms are responsible for eFA incorporation (10). *S. pneumoniae* wild-type and FabT mutant strains differ in their FA contents (20). The expression of $degV_{1638}$ is controlled by FabT in *S. pyogenes*. We thus hypothesized that an absence of DegV may influence the FA membrane composition in either FA supplemented or non-supplemented media and we determined the composition of the WT, mDegV and BWT strains grown in various media (Fig. 2A, B, D, Table S1). The composition of the WT and BWT strains were, with one exception of small amplitude, always identical. The FA composition was similar in WT, mDegV strains grown in THY (Fig. 2A, Table S1). The addition of Tween 80 strongly modified the composition of *S. pyogenes* membrane with strong diminution of 16:0 and 16:1 and rise of 18:1Δ9 relative concentrations, signing the influence eFA incorporation and FASII arrest. Again, no difference was observed between the WT and mDegV strain membranes (Fig. 2B, Table S1). This suggested that both strains incorporated similarly eFAs. This was checked by assessing the percentage of 17:1, that is not produced by the bacteria, after its addition to the culture medium (Fig. 2C). The percentage in both strain membranes was the same confirming the absence of eFA incorporation defect in the mDegV strain. However, 17:1 and 18:1Δ9, provided by Tween, 80 are monounsaturated FAs. We reasoned that if DegV was specific for other FAs, a difference may have been unnoticed. We consequently also determined the FA composition after growth in the presence of human plasma that also contains saturated and poly-unsaturated FAs (Fig. 2D, Table S1). Again, the membrane composition was different from those found in THY and THY-Tween 80 grown bacteria. The concentration of poly-unsaturated 18:2 and 20:4 strongly rose, indicating that, in contrast to *Staphylococcus aureus*, but as already shown for *S. pneumoniae*, *S. agalactiae* and *E. faecalis*, *S. pyogenes* incorporated poly-unsaturated FAs (5, 6, 13). However, the composition of both strains was again similar, indicating that, whatever the environment, the mDegV strain had no membrane FA composition defect. It also suggested that either the role of DegV is redundant with that of one of the FakB proteins or that DegV is not involved in eFA incorporation.

FakB proteins are involved in the transfer of eFAs to the FASII pathway for elongation or to the phospholipid synthesis pathway. The FA being unmodified in the mDegV strain, we analyzed the lipid contents in the strains (Fig. 2E-G, Table S2). Contrary to FA analysis that

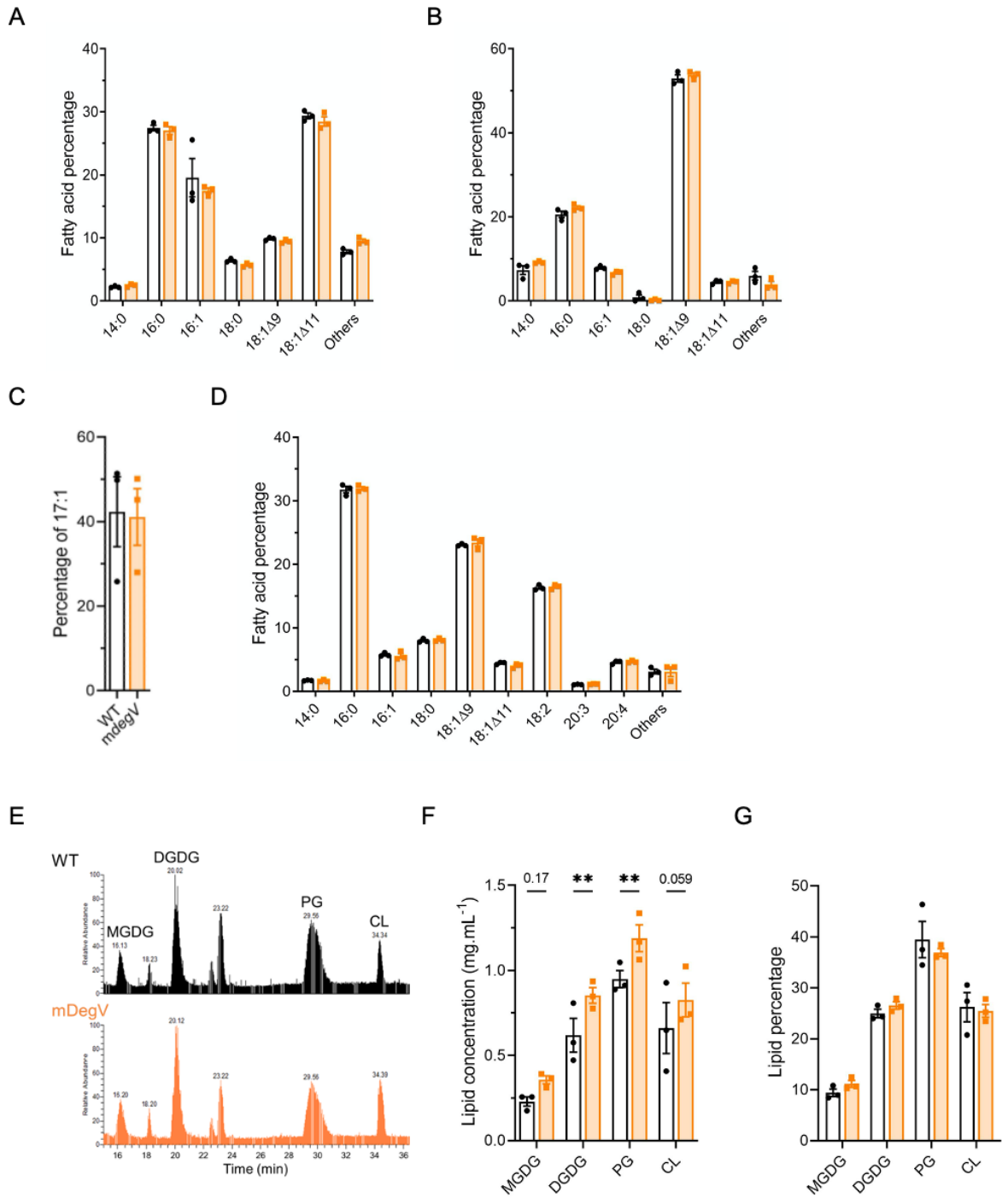

Figure 2. The WT and mDegV strains show identical relative FA and lipid compositions, but different lipid quantities. A, B, D) Membrane fatty acid percentage of WT and mDegV strains grown in A) THY, B) THY-Tween, D) THY-Plasma; C) Membrane 17:1 percentage in WT and mDegV strains grown in THY-17:1; A-D, N=3 (Table S1). E-G) Lipid content in the WT and mDegV strains grown in THY, by class of lipids: E-F) lipid composition; E) HPLC-MS profile representing the main lipid classes, F) lipid concentration, G) ratio of lipid classes; F-G) N=3 (Table S2). Bars and symbols, white, WT strain; orange, mDegV strain; MGDG, monogalactosyldiacylglycerol; DGDG, digalactosyldiacylglycerol; PG, phosphatidylglycerol; CL, cardiolipin. 2-way ANOVA, Bonferroni post-test, **p<0.01; p values are indicated when between 0.05 <p<0.2.

yields a relative composition within the bacterial membrane, the lipid analysis indicates the concentration of each class of lipid per volume of sample; since we normalized the samples per cfu, we obtained the quantity of lipid proportional to the number of cfus. (Fig. 2E, 2F). The digalactosyldiacylglycerol and phosphatidylglycerol concentrations were higher in the mDegV than in the WT strain and there was a trend to similar increases for the monogalactosyldiacylglycerol and the cardiolipins. To assay whether the concentration differences were due to differences in relative composition between strains or in total quantity of phospholipids per cfu, we calculated the former (Fig. 2G, Table S2). The ratios of the different phospholipid classes were, like those of the FAs, identical between both strains. Altogether, these results indicated that the mDegV strain harbors more phospholipids than the WT strain.

The mDegV strain expels an excess of extracellular vesicles. FA availability sets cell envelope capacity which in turn affects cell size (21). We consequently hypothesized that the phospholipid excess may give rise to a morphology variation or a diameter increase to compensate the material increase. Both strains were consequently observed by transmission electron microscopy (TEM) and the diameter of bacteria measured (Fig. 3A, 3B). Both strains displayed the same bacterial morphology (Fig. 3A). Also, the bacterial sizes were similar (Fig. 3B). A close examination of the TEM images indicated the presence of structures composed of double membranes, extracellular membrane vesicles (EMV), at the surface of *S. pyogenes* during the exponential phase (Fig. 3A). Their relative abundance in WT, mDegV and BWT strains was compared (Fig. 3C). There were 2.5-fold more EMVs at the surface of the mDegV strain than of the WT or BWT strains. We wondered whether an excess of EMVs could also be shed in the culture supernatants and quantified these by TEM images of pelleted supernatants (Fig. 3D, 3E). Three times more EMVs were found in the mDegV than in the WT or BWT strain supernatants. These data indicated that a *S. pyogenes* strain devoid of DegV expels phospholipid excess.

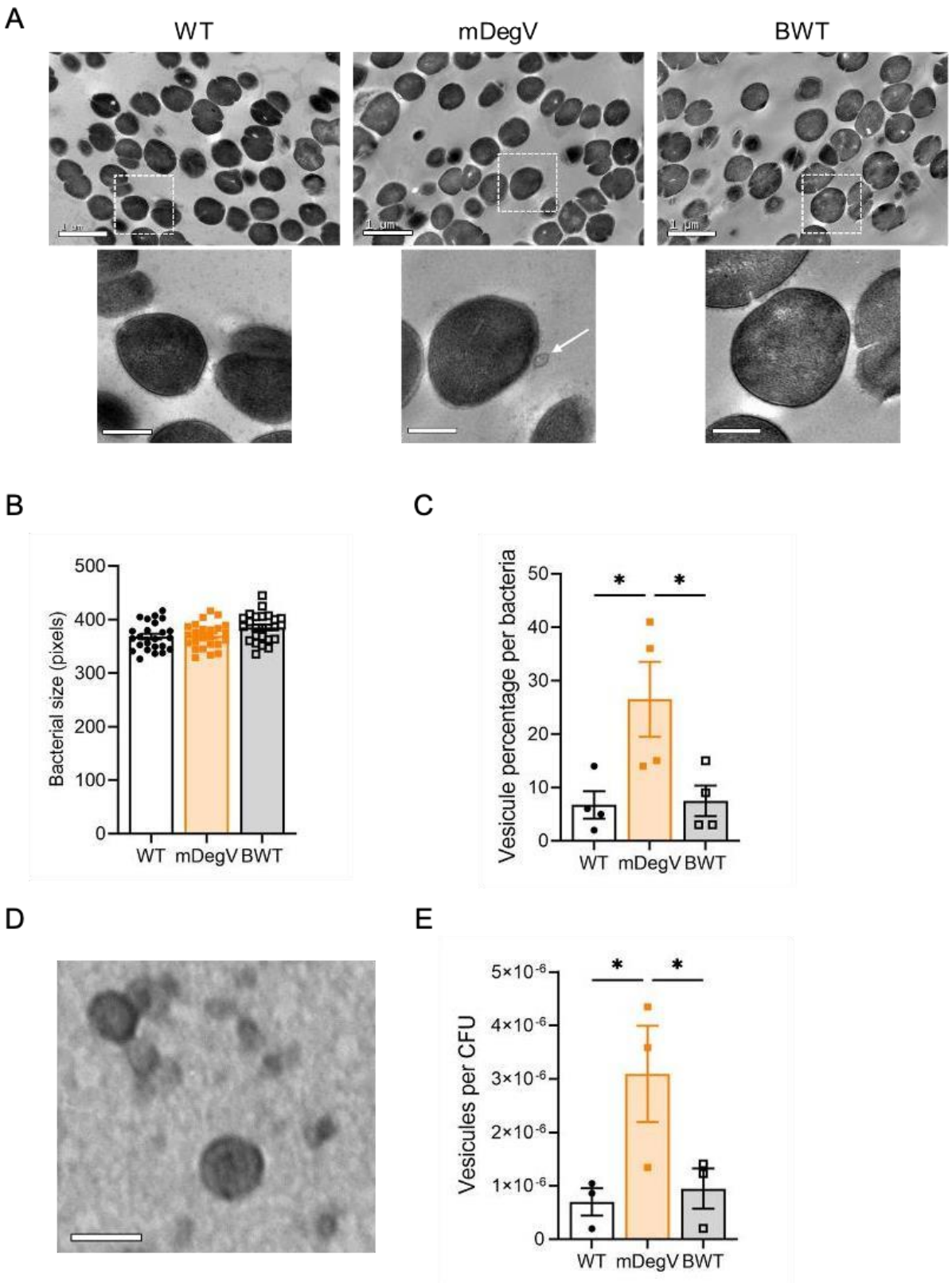

Figure 3. The mDegV strain secretes extracellular vesicles. A) TEM images of bacterial sections, left WT, middle, mDegV, right, BWT 4000X (scale = 1μm) (insets scale = 250 nm), B, C) Image analysis, B) bacterial diameter length, N=4, 24 independent images, C) percentage of vesicles per bacteria, N=4, 67 independent images. D) TEM images, of extracellular membrane vesicles contained in mDegV culture supernatant (scale = 40 nm); E) Image analysis N = 3, 30 independent images. B, C, E) One-way ANOVA, Bonferroni post-test, *$p<0.05$.

Discussion

FakB proteins, members of the DegV family of proteins, take up eFAs and within the FakA-FakB complexes, FakA, the kinase, phosphorylates the free FAs yielding substrates for PlsX or PlsY (9, 10, 13). The specific roles of FakB1, FakB2 and FakB3, when present, have been characterized in *S. aureus*, S. *pneumoniae* and *S. suis* (10, 13, 14). However, some species possess a fourth DegV protein whose role has not been demonstrated (14). The gene encoding *S. pyogenes* fourth DegV protein is coregulated with the FASII genes, whose products synthesize endogenous FAs. This suggests that, whereas FakBs are involved in eFA binding, the role of DegV is connected to endogenous FAs. It is consequently tempting to hypothesize that it binds free FAs that may be found in the cytosol (22).

The DegV mutant strain produced more lipids than its wild-type counter-part. This indicates that more acyl molecules are available in a *degV* mutant than in the wild-type strain. This strongly supports the binding of acyl molecules by DegV. It further indicates that, in contrast to FakB-bound acyl molecules, the DegV-bound acyl moieties are not subsequently transferred to the phospholipid biosynthetic pathway. As such, DegV would be an Acyl Carrier Protein that would not support the incorporation of the acyl moiety in phospholipids. Since unsaturated long chain FAs participate in the repression of the FASII pathway, they limit the *de novo* synthesis of both FA and DegV (4). Saturated FAs are less efficient as corepressors. The additional DegV molecules may have an important role in sequestering eventual saturated FA excess. Various FA detoxification mechanisms have been described [for review, (23)]. Among them, β-oxidation counteracts excess fatty acids in many bacteria. However, *S. aureus* that is unable to carry out this reaction possesses FarE, an efflux pump, which displays a detoxification function (24). None of these mechanisms have been described in streptococci. *S. pyogenes* possesses a hydratase, the myosin cross-reactive antigen, that catalyzes the hydration of *cis*-9 and *cis*-12 double bonds (25). Its gene is overexpressed in a *fabT* mutant strain in conditions that yield membrane composition modifications and hence FabT activity (15). The hydration of unsaturated FAs prevents their accumulation which is detrimental to the bacteria. However, this mechanism produces saturated FAs, which may thus accumulate inside the bacterium. This supports the hypothesis that DegV binds preferentially saturated FAs.

Microbial cell size is dependent on FA availability (21). In contrast to expectation, the enhanced phospholipid abundance in the *degV* mutant strain did not result in an increased cell size. However, the phospholipid excess was found in EMVs. EMV production has been reported in *S. pyogenes* (26-29). It is negatively regulated by the CovRS, a two-component system that controls the expression of 15 % of *S. pyogenes* genes and that is turned down in response to sub-lethal concentrations of antimicrobial peptide LL-37 (26, 30). In agreement with this regulation, extracellular membrane vesicles production was triggered by LL-37 (27). This indicates that EMV production is stimulated in the host, where *S. pyogenes* is in the presence of eFAs. EMV production may be a FA detoxification mechanism as in *S. aureus* that releases membrane vesicles. These act as decoys to protect bacteria against antimicrobial FAs (31). In *S.* pyogenes, EMVs are more abundant during late exponential or early stationary growth phase (26). In contrast, in the DegV mutant strain, the EMVs were abundant already during the exponential phase, in the absence of antimicrobial peptide, hence, in conditions where they are not normally highly produced as confirmed by the analysis of the wild-type strain. This suggests that DegV limits their production during exponential phase by binding supernumerary endogenous FAs. We suggest that expulsion of excess of FA *via* membrane vesicles can be a detoxification mechanism against an excess of endogenous FAs, as encountered in a DegV mutant strain.

Altogether, this study suggests that whereas, the FakBs are fatty acid binding proteins that exchange bound fatty acid/acyl-phosphate with fatty acid/acyl-phosphate presented in detergent micelles or liposomes (10), DegV prevents the formation of micelles or liposomes and, as such, is a protective factor against endogenous FA.

Materials and Methods

Bacterial strains and culture conditions. The strains used in this study are described in Table S3. *S. pyogenes* strains were grown under static condition at 37 °C in Todd Hewitt broth supplemented with 0.2 % Yeast Extract (THY) or on THY agar plates. To study, the role of eFA addition, the medium was supplemented with 0.1 % Tween 80 (THY-Tween 80) (Sigma-Aldrich, P1754), essentially composed of 18:1Δ9, or 100 µM 17:1 (Larodan, Sweden), or 10 % Fetal Bovine Serum (THY-FBS), essentially composed of, approx., 43 % saturated, 23 % mono-unsaturated and 8 % polyunsaturated FAs (Gibco), or 10% human plasma (Etablissement Français du Sang) (THY-Plasma). For all experiments, strains were prepared as follows. Overnight cultures were diluted to an OD_{600nm} = 0.05 and grown in THY to the exponential phase (OD_{600nm} comprised between 0.4 and 0.5). The mDegV strain was grown in the presence of 10 µg.ml^{-1} erythromycin. *E. coli* strains were grown in LB or on LB agar plates supplemented with 150 µg.ml^{-1} erythromycin when appropriate.

In silico analysis. *S. pyogenes* FakB protein sequences were extracted from the *S.* pyogenes M28PF1 strain, named WT in this study, using the Geneious software, searching for "DegV". The FakB sequences of the *S. pneumoniae* TIGR4 strain (WP_000762061, WP_000161399, WP_000219939) were collected from NCBI. The DegV protein sequence was used to search for a DegV homolog, a fourth DegV protein, in *S. pneumoniae* TIGR4 using Blast-P, on NCBI non-redundant protein sequences database, *S. pneumoniae* TIGR4 (taxid:170187). From this search were also extracted the identity and protein length coverage percentages. The presence of three or four DegV proteins in other *S. pneumoniae* strains, in *S. agalactiae* and in *E. faecalis* were carried out as follows. The DegV protein sequence was used to search *via* TBlast-N the entire genomes of strains contained in NCBI RefSeq Genome Database (refseq_genomes, September 2022) entering the name of a single species. The protein sequences of all the contigs of the first best matches were then searched by BlastP and the number of proteins highlighted and alignments analyzed.

The presence of putative FabT binding sequences on the M28PF1 genome was sought with the ANTTTGATTATCAAATT sequence as a probe, accepting up to 2 mismatches using Geneious prime Biomatters development, www.geneious.com (2).

RNA isolation *S. pyogenes* strains were cultured at 37 °C in THY or THY-Tween, and cells were harvested at exponential growth phase (OD comprised between 0.4 and 0.5). After adding 2 volumes of RNA protect* (Qiagen) Total RNA was extracted from three independent cultures for each condition after lysing the bacteria by a 30 min 15 $mg.ml^{-1}$ lysozyme, 300 $U.ml^{-1}$ mutanolysine treatment at 20°C followed by two cycles of Fast-prep (power 6, 30 s) at 4 °C, using the Macherey-Nagel RNA extraction kit, as indicated. RNA integrity was analyzed using an Agilent Bioanalyzer (Agilent Biotechnologies) and a PCR. Absence of DNA was further confirmed by PCR.

First-strand cDNA synthesis, quantitative PCR qPCR. Five hundred nanograms of total RNA was used for first-strand cDNA synthesis using SuperScriptTM II reverse transcriptase and random primers according to the manufacturer's instructions (Invitrogen, Life technologies).

Quantitative PCR was carried out with SYBR Green PCR kits (Applied Biosystems, Life technologies) using four pairs of primers (Table S4). *gyrA* and *rpoB* were used as the housekeeping reference genes. Relative quantification of specific gene expression was calculated with the $2^{-\Delta\Delta Ct}$ method using *gyrA* as the reference gene and expressed in log2-fold change. Each assay was performed in triplicate on each sample.

Strain construction. The primers used for the generation of the plasmids and verifying the different strains are described in Table S4. The mFabT strain harbors a point mutation in *fabT*; the mDegV strain corresponds to an insertion. They were obtained by homologous recombination of the plasmid pG1-mFabT or single cross-over with the plasmid pG1-DegVint2, respectively, following the same protocol as described previously (32, 33). Regarding the *fabT* mutation, the plasmid pG1-mFabT was obtained by amplifying nucleotides -222 to +805, relative to the translation start site from the chromosome of a spontaneous mutant from our collection, CCH1963, where the C in position 313 was replaced by a T, leading to the replacement of the histidine in position 105 by a tyrosine. For the mDegV strain, an internal fragment, from nucleotides 296 to 601 was amplified and cloned in pG1 using the In Fusion cloning kit® (Clonetech) giving rise to the plasmid pG1-DegVint2. The plasmid was then inserted by a single cross-over event in M28PF1 chromosome, resulting in the interruption of $degV_{1638}$. The mDegV back-to-the wild-type (BWT), *i.e.* reversion of the single cross-over and restauration of a wild-type $degV_{1638}$, was carried out as previously described (32, 33). The absence of surreptitious mutations in the strains was verified by whole genome sequencing.

Fatty acid analysis. Strains were grown in THY, THY-Tween 80, THY-Plasma or THY-17:1 until OD_{600nm} = 0.4 - 0.5. Fatty acids were extracted and analyzed as previously described (6).

Lipids analysis. Strains were grown in THY until OD_{600nm} = 0.4 - 0.5. Lipid extractions were performed as previously described (8). Lipids were identified following the method previously described (34). The lipids separation was realized by normal phase HPLC (U3000 ThermoFisher Scientific) using a Inertsil Si 5µm column (150 x 2.1 mm I.D.) from GL Sciences Inc (Tokyo, Japan). Lipids were quantified using a Corona-CAD Ultra and identified by mass-spectrometry negative ionization and MS^2/MS^3 fragmentation (LTQ-Orbitrap Velos Pro). The concentration of each lipid class was determined as previously described using as standards DGDG, 840524P-5MG; MGDG, 840523P-5MG; CL (heart CA), 840012P-25MG; PG (egg), 841138P-25MG (35). Lipids spectra were analyzed on Xcalibur™ software (ThermoFisher Scientific, version 4.2.47).

Bacterial morphology and size analysis. THY exponential phase cultures ($0.4 < OD_{600nm} < 0.5$) were centrifuged and the pellets resuspended in 1 ml phosphate buffer saline (PBS) twice and incubated at 4 °C with a fixative solution (4 % paraformaldehyde and 2.5 % glutaraldehyde). After 30 minutes, bacteria were washed three times in PBS then treated as previously described, with slight modifications (21). Secondary fixation was performed with 1 % osmium tetroxide in PBS for 1 h at room temperature, then bacteria were centrifuged, the pellets washed 3 times in H_2O and further dehydrated with increasing concentrations of ethanol (70 %, 90 %, and 100 % twice). After dehydration, pellets were infiltrated with sequential 3:1, 1:1, and 1:3 solutions of resin (Embed 812 kit; Electron Microscopy Sciences, Hatfield, PA) and 100 % ethanol for 1 h separately at room temperature. Finally, the samples were incubated with propylene oxide for 2 m and placed in the embedding molds with resin. The embedding resin blocks were polymerized in an oven at 60 °C for 24 h.Ultrathin sections (90 nm) were cut from the block surface using an ultramicrotome (Reichert Ultracut S ultramicrotome, Leica Microsystems) then stained with uranyl acetate and lead citrate (LFG, France) and observed by TEM (JEOL 1011, JEOL, Japan)) at 80 kV of acceleration voltage. Acquisitions were performed by an Orius 1000 CCD Camera (GATAN, USA) using Digital Micrograph software (GATAN, USA).

To determine the bacterial size, on each independent image, the larger bacteria were selected as representative of those sliced through the sphere diameter. The pixels along the diameter were then quantified.

Extracellular vesicle isolation and quantification. Extracellular vesicles were isolated from *S. pyogenes* strains cultured at 37 °C in THY as described previously (26). Phosphate buffer saline-washed pellets were further processed as follows. Small sample droplets (20 µl) were deposited on 200 mesh formvar coated copper grids for 2 min. The excess of sample solution was removed by blotting the grid with filter paper (Whatman). Grids were incubated with a drop of staining solution (uranyle acetate) for 2 min and blotted with a filter paper. The grid was deposited on a filter paper. Samples were immediatly examined in a JEOL 1011 transmission electron microscope (JEOL, Japan) with an ORIUS 1000 CCD camera (GATAN, France), operated with Digital Micrograph software (GATAN, France) for acquisition.

Acknowledgments

We thank A. Gruss for her constant interest and support. We thank Audrey Solgadi and Bastien Prost (UMS-IPSIT - Plateforme SAMM, Université Paris-Saclay) for performing HPLC-MS experiments and for their help with the lipid analysis; Sonia Abreu (LipSys², Université Paris-Saclay) for total lipids separation development. We thank Maëva Gauduin undergraduate in the laboratory for technical help.

CL was supported by Université Paris Cité (BioSPC, n°51809666), FRM (FDT202106012831) and FEMS (FEMS Congress Attendance Grant for poster n° 7875 in 2021 and FEMS grant - LISSSD 2022 n° LISS-213065). QZ was supported by bourse SSHN jeune chercheur and innovative research team of high-level local universities in Shanghai (SHSMU-ZDCX20212700). This work was supported by DIM One Health (RPH17043DJA)

References

1. Zhang YM, Rock CO. 2008. Membrane lipid homeostasis in bacteria. Nat Rev Microbiol 6:222-33.
2. Lambert C, Poyart C, Gruss A, Fouet A. 2022. FabT, a Bacterial Transcriptional Repressor That Limits Futile Fatty Acid Biosynthesis. Microbiol Mol Biol Rev 86:e0002922.
3. Jerga A, Rock CO. 2009. Acyl-Acyl carrier protein regulates transcription of fatty acid biosynthetic genes *via* the FabT repressor in *Streptococcus pneumoniae*. J Biol Chem 284:15364-8.
4. Zou Q, Zhu L, Cronan JE. 2022. The *Enterococcus faecalis* FabT transcription factor regulates fatty acid synthesis in response to exogenous fatty acids. Front Microbiol 13:877582.
5. Brinster S, Lamberet G, Staels B, Trieu-Cuot P, Gruss A, Poyart C. 2009. Type II fatty acid synthesis is not a suitable antibiotic target for Gram-positive pathogens. Nature 458:83-6.
6. Hays C, Lambert C, Brinster S, Lamberet G, du Merle L, Gloux K, Gruss A, Poyart C, Fouet A. 2021. Type II Fatty Acid Synthesis Pathway and Cyclopropane Ring Formation Are Dispensable during *Enterococcus faecalis* Systemic Infection. J Bacteriol 203:e0022121.
7. Parsons JB, Frank MW, Subramanian C, Saenkham P, Rock CO. 2011. Metabolic basis for the differential susceptibility of Gram-positive pathogens to fatty acid synthesis inhibitors. Proc Natl Acad Sci U S A 108:15378-83.
8. Kenanian G, Morvan C, Weckel A, Pathania A, Anba-Mondoloni J, Halpern D, Gaillard M, Solgadi A, Dupont L, Henry C, Poyart C, Fouet A, Lamberet G, Gloux K, Gruss A. 2019. Permissive Fatty Acid Incorporation Promotes Staphylococcal Adaptation to FASII Antibiotics in Host Environments. Cell Rep 29:3974-3982 e4.
9. Parsons JB, Frank MW, Jackson P, Subramanian C, Rock CO. 2014. Incorporation of extracellular fatty acids by a fatty acid kinase-dependent pathway in *Staphylococcus aureus*. Mol Microbiol 92:234-45.
10. Parsons JB, Broussard TC, Bose JL, Rosch JW, Jackson P, Subramanian C, Rock CO. 2014. Identification of a two-component fatty acid kinase responsible for host fatty acid incorporation by *Staphylococcus aureus*. Proc Natl Acad Sci U S A 111:10532-7.
11. Meier M, Sit RV, Quake SR. 2013. Proteome-wide protein interaction measurements of bacterial proteins of unknown function. Proc Natl Acad Sci U S A 110:477-82.
12. Schulze-Gahmen U, Pelaschier J, Yokota H, Kim R, Kim SH. 2003. Crystal structure of a hypothetical protein, TM841 of *Thermotoga maritima*, reveals its function as a fatty acid-binding protein. Proteins 50:526-30.
13. Gullett JM, Cuypers MG, Frank MW, White SW, Rock CO. 2019. A fatty acid-binding protein of *Streptococcus pneumoniae* facilitates the acquisition of host polyunsaturated fatty acids. J Biol Chem 294:16416-16428.
14. Shi Y, Zang N, Lou N, Xu Y, Sun J, Huang M, Zhang H, Lu H, Zhou C, Feng Y. 2022. Structure and mechanism for streptococcal fatty acid kinase (Fak) system dedicated to host fatty acid scavenging. Sci Adv 8:eabq3944.
15. Eraso JM, Olsen RJ, Beres SB, Kachroo P, Porter AR, Nasser W, Bernard PE, DeLeo FR, Musser JM. 2016. Genomic Landscape of Intrahost Variation in Group A *Streptococcus*: Repeated and Abundant Mutational Inactivation of the fabT Gene Encoding a Regulator of Fatty Acid Synthesis. Infect Immun 84:3268-3281.

16. Longo M, De Jode M, Plainvert C, Weckel A, Hua A, Chateau A, Glaser P, Poyart C, Fouet A. 2015. Complete Genome Sequence of *Streptococcus pyogenes emm28* Clinical Isolate M28PF1, Responsible for a Puerperal Fever. Genome Announc 3.
17. Cunningham MW. 2000. Pathogenesis of group A streptococcal infections. Clin Microbiol Rev 13:470-511.
18. Carapetis JR, Steer AC, Mulholland EK, Weber M. 2005. The global burden of group A streptococcal diseases. Lancet Infect Dis 5:685-94.
19. Rosinski-Chupin I, Sauvage E, Fouet A, Poyart C, Glaser P. 2019. Conserved and specific features of *Streptococcus pyogenes* and *Streptococcus agalactiae* transcriptional landscapes. BMC Genomics 20:236.
20. Lu YJ, Rock CO. 2006. Transcriptional regulation of fatty acid biosynthesis in *Streptococcus pneumoniae*. Mol Microbiol 59:551-66.
21. Vadia S, Tse JL, Lucena R, Yang Z, Kellogg DR, Wang JD, Levin PA. 2017. Fatty Acid Availability Sets Cell Envelope Capacity and Dictates Microbial Cell Size. Curr Biol 27:1757-1767 e5.
22. Sastre DE, Pulschen AA, Basso LGM, Benites Pariente JS, Marques Netto CGC, Machinandiarena F, Albanesi D, Navarro M, de Mendoza D, Gueiros-Filho FJ. 2020. The phosphatidic acid pathway enzyme PlsX plays both catalytic and channeling roles in bacterial phospholipid synthesis. J Biol Chem 295:2148-2159.
23. Kengmo Tchoupa A, Eijkelkamp BA, Peschel A. 2022. Bacterial adaptation strategies to host-derived fatty acids. Trends Microbiol 30:241-253.
24. Alnaseri H, Arsic B, Schneider JE, Kaiser JC, Scinocca ZC, Heinrichs DE, McGavin MJ. 2015. Inducible Expression of a Resistance-Nodulation-Division-Type Efflux Pump in *Staphylococcus aureus* Provides Resistance to Linoleic and Arachidonic Acids. J Bacteriol 197:1893-905.
25. Volkov A, Liavonchanka A, Kamneva O, Fiedler T, Goebel C, Kreikemeyer B, Feussner I. 2010. Myosin cross-reactive antigen of *Streptococcus pyogenes* M49 encodes a fatty acid double bond hydratase that plays a role in oleic acid detoxification and bacterial virulence. J Biol Chem 285:10353-61.
26. Resch U, Tsatsaronis JA, Le Rhun A, Stubiger G, Rohde M, Kasvandik S, Holzmeister S, Tinnefeld P, Wai SN, Charpentier E. 2016. A Two-Component Regulatory System Impacts Extracellular Membrane-Derived Vesicle Production in Group A *Streptococcus*. mBio 7.
27. Uhlmann J, Rohde M, Siemens N, Kreikemeyer B, Bergman P, Johansson L, Norrby-Teglund A. 2016. LL-37 Triggers Formation of *Streptococcus pyogenes* Extracellular Vesicle-Like Structures with Immune Stimulatory Properties. J Innate Immun 8:243-57.
28. Beerens D, Franch-Arroyo S, Sullivan TJ, Goosmann C, Brinkmann V, Charpentier E. 2021. Survival Strategies of *Streptococcus pyogenes* in Response to Phage Infection. Viruses 13.
29. Murase K, Aikawa C, Nozawa T, Nakatake A, Sakamoto K, Kikuchi T, Nakagawa I. 2021. Biological Effect of *Streptococcus pyogenes*-Released Extracellular Vesicles on Human Monocytic Cells, Induction of Cytotoxicity, and Inflammatory Response. Front Cell Infect Microbiol 11:711144.
30. Gryllos I, Tran-Winkler HJ, Cheng MF, Chung H, Bolcome R, 3rd, Lu W, Lehrer RI, Wessels MR. 2008. Induction of group A *Streptococcus* virulence by a human antimicrobial peptide. Proc Natl Acad Sci U S A 105:16755-60.
31. Kengmo Tchoupa A, Peschel A. 2020. *Staphylococcus aureus* Releases Proinflammatory Membrane Vesicles To Resist Antimicrobial Fatty Acids. mSphere 5.

32. Six A, Bellais S, Bouaboud A, Fouet A, Gabriel C, Tazi A, Dramsi S, Trieu-Cuot P, Poyart C. 2015. Srr2, a multifaceted adhesin expressed by ST-17 hypervirulent Group B *Streptococcus* involved in binding to both fibrinogen and plasminogen. Mol Microbiol 97:1209-22.
33. Weckel A, Ahamada D, Bellais S, Mehats C, Plainvert C, Longo M, Poyart C, Fouet A. 2018. The N-terminal domain of the R28 protein promotes emm28 group A *Streptococcus* adhesion to host cells *via* direct binding to three integrins. J Biol Chem 293:16006-16018.
34. Abreu S, Solgadi A, Chaminade P. 2017. Optimization of normal phase chromatographic conditions for lipid analysis and comparison of associated detection techniques. J Chromatogr A 1514:54-71.
35. Moulin M, Solgadi A, Veksler V, Garnier A, Ventura-Clapier R, Chaminade P. 2015. Sex-specific cardiac cardiolipin remodelling after doxorubicin treatment. Biol Sex Differ 6:20.

Supplementary figures

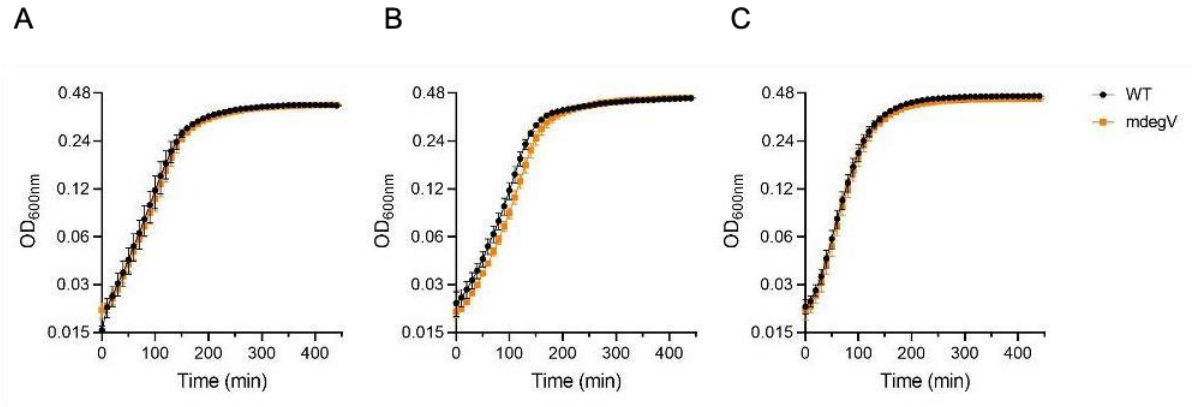

Figure S1. Influence of a *degV*$_{1638}$ mutation on bacterial growth in rich media. Bacterial growth in A) THY B), THY-Tween 80 and C) THY-FBS.

Supplementary Tables

Table S1. Consequences of a degV1638 mutation on fatty acid membrane composition in different media.

	THY			THY-Tween			THY-Plasma			Plasma
Strain	WT	mDegV	BWT	WT	mDegV	BWT	WT	mDegV	BWT	
14:0 [a]	2.19 ± 0.14	3.2 ± 0.16	2.16 ± 0.17	7.33 ± 1.80	9.14 ± 0.29	ND	1.73 ± 0.07	1.64 ± 0.18	1.64 ± 0.18	1.16
16:0	26.37 ± 1.47	29.91 ± 1.06	26.72 ± 0.16	20.61 ± 1.33	22.17 ± 0.73	ND	31.78 ± 0.89	31.95 ± 0.49	30.48 ± 0.04	25.58
16:1	16.83 ± 0.51	19.06 ± 0.10	15.38 ± 0.55	7.87 ± 0.43	6.66 ± 0.43	ND	5.79 ± 0.30	5.58 ± 0.64	5.8 ± 1.10	3.49
18:0	6.27 ± 0.25	5.79 ± 0.15	8.5 ± 0.34	0.84 ± 1.03	0.12 ± 0.20	ND	8.01 ± 0.30	8.09 ± 0.24	8.05 ± 0.30	8.14
18:1Δ9	9.9 ± 0.21	8.8 ± 0.07	10.3 ± 0.21	52.95 ± 1.47	53.76 ± 0.94	ND	23.06 ± 0.20	23.43 ± 0.96	21.79 ± 1.34	22.09
18:1Δ11	29.59 ± 1.96	26.33 ± 0.49	29.71 ± 0.60	4.52 ± 0.48	4.45 ± 0.32	ND	4.46 ± 0.18	4.01 ± 0.36	5.3 ± 1.24	0
18:2	0	0	0	0	0	ND	16.34 ± 0.43	16.45 ± 0.37	15.02 ± 1.14	33.72
20:3	0	0	0	0	0	ND	1.09 ± 0.04	1.13 ± 0.05	1.04 ± 0.06	0
20:4	0	0	0	0	0	ND	4.61 ± 0.27	4.65 ± 0.18	3.41 ± 1.76	5.81
Others [b]	8.03 ± 0.61	6.91 ± 1.14	7.32 ± 0.65	2.96 ± 0.77	1.25 ± 0.87	ND	3.14 ± 0.62	3.08 ± 1.30	6.39 ± 0.69	0
(C16):(C18) [c]	0.94	1.20	0.87	0.49	0.49	ND	0.72	0.72	0.72	0.45
UFA:SFA [d]	1.62	1.39	1.48	2.27	2.06	ND	1.33	1.33	1.30	1.87

[a] Percentage of total FAs.
[b] Fatty acids representing less than 2 % total FAs.
[c] Ratio of length chain = (C18:0 + C18:1)/(C16:0 + C16:1).
[d] Ratio unsaturated/saturated FAs = (16:1 + 18:1Δ9 + 18:1Δ11)/(14:0 + 16:0 + 18:0).

Table S2. Membrane lipid family composition and proportion in WT and mDegV strains.

	Lipid composition		Lipid proportion	
Lipids	**WT**	**mDegV**	**WT**	**mDegV**
MGDG	0.229 ± 0.05	0.357 ± 0.04	9.4% ± 1.3 %	11.1% ± 1.2 %
DGDG	0.619 ± 0.17	0.853 ± 0.08	25.0% ± 1.4 %	26.5% ± 1.3 %
PG	0.949 ± 0.09	1.189 ± 0.14	39.4% ± 6.2 %	36.9% ± 1.3 %
CL	0.661 ± 0.26	0.827 ± 0.17	26.2% ± 5.0 %	25.5% ± 2.2 %

MGDG, monogalactosyldiacylglycerol; DGDG, digalactosyldiacylglycerol ; PG, phosphatidylglycerol; CL, cardiolipin.

Table S3. Strains and plasmids used in this study.

Strains or plasmids	**Relevant properties**	**Source or references**
Streptococcus pyogenes		
WT	Wild-type representative *emm28* clinical isolate, M28PF1	1
mFabT	M28PF1 mutated in *fabT* C313T (H105Y)	This study
mDegV	M28PF1 mutated in $degV_{1638}$, interrupted by an insertion	This study
BWT	Back-to-the-wild-type, the reverting strain of the mDegV construction	This study
Escherichia coli		
Stellar™	F-, endA1, supE44, thi-1, recA1, gyrA96, phoA, Φ80d lacZΔ M15, Δ(lacZYA – argF) U169, Δ(mrr – hsdRMS –mcrBC), ΔmcrA, λ-	Clontech
Plasmids		
pG1	Thermosensitive broad-host-range vector	2
pG1-mFabT	pG1 containing the *fabT* gene with the point mutation C313T	This study
pG1-DegVint2	pG1 containing an internal fragment of $degV_{1638}$	This study

1. Longo M, De Jode M, Plainvert C, Weckel A, Hua A, Chateau A, Glaser P, Poyart C, Fouet A. 2015. Complete Genome Sequence of Streptococcus pyogenes emm28 Clinical Isolate M28PF1, Responsible for a Puerperal Fever. Genome Announc 3.
2. Biswas I, Gruss A, Ehrlich SD, Maguin E. 1993. High-efficiency gene inactivation and replacement system for gram-positive bacteria. J Bacteriol 175:3628-35.

Table S4. Primers used in this study for plasmid and strain construction and for PCR experiments.

Primer name	Sequence	Used for
P47	CGCCAGGGTTTTCCCAGTCACGAC	plasmid construction
RP48	AGCGGATAACAATTTCACACAGGA	plasmid construction
FabT-222_am	GACTCTAGA**GGATCC**GGTCTGGCAAAGCTTTTTCA	pG1-mFabT construction
Fabt+805_av	CATGATTAC**GAATTC**GGCACCTGATGCAATAAGCT	pG1-mFabT construction
degVintF2	CGACTCTAGA**GGATCC**GCGCTCTAATGGCACGCGAT	pG1-DegVint2 construction
degV intR2	CCATGATTAC**GAATTCC**CTTCCTCATCAATCCACA	pG1-DegVint2 construction
ermB-F	GAGTGTGTTGATAGTGCAGT	mDegV strain construction
ermB-R	TAGGCGCTAGGGACCTCTTTA	mDegV strain construction
gyrA1	CTGCTCGTATTACGGGTGATGT	qRT-PCR of *gyrA*
gyrA2	GGCGATAACTCCACCACTGA	qRT-PCR of *gyrA*
rpoB1	CCGTACACGTCGTAGCTTTT	qRT-PCR of *rpoB*
rpoB2	GCATCGTGGATACGAGCTTC	qRT-PCR of *rpoB*
FabT-3'	CCCTAGTCCACGCACCAATGCCT	qRT-PCR of *fabT*
FabT-5'	GGGACAGTAACGACTAGCTTAAATA	qRT-PCR of *fabT*
1638-Am	GCCAGCTTTCATCTTTTTCAAAAGG	qRT-PCR of $degV_{1638}$
1638-Av	GGGCAGAAGATCATGATATTGTC	qRT-PCR of $degV_{1638}$

* in bold, added restriction enzyme sites, EcoRI or BamH1.

Supplementary Material and Methods

Growth curves. *S. pyogenes* stationary precultures were diluted in THY, THY-Tween 80 or THY-FBS to an OD_{600nm} = 0.05 and transferred to 96-well plates. These were incubated at 37 °C in a Thermo Scientific Multiskan GO (ThermoFischer Scientific) and growth was determined by measuring absorbance at 600 nm every 10 min after shaking the plates.

Résultat additionel

Analyse de la poche de fixation de l'acide gras de DegV$_{1638}$.

Les analyses *in silico* des séquences protéiques de FakB1 et DegV$_{1638}$ ont permis de définir que DegV$_{1638}$ est plus proche de la protéine FakB1 que des autres protéines FakB. De plus, à partir de la description du site de fixation de l'acide gras sur FakB1 (311,312), nous avons constaté que les acides aminés impliqués dans cette interaction sont conservés entre les deux protéines (Figure 27). Ceci suggère fortement que de la protéine DegV$_{1638}$ fixe préférentiellement les acides gras saturés.

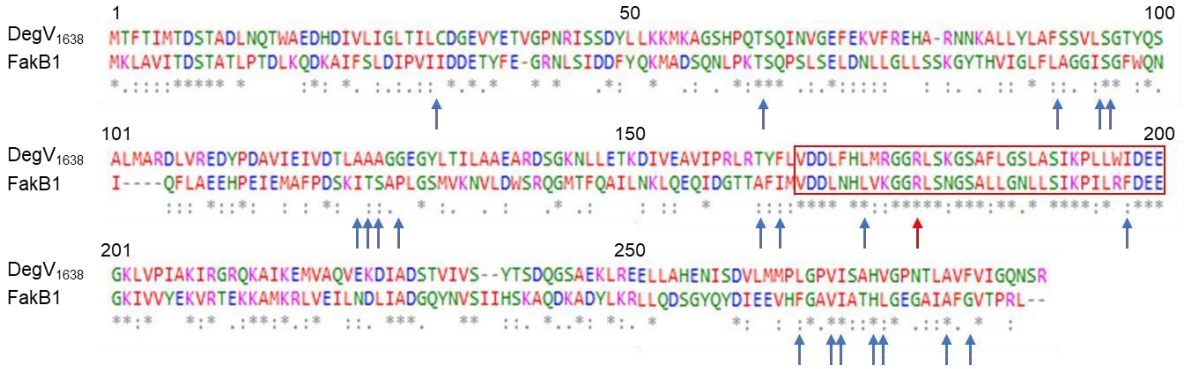

Figure 27. Conservation des acides aminés constituant le site de fixation des protéines FakB1 et DegV$_{1638}$. L'alignement des séquences de FakB1 et DegV$_{1638}$ a été effectué à l'aide de Clustal W (1.83), le code couleur suit la classification fonctionnelle ; *, identique chez les protéines ; : même classe structurelle ; les flèches grises verticales indiquent les résidus d'acides aminés, qui sont impliqués dans l'interaction avec l'acides gras.

Discussion et Perspectives

La membrane bactérienne, constituée d'une bicouche lipidique, forme une barrière perméable impliquée dans les échanges de la bactérie avec son environnement (270). Le maintien de l'équilibre des propriétés physiques de la membrane, dépendant de sa composition, est crucial pour le développement de la bactérie. Les lipides, principaux composants des membranes, sont des molécules amphiphiles comprenant une tête polaire spécifique à chaque famille lipidique et un corps apolaire, les acides gras. La longueur et la saturation de ces acides gras définissent les propriétés de la membrane et par conséquent influencent l'interaction de la bactérie avec son environnement (287). Les bactéries ont développé différents mécanismes pour maintenir l'homéostasie de leur membrane en contrôlant notamment le type d'acides gras synthétisés et leur quantité. Chez les streptocoques, *E. faecalis* et *L. lactis*, la voie de biosynthèse des acides gras, voie FASII, est régulée par FabT (294). Au cours de ce travail, nous avons caractérisé le rôle de FabT en tant que répresseur transcriptionnel de la voie FASII et les conséquences physiologiques d'une dérégulation chez *S. pyogenes* définissant ainsi le lien entre FabT et la virulence.

Pour la première fois, nous avons établi le rôle de FabT lorsque les bactéries sont cultivées en présence d'acides gras, corépresseurs de FabT. FabT réprime l'expression des gènes FASII et d'un unique autre gène codant une protéine de la famille DegV. La régulation des gènes FASII par FabT en réponse à l'ajout d'acides gras exogènes dans le milieu de culture a été décrite chez *E. faecalis* (302). Cette répression permet de contrôler la concentration d'acides gras présents dans la bactérie et de contourner un stress membranaire.

Le mécanisme de répression de FabT est dépendant d'un corépresseur l'acyl-ACP à chaîne longue (362). Chez *S. pneumoniae* et *E. faecalis*, tout comme chez *S. pyogenes*, il existe deux protéines ACP, AcpA et AcpB, (301,302,377). AcpA participe à la synthèse *de novo* des acides gras. AcpB joue un rôle dans la synthèse des phospholipides *via* PlsX. Leur implication dans la corépression de FabT est controversée. Nous avons montré que la protéine AcpB couplée à un acyl est le principal corépresseur de FabT chez *S. pyogenes*. La protéine AcpA joue également un rôle, mais celui-ci est minime par rapport à AcpB (Figure 28). Nos résultats soutiennent le modèle décrit chez *S. pneumoniae* (301). Ainsi, la corépression de FabT chez

des streptocoques serait différente de celle chez *E. faecalis* (302). L'acyl-AcpA issu de la synthèse *de novo* réprime en fonction de sa quantité. En revanche, l'acyl-AcpB qui est formé à partir d'un acyl-phosphate, réprime en fonction de la quantité d'acyl-phosphates, qu'ils soient produits à partir soit d'un acyl-AcpA endogène par PlsX ou d'acides gras exogènes par le complexe FakA/FakB. De plus, le niveau d'expression du gène codant AcpB est constant contrairement à celui codant AcpA qui diminue en présence d'acides gras exogènes (299). Ainsi l'acyl-AcpA et l'acyl-AcpB corépriment les gènes en absence d'acides gras exogènes. L'acyl-AcpB participe à la corépression de FabT en présence d'acides gras exogènes, mimant des conditions physiologiques dites « *in vivo* ».

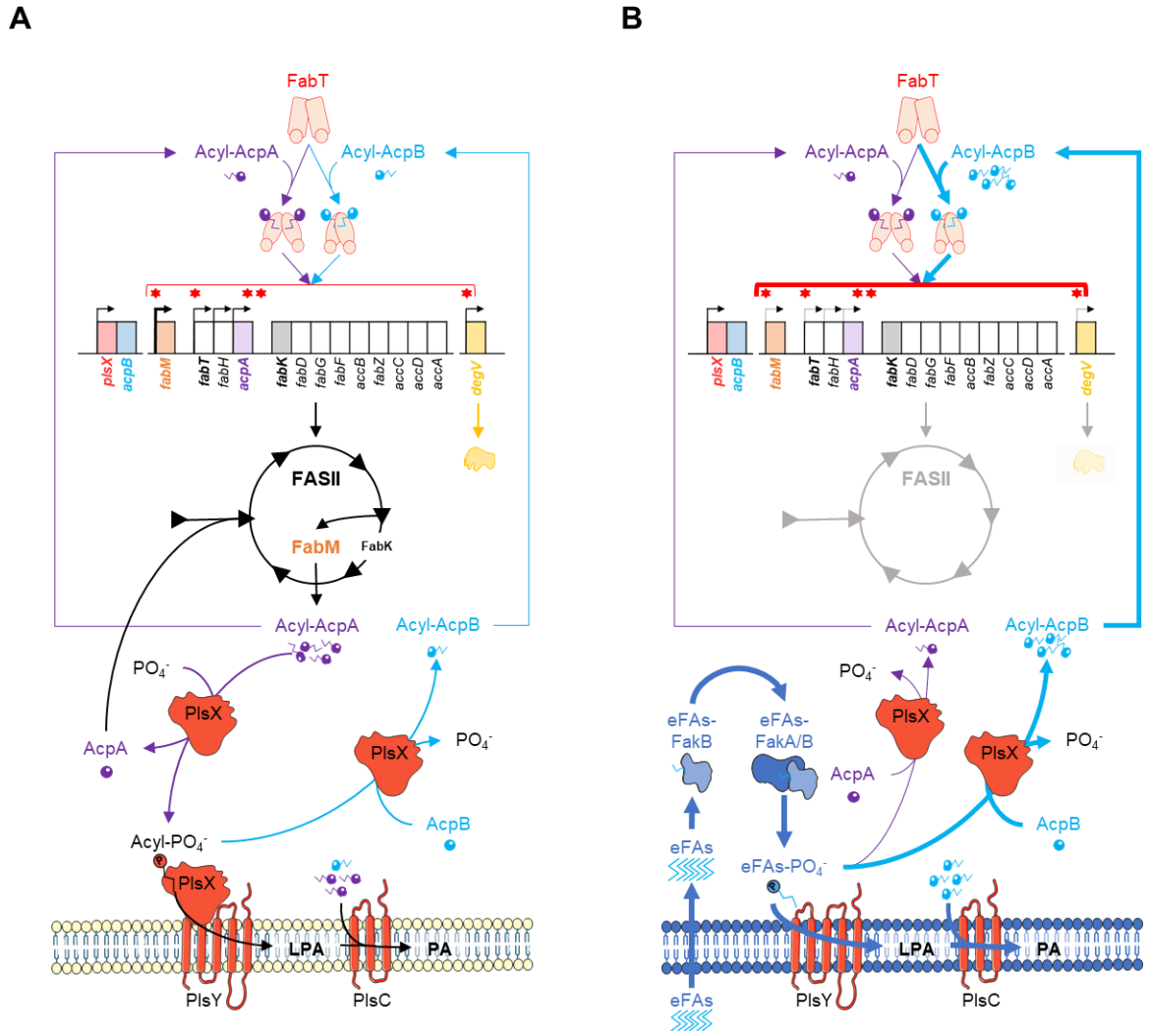

Figure 28. Mécanisme de répression de FabT chez *S. pyogenes* (A) en absence d'acides gras et (B) conditions physiologiques dites « *in vivo* », en présence d'acides gras exogènes. eFAs, Acides gras exogènes. LPA, Acide lysophosphatidique. PA, Acide phosphatidique.

Nous avons aussi montré que les gènes FASII ne sont pas régulés de la même manière, chez *S. pyogenes*. L'expression du gène *fabM*, participant à la formation des acides gras insaturés est moins réprimée que celle du gène *fabK*, qui est impliqué dans l'élongation. Cette différence permet de maintenir l'équilibre membranaire en ajustant les ratios d'acides gras saturés *versus* insaturés et chaînes longues *versus* chaînes courtes. Par la suite, nous avons confirmé que la dérégulation de FASII impacte la composition en acides gras de la membrane en faveur des acides gras saturés et à chaîne longue. La différence du niveau de régulation de ces gènes et les conséquences sur la composition en acides gras a également été décrite chez *S. pneumoniae* où le gène *fabM* n'est pas contrôlé par FabT (334). Toute modification de l'homéostasie de la membrane, par addition d'acides gras exogènes, par modification des conditions de culture (température, pH) ou par surexpression de FabT, nécessite un ajustement de la membrane faisant intervenir FabT (296,355,358). FabT régule alors la synthèse des acides gras en contrôlant l'élongation et le niveau de saturation des acides gras présents dans la membrane. De cette manière, une mutation dans FabT impacte la régulation de FASII ce qui modifie la composition de la membrane.

Contrairement à *L. lactis* (296), les modifications de la composition en acides gras n'impactent pas les propriétés de la membrane telles que la perméabilité. En revanche, elles impactent les capacités d'incorporation des acides gras dans la membrane. Ce défaut a également été rapporté chez *E. faecalis* (302). L'incorporation des acides gras dépend des complexes protéiques FakA-FakB (310). Lors de notre analyse transcriptomique, seul le gène codant la protéine FakB3 est ressorti négativement contrôlé par l'addition d'acides gras dans le milieu de culture et ce, quelle que soit la souche. Ces résultats indiquent que FabT n'est pas impliqué directement dans la régulation de l'incorporation des acides gras. La dérégulation de FASII impacte peut-être l'activité des complexes FakA-FakB, induisant le défaut d'incorporation. Plusieurs hypothèses peuvent être envisagées (Figure 29) : i) l'activité des complexes FakA-FakB est inhibée par la concentration en acyl-phosphates issus de la synthèse endogène, ii) l'acyl-phosphate formé par FakA-FakB est transféré, non pas à PlsY, mais à PlsX pour former de l'acyl-AcpB, interagissant avec FabT sans conséquence sur la répression de FASII, et iii) FakB ne peut pas transférer l'acyl-phosphate à PlsY, déjà monopolisée par PlsX. Chez *E. faecalis*, la surexpression du gène codant AcpB dans une souche par ailleurs délétée de *fabT* restaure en partie l'incorporation (302). La formation d'acyl-AcpB par PlsX permettrait de réduire la quantité d'acyl-phosphate endogène présent dans la bactérie. Cette diminution

induirait donc une activation partielle des protéines FakA/FakB. Ces observations sont en faveur de la première hypothèse. Afin de la tester, nous pouvons comparer les capacités d'incorporation de la souche mutante mFabT dans différentes conditions réduisant la quantité d'acyl-phosphate endogène. Pour ce faire, il serait intéressant de déléter le gène codant PlsX et/ou d'inhiber FASII par traitement avec un anti-FASII.

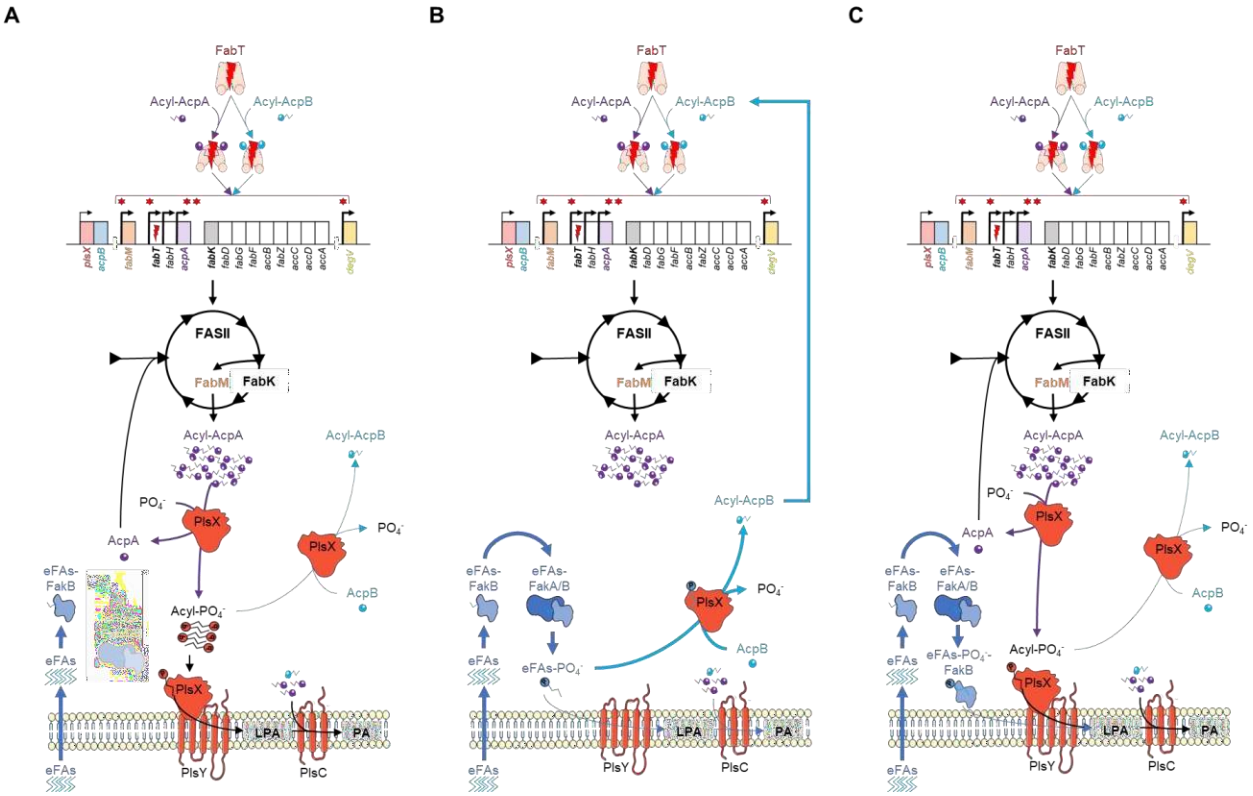

Figure 29. Différentes hypothèses *concernant* le défaut d'incorporation des acides gras exogènes dans la membrane de la souche mutante mFabT chez *S. pyogenes*. (A) Inhibition de l'activité des complexes FakA-FakB. (B) Conversion de l'acyl-phosphate exogène (eFAs-PO $^{-}$) par P_4lsX.
(C) Encombrement de PlsY par PlsX. L'éclair rouge indique l'inactivation de FabT. eFAs, Acides gras exogènes. LPA, Acide lysophosphatidique. PA, Acide phosphatidique.

La dérégulation de FASII couplée au défaut d'incorporation des acides gras exogènes peut compromettre la croissance d'une souche mutée dans *fabT*. La croissance de la souche délétée de *fabT* est controversée chez *S. pyogenes.* Port et al. n'ont pas pu obtenir de mutants délétés *fabT* sans mutations compensatrices (363). De même, les souches délétées, réalisées par Tatsuno *et al.* et par nous présentent un important défaut de croissance (359). Ainsi, chez *S. pyogenes*, la perte de *fabT* impacte la croissance en milieu riche de laboratoire. Cependant, Eraso *et al.* ont construit une souche délétée de *fabT* qui pousse comme la souche sauvage (355) ; nous supposons que cette souche possède des mutations compensatrices. Nous avons

également défini la croissance de ces souches en milieu riche de laboratoire supplémenté en acides gras. La souche délétée présente toujours un défaut de croissance. Ainsi, l'addition d'acides gras ne suffit pas à compenser la perte de *fabT* chez *S. pyogenes*, contrairement aux souches délétées des gènes FASII chez *S. agalactiae* et *E. faecalis* (297,373). Cette observation est une preuve supplémentaire permettant d'envisager sérieusement la surproduction de FASII comme nouvelle stratégie thérapeutique.

Un couplage de la synthèse des acides gras et du précurseur des lipides *via* PlsX a été décrit chez *B. subtilis* (273). Chez *S. pneumoniae*, une mutation dans FabT induit une modification de l'expression du gène codant PlsC dans le même sens que celle de FASII, suggérant le contrôle de PlsC par FabT (334). Ainsi, la dérégulation de FASII impacte la synthèse des lipides et par conséquent la composition lipidique de la membrane, mettant aussi en évidence le couplage des deux synthèses chez *S. pneumoniae*. Nous avons montré qu'une mutation dans FabT induit une diminution de la quantité de digalactosyldiacylglycérol et de cardiolipine chez *S. pyogenes*. Néanmoins, aucun gène codant une enzyme participant à la synthèse des lipides n'est apparu modifié lors de l'analyse transcriptomique. Chez *S. pyogenes*, FabT n'intervient pas directement dans la régulation de la synthèse des lipides. Cependant les variations de composition en lipides membranaires suggèrent fortement la présence d'un couplage entre les deux synthèses. Chez *E. coli*, l'activité des enzymes de synthèse des cardiolipines est contrôlée par l'acide phosphatidique, précurseur des lipides et par les cardiolipines elles-mêmes (378). La diminution de la quantité de cardiolipine et de digalactosyldiacylglycérol peut traduire une modification de l'activité des enzymes de synthèse en réponse à la dérégulation de FabT entrainant une augmentation de la concentration en acide phosphatidique. Afin de vérifier ces hypothèses nous pourrions comparer les quantités d'acide phosphatidique, précurseur des lipides, et des produits de la synthèse des digalactosyldiacylglycerols et des cardiolipines (cf. Introduction, 2.1. La synthèse des lipides membranaires), au sein des souches sauvage et mutante pour FabT. Par ailleurs, la modification de la concentration en cardiolipine peut permettre à la bactérie de s'adapter. En effet, une accumulation de cardiolipine permet à *B. subtilis* et à *S. aureus* de survivre à un stress salin et à la phagocytose par les neutrophiles polymorphonucléaires (PMNs) (379–381). De plus, chez *S. pyogenes*, les premières mutations dans FabT ont été sélectionnés au sein de

clones présentant une sensibilité moindre à la polymyxine B, antibiotique ciblant les lipides anioniques (363). Ainsi, le défaut de cardiolipine lié à la dérégulation de FASII permet à *S. pyogenes* de résister à ce traitement. D'autres apparitions de mutations dans FabT ont également été rapportées dans plusieurs études induisant des modifications de l'enveloppe de la bactérie, notamment chez *S. agalactiae* lors de la fragilisation du peptidoglycane due à l'ajout de glycine dans le milieu de culture (382) et lors de la diminution de l'épaisseur de la capsule liée à la variation de phase de colonie chez *S. pneumoniae* (360). Ainsi, la dérégulation de FASII permet à certains streptocoques de s'adapter à leur environnement ou à leur interaction avec celui-ci.

Nous avons caractérisé les conséquences *in vitro* d'une mutation perte de fonction *fabT* lors des premières étapes d'infection à *S. pyogenes*. Le spectre d'infection de *S. pyogenes* étant très large, nous avons analysé le mécanisme d'infection en présence de deux types cellulaires, endométriales et kératinocytes. La souche mutée présente un défaut d'adhésion aux cellules. *S. pyogenes* comporte de nombreux facteurs de virulence impliqués dans l'adhésion tels que les adhésines et le pilus (cf. Introduction, 1.4.1. Les adhésines). A partir des analyses transcriptomiques et protéomiques, nous avons constaté que sept adhésines dont la protéine M sont moins abondantes dans la souche mutante que dans la souche sauvage à l'inverse du pilus et de la protéine R28. Néanmoins, la surproduction de R28 et du pilus ne permet pas de compenser la perte des sept autres. Chez *S. pneumoniae*, une souche délétée *fabT* a, *in vivo*, un défaut de colonisation et présente également un défaut d'adhésion aux cellules (360). Ainsi les modifications indirectes de la dérégulation de FASII induisent un défaut d'adhésion de la bactérie ; ceci peut-être à l'origine de la virulence atténuée des souches mutantes *fabT*.

Par la suite, nous avons montré que les cellules endométriales et kératinocytes sécrètent des nutriments permettant la croissance de *S. pyogenes*. L'analyse métabolomique a souligné la consommation par les deux souches d'un métabolite sécrété par les cellules, l'ester de cholestérol CE(20:4). Néanmoins, l'addition de ce lipide au RPMI n'est pas suffisante à la croissance (données non montrées). La concentration d'autres produits étant en dessous du seuil de détection, nous ne pouvons pas définir avec certitudes leur utilisation par les bactéries. Nous envisageons donc que certains d'entre eux sont nécessaires à la multiplication

bactérienne. La croissance de *S. pyogenes* en présence de cellules est donc liée à la consommation d'une combinaison de produits cellulaires. Le cholestérol est un composant majeur des membranes des cellules eucaryotes assurant sa fluidité. Il est synthétisé par la voie du mévalonate qui à partir de l'acétyl-CoA produit du mévalonate puis du cholestérol (383). Enfin pour contrôler la concentration de cholestérol libre dans la cellule, il est estérifié par une acétyl-CoA cholestérol acyltransférase. L'ester de cholestérol est, soit stocké sous forme de gouttelettes lipidiques, soit sécrété *via* des lipoprotéines (384). Plusieurs enzymes assurant sa synthèse sont situées dans le réticulum endoplasmique, qui joue un rôle important dans la production de ce métabolite. L'utilisation des lipides de l'hôte par les bactéries plus particulièrement de l'ester de cholestérol a déjà été documentée. Il peut être incorporé dans la membrane bactérienne et/ou utilisé comme source de carbone et d'énergie (385,386). *Mycobacterium tuberculosis*, pathogène intracellulaire, utilise l'ester de cholestérol des gouttelettes lipidiques comme source primaire de carbone. Sa consommation est requise pour la persistance de la bactérie au sein de l'hôte (387). *M. tuberculosis* dégrade l'ester de cholestérol *via* différentes voies dont la β-oxydation qui permet la production de propionyl-CoA (388). Ce produit est ensuite transformé en succinate et pyruvate-CoA qui alimenteront le cycle de Krebs de la bactérie (389). Chez *Helicobacter pylori*, pathogène extracellulaire, l'addition *in vitro* de cholestérol dans le milieu de culture favorise sa croissance (390,391). Ainsi, d'autres produits sont impliqués dans la croissance de *H. pylori*, tout comme nous le supposons pour la croissance de *S. pyogenes* en présence de cellules. *H. pylori* peut également incorporer l'ester de cholestérol de l'environnement dans sa membrane. Après glycosylation, le glycosyl-cholestérol est incorporé *via* une α-glucosyltransférase (392).

S. pyogenes a également la capacité d'incorporer les lipides de l'hôte dans sa membrane lorsqu'il est cultivé dans du sérum humain (393). En revanche, l'utilisation des lipides comme source d'énergie par *S. pyogenes* n'avait pas encore été décrite. Aucune voie de dégradation connue n'ayant été mise en évidence chez *S. pyogenes*, le (ou les) mécanisme(s) impliqué(s) dans cette utilisation reste(nt) à être caractérisé(s). Néanmoins, certaines souches de *S. pyogenes*, dont la souche M28PF1 étudiée au laboratoire, possèdent le facteur d'opacité sérique (SOF) (cf. Introduction, 1.4.3. Les facteurs de virulence sécrétés : les toxines). Il est sécrété par les bactéries et perturbe les structures des lipoprotéines de haute densité, créant ainsi une émulsion riche en ester de cholestérol (69,394). L'acide gras présent sur le lipide pourra être libéré par l'action d'une phospholipase A puis incorporé dans la membrane de la

bactérie. Certaines souches de *S. pyogenes*, dont M28PF1, ont acquis un bactériophage codant une phospholipase A2, SlaA (395). SlaA est impliquée dans la colonisation de *S. pyogenes*, par conséquent dans la virulence de ce pathogène (199). Cette phospholipase a été retrouvée au niveau des sites de lésions indiquant que la production et la sécrétion de cette protéine ont lieu lors des premières étapes de l'infection. Nous supposons que cette protéine va permettre de cliver les acides gras de l'ester de cholestérol de l'hôte qui seront alors utilisés par la bactérie. Cependant, aucune variation d'expression du gène codant SlaA (M28_Spy1222) ou de l'accumulation de la protéine n'a été mise en évidence dans nos analyses *in vitro.* Il serait donc intéressant de regarder le niveau d'expression du gène codant SlaA et la quantité de protéines dans les souches sauvage et mutante en présence de cellules et de surnageant de cellules. On pourrait également étudier son activité phospholipase en présence de cellules pour voir s'il y a libération de l'acide arachidonique présent sur le CE(20:4). Par ailleurs, nous ne pouvons pas négliger que ces lipides peuvent être également incorporés dans la membrane de *S. pyogenes*. Malheureusement, la concentration bactérienne après croissance en présence de cellules ou en surnageant conditionné n'est pas suffisante pour analyser l'incorporation de l'ester de cholestérol CE(20:4) dans la membrane des souches sauvage et mutante. En nous basant sur les résultats de différence d'incorporation en milieu de laboratoire, nous supposons que la souche mutante a moins de cholestérol dans sa membrane que la souche sauvage.

Bien que les deux souches consomment similairement le CE(20:4), nous avons montré que la souche mutante présente un défaut de croissance par rapport à la souche sauvage. Elle consomme spécifiquement plus d'acides aminés et d'hexoses et produit plus d'ester de cholestérol CE(22:6). Nous émettons l'hypothèse que la souche mutante, dont FASII est active, participe à l'élongation des chaines d'acides gras présents dans l'ester de cholestérol CE(20:4) afin de produire du CE(22:6). Ceci renforce l'hypothèse que la souche mutante perd son énergie à produire ou allonger des acides gras, nécessitant la consommation d'autres sources d'énergie telles que les acides aminés et les hexoses. De plus, les cellules sécrètent également des produits toxiques. Nous avons mis en évidence que la souche mutante meurt plus que la souche sauvage. La souche mutante pourrait être plus sensible que la souche sauvage aux produits toxiques. Chez *H. pylori*, l'incorporation *in vitro* du cholestérol dans la membrane augmente la résistance à certains peptides antimicrobiens (LL37) et à certains antibiotiques

ciblant la synthèse de la paroi comme les pénicillines (396). En milieu de laboratoire, la souche mutante ne présente pas de différence de sensibilité au LL37 par rapport à la souche sauvage. Cependant, en présence de cellules, où sa membrane contiendrait potentiellement moins d'ester de cholestérol que la souche sauvage, elle pourrait être plus sensible à ce peptide antimicrobien. Cette hypothèse pourrait rendre compte de la plus grande mortalité de la souche mutante. Ainsi, le défaut de croissance de la souche mutante est la résultante d'une combinaison de deux facteurs, la perte d'énergie du mutant liée à la dérégulation de FASII, d'une part, et sa mortalité accrue, d'autre part.

En utilisant un modèle d'infection *ex vivo* de tissu humain endométrial, nous avons confirmé que la souche mutante présente un défaut de multiplication à la surface du tissu. En accord avec ces résultats, les souches perte de fonction *fabT* de *S. pyogenes* présentent un défaut de multiplication dans un modèle *in vivo* d'infection murin et de primate non-humain (355). Un défaut de colonisation d'une souche délétée *fabT* a également été décrit chez *S. pneumoniae* (360). Ainsi chez *S. pyogenes* et *S. pneumoniae*, une mutation dans FabT induit une diminution de la virulence de la souche mutante par rapport à la souche sauvage. Le défaut de croissance que nous avons montré en présence de cellules et confirmé sur tissu humain rend compte du défaut de virulence des souches mutées dans *fabT* chez certains streptocoques.

Le laboratoire a mis en évidence l'implication de deux facteurs de virulence, SLO et SpeB, lors des premières étapes d'infection de *S. pyogenes* (21). Par ailleurs, *S. pyogenes* modifie le métabolisme de son hôte par les hémolysines SLO et SLS pour favoriser sa croissance (215,253). Pendant la première étape d'interaction avec les cellules, les bactéries sécrètent SLO et SLS induisant un stress du réticulum endoplasmique et l'activation des voies « Unfolded Protein Response » (UPR). Cette activation a pour conséquence d'augmenter la synthèse d'asparagine et sa sécrétion dans le milieu de culture. La consommation de l'asparagine par *S. pyogenes* lui permet de proliférer au sein de l'hôte (215). Le réticulum endoplasmique est aussi le lieu de synthèse du cholestérol de la cellule. L'activation des voies UPR via un stress du réticulum endoplasmique a ainsi aussi pour conséquence une augmentation de la synthèse de cholestérol (397,398). Afin de contrer l'excès de cholestérol, la cellule le transforme en ester de cholestérol et l'exporte *via* des lipoprotéines. Ainsi, nous proposons que lors des premières étapes d'infection, le stress du réticulum endoplasmique

induit une surproduction de cholestérol augmentant l'abondance du CE(20:4) dans le milieu des cellules infectées par rapport aux cellules non infectées (Figure 30). Il sera ensuite pris en charge par SOF et des phospholipases et utilisé pour la croissance bactérienne. De plus, l'expression des gènes codant SLO et SOF est moins importante dans la souche mutante que dans la souche sauvage en condition de culture de laboratoire. Ces données suggèrent que ces facteurs sont moins sécrétés par la souche mutante qui induirait potentiellement une moindre production de CE(20:4), expliquant en partie le défaut de croissance à l'origine de la virulence atténuée.

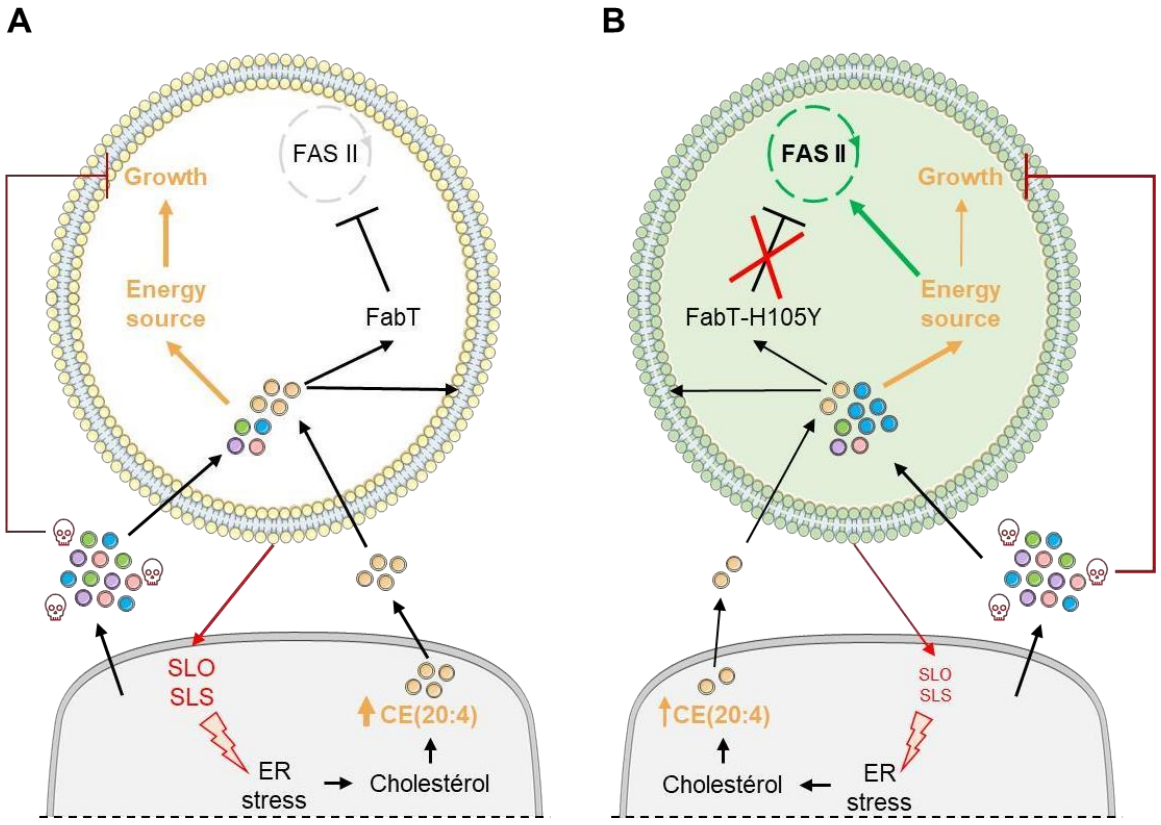

Figure 30. Modèle d'étude illustrant le défaut de virulence des souches *S. pyogenes* mutées dans *fabT*. *S. pyogenes* utilise les produits sécrétés par les cellules (cercles de couleur) notamment l'ester de cholestérol CE(20:4) (cercle jaune) comme source d'acides gras et d'énergie. (A) Au sein de la souche sauvage, le CE(20:4) participe à la répression FASII par FabT (barre T, cycle gris). (B) Du fait de l'absence de répression de FASII par FabT (croix rouge, cycle vert), la souche mutante mfabT dépense son énergie à synthétiser des acides gras, flèche verte, et consomme par conséquent plus de produits sécrétés par les cellules que la souche sauvage notamment des acides aminés et des hexoses (cercle bleu). SLO et SLS, hémolysines de *S. pyogenes*, augmentent la production d'esters de cholestérol. Celle-ci est probablement plus importante lors de l'infection par la souche sauvage.

Cette hypothèse reste à être consolidée en comparant notamment la concentration de SLO sécrétée dans les surnageants des deux souches et l'effet cytotoxique des deux souches sur les cellules. Nous pouvons également analyser la croissance en présence de surnageant de cellules infectées par la souche sauvage ou mutante. Cependant, il faut prendre en compte que les cellules et les bactéries consomment les produits au cours de leur synthèse, et qu'en présence de bactéries, les cellules sécrètent également plus de produits toxiques. Cela complexifie l'analyse de ces croissances. Afin de consolider le modèle, nous pourrions surtout envisager de réaliser un dual RNAseq. Cette analyse nous permettra d'établir les changements cellulaires en réponse à la présence bactérienne, et réciproquement les changements bactériens apportés par la réponse cellulaire. Elle soulignera aussi les voies métaboliques actives permettant de définir les nutriments consommés par les deux organismes et par les deux souches bactériennes, sauvage et mutante.

Lors de l'étude du régulon de FabT, nous avons montré qu'un unique gène, codant une protéine de la famille DegV, $DegV_{1638}$, est corégulé avec les gènes de FASII et donc exprimé en plus faible quantité en présence d'acides gras exogènes. Les protéines de la famille DegV se lient avec une forte affinité à un acide gras indiquant que les protéines DegV participent au transport et/ou au métabolisme des acides gras (376). La corégulation suggère que la protéine $DegV_{1638}$ est impliquée dans le maintien de l'équilibre membranaire. Nous avons mis en évidence qu'une mutation perte de fonction de $DegV_{1638}$ induit une surproduction de lipides dont les conséquences sont très probablement limitées par la production de vésicules extracellulaires. Les vésicules extracellulaires, principalement étudiées chez les bactéries Gram-négatives, sont impliquées dans de nombreuses fonctions de la physiologie bactérienne, notamment la réponse au stress pariétal (399). La présence de ces structures chez les bactéries Gram-positives a longtemps été controversée du fait de l'absence de membrane externe. Depuis les années 2000, la production de vésicules extracellulaires par des bactéries pathogènes Gram-positives a été démontrée notamment chez *S. aureus*, *S. pneumoniae* et *S. pyogenes* (400–402). Chez *S. pyogenes*, l'augmentation de la présence de vésicules extracellulaire a été rapportée lors de culture en présence de pénicilline et du peptide antimicrobien LL37 (402,403). Ces conditions ont en commun d'induire un stress pariétal, modifiant l'équilibre de l'enveloppe bactérienne et conduisant à l'augmentation de

la synthèse des lipides de la membrane. Ceci est également le cas chez les bactéries « L-form » de *B. subtilis* qui ne possédant plus de peptidoglycane surproduisent leur membrane (404). Par ailleurs, la production de vésicules chez *S. aureus* participe à la résistance aux acides gras toxiques de l'hôte (405). *S. aureus* incorpore les acides gras de l'hôte et les expulse en formant des vésicules. La production de vésicules extracellulaires par la bactérie est donc un mécanisme de détoxification en réponse à un stress membranaire. Chez *S. pyogenes* et *S. pneumoniae*, les vésicules extracellulaires sont principalement produites en fin de phase exponentielle ou début de phase stationnaire (401,406). Or les vésicules extracellulaires sont présentes en forte concentration dès la phase exponentielle chez la souche mutante mDegV cultivée en milieu classique de laboratoire et sans stress extérieur. Nos résultats suggèrent que la protéine $DegV_{1638}$ participerait à un mécanisme de détoxification contrôlant la quantité d'acides gras afin d'éviter un stress membranaire chez *S. pyogenes*.

Pour aller plus loin dans la compréhension de ce mécanisme de détoxification, nous avons entrepris de définir le rôle de cette protéine dans le métabolisme des acides gras chez *S. pyogenes*. Les protéines de la famille DegV les plus connues sont les protéines FakB, FakB1, FakB2 et FakB3, impliquées dans l'incorporation des acides gras exogènes (310). Le rôle spécifique de ces protéines a été étudié chez *S. aureus*, *S. pneumoniae* et *S. suis* (310–312). Certaines bactéries, comme *E. faecalis* et *S. suis*, possèdent une quatrième protéine DegV dont le rôle n'a pas encore été défini (302,311). La protéine $DegV_{1638}$ est également une quatrième protéine de la famille DegV chez *S. pyogenes*. Les capacités d'incorporation d'acides gras exogènes de la souche mutée mDegV ne sont pas modifiées. Ainsi, contrairement aux autres protéines DegV, $DegV_{1638}$ ne serait pas impliquée dans le métabolisme des acides gras exogènes. Les protéines DegV, tout comme les protéines ACP, transportent une molécule d'acyle à une autre protéine ; nous avons alors imaginé l'implication de $DegV_{1638}$ dans la régulation de FASII. Or, nos résultats de composition en acides gras montrent que $DegV_{1638}$ n'est pas impliquée dans la régulation de la synthèse des acides gras endogènes. A partir des analyses *in silico* des séquences protéiques, nous avons défini que la protéine $DegV_{1638}$ est plus proche de la protéine FakB1 que des autres protéines FakB. Nous avons également constaté que les acides aminés du site de fixation de l'acide gras saturé sont conservés entre les deux protéines (cf. Résultats, Partie 3, Résultat additionel). L'ensemble de ces observations suggère que $DegV_{1638}$ fixe préférentiellement les acides gras saturés issus de la synthèse *de*

novo qui, présents en forte concentration dans la bactérie, sont toxiques. Chez *S. pneumoniae*, la thioestérase TesS permet de contourner l'accumulation d'acyl-ACP liée à la délétion de PlsX en les dégradant et en produisant des acides gras libres (317). Une analyse *in silico*, a montré que *S. pyogenes* possède une thioestérase présentant 52,24 % d'identité de séquence avec TesS. Ainsi deux hypothèses non exclusives sont envisagées : i) $DegV_{1638}$ interagit avec PlsX lors de la réaction inverse, acyl-phosphate saturé vers acyl-DegV saturé, et/ou ii) une thioestérase libère l'acyle saturé présent sur l'acyl-AcpA ou l'acyl-AcpB permettant à $DegV_{1638}$ de se lier à l'acyle saturé libre (Figure 31).

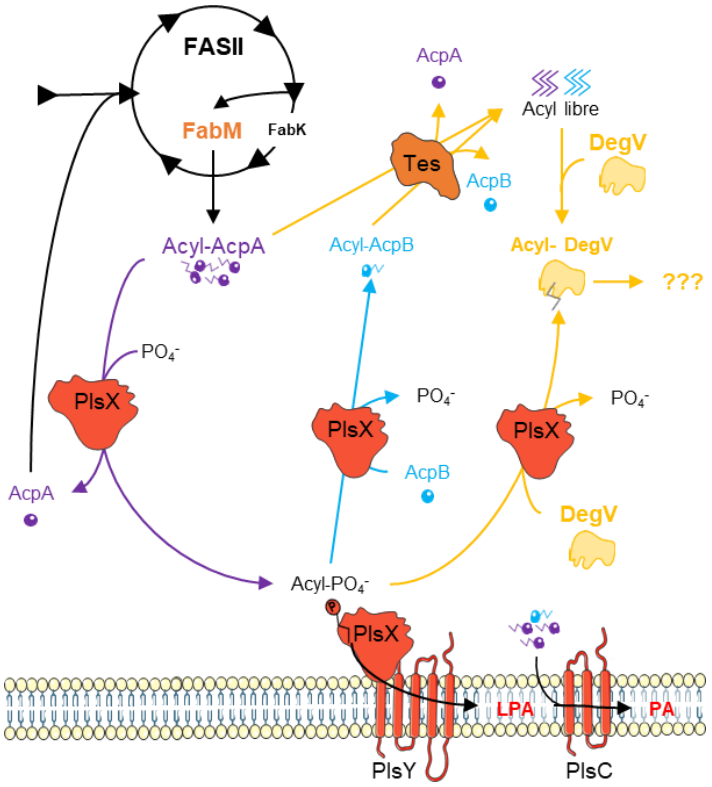

Figure 31. Proposition de rôle de la protéine $DegV_{1638}$ dans le métabolisme des acides gras endogènes chez *S. pyogenes*. Tes, Thioestérase. LPA, Acide lysophosphatidique. PA, Acide phosphatidique.

Afin de tester ces hypothèses, nous pourrions définir le type d'acides gras se liant préférentiellement à $DegV_{1638}$ par des expériences biochimiques telles que décrites pour l'identification du ligand de FabT (cf. Introduction, 3.2.3. Le mécanisme de répression de FabT) et comparer la composition en acides gras des lipides provenant des vésicules extracellulaires et des membranes bactériennes. Puis il serait intéressant d'étudier l'origine de l'acyle, acyl-ACP ou acyl-phosphate, en définissant les interactions de $DegV_{1638}$ avec d'autres

protéines telles que PlsX et l'activité du potentiel complexe protéique, $DegV_{1638}$-PlsX ou $DegV_{1638}$-Thioestérase, en le reproduisant *in vitro*. Nous pourrions également comparer la synthèse des lipides et la formation de vésicules extracellulaires dans le double mutant mFabT-mDegV et dans le mutant PlsX. Il faudrait également étudier le rôle de la protéine thioestérase chez *S. pyogenes* qui pourrait contrer les effets de l'accumulation d'acyl-ACP dans la bactérie. Enfin la combinaison de l'ensemble de ces données permettra d'envisager le devenir des acides gras pris en charge par $DegV_{1638}$.

En conclusion, nous avons montré qu'une mutation dans FabT impacte la composition de la membrane de *S. pyogenes* et son interaction avec l'hôte expliquant son défaut de virulence. Ce travail a également permis de découvrir un nouveau mécanisme de détoxification des acides gras endogènes contrôlé par FabT chez *S. pyogenes*. Par ailleurs, il a été montré que la surproduction des acides gras est une nouvelle voie thérapeutique exploitable. Cette découverte peut être appliquée dans le but de contrer spécifiquement les infections à certaines bactéries Gram-positives. La majorité des bactéries Gram-positives possèdent un unique régulateur de la synthèse des acides gras, soit FabT, soit FapR, selon les espèces (cf. Introduction, 2.3. Le maintien de l'équilibre membranaire). Nous pourrions envisager la surexpression de FASII par l'inactivation de leur répresseur, le bloquant dans sa configuration inactive. Celle-ci peut être réalisée *via* des analogues d'acyl, corépresseur de FabT chez les Streptocoques et les Entérocoques ou par des analogues de malonyl-CoA, inducteur de FapR chez *S. aureus.*

La persistance et la contre sélection des mutants FabT dans les infections non invasives restent, par ailleurs, encore à être caractérisées au niveau de la bactérie, « single-cell ». La pression de sélection exercée sur ces bactéries permet leur survie via la dérégulation de la synthèse de leur membrane. Chez *S. pyogenes*, la multiplication en présence de cellules est caractérisée par la formation d'une structure de type biofilm-like qui pourrait permettre de protéger les bactéries mutées au niveau du point d'infection. Certaines bactéries finissent néanmoins par envahir l'hôte (355). Nous pouvons nous questionner sur leur nature génétique, est-ce que ces isolats sont des révertants ou est-ce qu'elles ont acquis d'autres mutations notamment au niveau de la synthèse du peptidoglycane. Cette étude renforce également le lien existant entre la synthèse de la membrane et celle du peptidoglycane chez

les streptocoques et chez toutes bactéries Gram-positives. En effet, lors de cette discussion, nous avons fait référence notamment aux bactéries « L-form » de *B. subtilis*. *B. subtilis* ne possède pas le même système de régulation de FASII que *S. pyogenes*. Les répresseurs transcriptionnels de FASII chez *B. subtilis* sont FapR, tout comme chez *S. aureus* et FadR, tout comme chez *E. coli* (cf. Introduction, 2.3. Le maintien de l'équilibre membranaire). Ainsi, de manière générale, la régulation de la synthèse des acides gras fait partie d'un énorme réseau de régulation de la synthèse de l'intégralité de l'enveloppe permettant à la bactérie de s'adapter à son environnement.

Références bibliographiques

1. Prescott LM, Willey JM, Sherwood LM, Woolverton CJ. Microbiologie. 4ème édition. De Boeck; 2013.
2. Hamada S, Kawabata S, Nakagawa I. Molecular and genomic characterization of pathogenic traits of group A *Streptococcus*. Proc Jpn Acad Ser B Phys Biol Sci. 2015;91(10):539-59.
3. Lancefield RC. A Serological Differentiation of Human and Other Groups of Hemolytic Streptococci. J Exp Med. 1933;57(4):571-95.
4. Carapetis JR, Steer AC, Mulholland EK, Weber M. The global burden of group A streptococcal diseases. Lancet Infect Dis. 2005;5(11):685-94.
5. Mason KL, Aronoff DM. Postpartum Group A *Streptococcus* Sepsis and Maternal Immunology. Am J Reprod Immunol. 2012;67(2):91-100.
6. Mead PB, Winn WC. Vaginal-Rectal Colonization With Group A Streptococci in Late Pregnancy. Infect Dis Obstet Gynecol. 2000;8(5-6):217-9.
7. Martin J. The Streptococcus pyogenes Carrier State. In: *Streptococcus pyogenes*: Basic Biology to Clinical Manifestations. Ferretti JJ, Stevens DL, Fischetti VA, editors. Oklahoma City (OK): University of Oklahoma Health Sciences Center; 2016. p. 11.
8. Avire NJ, Whiley H, Ross K. A Review of *Streptococcus pyogenes*: Public Health Risk Factors, Prevention and Control. Pathogens. 2021;10(2):248.
9. Lamagni TL, Darenberg J, Luca-Harari B, Siljander T, Efstratiou A, Henriques-Normark B, et al. Epidemiology of Severe *Streptococcus pyogenes* Disease in Europe. J Clin Microbiol. 2008;46(7):2359-67.
10. Morens DM, Taubenberger JK, Fauci AS. Predominant Role of Bacterial Pneumonia as a Cause of Death in Pandemic Influenza: Implications for Pandemic Influenza Preparedness. J Infect Dis. 2008;198(7):962-70.
11. Okamoto S, Nagase S. Pathogenic mechanisms of invasive group A *Streptococcus* infections by influenza virus-group A *Streptococcus* superinfection: Invasive GAS infection by superinfection. Microbiol Immunol. 2018;62(3):141-9.
12. Lamagni TL, Neal S, Keshishian C, Alhaddad N, George R, Duckworth G, et al. Severe *Streptococcus pyogenes* Infections, United Kingdom, 2003–2004. Emerg Infect Dis. 2008;14(2):202-9.
13. Luo R, Sickler J, Vahidnia F, Lee YC, Frogner B, Thompson M. Diagnosis and Management of Group a Streptococcal Pharyngitis in the United States, 2011–2015. BMC Infect Dis. 2019;19(1):193.
14. Bulut ME, Kına N, Büyükyanbolu E, Özer VY, Aktaş E, Bayraktar B. A highly-sensitive rapid test for the diagnosis of streptococcal pharyngitis: BD veritor ™ system. Int J Pediatr Otorhinolaryngol. 2020;133:109980.
15. Van Brusselen D, Vlieghe E, Schelstraete P, De Meulder F, Vandeputte C, Garmyn K, et al. Streptococcal pharyngitis in children: to treat or not to treat? Eur J Pediatr. 2014;173(10):1275-83.
16. Stevens DL, Bryant AE. Impetigo, Erysipelas and Cellulitis. In: *Streptococcus pyogenes*: Basic Biology to Clinical Manifestations. Ferretti JJ, Stevens DL, Fischetti VA, editors. Oklahoma City (OK): University of Oklahoma Health Sciences Center; 2016. p.18.

17. Hay RJ, Johns NE, Williams HC, Bolliger IW, Dellavalle RP, Margolis DJ, et al. The Global Burden of Skin Disease in 2010: An Analysis of the Prevalence and Impact of Skin Conditions. J Invest Dermatol. 2014;134(6):1527-34.
18. Barton LL, Friedman AD, Sharkey AM, Schneller DJ, Swierkosz EM. Impetigo Contagiosa III. Comparative Efficacy of Oral Erythromycin and Topical Mupirocin. Pediatr Dermatol. 1989;6(2):134-8.
19. Stevens DL, Bryant AE. Severe Group A Streptococcal Infections. In: *Streptococcus pyogenes*: Basic Biology to Clinical Manifestations. Ferretti JJ, Stevens DL, Fischetti VA, editors. Oklahoma City (OK): University of Oklahoma Health Sciences Center; 2016. p. 29.
20. Gottlieb M, Long B, Koyfman A. The Evaluation and Management of Toxic Shock Syndrome in the Emergency Department: A Review of the Literature. J Emerg Med. 2018;54(6):807-14.
21. Weckel A, Guilbert T, Lambert C, Plainvert C, Goffinet F, Poyart C, et al. *Streptococcus pyogenes* infects human endometrium by limiting the innate immune response. J Clin Invest. 2021;131(4):e130746.
22. Phillips C, Walsh E. Group A Streptococcal Infection During Pregnancy and the Postpartum Period. Nurs Womens Health. 2020;24(1):13-23.
23. Hamilton SM, Stevens DL, Bryant AE. Pregnancy-Related Group A Streptococcal Infections: Temporal Relationships Between Bacterial Acquisition, Infection Onset, Clinical Findings, and Outcome. Clin Infect Dis. 2013;57(6):870-6.
24. Gendron N, Joubrel C, Nedellec S, Campagna J, Agostini A, Doucet-Populaire F, et al. Group A *Streptococcus* Endometritis following Medical Abortion. J Clin Microbiol. 2014;52(7):2733-5.
25. Cunningham MW. Molecular Mimicry, Autoimmunity, and Infection: The Cross-Reactive Antigens of Group A Streptococci and their Sequelae. Microbiol Spectr. 2019;7(4):10.1128.
26. Rodriguez-Iturbe B, Haas M. Post-Streptococcal Glomerulonephritis. In: *Streptococcus pyogenes*: Basic Biology to Clinical Manifestations. Ferretti JJ, Stevens DL, Fischetti VA, editors. Oklahoma City (OK): University of Oklahoma Health Sciences Center; 2016. p. 24.
27. Montseny JJ, Meyrier A, Kleinknecht D, Callard P. The Current Spectrum of Infectious Glomerulonephritis: Experience with 76 Patients and Review of the Literature. Medicine. 1995;74(2):63-73.
28. Parnaby MG, Carapetis JR. Rheumatic fever in Indigenous Australian children: Rheumatic fever in Indigenous Australian children. J Paediatr Child Health. 2010;46(9):527-33.
29. Bryant PA, Robins-Browne R, Carapetis JR, Curtis N. Some of the People, Some of the Time: Susceptibility to Acute Rheumatic Fever. Circulation. 2009;119(5):742-53.
30. Sika-Paotonu D, Beaton A, Raghu A, Steer A, Carapetis J. Acute Rheumatic Fever and Rheumatic Heart Disease. In: *Streptococcus pyogenes*: Basic Biology to Clinical Manifestations. Ferretti JJ, Stevens DL, Fischetti VA, editors. Oklahoma City (OK): University of Oklahoma Health Sciences Center; 2016. p. 57.
31. Saxena A. Echocardiographic Diagnosis of Chronic Rheumatic Valvular Lesions. Glob Heart. 2013;8(3):203.
32. Gewitz MH, Baltimore RS, Tani LY, Sable CA, Shulman ST, Carapetis J, et al. Revision of the Jones Criteria for the Diagnosis of Acute Rheumatic Fever in the Era of Doppler Echocardiography: A Scientific Statement From the American Heart Association. Circulation. 2015;131(20):1806-18.

33. Neff A, Chok L, von Both U, Matt U, Tarnutzer A, Andreoni F, et al. Characterisation of clinical manifestations and treatment strategies for invasive beta-haemolytic streptococcal infections in a Swiss tertiary hospital. Swiss Med Wkly. 2020;150:w20378.
34. Silva-Costa C, Friães A, Ramirez M, Melo-Cristino J. Macrolide-resistant *Streptococcus pyogenes* : prevalence and treatment strategies. Expert Rev Anti Infect Ther. 2015;13(5):615-28.
35. Castro SA, Dorfmueller HC. A brief review on Group A *Streptococcus* pathogenesis and vaccine development. R Soc open sci. 2021;8(3):201991.
36. Mahmoud A, Toth I, Stephenson R. Developing an Effective Glycan-Based Vaccine for *Streptococcus pyogenes*. Angew Chem Int Ed Engl. 2022;61(11):e202115342.
37. Dale JB, Batzloff MR, Cleary PP, Good MF, Grandi G, Halperin S, et al. Current Approaches to Group A Streptococcal Vaccine Development. In: *Streptococcus pyogenes*: Basic Biology to Clinical Manifestations. Ferretti JJ, Stevens DL, Fischetti VA, editors. Oklahoma City (OK): University of Oklahoma Health Sciences Center; 2016. p. 36.
38. Efstratiou A, Lamagni T. Epidemiology of *Streptococcus pyogenes*. In: *Streptococcus pyogenes*: Basic Biology to Clinical Manifestations. Ferretti JJ, Stevens DL, Fischetti VA, editors. Oklahoma City (OK): University of Oklahoma Health Sciences Center; 2016. p. 21.
39. Ferretti JJ, McShan WM, Ajdic D, Savic DJ, Savic G, Lyon K, et al. Complete genome sequence of an M1 strain of *Streptococcus pyogenes*. PNAS. 2001;98(8):4658-63.
40. Streptococcus pyogenes (ID 175) - Genome - NCBI.
41. Todd EW, Lancefield RC. Variants of hemolytic streptococci; their relation to type-specific substance, virulence, and toxin. J Exp Med. 1928;48(6):751-67.
42. McMillan DJ, Drèze PA, Vu T, Bessen DE, Guglielmini J, Steer AC, et al. Updated model of group A Streptococcus M proteins based on a comprehensive worldwide study. Clin Microbiol Infect. 2013;19(5):E222-9.
43. Plainvert C, Poyart C, Tazi A. Rapport d'activité du CNR 2019. Centre National de Référence des Streptocoques. https://cnr-strep.fr/.
44. Plainvert C, Poyart C, Tazi A. Rapport d'activité du CNR 2020. Centre National de Référence des Streptocoques. https://cnr-strep.fr/.
45. Bessen DE, McShan WM, Nguyen SV, Shetty A, Agrawal S, Tettelin H. Molecular epidemiology and genomics of group A *Streptococcus*. Infect Genet Evol. 2015;33:393-418.
46. Frost HR, Davies MR, Delforge V, Lakhloufi D, Sanderson-Smith M, Srinivasan V, et al. Analysis of Global Collection of Group A *Streptococcus* Genomes Reveals that the Majority Encode a Trio of M and M-Like Proteins. mSphere. 2020;5(1).
47. Efstratiou A. Group A streptococci in the 1990s. J Antimicrob Chemother. 2000;45 suppl:3-12.
48. Koller T, Manetti AGO, Kreikemeyer B, Lembke C, Margarit I, Grandi G, et al. Typing of the pilus-protein-encoding FCT region and biofilm formation as novel parameters in epidemiological investigations of Streptococcus pyogenes isolates from various infection sites. J Med Microbiol. 2010;59(4):442-52.
49. Nakata M, Koller T, Moritz K, Ribardo D, Jonas L, McIver KS, et al. Mode of Expression and Functional Characterization of FCT-3 Pilus Region-Encoded Proteins in *Streptococcus pyogenes* Serotype M49. Infect Immun. 2009;77(1):32-44.
50. Enright MC, Spratt BG, Kalia A, Cross JH, Bessen DE. Multilocus Sequence Typing of *Streptococcus pyogenes* and the Relationships between emm Type and Clone. Infect Immun. 2001;69(4):2416-27.

51. Sumby P, Porcella SF, Madrigal AG, Barbian KD, Virtaneva K, Ricklefs SM, et al. Evolutionary Origin and Emergence of a Highly Successful Clone of Serotype M1 Group A *Streptococcus* Involved Multiple Horizontal Gene Transfer Events. J Infect Dis. 2005;192(5):771-82.
52. Nasser W, Beres SB, Olsen RJ, Dean MA, Rice KA, Long SW, et al. Evolutionary pathway to increased virulence and epidemic group A *Streptococcus* disease derived from 3,615 genome sequences. PNAS. 2014;111(17):E1768-76.
53. Sitkiewicz I, Green NM, Guo N, Mereghetti L, Musser JM. Lateral gene transfer of streptococcal ICE element RD2 (region of difference 2) encoding secreted proteins. BMC Microbiology. 2011;11(1):65.
54. Weckel A, Ahamada D, Bellais S, Méhats C, Plainvert C, Longo M, et al. The N-terminal domain of the R28 protein promotes *emm28* group A *Streptococcus* adhesion to host cells *via* direct binding to three integrins. J Biol Chem. 2018;293(41):16006-18.
55. Jain I, Sarkar P, Danger JL, Medicielo J, Roshika R, Calfee G, et al. A Mobile Genetic Element Promotes the Association Between Serotype M28 Group A *Streptococcus* Isolates and Cases of Puerperal Sepsis. J Infect Dis. 2019;220(5):882-91.
56. Brouwer S, Barnett TC, Rivera-Hernandez T, Rohde M, Walker MJ. *Streptococcus pyogenes* adhesion and colonization. FEBS Letters. 2016;590(21):3739-57.
57. Courtney HS, Hasty DL, Dale JB. Molecular mechanisms of adhesion, colonization, and invasion of group A streptococci. Annals of Medicine. 2002;34(2):77-87.
58. Kreikemeyer B, Klenk M, Podbielski A. The intracellular status of *Streptococcus pyogenes*: role of extracellular matrix-binding proteins and their regulation. Int J Med Microbiol. 2004;294(2-3):177-88.
59. Molinari G, Talay SR, Valentin-Weigand P, Rohde M, Chhatwal GS. The fibronectin-binding protein of *Streptococcus pyogenes*, SfbI, is involved in the internalization of group A streptococci by epithelial cells. Infect Immun. 1997;65(4):1357-63.
60. Kreikemeyer B, Nakata M, Oehmcke S, Gschwendtner C, Normann J, Podbielski A. *Streptococcus pyogenes* Collagen Type I-binding Cpa Surface Protein. J Biol Chem. 2005;280(39):33228-39.
61. Mora M, Bensi G, Capo S, Falugi F, Zingaretti C, Manetti AGO, et al. Group A *Streptococcus* produce pilus-like structures containing protective antigens and Lancefield T antigens. PNAS. 2005;102(43):15641-6.
62. Nakata M, Kimura KR, Sumitomo T, Wada S, Sugauchi A, Oiki E, et al. Assembly Mechanism of FCT Region Type 1 Pili in Serotype M6 *Streptococcus pyogenes*. J Biol Chem. 2011;286(43):37566-77.
63. Manetti AGO, Zingaretti C, Falugi F, Capo S, Bombaci M, Bagnoli F, et al. *Streptococcus pyogenes* pili promote pharyngeal cell adhesion and biofilm formation. Mol Microbiol. 2007;64(4):968-83.
64. Kimura KR, Nakata M, Sumitomo T, Kreikemeyer B, Podbielski A, Terao Y, et al. Involvement of T6 Pili in Biofilm Formation by Serotype M6 *Streptococcus pyogenes*. J Bacteriol. 2012;194(4):804-12.
65. Rohde M. Adhesion and invasion of *Streptococcus pyogenes* into host cells and clinical relevance of intracellular streptococci. In: *Streptococcus pyogenes*: Basic Biology to Clinical Manifestations. Ferretti JJ, Stevens DL, Fischetti VA, editors. Oklahoma City (OK): University of Oklahoma Health Sciences Center; 2016. p.39.

66. Almengor AC, Walters MS, McIver KS. Mga Is Sufficient To Activate Transcription In Vitro of *sof-sfbX* and Other Mga-Regulated Virulence Genes in the Group A Streptococcus. J Bacteriol. 2006;188(6):2038-47.
67. Beall B, Gherardi G, Lovgren M, Facklam RR, Forwick BA, Tyrrell GJ. *emm* and *sof* gene sequence variation in relation to serological typing of opacity-factor-positive group A streptococci. Microbiology. 2000;146(5):1195-209.
68. Gillen CM, Courtney HS, Schulze K, Rohde M, Wilson MR, Timmer AM, et al. Opacity Factor Activity and Epithelial Cell Binding by the Serum Opacity Factor Protein of *Streptococcus pyogenes* Are Functionally Discrete. J Biol Chem. 2008;283(10):6359-66.
69. Courtney HS, Li Y, Twal WO, Argraves WS. Serum Opacity Factor Is a Streptococcal Receptor for the Extracellular Matrix Protein Fibulin-1. J Biol Chem. 2009;284(19):12966-71.
70. Courtney HS, Zhang YM, Frank MW, Rock CO. Serum Opacity Factor, a Streptococcal Virulence Factor That Binds to Apolipoproteins A-I and A-II and Disrupts High Density Lipoprotein Structure. J Biol Chem. 2006;281(9):5515-21.
71. Jeng A, Sakota V, Li Z, Datta V, Beall B, Nizet V. Molecular Genetic Analysis of a Group A Streptococcus Operon Encoding Serum Opacity Factor and a Novel Fibronectin-Binding Protein, SfbX. J Bacteriol. 2003;185(4):1208-17.
72. Rasmussen M, Eden A, Bjorck L. SclA, a Novel Collagen-Like Surface Protein of *Streptococcus pyogenes*. Infect Immun. 2000;68(11):6370-7.
73. McNitt DH, Choi SJ, Keene DR, Van De Water L, Squeglia F, Berisio R, et al. Surface-exposed loops and an acidic patch in the Scl1 protein of group A *Streptococcus* enable Scl1 binding to wound-associated fibronectin. J Biol Chem. 2018;293(20):7796-810.
74. Oliver-Kozup HA, Elliott M, Bachert BA, Martin KH, Reid SD, Schwegler-Berry DE, et al. The streptococcal collagen-like protein-1 (Scl1) is a significant determinant for biofilm formation by group A *Streptococcus*. BMC Microbiol. 2011;11(1):262.
75. Zhang S, Green NM, Sitkiewicz I, LeFebvre RB, Musser JM. Identification and Characterization of an Antigen I/II Family Protein Produced by Group A Streptococcus. Infect Immun. 2006;74(7):4200-13.
76. Maddocks SE, Wright CJ, Nobbs AH, Brittan JL, Franklin L, Strömberg N, et al. *Streptococcus pyogenes* antigen I/II-family polypeptide AspA shows differential ligand-binding properties and mediates biofilm formation: *Streptococcus pyogenes* AspA. Mol Microbiol. 2011;81(4):1034-49.
77. Franklin L, Nobbs AH, Bricio-Moreno L, Wright CJ, Maddocks SE, Sahota JS, et al. The AgI/II Family Adhesin AspA Is Required for Respiratory Infection by *Streptococcus pyogenes*. PLoS ONE. 2013;8(4):e62433.
78. Terao Y, Kawabata S, Kunitomo E, Murakami J, Nakagawa I, Hamada S. Fba, a novel fibronectin-binding protein from *Streptococcus pyogenes*, promotes bacterial entry into epithelial cells, and the fba gene is positively transcribed; under the Mga regulator: Fba is a novel Fn-binding protein of *S. pyogenes*. Mol Microbiol. 2008;42(1):75-86.
79. Pandiripally V, Gregory E, Cue D. Acquisition of Regulators of Complement Activation by *Streptococcus pyogenes* Serotype M1. Infect Immun. 2002;70(11):6206-14.
80. Courtney HS, Dale JB, Hasty DI. Differential effects of the streptococcal fibronectin-binding protein, FBP54, on adhesion of group A streptococci to human buccal cells and HEp-2 tissue culture cells. Infect Immun. 1996;64(7):2415-9.

81. Jin H, Song YP, Boel G, Kochar J, Pancholi V. Group A Streptococcal Surface GAPDH, SDH, Recognizes uPAR/CD87 as its Receptor on the Human Pharyngeal Cell and Mediates Bacterial Adherence to Host Cells. J Mol Biol. 2005;350(1):27-41.
82. Jin H, Agarwal S, Agarwal S, Pancholi V. Surface Export of GAPDH/SDH, a Glycolytic Enzyme, Is Essential for Streptococcus pyogenes Virulence. mBio. 2011; 2(3):e00068-11.
83. Terao Y, Yamaguchi M, Hamada S, Kawabata S. Multifunctional Glyceraldehyde-3-phosphate Dehydrogenase of *Streptococcus pyogenes* Is Essential for Evasion from Neutrophils. J Biol Chem. 2006;281(20):14215-23.
84. Seidler KA, Seidler NW. Role of extracellular GAPDH in *Streptococcus pyogenes* virulence. Mo Med. 2013;110(3):236-40.
85. Linke C, Caradoc-Davies TT, Young PG, Proft T, Baker EN. The Laminin-Binding Protein Lbp from *Streptococcus pyogenes* Is a Zinc Receptor. J Bacteriol. 2009;191(18):5814-23.
86. Berge A, Sjöbring U. PAM, a novel plasminogen-binding protein from *Streptococcus pyogenes*. J Biol Chem. 1993;268(34):25417-24.
87. Wistedt AC, Ringdahl U, Muller-Esterl W, Sjobring U. Identification of a plasminogen-binding motif in PAM, a bacterial surface protein. Mol Microbiol. 1995;18(3):569-78.
88. Figuera-Losada M, Ranson M, Sanderson-Smith ML, Walker MJ, Castellino FJ, Prorok M. Effects on human plasminogen conformation and activation rate caused by interaction with VEK-30, a peptide derived from the group A streptococcal M-like protein (PAM). Biochim Biophys Acta. 2010;1804(6):1342-9.
89. Qiu C, Yuan Y, Liang Z, Lee SW, Ploplis VA, Castellino FJ. Variations in the secondary structures of PAM proteins influence their binding affinities to human plasminogen. J Struct Biol. 2019;206(2):193-203.
90. Abbot EL, Smith WD, Siou GPS, Chiriboga C, Smith RJ, Wilson JA, et al. Pili mediate specific adhesion of *Streptococcus pyogenes* to human tonsil and skin. Cell Microbiol. 2007;9(7):1822-33.
91. Podbielski A, Schnitzler N, Beyhs P, Boyle MDP. M-related protein (Mrp) contributes to group A streptococcal resistance to phagocytosis by human granulocytes. Mol Microbiol. 1996;19(3):429-41.
92. Ji Y, Schnitzler N, DeMaster E, Cleary P. Impact of M49, Mrp, Enn, and C5a Peptidase Proteins on Colonization of the Mouse Oral Mucosa by *Streptococcus pyogenes*. McGhee JR, éditeur. Infect Immun. 1998;66(11):5399-405.
93. Staali L, Morgelin M, Bjorck L, Tapper H. *Streptococcus pyogenes* expressing M and M-like surface proteins are phagocytosed but survive inside human neutrophils. Cell Microbiol. 2003;5(4):253-65.
94. Bauer S, Tapper H. Membrane retrieval in neutrophils during phagocytosis: inhibition by M protein-expressing *S. pyogenes* bacteria. J Leukoc Biol. 2004;76(6):1142-50.
95. Sanderson-Smith ML, Dinkla K, Cole JN, Cork AJ, Maamary PG, McArthur JD, et al. M protein-mediated plasminogen binding is essential for the virulence of an invasive *Streptococcus pyogenes* isolate. FASEB J. 2008;22(8):2715-22.
96. Anderson EL, Cole JN, Olson J, Ryba B, Ghosh P, Nizet V. The Fibrinogen-binding M1 Protein Reduces Pharyngeal Cell Adherence and Colonization Phenotypes of M1T1 Group A *Streptococcus*. J Biol Chem. 2014;289(6):3539-46.
97. LaRock CN, Döhrmann S, Todd J, Corriden R, Olson J, Johannssen T, et al. Group A Streptococcal M1 protein sequesters cathelicidin to evade innate immune killing. Cell Host Microbe. 2015;18(4):471-7.

98. Kilsgård O, Karlsson C, Malmström E, Malmström J. Differential compartmentalization of *Streptococcus pyogenes* virulence factors and host protein binding properties as a mechanism for host adaptation. Int J Med Microbiol. 2016;306(7):504-16.
99. Herrera AL, Suso K, Allison S, Simon A, Schlenker E, Huber VC, et al. Binding host proteins to the M protein contributes to the mortality associated with influenza–*Streptococcus pyogenes* superinfections. Microbiology. 2017;163(10):1445-56.
100. De Oliveira DMP, Hartley-Tassell L, Everest-Dass A, Day CJ, Dabbs RA, Ve T, et al. Blood Group Antigen Recognition *via* the Group A Streptococcal M Protein Mediates Host Colonization. mBio. 2017;8(1):e02237-16.
101. Döhrmann S, LaRock CN, Anderson EL, Cole JN, Ryali B, Stewart C, et al. Group A Streptococcal M1 Protein Provides Resistance against the Antimicrobial Activity of Histones. Sci Rep. 2017;7:43039.
102. Yuan Y, Zajicek J, Qiu C, Chandrahas V, Lee SW, Ploplis VA, et al. Conformationally organized lysine isosteres in *Streptococcus pyogenes* M protein mediate direct high-affinity binding to human plasminogen. J Biol Chem. 2017;292(36):15016-27.
103. Valderrama JA, Riestra AM, Gao NJ, LaRock CN, Gupta N, Ali SR, et al. Group A streptococcal M protein activates the NLRP3 inflammasome. Nat Microbiol. 2017;2(10):1425-34.
104. Sanderson-Smith M, De Oliveira DMP, Guglielmini J, McMillan DJ, Vu T, Holien JK, et al. A Systematic and Functional Classification of *Streptococcus pyogenes* That Serves as a New Tool for Molecular Typing and Vaccine Development. J Infect Dis. 2014;210(8):1325-38.
105. Edwards ML, Fagan PK, Towers RJ, Currie BJ, Sriprakash KS. Inhibition of *Streptococcus pyogenes* adherence to HaCaT cells by a peptide corresponding to the streptococcal fibronectin-binding protein, SfbI, is strain dependent. Microbes Infect. 2004;6(10):926-8.
106. Hyland KA, Wang B, Cleary PP. Protein F1 and *Streptococcus pyogenes* Resistance to Phagocytosis. Infect Immun. 2007;75(6):3188-91.
107. Jaffe J, Natanson-Yaron S, Caparon MG, Hanski E. Protein F2, a novel fibronectin-binding protein from *Streptococcus pyogenes*, possesses two binding domains. Mol Microbiol. 1996;21(2):373-84.
108. Kreikemeyer B, Oehmcke S, Nakata M, Hoffrogge R, Podbielski A. *Streptococcus pyogenes* Fibronectin-binding Protein F2. J Biol Chem. 2004;279(16):15850-9.
109. Gorton D, Norton R, Layton R, Smith H, Ketheesan N. Presence of fibronectin-binding protein gene *prtF2* in invasive group A streptococci in tropical Australia is associated with increased internalisation efficiency. Microbes Infect. 2005;7(3):421-6.
110. Caswell CC, Oliver-Kozup H, Han R, Lukomska E, Lukomski S. Scl1, the multifunctional adhesin of group A *Streptococcus* , selectively binds cellular fibronectin and laminin, and mediates pathogen internalization by human cells. FEMS Microbiol Lett. 2010;303(1):61-8.
111. Oliver-Kozup H, Martin KH, Schwegler-Berry D, Green BJ, Betts C, Shinde AV, et al. The group A streptococcal collagen-like protein-1, Scl1, mediates biofilm formation by targeting the extra domain A-containing variant of cellular fibronectin expressed in wounded tissue: Scl1 binding to cellular fibronectin. Mol Microbiol. 2013;87(3):672-89.
112. Siemens N, Patenge N, Otto J, Fiedler T, Kreikemeyer B. *Streptococcus pyogenes* M49 Plasminogen/Plasmin Binding Facilitates Keratinocyte Invasion *via* Integrin-Integrin-linked Kinase (ILK) Pathways and Protects from Macrophage Killing. J Biol Chem. 2011;286(24):21612-22.

113. Bergmann S, Schoenen H, Hammerschmidt S. The interaction between bacterial enolase and plasminogen promotes adherence of *Streptococcus pneumoniae* to epithelial and endothelial cells. Int J Med Microbiol. 2013;303(8):452-62.
114. Fulde M, Steinert M, Bergmann S. Interaction of streptococcal plasminogen binding proteins with the host fibrinolytic system. Front Cell Infect Microbiol. 2013;3:85.
115. Courtney HS, Hasty DL, Dale JB. Anti-phagocytic mechanisms of *Streptococcus pyogenes*: binding of fibrinogen to M-related protein. Mol Microbiol. 2006;59(3):936-47.
116. Fisher M, Huang YS, Li X, McIver KS, Toukoki C, Eichenbaum Z. Shr Is a Broad-Spectrum Surface Receptor That Contributes to Adherence and Virulence in Group A *Streptococcus*. Infect Immun. 2008;76(11):5006-15.
117. Dahesh S, Nizet V, Cole JN. Study of streptococcal hemoprotein receptor (Shr) in iron acquisition and virulence of M1T1 group A *Streptococcus*. Virulence. 2012;3(7):566-75.
118. Oehmcke S, Podbielski A, Kreikemeyer B. Function of the Fibronectin-Binding Serum Opacity Factor of *Streptococcus pyogenes* in Adherence to Epithelial Cells. Infect Immun. 2004;72(7):4302-8.
119. Timmer AM, Kristian SA, Datta V, Jeng A, Gillen CM, Walker MJ, et al. Serum opacity factor promotes group A streptococcal epithelial cell invasion and virulence. Mol Microbiol. 2006;62(1):15-25.
120. Percy MG, Gründling A. Lipoteichoic Acid Synthesis and Function in Gram-Positive Bacteria. Annu Rev Microbiol. 2014;68:81-100.
121. Denapaite D, Brückner R, Hakenbeck R, Vollmer W. Biosynthesis of Teichoic Acids in *Streptococcus pneumoniae* and Closely Related Species: Lessons from Genomes. Microb Drug Resist. 2012;18(3):344-58.
122. Sela S, Marouni MJ, Perry R, Barzilai A. Effect of lipoteichoic acid on the uptake of *Streptococcus pyogenes* by HEp-2 cells. FEMS Microbiol Lett. 2000;193(2):187-93.
123. Cywes C, Wessels MR. Group A *Streptococcus* tissue invasion by CD44-mediated cell signalling. Nature. 2001;414(6864):648-52.
124. Purushothaman SS, Park HS, Cleary PP. Promotion of fibronectin independent invasion by C5a peptidase into epithelial cells in group A *Streptococcus*. Indian J Med Res. 2004;119 Suppl:44-7.
125. Lynskey NN, Reglinski M, Calay D, Siggins MK, Mason JC, Botto M, et al. Multi-functional mechanisms of immune evasion by the streptococcal complement inhibitor C5a peptidase. PLOS Pathogens. 2017;13(8):e1006493.
126. Wessels MR, Bronze MS. Critical role of the group A streptococcal capsule in pharyngeal colonization and infection in mice. PNAS. 1994;91(25):12238-42.
127. Dale JB, Washburn RG, Marques MB, Wessels MR. Hyaluronate capsule and surface M protein in resistance to opsonization of group A streptococci. Infect Immun. 1996;64(5):1495-501.
128. Moses AE, Wessels MR, Zalcman K, Albertí S, Natanson-Yaron S, Menes T, et al. Relative contributions of hyaluronic acid capsule and M protein to virulence in a mucoid strain of the group A *Streptococcus*. Infect Immun. 1997;65(1):64-71.
129. Husmann LK, Yung DL, Hollingshead SK, Scott JR. Role of putative virulence factors of *Streptococcus pyogenes* in mouse models of long-term throat colonization and pneumonia. Infect Immun. 1997;65(4):1422-30.
130. Kawabata S, Kuwata H, Nakagawa I, Morimatsu S, Sano K, Hamada S. Capsular hyaluronic acid of Group A Streptococci hampers their invasion into human pharyngeal epithelial cells. Microb Pathog. 1999;27(2):71-80.

131. Okamoto S, Kawabata S, Terao Y, Fujitaka H, Okuno Y, Hamada S. The *Streptococcus pyogenes* Capsule Is Required for Adhesion of Bacteria to Virus-Infected Alveolar Epithelial Cells and Lethal Bacterial-Viral Superinfection. Infect Immun. 2004;72(10):6068-75.
132. Dinkla K, Sastalla I, Godehardt AW, Janze N, Chhatwal GS, Rohde M, et al. Upregulation of capsule enables *Streptococcus pyogenes* to evade immune recognition by antigen-specific antibodies directed to the G-related α2-macroglobulin-binding protein GRAB located on the bacterial surface. Microbes Infect. 2007;9(8):922-31.
133. Matysik A, Kline KA. *Streptococcus pyogenes* Capsule Promotes Microcolony-Independent Biofilm Formation. J Bacteriol. 2019;201(18):e00052-19.
134. O'Connor SP, Cleary PP. Localization of the streptococcal C5a peptidase to the surface of group A streptococci. Infect Immun. 1986;53(2):432-4.
135. Zhu L, Olsen RJ, Beres SB, Ojeda Saavedra M, Kubiak SL, Cantu CC, et al. Genome-Wide Screens Identify Group A *Streptococcus* Surface Proteins Promoting Female Genital Tract Colonization and Virulence. Am J Pathol. 2020;190(4):862-73.
136. Bateman A, Rawlings ND. The CHAP domain: a large family of amidases including GSP amidase and peptidoglycan hydrolasesq. Trends Biochem Sci. 2003;28(5):234-7.
137. Beachey EH, Ofek I. Epithelial cell binding of group A streptococci by lipoteichoic acid on fimbriae denuded of M protein. J Exp Med. 1976;143(4):759-71.
138. Ofek I, Zafriri D. Inability of Toxin Inhibitors To Neutralize Enhanced Toxicity Caused by Bacteria Adherent to Tissue Culture Cells. Infect Immun. 1990;58(11):3737-42.
139. Hasty DL, Ofek I, Courtney HS, Doyle RJ. Multiple adhesins of streptococci. Infect Immun. 1992;60(6):2147-52.
140. Courtney HS, Ofek I, Penfound T, Nizet V, Pence MA, Kreikemeyer B, et al. Relationship between Expression of the Family of M Proteins and Lipoteichoic Acid to Hydrophobicity and Biofilm Formation in *Streptococcus pyogenes*. PLoS One. 2009;4(1):e4166.
141. Imai T, Matsumura T, Mayer-Lambertz S, Wells CA, Ishikawa E, Butcher SK, et al. Lipoteichoic acid anchor triggers Mincle to drive protective immunity against invasive group A *Streptococcus* infection. PNAS. 2018;115(45):E10662-71.
142. Coye LH, Collins CM. Identification of SpyA, a novel ADP-ribosyltransferase of *Streptococcus pyogenes*: Identification of SpyA. Mol Microbiol. 2004;54(1):89-98.
143. Icenogle LM, Hengel SM, Coye LH, Streifel A, Collins CM, Goodlett DR, et al. Molecular and Biological Characterization of Streptococcal SpyA-mediated ADP-ribosylation of Intermediate Filament Protein Vimentin. J Biol Chem. 2012;287(25):21481-91.
144. Gallotta M, Gancitano G, Pietrocola G, Mora M, Pezzicoli A, Tuscano G, et al. SpyAD, a Moonlighting Protein of Group A *Streptococcus* Contributing to Bacterial Division and Host Cell Adhesion. Infect Immun. 2014;82(7):2890-901.
145. Zinkernagel AS, Timmer AM, Pence MA, Locke JB, Buchanan JT, Turner CE, et al. The IL-8 Protease SpyCEP/ScpC of Group A *Streptococcus* Promotes Resistance to Neutrophil Killing. Cell Host Microbe. 2008;4(2):170-8.
146. Kurupati P, Turner CE, Tziona I, Lawrenson RA, Alam FM, Nohadani M, et al. Chemokine-cleaving *Streptococcus pyogenes* protease SpyCEP is necessary and sufficient for bacterial dissemination within soft tissues and the respiratory tract: SpyCEP and *S. pyogenes* dissemination. Mol Microbiol. 2010;76(6):1387-97.
147. Zingaretti C, Falugi F, Nardi-Dei V, Pietrocola G, Mariani M, Liberatori Marilena Gallotta S, et al. *Streptococcus pyogenes* SpyCEP: a chemokine-inactivating protease with unique structural and biochemical features. FASEB J. 2010;24(8):2839-48.

148. Kaur SJ, Nerlich A, Bergmann S, Rohde M, Fulde M, Zähner D, et al. The C *X* C Chemokine-degrading Protease SpyCep of *Streptococcus pyogenes* Promotes Its Uptake into Endothelial Cells. J Biol Chem. 2010;285(36):27798-805.
149. Chiappini N, Seubert A, Telford JL, Grandi G, Serruto D, Margarit I, et al. *Streptococcus pyogenes* SpyCEP Influences Host-Pathogen Interactions during Infection in a Murine Air Pouch Model. PLoS One. 2012;7(7):e40411.
150. Soderholm AT, Barnett TC, Korn O, Rivera-Hernandez T, Seymour LM, Schulz BL, et al. Group A *Streptococcus* M1T1 Intracellular Infection of Primary Tonsil Epithelial Cells Dampens Levels of Secreted IL-8 Through the Action of SpyCEP. Front Cell Infect Microbiol. 2018;8:160.
151. Goldblatt J, Lawrenson RA, Muir L, Dattani S, Hoffland A, Tsuchiya T, et al. A Requirement for Neutrophil Glycosaminoglycans in Chemokine: Receptor Interactions Is Revealed by the Streptococcal Protease SpyCEP. J Immunol. 2019;202(11):3246-55.
152. Gubba S, Low DE, Musser JM. Expression and Characterization of Group A *Streptococcus* Extracellular Cysteine Protease Recombinant Mutant Proteins and Documentation of Seroconversion during Human Invasive Disease Episodes. Infect Immun. 1998;66(2):765-70.
153. Stockbauer KE, Magoun L, Liu M, Burns EH, Gubba S, Renish S, et al. A natural variant of the cysteine protease virulence factor of group A *Streptococcus* with an arginine-glycine-aspartic acid (RGD) motif preferentially binds human integrins v 3 and IIb 3. PNAS. 1999;96(1):242-7.
154. Barnett TC, Cole JN, Rivera-Hernandez T, Henningham A, Paton JC, Nizet V, et al. Streptococcal toxins: role in pathogenesis and disease: Streptococcal toxins role in pathogenesis and disease. Cell Microbiol. 2015;17(12):1721-41.
155. Shannon BA, McCormick JK, Schlievert PM. Toxins and Superantigens of Group A Streptococci. Microbiol Spectr. 2019;7(1).
156. Collin M, Svensson MD, Sjoholm AG, Jensenius JC, Sjobring U, Olsen A. EndoS and SpeB from *Streptococcus pyogenes* Inhibit Immunoglobulin-Mediated Opsonophagocytosis. Infect Immun. 2002;70(12):6646-51.
157. Honda-Ogawa M, Ogawa T, Terao Y, Sumitomo T, Nakata M, Ikebe K, et al. Cysteine Proteinase from *Streptococcus pyogenes* Enables Evasion of Innate Immunity *via* Degradation of Complement Factors. J Biol Chem. 2013;288(22):15854-64.
158. Michos A, Gryllos I, Håkansson A, Srivastava A, Kokkotou E, Wessels MR. Enhancement of Streptolysin O Activity and Intrinsic Cytotoxic Effects of the Group A Streptococcal Toxin, NAD-Glycohydrolase. J Biol Chem. 2006;281(12):8216-23.
159. Magassa N, Chandrasekaran S, Caparon MG. *Streptococcus pyogenes* cytolysin-mediated translocation does not require pore formation by streptolysin O. EMBO Rep. 2010;11(5):400-5.
160. Boxrud PD, Verhamme IM, Bock PE. Resolution of Conformational Activation in the Kinetic Mechanism of Plasminogen Activation by Streptokinase. J Biol Chem. 2004;279(35):36633-41.
161. Boxrud PD, Bock PE. Coupling of Conformational and Proteolytic Activation in the Kinetic Mechanism of Plasminogen Activation by Streptokinase. J Biol Chem. 2004;279(35):36642-9.
162. Gase K, Ferretti JJ, Primeaux C, McShan WM. Identification, Cloning, and Expression of the CAMP factor gene (cfa) of Group A Streptococci. Fischetti VA, éditeur. Infect Immun. 1999;67(9):4725-31.

163. Kurosawa M, Oda M, Domon H, Saitoh I, Hayasaki H, Terao Y. *Streptococcus pyogenes* CAMP factor attenuates phagocytic activity of RAW 264.7 cells. Microbes Infect. 2016;18(2):118-27.
164. Kurosawa M, Oda M, Domon H, Isono T, Nakamura Y, Saitoh I, et al. Streptococcus pyogenes CAMP factor promotes bacterial adhesion and invasion in pharyngeal epithelial cells without serum *via* PI3K/Akt signaling pathway. Microbes Infect. 2018;20(1):9-18.
165. Pietrocola G, Rindi S, Rosini R, Buccato S, Speziale P, Margarit I. The Group B *Streptococcus* –Secreted Protein CIP Interacts with C4, Preventing C3b Deposition *via* the Lectin and Classical Complement Pathways. J Immunol. 2016;196(1):385-94.
166. Collin M, Olsén A. EndoS, a novel secreted protein from *Streptococcus pyogenes* with endoglycosidase activity on human IgG. EMBO J. 2001;20(12):3046-55.
167. Collin M, Olsén A. Effect of SpeB and EndoS from *Streptococcus pyogenes* on Human Immunoglobulins. Infect Immun. 2001;69(11):7187-9.
168. Toppel AW, Rasmussen M, Rohde M, Medina E, Chhatwal GS. Contribution of Protein G–Related α2-Macroglobulin–Binding Protein to Bacterial Virulence in a Mouse Skin Model of Group A Streptococcal Infection. J Infect Dis. 2003;187(11):1694-703.
169. Rasmussen M. Protein GRAB of *Streptococcus pyogenes* Regulates Proteolysis at the Bacterial Surface by Binding α2-Macroglobulin. 1999;274(22):15336-44.
170. Rivera Starr C, Engleberg NC. Role of Hyaluronidase in Subcutaneous Spread and Growth of Group A *Streptococcus*. Infect Immun. 2006;74(1):40-8.
171. Lei B, DeLeo FR, Hoe NP, Graham MR, Mackie SM, Cole RL, et al. Evasion of human innate and acquired immunity by a bacterial homolog of CD11b that inhibits opsonophagocytosis. Nat Med. 2001;7(12):1298-305.
172. von Pawel-Rammingen U. IdeS, a novel streptococcal cysteine proteinase with unique specificity for immunoglobulin G. EMBO J. 2002;21(7):1607-15.
173. Wenig K, Chatwell L, von Pawel-Rammingen U, Bjorck L, Huber R, Sondermann P. Structure of the streptococcal endopeptidase IdeS, a cysteine proteinase with strict specificity for IgG. PNAS. 2004;101(50):17371-6.
174. Âkesson P, Moritz L, Truedsson M, Christensson B, von Pawel-Rammingen U. IdeS, a highly specific immunoglobulin g (igg)-cleaving enzyme from *Streptococcus pyogenes*, is inhibited by specific igg antibodies generated during infection. Infect Immun. 2006;74(1):497-503.
175. Okumura CYM, Anderson EL, Döhrmann S, Tran DN, Olson J, von Pawel-Rammingen U, et al. IgG Protease Mac/IdeS Is Not Essential for Phagocyte Resistance or Mouse Virulence of M1T1 Group A *Streptococcus*. mBio. 2013;4(4):e00499-13.
176. Bricker AL, Cywes C, Ashbaugh CD, Wessels MR. NAD^+-glycohydrolase acts as an intracellular toxin to enhance the extracellular survival of group A streptococci. Mol Microbiol. 2002;44(1):257-69.
177. Bricker AL, Carey VJ, Wessels MR. Role of NADase in Virulence in Experimental Invasive Group A Streptococcal Infection. Infect Immun. 2005;73(10):6562-6.
178. Ghosh J, Caparon MG. Specificity of *Streptococcus pyogenes* NAD^+-glycohydrolase in cytolysin-mediated translocation. Mol Microbiol. 2006;62(4):1203-14.
179. Tatsuno I, Sawai J, Okamoto A, Matsumoto M, Minami M, Isaka M, et al. Characterization of the NAD^+-glycohydrolase in streptococcal strains. Microbiology. 2007;153(12):4253-60.

180. Bastiat-Sempe B, Love JF, Lomayesva N, Wessels MR. Streptolysin O and NAD^+-Glycohydrolase Prevent Phagolysosome Acidification and Promote Group A *Streptococcus* Survival in Macrophages. mBio. 2014;5(5):e01690-14.
181. Sharma O, O'Seaghdha M, Velarde JJ, Wessels MR. NAD+-Glycohydrolase Promotes Intracellular Survival of Group A Streptococcus. PLOS Pathogens. 2016;12(3):e1005468.
182. Velarde JJ, O'Seaghdha M, Baddal B, Bastiat-Sempe B, Wessels MR. Binding of NAD^+-Glycohydrolase to Streptolysin O Stabilizes Both Toxins and Promotes Virulence of Group A *Streptococcus*. mBio. 2017;8(5):e01382-17.
183. Sumby P, Barbian KD, Gardner DJ, Whitney AR, Welty DM, Long RD, et al. Extracellular deoxyribonuclease made by group A *Streptococcus* assists pathogenesis by enhancing evasion of the innate immune response. PNAS. 2005;102(5):1679-84.
184. Buchanan JT, Simpson AJ, Aziz RK, Liu GY, Kristian SA, Kotb M, et al. DNase Expression Allows the Pathogen Group A *Streptococcus* to Escape Killing in Neutrophil Extracellular Traps. Curr Biol. 2006;16(4):396-400.
185. Uchiyama S, Andreoni F, Schuepbach RA, Nizet V, Zinkernagel AS. DNase Sda1 Allows Invasive M1T1 Group A *Streptococcus* to Prevent TLR9-Dependent Recognition. PLoS Pathog. 2012;8(6):e1002736.
186. Åkesson P, Sjöholm AG, Björck L. Protein SIC, a novel extracellular protein of *Streptococcus pyogenes* interfering with complement function. J Biol Chem. 1996;271(2):1081-8.
187. Lukomski S, Hoe NP, Abdi I, Rurangirwa J, Kordari P, Liu M, et al. Nonpolar Inactivation of the Hypervariable Streptococcal Inhibitor of Complement Gene (sic) in Serotype M1 *Streptococcus pyogenes* Significantly Decreases Mouse Mucosal Colonization. Infect Immun. 2000;68(2):535-42.
188. Hoe NP, Ireland RM, DeLeo FR, Gowen BB, Dorward DW, Voyich JM, et al. Insight into the molecular basis of pathogen abundance: Group A *Streptococcus* inhibitor of complement inhibits bacterial adherence and internalization into human cells. PNAS. 2002;99(11):7646-51.
189. Fernie-King BA, Seilly DJ, Davies A, Lachmann PJ. Streptococcal Inhibitor of Complement Inhibits Two Additional Components of the Mucosal Innate Immune System: Secretory Leukocyte Proteinase Inhibitor and Lysozyme. Infect Immun. 2002;70(9):4908-16.
190. Frick IM, Åkesson P, Rasmussen M, Schmidtchen A, Björck L. SIC, a Secreted Protein of *Streptococcus pyogenes* That Inactivates Antibacterial Peptides. J Biol Chem. 2003;278(19):16561-6.
191. Shelburne SA, Granville C, Tokuyama M, Sitkiewicz I, Patel P, Musser JM. Growth Characteristics of and Virulence Factor Production by Group A *Streptococcus* during Cultivation in Human Saliva. Infect Immun. 2005;73(8):4723-31.
192. Fernie-King BA, Seilly DJ, Binks MJ, Sriprakash KS, Lachmann PJ. Streptococcal DRS (distantly related to SIC) and SIC inhibit antimicrobial peptides, components of mucosal innate immunity: a comparison of their activities. Microbes Infect. 2007;9(3):300-7.
193. Åkesson P, Herwald H, Rasmussen M, HÅkansson K, Abrahamson M, Hasan AAK, et al. Streptococcal inhibitor of complement-mediated lysis (SIC): an anti-inflammatory virulence determinant. Microbiology. 2010;156(12):3660-8.
194. Pence MA, Rooijakkers SHM, Cogen AL, Cole JN, Hollands A, Gallo RL, et al. Streptococcal Inhibitor of Complement Promotes Innate Immune Resistance Phenotypes of Invasive M1T1 Group A *Streptococcus*. J Innate Immun. 2010;2(6):587-95.

195. Frick IM, Shannon O, Åkesson P, Mörgelin M, Collin M, Schmidtchen A, et al. Antibacterial Activity of the Contact and Complement Systems Is Blocked by SIC, a Protein Secreted by *Streptococcus pyogenes*. J Biol Chem. 2011;286(2):1331-40.
196. Westman J, Chakrakodi B, Snäll J, Mörgelin M, Bruun Madsen M, Hyldegaard O, et al. Protein SIC Secreted from *Streptococcus pyogenes* Forms Complexes with Extracellular Histones That Boost Cytokine Production. Front Immunol. 2018;9:236.
197. Nitzsche R, Rosenheinrich M, Kreikemeyer B, Oehmcke-Hecht S. *Streptococcus pyogenes* Triggers Activation of the Human Contact System by Streptokinase. Infect Immun. 2015;83(8):3035-42.
198. Nitzsche R, Köhler J, Kreikemeyer B, Oehmcke-Hecht S. *Streptococcus pyogenes* Escapes Killing from Extracellular Histones through Plasminogen Binding and Activation by Streptokinase. J Innate Immun. 2016;8(6):589-600.
199. Sitkiewicz I, Nagiec MJ, Sumby P, Butler SD, Cywes-Bentley C, Musser JM. Emergence of a bacterial clone with enhanced virulence by acquisition of a phage encoding a secreted phospholipase A2. PNAS. 2006;103(43):16009-14.
200. Ruiz N, Wang B, Pentland A, Caparon M. Streptolysin O and adherence synergistically modulate proinflammatory responses of keratinocytes to group A streptococci. Mol Microbiol. 1998;27(2):337-46.
201. Limbago B, Penumalli V, Weinrick B, Scott JR. Role of Streptolysin O in a Mouse Model of Invasive Group A Streptococcal Disease. Infect Immun. 2000;68(11):7.
202. Sierig G, Cywes C, Wessels MR, Ashbaugh CD. Cytotoxic Effects of Streptolysin O and Streptolysin S Enhance the Virulence of Poorly Encapsulated Group A Streptococci. Infect Immun. 2003;71(1):446-55.
203. Nilsson M, Sørensen O, Mörgelin M, Weineisen M, Sjöbring U, Herwald H. Activation of human polymorphonuclear neutrophils by streptolysin O from *Streptococcus pyogenes* leads to the release of proinflammatory mediators. Thromb Haemost. 2006;95(06):982-90.
204. Timmer AM, Timmer JC, Pence MA, Hsu LC, Ghochani M, Frey TG, et al. Streptolysin O Promotes Group A *Streptococcus* Immune Evasion by Accelerated Macrophage Apoptosis. J Biol Chem. 2009;284(2):862-71.
205. Logsdon LK, Håkansson AP, Cortés G, Wessels MR. Streptolysin O Inhibits Clathrin-Dependent Internalization of Group A *Streptococcus*. mBio. 2011;2(1):e00332-10.
206. Baruch M, Hertzog BB, Ravins M, Anand A, Catherine Youting C, Biswas D, et al. Induction of endoplasmic reticulum stress and unfolded protein response constitutes a pathogenic strategy of group A streptococcus. Front. Cell. Infect. Microbiol. 2014;4:105.
207. Uchiyama S, Döhrmann S, Timmer AM, Dixit N, Ghochani M, Bhandari T, et al. Streptolysin O Rapidly Impairs Neutrophil Oxidative Burst and Antibacterial Responses to Group A *Streptococcus*. Front Immunol. 2015;6(581).
208. Zhu L, Olsen RJ, Lee JD, Porter AR, DeLeo FR, Musser JM. Contribution of Secreted NADase and Streptolysin O to the Pathogenesis of Epidemic Serotype M1 *Streptococcus pyogenes* Infections. Am J Pathol. 2017;187(3):605-13.
209. Lin A, Loughman JA, Zinselmeyer BH, Miller MJ, Caparon MG. Streptolysin S Inhibits Neutrophil Recruitment during the Early Stages of *Streptococcus pyogenes* Infection. Infect Immun. 2009;77(11):5190-201.
210. Sumitomo T, Nakata M, Higashino M, Jin Y, Terao Y, Fujinaga Y, et al. Streptolysin S Contributes to Group A Streptococcal Translocation across an Epithelial Barrier. J Biol Chem. 2011;286(4):2750-61.

211. Flaherty RA, Puricelli JM, Higashi DL, Park CJ, Lee SW. Streptolysin S Promotes Programmed Cell Death and Enhances Inflammatory Signaling in Epithelial Keratinocytes during Group A *Streptococcus* Infection. Infect Immun. 2015;83(10):4118-33.
212. Feng W, Minor D, Liu M, Lei B. Requirement and Synergistic Contribution of Platelet-Activating Factor Acetylhydrolase Sse and Streptolysin S to Inhibition of Neutrophil Recruitment and Systemic Infection by Hypervirulent *emm3* Group A *Streptococcus* in Subcutaneous Infection of Mice. Infect Immun. 2017;85(12):e00530-17.
213. Flaherty RA, Donahue DL, Carothers KE, Ross JN, Ploplis VA, Castellino FJ, et al. Neutralization of Streptolysin S-Dependent and Independent Inflammatory Cytokine IL-1β Activity Reduces Pathology During Early Group A Streptococcal Skin Infection. Front Cell Infect Microbiol. 2018;8:211.
214. Tsao N, Kuo CF, Cheng MH, Lin WC, Lin CF, Lin YS. Streptolysin S induces mitochondrial damage and macrophage death through inhibiting degradation of glycogen synthase kinase-3β in *Streptococcus pyogenes* infection. Sci Rep. 2019;9(1):5371.
215. Vajjala A, Biswas D, Tay WH, Hanski E, Kline KA. Streptolysin-induced endoplasmic reticulum stress promotes group A Streptococcal host-associated biofilm formation and necrotising fasciitis. Cell Microbiol. 2019;21(1):e12956.
216. Kline JB, Collins CM. Analysis of the interaction between the bacterial superantigen streptococcal pyrogenic exotoxin A (SpeA) and the human T-cell receptor. Mol Microbiol. 1997;24(1):191-202.
217. Papageorgiou AC, Collins CM, Gutman DM, Kline JB, O'Brien SM, Tranter HS, et al. Structural basis for the recognition of superantigen streptococcal pyrogenic exotoxin A (SpeA1) by MHC class II molecules and T-cell receptors. EMBO J. 1999;18(1):9-21.
218. Bhatnagar, Grover, Ganguly. Superantigen-induced T cell responses in acute rheumatic fever and chronic rheumatic heart disease patients. Clin Exp Immunol. 1999;116(1):100-6.
219. Sriskandan S, Unnikrishnan M, Krausz T, Cohen J. Molecular analysis of the role of streptococcal pyrogenic exotoxin A (SPEA) in invasive soft-tissue infection resulting from *Streptococcus pyogenes*. Mol Microbiol. 1999;33(4):778-90.
220. Norrby-Teglund A, Thulin P, Gan BS, Kotb M, McGeer A, Andersson J, et al. Evidence for Superantigen Involvement in Severe Group A Streptococcal Tissue Infections. J Infect Dis. 2001;184(7):853-60.
221. Proft T, Arcus VL, Handley V, Baker EN, Fraser JD. Immunological and Biochemical Characterization of Streptococcal Pyrogenic Exotoxins I and J (SPE-I and SPE-J) from *Streptococcus pyogenes*. J Immunol. 2001;166(11):6711-9.
222. Muller-Alouf H, Proft T, Zollner TM, Gerlach D, Champagne E, Desreumaux P, et al. Pyrogenicity and Cytokine-Inducing Properties of *Streptococcus pyogenes* Superantigens: Comparative Study of Streptococcal Mitogenic Exotoxin Z and Pyrogenic Exotoxin A. Infect Immun. 2001;69(6):4141-5.
223. Unnikrishnan M, Altmann DM, Proft T, Wahid F, Cohen J, Fraser JD, et al. The Bacterial Superantigen Streptococcal Mitogenic Exotoxin Z Is the Major Immunoactive Agent of *Streptococcus pyogenes*. J Immunol. 2002;169(5):2561-9.
224. Sriskandan S, Faulkner L, Hopkins P. *Streptococcus pyogenes*: Insight into the function of the streptococcal superantigens. Int J Biochem Cell Biol. 2007;39(1):12-9.
225. Ganem MB, De Marzi MC, Fernández-Lynch MJ, Jancic C, Vermeulen M, Geffner J, et al. Uptake and Intracellular Trafficking of Superantigens in Dendritic Cells. PLoS One. 2013;8(6):e66244.

226. Kasper KJ, Zeppa JJ, Wakabayashi AT, Xu SX, Mazzuca DM, Welch I, et al. Bacterial Superantigens Promote Acute Nasopharyngeal Infection by *Streptococcus pyogenes* in a Human MHC Class II-Dependent Manner. PLoS Pathog. 2014;10(5):e1004155.
227. Zeppa JJ, Kasper KJ, Mohorovic I, Mazzuca DM, Haeryfar SMM, McCormick JK. Nasopharyngeal infection by *Streptococcus pyogenes* requires superantigen-responsive Vβ-specific T cells. PNAS. 2017;114(38):10226-31.
228. Tsai PJ, Kuo CF, Lin KY, Lin YS, Lei HY, Chen FF, et al. Effect of Group A Streptococcal Cysteine Protease on Invasion of Epithelial Cells. Infect Immun. 1998;66(4):1460-6.
229. Lukomski S, Burns EH, Wyde PR, Podbielski A, Rurangirwa J, Moore-Poveda DK, et al. Genetic Inactivation of an Extracellular Cysteine Protease (SpeB) Expressed by *Streptococcus pyogenes* Decreases Resistance to Phagocytosis and Dissemination to Organs. Infect Immun. 1998;66(2):771-6.
230. Liu M, Zhu H, Zhang J, Lei B. Active and Passive Immunizations with the Streptococcal Esterase Sse Protect Mice against Subcutaneous Infection with Group A Streptococci. Infect Immun. 2007;75(7):3651-7.
231. Liu M, Zhu H, Li J, Garcia CC, Feng W, Kirpotina LN, et al. Group A *Streptococcus* Secreted Esterase Hydrolyzes Platelet-Activating Factor to Impede Neutrophil Recruitment and Facilitate Innate Immune Evasion. PLoS Pathog. 2012;8(4):e1002624.
232. Nobbs AH, Lamont RJ, Jenkinson HF. *Streptococcus* Adherence and Colonization. Microbiol Mol Biol Rev. 2009;73(3):407-50.
233. Nitsche-Schmitz P, Rohde M, Chhatwal G. Invasion mechanisms of Gram-positive pathogenic cocci. Thromb Haemost. 2007;98(09):488-96.
234. Manetti AGO, Köller T, Becherelli M, Buccato S, Kreikemeyer B, Podbielski A, et al. Environmental Acidification Drives *S. pyogenes* Pilus Expression and Microcolony Formation on Epithelial Cells in a FCT-Dependent Manner. PLoS One. 2010;5(11):e13864.
235. Fiedler T, Köller T, Kreikemeyer B. *Streptococcus pyogenes* biofilms - formation, biology, and clinical relevance. Front Cell Infect Microbiol. 2015;5:15.
236. Dombek PE, Cue D, Sedgewick J, Lam H, Ruschkowski S, Finlay BB, et al. High-frequency intracellular invasion of epithelial cells by serotype M1 group A streptococci: M1 protein-mediated invasion and cytoskeletal rearrangements. Mol Microbiol. 1999;31(3):859-70.
237. Molinari G, Rohde M, Guzman CA, Chhatwal GS. Two distinct pathways for the invasion of *Streptococcus pyogenes* in non-phagocytic cells. Cellr Microbiol. 2000;2(2):145-54.
238. Rohde M, Muller E, Chhatwal GS, Talay SR. Host cell caveolae act as an entry-port for Group A streptococci. Cell Microbiol. 2003;5(5):323-42.
239. Wexler DE, Chenoweth DE, Cleary PP. Mechanism of action of the group A streptococcal C5a inactivator. PNAS. 1985;82(23):8144-8.
240. Voyich JM, Sturdevant DE, Braughton KR, Kobayashi SD, Lei B, Virtaneva K, et al. Genome-wide protective response used by group A *Streptococcus* to evade destruction by human polymorphonuclear leukocytes. PNAS. 2003;100(4):1996-2001.
241. Kobayashi SD, Braughton KR, Whitney AR, Voyich JM, Schwan TG, Musser JM, et al. Bacterial pathogens modulate an apoptosis differentiation program in human neutrophils. PNAS. 2003;100(19):10948-53.
242. Dinkla K, Rohde M, Jansen WTM, Carapetis JR, Chhatwal GS, Talay SR. *Streptococcus pyogenes* recruits collagen *via* surface-bound fibronectin: a novel colonization and immune evasion mechanism: *S. pyogenes* collagen recruitment. Mol Microbiol. 2003;47(3):861-9.

243. Brinkmann V, Reichard U, Goosmann C, Fauler B, Uhlemann Y, Weiss DS, et al. Neutrophil Extracellular Traps Kill Bacteria. Science. 2004;303(5663):1532-5.
244. Tanaka M, Kinoshita-Daitoku R, Kiga K, Sanada T, Zhu B, Okano T, et al. Group A *Streptococcus* establishes pharynx infection by degrading the deoxyribonucleic acid of neutrophil extracellular traps. Sci Rep. 2020;10(1):3251.
245. Pancholi V, Caparon M. *Streptococcus pyogenes* Metabolism. In: *Streptococcus pyogenes*: Basic Biology to Clinical Manifestations. Ferretti JJ, Stevens DL, Fischetti VA, editors. Oklahoma City (OK): University of Oklahoma Health Sciences Center; 2016. p. 49.
246. Shelburne SA, Sumby P, Sitkiewicz I, Okorafor N, Granville C, Patel P, et al. Maltodextrin Utilization Plays a Key Role in the Ability of Group A *Streptococcus* To Colonize the Oropharynx. Infect Immun. 2006;74(8):4605-14.
247. Loughman JA, Caparon MG. Comparative functional analysis of the lac operons in *Streptococcus pyogenes*: Comparison of paralogous streptococcal pathways. Mol Microbiol. 2007;64(2):269-80.
248. Loughman JA, Caparon MG. A novel adaptation of aldolase regulates virulence in *Streptococcus pyogenes*. EMBO J. 2006;25(22):5414-22.
249. Paluscio E, Caparon MG. *Streptococcus pyogenes* Malate Degradation Pathway Links pH Regulation and Virulence. Infect Immun. 2015;83(3):1162-71.
250. Steiner K, Malke H. Life in protein-rich environments: the relA-independent response of *Streptococcus pyogenes* to amino acid starvation. Mol Microbiol. 2000;38(5):1004-16.
251. Steiner K, Malke H. relA-Independent amino acid starvation response network of *Streptococcus pyogenes*. J Bacteriol. 2001;183(24):7354-64.
252. Hirose Y, Yamaguchi M, Sumitomo T, Nakata M, Hanada T, Okuzaki D, et al. *Streptococcus pyogenes* upregulates arginine catabolism to exert its pathogenesis on the skin surface. Cell Rep. 2021;34(13):108924.
253. Baruch M, Belotserkovsky I, Hertzog BB, Ravins M, Dov E, McIver KS, et al. An Extracellular Bacterial Pathogen Modulates Host Metabolism to Regulate Its Own Sensing and Proliferation. Cell. 2014;156(1-2):97-108.
254. Brouwer S, Jespersen MG, Ong C lynn Y, De Oliveira DMP, Keller B, Cork AJ, et al. *Streptococcus pyogenes* Hijacks Host Glutathione for Growth and Innate Immune Evasion. mBio. 2022;13(3):e00676-22.
255. Almengor AC, Kinkel TL, Day SJ, McIver KS. The Catabolite Control Protein CcpA binds to p *mga* and influences expression of the virulence regulator Mga in the group A *Streptococcus*. J Bacteriol. 2007;189(23):8405-16.
256. Patenge N, Fiedler T, Kreikemeyer B. Common Regulators of Virulence in Streptococci. Curr Top Microbiol Immunol. 2012;368:111-53.
257. Kinkel TL, McIver KS. CcpA-Mediated Repression of Streptolysin S Expression and Virulence in the Group A *Streptococcus*. Infect Immun. 2008;76(8):3451-63.
258. Deutscher J, Küster E, Bergstedt U, Charrier V, Hillen W. Protein kinase-dependent HPr/CcpA interaction links glycolytic activity to carbon catabolite repression in Gram-positive bacteria. Mol Microbiol. 1995;15(6):1049-53.
259. Vega LA, Malke H, McIver KS. Virulence-Related Transcriptional Regulators of *Streptococcus pyogenes*. In: *Streptococcus pyogenes*: Basic Biology to Clinical Manifestations. Ferretti JJ, Stevens DL, Fischetti VA, editors. Oklahoma City (OK): University of Oklahoma Health Sciences Center; 2016. p. 52.

260. Graham MR, Smoot LM, Migliaccio CAL, Virtaneva K, Sturdevant DE, Porcella SF, et al. Virulence control in group A *Streptococcus* by a two-component gene regulatory system: Global expression profiling and *in vivo* infection modeling. PNAS. 2002;99(21):13855-60.
261. Kreikemeyer B, McIver KS, Podbielski A. Virulence factor regulation and regulatory networks in *Streptococcus pyogenes* and their impact on pathogen–host interactions. Trends Microbiol. 2003;11(5):224-32.
262. Hondorp ER, McIver KS. The Mga virulence regulon: infection where the grass is greener. Mol Microbiol. 2007;66(5):1056-65.
263. Kreikemeyer B, Beckert S, Braun-Kiewnick A, Podbielski A. Group A streptococcal RofA-type global regulators exhibit a strain-specific genomic presence and regulation pattern. Microbiology. 2002;148(5):1501-11.
264. Fogg GC, Caparon MG. Constitutive expression of fibronectin binding in *Streptococcus pyogenes* as a result of anaerobic activation of *rofA*. J Bacteriol. 1997;179(19):6172-80.
265. Fogg GC, Gibson CM, Caparon MG. The identification of *rofA*, a positive-acting regulatory component of prtF expression: use of an m γ δ-based shuttle mutagenesis strategy in *Streptococcus pyogenes*. Mol Microbiol. 1994;11(4):671-84.
266. Kreikemeyer B, Nakata M, Köller T, Hildisch H, Kourakos V, Standar K, et al. *Streptococcus pyogenes* Serotype M49 Nra-Ralp3 Transcriptional Regulatory Network and Its Control of Virulence Factor Expression from the Novel *eno ralp3 epf sagA* Pathogenicity Region. Infect Immun. 2007;75(12):5698-710.
267. Chaussee MS, Watson RO, Smoot JC, Musser JM. Identification of Rgg-Regulated Exoproteins of *Streptococcus pyogenes*. Infect Immun. 2001;69(2):822-31.
268. Kappeler KV, Anbalagan S, Dmitriev AV, McDowell EJ, Neely MN, Chaussee MS. A Naturally Occurring Rgg Variant in Serotype M3 *Streptococcus pyogenes* Does Not Activate speB Expression Due to Altered Specificity of DNA Binding. Infect Immun. 2009;77(12):5411-7.
269. Chaussee MS, Sylva GL, Sturdevant DE, Smoot LM, Graham MR, Watson RO, et al. Rgg Influences the Expression of Multiple Regulatory Loci To Coregulate Virulence Factor Expression in *Streptococcus pyogenes*. Infect Immun. 2002;70(2):762-70.
270. Zhang YM, Rock CO. Membrane lipid homeostasis in bacteria. Nat Rev Microbiol. 2008;6(3):222-33.
271. Sohlenkamp C, Geiger O. Bacterial membrane lipids: diversity in structures and pathways. FEMS Microbiol Rev. 2016;40(1):133-59.
272. López-Lara IM, Geiger O. Bacterial lipid diversity. Biochim Biophys Acta Mol Cell Biol Lipids. 2017;1862(11):1287-99.
273. Paoletti L, Lu YJ, Schujman GE, de Mendoza D, Rock CO. Coupling of Fatty Acid and Phospholipid Synthesis in *Bacillus subtilis*. J Bacteriol. 2007;189(16):5816-24.
274. Jerga A, Lu YJ, Schujman GE, de Mendoza D, Rock CO. Identification of a Soluble Diacylglycerol Kinase Required for Lipoteichoic Acid Production in *Bacillus subtilis*. J Biol Chem. 2007;282(30):21738-45.
275. Hölzl G, Dörmann P. Structure and function of glycoglycerolipids in plants and bacteria. Prog Lipid Res. 2007;46(5):225-43.
276. Niemi AR, Rilfors L, Lindblom G. Influence of monoglucosyldiacylglycerol and monoacylmonoglucosyldiacylglycerol on the lipid bilayer of the membrane from Acholeplasma laidlawii strain A-EF22. Biochim Biophys Acta. 1995;1239(2):186-94.
277. Malanovic N, Lohner K. Gram-positive bacterial cell envelopes: The impact on the activity of antimicrobial peptides. Biochim Biophys Acta. 2016;1858(5):936-46.

278. Heß N, Waldow F, Kohler TP, Rohde M, Kreikemeyer B, Gómez-Mejia A, et al. Lipoteichoic acid deficiency permits normal growth but impairs virulence of *Streptococcus pneumoniae*. Nat Commun. 2017;8(1):2093.
279. Rosch JW, Hsu FF, Caparon MG. Anionic Lipids Enriched at the ExPortal of Streptococcus pyogenes. J Bacteriol. 2007;189(3):801-6.
280. Rosch JW, Caparon MG. The ExPortal: an organelle dedicated to the biogenesis of secreted proteins in *Streptococcus pyogenes*. Mol Microbiol. 2005;58(4):959-68.
281. Matsumoto K, Kusaka J, Nishibori A, Hara H. Lipid domains in bacterial membranes. Mol Microbiol. 2006;61(5):1110-7.
282. Mukhopadhyay R, Huang KC, Wingreen NS. Lipid Localization in Bacterial Cells through Curvature-Mediated Microphase Separation. Biophys J. 2008;95(3):1034-49.
283. Frolov VA, Shnyrova AV, Zimmerberg J. Lipid Polymorphisms and Membrane Shape. Cold Spring Harb Perspect Biol. 2011;3(11):a004747.
284. Port GC, Vega LA, Nylander AB, Caparon MG. Streptococcus pyogenes Polymyxin B-Resistant Mutants Display Enhanced ExPortal Integrity. J Bacteriol. 2014;196(14):2563-77.
285. Zhang YM, Rock CO. Thematic Review Series: Glycerolipids. Acyltransferases in bacterial glycerophospholipid synthesis. J Lipid Res. 2008;49(9):1867-74.
286. Lu YJ, Zhang YM, Grimes KD, Qi J, Lee RE, Rock CO. Acyl-Phosphates Initiate Membrane Phospholipid Synthesis in Gram-Positive Pathogens. Mol Cell. 2006;23(5):765-72.
287. Parsons JB, Rock CO. Bacterial lipids: Metabolism and membrane homeostasis. Prog Lipid Res. 2013;52(3):249-76.
288. Sastre DE, Pulschen AA, Basso LGM, Benites Pariente JS, Marques Netto CGC, Machinandiarena F, et al. The phosphatidic acid pathway enzyme PlsX plays both catalytic and channeling roles in bacterial phospholipid synthesis. J Biol Chem. 2020;295(7):2148-59.
289. Sastre DE, Basso LGM, Trastoy B, Cifuente JO, Contreras X, Gueiros-Filho F, et al. Membrane fluidity adjusts the insertion of the transacylase PlsX to regulate phospholipid biosynthesis in Gram-positive bacteria. J Biol Chem. 2020;295(7):2136-47.
290. Lu YJ, Zhang F, Grimes KD, Lee RE, Rock CO. Topology and active site of PlsY: the bacterial acylphosphate:glycerol-3-phosphate acyltransferase. J Biol Chem. 2007;282(15):11339-46.
291. Grogan DW, Cronan JE. Cyclopropane ring formation in membrane lipids of bacteria. Microbiol Mol Biol Rev. 1997;61(4):429-41.
292. Lai CY, Cronan JE. β-Ketoacyl-Acyl Carrier Protein Synthase III (FabH) Is Essential for Bacterial Fatty Acid Synthesis. J Biol Chem. 2003;278(51):51494-503.
293. Fujita Y, Matsuoka H, Hirooka K. Regulation of fatty acid metabolism in bacteria. Mol Microbiol. 2007;66(4):829-39.
294. Lambert C, Poyart C, Gruss A, Fouet A. FabT, a Bacterial Transcriptional Repressor That Limits Futile Fatty Acid Biosynthesis. Microbiol Mol Biol Rev. 2022;86(3):e00029-22.
295. Marrakchi H, Choi KH, Rock CO. A New Mechanism for Anaerobic Unsaturated Fatty Acid Formation in *Streptococcus pneumoniae*. J Biol Chem. 2002;277(47):44809-16.
296. Eckhardt TH, Skotnicka D, Kok J, Kuipers OP. Transcriptional Regulation of Fatty Acid Biosynthesis in *Lactococcus lactis*. J Bacteriol. 2013;195(5):1081-9.
297. Hays C, Lambert C, Brinster S, Lamberet G, du Merle L, Gloux K, et al. Type II Fatty Acid Synthesis Pathway and Cyclopropane Ring Formation Are Dispensable during *Enterococcus faecalis* Systemic Infection. J Bacteriol. 2021;203(20):e00221-21.

298. Roujeinikova A, Simon WJ, Gilroy J, Rice DW, Rafferty JB, Slabas AR. Structural Studies of Fatty Acyl-(Acyl Carrier Protein) Thioesters Reveal a Hydrophobic Binding Cavity that Can Expand to Fit Longer Substrates. J Mol Biol. 2007;365(1):135-45.
299. Zhu L, Zou Q, Cao X, Cronan JE. *Enterococcus faecalis* Encodes an Atypical Auxiliary Acyl Carrier Protein Required for Efficient Regulation of Fatty Acid Synthesis by Exogenous Fatty Acids. mBio. 2019;10(3):e00577-19.
300. Bi H, Zhu L, Wang H, Cronan JE. Inefficient Translation Renders the *Enterococcus faecalis* fabK Enoyl-Acyl Carrier Protein Reductase Phenotypically Cryptic. J Bacteriol. 2014;196(1):170-9.
301. Zuo G, Chen Z, Jiang Y, Zhu Z, Ding C, Zhang Z, et al. Structural insights into repression of the *Pneumococcal* fatty acid synthesis pathway by repressor FabT and co-repressor acyl-ACP. FEBS Lett. 2019;593(19):2730-41.
302. Zou Q, Dong H, Zhu L, Cronan JE. The *Enterococcus faecalis* FabT Transcription Factor Regulates Fatty Acid Biosynthesis in Response to Exogeneous Fatty Acids. Front Microbiol. 2022;13:877582.
303. Juneja VK, Foglia TA, Marmer BS. Heat Resistance and Fatty Acid Composition of *Listeria monocytogenes*: Effect of pH, Acidulant, and Growth Temperature. J Food Prot. 1998;61(6):683-7.
304. Dubois-Brissonnet F, Naïtali M, Mafu AA, Briandet R. Induction of Fatty Acid Composition Modifications and Tolerance to Biocides in *Salmonella enterica* Serovar *Typhimurium* by Plant-Derived Terpenes. Appl Environ Microbiol. 2011;77(3):906-10.
305. Tiwari KB, Gatto C, Wilkinson BJ. Interrelationships among Fatty Acid Composition, Staphyloxanthin Content, Fluidity, and Carbon Flow in the *Staphylococcus aureus* Membrane. Molecules. 2018;23(5):1201.
306. Aguilar PS, Lopez P, de Mendoza D. Transcriptional control of the low-temperature-inducible des gene, encoding the delta5 desaturase of *Bacillus subtilis*. J Bacteriol. 1999;181(22):7028-33.
307. Cybulski LE, Albanesi D, Mansilla MC, Altabe S, Aguilar PS, De Mendoza D. Mechanism of membrane fluidity optimization: isothermal control of the Bacillus subtilis acyl-lipid desaturase: B. subtilis membrane fluidity sensing. Mol Microbiol. 2002;45(5):1379-88.
308. Chang YY, Cronan JE. Membrane cyclopropane fatty acid content is a major factor in acid resistance of *Escherichia coli*. Mol Microbiol. 1999;33(2):249-59.
309. Yao J, Rock CO. Exogenous fatty acid metabolism in bacteria. Biochimie. 2017;141:1-10.
310. Parsons JB, Frank MW, Jackson P, Subramanian C, Rock CO. Incorporation of extracellular fatty acids by a fatty acid kinase-dependent pathway in *Staphylococcus aureus*. Mol Microbiol. 2014;92(2):234-45.
311. Shi Y, Zang N, Lou N, Xu Y, Sun J, Huang M, et al. Structure and mechanism for streptococcal fatty acid kinase (Fak) system dedicated to host fatty acid scavenging. Sci Adv. 2022;8(35):eabq3944.
312. Gullett JM, Cuypers MG, Frank MW, White SW, Rock CO. A fatty acid-binding protein of *Streptococcus pneumoniae* facilitates the acquisition of host polyunsaturated fatty acids. J Biol Chem. 2019;294(44):16416-28.
313. Broussard TC, Miller DJ, Jackson P, Nourse A, White SW, Rock CO. Biochemical Roles for Conserved Residues in the Bacterial Fatty Acid-binding Protein Family. J Biol Chem. 2016;291(12):6292-303.

314. Saito HE, Harp JR, Fozo EM. Incorporation of Exogenous Fatty Acids Protects *Enterococcus faecalis* from Membrane-Damaging Agents. Drake HL, éditeur. Appl Environ Microbiol. 2014;80(20):6527-38.
315. Saito HE, Harp JR, Fozo EM. *Enterococcus faecalis* Responds to Individual Exogenous Fatty Acids Independently of Their Degree of Saturation or Chain Length. Appl Environ Microbiol. 2017;84(1).
316. DeMars ZR, Singh VK, Bose JL. Exogenous Fatty Acids Remodel *Staphylococcus aureus* Lipid Composition through Fatty Acid Kinase. J Bacteriol. 2020;202(14):e00128-20.
317. Parsons JB, Frank MW, Eleveld MJ, Schalkwijk J, Broussard TC, de Jonge MI, et al. A thioesterase bypasses the requirement for exogenous fatty acids in the *plsX* deletion of *Streptococcus pneumoniae*: Role of PlsX in *S. pneumoniae* fatty acid metabolism. Mol Microbiol. 2015;96(1):28-41.
318. Machinandiarena F, Nakamatsu L, Schujman GE, de Mendoza D, Albanesi D. Revisiting the coupling of fatty acid to phospholipid synthesis in bacteria with FapR regulation. Mol Microbiol. 2020;114(4):653-63.
319. Fujihashi M, Nakatani T, Hirooka K, Matsuoka H, Fujita Y, Miki K. Structural characterization of a ligand-bound form of *Bacillus subtilis* FadR involved in the regulation of fatty acid degradation: Structural Characterization of FadR $_{Bs}$. Proteins. 2014;82(7):1301-10.
320. Alnaseri H, Arsic B, Schneider JET, Kaiser JC, Scinocca ZC, Heinrichs DE, et al. Inducible expression of a resistance-nodulation-division-type efflux pump in *Staphylococcus aureus* provides resistance to linoleic and arachidonic acids. J Bacteriol. 2015;197(11):1893-905.
321. Alnaseri H, Kuiack RC, Ferguson KA, Schneider JET, Heinrichs DE, McGavin MJ. DNA binding and sensor specificity of FarR, a novel TetR family regulator required for induction of the fatty acid efflux pump in *Staphylococcus aureus*. J Bacteriol. 2018;201(3):e00602-18.
322. Volkov A, Liavonchanka A, Kamneva O, Fiedler T, Goebel C, Kreikemeyer B, et al. Myosin Cross-reactive Antigen of *Streptococcus pyogenes* M49 Encodes a Fatty Acid Double Bond Hydratase That Plays a Role in Oleic Acid Detoxification and Bacterial Virulence. J Biol Chem. 2010;285(14):10353-61.
323. Zhang YM, Rock CO. Transcriptional regulation in bacterial membrane lipid synthesis. J Lipid Res. 2009;50Suppl(Suppl):S115-9.
324. Albanesi D, de Mendoza D. FapR: From control of membrane lipid homeostasis to a biotechnological tool. Front Mol Biosci. 2016;3:64.
325. Schujman GE, Paoletti L, Grossman AD, de Mendoza D. FapR, a Bacterial Transcription Factor Involved in Global Regulation of Membrane Lipid Biosynthesis. Dev Cell. 2003;4(5):663-72.
326. Zhang YM, Marrakchi H, Rock CO. The FabR (YijC) Transcription Factor Regulates Unsaturated Fatty Acid Biosynthesis in *Escherichia coli*. J Biol Chem. 2002;277(18):15558-65.
327. Zhu K, Zhang YM, Rock CO. Transcriptional Regulation of Membrane Lipid Homeostasis in *Escherichia coli*. J Biol Chem. 2009;284(50):34880-8.
328. Gui L, Sunnarborg A, LaPorte DC. Regulated expression of a repressor protein: FadR activates iclR. J Bacteriol. 1996;178(15):4704-9.
329. Campbell JW, Cronan JE. *Escherichia coli* FadR Positively Regulates Transcription of the fabB Fatty Acid Biosynthetic Gene. J Bacteriol. 2001;183(20):5982-90.

330. Feng Y, Cronan JE. *Escherichia coli* unsaturated fatty acid synthesis: complex transcription of the *fabA* gene and in vivo identification of the essential reaction catalyzed by FabB. J Biol Chem. 2009;284(43):29526-35.
331. Feng Y, Cronan JE. The *Vibrio cholerae* fatty acid regulatory protein, FadR, represses transcription of *plsB*, the gene encoding the first enzyme of membrane phospholipid biosynthesis. Mol Microbiol. 2011;81(4):1020-33.
332. Zhang YM, Zhu K, Frank MW, Rock CO. A *Pseudomonas aeruginosa* transcription factor that senses fatty acid structure. Mol Microbiol. 2007;66(3):622-32.
333. Subramanian C, Rock CO, Zhang YM. DesT Coordinates the Expression of Anaerobic and Aerobic Pathways for Unsaturated Fatty Acid Biosynthesis in *Pseudomonas aeruginosa*. J Bacteriol. 2010;192(1):280-5.
334. Lu YJ, Rock CO. Transcriptional regulation of fatty acid biosynthesis in *Streptococcus pneumoniae*: Regulation of fatty acid composition in *S. pneumoniae*. Mol Microbiol. 2006;59(2):551-66.
335. Martinez MA, Zaballa ME, Schaeffer F, Bellinzoni M, Albanesi D, Schujman GE, et al. A Novel Role of Malonyl-ACP in Lipid Homeostasis. Biochemistry. 2010;49(14):3161-7.
336. Pérez-Rueda E, Collado-Vides J. Common History at the Origin of the Position-Function Correlation in Transcriptional Regulators in Archaea and Bacteria. J Mol Evol. 2001;53(3):172-9.
337. Pérez-Rueda E, Collado-Vides J, Segovia L. Phylogenetic distribution of DNA-binding transcription factors in bacteria and archaea. Comput Biol Chem. 2004;28(5-6):341-50.
338. Will WR, Fang FC. The evolution of MarR family transcription factors as counter-silencers in regulatory networks. Curr Opin Microbiol. 2020;55:1-8.
339. Wilkinson SP, Grove A. Ligand-responsive Transcriptional Regulation by Members of the MarR Family of Winged Helix Proteins. Curr Issues Mol Biol. 2006;8:51-62.
340. Sulavik MC, Gambino LF, Miller PF, Arbor A. The MarR Repressor of the Multiple Antibiotic Resistance (mar) Operon in Escherichia coli: Prototypic Member of a Family of Bacterial Regulatory Proteins Involved in Sensing Phenolic Compounds. Mol Med. 1995;1(4):11.
341. Daigle DM, Cao L, Fraud S, Wilke MS, Pacey A, Klinoski R, et al. Protein Modulator of Multidrug Efflux Gene Expression in *Pseudomonas aeruginosa*. J Bacteriol. 2007;189(15):5441-51.
342. Chen H, Yi C, Zhang J, Zhang W, Ge Z, Yang C, et al. Structural insight into the oxidation-sensing mechanism of the antibiotic resistance of regulator MexR. EMBO Rep. 2010;11(9):685-90.
343. Oh SY, Shin JH, Roe JH. Dual Role of OhrR as a Repressor and an Activator in Response to Organic Hydroperoxides in *Streptomyces coelicolor*. J Bacteriol. 2007;189(17):6284-92.
344. Ingavale S, van Wamel W, Luong TT, Lee CY, Cheung AL. Rat/MgrA, a Regulator of Autolysis, Is a Regulator of Virulence Genes in *Staphylococcus aureus*. Infect Immun. 2005;73(3):1423-31.
345. Chen PR, Bae T, Williams WA, Duguid EM, Rice PA, Schneewind O, et al. An oxidation-sensing mechanism is used by the global regulator MgrA in *Staphylococcus aureus*. Nat Chem Biol. 2006;2(11):591-5.
346. Ellison DW, Miller VL. Regulation of virulence by members of the MarR/SlyA family. Curr Opin Microbiol. 2006;9(2):153-9.

347. Galan B, Kolb A, Sanz JM, Garcia JL, Prieto MA. Molecular determinants of the hpa regulatory system of Escherichia coli: the HpaR repressor. Nucleic Acids Research. 2003;31(22):6598-609.
348. Wilkinson SP, Grove A. HucR, a Novel Uric Acid-responsive Member of the MarR Family of Transcriptional Regulators from *Deinococcus radiodurans*. J Biol Chem. 2004;279(49):51442-50.
349. Alekshun MN, Levy SB. The mar regulon: multiple resistance to antibiotics and other toxic chemicals. Trends Microbiol. 1999;7(10):410-3.
350. Andrésen C, Jalal S, Aili D, Wang Y, Islam S, Jarl A, et al. Critical biophysical properties in the *Pseudomonas aeruginosa* efflux gene regulator MexR are targeted by mutations conferring multidrug resistance. Protein Sci. 2010;19(4):680-92.
351. Deochand DK, Grove A. MarR family transcription factors: dynamic variations on a common scaffold. Crit Rev Biochem Mol Biol. 2017;52(6):595-613.
352. Kumarevel T, Tanaka T, Umehara T, Yokoyama S. ST1710–DNA complex crystal structure reveals the DNA binding mechanism of the MarR family of regulators. Nucleic Acids Res. 2009;37(14):4723-35.
353. Alekshun MN, Levy SB, Mealy TR, Seaton BA, Head JF. The crystal structure of MarR, a regulator of multiple antibiotic resistance, at 2.3 Å resolution. Nat Struct Mol Biol. 2001;8(8):710-4.
354. Alekshun MN, Levy SB. Regulation of chromosomally mediated multiple antibiotic resistance: the mar regulon. Antimicrob Agents Chemother. 1997;41(10):2067-75.
355. Eraso JM, Olsen RJ, Beres SB, Kachroo P, Porter AR, Nasser W, et al. Genomic Landscape of Intrahost Variation in Group A *Streptococcus*: Repeated and Abundant Mutational Inactivation of the *fabT* Gene Encoding a Regulator of Fatty Acid Synthesis. Infect Immun. 2016;84(12):3268-81.
356. Lu YJ, White SW, Rock CO. Domain Swapping between *Enterococcus faecalis* FabN and FabZ Proteins Localizes the Structural Determinants for Isomerase Activity. J Biol Chem. 2005;280(34):30342-8.
357. Rosinski-Chupin I, Sauvage E, Fouet A, Poyart C, Glaser P. Conserved and specific features of *Streptococcus pyogenes* and *Streptococcus agalactiae* transcriptional landscapes. BMC Genomics. 2019;20(1):236.
358. Faustoferri RC, Hubbard CJ, Santiago B, Buckley AA, Seifert TB, Quivey RG. Regulation of fatty acid biosynthesis by the global regulator CcpA and the local regulator FabT in *Streptococcus mutans*. Mol Oral Microbiol. 2015;30(2):128-46.
359. Tatsuno I, Okada R, Matsumoto M, Hata N, Matsui H, Zhang Y, et al. Relevance of spontaneous *fabT* mutations to a streptococcal toxic shock syndrome to non-streptococcal toxic shock syndrome transition in the novel-type *Streptococcus pyogenes* isolates that lost a *salRK*. APMIS. 2016;124(5):414-24.
360. Zhang J, Ye W, Wu K, Xiao S, Zheng Y, Shu Z, et al. Inactivation of Transcriptional Regulator FabT Influences Colony Phase Variation of *Streptococcus pneumoniae*. mBio. 2021;12(4):e0130421.
361. Reichmann NT, Gründling A. Location, synthesis and function of glycolipids and polyglycerolphosphate lipoteichoic acid in Gram-positive bacteria of the phylum Firmicutes: Synthesis and function of glycolipid and PGP-LTA. FEMS Microbiol Lett. 2011;319(2):97-105.

362. Jerga A, Rock CO. Acyl-Acyl Carrier Protein Regulates Transcription of Fatty Acid Biosynthetic Genes *via* the FabT Repressor in *Streptococcus pneumoniae*. J Biol Chem. 2009;284(23):15364-8.
363. Port GC, Vega LA, Nylander AB, Caparon MG. *Streptococcus pyogenes* Polymyxin B-Resistant Mutants Display Enhanced ExPortal Integrity. J Bacteriol. 2014;196(14):2563-77.
364. Mohedano ML, Overweg K, de la Fuente A, Reuter M, Altabe S, Mulholland F, et al. Evidence that the Essential Response Regulator YycF in Streptococcus pneumoniae Modulates Expression of Fatty Acid Biosynthesis Genes and Alters Membrane Composition. J Bacteriol. 2005;187(7):2357-67.
365. Wayne KJ, Li S, Kazmierczak KM, Tsui HCT, Winkler ME. Involvement of WalK (VicK) phosphatase activity in setting WalR (VicR) response regulator phosphorylation level and limiting cross-talk in *Streptococcus pneumoniae* D39 cells. Mol Microbiol. 2012;86(3):645-60.
366. Mohedano ML, Amblar M, de la Fuente A, Wells JM, López P. The Response Regulator YycF Inhibits Expression of the Fatty Acid Biosynthesis Repressor FabT in *Streptococcus pneumoniae*. Front Microbiol. 2016; 7:1326.
367. Mileykovskaya E, Fishov I, Fu X, Corbin BD, Margolin W, Dowhan W. Effects of Phospholipid Composition on MinD-Membrane Interactions *in Vitro* and *in Vivo*. J Biol Chem. 2003;278(25):22193-8.
368. Bugrysheva J, Froehlich BJ, Freiberg JA, Scott JR. Serine/Threonine Protein Kinase Stk Is Required for Virulence, Stress Response, and Penicillin Tolerance in *Streptococcus pyogenes*. Infect Immun. 2011;79(10):4201-9.
369. Dramsi S, Bierne H. Spatial Organization of Cell Wall-Anchored Proteins at the Surface of Gram-Positive Bacteria. Curr Top Microbiol Immunol. 2016;404:177-201.
370. Heath RJ, Su N, Murphy CK, Rock CO. The Enoyl-[acyl-carrier-protein] Reductases FabI and FabL from *Bacillus subtilis*. J Biol Chem. 2000;275(51):40128-33.
371. Heath RJ, Li J, Roland GE, Rock CO. Inhibition of the *Staphylococcus aureus* NADPH-dependent Enoyl-Acyl Carrier Protein Reductase by Triclosan and Hexachlorophene. J Biol Chem. 2000;275(7):4654-9.
372. Sukhishvili SA, Chen Y, Müller JD, Gratton E, Schweizer KS, Granick S. Diffusion of a polymer 'pancake'. Nature. 2000;406(6792):146-146.
373. Brinster S, Lamberet G, Staels B, Trieu-Cuot P, Gruss A, Poyart C. Type II fatty acid synthesis is not a suitable antibiotic target for Gram-positive pathogens. Nature. 2009;458(7234):83-6.
374. Parsons JB, Frank MW, Subramanian C, Saenkham P, Rock CO. Metabolic basis for the differential susceptibility of Gram-positive pathogens to fatty acid synthesis inhibitors. PNAS. 2011;108(37):15378-83.
375. Kénanian G, Morvan C, Weckel A, Pathania A, Anba-Mondoloni J, Halpern D, et al. Permissive Fatty Acid Incorporation Promotes Staphylococcal Adaptation to FASII Antibiotics in Host Environments. Cell Rep. 2019;29(12):3974-3982.e4.
376. Schulze-Gahmen U, Pelaschier J, Yokota H, Kim R, Kim SH. Crystal structure of a hypothetical protein, TM841 of *Thermotoga maritima*, reveals its function as a fatty acid-binding protein. Proteins. 2003;50(4):526-30.
377. Longo M, De Jode M, Plainvert C, Weckel A, Hua A, Château A, et al. Complete Genome Sequence of *Streptococcus pyogenes emm28* Clinical Isolate M28PF1, Responsible for a Puerperal Fever. Genome Announc. 2015;3(4):e00750-15.

378. Ragolia L, Tropp BE. The effects of phosphoglycerides on *Escherichia coli* cardiolipin synthase. Biochim Biophys Acta. 1994;1214(3):323-32.
379. Lopez CS, Alice AF, Heras H, Rivas EA, Sanchez-Rivas C. Role of anionic phospholipids in the adaptation of *Bacillus subtilis* to high salinity. Microbiology. 2006;152(Pt 3):605-16.
380. Tsai M, Ohniwa RL, Kato Y, Takeshita SL, Ohta T, Saito S, et al. *Staphylococcus aureus* requires cardiolipin for survival under conditions of high salinity. BMC Microbiol. 2011;11(1):1-12.
381. Koprivnjak T, Zhang D, Ernst CM, Peschel A, Nauseef WM, Weiss JP. Characterization of *Staphylococcus aureus* Cardiolipin Synthases 1 and 2 and Their Contribution to Accumulation of Cardiolipin in Stationary Phase and within Phagocytes. J Bacteriol. 2011;193(16):4134-42.
382. Devaux L, Sleiman D, Mazzuoli MV, Gominet M, Lanotte P, Trieu-Cuot P, et al. Cyclic di-AMP regulation of osmotic homeostasis is essential in Group B *Streptococcus*. PLoS Genet. 2018;14(4):e1007342.
383. Espenshade PJ, Hughes AL. Regulation of Sterol Synthesis in Eukaryotes. Annu Rev Genet. 2007;41(1):401-27.
384. Ikonen E. Cellular cholesterol trafficking and compartmentalization. Nat Rev Mol Cell Biol. 2008;9(2):125-38.
385. Toledo A, Benach JL. Hijacking and Use of Host Lipids by Intracellular Pathogens. Microbiol Spectr. 2014;3(6):10.2228.
386. Vromman F, Subtil A. Exploitation of host lipids by bacteria. Curr Opin Microbiol. 2014;17:38-45.
387. Pandey AK, Sassetti CM. Mycobacterial persistence requires the utilization of host cholesterol. PNAS. 2008;105(18):4376-80.
388. Thomas ST, VanderVen BC, Sherman DR, Russell DG, Sampson NS. Pathway Profiling in *Mycobacterium tuberculosis*. J Biol Chem. 2011;286(51):43668-78.
389. Lee W, VanderVen BC, Fahey RJ, Russell DG. Intracellular *Mycobacterium tuberculosis* Exploits Host-derived Fatty Acids to Limit Metabolic Stress. J Biol Chem. 2013;288(10):6788-800.
390. Albertson N, Wenngren I, Sjöström JE. Growth and Survival of *Helicobacter pylori* in Defined Medium and Susceptibility to Brij 78. J Clin Microbiol. 1998;36(5):1232-5.
391. Testerman TL, McGee DJ, Mobley HLT. *Helicobacter pylori* Growth and Urease Detection in the Chemically Defined Medium Ham's F-12 Nutrient Mixture. J Clin Microbiol. 2001;39(11):3842-50.
392. Lebrun AH, Wunder C, Hildebrand J, Churin Y, Zähringer U, Lindner B, et al. Cloning of a Cholesterol-α-glucosyltransferase from *Helicobacter pylori*. J Biol Chem. 2006;281(38):27765-72.
393. Joyce LR, Guan Z, Palmer KL. *Streptococcus pneumoniae*, *S. pyogenes* and *S. agalactiae* membrane phospholipid remodelling in response to human serum. Microbiology. 2021;167(5):001048.
394. Pownall HJ, Courtney HS, Gillard BK, Massey JB. Properties of the products formed by the activity of serum opacity factor against human plasma high-density lipoproteins. Chem Phys Lipids. 2008;156(1-2):45-51.
395. Nagiec MJ, Lei B, Parker SK, Vasil ML, Matsumoto M, Ireland RM, et al. Analysis of a Novel Prophage-encoded Group A *Streptococcus* Extracellular Phospholipase A2. J Clin Microbiol. 2004;279(44):45909-18.

396. McGee DJ, George AE, Trainor EA, Horton KE, Hildebrandt E, Testerman TL. Cholesterol Enhances *Helicobacter pylori* Resistance to Antibiotics and LL-37. Antimicrob Agents Chemother. 2011;55(6):2897-904.
397. Lauressergues E, Bert E, Duriez P, Hum D, Majd Z, Staels B, et al. Does endoplasmic reticulum stress participate in APD-induced hepatic metabolic dysregulation? Neuropharmacology. 2012;62(2):784-96.
398. Moncan M, Mnich K, Blomme A, Almanza A, Samali A, Gorman AM. Regulation of lipid metabolism by the unfolded protein response. J Cell Mol Med. 2021;25(3):1359-70.
399. McBroom AJ, Kuehn MJ. Release of outer membrane vesicles by Gram-negative bacteria is a novel envelope stress response. Mol Microbiol. 2007;63(2):545-58.
400. Lee EY, Choi DY, Kim DK, Kim JW, Park JO, Kim S, et al. Gram-positive bacteria produce membrane vesicles: Proteomics-based characterization of *Staphylococcus aureus*µ-derived membrane vesicles. Proteomics. 2009;9(24):5425-36.
401. Olaya-Abril A, Prados-Rosales R, McConnell MJ, Martín-Peña R, González-Reyes JA, Jiménez-Munguía I, et al. Characterization of protective extracellular membrane-derived vesicles produced by *Streptococcus pneumoniae*. J Proteomics. 2014;106:46-60.
402. Biagini M, Garibaldi M, Aprea S, Pezzicoli A, Doro F, Becherelli M, et al. The Human Pathogen *Streptococcus pyogenes* Releases Lipoproteins as Lipoprotein-rich Membrane Vesicles. Mol Cell Proteomics. 2015;14(8):2138-49.
403. Uhlmann J, Rohde M, Siemens N, Kreikemeyer B, Bergman P, Johansson L, et al. LL-37 Triggers Formation of *Streptococcus pyogenes* Extracellular Vesicle-Like Structures with Immune Stimulatory Properties. J Innate Immun. 2016;8(3):243-57.
404. Mercier R, Kawai Y, Errington J. Excess Membrane Synthesis Drives a Primitive Mode of Cell Proliferation. Cell. 2013;152(5):997-1007.
405. Tchoupa AK, Peschel A. *Staphylococcus aureus* Releases Proinflammatory Membrane Vesicles To Resist Antimicrobial Fatty Acids. mSphere. 2020;5(5):e00804-20.
406. Resch U, Tsatsaronis JA, Le Rhun A, Stübiger G, Rohde M, Kasvandik S, et al. A Two-Component Regulatory System Impacts Extracellular Membrane-Derived Vesicle Production in Group A *Streptococcus*. mBio. 2016;7(6):e00207-16.

Annexes

Annexe 1

FabT, a Bacterial Transcriptional Repressor That Limits Futile Fatty Acid Biosynthesis.
Lambert Clara, Claire Poyart, Alexandra Gruss, et Agnès Fouet.
Microbiology and Molecular Biology Reviews 86, nº 3 (2022): e00029-22.
https://doi.org/10.1128/mmbr.00029-22.

Annexe 2

Streptococcus Pyogenes Infects Human Endometrium by Limiting the Innate Immune Response.
Weckel, Antonin, Thomas Guilbert, **Clara Lambert**, Céline Plainvert, Francois Goffinet, Claire Poyart, Céline Méhats, et Agnès Fouet.
The Journal of Clinical Investigation 131, nº 4 (2021): e130746.
https://doi.org/10.1172/JCI130746.

Annexe 3

Type II Fatty Acid Synthesis Pathway and Cyclopropane Ring Formation Are Dispensable during *Enterococcus Faecalis* Systemic Infection.
Hays Constantin, **Clara Lambert**, Sophie Brinster, Gilles Lamberet, Laurence du Merle, Karine Gloux, Alexandra Gruss, Claire Poyart, et Agnès Fouet.
Journal of Bacteriology 203, nº 20 (2021): e00221-21.
https://doi.org/10.1128/JB.00221-21.

Annexe 4

A novel CovS variant harbored by a colonization strain reduces *Streptococcus pyogenes* virulence.
Céline Plainvert, Isabelle Rosinski-Chupin, Antonin Weckel, **Clara Lambert**, Gérald Touak, Elisabeth Sauvage, Claire Poyart, Philippe Glaser, Agnès Fouet.
En cours de soumission.

AMERICAN SOCIETY FOR MICROBIOLOGY | Microbiology and Molecular Biology Reviews®

REVIEW

FabT, a Bacterial Transcriptional Repressor That Limits Futile Fatty Acid Biosynthesis

Clara Lambert,[a] Claire Poyart,[a,b] Alexandra Gruss,[c] Agnes Fouet[a]

[a]Université Paris Cité, Institut Cochin, INSERM, U1016, CNRS, UMR8104, Paris, France
[b]AP-HP Centre–Université Paris Cité, Paris, France
[c]Micalis Institute, INRAE, AgroParisTech, Université Paris-Saclay, Jouy en Josas, France

Alexandra Gruss and Agnes Fouet share senior authorship.

SUMMARY 1
INTRODUCTION 1
FABT INVOLVEMENT IN *STREPTOCOCCUS PYOGENES* VIRULENCE 2
IDENTIFICATION OF FABT AS THE FASII REGULATOR 4
THE FABT REGULON 4
FASII Gene Regulation by the FabT Repressor 4
Non-FASII Gene Regulation by the FabT Repressor 5
FABT MECHANISM OF REPRESSION 6
FabT Dimerization and Target Gene Interaction 6
The FabT Corepressor 7
The FabT ligand, acyl-ACP 7
Why are there two ACPs in some species? 8
REGULATION OF *FABT* TRANSCRIPTION AND FABT ACTIVITY 9
FABT AND BACTERIAL PHYSIOLOGY 11
CONCLUSIONS 13
ACKNOWLEDGMENTS 13
REFERENCES 13
AUTHOR BIOS 15

SUMMARY Phospholipids are vital membrane constituents that determine cell functions and interactions with the environment. For bacterial pathogens, rapid adjustment of phospholipid composition to changing conditions during infection can be crucial for growth and survival. Fatty acid synthesis (FASII) regulators are central to this process. This review puts the spotlight on FabT, a MarR-family regulator of FASII characterized in streptococci, enterococci, and lactococci. Roles of FabT in virulence, as reported in mouse and nonhuman primate infection models, will be discussed. We present FabT structure, the FabT regulon, and changes in FabT regulation according to growth conditions. A unique feature of FabT concerns its modulation by an unconventional corepressor, acyl-acyl-carrier protein (ACP). Some bacteria express two ACP proteins, which are distinguished by their interactions with endogenous or exogenous fatty acid sources, one of which causes strong FabT repression. This system seems to allow preferred use of environmental fatty acids, thereby saving energy by limiting futile FASII activity. Control of *fabT* expression and FabT activity link various metabolic pathways to FASII. The various physiological consequences of FabT loss summarized here suggest that FabT has potential as a narrow range therapeutic target.

KEYWORDS fatty acid synthesis, FabT, repressor, feedback regulation, acyl-ACP, binding sites

INTRODUCTION

All cells are delimited by lipid membranes, which form a selective permeable barrier that regulates the transport of nutrients and waste and receives and transmits environmental signals that adjust metabolic processes according to environmental

Copyright © 2022 American Society for Microbiology. All Rights Reserved.

Address correspondence to Agnes Fouet, agnes.fouet@inserm.fr, or Alexandra Gruss, alexandra.gruss@inrae.fr.

The authors declare no conflict of interest.

Published 21 June 2022

Downloaded from https://journals.asm.org/journal/mmbr on 12 October 2022 by 193.54.110.61.

conditions. Cell membranes commonly comprise a phospholipid bilayer composed of a polar head and an apolar body comprising two fatty acid (FA) chains per glycerol-phosphate backbone, whose features contribute to membrane composition and dynamics. FA structure and length are decisive for membrane topology and properties such as fluidity, permeability, and integrity. These features are crucial for the adaptation of bacteria to various environments (1).

Phospholipids comprise two main FA classes, saturated (straight and branched chain FA) and unsaturated (including mono- and poly-unsaturated FA). The FA synthesis pathway (FASII) comprises an initiation phase followed by a recursive elongation cycle, which produces acyl-acyl carrier protein (acyl-ACP) (Fig. 1A). Various bacteria including streptococci, *Enterococcus faecalis*, and *Lactococcus lactis* produce monounsaturated FAs, which are synthesized *via* a shunt within the cycle (Fig. 1A). Many bacteria also generate cyclic FA *via* an enzyme that acts postsynthetically on membrane phospholipids (2). The process of cyclopropanation generates a three-membered ring at the site of an unsaturation on the carbon chain. The numerous possible FA products (different chain lengths, saturated or unsaturated, cyclized) may facilitate membrane adjustments according to shifts in environmental conditions.

FASII is widespread among bacteria, but genetic organization and regulation of FASII genes are not that conserved. However, these features are conserved among lactic acid bacteria (Fig. 1B). A gene within the main FASII locus encodes a member of the MarR family of regulators, named FabT (Fig. 1B) (3). FASII regulation plays a crucial role in adjusting FA production under different conditions. Both feedback and feedforward mechanisms of FASII regulation are described for different bacterial species (4, 5). In this review, we summarize the current state of knowledge concerning FabT, a FASII regulator studied in streptococci, enterococci, and lactococci. While lactococci are mainly known as food-fermenting bacteria, the genus includes a fish pathogen, and commensals of plants, intestinal tracts, and the vagina, where FabT is highly conserved; its characterization in lactococci thus contributes to understanding FabT functionality. The unique features of FabT-family regulators will be highlighted, and findings linking FabT and virulence will be discussed.

FABT INVOLVEMENT IN *STREPTOCOCCUS PYOGENES* VIRULENCE

The natural occurrence and potential consequences of *fabT* mutations during *Streptococcus pyogenes in vivo* infections motivated us to write this review. *S. pyogenes* (group A *Streptococcus* [GAS]) is an important human pathogen responsible for a large variety of clinical manifestations ranging from mild superficial infections to more life-threatening invasive infections including necrotizing fasciitis or streptococcal toxic shock syndrome. GAS infections are also responsible for postinfectious complications such as rheumatic arthritis and glomerulonephritis and, altogether, GAS infections are responsible for 517,000 deaths annually worldwide (6, 7). In one study, 74 clinical isolates of the same genotype, from either invasive infections (mainly streptococcal toxic shock syndrome), or noninvasive infections, were analyzed (8). *fabT* point mutations were only detected in noninvasive infections (2 out of 38 isolates). This suggested that spontaneous mutations in *fabT* are counterselected in invasive infections and infrequent in noninvasive ones. Similarly, another study identified only nine single nucleotide polymorphisms or nonsynonymous insertions/deletions in *fabT* when comparing the genomic sequences of more than 3,615 clinical isolates of *S. pyogenes* of the same genotype from invasive and noninvasive infections (9, 10). In the study of Eraso et al. (10), *fabT* mutant distribution between invasive and noninvasive infections was not considered. In striking contrast with the low incidence of *fabT* polymorphisms among invasive isolates, their occurrence rose to 12% among isolates recovered at the site of infection from nonhuman primates in necrotizing fasciitis experiments (44 amino acid replacements at 30 different FabT positions were identified). Infection was then compared using a reference strain and its isogenic *fabT* deletion mutant in the nonhuman primate necrotizing fasciitis model. The mutant strain multiplied less at the inoculation

Downloaded from https://journals.asm.org/journal/mmbr on 12 October 2022 by 193.54.110.61.

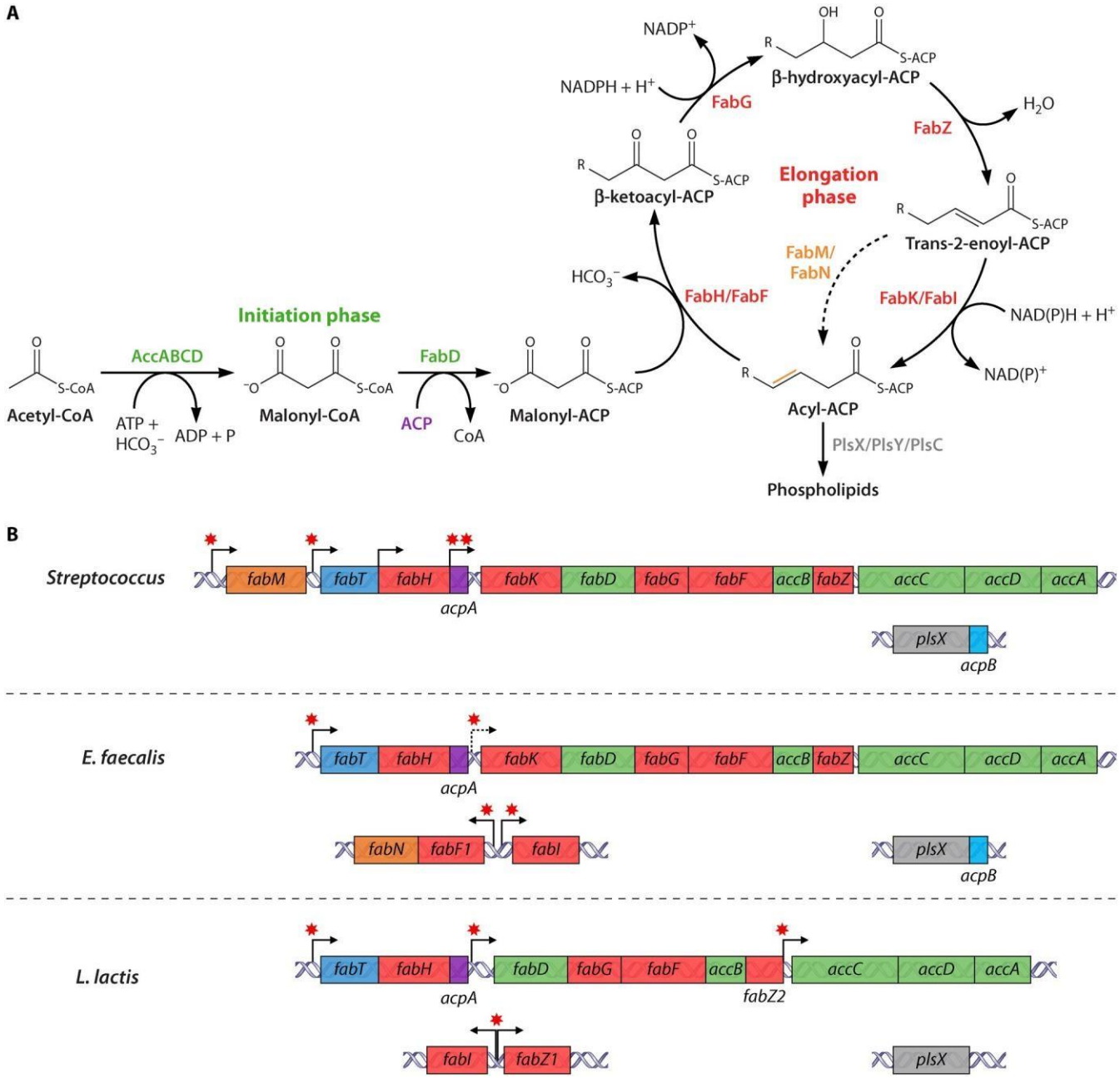

FIG 1 Fatty acid synthesis pathway (FASII) in food and pathogenic *Lactobacillales*. (A) FASII comprises a first initiation phase for precursor synthesis, followed by the recursive elongation cycle. The mature acyl-ACP products supply fatty acids for phospholipid synthesis. Products of FabM/FabN are unsaturated (in gold), while those of FabI/FabK are saturated. Proteins performing the same functions may vary according to species. (B) FASII genes are clustered in streptococci (*S. pneumoniae*, *S. agalactiae*, *S. pyogenes*), *E. faecalis*, and *L. lactis*, and share a similar genetic organization. Proteins (in panel A) or coding genes (in panel B) are in green for initiation functions, red for elongation functions, brown for FA-modifying functions, and gray for phospholipid synthesis functions. *fabF1* is also named *fabO.* In panel A, the dashed arrow represents the shunt leading to unsaturated FA synthesis; in (B) dark blue, *fabT*; purple and light blue, *acpA* and *acpB*, respectively. Bent arrows, transcription start sites (12, 15); dashed bent arrow, suggested transcription reinitiation site (11); *FabT binding sites; a single star represents one or two closely localized consensus sequences.

point and caused significantly less spread, smaller lesions, and less tissue destruction than the wild-type strain; it was also more sensitive to killing in blood and in polymorphonuclear neutrophils (10). Another study in a murine subcutaneous infection model used wild-type strains, their *fabT* deleted derivatives, or clinical isolates harboring spontaneous *fabT* point mutations and a *fabT*-complemented strain. Virulence was strongly attenuated for all *fabT* mutant strains (8), in support of the above observations.

Downloaded from https://journals.asm.org/journal/mmbr on 12 October 2022 by 193.54.110.61.

In conclusion, *fabT* mutants appear spontaneously among noninvasive isolates and, when mutated, may compromise bacterial virulence. Characterization of the genes controlled by FabT and FabT repression mechanisms and how FabT influences bacterial physiology will shed light on how and why *fabT* mutants emerge in weakly pathogenic isolates.

IDENTIFICATION OF FABT AS THE FASII REGULATOR

Bioinformatics analysis revealed a similar genetic organization of the FASII main cluster in three *Streptococcus* species, and in *Clostridium acetobutylicum* (3, 11), *L. lactis*, and *E. faecalis* (Fig. 1B). In streptococci, FASII genes are grouped in a single locus, whereas in *L. lactis* and *E. faecalis*, they are found in two distinct loci. The main acyl carrier protein (ACP) encoded by *acpA* is always present on the main locus, in an operon comprising three or more genes, the first of which is the MarR family regulator FabT (Fig. 1B) (12–14). A second transcript starting with *acpA* may indicate the existence of a second operon, or of a stabilized part of a longer mRNA (12, 15). When present, a second ACP encoded by *acpB* is colocalized with *plsX* and will be discussed below.

FabT was shown in *S. pneumoniae* by the Rock laboratory to be a FASII transcriptional regulator (12, 16). Its role was further demonstrated in *S. pyogenes*, *E. faecalis*, and *L. lactis* and suggested by synteny and sequence similarity analyses in *C. acetobutylicum* (3). FabT is conserved among the streptococci; the 144 amino acid *S. pneumoniae* FabT protein, respectively, shares 64%, 62%, 51%, 59%, and 45% sequence identity with *S. pyogenes*, *Streptococcus agalactiae*, *E. faecalis*, *L. lactis*, and *C. acetobutylicum* FabT (unpublished data). FabT is distinct from FapR-type regulators as described in *Bacillus*, *Staphylococcus*, and *Listeria*, which involve a feed-forward-type regulation (17). In that system, FapR repression is alleviated by binding to FASII precursors malonyl-CoA or malonyl-ACP (4, 5, 18).

THE FABT REGULON

The roles of FabT and the breadth of its regulon, which includes FASII and non-FASII genes, were reported in different transcriptional studies. For this, expression was compared in wild-type and *fabT* deleted or overproducing mutants, using various growth conditions, including those requiring adjustments in membrane composition (10, 12, 19–21).

FASII Gene Regulation by the FabT Repressor

FASII genes are organized in three to five transcriptional units in *Streptococcus* and four and five in *E. faecalis* and *L. lactis*, respectively (Fig. 1B). Internal transcriptional start sites within the operon beginning with *fabT* were uncovered in *S. pneumoniae* and *S. pyogenes*, suggesting that expression may be finely controlled (12, 15). In *E. faecalis*, overlapping RT-PCR demonstrated that the 12-gene cluster is organized as a single operon that accommodates a putative transcription reinitiation site upstream from *fabK* (13).

In *S. pneumoniae* and *S. pyogenes*, at 37°C, *fabT* loss of function mutants showed 2- to 9-fold increases in FASII gene expression compared to the wild-type strain, although species differences were observed (12, 21). Those studies showed that in *S. pneumoniae*, FabT represses expression of all FASII genes with the exception of *fabM* (required for FA unsaturation) (12). In *L. lactis*, only three genes from the main locus, *fabD*, *fabG1*, and *accB*, and two genes in a separate locus, *fabZ1* and *fabI*, displayed increased expression in a *fabT* deleted strain, suggesting that repression was too weak to be detected for other FASII genes in the test condition (19). Indeed, in an *L. lactis* strain overproducing *fabT* by ~135-fold, all FASII genes except *fabH* were repressed by a factor of 2.5 to 5.3, indicating that these genes are controlled by FabT (19). The moderate effects of FabT on FASII gene expression in these extreme conditions, evokes the possibility that FabT activity is modulated by a cofactor (see The FabT corepressor). In *Streptococcus mutans*, FASII gene derepression in a *fabT* deletion mutant was observed under both neutral and acidic pH conditions (20). In *S. pyogenes*, variations in FASII

Downloaded from https://journals.asm.org/journal/mmbr on 12 October 2022 by 193.54.110.61.

gene transcription were analyzed between wild-type and *fabT* deletion strains, at different temperatures and growth phases. The authors concluded that FabT controls all FASII pathway genes, although *fabM* was less tightly controlled at 35°C than the other genes (10). Weaker control of *fabM* is reminiscent of results obtained in *S. pneumoniae*, where it was not repressed by FabT (12). In conclusion, FabT represses FASII genes in a coordinated but nonidentical way. Differential regulation of fluidifying fatty acids (requiring FabM) might be important for adjustment to stress conditions.

Non-FASII Gene Regulation by the FabT Repressor

Transcriptomic studies revealed numerous non-FASII genes whose expression is affected by the FabT status. In *S. pneumoniae*, comparison of transcription profiles between strains grown in laboratory medium showed that *fabT* deletion led to mostly minor (up to 5-fold) and 4 major (12- to 50-fold) expression changes for 85 upregulated and 4 downregulated genes, involved in transport, DNA metabolism and protein synthesis, and proteins of unknown function (12). The likely indirect effects of the *fabT* deletion may reflect bacterial adaptation to the altered ratio of saturated to unsaturated FAs (see reference 7; FabT and *in vitro* bacterial physiology). In support of this finding, comparing transcriptomes of wild-type and *fabT* deleted strains in *L. lactis* revealed expression changes of only 10 non-FASII genes (19). The use of dairy strains in that study may limit the identified targets when compared to a lactococcal pathogen (*Lactococcus garvieae*), or *L. lactis* plant, vaginal, or intestinal isolates, which express identical FabT proteins. However, *fabT* overexpression affected 125 genes belonging to the same functional categories as those identified in *S. pneumoniae*. It is likely that most expression changes are indirect consequences of FabT control.

Interestingly, FabT represses the expression of two non-FASII genes involved in FA and phospholipid metabolism. i- *fakB3* encodes FakB3, which is involved in the incorporation of polyunsaturated FAs, which are not synthesized by *Firmicutes* (22, 23); and ii- *plsC* encodes PlsC, which catalyzes joining of a second FA to the 1-acyl-*sn*-glycerol 3-phosphate (bearing a single FA) to complete phospholipid acylation. *S. pneumoniae* FabT thus couples regulation of FA and phospholipid synthesis, similar to FapR regulation in *B. subtilis* and *Staphylococcus aureus*, where the regulatory mechanisms are different (24, 25). A direct or indirect role of FabT in regulating *fakB3* and *plsC* expression remains to be shown.

In *S. mutans*, transcription profile comparisons of wild-type and *fabT* deleted strains were performed after growth at pH 7 or pH 5 (20). The expression of 25% of *S. mutans* genes was altered at pH 7 and 7% at pH 5. They also belonged to the same functional categories as described in *S. pneumoniae*. Deletion of *fabT* may thus have more consequences at neutral pH, as normally found in the oral cavity, than at acidic pH, as produced during *S. mutans* growth. Alternatively, low pH already creates the membrane perturbations that are similarly generated by FabT mutation, so that the changes are already in place.

Transcriptional analyses of a *fabT* deletion strain were also performed in *S. pyogenes*, in which growth phase and temperature were varied. Stationary growth phase and to a lesser extent 40°C induced the highest number of differentially expressed genes, i.e., up to 28.5%, between wild-type and *fabT* strains. The majority of affected genes was less expressed in the *fabT* mutant (10). Significantly, expression of many genes of carbohydrate metabolism and purine and pyrimidine synthesis pathways was modified, particularly during the stationary phase. This suggests that *fabT* mutations may lead to metabolic dysbiosis. Temperature, growth phase, biofilm status, and the nutritional environment were documented to affect bacterial FA composition and thereby impact membrane fluidity (26–29). Thus, in bacteria using FabT as the FASII regulator, FabT would ensure the maintenance of membrane homeostasis in response to membrane stress.

Altogether, these studies indicate that FabT likely has similar roles in different streptococcaceae. They show that the consequences of *fabT* mutation on bacterial physiology are numerous; possibly, these pleiotropic effects are triggered by changes in

Downloaded from https://journals.asm.org/journal/mmbr on 12 October 2022 by 193.54.110.61.

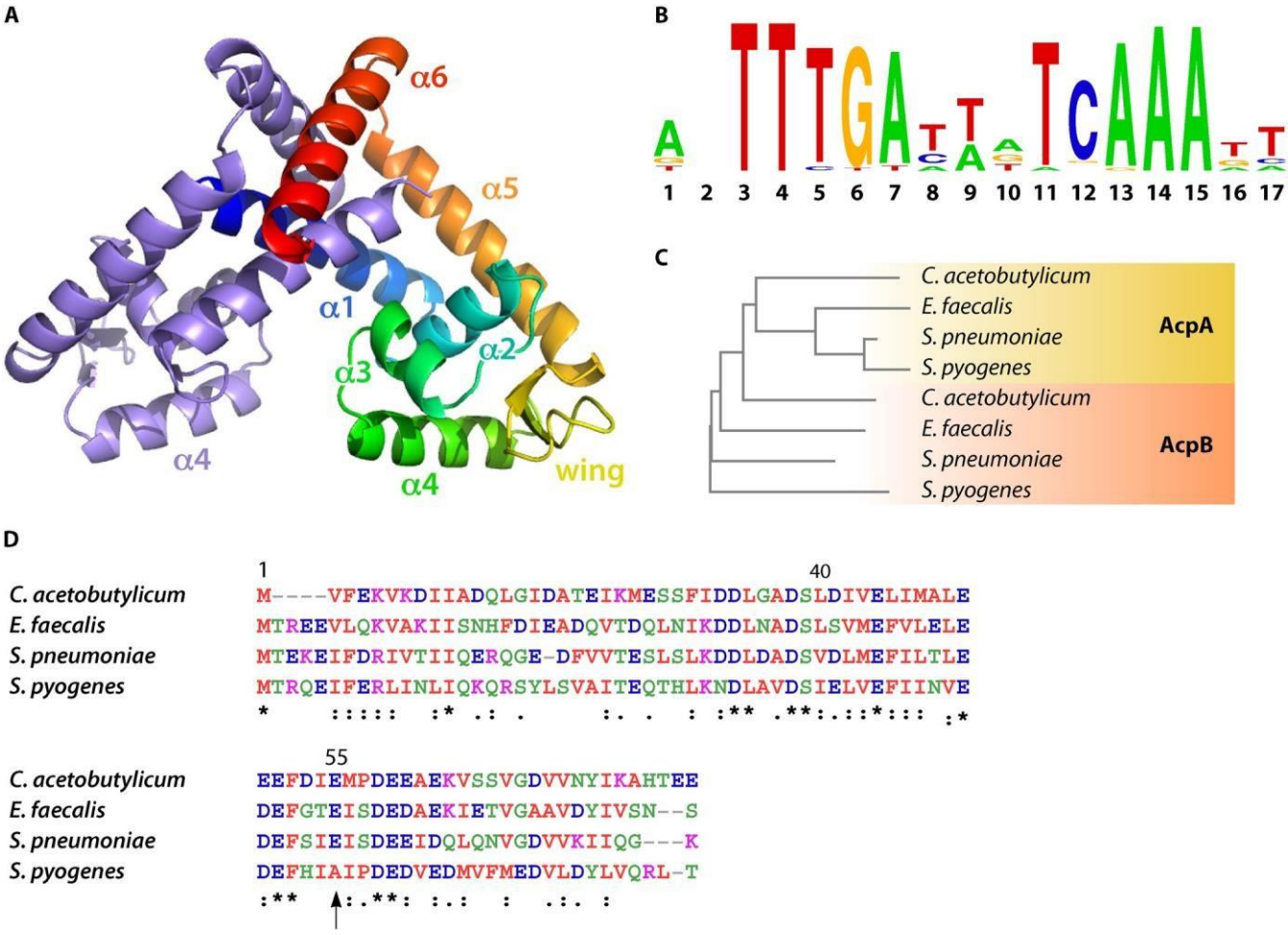

FIG 2 Structural features of FabT, the ACP corepressor, and the FabT-DNA binding motif. (A) Overall structure of MarR family member dimer; one monomer is represented multicolored and the other in blue. Reprinted from reference 30 with permission. (B) FabT DNA binding motif; top, calculated from 56 FabT DNA binding sequences (https://regprecise.lbl.gov/regulog.jsp?regulog_id=3571). The relative size of letters corresponds to the relative frequency at which each nucleotide is present. (C) Phylogenetic neighbor-joining tree obtained from a multiple sequence alignment carried out using Clustal W (1.83). Branch lengths correspond to: *C. acetobutylicum* AcpA, 0.28257; *E. faecalis* AcpA, 0.19187; *S. pneumoniae*, AcpA 0.0325; *S. pyogenes*, AcpA 0.04858; *C. acetobutylicum* AcpB, 0.25594; *E. faecalis* AcpB, 0.29157; *S. pneumonia*, AcpB, 0.25143; *S. pyogenes*, AcpA, 0.35383. (D) AcpB alignment; multiple sequence alignment was carried out using Clustal W (1.83) (unpublished results), color code follows functional classification; *, identical in all four species: the same structural class; vertical arrow highlights amino acid residue 55, which is adjacent to the FabT-AcpB binding (32) but is not conserved in *S. pyogenes*.

membrane composition. Our previous works showed that FASII transcription is turned off in FA-rich environments (11); in light of current knowledge, this repression involves FabT. The above observations show the far-reaching consequences of FASII regulation by FabT in bacterial lifestyle.

FABT MECHANISM OF REPRESSION

Like other MarR-family proteins, the FabT regulator comprises six alpha helices and three beta strands: *a*1-*a*2-*b*1-*a*3-*a*4-*b*2-*b*3-*a*5-*a*6. These regulators exist as homodimers both in their free or DNA-bound forms, and each subunit contributes a winged helix-turn-helix DNA-binding motif (Fig. 2A) (30, 31). MarR regulators have varying DNA targets and interact with either an inducer or a corepressor that modulates their affinity for their targets. Identification of these cofactors has been invaluable for understanding FabT regulatory mechanisms.

FabT Dimerization and Target Gene Interaction

The crystal structure of the *S. pneumoniae* FabT-DNA complex revealed that FabT structure is similar to that of the MarR prototype protein (32). The FabT *a* helix 1 on

Downloaded from https://journals.asm.org/journal/mmbr on 12 October 2022 by 193.54.110.61.

one subunit intertwines with *a* helices 5 and 6 of the second subunit, creating a very compact and stable dimer; its *a*2, *a*3, and *a*4 helices, together with the hairpin comprising the *b*1-*b*2 strands, compose the DNA binding domain. However, the acyl-Acp-FabT complex binds DNA with more affinity than FabT alone. Weak FabT-DNA binding could be nonspecific, as only a single amino acid residue (Arg89)-nucleotide (T) interaction was highlighted (32). Further structural analysis will be needed to determine the biological relevance and molecular interactions involved in an effective FabT-DNA binding.

In *S. pneumoniae*, palindromes upstream of FASII operon genes *fabM*, *fabT*, and *fabK* were detected (Fig. 1B) (16). Their roles as FabT binding sites were confirmed by electrophoretic mobility shift assays (12). The positions of these binding sequences in *S. pneumoniae*, 10 and 30 bp from the ribosome binding sites of *fabT* and *fabK*, respectively, suggested that FabT inhibits RNA polymerase recruitment. Alternatively, the palindrome close to the *fabK* ribosome binding site could stop elongation of an RNA whose transcription starts upstream of *acpA* (12). FabT binding sites were also identified *in silico* in *L. lactis*, *S. mutans*, *S. pyogenes*, and *E. faecalis*, and were confirmed for *L. lactis* and *S. mutans* (10, 19–21, 33, 34). They were found upstream of various FASII genes *fabM*, *fabT*, and *fabK* or *fabD*, further supporting the existence of two or more FabT-regulated transcriptional units in the main cluster (Fig. 1B). A consensus FabT binding motif was proposed, based on 56 predicted or confirmed sequences (https://regprecise.lbl.gov/regulog.jsp?regulog_id=3571) (Fig. 2B). Most MarR proteins are sequence specific but may still show some degeneracy (31). More data are needed to determine whether FabT binds to degenerate motifs.

The presence of FabT binding sites adjacent to transcriptional start sites of specific genes is indicative of direct FabT regulation. Interestingly, FabT binding sites outside the main FASII locus are present in the intergenic regions between divergent FASII genes, such that FabT likely controls both transcriptional units. This organization was described for other MarR targets (31). Hence, while the location of the FabT binding sites appear to vary according to the species, a common feature of FabT is that it regulates all FASII genes, albeit at different levels, and depending on the growth conditions. Moreover, the low number of additional binding sites predicted in different species suggests that the FabT direct target genes are almost exclusively FASII genes.

The FabT Corepressor

The FabT ligand, acyl-ACP. MarR family regulators generally possess a ligand acting as a corepressor or inducer. However, screening for known effectors of other MarR regulators failed to identify the FabT ligand (35). FabT was found to bind a unique ligand, acyl-ACP, the FASII end product, to modulate FASII expression. FabT-(acyl-ACP) binds DNA with high affinity. This feedback regulation strategy contrasts with the feed-forward strategy used by other *Firmicutes* (see Identification of FabT as the FASII Regulator). However, it is not a simple feedback regulation. AcpA is encoded in the FASII main locus and *acpA* expression is controlled by FabT, implying that the excess of acyl-AcpA stops *acpA* synthesis. This in turn leads to lower production of acyl-AcpA-FabT production and subsequent derepression of the FASII genes. This regulation favors fine tuning of the available pools of Acyl-AcpA.

It is notable that FabT-(acyl-ACP) is not a unique molecule, and its binding to DNA targets varies according to the acyl moiety (32). While FabT reportedly has the same affinity for all acyl-ACPs, the affinity of the FabT-acyl-ACP interaction with DNA increases with the length of the acyl carbon chain, with a marked increase beyond 14 carbons in *S. pneumoniae* (35). Thus, the length of the acyl-ACP chain is essential for consolidating FabT binding to DNA. Also, FabT-DNA binding is greater when FabT is complexed with C18:1-ACP than with C16:0-ACP. This suggested that chain length, and/or saturation status of the bound fatty acid might determine FabT-DNA binding affinity. In *E. faecalis*, FabT-mediated repression of FA synthesis is similarly exacerbated by C16:1 and C18:1 (*cis*-9), but less so in C18:1 (*trans*-9) and even less so in C16:0 (36). This argues in the favor of *cis* unsaturated FA maximizing FabT-DNA binding affinity.

Downloaded from https://journals.asm.org/journal/mmbr on 12 October 2022 by 193.54.110.61.

The corepression mechanism mediated by *S. pneumoniae* FabT and acyl-ACP was characterized by combining crystallographic, biochemical, and genetic approaches (32). One acyl-ACP molecule binds to each subunit of the FabT dimer. It was suggested that acyl-ACP more readily binds FabT than does free ACP and that the acyl-ACP-FabT complex provokes a change in FabT conformation favoring the interaction with DNA (32, 35). Evidence for this interaction was obtained by replacing FabT lysine 97 and ACP aspartate 50 by cysteine residues; protein interactions and DNA binding were observed in the absence but not in the presence of DTT (32). The acyl moiety binds directly within a hydrophobic pocket of FabT, favoring ACP interaction within the FabT *a*5 helix, leading to formation of a stable FabT-acyl-ACP complex (32). The length of the acyl moiety increases stability of the acyl-ACP-FabT complex; this makes physiological sense, as accumulation of full-length phospholipid precursors should arrest FASII.

An increased concentration of 18:1-ACP during electrophoretic mobility shift assays performed with a fixed concentration of FabT protein led to a more intense FabT-DNA band (35). Possibly, the acyl-ACP cofactor could be a limiting factor for interactions between FabT-(acyl-ACP) and DNA in the bacterium (32). This would explain the modest difference in repression of FASII genes in *L. lactis* when FabT was overproduced 135-fold (19).

Why are there two ACPs in some species? Numerous species of the order *Lactobacillales*, which comprise the *Streptococcaceae*, possess two ACPs. AcpA is encoded within the FASII locus; AcpB is encoded in the same operon as PlsX (glycerol-3-phosphate acyltransferase), required for phospholipid synthesis (Fig. 1B) (14, 32, 37). *E. faecalis* and *S. pneumoniae* encode the second ACP, AcpB, while *L. lactis* does not. AcpB is also found in *C. acetobutylicum* in the same operon as *plsX* (unpublished result). AcpA and AcpB share approximately 40%, 24%, 30%, and 45% sequence identity in *S. pneumoniae*, *S. pyogenes*, *E. faecalis*, and *C. acetobutylicum*, respectively (unpublished results; references 14, 32, 37). A phylogenetic tree based on multialignment comparison of AcpA and AcpB shows clustering of the four AcpA proteins but not of the four AcpBs. In *C. acetobutylicum*, AcpB is more closely related to the AcpA proteins than to the other AcpB proteins (Fig. 2C). Closer homology between AcpA proteins suggests that it may have more functional constraints than AcpB. Multialignment comparison of AcpB sequences highlights clusters of similarity (Fig. 2D). However, BLASTP analysis indicates that AcpB is absent or severely truncated in over half of sequenced *S. agalactiae* strains available in NCBI (unpublished results). These observations raise questions about the need for a second acyl carrier protein in some species.

Distinguishing features of AcpA and AcpB with respect to FASII and to interactions with FabT were investigated in *E. faecalis* (14). Whereas the *acpA* gene is essential, *acpB* is not. Furthermore, the *acpB* mutant grows without exogenous FA supplementation, unlike FASII mutants (13). AcpA and AcpB involvement in FA synthesis was assessed by studying their interactions with FabI and FabK enoyl-ACP reductases, which catalyze the last step in FASII synthesis to produce acyl-ACP (38) (Fig. 1A). FabI was reportedly more effective than FabK in reducing the acyl-AcpA precursor; conversely, FabK reduced the acyl-AcpB precursor more effectively than FabI (14). However, interactions of AcpA and AcpB were not studied in streptococci, which possess only FabK. These results suggested that FabI and AcpA are main actors in FA *de novo* synthesis in *E. faecalis*, whereas the role of AcpB in FA synthesis remains in question. To define the involvement of AcpA and AcpB in the phospholipid synthesis step, the authors then followed the activity of PlsX, which catalyzes reversible transfer of the acyl moiety between ACP and a phosphate group. Acyl transfer from AcpA proved much more efficient than from AcpB. In contrast, in the presence of exogenous FAs and PlsX, acyl transfer to AcpB (the reverse reaction) was the more efficient. This indicated that acyl-AcpA is the preferred PlsX substrate to synthesize acyl-phosphate, which then initiates phospholipid production *via* PlsY. In contrast, free AcpB would be a PlsX substrate, which produces Acyl-AcpB in the reverse reaction. Acyl-AcpB would then act as corepressor of FabT, signaling availability of the exogenous FA sources. Acyl-AcpB could

Downloaded from https://journals.asm.org/journal/mmbr on 12 October 2022 by 193.54.110.61.

additionally be a precursor for phospholipid synthesis that favors entry of exogenous fatty acids (14) Altogether, this suggested that AcpA is the main FASII enzyme needed for FA *de novo* synthesis, but may also regulate FASII repression in the presence of exogenous FA; AcpB, which is encoded in the same operon as *plsX* and is nonessential, may only have a role in facilitating exogenous FA utilization for phospholipid synthesis (14, 36). However, part of these conclusions were recently revised (36; see below).

Although some features of AcpB have been elucidated, our understanding of its role in fatty acid metabolism remains incomplete: a comparison of membrane FA composition and FASII gene repression in the presence of exogenous FAs indicated that *acpB* and *fabT* mutant strains had the same phenotypes, suggesting that AcpB is a corepressor of FabT (14). In keeping with this observation, acyl-AcpB, but not AcpB alone, increased FabT-(acyl-ACP) binding to DNA in *S. pneumoniae* (32). *In silico* comparison of AcpB sequences shows that amino acid residues involved in interactions with FabT are only partially conserved in *S. pyogenes*. AcpB Asp^{50} interacts with the FabT Lys^{97}; however, the spatially adjacent AcpB Glu^{55} is not conserved, which may weaken the interaction (Fig. 2D) (unpublished results); reference (32). Moreover, AcpB is absent in about half the *S. agalactiae* strains and in *L. lactis*. Consistent with the above observations, a recent report clarified that the role of AcpB in controlling FabT repression was minor, compared to earlier conclusions that the *acpB* mutant exerted a dominant effect on FabT repression; a secondary mutation in *fabT* was identified, which accounted for this revised explanation (14, 36). In a reconstructed *E. faecalis acpB* deletion strain, addition of exogenous FA showed just partial repression of *fabT* promoter expression (36). Also, and in contrast to the situation in *S. pneumoniae*, in *E. faecalis*, acyl-AcpA enhances FabT binding to the *fabT* promoter *in vitro* (32, 36). This confirms that in *E. faecalis*, AcpA is also a FabT corepressor. Altogether, these results suggest that AcpA and AcpB as studied in *E. faecalis* and *S. pneumoniae* do not have totally distinct functions and that their properties may not be conserved in all related strains and species (14). The differential roles of the two ACP proteins merit further study.

Since AcpB is constitutively synthesized in exponential growth (10, 12, 21), the concentration of acyl-AcpB and consequently its repression efficiency may depend primarily on the amounts and composition of exogenous FAs. A regulatory model was proposed based on the above considerations (Fig. 3). It is likely that the repressive effects of exogenous FA on FASII gene transcription, as we previously described (11, 13), are carried out at least in part *via* AcpB.

REGULATION OF *FABT* TRANSCRIPTION AND FABT ACTIVITY

FabT regulates FASII synthesis and, concomitantly, exogenous FA utilization and phospholipid synthesis. To understand how this regulon responds to bacterial metabolism, we must first know how FabT itself is regulated.

In *S. mutans*, in-depth analysis of genes affected by deletion of *fabT* suggested that catabolite control protein CcpA, a master regulator of catabolic repression in Gram-positive bacteria, also controls their expression. CcpA DNA binding motifs were identified upstream of different *fab* genes and confirmed to be active. Importantly, *fabT* is regulated by CcpA (20). By controlling *fabT* expression, CcpA links carbon and FA metabolism. Whether CcpA exerts similar roles in *fabT* regulation in species related to *S. mutans* remains to be confirmed.

In *S. pneumoniae*, *fabT* expression is regulated by a two-component system called VicKR (also known as WalKR), which responds to parietal stress. Upon membrane stress, the VicK kinase autophosphorylates and then phosphorylates the VicR regulator, leading to repression of VicRK regulon genes within 10 min (39, 40). In the absence of parietal stress, the nonphosphorylated VicR regulator binds to the *fabT* promoter region, thus directly repressing its transcription (41). *fabT* repression in the nonstress state leads to upregulation of the *fabK* operon, which results in longer FA chains (39). These findings indicate that bacterial membranes would comprise a higher proportion of long-chain FAs in the absence than in the presence of parietal stress; this regulation

Downloaded from https://journals.asm.org/journal/mmbr on 12 October 2022 by 193.54.110.61.

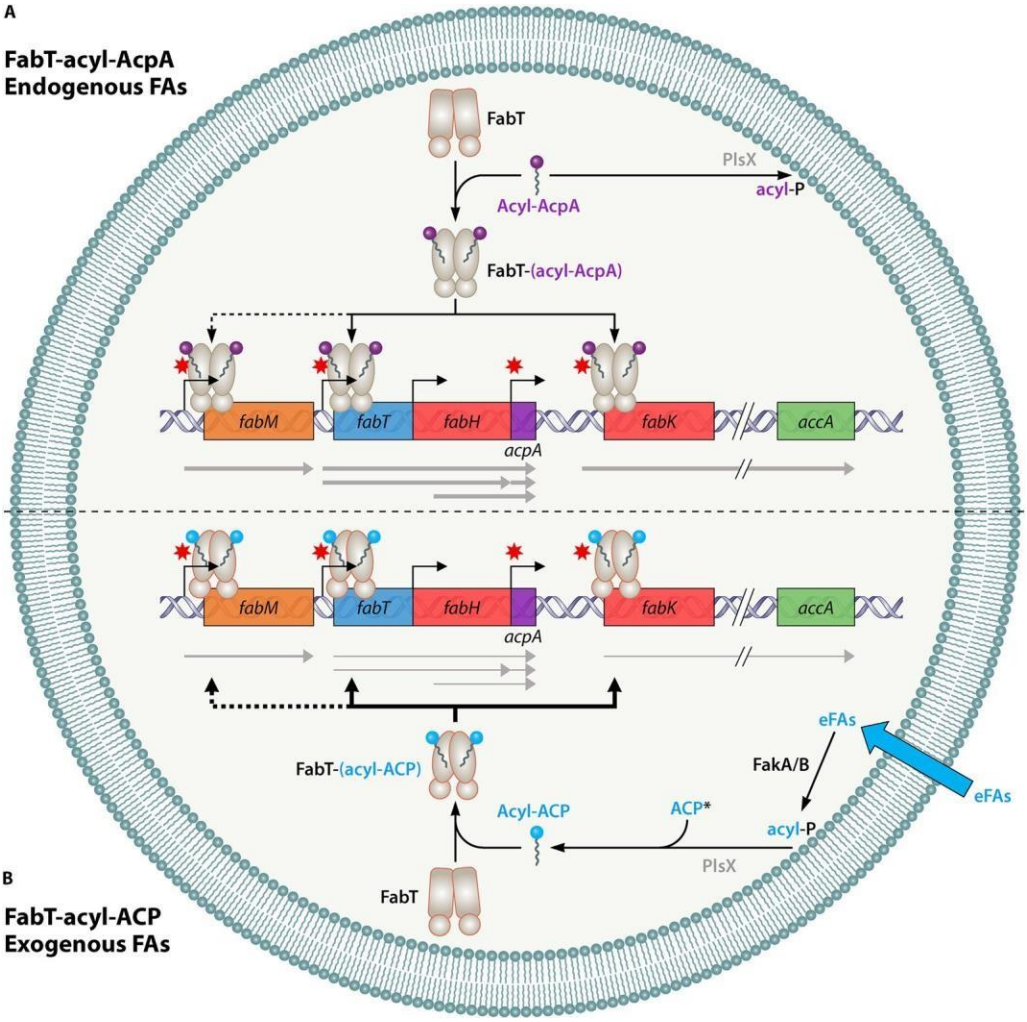

FIG 3 Model of the FabT repression mechanism in *S. pneumoniae* and *E. faecalis*. (A) Endogenous fatty acid (FA) synthesis: an excess of FA synthesis generates acyl-AcpA, which binds to FabT; the complex binds with low affinity to the promoter regions of its target transcriptional units, leading to weak repression of FabT directly controlled genes, including *acpA*. Acyl-AcpA is also a substrate for the bidirectional glycerol-3-phosphate acyltransferase PlsX, leading to phospholipid synthesis (not shown). The minor apparent regulatory role of FabT when interacting with acyl-AcpA contrasts with its prominent role when exogenous FAs are present, e.g., as is common *in vivo*. (B) Exogenous FA utilization: entering FAs may be phosphorylated by fatty acid kinase complex FakA coupled to one of the FA-binding FakB subunits, each of which has FA preferences (22). Acyl-P is then converted to acyl-AcpB or AcpA (36) by a reverse PlsX reaction. Acyl-ACP binds to FabT, and the complex binds with high affinity to the promoter regions of its transcriptional unit targets, strongly repressing gene expression. The information contained in this figure corresponds to results shown in at least one species. Gray arrows under the genes represent the various transcriptional units described; their thickness symbolizes the level of transcription. Black arrows above or below the genes represent the binding of acyl-Acp to promoter regions; their thickness indicates repression efficiency; dotted arrows indicate that the repression level is species dependent. Note that only FabT-related functions are indicated. eFAs: exogenous FAs; acyl-P, acyl-phosphate. Note that acyl-AcpA is the FASII product; both acyl-AcpB and acyl-AcpA appear to be involved in eFA incorporation and reverse activity of PlsX.

would contribute to bacterial adaptation to each condition. This adjustment of membrane composition at the *fabT* transcriptional level may bypass the need for FASII regulation *via* (acyl-Acp)-FabT during parietal stress.

In *S. pyogenes*, Stk is the kinase of a two-component histidine kinase/regulator system (33). Transcriptomic analysis of the *stk* deleted strain suggested that Stk indirectly activates expression of FASII pathway genes. Two hypotheses were proposed. The simplest is that Stk phosphorylates FabT, preventing it from exerting its role as a transcriptional repressor. The second postulates that Stk phosphorylates FASII enzymes and

Downloaded from https://journals.asm.org/journal/mmbr on 12 October 2022 by 193.54.110.61.

that a loss of function leads to feedback activation of FASII gene expression. Kinases may have important roles in modulating FASII activity that warrant further studies.

Taken together, FabT is subject to various selective pressures and types of regulation, which seem to differ according to the *Streptococcus* species. Whether regulatory controls on *fabT* cross species boundaries remains to be tested. However, these reports underscore the importance of FabT in coordinating FASII-mediated membrane biogenesis with other metabolic processes to optimize bacterial fitness.

FABT AND BACTERIAL PHYSIOLOGY

Invasive *S. pyogenes* infections cause ~150,000 deaths/year, thus calling for new treatment targets and strategies. We discussed above that emergence of *fabT* variants correlated with noninvasive infections (see Identification of FabT as the FASII Regulator). Mutations in *fabT* may thus be counterselected in invasive infections due to lower virulence of these mutants. Assessing the consequences of mutating *fabT* on bacterial physiology and on potential penalties and/or benefits during infection could give insight into the use of FabT as a therapeutic target to reduce severity of infection.

The extent to which FabT affects bacterial survival *in vitro* varies with the species and possibly with test conditions. In *E. faecalis* and *L. lactis*, *fabT* deleted strains are viable, although the *E. faecalis* mutant displays a growth delay (14, 19). An *S. pneumoniae fabT* mutant containing a stop codon early in the *orf* is viable, with no growth defects reported in rich medium (12). In contrast, construction of *S. pyogenes fabT* deletion mutants, as attempted in three separate studies, suggested that *fabT* has an important role: *fabT* mutants could not be obtained without deleting *clpX* (a protease ATP-binding subunit) or *gdpP* (encoding a c-di-AMP phosphodiesterase) (21). In a second study, a *S. pyogenes fabT* deleted strain displayed highly altered growth: longer latency time, slower growth and lower bacterial yield in rich medium (8). Growth was restored in medium supplemented with unsaturated FAs (*cis*-vaccenic acid, C18:1, or *cis*-eicosenoic acid, C20:1). Unlike *fabT* deletion mutants, *fabT* point mutants were obtained with no effects on *in vitro* growth. In a third study, a *S. pyogenes fabT* deletion mutant displayed no major doubling time defect but did show a longer latency period (10). All the *S. pyogenes* constructs respected the integrity of *fabH*, the gene directly downstream of *fabT* (Fig. 1B); hence, the discrepancies between reports can best be explained by wild-type strain differences and/or variations in test conditions. Despite these phenotypic differences, a common feature of the *fabT* point mutant and deleted strains was that both displayed attenuated virulence (8, 10).

Since FabT regulates the quasi-ensemble of FASII pathway genes (see The FabT Regulon), its inactivation should have direct consequences on membrane FA composition. In *S. pneumoniae* and *L. lactis*, the proportion of long-chain FAs is higher in the *fabT* mutant than in the wild-type strain, in keeping with derepression of FASII (12, 19). A greater proportion of saturated FAs was also reported. Interestingly, *fabT* inactivation leads to greater upregulation of *fabK* than *fabM.* FabM (required for unsaturated FA synthesis) and FabK compete for the same substrate (Fig. 1A); the relative increase in FabK expression compared to FabM accounts for this ratio variation. Moreover, in *S. pneumoniae*, FabT also controls phospholipid synthesis gene *plsC* (see The FabT Regulon). These observations are consistent with findings described above, that *fabT* repression results in longer FA chains (39) (see Regulation of *FabT* Transcription and FabT Activity).

Membrane permeability studies were performed to determine how FabT mutation-induced alterations of FA ratios impact membrane properties. Measurements of ethidium bromide incorporation in *L. lactis* indicated that permeability of the *fabT* membrane is greater than that of the wild-type strain (19). Membrane rigidity is known to depend in part on the ratio of saturated/unsaturated FAs. Different ratios in wild-type and *fabT* strains can explain the reported differences in membrane permeability.

Osmotic homeostasis is critical for all cells, and membrane FA composition is a key determinant of bacterial survival under osmotic pressure. Interestingly, *fabT* mutations

Downloaded from https://journals.asm.org/journal/mmbr on 12 October 2022 by 193.54.110.61.

arose when *S. agalactiae* was submitted to osmotic stress conditions: in that work, strains were grown in a minimal medium supplemented with 0.5 mM potassium (42). One could speculate that higher relative amounts of saturated FAs in the *fabT* mutant and consequent modified permeability may be responsible for this natural selection. Alternatively, but not exclusively, altered membrane protein composition may contribute to the response to potassium excess (see below).

Modifying membrane composition by environmental FAs that are not normally present may affect bacterial growth or survival. For example, ;20 *m*g/mL free linoleic acid (C18:2), a main FA constituent of soy bean oil, inhibits growth of lactobacilli. Increased consumption of soybeans in the USA and Europe was suggested to correlate with a decrease of *L. reuteri* and *Lactobacillus johnsonii* prevalence in the human intestinal microbiota (43). Di Rienzi et al. (43) considered a possible link between this decrease and enriched linoleic acid in the diet. Isolation of linoleic acid-resistant *L. reuteri* mutants identified mutations in *fabT*. In hindsight, the selection of *fabT* mutations would lead to increased proportions of membrane saturated FAs, which could equilibrate FA composition in linoleic-acid-rich environments.

During a search for a narrow-spectrum antibiotic, the alkylated dicyclohexyl carboxylic acid 2CCA-1, a polyunsaturated FA mimetic, was identified as targeting *S. pneumoniae*. Investigation of its bactericidal effect led to the isolation of resistant mutants (23). One mutation mapped to *fakB3*, encoding a FA binding protein involved in the uptake of polyunsaturated FAs. The second mapped to *fabT*. *fakB3* is less expressed in the *fabT* mutant than in the wild-type strain. Consequently, in both mutant strains, 2CCA-1 incorporation would be reduced, rendering the strain resistant to the FA analog.

S. pyogenes strains were selected for resistance to polymyxin B, an antibiotic targeting anionic lipids (21). Sequencing showed that *fabT* point mutants displayed high polymyxin B resistance. In line with this result, *fabT* deleted strains are more resistant to polymyxin B (10, 19). Thus, changes in FA synthesis associated with *fabT* mutations may alter lipid composition, with consequences on antibiotic resistance, particularly to antibiotics targeting membrane constituents.

Deletion of *fabT* impacts *S. pneumoniae* adaptation to different known stresses (pH, reactive oxygen species [ROS], and detergents) (12). The *fabT* mutant proved to be more sensitive than the wild-type strain to acidic pH and detergents such as deoxycholate, suggesting that FabT may have specific roles in bacterial adaptation to these conditions. Resistance to ampicillin, vancomycin, and ROS was unchanged. Mutations in the FabT partner AcpB would expectedly give similar effects as the *fabT* mutant, and could further strengthen these findings.

Membrane modifications may also affect structure, function, and abundance of membrane, parietal, and secreted proteins. Indeed, some membrane protein complexes, such as the general secretion system Sec or sortases, are involved in the secretion and/or surface-anchoring of numerous proteins (44). Changes in phospholipid characteristics could affect both expression levels and activities of membrane proteins, and thereby impact bacterial adaptation to environmental changes. Studies based on exogenous FA incorporation capacities of *E. faecalis* confirm that disturbance of the membrane FA ratio modifies bacterial morphology, growth, and adaptation capacities (45, 46). Current studies in our laboratory will monitor the effects of *S. pyogenes fabT* mutations (which alter the membrane FA ratio) on protein expression and bacterial fitness. This study might help explain the emergence of mutations under some stress conditions.

Studies thus far show that FASII deregulation when FabT is mutated has direct and indirect consequences on membrane composition and modifies bacterial adaptation to its environment. Selective advantages driven by *fabT* mutations during noninvasive infection remain to be assessed. Accumulation of pathogen mutations during infection raises the possibility that *fabT* revertants might be selected because they restore bacterial invasive capacity.

Downloaded from https://journals.asm.org/journal/mmbr on 12 October 2022 by 193.54.110.61.

CONCLUSIONS

The emergence of multiresistant bacteria and growing awareness of the need to preserve the microbiota have spurred development of therapeutic targets specific to bacterial pathogens. FASII was thought to be essential for bacterial survival, which drove the development of numerous FASII inhibitors. The understanding that Gram-positive bacteria, such as *S. aureus*, *E. faecalis*, and streptococci, incorporate exogenous FAs that allow these bacteria to bypass FASII inhibition has modified the rationale of monotherapy, as anti-FASII reaches its targets but fails to block streptococcal, staphylococcal, and enterococcal growth in FA-rich host environments (11, 13, 47–50). Thus, anti-FASII are ineffective as stand-alone *in vivo* antibacterial agents against these bacteria.

Here we summarized the roles of FabT as a major regulator that acts as repressor in the presence of long chain acyl-ACP. Whether acyl-ACP comprises AcpA or AcpB, which are stakeholders of a feedback or an exogenous FA-sensing mechanism, respectively, FabT-acyl-Acp-mediated repression limits futile FASII activity. FabT mutants arise spontaneously when bacteria undergo osmotic stress and seem to emerge in noninvasive infections, suggesting that *fabT* mutations may improve bacterial fitness in certain conditions. Since FabT controls FA length and the saturated to unsaturated FA ratio, the state of FabT is a key factor in bacterial fitness and adaptation. Development of FabT inhibitors, such as FAs leading to acyl-Acp toxic analogues, could pave the way for new narrow-spectrum therapeutic tools.

ACKNOWLEDGMENTS

We thank A. Grove for permission to reproduce a figure from her article (30).

Research of authors on the topic of this review was funded by the following French granting agencies: the regional DIM-Malinf, DIM-OneHealth Projet 00002247, the Agence Nationale de la Recherche (StaphEscape project ANR-16-CE15-0013), and the Fondation pour la Recherche Medicale (DBF20161136769), the Université de Paris (to C.L.).

REFERENCES

1. Zhang YM, Rock CO. 2008. Membrane lipid homeostasis in bacteria. Nat Rev Microbiol 6:222–233. https://doi.org/10.1038/nrmicro1839.
2. Grogan DW, Cronan JE, Jr. 1997. Cyclopropane ring formation in membrane lipids of bacteria. Microbiol Mol Biol Rev 61:429–441. https://doi.org/10.1128/mmbr.61.4.429-441.1997.
3. Osterman A, Overbeek R. 2003. Missing genes in metabolic pathways: a comparative genomics approach. Curr Opin Chem Biol 7:238–251. https://doi.org/10.1016/S1367-5931(03)00027-9.
4. Cronan JE. 2020. The *Escherichia coli* FadR transcription factor: too much of a good thing? Mol Microbiol 15:1080–1085. https://doi.org/10.1111/mmi.14663.
5. Zhang YM, Rock CO. 2009. Transcriptional regulation in bacterial membrane lipid synthesis. J Lipid Res 50 Suppl:S115–S119. https://doi.org/10.1194/jlr.R800046-JLR200.
6. Cunningham MW. 2000. Pathogenesis of group A streptococcal infections. Clin Microbiol Rev 13:470–511. https://doi.org/10.1128/CMR.13.3.470.
7. Carapetis JR, Steer AC, Mulholland EK, Weber M. 2005. The global burden of group A streptococcal diseases. Lancet Infect Dis 5:685–694. https://doi.org/10.1016/S1473-3099(05)70267-X.
8. Tatsuno I, Okada R, Matsumoto M, Hata N, Matsui H, Zhang Y, Isaka M, Hasegawa T. 2016. Relevance of spontaneous *fabT* mutations to a streptococcal toxic shock syndrome to non-streptococcal toxic shock syndrome transition in the novel-type *Streptococcus pyogenes* isolates that lost a salRK. APMIS 124:414–424. https://doi.org/10.1111/apm.12521.
9. Nasser W, Beres SB, Olsen RJ, Dean MA, Rice KA, Long SW, Kristinsson KG, Gottfredsson M, Vuopio J, Raisanen K, Caugant DA, Steinbakk M, Low DE, McGeer A, Darenberg J, Henriques-Normark B, Van Beneden CA, Hoffmann S, Musser JM. 2014. Evolutionary pathway to increased virulence and epidemic group A *Streptococcus* disease derived from 3,615 genome sequences. Proc Natl Acad Sci U S A 111:E1768–76. https://doi.org/10.1073/pnas.1403138111.
10. Eraso JM, Olsen RJ, Beres SB, Kachroo P, Porter AR, Nasser W, Bernard PE, DeLeo FR, Musser JM. 2016. Genomic landscape of intrahost variation in group A *Streptococcus*: repeated and abundant mutational inactivation of the *fabT* gene encoding a regulator of fatty acid synthesis. Infect Immun 84:3268–3281. https://doi.org/10.1128/IAI.00608-16.
11. Brinster S, Lamberet G, Staels B, Trieu-Cuot P, Gruss A, Poyart C. 2009. Type II fatty acid synthesis is not a suitable antibiotic target for Gram-positive pathogens. Nature 458:83–86. https://doi.org/10.1038/nature07772.
12. Lu YJ, Rock CO. 2006. Transcriptional regulation of fatty acid biosynthesis in *Streptococcus pneumoniae*. Mol Microbiol 59:551–566. https://doi.org/10.1111/j.1365-2958.2005.04951.x.
13. Hays C, Lambert C, Brinster S, Lamberet G, Du Merle L, Gloux K, Gruss A, Poyart C, Fouet A. 2021. Type II fatty acid synthesis pathway and cyclopropane ring formation are dispensable during *Enterococcus faecalis* systemic infection. J Bacteriol 203:e0022121. https://doi.org/10.1128/JB.00221-21.
14. Zhu L, Zou Q, Cao X, Cronan JE. 2019. *Enterococcus faecalis* encodes an atypical auxiliary acyl carrier protein required for efficient regulation of fatty acid synthesis by exogenous fatty acids. mBio 10:e00577-19. https://doi.org/10.1128/mBio.00577-19.
15. Rosinski-Chupin I, Sauvage E, Fouet A, Poyart C, Glaser P. 2019. Conserved and specific features of *Streptococcus pyogenes* and *Streptococcus agalactiae* transcriptional landscapes. BMC Genomics 20:236. https://doi.org/10.1186/s12864-019-5613-5.
16. Marrakchi H, Choi KH, Rock CO. 2002. A new mechanism for anaerobic unsaturated fatty acid formation in *Streptococcus pneumoniae*. J Biol Chem 277:44809–44816. https://doi.org/10.1074/jbc.M208920200.
17. Albanesi D, Reh G, Guerin ME, Schaeffer F, Debarbouille M, Buschiazzo A, Schujman GE, de Mendoza D, Alzari PM. 2013. Structural basis for feed-forward transcriptional regulation of membrane lipid homeostasis in *Staphylococcus aureus*. PLoS Pathog 9:e1003108. https://doi.org/10.1371/journal.ppat.1003108.

Downloaded from https://journals.asm.org/journal/mmbr on 12 October 2022 by 193.54.110.61.

18. Martinez MA, Zaballa ME, Schaeffer F, Bellinzoni M, Albanesi D, Schujman GE, Vila AJ, Alzari PM, de Mendoza D. 2010. A novel role of malonyl-ACP in lipid homeostasis. Biochemistry 49:3161–3167. https://doi.org/10.1021/bi100136n.
19. Eckhardt TH, Skotnicka D, Kok J, Kuipers OP. 2013. Transcriptional regulation of fatty acid biosynthesis in *Lactococcus lactis*. J Bacteriol 195:1081–1089. https://doi.org/10.1128/JB.02043-12.
20. Faustoferri RC, Hubbard CJ, Santiago B, Buckley AA, Seifert TB, Quivey RG Jr, 2015. Regulation of fatty acid biosynthesis by the global regulator CcpA and the local regulator FabT in *Streptococcus mutans*. Mol Oral Microbiol 30:128–146. https://doi.org/10.1111/omi.12076.
21. Port GC, Vega LA, Nylander AB, Caparon MG. 2014. *Streptococcus pyogenes* polymyxin B-resistant mutants display enhanced ExPortal integrity. J Bacteriol 196:2563–2577. https://doi.org/10.1128/JB.01596-14.
22. Gullett JM, Cuypers MG, Frank MW, White SW, Rock CO. 2019. A fatty acid-binding protein of *Streptococcus pneumoniae* facilitates the acquisition of host polyunsaturated fatty acids. J Biol Chem 294:16416–16428. https://doi.org/10.1074/jbc.RA119.010659.
23. Reithuber E, Nannapaneni P, Rzhepishevska O, Lindgren AEG, Ilchenko O, Normark S, Almqvist F, Henriques-Normark B, Mellroth P. 2020. The bactericidal fatty acid mimetic 2CCA-1 selectively targets pneumococcal extracellular polyunsaturated fatty acid metabolism. mBio 11:e03027-20. https://doi.org/10.1128/mBio.03027-20.
24. Paoletti L, Lu YJ, Schujman GE, de Mendoza D, Rock CO. 2007. Coupling of fatty acid and phospholipid synthesis in *Bacillus subtilis*. J Bacteriol 189:5816–5824. https://doi.org/10.1128/JB.00602-07.
25. Pathania A, Anba-Mondoloni J, Gominet M, Halpern D, Dairou J, Dupont L, Lamberet G, Trieu-Cuot P, Gloux K, Gruss A. 2021. (p)ppGpp/GTP and malonyl-CoA modulate *Staphylococcus aureus* adaptation to FASII antibiotics and provide a basis for synergistic bi-therapy. mBio 12:e03193-20. https://doi.org/10.1128/mBio.03193-20.
26. Dubois-Brissonnet F, Naitali M, Mafu AA, Briandet R. 2011. Induction of fatty acid composition modifications and tolerance to biocides in *Salmonella enterica* serovar Typhimurium by plant-derived terpenes. Appl Environ Microbiol 77:906–910. https://doi.org/10.1128/AEM.01480-10.
27. Juneja VK, Foglia TA, Marmer BS. 1998. Heat resistance and fatty acid composition of *Listeria monocytogenes*: effect of pH, acidulant, and growth temperature. J Food Prot 61:683–687. https://doi.org/10.4315/0362-028X-61.6.683.
28. Dubois-Brissonnet F, Trotier E, Briandet R. 2016. The biofilm lifestyle involves an increase in bacterial membrane saturated fatty acids. Front Microbiol 7:1673. https://doi.org/10.3389/fmicb.2016.01673.
29. Tiwari KB, Gatto C, Wilkinson BJ. 2018. Interrelationships between fatty acid composition, staphyloxanthin content, fluidity, and carbon flow in the *Staphylococcus aureus* membrane. Molecules 23:1201. https://doi.org/10.3390/molecules23051201.
30. Gupta A, Pande A, Sabrin A, Thapa SS, Gioe BW, Grove A. 2019. MarR Family transcription factors from *Burkholderia* species: hidden clues to control of virulence-associated genes. Microbiol Mol Biol Rev 83:e00039-18. https://doi.org/10.1128/MMBR.00039-18.
31. Deochand DK, Grove A. 2017. MarR family transcription factors: dynamic variations on a common scaffold. Crit Rev Biochem Mol Biol 52:595–613. https://doi.org/10.1080/10409238.2017.1344612.
32. Zuo G, Chen ZP, Jiang YL, Zhu Z, Ding C, Zhang Z, Chen Y, Zhou CZ, Li Q. 2019. Structural insights into repression of the Pneumococcal fatty acid synthesis pathway by repressor FabT and co-repressor acyl-ACP. FEBS Lett 593:2730–2741. https://doi.org/10.1002/1873-3468.13534.
33. Bugrysheva J, Froehlich BJ, Freiberg JA, Scott JR. 2011. Serine/threonine protein kinase Stk is required for virulence, stress response, and penicillin tolerance in *Streptococcus pyogenes*. Infect Immun 79:4201–4209. https://doi.org/10.1128/IAI.05360-11.
34. Lu YJ, White SW, Rock CO. 2005. Domain swapping between *Enterococcus faecalis* FabN and FabZ proteins localizes the structural determinants for isomerase activity. J Biol Chem 280:30342–30348. https://doi.org/10.1074/jbc.M504637200.
35. Jerga A, Rock CO. 2009. Acyl-Acyl carrier protein regulates transcription of fatty acid biosynthetic genes via the FabT repressor in *Streptococcus pneumoniae*. J Biol Chem 284:15364–15368. https://doi.org/10.1074/jbc.C109.002410.
36. Zou Q, Dong H, Zhu L, Cronan JE. 2022. The *Enterococcus faecalis* FabT transcription factor regulates fatty acid synthesis in response to exogenous fatty acids. Front Microbiol 13:877582. https://doi.org/10.3389/fmicb.2022.877582.
37. Longo M, De Jode M, Plainvert C, Weckel A, Hua A, Chateau A, Glaser P, Poyart C, Fouet A. 2015. Complete genome sequence of *Streptococcus pyogenes emm28* clinical isolate M28PF1, responsible for a puerperal fever. Genome Announc 3:e00750-15. https://doi.org/10.1128/genomeA.00750-15.
38. Bi H, Zhu L, Wang H, Cronan JE. 2014. Inefficient translation renders the *Enterococcus faecalis* fabK enoyl-acyl carrier protein reductase phenotypically cryptic. J Bacteriol 196:170–179. https://doi.org/10.1128/JB.01148-13.
39. Mohedano ML, Overweg K, de la Fuente A, Reuter M, Altabe S, Mulholland F, de Mendoza D, Lopez P, Wells JM. 2005. Evidence that the essential response regulator YycF in *Streptococcus pneumoniae* modulates expression of fatty acid biosynthesis genes and alters membrane composition. J Bacteriol 187:2357–2367. https://doi.org/10.1128/JB.187.7.2357-2367.2005.
40. Wayne KJ, Li S, Kazmierczak KM, Tsui HC, Winkler ME. 2012. Involvement of WalK (VicK) phosphatase activity in setting WalR (VicR) response regulator phosphorylation level and limiting cross-talk in *Streptococcus pneumoniae* D39 cells. Mol Microbiol 86:645–660. https://doi.org/10.1111/mmi.12006.
41. Mohedano ML, Amblar M, de la Fuente A, Wells JM, Lopez P. 2016. The response regulator YycF inhibits expression of the fatty acid biosynthesis repressor FabT in *Streptococcus pneumoniae*. Front Microbiol 7:1326. https://doi.org/10.3389/fmicb.2016.01326.
42. Devaux L, Sleiman D, Mazzuoli MV, Gominet M, Lanotte P, Trieu-Cuot P, Kaminski PA, Firon A. 2018. Cyclic di-AMP regulation of osmotic homeostasis is essential in Group B *Streptococcus*. PLoS Genet 14:e1007342. https://doi.org/10.1371/journal.pgen.1007342.
43. Di Rienzi SC, Jacobson J, Kennedy EA, Bell ME, Shi Q, Waters JL, Lawrence P, Brenna JT, Britton RA, Walter J, Ley RE. 2018. Resilience of small intestinal beneficial bacteria to the toxicity of soybean oil fatty acids. Elife 7:e32581. https://doi.org/10.7554/eLife.32581.
44. Dramsi S, Bierne H. 2017. Spatial organization of cell wall-anchored proteins at the surface of gram-positive bacteria. Curr Top Microbiol Immunol 404:177–201. https://doi.org/10.1007/82_2016_4.
45. Saito HE, Harp JR, Fozo EM. 2014. Incorporation of exogenous fatty acids protects *Enterococcus faecalis* from membrane-damaging agents. Appl Environ Microbiol 80:6527–6538. https://doi.org/10.1128/AEM.02044-14.
46. Saito HE, Harp JR, Fozo EM. 2018. *Enterococcus faecalis* responds to individual exogenous fatty acids independently of their degree of saturation or chain length. Appl Environ Microbiol 84:e01633-17. https://doi.org/10.1128/AEM.01633-17.
47. Morvan C, Halpern D, Kenanian G, Hays C, Anba-Mondoloni J, Brinster S, Kennedy S, Trieu-Cuot P, Poyart C, Lamberet G, Gloux K, Gruss A. 2016. Environmental fatty acids enable emergence of infectious *Staphylococcus aureus* resistant to FASII-targeted antimicrobials. Nat Commun 7:12944. https://doi.org/10.1038/ncomms12944.
48. Morvan C, Halpern D, Kenanian G, Pathania A, Anba-Mondoloni J, Lamberet G, Gruss A, Gloux K. 2017. The *Staphylococcus aureus* FASII bypass escape route from FASII inhibitors. Biochimie 141:40–46. https://doi.org/10.1016/j.biochi.2017.07.004.
49. Gloux K, Guillemet M, Soler C, Morvan C, Halpern D, Pourcel C, Vu Thien H, Lamberet G, Gruss A. 2017. Clinical relevance of type II fatty acid synthesis bypass in *Staphylococcus aureus*. Antimicrob Agents Chemother 61:e02515-16. https://doi.org/10.1128/AAC.02515-16.
50. Kenanian G, Morvan C, Weckel A, Pathania A, Anba-Mondoloni J, Halpern D, Gaillard M, Solgadi A, Dupont L, Henry C, Poyart C, Fouet A, Lamberet G, Gloux K, Gruss A. 2019. Permissive fatty acid incorporation promotes staphylococcal adaptation to fasii antibiotics in host environments. Cell Rep 29:3974–3982.e4. https://doi.org/10.1016/j.celrep.2019.11.071.

Downloaded from https://journals.asm.org/journal/mmbr on 12 October 2022 by 193.54.110.61.



Clara Lambert is a fourth-year PhD student in Pr. Claire Poyart and Dr. Agnès Fouet's laboratory at Institut Cochin, Paris, France. She received her bachelor's degree in biology from Université Paris Saclay in 2016 and in 2018 her master's in fundamental microbiology from Université Paris Cité in collaboration with Institut Pasteur. She is currently investigating the role of FabT in *Streptococcus pyogenes* invasive infections. She characterizes the link between the deregulation of fatty acid synthesis and the virulence defect in *S. pyogenes*. Using various approaches, her project provides a holistic view of the consequences of FabT mutations on bacterial environmental adaptation. She has expertise in bacterial physiology, omic techniques such as transcriptomic, proteomic, lipidomic and metabolomic, and *in vivo* and *ex vivo* analysis of bacteria-host interaction. She will defend her thesis in December 2022. After graduating, she would like to investigate the importance of the bacterial cell-wall in bacterial adaptation.



Claire Poyart, MD, PhD, studied medicine at the Universities Pierre&Marie Curie and Paris Descartes and her PhD at Institut Pasteur. In 2003, nominated Professor at Hospital Cochin, she heads the Clinical bacteriological laboratory. Since 2006, she heads the National Reference Center for Streptococci and codirects an INSERM Team at the Institut Cochin affiliated to Université Paris Cité. Her research combines clinical and fundamental approaches towards characterizing the virulence factors of group A and B *Streptococcus*. The main fundamental research topics are: surface proteins, environmental adaptation and expression of virulence genes, genetic variability, and virulence. She showed, together with Alexandra Gruss, that fatty acid synthesis is not a suitable antibiotic target for Gram-positive pathogens. As a clinical microbiologist her clinical research aims at the epidemiological characterization of GAS and GBS strains responsible for invasive infections and colonization, the development of diagnostic tools for the detection, and the identification of Gram-positive bacteria.



Alexandra Gruss obtained her PhD in Microbiology from the New York University Medical Center, where she worked on plasmid replication determinants in *Staphylococcus aureus*. She then established her lab at the French National Institute for Agriculture, Food and Environment (INRAE, Jouy en Josas). Her research team identified the recombination "crossover hotspot instigator" motif Chi in various Gram-positive bacteria; it also isolated thermosensitive plasmids currently used for genetic manipulation. Her subsequent research on dairy bacteria uncovered that exogenous heme activated respiratory metabolism, greatly improving lactococcal biomass and stability; this fundamental observation was successfully applied to industrial starter culture production. Fatty acid utilization has been a research focus of authors' labs since 2006. A major finding was that environmental fatty acids, as used by essentially all *Firmicutes*, can overcome antibiotics targeting the fatty acid synthesis (FASII) pathway. A current focus is on combinatorial therapy approaches that block *S. aureus* development.



Agnes Fouet obtained her PhD at the Pasteur Institute, Paris, on the regulation of genes encoding proteins involved in sucrose transport and catabolism in *Bacillus subtilis*. She then moved to Tufts Medical School, Boston, as a post-doc where she studied the relationship between catabolic repression and repression of sporulation initiation in *B. subtilis*. In 1990, she established her group at the Pasteur Institute, where her research focused on surface components and regulation of synthesis of virulence factors in *Bacillus anthracis*. In 2011, she moved to the Institut Cochin, Paris, and initiated an entirely new project, investigating the mechanisms involved in initial steps of *Streptococcus pyogenes* infection. In this context, she uncovered a pivotal role of fatty acid metabolism in *S. pyogenes*-host cell interaction. She collaborates with Alexandra Gruss at the Micalis Institute, Jouy en Josas, France, on fatty acid metabolism in other *Firmicutes*, including *Enterococcus faecalis*.

Downloaded from https://journals.asm.org/journal/mmbr on 12 October 2022 by 193.54.110.61.

JCI The Journal of Clinical Investigation

Streptococcus pyogenes infects human endometrium by limiting the innate immune response

Antonin Weckel, … , Céline Méhats, Agnès Fouet

J Clin Invest. 2021;131(4):e130746. https://doi.org/10.1172/JCI130746.

Research Article | Infectious disease | Microbiology

Graphical abstract

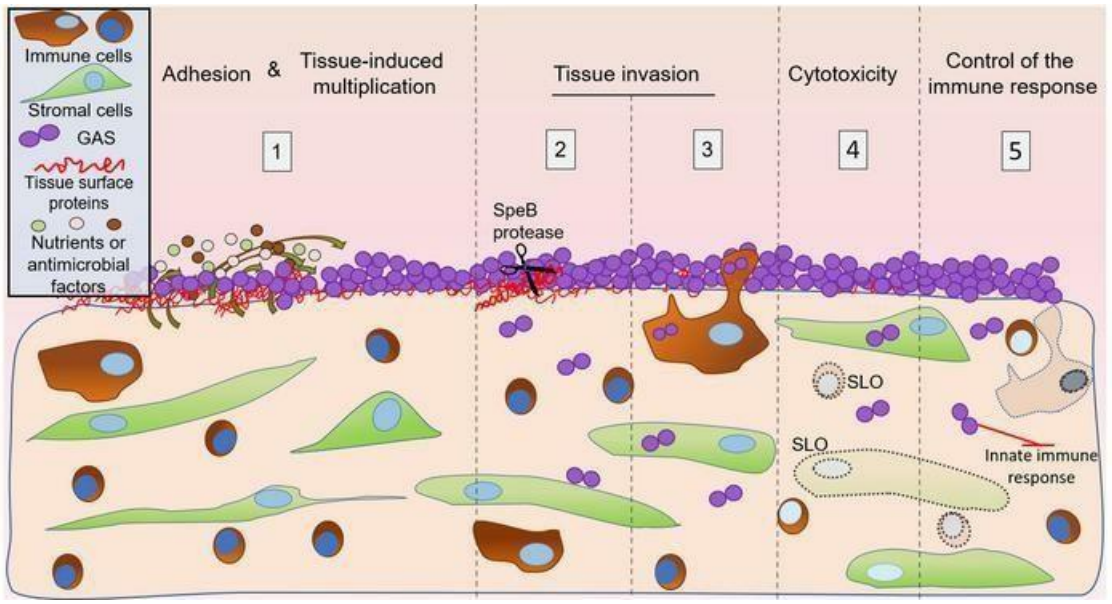

Find the latest version:

https://jci.me/130746/pdf

Streptococcus pyogenes infects human endometrium by limiting the innate immune response

Antonin Weckel,[1,2] Thomas Guilbert,[1] Clara Lambert,[1,2] Céline Plainvert,[1,2,3,4] François Goffinet,[2,5,6] Claire Poyart,[1,2,3,4] Céline Méhats,[1,2] and Agnès Fouet[1,2,3]

[1]Université de Paris, Institut Cochin, INSERM, U1016, CNRS, UMR8104, Paris, France. [2]Département Hospitalo-Universitaire Risk & Pregnancy, Port Royal Maternity, Paris, France. [3]Centre National de Référence des Streptocoques, [4]Hôpitaux Universitaires Paris Centre, Cochin, Assistance Publique Hôpitaux de Paris, [5]Faculté de Médecine, Université Paris Descartes, and [6]Service de Gynécologie Obstétrique I, Maternité Port Royal, Assistance Publique-Hôpitaux de Paris, Paris, France.

Group A *Streptococcus* (GAS), a Gram-positive human-specific pathogen, yields 517,000 deaths annually worldwide, including 163,000 due to invasive infections and among them puerperal fever. Before efficient prophylactic measures were introduced, the mortality rate for mothers during childbirth was approximately 10%; puerperal fever still accounts for over 75,000 maternal deaths annually. Yet, little is known regarding the factors and mechanisms of GAS invasion and establishment in postpartum infection. We characterized the early steps of infection in an ex vivo infection model of the human decidua, the puerperal fever portal of entry. Coordinate analysis of GAS behavior and the immune response led us to demonstrate that (a) GAS growth was stimulated by tissue products; (b) GAS invaded tissue and killed approximately 50% of host cells within 2 hours, and these processes required SpeB protease and streptolysin O (SLO) activities, respectively; and (c) GAS impaired the tissue immune response. Immune impairment occurred both at the RNA level, with only partial induction of the innate immune response, and protein level, in an SLO- and SpeB-dependent manner. Our study indicates that efficient GAS invasion of the decidua and the restricted host immune response favored its propensity to develop rapid invasive infections in a gynecological-obstetrical context.

Introduction

Puerperal fever currently accounts for more than 75,000 maternal deaths annually. The Gram-positive human-specific pathogen *Streptococcus pyogenes*, also known as group A *Streptococcus* (GAS), is responsible for the most severe forms of infection (1). Between 2010 and 2016, GAS was responsible for over 50 and 100 postpartum infections per 100,000 persons per year in the United States and the United Kingdom, respectively (2, 3). In France in 2017–2018, every year an average of 60% of GAS invasive infections occurred in the gyneco-obstetrical sphere for women between 18 and 40 years of age. In addition to puerperal fever, GAS causes a wide range of infections, from noninvasive infections, such as pharyngitis and impetigo, to invasive infections, such as necrotizing fasciitis, bacteremia, and streptococcic toxic shock syndrome, altogether responsible for 163,000 deaths annually (4).

GAS is genetically diverse (5). Strain genotyping relies on the sequence of the 5′ end of the *emm* gene and more than 200 *emm* types exist (6). *emm28* strains are associated with obstetrical and gynecological infections and the *emm28* type is among the 3 most prevalent *emm* types involved in invasive infections in Europe (7–9). Virulence factors contributing to invasive diseases, including the extracellular cysteine protease SpeB and cytotoxin streptolysin O (SLO), have been described in vitro and confirmed in vivo in animal models of infection (10–12). SpeB cleaves many host molecules including matrix proteins; its in vivo importance has been inferred from its prevalence and demonstrated by in vivo experiments (13–15). SLO, in addition to being a pore-forming toxin, facilitates the entry of the NAD-glycohydrolase into eukaryotic cells and together these toxins contribute to cell lysis and to GAS pathogenesis (16, 17).

In contrast with commensals or other pathogens, GAS colonizes only rarely the vagina of healthy individuals (0.03%; ref. 18). Yet, before the introduction of efficient hygienic prophylactic measures, up to 10% of postpartum women died of puerperal fever. Furthermore, half of the cases of GAS-related puerperal fever occur within the first 2 days postpartum, with rapid progression to severe sepsis (19). We hypothesized that GAS efficiently and promptly infects the decidua, which is the mucosal uterine lining during pregnancy. This tissue is composed of roughly 60% endometrial decidualized stromal cells and 40% resident leucocytes (20). The immunological status of the decidua at the time of term birth is unique as compared with earlier terms, with higher abundance of T cells, macrophages, and dendritic cells and a decline in the NK cell number (20, 21). We recently showed that GAS readily adheres to primary human decidual stromal cells (22). However, to our knowledge, the early steps of human decidua infection by GAS or more generally, of GAS human tissue invasion, have not been characterized.

The current model describing the early steps of GAS invasive infections suggests adhesion to host tissue, growth, and invasion of the tissue within 24 hours postinfection (hpi) (23). These steps

Authorship note: CM and AF contributed equally to this work.
Conflict of interest: The authors have declared that no conflict of interest exists.
Copyright: © 2021, American Society for Clinical Investigation.
Submitted: June 3, 2019; **Accepted:** December 10, 2020; **Published:** February 15, 2021.
Reference information: *J Clin Invest*. 2021;131(4):e130746.
https://doi.org/10.1172/JCI130746.

are followed by resistance to immune responses, tissue destruction, and systemic GAS infection (24). The observations of necrotizing fasciitis biopsy support the clinical relevance of these results (23). However, questions remain regarding the events occurring during the first hours of tissue infection, particularly when GAS reaches nonepithelial tissues such as the decidua.

In this work, we investigated the early events of GAS infection, and identified factors leading to the rapid progression of infection. To that end, we developed an integrated experimental model that simultaneously studies diverse aspects of the infection including the bacterial outcome and the host immune response. We show that GAS multiplies at the decidual surface and benefits from tissue-secreted products to do so, that it invades the tissue in the first 8 hours of infection, and that it kills half of the cells within 2 hours. SpeB and SLO, 2 major virulence factors, are implicated in these early infection steps. The host tissue immune response is restricted during these first infection steps.

Results

GAS grows on human decidua during the early steps of infection. We used 2 complementary approaches to follow tissue colonization and invasion: static and flow conditions (Figure 1). Human decidual explants were infected within hours of surgery with a wild-type (WT) isolate or its derivative expressing GFP (GFP-WT). When static conditions were used fixation was carried out at different time points; flow conditions were used for live microscopy. The decidua is composed of a fibronectin layer that covers the cells which are embedded in an extracellular matrix containing type IV collagen (Figure 1A, Supplemental Figure 1, and Supplemental Figure 3B; supplemental material available online with this article; https://doi.org/10.1172/JCI130746DS1). GAS efficiently adheres to the tissue surface. Furthermore, in flow and static conditions, GAS-covered surface or the thickness of bacterial microcolonies increased in a time-dependent fashion, indicating the successful tissue surface colonization by GAS (11 out of 11 tissues) (Figure 1, Supplemental Figure 2, and Supplemental Table 1). GAS was observed to cover the entire tissue surface (Figure 1C and Supplemental Video 1). We precisely quantified GAS multiplication at the tissue surface during the first hours after infection in flow conditions (Figure 1D and Supplemental Table 1). GAS grew exponentially at the tissue surface, with doubling of the colonized surface every 82 minutes (Figure 1, E and F, and Supplemental Video 2). Determination of the thickness of bacterial microcolonies further showed that the mean value doubled in 4 hours, reaching a mean value of 4.2 μm (Figure 1, G and H). However, GAS thickness was locally heterogeneous, and at 6 hpi reached 10 μm in some hot spots and up to 16 μm at 24 hpi (Figure 1G and data not shown). Yet, the overall thickness increase was similar in all tissue samples considered (Figure 1, G and H). Hence, growth occurs in all 3 dimensions and GAS doubling time in contact with the decidua is close to 60 minutes; this accounts for GAS's robust capacity to infect human decidua.

To analyze if diffusible host factors promoted GAS growth, we compared GAS growth in RPMI medium and in tissue-conditioned supernatants from 8 samples (Supplemental Table 1 and Figure 1I). Whereas GAS does not multiply in RPMI, it multiplied in some conditioned supernatants (Supplemental Table 1 and Figure 1I). In contrast with the tissues, not all conditioned supernatants elicited growth; GAS grew in 5 out of the 8 samples. However, both tissues with supernatants that did not elicit growth and for which surface colonization was analyzed proved to support GAS multiplication (Supplemental Table 1). Since women were excluded if prescription antibiotics were used during the 2 weeks preceding delivery, except for preoperatively administered cephalosporin, and tissues were all similarly extensively rinsed in PBS, we excluded a role for antibiotic interference in GAS growth in supernatants. We therefore considered that nutrients secreted by uninfected tissues and bactericidal molecules might impact GAS growth. Antimicrobial peptides (AMPs), including human β defensins (hBD1 and -2) and LL-37, were previously detected in the decidua during pregnancy (25). To determine whether their presence could explain GAS growth limitation, we measured the concentrations of these AMPs in conditioned supernatants (Figure 1J). No significant differences were detected between tissue samples, indicating that AMP concentrations are not predictive of GAS growth potential in tissue supernatants (Figure 1I). That GAS multiplies on all tested tissues but only in some conditioned supernatants needs to be further investigated.

GAS invades human decidua ex vivo. We then characterized GAS penetration of the tissue. Although GAS is nonmotile, bacteria were found below the tissue surface as soon as 4 hpi in static conditions (Supplemental Figure 3A). We quantified invasion events using automated image analysis (Figure 2, A and B, and Supplemental Figure 3B). As soon as 4 hpi, we observed an average of 600 invasion events per mm^2; this corresponds to approximately 2 invading chains per 1000 surface chains. Furthermore, there were 3 times more intratissular bacteria at 8 hpi than at 4 hpi (Figure 2C). At 16 hpi, GAS were observed in direct contact with and inside stromal cells (Supplemental Figure 3C). We hypothesized that GAS invasion is an active process that is at least partly due to tissue degradation, especially fibronectin degradation, which is the upper layer of the tissue (Figure 1). SpeB, the major GAS protease, which is expressed in vivo and degrades fibronectin (26), may be involved in tissue penetration. To test this hypothesis, we infected decidua with either the WT or a ΔSpeB strain. At 4 hpi, the efficiency of tissue invasion of the ΔSpeB strain was approximately 50% of that of the WT strain, indicating that SpeB or products derived from SpeB activity contribute to the initial tissue invasion step (Figure 2C).

Another potential source of bacterial invasion is internalization into host motile cells. We observed phagocytosis of GAS by immune cells, presumably macrophages given the fairly large size of the cells, 15 minutes after infection in flow conditions. Intracellular bacteria were localized 6 μm below the tissue surface for at least 4 hpi (Figure 2, D and E, Supplemental Figure 3D), indicating that GAS may invade the decidua as intracellular bacteria. Our results indicate that GAS can rapidly and actively invade the decidua and may exploit survival in decidual immune cells.

GAS induces cell death. GAS strains are cytotoxic to immune or epithelial cells in vitro. The factors responsible for toxicity may vary with GAS *emm* type (27). However, whether GAS cytotoxicity is involved in the early infection steps, particularly in decidua invasion, remains largely undocumented. We thus analyzed the consequences of ex vivo GAS infection of the human decidua on the physical state of cells in static conditions. As early as 4 hpi, we observed cell blebbing and dying immune cells, as indicated

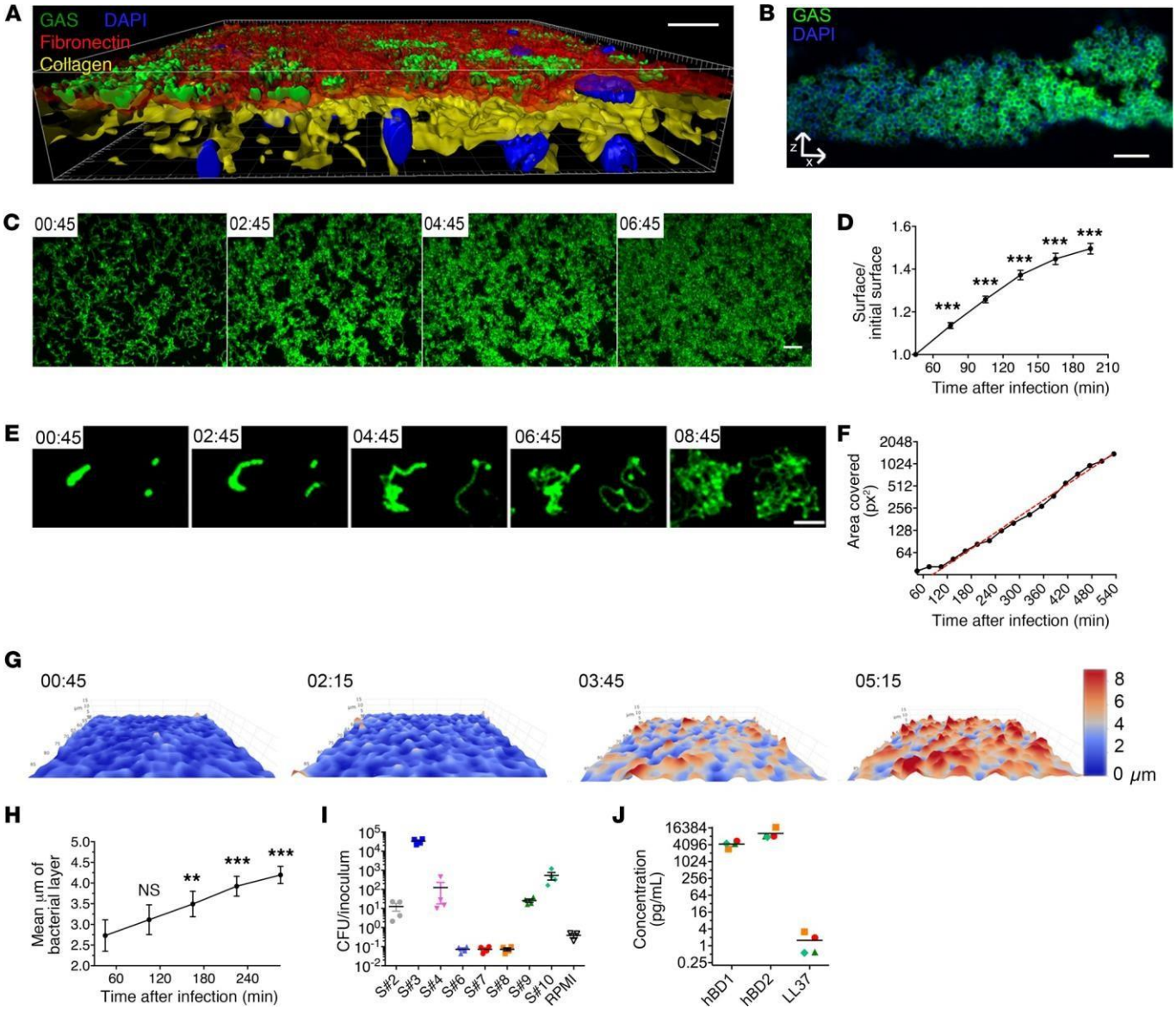

Figure 1. GAS adheres to the decidua and grows on it using tissue-secreted products. (**A**) Imaris 3D representation of a tissue infected 16 hours and imaged en face. Fibronectin, red; type IV collagen, yellow; GFP-GAS, green; DAPI, blue. Scale bar: 20 μm. Magnification: ×40. (**B**) Immunofluorescence of a paraffin-embedded tissue transverse slice (24 hpi). Anti-GAS, green; DAPI, blue. Scale bar: 10 μm. Magnification: ×100. (**C** and **E**) *z*-Max intensity projections of GFP signals from live en face acquisition images of GFP-WT at the tissue surface, at indicated time points (hr:min). Scale bars: 10 μm (**C**) and 20 μm (**E**). Magnification: ×25. (**D**) Ratio over time of the area covered by WT GFP-GAS signal area in tissues from 5 samples including those in **C**. Mean values of 3 to 11 fields for each of the 5 tissues are plotted. (**F**) Quantification of the surface covered by GFP-GAS from the image in **E**. Red dotted line, exponential curve fitted starting at 105 minutes; R^2 = 0.9948. (**G**) 3D surface heatmap of the bacterial layer thickness at different time points (hr:min) (live imaging). The *x*, *y*, and *z* axes are scaled, color code in micrometers. Image size: 303 × 190 μm. (**H**) Quantification of bacterial layer mean thickness; mean values of 2 to 13 fields for each of 5 tissues are plotted. (**I**) Multiplication factor after GAS incubation for 8 hours in tissue-conditioned medium or RPMI. S# indicates the sample number. (**J**) Basal levels of accumulation of the indicated antimicrobial peptide in the supernatant of noninfected decidual tissues 8 hours after addition of fresh RPMI. Symbols are the same as in panel **I**. For all panels, error bars are standard error of the mean. $^{**}P < 0.005$, $^{***}P < 0.001$ by 2-way ANOVA at the initial time points (**D** and **H**).

by $CD45^+$ membranes and DAPI staining (Figure 3A and Supplemental Video 3). At 16 hpi, a TUNEL assay indicated the presence of nuclei with altered morphology and DNA damage (Figure 3B); moreover, all cell types, immune ($CD45^+$) and nonimmune ($CD45^-$), were damaged (Figure 3C). GAS-induced cytotoxicity increased with time after infection; 27% and 57% of cells were TUNEL positive at 2 hpi and 8 hpi, respectively, compared with 7% and 11% without infection (Figure 3, D and E). To determine if cell death was induced by a GAS-secreted factor, we measured cytotoxicity when bacteria were physically separated from the tissue via a Transwell insert (Figure 3E). In these conditions, GAS was still able to induce 21% and 37% of cell death at 2 hpi and 8 hpi, respectively, which demonstrates that GAS-secreted factors induce cell death without bacterial contact of host cells (at a

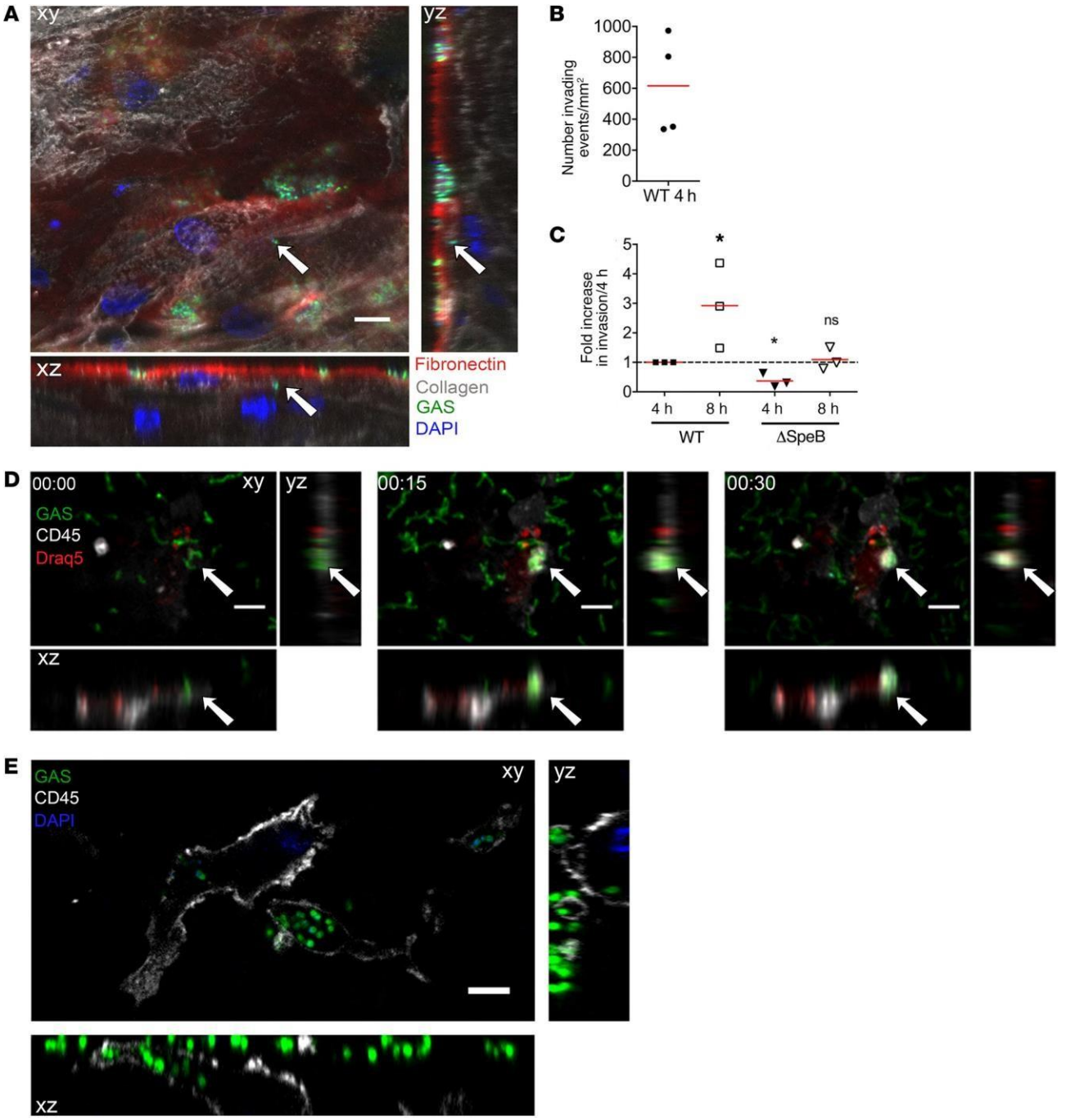

Figure 2. GAS actively invades the decidual tissue. (**A**) Orthogonal view of a tissue 16 hpi, static conditions; see also Supplemental Figure 3B. Arrows indicate an invading particle. Fibronectin, red; type IV collagen, gray; GAS, green; DAPI, blue. Scale bar: 10 μm. Magnification: ×40. (**B**) Mean number of invading events per mm² at 4 hpi under static conditions with the GFP-WT strain calculated using high-throughput image analysis. Four samples are shown. (**C**) Ratio of GFP-WT and GFP-ΔSpeB invading events 4 and 8 hpi under static conditions. *P < 0.05 by 1-sample t test vs. the WT at 4 hpi for WT 8 hpi and ΔSpeB 4 hpi, and vs. ΔSpeB 4 hpi for ΔSpeB 8 hpi (n = 3). (**D**) Time-lapse (hr:min), flow conditions, of an immune cell phagocytosing GAS in situ, with orthogonal view. Anti-CD45 (immune cells), gray; GAS, green; DRAQ5 (DNA), red. White arrows indicate the localization of the phagocytosis event. Scale bar: 10 μm. Magnification: ×25. (**E**) Orthogonal views of GFP-WT bacteria inside the tissue and within an immune cell; image taken 6 μm under the tissue surface 3 hpi under flow conditions; see also Supplemental Figure 3D. Anti-CD45, gray; bacteria, green; DAPI, blue. Scale bar: 5 μm. Magnification: ×100.

distance >250 μm). As these values are lower than when bacteria are in contact with tissues, it is possible that direct contact or proximity increases cytotoxicity efficiency.

SLO is a pore-forming toxin described to induce cell death (28, 29). We tested to what extent SLO was involved in GAS cytotoxicity in primary decidualstromal cells, and in whole decidua, at 2 and 4 hpi (Figure3, F and G). In primary decidual stromal cells at 4 hpi, the WT and isogenic revertant (BTSLO) strains induced 60% and 54% cytotoxicity. In striking contrast, the isogenic SLO-deleted mutant strain (ΔSLO) induced only 14% cytotoxicity (Figure 3F). In comparison,

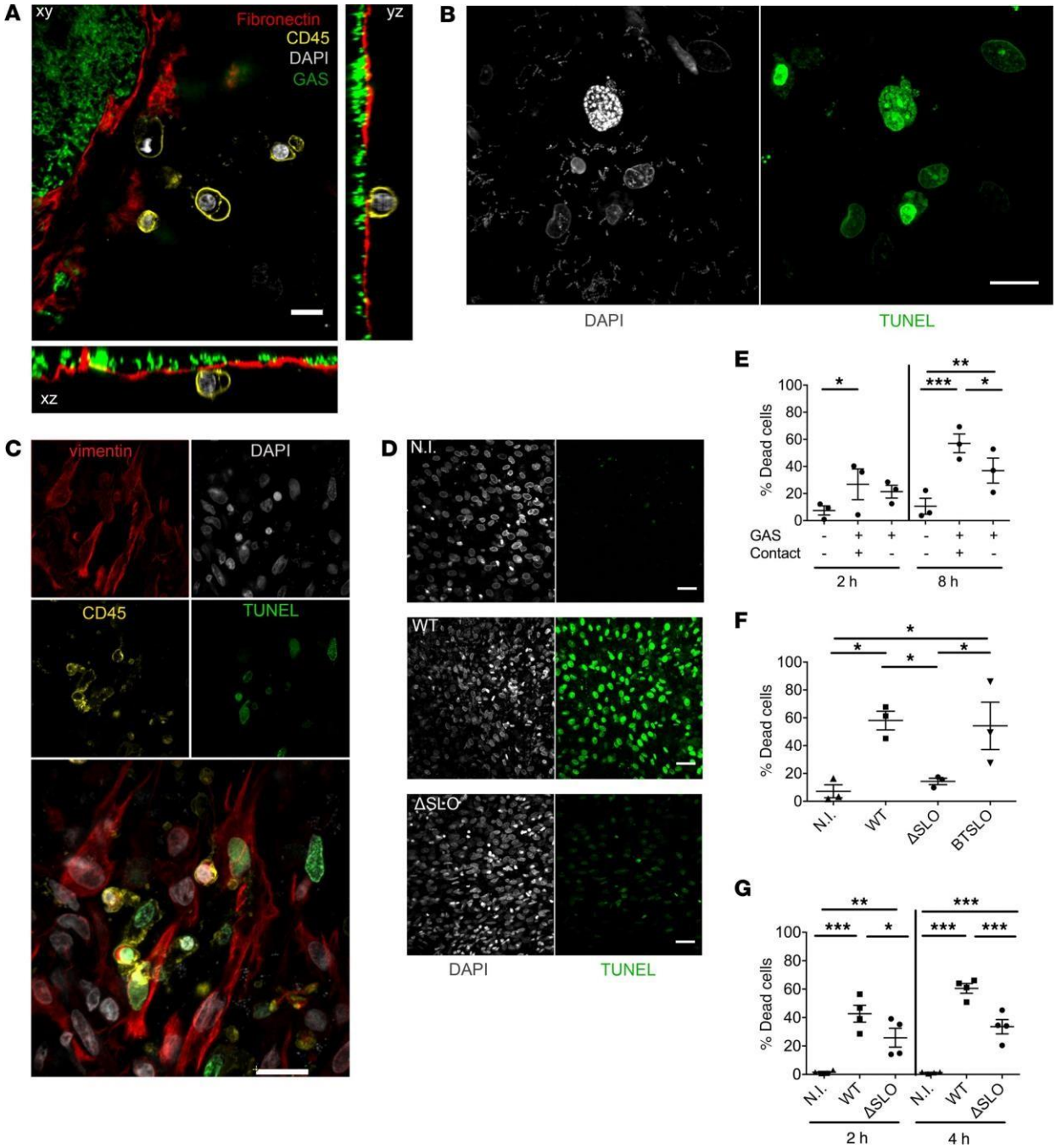

Figure 3. GAS induces stromal and immune cell death via processes involving SLO and other secreted factors. (**A**) Orthogonal view of a sample 5 hpi under static conditions prestained with anti-fibronectin (red), anti-CD45 (yellow), WT-GFP bacteria (green), and DAPI (gray). Scale bar: 10 μm. Magnification: ×40. (**B**) Immunofluorescence of the decidua 16 hpi under static conditions. DAPI, gray; TUNEL, green. Scale bar: 10 μm. Magnification: ×63. (**C**) Immunofluorescence of a sample 16 hpi under static conditions. Stromal cells are vimentin$^+$CD45$^-$ and immune cells are CD45$^+$. Vimentin, red; DAPI, gray; CD45, yellow; TUNEL, green. Scale bar: 10 μm. Magnification: ×40. (**D**) Immunofluorescence of a sample 4 hpi under static conditions with the indicated strains. N.I., not infected. DAPI, gray; TUNEL, green. Scale bar: 40 μm. Magnification: ×20. (**E**–**G**) Quantification of cytotoxicity by determination of the percentage of dead cells (**E**) on decidua with 3 samples, in the absence, contact (+), or the presence, contact (−), of a Transwell insert at indicated times; (**F**) on primary decidual cells from 3 different samples with indicated strains 4 hpi; and (**G**) on decidua with 4 samples with indicated strains, at indicated times. *P < 0.05; **P < 0.005; ***P < 0.001 by 2-way ANOVA with Bonferroni's post hoc test (**E** and **G**) or paired 1-way ANOVA (**F**).

cytotoxicity in control noninfected cells was 7%. These results confirm the involvement of SLO in the GAS cytotoxic effect. In decidual tissue, the ΔSLO strain was approximately 50% as cytotoxic as the WT strain (25% vs. 43% at 2 hpi, and 33% vs. 60% at 4 hpi, respectively; Figure 3G). However, at both time points, the ΔSLO strain still induced significant cytotoxicity compared with the noninfected control (1.6% and 1.4% at 2 and 4 hpi, respectively), indicating that GAS produces cytotoxic molecules in addition to SLO. In conclusion, GAS yields dramatic cell damages within a few hours of infection of the decidua, and SLO has an important role in toxicity.

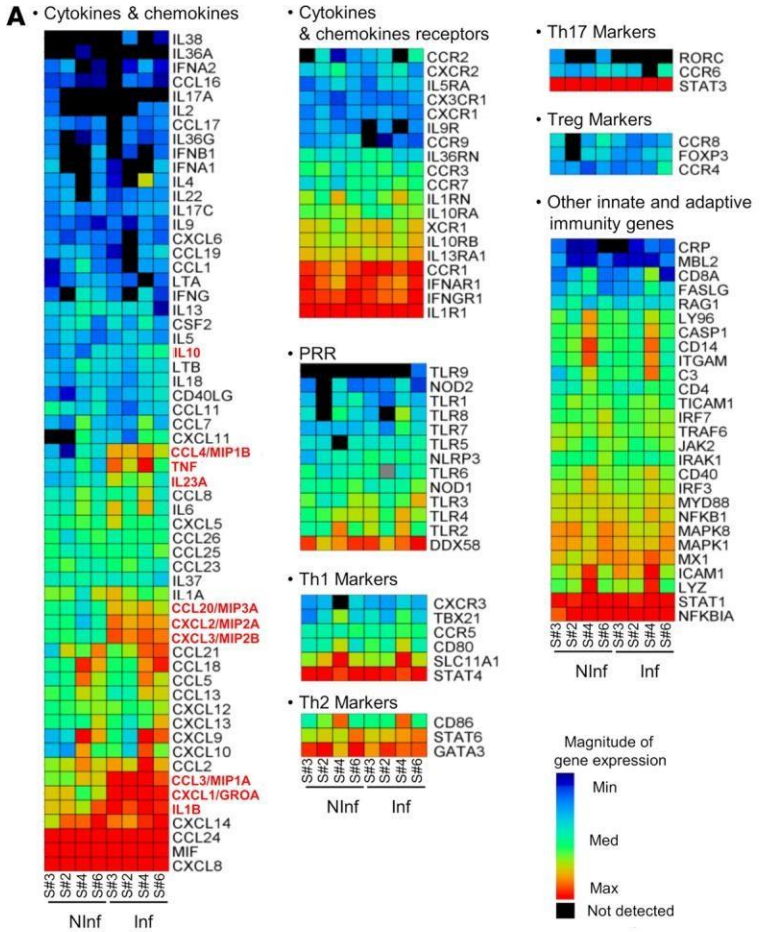

Figure 4. Host cytokine responses to GAS infection. (**A**) Heatmap of the results from the qRT-PCR screening using Qiagen RT^2 Profiler PCR Arrays "Inflammatory cytokines and receptors" and "Human innate & adaptive response" on 4 samples, noninfected (NInf) or infected 8 hours under static conditions with the WT strain (Inf). Cytokines significantly overexpressed in the infected compared with noninfected condition are shown in red. (**B** and **C**) Fold-change variation of the expression of the immune-related genes (**B**) 4 hpi (left) and 8 hpi (right) compared with the noninfected expression. $^aP < 0.05$ compared with noninfected by 1-way Mann-Whitney *U* test. (**C**) The concentration of the indicated cytokines compared with the noninfected condition (left, 4 hpi; right, 8 hpi) from 4 different samples. $^aP < 0.05$ compared with noninfected; $^bP < 0.05$ compared with WT; Friedman's test with Dunn's post hoc multiple-comparison test. Axes in **B** and **C** are $\log_2$ transformed. Symbols are as in Figure 1I. The infecting strain, WT, ΔSLO, or ΔSpeB is indicated below the *x* axis. Means are indicated with black lines. Dotted lines correspond to a ratio of 1.

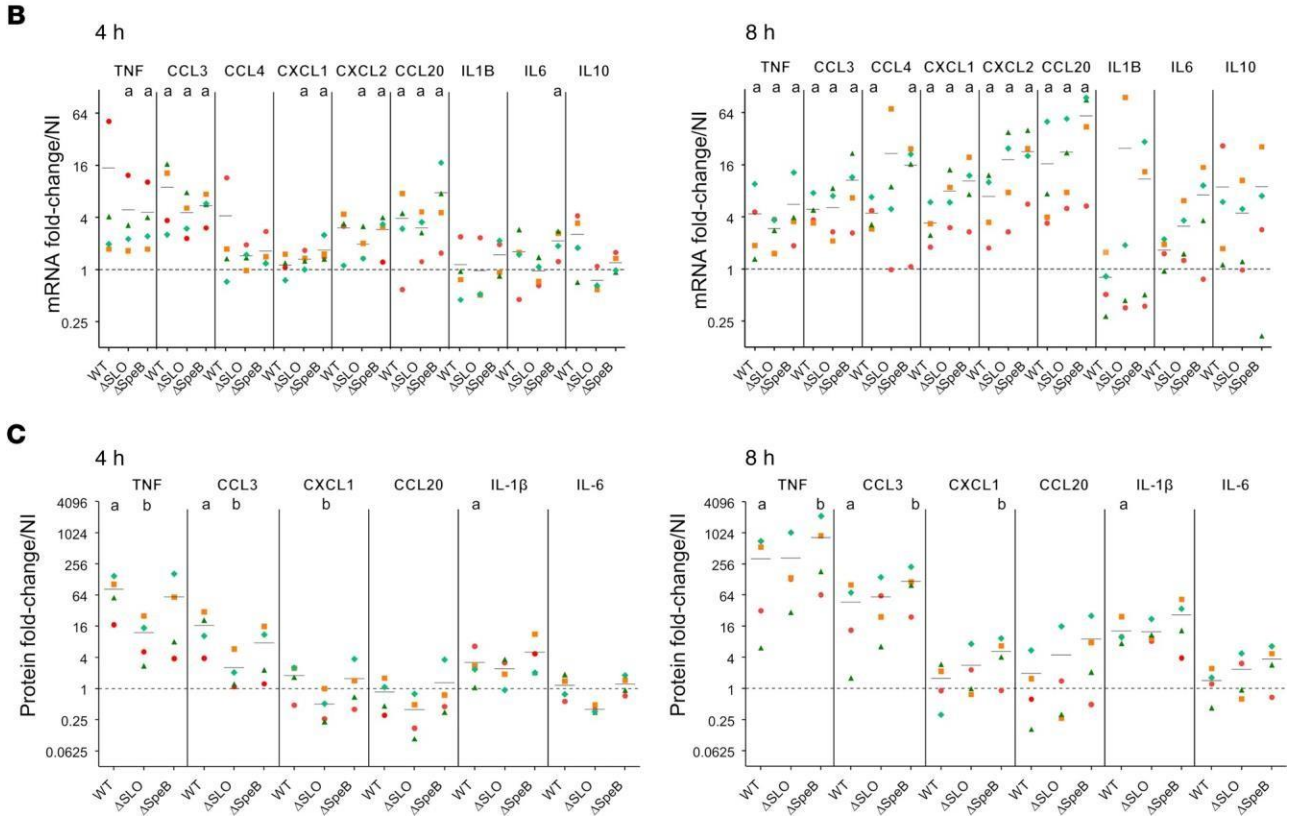

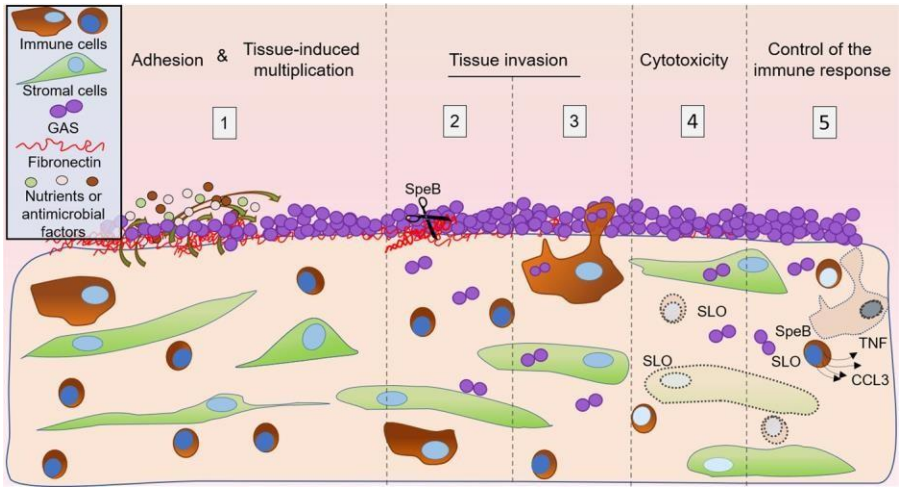

Figure 5. Schematic representation of the initial steps of decidual invasive infection by GAS. The successive steps are represented. 1: The decidua secretes nutrients and antimicrobial peptides (Figure 1I), promoting GAS multiplication at the tissue surface (Figure 1, C–H). 2: GAS invades the tissue in, among others, an SpeB-dependent manner, most likely through its capacity to degrade fibronectin (Figure 2, A–C). 3: GAS is phagocytosed at the surface and is present inside decidual immune cells at least 6 μm below the surface and 4 hpi, suggesting GAS may use immune decidual cells to invade the decidua (Figure 2, D and E). 4: GAS induces the death of decidual stromal and immune cells in an SLO-dependent mechanism (Figure 3). 5: GAS limits the innate immune response, impairing the response amplification (Figure 4). Decidual immune and stromal cells are represented as observed in the tissue; curved arrows = nutrients, AMP, or growth signaling factor secretion and diffusion; dotted line objects = damaged cells; dotted arrows = cytokine secretion.

GAS limits the tissue inflammatory response. Efficient GAS multiplication in immune decidual cells led us to question whether the host mounted an inflammatory response to GAS. Expression was first analyzed for 133 unique immune genes related to inflammatory cytokines and receptors, and human innate and adaptive response pathways, using 2 commercial RT-PCR arrays, in noninfected decidua. This analysis provided the steady-state levels of immune response factors (Figure 4). As expected, the majority of the genes tested showed low to moderate expression, as compared with housekeeping genes (Figure 4A, Supplemental Table 1, and ref. 30). Infection with GAS led to the induction of only 10 genes at 8 hpi. Nine genes encode cytokines and chemokines related to acute inflammatory response, including TNF, CXCL1, CXCL2, and IL-23A that are characteristic of an immediate-early-gene primary response (Figure 4A, Supplemental Table 2, and refs. 31, 32). The tenth gene encodes the antiinflammatory cytokine IL-10. This expression pattern suggested that either ex vivo decidua is unable to mount an immune response or that GAS infection restrains this response. The low induction level of GAS contrasts with much higher induction levels by group B *Streptococcus* (GBS) in a similar setup of infection (33). GBS infection modified the expression of 32 out of these 133 genes, and furthermore, the most activated genes compared with uninfected tissue are related to cellular response to cytokine stimulus (33). This supports the capacity of the decidua to elicit an immune response. Notably, in contrast with GBS, GAS infection fails to induce certain secondary response genes, such as NFKB1, CCR7, CD80, and ICAM1. This comparison indicates that GAS may impair the robust immune response in tissue that is elicited by GBS, a *Streptococcus* that elicits milder endometritis (34). Altogether, these results show that GAS specifically induces a low and limited inflammation at 8 hpi.

We performed qRT-PCR on 4 other uninfected and GAS-infected tissues at 4 hpi and 8 hpi to confirm the changes in gene expression. Expression was followed for 8 of the 10 genes overexpressed after GAS infection, as well as IL-6, the classical proinflammatory cytokine, the expression of which did not appear modified in the arrays (Figure 4B and Supplemental Figure 4A). Overexpression of 2 genes, encoding CCL3 and CCL20, occurred as soon as 4 hpi; at 8 hpi the expression of TNF, CCL4, CXCL1, and CXCL2 was also increased (Figure 4B). Overexpression of IL-10 was not statistically different in this set of tissues. However, an analysis of the 8 samples together indicated a statistically different overexpression of IL-10 (fold-change 5.45 ± 3.07, $P = 0.0156$). This suggests that IL-10 is induced by GAS infection. Notably, qRT-PCR assays confirmed that IL-6 is not significantly overexpressed after GAS infection, in contrast with its observed overexpression with GBS at 8 hpi (Supplemental Table 2 and ref. 33).

As GAS also modulates the in vitro accumulation of cytokines at the protein level (35–37), we asked whether the overexpression of 6 cytokine genes correlated with an increase in protein concentrations in tissue supernatants (Figure 4C and Supplemental Figure 4B). The basal level of accumulation of the 6 cytokines in the uninfected tissues 4 hpi and 8 hpi had the same pattern, independently of the sample, with high concentrations of IL-6 and CXCL2 (Supplemental Figure 4B and Supplemental Tables 3 and 4), known to be highly expressed in different subsets of decidual cells during pregnancy (30). After infection, the levels of TNF, CCL3, and IL-1β were higher as early as 4 hpi and further increased at 8 hpi (Figure 4C and Supplemental Tables 3 and 4). However, overexpression of the CXCL2 gene at 4 hpi and of the CXCL2 and CCL20 genes at 8 hpi (Figure 4B) were not paralleled by an increase in the amounts of these 2 proteins (Figure 4C), suggesting that GAS may control the immune response at a posttranscriptional level.

Modulation of the immune response might be a key step during GAS invasive infection, and appears to be controlled on transcriptional and posttranscriptional levels. We assessed the potential roles of SLO and SpeB on that limitation in the decidua (35, 38). Transcriptional activation of the tested genes was similar in the WT strain and the ΔSLO and ΔSpeB mutant strains (Figure 4B). Remarkably, accumulation of some cytokines was different after infection with the mutant strains. The SLO-deficient strain showed reduced accumulation of TNF, CCL3, CXCL2, and IL-6 at 4 hpi (Figure 4C). The ΔSpeB mutant induced a cytokine accumulation comparable to that of the WT at 4 hpi. However, accumulation of TNF, CCL3, and CXCL2 was significantly greater in the ΔSpeB- than in the WT-infected condition at 8 hpi (Figure 4C). This indicates that SLO is, at least in part, responsible for

the accumulation of these cytokines, whereas the production of SpeB, directly or indirectly, increases GAS's capacity to inhibit cytokine accumulation.

These results suggest that the moderate accumulation of cytokines after GAS infection is the result of a fine balance between pro- and antiinflammatory responses induced by GAS. Also, during GAS's efficient colonization and invasion of the human decidua, SLO accentuates the inflammatory response while SpeB attenuates it.

Discussion

GAS is established as the major etiological agent of puerperal fever and maternal death. A key element of GAS infection is the rapid onset, i.e., development of fever within 2 days following delivery. To bypass the roadblock brought by GAS human specificity, studies of GAS noninvasive and invasive infections, and host responses during *emm1*-elicited pharyngitis were conducted in nonhuman primates (14, 39–42). However, these models do not permit direct visualization of colonization nor of early invasion steps. We overcame this limitation by using the original conjunction of ex vivo infection of human decidua, bacterial genetic manipulation, state-of-the-art imaging, and immune response analyses. Our main findings are that (a) GAS adheres and grows on human decidual tissue within the first hours of infection; (b) GAS actively kills cells and invades this tissue, a process that requires SLO and SpeB, respectively; and (c) GAS limits the host immune response (Figure 5). The ex vivo setup developed here enabled us to dissect GAS's capacity to establish decidua infection in real time and to simulate an in vivo situation.

We observed significant GAS growth; to our knowledge, our study provides the first estimate of GAS doubling time in contact with a human tissue, roughly 60 minutes; it corresponds to a 10^7 multiplication in 24 hours, and could account for the rapidity with which puerperal fever occurs. Our results indicate that the decidua secretes nutrients and/or growth signaling molecules (Figure 5). The secreted nutrient(s)/growth signal(s) may be numerous. That in some cases GAS grows on a tissue but not in the corresponding conditioned supernatant suggests that compounds may be secreted in response to infection or that cell lysis releases nutrients. Also, growth factors are present in several conditioned supernatants and are most likely not asparagine, which is used by GAS for sensing and proliferation (43). In our study, the 15 amino acids for which GAS is auxotrophic are supplied in the medium (44). Also, the described mechanism required bacteria–host cell contact that is absent when preparing conditioned supernatants. Furthermore, GAS grows on all tissues and some conditioned supernatants and dies in other supernatants, suggesting that secreted nutrients and/or bactericidal products may differ between individuals, even before infection. A difference in quantities of the human defensins or AMPs did not explain a difference in growth. Indeed, hBD1 and hBD2 concentrations were identical in all tissues. As for LL-37, its concentration varied between individuals, but this would probably have few consequences for GAS killing since SpeB inactivates LL-37 at the bacterial surface, representing a resistance mechanism (45).

Invasion initiation on human decidua by GAS has not been previously documented to the best of our knowledge (Figure 5). Our findings show that factors produced by GAS actively promote its penetration into human tissue. SpeB has broad proteolytic activity, including the degradation of extracellular matrix proteins; its role in tissue invasion may be linked to this capacity (13). Yet, considering the pleiotropic effects of the absence of SpeB on the GAS surfactome and on GAS virulence mechanisms (13), including the modified SLO production in the ΔSpeB strain, our data do not exclude a role for other virulence factors in the decreased invasion of the ΔSpeB mutant strain. As the decidua parietalis is not covered by epithelial cells, bacteria that cross the extracellular matrix are in direct contact with stromal and immune cells, among which neutrophils are scarce (46). GAS at the cell surface readily invaded phagocytic cells in the first minutes of infection and were still present at 4 hpi (Figure 5). GAS-charged phagocytes may facilitate penetration of decidua in agreement with previous reports (47–49).

GAS induces the death of about half the stromal and immune cells in the decidua (Figure 5). The ΔSLO mutant strain is less cytotoxic than the WT strain, supporting in vitro–obtained conclusions (50). Moreover, the ΔSLO mutant strain still induced cell death, suggesting the cytotoxic action of other GAS-secreted products, such as streptolysin S (51). Hence, GAS cytotoxicity could account for the failure of cells to clear GAS infection (52).

Dense macrophage and neutrophil infiltrations are observed during established GAS severe invasive soft tissue infections in humans (48), which would be absent in ex vivo infection models (52). However, as seen upon GBS infection, such a setup does allow assessment of IL-6 and CXCL8 production by tissue cells, which attracts neutrophils (53). The ex vivo setup is thus a key readout for the in vivo situation. In our study, GAS jeopardized the upregulation of inflammatory mediators for neutrophil and macrophage recruitment (Figure 5). Also, the GAS-specific concomitant absence of signaling mediators, especially from the NF-κB family, indicates that GAS limits the decidua innate response, including the response amplification. Our results regarding GAS's ability to prevent the activation of the immune response support and expand the conclusion that cytokine production is decreased during an experimental pharyngeal infection of nonhuman primates (40). GAS is less common than GBS in the female reproductive tract, but typically causes more severe maternal infection. In a comparable study, GBS did not readily cross healthy-term maternal-fetal membranes (54). Altogether, these data indicate that limited inflammation may favor GAS infection initiation by delaying or decreasing the recruitment of immune cells. These responses may account for the GAS–puerperal fever association.

The integrated model, comprising an in situ setup and multiple analyses developed in this study, offers a valuable tool to study bacterial tissue invasion and toxicity, which is applicable to various invasive pathogens and tissue types. Other GAS virulence factors implicated via in vitro studies in nonimmune cell entry, phagocytosis, and inflammation modulation could be tested by our holistic approach (13, 24). Transposon libraries could also be screened as a means of identifying novel colonization or invasion factors.

In conclusion, GAS actively multiplies, hides intracellularly, and diverts the host response during the very first hours following decidua infection. This rapidity may account both for the particu-

lar capacity of GAS, despite its quasi-absence from the female genital tract microbiota, to elicit puerperal fever and for its swift establishment. Our elucidation of GAS infection of the human decidua supports epidemiological conclusions underlining the need for prophylactic measures (2, 55) and vaccine development to prevent life-threatening GAS infections such as puerperal fevers.

Methods

Strains and culture conditions. The strains used in this study are described in Supplemental Table 7. The M28PF1 strain is an *emm28* clinical isolate responsible for an endometritis (French National Reference Center [CNR] for Streptococci; https://cnr-strep.fr/) that was selected on phenotypic and genotypic bases (56). More precisely, a collection of 50 *emm28* independent endometrial clinical isolates from different geographic locations and sampling years was constituted. For each strain, the presence of the specific RD2 sequence was tested, the sequence of the *covR*, *covS*, and *ropB* genes, genes amenable to mutations in other *emm* types, was defined and the capacity to form a biofilm was measured (7, 57–59). A subgroup of 20 $RD2^+$ strains, WT for *covR*, *covS*, and *ropB* (since this was the most frequently observed genotype) and displaying an average biofilm formation capacity was constituted. To define isolates that possessed the same genes as most of the other *emm28* endometrial isolates, the 20 strains were analyzed by DNA arrays covering the GAS pangenome. A subgroup of 8 representative isolates was then constituted and growth in THY supplemented with 20% human plasma, in the presence of cervical cells (HeLa), endometrial cells (HEC-1A), and pulmonary cells (A549), as well as their adhesion to these cell lines, were further analyzed. M28PF1 displays mean growth and adhesion values; therefore, it is a genetically and phenotypically representative *emm28* endometrial isolate. GAS strains were grown under static conditions at 37°C in Todd Hewitt broth supplemented with 0.2% yeast extract (THY) or on THY agar (THYA) plates. For GFP strains, the medium was supplemented with 10 μg/mL erythromycin. Prior to the infection, the bacterial solution was vortexed to disrupt bacterial cell chains.

Genetic constructions and generation of GFP-producing and SLO- and SpeB-deleted mutant strains. The plasmids used in this study are described in Supplemental Table 7. The primers used for the generation of the plasmids and verifying the different strains are described in Supplemental Table 8. The strains harboring an integrated inducible *Gfp* gene were constructed as follows. We sequentially cloned into the pG1 vector (60) the Perm–*Gfp* transcriptional fusion surrounded by the KpnI and HindIII sites from pATGfp (61), giving rise to pG1-Perm-Gfp. The *lacA-lacR* intergenic sequence, enabling a single cross-over in M28PF1 and derivatives, was amplified using the primers F_lacA and R_lacA and cloned by In-Fusion (Clontech) into pG1-Perm-Gfp digested with EcoRI, giving rise to pG1-lacA-Perm-Gfp. The *erm* promoter was replaced by the *tetO tetR Pxyl* promoter region by amplifying it from pTCV_TetO (62) using the primers F_tetO and R_tetO and cloning it into pG1-lacA-Perm-Gfp previously digested with EcoRI-EcoRV, giving rise to pG1-lacA-PTetO-Gfp. The plasmid was checked by sequencing and transferred into M28PF1 or derivatives by electroporation as previously described (63). The correct localization of the construct was confirmed by sequencing the region using a primer outside the construct (R_extlacA) and one hybridizing to the vector, RP48. The uninduced GFP-producing strains grew like M28PF1 in laboratory THY. The construct was stable even in the absence of erythromycin for at least 12 generations. The anhydrotetracycline (Sigma-Aldrich) concentration required for full expression of GFP was 20–50 ng/mL and all bacteria were fluorescent after 90 minutes of induction; the fluorescence was stable for at least 6 hours when the bacteria were in the stationary growth phase. GFP fluorescence is observable when GAS is intracellular; induction of GFP does not affect strain growth.

The ΔSLO and ΔSpeB strains correspond to in-frame deletion mutants of the *slo* and *speB* genes and were obtained by homologous recombination of the plasmids pG1-SLO and pG1-SpeB following the same protocol as described previously (22, 64). The DNA fragments encompassing *speB* and *slo* were cloned in BamHI-EcoRI–digested pG1 using the In-Fusion cloning kit (Clontech). This led to deletion of nucleotides 72–1155 and 76–1690 for *speB* and *slo*, respectively. The back-to-the-WT (BTSLO and BTSpeB) strains were obtained during the second cross-over, which leads to the mutant or back to the WT strain. The strains were entirely sequenced and no spurious mutation were found. The absence of the cognate protein in the mutant strains was confirmed by Western blot or dot blot. The SLO and SpeB production in the ΔSpeB and ΔSLO strains, respectively, was assessed by Western blot or dot blot. The ΔSLO strain produced similar amounts of SpeB as the WT strain. In contrast, the SLO production in the ΔSpeB strain was one-tenth of that of the WT.

For all experiments, GAS strains were prepared as follows. Overnight cultures were diluted to OD = 0.05 and grown in THY to the exponential phase (OD = 0.5), centrifuged, and diluted in RPMI. For GFP expression, exponential-phase bacteria were further diluted to OD = 0.1 in THY supplemented with 10 μg/mL erythromycin and 20 ng/mL anhydrotetracyclin, grown for 90 minutes at 37°C, and diluted in RPMI.

Human tissue collection. Human placenta with attached maternal-fetal membranes were collected from healthy women with an uncomplicated singleton pregnancy, undergoing a planned cesarean delivery prior to the onset of active labor at term (between 38 and 40 weeks of pregnancy). Except for per-operatively administered cephalosporin, women were excluded if prescription antibiotics were used during the 2 weeks preceding delivery. Supplemental Table 1 indicates in which experiment each sample tissue was used.

Maternal-fetal membrane processing. Within 15 minutes of collection, biological samples were processed in the laboratory. Maternal-fetal membranes were detached from placenta under sterile conditions. All membranes were similarly extensively rinsed in PBS and carefully examined. Pieces of membrane that were not in the vicinity of either the placenta or the remodeled zone overlying the cervix (20), free of surface blood clots, were cut and glued to Petri dishes or coverslips with veterinary glue (3M Vetbond glue), with the fetal side sticking to the plastic or glass, and covered with RPMI.

In vitro bacterial growth measurement. Conditioned supernatants were prepared as follows. RPMI was added to maternal-fetal tissues for 8 hours at 37°C, 5% CO_2; the supernatants were subsequently filtered and diluted 1:5 with RPMI. Bacteria (1000/mL) were added to these diluted supernatants or to RPMI alone. After 8 hours of incubation at 37°C, 5% CO_2, solutions were serially diluted and plated. After 24 hours at 37°C, CFU were counted.

Primary decidual stromal cell culture, infection, and analyses. Cells from 3 samples were isolated from the decidua parietalis obtained and processed as described above and cultured as previously

described (22). One milliliter of GAS in RPMI at a bacterial density corresponding to an MOI of 100 was added to confluent decidual stromal cells for 4 hours at 37°C, 5% CO_2. Cells were extensively washed with PBS and fixed for 15 minutes at 20°C with 4% paraformaldehyde. Cytotoxicity was assessed using TUNEL staining following the manufacturer's protocol (DeadEnd Fluorometric TUNEL System, Promega) and a LEICA DMI 6000 microscope with a 20× objective (NA 0.5) for measurement.

Antibodies. The following antibodies were used during this study: Alexa Fluor 594 mouse anti-CD45 (Biolegend, clone M5E2), rabbit anti-fibronectin (Sigma-Aldrich, F3648), rabbit anti-vimentin (Abcam, ab92547), mouse anti–type IV collagen (DSHB, M3F7), and rabbit anti–whole GAS, gift from I. Julkunen (Department of Vaccination and Immune Protection, National Institute for Health and Welfare [THL], University of Helsinki, Finland). Secondary antibodies used were Alexa Fluor 594–conjugated anti-rabbit and Alexa Fluor 647–conjugated anti-mouse antibodies (Invitrogen).

Experiments in static conditions

Immunofluorescence. Maternal-fetal membranes (8 cm^2 or 1.5 cm^2) were glued to a 35-mm-diameter Petri dish or on a 12-mm-diameter glass coverslip, respectively. When specified, tissues were prestained with anti-CD45 (1:100) for 30 minutes at 37°C, 5% CO_2. Tissues were infected with 0.2 mL/cm^2 of a solution of 1.7×10^8 bacteria/mL in RPMI, supplemented with 10 μg/mL erythromycin and 50 ng/mL anhydrotetracycline (infection medium) when GFP strains were used. After infection, tissues were washed and fixed in formalin for 24 hours, and then stored in 70% ethanol at 4°C until use. Fixed tissues were further cut into 0.5 cm^2 pieces and glued to coverslips, and permeabilized with 0.2% Triton X-100 (Sigma-Aldrich) for 30 minutes at 20°C. Blocking solution (PBS + 3% BSA) was added for 1 hour at 20°C, and tissues were stained for 4 hours at 20°C with blocking solution containing primary antibodies: anti-GAS (1:250), anti-fibronectin (1:250), anti–type IV collagen (1:50), and anti-vimentin (1:250). Tissues were washed with PBS and secondary antibodies and DAPI (1:1000) in blocking solution were added for 1 hour at 20°C.

Immunofluorescence was performed on paraffin-embedded tissues as described previously (65). Slices were cut (10 μm thick) and stained with whole GAS rabbit antiserum (laboratory stock, 1:250).

TUNEL assay. RPMI (500 μL) was added to 1.5 cm^2 tissue glued to a 12-mm glass coverslip. One hundred microliters of M28PF1 at 5×10^8 bacteria/mL was added directly to the tissue or in the upper chamber of a 6.5 mm Transwell insert (polycarbonate, 0.4 μm membrane, Costar). For the noninfected condition, 100 μL of RPMI was added directly to the tissue. After the specified infection time, tissues were washed with PBS and fixed in formalin for 24 hours, and then stored in 70% ethanol at 4°C until use.

Slight modifications were brought to the TUNEL manufacturer's protocol. Pieces of tissue (0.5 cm^2) were fixed and glued to coverslips and permeabilized with 500 μL PBS with 0.2% Triton X-100 for 30 minutes at 20°C. One hundred microliters of equilibration buffer (from the manufacturer's kit) was added to the tissues in a wet chamber for 15 minutes, after which the liquid was removed and 50 μL of labeling solution was added for 3–4 hours at 37°C. Tissues were washed twice with saline–sodium citrate 2× buffer (from the manufacturer's kit) and stained with DAPI (1:2000) for 15 minutes. For double vimentin and TUNEL staining, TUNEL staining was performed first.

Static condition image acquisition. The maternal side of tissues was placed facing a 35-mm high glass-bottom μ-dish (IBIDI) and imaged en face using a Yokogawa CSU-X1 Spinning Disk coupled with a Leica DMI6000B microscope. Acquisitions were made with MetaMorph 7 software (Molecular Devices). For measurement of surface coverage, the thickness of bacterial microcolonies, and quantification of bacterial invasion, images were acquired with a 40× objective (NA 1.25). For the latter, 0.3 μm *z*-steps and approximatively 90 slices per stack were acquired. For cytotoxicity quantification, images were acquired with a 20× objective (NA 0.7), 1 μm *z*-steps and for tissues approximatively 70 slices per stack were acquired.

Static condition imagetreatmentsanddata analysis. All images were processed with ImageJ (NIH). For cytotoxicity measurements, TUNEL- and DAPI-positive nuclei of images were segmented and automatically counted. At least 5 fields per condition were analyzed for tissues, and 10 fields for decidualstromalcells. To measurebacterialinvasion,another ImageJmacro was used to segment bacterial particles on *z*-max projection images of GFP signals. For each bacterial particle, the axial localization was determined and compared to fibronectin and type IV collagen localization. Any bacterial particle whose signal was 1.2 μm below fibronectin or collagen signals was considered as an invasion event. Five to 8 fields (153 × 169 × 30 μm) per condition were analyzed. A GAS chain was considered to be on average 4 cocci, corresponding to the mean size of invading particles. We estimated the amount of invading chains by considering bacterial chain surface and thickness (mean thickness, 4 μm; bacterialcoverageofafield, 90%).

For local thickness measurement of the GFP signals corresponding to bacteria, the whole field was subdivided into regions of interest and a custom ImageJ macro measured the full width at half maximum (FWHM) of the *z*-axis GFP signal. The thickness value obtained by measuring the FWHM was then converted to micrometers by measuring the mean FWHM of 20 single bacteria, considered to be 1 μm thick. Five to 7 fields per tissue were analyzed, with samples treated and acquired using the same procedure as for bacterial invasion. A 3D image representation of the tissue was performed using Imaris 7.4 (Bitplane AG).

Experiments in flow conditions

Maternal-fetal explants (8 cm^2) were glued to a 35-mm Petri dish and stained with DRAQ5 (1:2000) and anti-CD45 (1:100) in infection medium containing DAPI (1:30,000) (flow condition infection medium) for 30 minutes at 37°C, 5% CO_2. Tissues were extensively washed with flow condition infection medium and 3 mL of GFP-producing bacteria (1×10^8 CFU/mL) in flow condition infection medium were added to the tissues in a 37°C microscopy chamber for 45 minutes until 20%–30% of the tissue surface was covered by bacteria. The supernatant was then discarded, tissue was washed with infection medium to remove unattached bacteria, and a peristaltic pump with circulating infection medium bubbled with 95% O_2 and 5% CO_2 was activated in an open circuit at 0.3 mL/min.

Flow condition image acquisition. Images of infected tissues were acquired en face with an upright DM6000FS Leica confocal microscope coupled with a Yokogawa CSU-X1 Spinning Disk, with a 25× objective (NA 0.95, Leica Microsystems). Acquisitions were made with MetaMorph 7 software and images were taken every 30 minutes for 3 hours with a *z*-step of 2 μm. For long-term acquisition, axial drift was manually compensated for after 3 hours and acquisition was resumed for another 3 hours.

Flow condition image treatments and data analysis. All images were processed with ImageJ. 3D drifts of live images were corrected with custom routines. For surface area measurements of bacterial colonization, bacteria were segmented based on a threshold on the maximum intensity *z*-projection images of the GFP signal at the different time points, with the same threshold for each time point. Measurements of the local thickness was performed on images acquired in real time as described above for static images. Three to 12 fields per tissue were analyzed.

Bacterial layer thickness. A 3D surface heatmap was generated by a custom R code based on the plot-ly library.

Computer code availability. Computer codes used for this work will be transferred upon request.

RNA extraction. Static condition–obtained tissues were washed once and stored in TRI Reagent (Sigma-Aldrich) at –80°C until used. Total RNA was isolated using a Qiagen RNeasy Kit according to the manufacturer's instructions. The purity and concentration of total RNA were evaluated using a NanoDrop spectrophotometer (Thermo Fisher Scientific), by measuring the absorbance at 260 nm and the ratio of absorbance at 260 nm and 280 nm.

qRT-PCR analysis. RNAs were treated with deoxyribonuclease (Invitrogen, Life Technologies) to remove any contaminating DNA. Total RNA (4 μg) was reverse transcribed using random primers and M-MLV Reverse Transcriptase (Invitrogen), according to the manufacturer's instructions. Quantitative PCR was carried out on a Light Cycler 480, 96-well apparatus (Roche Diagnostics), with 160 ng of cDNA as a template, using the amplification kit SensiFAST SYBR No-Rox kit (Bioline), according to the manufacturer's instructions. The RT^2 Profiler PCR Arrays (Qiagen) for inflammatory cytokines and receptors and human innate and adaptive response were performed according to the manufacturer's instructions. Gene expression was normalized using a panel of 5 housekeeping genes: ACTB, B2M, GAPDH, HPRT1, and RPLP0. ΔCt ranging from 0 to 6.0 was considered as the maximum magnitude of gene expression, from 6.1 to 9.9 as moderate, and from 10 to 15 as low. Genes with a nominal P value ≤ 0.05 were considered to be differentially expressed. Genes showing greater than 2-fold variation were further considered in the analysis. Heatmaps were created using the MeV Package (http://mev.tm4.org/). Enrichr (https://maayanlab.cloud/Enrichr/) was used for pathways enrichment analysis, restricted to Gene Ontology (GO) terms and ARCHS4 databases.

GBS infection of maternal-fetal membrane microarray subanalysis. Data were extracted using GEO2R from Park et al. (33). After conversion of the gene annotation using the DAVID gene ID Conversion tool (https://david.ncifcrf.gov/conversion.jsp), fold-changes and P values for the 133 immune-related genes we previously analyzed with the RT^2 Profiler Arrays were retrieved from 8-hour incubation samples (4 controls and 4 GBS-treated).

Protein and AMP analysis. Static condition–obtained supernatants of explants were stored at −80°C until use. The levels of IL-6, TNF, CCL20, CXCL2, CCL3, and IL-1 were measured with a Bio-Plex custom assay (Bio-Rad) using a Bio-Plex 200. AMP concentrations were analyzed in the same supernatants by ELISA with the following kits: LL-37 (Hycult Biotech), hBD1 (R&D Systems, Novus), and hBD2 (Elabscience). The concentrations are reported as pg/mL medium. The samples were quantified in duplicate according to the manufacturers' instructions.

Statistics. Data were analyzed by Prism 6 software (GraphPad Software) or Xlstat version 2018.1 (Addinsoft). Where indicated, we used 2-way ANOVA. We used Student's t test or nonparametric tests for quantitative variables as indicated in the text and Pearson's χ^2 test for qualitative variables, as appropriate. A P value of less than 0.05 was considered to be significant.

Study approval. The study of the human maternal-fetal membranes was approved by the local ethics committee (Comité de Protection des Personnes Ile de France III, no. Am5724-1-COL2991, 05/02/2013). All participants provided written informed consent prior to inclusion in the study at the Department of Obstetrics, Port Royal Maternity, Cochin University Hospital, Paris, France.

Author contributions

AW, TG, CL, CM, and AF designed experiments, carried out experiments and performed data analysis. C Plainvert, FG, and C Poyart provided essential reagents and scientific advice. CM and AF supervised the project. AW, CM, and AF wrote the manuscript.

Acknowledgments

We thank Louis Réot for the RT-PCR screening; Karine Bailly of Cochin Cytometry and Immunology (CYBIO) for the Luminex cytokine quantification; S. Brochet, Q. Cece, and M. Gaillard from AF and C Poyart's laboratory and T. Meylheuc from the Imaging Facility at the Microscopy and Imaging Platform (ISC MIMA2, INRAE, Jouy-en-Josas-Antony research center France, DOI: MIMA2, INRAE, 2018. Microscopy and Imaging Facility for Microbes, Animals and Foods, https://doi.org/10.15454/1.5572348210007727E12) for assistance with in vitro experiments; E. Donnadieu, S. Barrin, E. Peranzoni, V. Feuillet, and A. Trautmann for advice in the imaging setup and helpful discussions; A. Gruss for helpful discussions and correcting the manuscript; I. Julkunen for the gift of anti-GAS antibodies; the Imag'IC facility of the Cochin Institute; and all the personnel of the CIC Mère-Enfant Cochin-Necker. This work was supported by Université Paris Descartes (contract no. KL2UD to AW) the Département Hospitalo-Universitaire Risks in Pregnancy (PRIDE 2014, to AF and CM), INSERM, CNRS, Université de Paris, Centre National de Référence des Streptocoques.

Address correspondence to: Agnes Fouet, 22 rue Méchain, Paris 75014, France. Phone: 33.1.40.51.64.50; Email: agnes.fouet@inserm.fr.

AW's current address: University of California, San Francisco, 513 Parnassus Ave, San Francisco, California 94143, USA.

1. Sriskandan S. Severe peripartum sepsis. *J R Coll Physicians Edinb*. 2011;41(4):339–346.
2. Leonard A, et al. Severe group A streptococcal infections in mothers and their newborns in London and the South East, 2010-2016: assessment of risk and audit of public health management. *BJOG*. 2019;126(1):44–53.
3. Deutscher M, et al. Incidence and severity of invasive Streptococcus pneumoniae, group A Streptococcus, and group B Streptococcus infections among pregnant and postpartum women. *Clin Infect Dis*. 2011;53(2):114–123.
4. Carapetis JR, et al. The global burden of group A streptococcal diseases. *Lancet Infect Dis*. 2005;5(11):685–694.

5. Bessen DE, et al. Genetic correlates of throat and skin isolates of group A streptococci. *J Infect Dis*. 1996;173(4):896–900.
6. Beall B, et al. Sequencing emm–specific polymerase chain reaction products for routine and accurate typing of group A Streptococci. *J Clin Microbiol*. 1995;34(4):953–958.
7. Green NM et al. Genetic diversity among type emm28 group A Streptococcus strains causing invasive infections and pharyngitis. *J Clin Microbiol*. 2005;43(8):4083–4091.
8. Plainvert C et al. Invasive group A streptococcal infections in adults, France (2006-2010). *Clin Microbiol Infect*. 2012;18(7):702–710.
9. Gherardi G, et al. Prevalent emm types among invasive GAS in Europe and North America since year 2000. *Front Public Health*. 2018;6(3):59.
10. Hung CH et al. Synergistic effects of streptolysin S and streptococcal pyrogenic exotoxin B on the mouse model of group A streptococcal infection. *Med Microbiol Immunol*. 2012;201(3):357–369.
11. Limbago B, et al. Role of streptolysin O in a mouse model of invasive group A streptococcal disease. *Infect Immun*. 2000;68(11):6384–6390.
12. Walker MJ et al. Disease manifestations and pathogenic mechanisms of Group A Streptococcus. *Clin Microbiol Rev*. 2014;27(2):264–301.
13. Shannon BA, et al. Toxins and superantigens of Group A Streptococci. *Microbiol Spectr*. 2019;7(1):47–58.
14. Olsen RJ et al. The majority of 9,729 group A Streptococcus strains causing disease secrete SpeB cysteine protease: pathogenesis implications. *Infect Immun*. 2015;83(12):4750–4758.
15. Lukomski S et al. Inactivation of Streptococcus pyogenes extracellular cysteine protease significantly decreases mouse lethality of serotype M3 and M49 strains. *JClin Invest*. 1997;99(11):2574–2580.
16. Madden JC, et al. Cytolysin-mediated translocation (CMT): a functional equivalent of type III secretion in gram-positive bacteria. *Cell*. 2001;104(1):143–152.
17. Zhu L et al. Contribution of secreted NADase and Streptolysin O to the pathogenesis of epidemic serotype M1 Streptococcus pyogenes infections. *Am J Pathol*. 2017;187(3):605–613.
18. Mead PB, Winn WC. Vaginal-rectal colonization with group A streptococci in late pregnancy. *Infect Dis Obstet Gynecol*. 2000;8(5–6):217–219.
19. Hamilton SM, et al. Pregnancy-related group a streptococcal infections: Temporal relationships between bacterial acquisition, infection onset, clinical findings, and outcome. *Clin Infect Dis*. 2013;57(6):870–876.
20. Marcellin L, et al. Immune modifications in fetal membranes overlying the cervix precede parturition in humans. *J Immunol*. 2017;198(3):1345–1356.
21. Bartmann C, et al. Quantification of the predominant immune cell populations in decidua throughout human pregnancy. *Am J Reprod Immunol*. 2014;71(2):109–119.
22. Weckel A, et al. The N-terminal domain of the R28 protein promotes emm28 group A Streptococcus adhesion to host cells via direct binding to three integrins. *J Biol Chem*. 2018;293(41):16006–16018.
23. Siemens N, et al. Biofilm in group A streptococcal necrotizing soft tissue infections. *JCI Insight*. 2016;1(10):151–157.
24. Cole JN, et al. Molecular insight into invasive group A streptococcal disease. *Nat Rev Microbiol*. 2011;9(10):724–736.
25. Yarbrough VL, et al. Antimicrobial peptides in the female reproductive tract: a critical component of the mucosal immune barrier with physiological and clinical implications. *Hum Reprod Update*. 2015;21(3):353–377.
26. Carroll RK, Musser JM. From transcription to activation: how group A Streptococcus, the flesh-eating pathogen, regulates SpeB cysteine protease production. *Mol Microbiol*. 2011;81(3):588–601.
27. Goldmann O, et al. Streptococcus pyogenes induces oncosis in macrophages through the activation of an inflammatory programmed cell death pathway. *Cell Microbiol*. 2009;11(1):138–155.
28. Bricker AL, et al. NAD^+-glycohydrolase acts as an intracellular toxin to enhance the extracellular survival of group A streptococci. *Mol Microbiol*. 2002;44(1):257–269.
29. Timmer AM, et al. Streptolysin O promotes group A Streptococcus immune evasion by accelerated macrophage apoptosis. *J Biol Chem*. 2009;284(2):862–871.
30. Suryawanshi H, et al. A single-cell survey of the human first-trimester placenta and decidua. *Sci Adv*. 2018;4(10):eaau4788.
31. Goldfeld AE, et al. Transcription of the tumor necrosis factor alpha gene is rapidly induced by anti-immunoglobulin and blocked by cyclosporin A and FK506 in human B cells. *Proc Natl Acad Sci U S A*. 1992;89(24):12198–12201.
32. Smale ST. Selective transcription in response to an inflammatory stimulus. *Cell*. 2010;140(6):833–844.
33. Park H-R, et al. Group B Streptococcus activates transcriptomic pathways related to premature birth in human extraplacental membranes in vitro. *Biol Reprod*. 2018;98(3):396–407.
34. Cicinelli E, et al. Chronic endometritis due to common bacteria is prevalent in women with recurrent miscarriage as confirmed by improved pregnancy outcome after antibiotic treatment. *Reprod Sci*. 2014;21(5):640–647.
35. Egesten A, et al. SpeB of Streptococcus pyogenes differentially modulates antibacterial and receptor activating properties of human chemokines. *PLoS One*. 2009;4(3):1–9.
36. Zingaretti C, et al. Streptococcus pyogenes SpyCEP: a chemokine-inactivating protease with unique structural and biochemical features. *FASEB J*. 2010;24(8):2839–2848.
37. Klenk M, et al. Global epithelial cell transcriptional responses reveal Streptococcus pyogenes Fas regulator activity association with bacterial aggressiveness. *Cell Microbiol*. 2005;7(9):1237–1250.
38. Harder J, et al. Activation of the Nlrp3 inflammasome by Streptococcus pyogenes requires Streptolysin O and NF- κB activation but proceeds independently of TLR signaling and P2X7 receptor. *J Immunol*. 2009;183(9):5823–5829.
39. Virtaneva K, et al. Longitudinal analysis of the group A Streptococcus transcriptome in experimental pharyngitis in cynomolgus macaques. *Proc Natl Acad Sci U S A*. 2005;102(25):9014–9019.
40. Shea PR, et al. Interactome analysis of longitudinal pharyngeal infection of cynomolgus macaques by group A Streptococcus. *Proc Natl Acad Sci U S A*. 2010;107(10):4693–4698.
41. Zhu L, et al. Streptococcus pyogenes genes that promote pharyngitis in primates. *JCI Insight*. 2020;5(11):e137686.
42. Zhu L, et al. Genome-wide screens identify group A Streptococcus surface proteins promoting female genital tract colonization and virulence. *Am J Pathol*. 2020;190(4):862–873.
43. Baruch M, et al. An extracellular bacterial pathogen modulates host metabolism to regulate its own sensing and proliferation. *Cell*. 2014;156(1–2):97–108.
44. Davies HC, et al. Effect of amino acids on steady-state growth of a group a hemolytic Streptococcus. *J Bacteriol*. 1965;89(2):421–427.
45. Johansson L, et al. Cathelicidin LL-37 in severe Streptococcus pyogenes soft tissue infections in humans. *Infect Immun*. 2008;76(8):3399–3404.
46. Presicce P, et al. IL-1 signaling mediates intrauterine inflammation and chorio-decidua neutrophil recruitment and activation. *JCI Insight*. 2018;3(6):e98306.
47. Rohde M, Cleary PP. Adhesion and invasion of Streptococcus pyogenes into host cells and clinical relevance of intracellular streptococci. In: Ferretti JJ, Stevens DL, Fischetti VA, eds. *Streptococcus pyogenes: Basic Biology to Clinical Manifestations*. University of Oklahoma Health Sciences Center; 2016: 1–39.
48. Thulin P, et al. Viable Group A Streptococci in macrophages during acute soft tissue infection. *PLoS Med*. 2006;3(3):e53.
49. Medina E, et al. Survival of Streptococcus pyogenes within host phagocytic cells: a pathogenic mechanism for persistence and systemic invasion. *J Infect Dis*. 2003;187(4):597–603.
50. O'Neill AM, et al. Cytosolic replication of Group A Streptococcus in human macrophages. *MBio*. 2016;7(2):e00020–16.
51. Flaherty RA, et al. Streptolysin S promotes programmed cell death and enhances inflammatory signaling in epithelial keratinocytes during Group A Streptococcus infection. *Infect Immun*. 2015;83(10):4118–4133.
52. Valderrama JA, Nizet V. Group A Streptococcus encounters with host macrophages. *Future Microbiol*. 2018;13(1):119–134.
53. Griffith JW, et al. Chemokines and chemokine receptors: positioning cells for host defense and immunity. *Annu Rev Immunol*. 2014;32(1):659–702.
54. Boldenow E, et al. Antimicrobial peptide response to group B Streptococcus in human extraplacental membranes in culture. *Placenta*. 2013;34(6):480–485.
55. Cohen R, et al. Screening asymptomatic households for Streptococcus pyogenes pharyngeal carriage as a part of in-hospital investigation of puerperal sepsis. *Am J Infect Control*. 2019;47(12):1493–1499.
56. Longo M, et al. Complete genome sequence of Streptococcus pyogenes emm28 strain M28PF1, responsible of a puerperal fever. *Genome Announc*. 2015;3(4):e00750–15.
57. Graham MR, et al. Virulence control in Group A Streptococcus by a two-component gene regu-

latory system: global expression profiling and in vivo infection modeling. *Proc Natl Acad Sci U S A*. 2002;99(21):13855–13860.
58. Köller T, et al. Typing of the pilus-protein-encoding FCT region and biofilm formation as novel parameters in epidemiological investigations of Streptococcus pyogenes isolates from various infection sites. *J Med Microbiol*. 2010;59(pt 4):442–452.
59. Ikebe T, et al. Highly frequent mutations in negative regulators of multiple virulence genes in Group A Streptococcal toxic shock syndrome isolates. *PLoS Pathog*. 2010;6(4):e1000832.
60. Biswas I, et al. High-efficiency gene inactivation and replacement system for gram-positive bacteria. *J Bacteriol*. 1993;175(11):3628–3635.
61. Clarebout G, Leclercq R. Fluorescence assay for studying the ability of macrolides to induce production of ribosomal methylase. *Antimicrob Agents Chemother*. 2002;46(7):2269–2272.
62. Buscetta M, et al. FbsC, a novel fibrinogen-binding protein, promotes Streptococcus agalactiae-host cell interactions. *J Biol Chem*. 2014;289(30):21003–21015.
63. Caparon MG, Scott JR. Genetic manipulation of pathogenic streptococci. *Methods Enzymol*. 1991;204:556–586.
64. Six A, et al. Srr2, a multifaceted adhesin expressed by ST-17 hypervirulent Group B Streptococcus involved in binding to both fibrinogen and plasminogen. *Mol Microbiol*. 2015;97(6):1209–1222.
65. Marcellin L et al. Endometriosis also affects the decidua in contact with the fetal membranes during pregnancy. *Hum Reprod*. 2015;30(2):392–405.

AMERICAN SOCIETY FOR MICROBIOLOGY | Journal of Bacteriology®

RESEARCH ARTICLE

Type II Fatty Acid Synthesis Pathway and Cyclopropane Ring Formation Are Dispensable during Enterococcus faecalis Systemic Infection

Constantin Hays,[a,b,c*] Clara Lambert,[a] Sophie Brinster,[a] Gilles Lamberet,[d†] Laurence du Merle,[e,f] Karine Gloux,[d] Alexandra Gruss,[d] Claire Poyart,[a,b,c] Agnes Fouet[a,b]

[a]Université de Paris, Institut Cochin, INSERM, CNRS, Paris, France
[b]Centre National de Référence des Streptocoques, Paris, France
[c]Hôpitaux Universitaires Paris Centre, Site Cochin, Assistance Publique Hôpitaux de Paris, Paris, France
[d]MICALIS, UMR1319, Institut National de Recherche pour l'Agriculture, l'Alimentation et l'Environnement, Domaine de Vilvert, Jouy en Josas, France
[e]Institut Pasteur, Unité de Biologie des Bactéries Pathogènes à Gram Positif, Paris, France
[f]CNRS ERL3526, Paris, France

Agnes Fouet and Claire Poyart contributed equally to this work.

ABSTRACT *Enterococcus faecalis*, a multiple antibiotic-resistant Gram-positive bacterium, has emerged as a serious nosocomial pathogen. Here, we used a genetic approach to characterize the strategies used by *E. faecalis* to fulfill its requirements for endogenous fatty acid (FA) synthesis *in vitro* and *in vivo*. The type II fatty acid synthesis (FASII) pathway is encoded by two operons and two monocistronic genes. Expression of all of these genes is repressed by exogenous FAs, which are incorporated into the *E. faecalis* membrane and modify its composition. Deletion of nine genes of the 12-gene operon abolished growth in an FA-free medium. Addition of serum, which is lipid rich, restored growth. Interestingly, the *E. faecalis* membrane contains cyclic fatty acids that modify membrane properties but that are unavailable in host serum. The *cfa* gene that encodes the cyclopropanation process is located in a locus independent of the FASII genes. Its deletion did not alter growth under the conditions tested, but yielded bacteria devoid of cyclic FAs. No differences were observed between mice infected with wild-type (WT) or with FASII or cyclopropanation mutant strains, in terms of bacterial loads in blood, liver, spleen, or kidneys. We conclude that in *E. faecalis*, neither FASII nor cyclopropanation enzymes are suitable antibiotic targets.

IMPORTANCE Membrane lipid homeostasis is crucial for bacterial physiology, adaptation, and virulence. Fatty acids are constituents of the phospholipids that are essential membrane components. Most bacteria incorporate exogenous fatty acids into their membranes. *Enterococcus faecalis* has emerged as a serious nosocomial pathogen that is responsible for urinary tract infections, bacteremia, and endocarditis and is intrinsically resistant to numerous antibiotics. *E. faecalis* synthesizes saturated and unsaturated fatty acids, as well as cyclic fatty acids that are not found in the human host. Here, we characterized mutant strains deficient in fatty acid synthesis and modification using genetic, biochemical, and *in vivo* approaches. We conclude that neither the fatty acid synthesis pathway nor the cyclopropanation enzyme are suitable targets for *E. faecalis* antibiotic development.

KEYWORDS *Enterococcus faecalis*, FASII pathway, antibiotic target, cyclopropane ring formation, fatty acids, septicemic infection

Bacterial fatty acids (FAs) are usually synthesized by the type II fatty acid synthesis (FASII) pathway. FAs constitute two hydrophobic tails, which, together with a

Citation Hays C, Lambert C, Brinster S, Lamberet G, du Merle L, Gloux K, Gruss A, Poyart C, Fouet A. 2021. Type II fatty acid synthesis pathway and cyclopropane ring formation are dispensable during *Enterococcus faecalis* systemic infection. J Bacteriol 203: e00221-21. https://doi.org/10.1128/JB.00221-21.

Editor William W. Metcalf, University of Illinois at Urbana Champaign

Copyright © 2021 American Society for Microbiology. All Rights Reserved.

Address correspondence to Claire Poyart, claire.poyart@inserm.fr, or Agnes Fouet, agnes.fouet@inserm.fr.

* Present address: Constantin Hays, Laboratoire d'Immunologie et Histocompatibilité, Saint-Louis Hospital, Paris, France.

†Deceased.

Received 29 April 2021
Accepted 20 July 2021

Accepted manuscript posted online 26 July 2021
Published 23 September 2021

Downloaded from https://journals.asm.org/journal/jb on 27 September 2021 by 193.52.79.218.

hydrophilic head, comprise phospholipids (PL) that are essential components of cell membranes. *Enterococcus faecalis* synthesizes both saturated and unsaturated fatty acids (SFA and UFA, respectively), as do numerous streptococci (1–3). Additionally, *E. faecalis* and numerous other bacteria encode a cyclopropane fatty acid synthase (Cfa), which catalyzes the transfer of a methyl group from *S*-adenosyl-L-methionine to the double bond of a lipid chain, thereby forming a cyclopropane ring (4). Recent studies uncovered that *E. faecalis* also synthesizes *trans*-UFA, further expanding the variety of fatty acids produced by this bacterium (5). Both cyclopropane and *trans* fatty acids are more rigid than their nonmodified substrates, and they contribute to *E. faecalis* membrane homeostasis under starvation and stress conditions (6–8).

The FASII pathway defects prevent bacterial growth *in vitro* in medium not supplemented with FA; this suggests that FASII enzymes may be essential for bacterial viability and are therefore feasible targets for antibiotic design (9–15). However, most bacteria incorporate exogenous FA into their membranes. FA abundance in host compartments and in serum led us to hypothesize and then prove that FA incorporation can bypass FASII-targeted antibiotics in the neonatal pathogen *Streptococcus agalactiae*, as well as in other *Streptococcaceae* taxa (1). Nevertheless, antibiotic bypass may differ according to whether bacteria can survive on exclusively exogenous FAs; for example, *Mycobacterium tuberculosis* remains sensitive to the anti-FASII isoniazid because of its complex lipid requirement (16). In contrast, *Staphylococcus aureus*, which synthesizes FAs not produced by humans, can nevertheless bypass FASII inhibitors with host-derived fatty acids (17–19).

Enterococcus faecalis is a Gram-positive bacterium that inhabits the gastrointestinal tract of humans and animals (20) and has long been associated with food fermentations. *E. faecalis* has emerged as a serious nosocomial pathogen and is the second most frequently isolated Gram-positive pathogen isolated in hospitals after *S. aureus* (21, 22). *E. faecalis* is responsible for urinary tract infections, bacteremia, and endocarditis (23). It is intrinsically resistant to many antibiotics, and its acquisition of antibiotic resistance genes has made it a public health concern worldwide (23). This situation prompts the search for new antibiotic targets, notably within the FASII pathway (24, 25).

Whether targeting of the FASII pathway or cyclopropanation enzymes could lead to treatment of *E. faecalis* systemic infection is not resolved. *E. faecalis* was previously shown to use environmental fatty acids (26). In the presence of 15% human serum, the *E. faecalis* membrane comprises about 10% vaccenic acid (VA; $C_{18:1D11}$), an FA not present in serum (26). Thus, the *E. faecalis* FASII pathway is likely active even in the presence of exogenous FAs. The *E. faecalis* FASII pathway is encoded by the 12-gene cluster *fabT* to *accA*, whose genes are present in numerous Gram-positive species, and by a set of three genes, *fabO-fabN* and the divergent *fabI* gene, which encode enzymes involved in UFA and SFA synthesis, respectively (14, 27). Finally, *cfa* encodes the cyclopropanation reaction. In one study, deletion of *fabN* resulted in *E. faecalis* UFA auxotrophy (28). In *E. faecalis*, expression of FASII genes is controlled by FabT, the transcriptional repressor. An auxiliary acyl carrier protein (ACP) carrying long-chain FAs binds to FabT and facilitates repression of a consensus sequence that regulates FASII gene expression (14, 29, 30).

Although *E. faecalis* incorporates FA from its environment, the FA synthesis requirement in an FA-rich environment cannot be deduced (31, 32). In this study, we characterized the repressive effect of serum on expression of FASII and FA-related genes. We also tested whether FASII pathway and/or cyclopropanation functions are possible antibiotic targets in a murine model of *E. faecalis* systemic infection.

RESULTS AND DISCUSSION

FASII pathway genetic organization and regulation of expression. In *E. faecalis*,a total of 15 genes belonging to the FASII pathway have been previously identified (14, 27, 33). However, a 16th gene, *ef1773* (NCBI GenPept accession number WP_010706667), named *fabG*, is present in the annotated V583 genome. This gene is conserved among *E. faecalis* isolates. As two genes were assigned the same annotation, we suggest renaming

Downloaded from https://journals.asm.org/journal/jb on 27 September 2021 by 193.52.79.218.

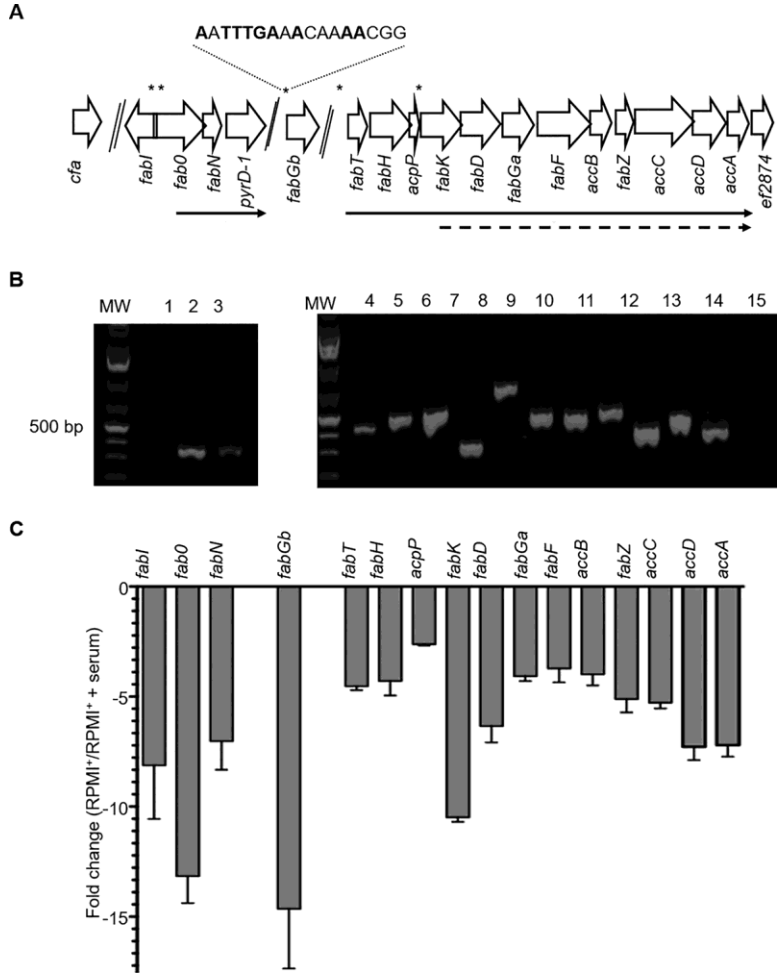

FIG 1 Genetic organization of the *Enterococcus faecalis* type II fatty acid synthesis (FASII) pathway and impact of exogenous fatty acids (FAs) on *E. faecalis* FASII gene expression. (A) Schematic representation of *E. faecalis* VE14089 FASII pathway genes. Gene positions with names below are represented with open arrows. Two genes in the locus, *pyrD-1* (*ef0285*), and *ef2874*, are unrelated to FASII. Above, asterisks indicate putative FabT binding sites; below, solid arrows indicate transcripts predicted by PCRs, and dotted arrows indicate transcripts identified by predicted FabT binding sequence and expression levels. (B) Agarose gel of the real-time PCR (RT-PCR) amplification products on cDNA using primer pairs from neighboring genes. The order is the same as that in panel A. Lane 1, *fabI-fabO*; 2, *fabO-fabN*; 3, *fabN-ef0285*; 4, *fabT-fabH*; 5, *fabH-acpP*; 6, *acpP-fabK*; 7, *fabK-fabD*; 8, *fabD-fabGa*; 9, *fabGa-fabF*; 10, *fabF-accB*; 11, *accB-fabZ*; 12, *fabZ-accC*; 13, *accC-accD*; 14, *accD-accA*; and 15, *accA-ef2874*. MW, molecular weight standard. (C) FASII gene expression fold change in *E. faecalis* grown in RPMI1 medium in the absence or the presence of 40% human serum. The means 6 standard deviation (SD) from three independent experiments are represented.

ef2881, which belongs to the 12-gene cluster, to *fabGa*, and *ef1773* to *fabGb*. The FabGa and FabGb proteins share 32% identity and 65% similarity. The physiological and enzymatic properties of the two FabG homologues remain unknown, and we hypothesized that they may catalyze the same 3-oxoacyl-ACP reduction step but with different substrate preferences or conditions of expression. *In silico* analysis using the *E. faecalis* FabT consensus sequence indicated the presence of a putative FabT binding site, AATTTGAAAC AAAACG (palindromic nucleotides shown in bold) 10 bp downstream of the *fabGb* translation start codon (Fig. 1A) (33). FabT belongs to the family of MarR regulators (34). An HpaR binding site, HpaR also belonging to the MarR family, is centered 47 bp downstream of the *hpaG* to *hpaI* operon start site, and it was suggested that HpaR interferes with transcription elongation (35). Based on this precedent, we suggest that *fabGb* is controlled by FabT and, furthermore, that FabGb is involved in FA synthesis.

Genetic organization of the 12-gene cluster was initially defined *in silico* on the

Downloaded from https://journals.asm.org/journal/jb on 27 September 2021 by 193.52.79.218.

basis of an upstream FabT consensus binding sequence (27). Depending on the species, an organization in two or three operons was suggested (14, 27, 33). In *E. faecalis*, FabT consensus binding sequences are present upstream of *fabT* and *fabK* (Fig. 1A), suggesting a two-operon organization. Also, the UFA synthesis genes *fabO* and *fabN* may constitute another operon (14, 27, 33). This organization was tested by overlapping real-time PCR (RT-PCR) mapping (Fig. 1A and B). Results show that the 12-gene cluster is organized as a single operon that ends before *ef2874*. A transcription reinitiation site may be linked to the FabT consensus binding sequence upstream of *fabK*. Furthermore, intense and faint bands, respectively, were obtained for *fabO-fabN* and *fabN-pyrD-1* (= *ef0285*), suggesting that *fabO* and *fabN* constitute an operon and that there may be some read-through downstream of *fabN*. Together, our data show that *E. faecalis* FASII genes are organized in two operons (*fabT* to *accA* and *fabO-fabN*) and two monocistronic transcriptional units (*fabI* and *fabGb*) (Fig. 1A and B).

The FASII pathway can be strongly repressed by exogenous fatty acids, such that phospholipid synthesis relies on exogenous FA substrates (1, 36). Human serum is rich in lipids comprising long-acyl-chain fatty acids such as 18:1 (15%) and 16:0 (25%), which can act as FabT corepressors (29). To our knowledge, the regulation of *E. faecalis* FASII gene expression elicited by the addition of FAs has not been studied. To address this question, and after checking that there was no growth difference in RPMI1 medium in the presence or absence of added human serum (data not shown), we used real-time quantitative PCR (qRT-PCR) to analyze the effect of 40% human serum on *E. faecalis* FASII gene expression (Fig. 1A and C). Serum addition resulted in decreased expression of all FASII genes, ranging from 2.5- to 14-fold depending on the gene. Interestingly, a putative FabT binding site was found close to the most strongly repressed genes, *fabGb*, *fabO*, and *fabK*. This suggests that a FabT-controlled transcription initiation site or a transcription repression site exists upstream of these genes. Together, our data show that the 12-gene operon (from *fabT* to *accA*), as defined above, is strongly repressed in the presence of a physiological concentration of serum.

The *E. faecalis* FASII pathway and cyclopropanation are dispensable for growth in the presence of serum. Supplementation with serum or unsaturated FA overcomes growth inhibition mediated by cerulenin, a FASII inhibitor (1, 17, 37). We confirmed these results with the wild-type (WT) strain VE14089 (data not shown). The consequences of a nonfunctional FASII pathway were then examined by constructing the EfDFASII mutant, in which 9 genes of the 12-gene operon, from *fabK* to *accA* (*ef2883* to *ef2875*) were deleted. The genes that were removed encode products implicated in the initiation and elongation modules (Fig. 1A). Growth of the WT, the EfDFASII mutant, and back-to-the-wild-type (BWT-FASII) (see Materials and Methods) strains was first compared in RPMI1 (Fig. 2A). The WT and the BWT-FASII strains behaved similarly. In contrast, growth of the EfDFASII strain was essentially arrested in RPMI1. To test whether the slight growth observed with the EfDFASII strain was due to fatty acids carried over from the preculture, we rediluted the cultures to an absorbance at 600 nm (OD_{600}) of 0.01 in RPMI1 when the EfDFASII culture reached a plateau (Fig. 2B). Although the WT and BWT strains resumed growth, the EfDFASII strain barely did (OD_{600} change from 0.01 to 0.015). These results confirm that an active FASII pathway is required for growth in FA-free medium. Addition of 40% human serum to growth medium led to equivalent growth of all strains (Fig. 2A), indicating that serum is sufficient to fully restore growth of the EfDFASII mutant strain. Together, these results indicate that the exogenous FAs present in serum are necessary and sufficient to restore growth when *E. faecalis* FASII pathway is abolished, either via the addition of an FASII inhibitor (1) or by deletion of FASII genes.

The role of cyclopropanation in *E. faecalis* growth in the presence of exogenous FAs remained an open question. *E. faecalis* produces cyclopropane FAs, which are produced from both endogenous and exogenous substrates, presumably to mediate membrane fluidity adjustment by modifying UFA (8). A *cfa* in-frame deletion mutant was constructed to assess the role of cyclopropane FA synthesis in *E. faecalis* growth in medium without or with host serum. The mutant strain grew like the WT and BWT-*cfa*

Downloaded from https://journals.asm.org/journal/jb on 27 September 2021 by 193.52.79.218.

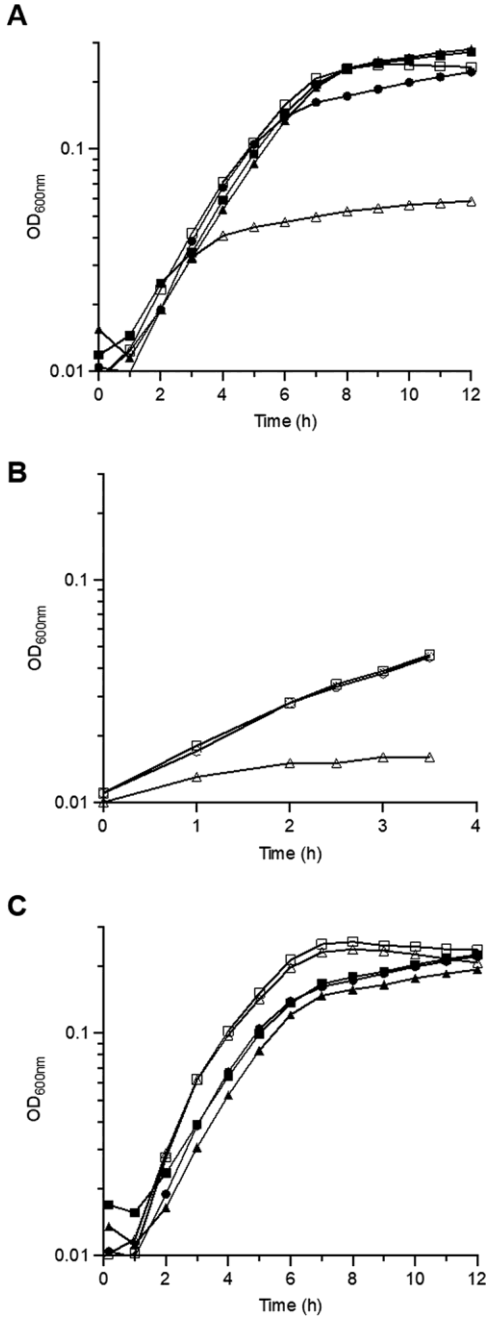

FIG 2 Impact of FASII pathway mutations on *E. faecalis* growth. (A) Growth curves of VE14089 (WT) (▮), EfDFASII (ꙅ), and BWT-FASII (■) strains in RPMI1 in the absence (empty symbols) or presence (closed symbols) of 40% human serum. (B) Growth curves of VE14089 (WT) (*), EfDFASII (D) and BWT-FASII (h) and diluted in RPMI1 to an absorbance at 600 nm (OD_{600}) of 0.01 when EfDFASII strain growth reached a plateau. (C) Growth curves of VE14089 (▮), EfD*cfa* (■), and BWT-*cfa* (ꙅ) strains in RPMI1 in the absence (empty symbols) or presence (closed symbols) of 40% human serum. Growth curves shown are representative of at least 3 independent experiments. Note change of scales for panel B.

strains in both media, indicating that the presence or absence of cyclic FA does not impact *E. faecalis* growth *in vitro* (Fig. 2C).

E. faecalis WT and EfDFASII strains show identical FA composition upon growth in serum. Strong repression of *E. faecalis* FASII genes in the presence of human serum correlates with incorporation of FAs, as previously observed under the same culture conditions (26). We determined the FA compositions of WT VE14089 and BWT-derivative (BWT-FASII) strains grown in the absence or presence of 40% serum (Fig. 3A; see

Downloaded from https://journals.asm.org/journal/jb on 27 September 2021 by 193.52.79.218.

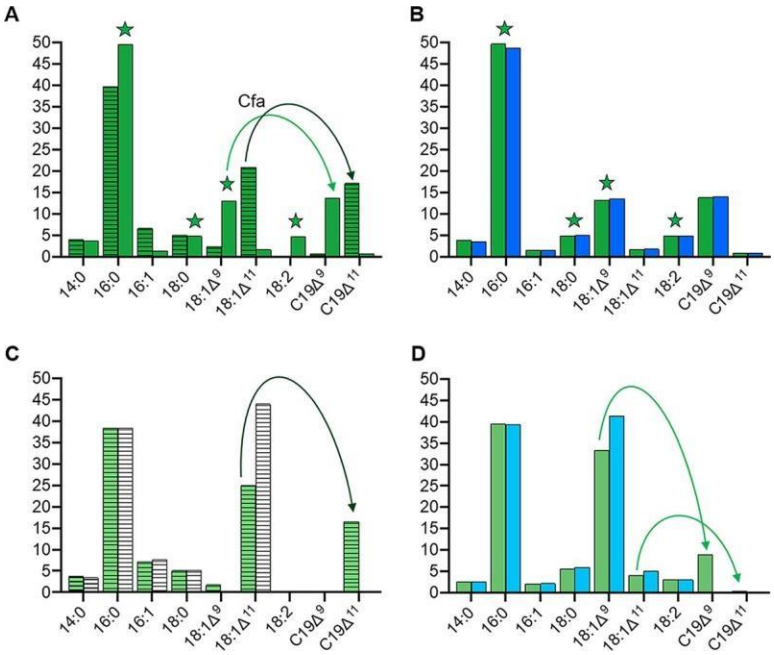

FIG 3 Fatty acid profiles of *E. faecalis* WT, DFASII, and D*cfa* strains grown without and with serum. *E. faecalis* was grown in RPMI1 or in RPMI1 containing 40% human serum to the stationary phase. FA composition was compared to assess the roles of medium FA content and genetic background. The means of the percentages of each FA found in *E. faecalis* BWT or mutant strains grown to the stationary phase in the presence or absence of 40% serum of three independent experiments are presented (see also Tables S2 to S4 in the supplemental material). (A) BWT-FASII grown in the absence or presence of serum. (B). BWT-FASII and EfDFASII strains grown in 40% serum. (C) BWT-*cfa* and EfD*cfa* strains grown in RPMI1. (D) BWT-*cfa* and EfD*cfa* strains grown in 40% human serum. Only major fatty acids (≥2% of total in at least one profile) are shown. Stars, fatty acids derived from serum. Green arrows, cyclopropanation in the BWT strains of unsaturated fatty acids; dark green, produced by *E. faecalis* (mainly 18:1D11); light green, incorporated from serum (mainly 18:1D9). Columns are colored as follows: dark green, BWT-FASII; dark blue, EfDFASII; light green, BWT-*cfa*; light blue, EfD*cfa*; hatched, strains grown in RPMI1; empty, strains in RPMI1 supplemented with 40% human serum.

also Tables S2 and S3 in the supplemental material). BWT-FASII profiles were similar to those of the WT; the slight differences probably arose from growth variations that could alter the efficiency of conversion between the UFA and cyclo forms. As previously described, FA of cells grown in FA-free medium (RPMI1) comprised mainly palmitic acid (PA; 16:0) (40%), vaccenic acid (VA; 18:1D11) (20%), and cyclopropanated VA form (19D11) (20%) (Fig. 3A). In contrast, membrane FA composition of bacteria grown in serum resembled the profiles of serum alone (Table S3 and Fig. 3A) (14, 26, 31). Thus, the proportion of endogenously produced 18:1D11 dropped to 1.7%, and that of serum-provided oleic acid (OA; 18:1D9) rose to 13.5%. These latter percentages are different from previously reported ones (26, 31); this could be due to the use here of 40% rather than 15% serum. Thus, VE14089, like other *E. faecalis* isolates, incorporates serum-supplied exogeneous FA (6). Another notable change in the presence of serum was a decrease in the amount of C19D11, as reported previously (26), while cyclopropanated OA (C19D9), which is not found in serum, rose to 15%, indicating that *E. faecalis* CFA synthase cyclizes both 18:1D9 and 18:1D11. This indicates that *E. faecalis* CFA synthase is active on different substrates, which is in agreement with the fact that bacterial CFAs display lax requirements for positioning of the *cis* double bond, except for *cis* double-bond positions at FA extremities, or *trans* double bonds, which are generally not converted (4).

We also established the FA content of the EfDFASII mutant strain grown in 40% human serum (Fig. 3B). The FA profiles of the EfDFASII and BWT-FASII strains were

Downloaded from https://journals.asm.org/journal/jb on 27 September 2021 by 193.52.79.218.

similar (Fig. 3B). Both strains similarly incorporated serum FAs and generated C19D9. These data demonstrate that FASII activity has no impact on membrane composition in the presence of human serum.

E. faecalis cyclopropane fatty acid synthase impacts cellular FA composition. To characterize the impact of the *cfa* deletion on *E. faecalis* membrane FA composition, we compared the FA profiles of EfD*cfa*, BWT-*cfa*, and WT strains grown in FA-free medium and in the presence of human serum (Fig. 3C and D; see also Tables S2 and S4 in the supplemental material). The BWT-*cfa* profiles were nearly identical to those of the WT (Tables S2 and S4). Compared to the BWT-*cfa* control strain in RPMI1, the EfD*cfa* mutant strain was devoid of C19D11 and was enriched in 18:1D11 (Fig. 3C). In serum-supplemented medium, the EfD*cfa* strain was devoid of C19D9 and enriched in 18:1D9 (Fig. 3D). These data confirm that the EfD*cfa* strain is defective for cyclopropanation of unsaturated fatty acids, mainly 18:1D11 in RPMI1 and 18:1D9 in the presence of serum. This implies that, *in vivo*, the fatty acid composition of *cfa*-defective strains may be different from those of wild-type strains, and this could have physiological consequences.

E. faecalis septicemic infection is independent of both the FASII pathway and fatty acid cyclopropanation. The WT, EfDFASII, and BWT-FASII strains grew similarly and displayed the same FA composition when grown in the presence of human serum. During infection, however, *E. faecalis* infects organs whose FA contents are variable (38, 39). We therefore asked whether exogenous FAs in the host may compensate the loss of the active FASII pathway *in vivo*.

We first followed the infection process, looking at the physiological consequences of intravenous infection with the BWT-FASII strain. CFU counts and organ weights were examined at 1, 7, and 14 days postinfection (dpi) (Fig. 4A and B). Throughout the course of the experiment, the CFU counts in blood were below the detection threshold (data not shown). The CFU counts in the liver diminished 31-fold, at 14 dpi, with no change in the weight of livers throughout the experiment. In the spleen, the bacterial levels strongly decreased over a 2-week period, from approximately 10^4 CFU 24 h postinfection (hpi) to 66% of spleens being sterile at the end of the experiment. However, day 14 spleens weighed twice as much as day 1 spleens (Fig. 4B). Finally, kidney weights increased between day 7 to day 14 (Fig. 4B). This correlated, albeit with a time lag, to the tendency in the CFU counts to increase at day 7 in BWT-FASII-infected mice (15-fold) and is in agreement with *E. faecalis* tropism for the kidneys (31, 32).

We then assessed the consequences of the FASII gene deletion by comparing the BWT-FASII- and EfDFASII-infected mice. Bacterial counts in liver, spleen, and kidneys, as well as organ weights, were similar for BWT-FASII- and EfDFASII-infected mice at all time points (Fig. 4A and B). This demonstrates that, as in other species, targeting the FASII pathway would be ineffective for the treatment of *E. faecalis* septicemic infection (1).

The consequences of a *cfa* deletion were also examined in the mouse septicemia infection model. *cfa* is reportedly more expressed in the stationary phase (40). We reasoned that differences, if any, between EfDcfa and BWT-*cfa* strains would be more pronounced after CFU counts reached their highest level in the wild-type strain (here BWT)-infected mice, i.e., at day 7. No differences were observed in terms of bacterial loads in the different organs between EfDcfa- and BWT-*cfa*-infected mice (Fig. 4C). This indicates that cyclopropanation activity does not confer an advantage to *E. faecalis* during systemic infection in this model.

In conclusion, our data demonstrate that targeting the FASII pathway or the cyclopropanation process would be ineffective for the treatment of *E. faecalis* septicemic infection.

MATERIALS AND METHODS

Bacterial strains, media, and culture conditions. The vancomycin-resistant *E. faecalis* V583 strain was isolated from a bloodstream infection and sequenced. It was used for the *in silico* analysis. VE14089, a plasmid-cured derivative of the V583 strain, was the wild type (WT) reference strain used for the construction of mutant and back-to-the-wild-type (BWT [see "Strain construction," below]) strains (41–43). Two mutants were constructed, EfDFASII and EfD*cfa*, corresponding to the in-frame deletion of nine genes from *fabK* to *accA* (7,863 bp) and of *cfa* (1,176 bp), respectively. The respective isogenic BWT strains BWT-FASII and BWT-*cfa* were obtained. *Escherichia coli* TG1 (Invitrogen) was used for cloning

Downloaded from https://journals.asm.org/journal/jb on 27 September 2021 by 193.52.79.218.

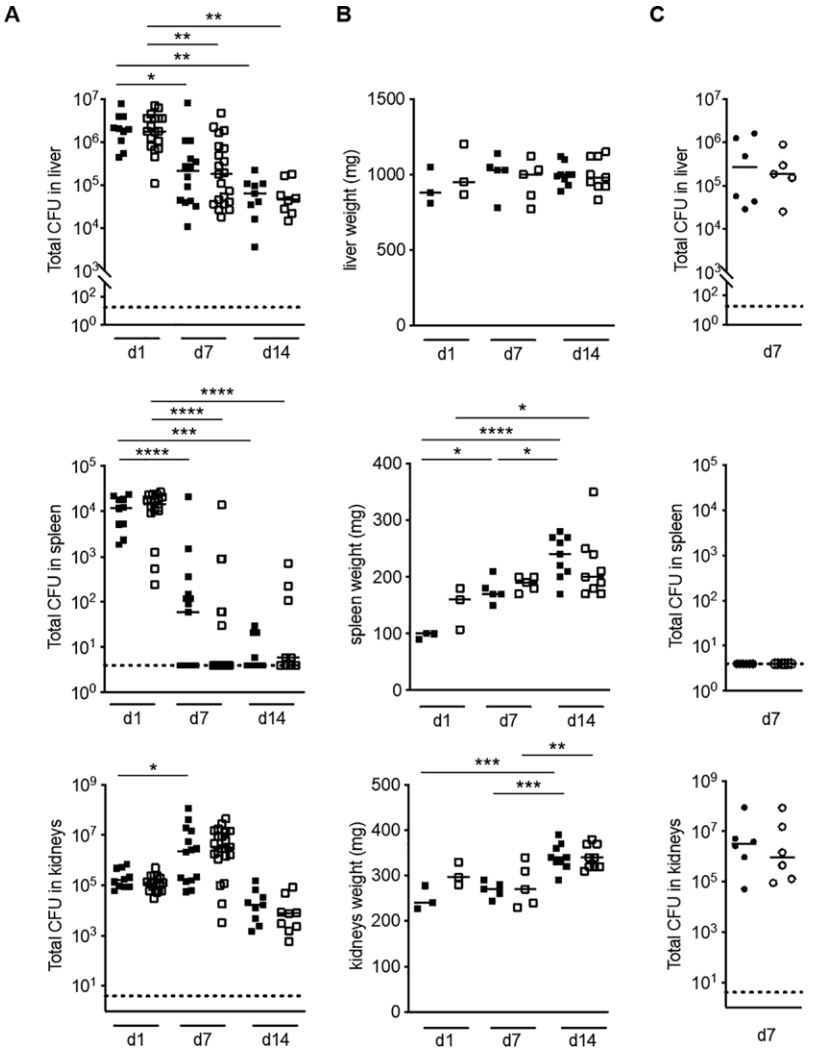

FIG 4 EfDFASII and BWT-FASII infection in a mouse septicemic model. (A) CFU shown by scatter graph plots at 1, 7, and 14 days postinfection (dpi) of bacteria recovered from BWT-FASII- and EfDFASII-infected mice. Nine to 20 mice were intravenously infected with 6×10^8 to 8×10^8 CFU *E. faecalis* BWT-FASII (closed squares) or EfDFASII (open squares) strains. (B) Organ weights shown by scatter graph plots at 1, 7, and 14 dpi of 3 to 9 mice infected by the EfDFASII or BWT-FASII strains. Symbols are as in panel A. (C) CFU shown by scatter graph plots at 7 dpi of viable bacteria recovered from EfD*cfa*- and BWT-*cfa*-infected mice. Six mice were intravenously infected with 6×10^8 to 8×10^8 CFU *E. faecalis* BWT-*cfa* (closed circles) or EfD*cfa* (open circles) strains. Upper panels, liver; middle panels, spleen; lower panels, kidneys. Each symbol represents the number of CFU per organ of one infected mouse or the weight of one organ. Median ranges are represented. Statistical analysis was as follows: 2-way analysis of variance (ANOVA) and a Bonferroni posttest (A and B) Mann-Whitney test (C). *, P , 0.05; **, P , 0.01; ***, P , 0.005; ****, P , 0.0001.

experiments. *E. faecalis* was cultured in Todd-Hewitt (TH) broth or agar (Difco Laboratories, Detroit, MI), supplemented with 0.1% Tween 80 (Sigma) when appropriate, or in RPMI1 medium (RPMI 1640 supplemented with 1× amino acids; Gibco, Life Technologies), 1× vitamins (Sigma-Aldrich), 1% glucose, and 0.1 mM HEPES (Gibco, Life Technologies). *E. coli* was cultured in trypticase soy (TS) medium (Difco Laboratories,). When needed, antibiotics were used at the following concentrations: for *E. coli*, ticarcillin, 100 *m*g/ml, and erythromycin, 160 *m*g/ml; and for *E. faecalis*, erythromycin, 50 *m*g/ml. Cerulenin (Sigma) was added at 8 *m*g/ml final concentration.

In silico analysis. The AGTTTGATAATCAAATT sequence was used to seek potential FabT binding sites in the regulatory regions or within the FASII genes (27).

General DNA techniques. *E. coli* plasmid DNA was prepared by rapid alkaline lysis using the QIAprep spin miniprep kit (Qiagen). Genomic DNA from *E. faecalis* was prepared using the DNeasy blood and tissue kit (Qiagen) with pretreatment for Gram-positive bacteria, as recommended by the manufacturer. PCR was carried out with Ampli*Taq* Gold polymerase as described by the manufacturer (Applied Biosystems). The molecular weight standard used in agarose gels is the 1 kb Plus DNA ladder (Life Technologies). Amplification products were purified using a QIAquick PCR purification kit (Qiagen). PCR

Downloaded from https://journals.asm.org/journal/jb on 27 September 2021 by 193.52.79.218.

products and plasmids used were sequenced with an ABI 310 automated DNA sequencer, using the Prism dye terminator cycle sequencing kit (Applied Biosystems). To determine the genetic and transcriptional organization of VE14089 FASII genes, primer pairs were designed to flank neighboring FASII genes. Primers are listed in Table S1 in the supplemental material.

Strain construction. The primers used for the construction of the in-frame EfDFASII and EfD*cfa* mutant strains are listed in Table S1. Primers used are based on the published genome sequence of *E. faecalis* V583 (GenBank accession number NC_004668.1) (41). The DFASII deletion was constructed by using splicing by overlap extension PCR as described previously (44). The corresponding PCR fragment was cloned into the thermosensitive shuttle plasmid pG1. The D*cfa* (*ef0203*; NCBI reference sequence NC_004668.1) deletion was constructed using the In-Fusion PCR cloning kit (Clontech), cloning the two PCR-amplified fragments into pG1, previously linearized in a one-step reaction, following the manufacturer's recommendations. The resulting intermediate plasmids, pG1DFASII and pG1D*cfa*, were checked by sequencing the inserts. Electroporation of VE14089 and allelic exchange were performed as described previously with minor modifications (44, 45). For each construction, starting from a single clone in which the intermediate plasmid was integrated by homologous recombination, we selected clones in which the second homologous recombination event had taken place. One class of clones was deleted for the considered gene, and the other reverted to the wild-type genotype. An isolated reverted clone was termed back-to-the-wild type (BWT). The BWT strains are isogenic to their deleted counterparts, i.e., they should possess the same secondary mutations if any came up during the construction steps (43). That they displayed the WT phenotype was checked for all *in vitro* phenotypes. For the EfDFASII strain construction, 0.1% Tween 80 (Sigma), a rich source of FA containing 70% oleic acid (OA; 18:1D9), was added during all steps of the experiment after the electroporation. The in-frame deletion mutants and BWT strains were confirmed by PCR and sequence analysis.

Growth curves. *E. faecalis* strains were inoculated into RPMI1 supplemented with Tween 80 (0.1%) and cultured overnight at 37°C. Overnight cultures were washed twice in phosphate-buffered saline (PBS) and subcultured (1:100) in RPMI1 and in RPMI1 supplemented with 40% human serum. In these experiments, the bacterial cultures carried out in RPMI1 were further diluted in RPMI1 before assessing growth. Growth was determined by measuring absorbance at 600 nm (OD_{600}). Experiments were repeated three times.

RNA extraction and RT-PCR. RNA was extracted from bacteria by the phenol-chloroform technique as described previously (46). RNA (2 to 5 *m*g) was treated with DNase I (Promega) according to the manufacturer's recommendations. RNA was quantified by absorbance at 260 and 280 nm. RNA purity and integrity were controlled, and RNA was stored at 280°C until use.

Reverse transcription was carried out using the SuperScript II kit (Invitrogen) and random hexamer primers (Fermentas) according to the manufacturers' instructions. PCRs were carried out on cDNA, as well as on genomic DNA (gDNA) and RNA as positive and negative controls, using primer pairs flanking neighboring FASII genes (Table S1). PCR amplicons were examined on a 1% agarose gel.

Real-time quantitative PCRs. Overnight VE14089 RPMI1 cultures were then subcultured (1:100) to the mid-log phase (OD_{600} = 0.3) in RPMI1 with or without the addition of 40% human serum. RNAs were extracted, and cDNA samples were diluted to 50 ng/*m*l. qPCR was performed using the LightCycler (Roche) and the SYBR green PCR kits (Applied Biosystems) using primers listed in Table S1. Each assay was performed in duplicate, with two independently prepared total RNA samples. The relative quantification in gene expression was determined by the comparative threshold cycle (2^{2DDCT}) method, using *rpoB* as the reference gene (47).

Fatty acid analysis. Strains were inoculated into RPMI1 supplemented with Tween 80 (0.1%) and grown overnight at 37°C. Cells were washed three times in RPMI1 and diluted 100-fold in fresh RPMI1 cultures with or without 40% human serum. Cells were harvested after 14 h of growth (stationary phase) under static conditions at 37°C and washed once in NaCl 0.9% containing 0.01% Triton X-100 and twice in NaCl 0.9%. Cell pellets were stored at 220°C until analysis. The FA composition of serum used for experiments was also determined. Whole-cell esterified fatty acid determinations were done on an AutoSystem XL gas chromatograph (Perkin-Elmer) equipped with a DB-Wax column (30 m × 30.25 mm × 30.25 mm; Agilent, France), for all analyses except those shown in Fig. 3D, or on a ZB-Wax capillary column (30 m × 0.25 mm × 0.25 mm; Phenomenex, France), for that shown in Fig. 3D, as described previously (1, 17). Bacterial fatty acid composition of each sample was analyzed in three independent experiments.

Ethics statement. All animal experiments described in this study were conducted in accordance with the guidelines of Paris Descartes University, in compliance with the European animal welfare regulation (http://ec.europa.eu/environment/chemicals/lab_animals/home_en.html), and were approved by the Paris Descartes University animal care and use committee and by the Ministère de l'Education Nationale, l'Enseignement Supérieur et la Recherche (2015032714098562_v1, APAFIS no. 390).

Intravenous infection of mice. All *in vivo* infections in this study were performed with 6-week-old female BALB/c mice (Charles River, L'Arbresle, France). Bacterial suspensions used for intravenous (i.v.) infection were prepared as follows. Overnight broth cultures of mutant and isogenic BWT strains, grown in TH medium supplemented with 0.1% Tween 80, were diluted 1:100 into 50 ml of TH-Tween 80 medium and grown until an OD_{600} of 0.6. The bacterial suspensions were washed twice in 0.9% NaCl and resuspended in 0.9% NaCl to obtain a final concentration of 6×10^8 to 8×10^8 CFU/ml in 500 *m*l for intravenous injections. Mice were injected in the tail vein using a 28-gauge 0.5-in. needle.

Dissemination assay and organ analysis. Randomized groups of 9 to 21 mice or of 6 mice were infected with the BWT-FASII and EfDFASII or BWT-*cfa* and EfD*cfa* strains, respectively, and mice were sacrificed by cervical dislocation at days 1, 7, and 14 postinfection or at day 7, postinfection; blood, liver, spleen, and kidneys were harvested. All organs were weighed prior to further experimentation. Liver,

Downloaded from https://journals.asm.org/journal/jb on 27 September 2021 by 193.52.79.218.

spleen, and kidneys were homogenized in 0.9% NaCl. Serial dilutions were immediately plated on TH agar plates containing 0.1% Tween 80 (TH-Tween agar). CFU were enumerated after 24 h of incubation at 37°C.

Statistical analysis. Statistical analyses were performed using a 2-way analysis of variance (ANOVA) and a Bonferroni posttest or a Mann-Whitney test (Prism 8). A *P* value of #0.05 was considered statistically significant.

SUPPLEMENTAL MATERIAL

Supplemental material is available online only.

SUPPLEMENTAL FILE 1, XLSX file, 0.02 MB.

ACKNOWLEDGMENTS

We fondly acknowledge our colleague G. Lamberet, who passed away 23 Dec 2019. We thank A. Tazi for helpful discussions.

This work was supported by funding from the Agence Nationale de la Recherche (ANR-13001038), the Fondation pour la recherche Médicale (DBF20161136769), and from INSERM, CNRS, and Université de Paris.

REFERENCES

1. Brinster S, Lamberet G, Staels B, Trieu-Cuot P, Gruss A, Poyart C. 2009. Type II fatty acid synthesis is not a suitable antibiotic target for Gram-positive pathogens. Nature 458:83–86. https://doi.org/10.1038/nature07772.
2. Altabe S, Lopez P, de Mendoza D. 2007. Isolation and characterization of unsaturated fatty acid auxotrophs of *Streptococcus pneumoniae* and *Streptococcus mutans*. J Bacteriol 189:8139–8144. https://doi.org/10.1128/JB.01275-07.
3. Montgomerie JZ, Kalmanson GM, Guze LB. 1973. Fatty acid composition of L-forms of *Streptococcus faecalis* cultured at different osmolalities. J Bacteriol 115:73–75. https://doi.org/10.1128/jb.115.1.73-75.1973.
4. Grogan DW, Cronan JE. 1997. Cyclopropane ring formation in membrane lipids of bacteria. Microbiol Mol Biol Rev 61:429–441. https://doi.org/10.1128/mmbr.61.4.429-441.1997.
5. Kondakova T, Kumar S, Cronan JE. 2019. A novel synthesis of trans-unsaturated fatty acids by the Gram-positive commensal bacterium *Enterococcus faecalis* FA2–2. Chem Phys Lipids 222:23–35. https://doi.org/10.1016/j.chemphyslip.2019.04.010.
6. Zhang Y-M, Rock CO. 2008. Membrane lipid homeostasis in bacteria. Nat Rev Microbiol 6:222–233. https://doi.org/10.1038/nrmicro1839.
7. Parsons JB, Rock CO. 2013. Bacterial lipids: metabolism and membrane homeostasis. Prog Lipid Res 52:249–276. https://doi.org/10.1016/j.plipres.2013.02.002.
8. Poger D, Mark AE. 2015. A ring to rule them all: the effect of cyclopropane fatty acids on the fluidity of lipid bilayers. J Phys Chem B 119:5487–5495. https://doi.org/10.1021/acs.jpcb.5b00958.
9. Heath RJ, White SW, Rock CO. 2001. Lipid biosynthesis as a target for antibacterial agents. Prog Lipid Res 40:467–497. https://doi.org/10.1016/s0163-7827(01)00012-1.
10. Parsons JB, Rock CO. 2011. Is bacterial fatty acid synthesis a valid target for antibacterial drug discovery? Curr Opin Microbiol 14:544–549. https://doi.org/10.1016/j.mib.2011.07.029.
11. Zhang Y-M, White SW, Rock CO. 2006. Inhibiting bacterial fatty acid synthesis. J Biol Chem 281:17541–17544. https://doi.org/10.1074/jbc.R600004200.
12. Heath RJ, White SW, Rock CO. 2002. Inhibitors of fatty acid synthesis as antimicrobial chemotherapeutics. Appl Microbiol Biotechnol 58:695–703. https://doi.org/10.1007/s00253-001-0918-z.
13. Lu H, Tonge PJ. 2008. Inhibitors of FabI, an enzyme drug target in the bacterial fatty acid biosynthesis pathway. Acc Chem Res 41:11–20. https://doi.org/10.1021/ar700156e.
14. Zhu L, Bi H, Ma J, Hu Z, Zhang W, Cronan JE, Wang H. 2013. The two functional enoyl-acyl carrier protein reductases of *Enterococcus faecalis* do not mediate triclosan resistance. mBio 4:e00613-13–e00613. https://doi.org/10.1128/mBio.00613-13.
15. Parsons JB, Frank MW, Rosch JW, Rock CO. 2013. *Staphylococcus aureus* fatty acid auxotrophs do not proliferate in mice. Antimicrob Agents Chemother 57:5729–5732. https://doi.org/10.1128/AAC.01038-13.
16. Bhatt A, Molle V, Besra GS, Jacobs WR, Kremer L. 2007. The *Mycobacterium tuberculosis* FAS-II condensing enzymes: their role in mycolic acid biosynthesis, acid-fastness, pathogenesis and in future drug development: the mycobacterial FAS-II condensing enzymes. Mol Microbiol 64:1442–1454. https://doi.org/10.1111/j.1365-2958.2007.05761.x.
17. Kénanian G, Morvan C, Weckel A, Pathania A, Anba-Mondoloni J, Halpern D, Gaillard M, Solgadi A, Dupont L, Henry C, Poyart C, Fouet A, Lamberet G, Gloux K, Gruss A. 2019. Permissive fatty acid incorporation promotes staphylococcal adaptation to FASII antibiotics in host environments. Cell Rep 29:3974–3982.e4. https://doi.org/10.1016/j.celrep.2019.11.071.
18. Gloux K, Guillemet M, Soler C, Morvan C, Halpern D, Pourcel C, Vu Thien H, Lamberet G, Gruss A. 2017. Clinical relevance of type II fatty acid synthesis bypass in *Staphylococcus aureus*. Antimicrob Agents Chemother 61:e02515-16. https://doi.org/10.1128/AAC.02515-16.
19. Morvan C, Halpern D, Kénanian G, Hays C, Anba-Mondoloni J, Brinster S, Kennedy S, Trieu-Cuot P, Poyart C, Lamberet G, Gloux K, Gruss A. 2016. Environmental fatty acids enable emergence of infectious *Staphylococcus aureus* resistant to FASII-targeted antimicrobials. Nat Commun 7:12944. https://doi.org/10.1038/ncomms12944.
20. Fisher K, Phillips C. 2009. The ecology, epidemiology and virulence of *Enterococcus*. Microbiology (Reading) 155:1749–1757. https://doi.org/10.1099/mic.0.026385-0.
21. Karchmer AW. 2000. Nosocomial bloodstream infections: organisms, risk factors, and implications. Clin Infect Dis 31(Suppl 4):S139–S143. https://doi.org/10.1086/314078.
22. Wisplinghoff H, Bischoff T, Tallent SM, Seifert H, Wenzel RP, Edmond MB. 2004. Nosocomial bloodstream infections in US hospitals: analysis of 24,179 cases from a prospective nationwide surveillance study. Clin Infect Dis 39:309–317. https://doi.org/10.1086/421946.
23. Arias CA, Murray BE. 2012. The rise of the *Enterococcus*: beyond vancomycin resistance. Nat Rev Microbiol 10:266–278. https://doi.org/10.1038/nrmicro2761.
24. Feng Z, Chakraborty D, Dewell SB, Reddy BVB, Brady SF. 2012. Environmental DNA-encoded antibiotics fasamycins A and B inhibit FabF in type II fatty acid biosynthesis. J Am Chem Soc 134:2981–2987. https://doi.org/10.1021/ja207662w.
25. Gerusz V. 2010. Recent advances in the inhibition of bacterial fatty acid biosynthesis. Annu Rep Med Chem 45:295–311.
26. Saito HE, Harp JR, Fozo EM. 2014. Incorporation of exogenous fatty acids protects *Enterococcus faecalis* from membrane-damaging agents. Appl Environ Microbiol 80:6527–6538. https://doi.org/10.1128/AEM.02044-14.
27. Eckhardt TH, Skotnicka D, Kok J, Kuipers OP. 2013. Transcriptional regulation of fatty acid biosynthesis in *Lactococcus lactis*. J Bacteriol 195:1081–1089. https://doi.org/10.1128/JB.02043-12.
28. Diederich A-K, Duda KA, Romero-Saavedra F, Engel R, Holst O, Huebner J. 2016. Deletion of *fabN* in *Enterococcus faecalis* results in unsaturated fatty acid auxotrophy and decreased release of inflammatory cytokines. Innate Immun 22:284–293. https://doi.org/10.1177/1753425916639669.
29. Jerga A, Rock CO. 2009. Acyl-Acyl carrier protein regulates transcription of fatty acid biosynthetic genes via the FabT repressor in *Streptococcus pneumoniae*.J Biol Chem 284:15364–15368. https://doi.org/10.1074/jbc.C109.002410.

Downloaded from https://journals.asm.org/journal/jb on 27 September 2021 by 193.52.79.218.

30. Zhu L, Zou Q, Cao X, Cronan JE. 2019. *Enterococcus faecalis* encodes an atypical auxiliary acyl carrier protein required for efficient regulation of fatty acid synthesis by exogenous fatty acids. mBio 10:e00577-19. https://doi.org/10.1128/mBio.00577-19.
31. Harp JR, Saito HE, Bourdon AK, Reyes J, Arias CA, Campagna SR, Fozo EM. 2016. Exogenous fatty acids protect *Enterococcus faecalis* from daptomycin-induced membrane stress independently of the response regulator LiaR. Appl Environ Microbiol 82:4410–4420. https://doi.org/10.1128/AEM.00933-16.
32. Kau AL, Martin SM, Lyon W, Hayes E, Caparon MG, Hultgren SJ. 2005. *Enterococcus faecalis* tropism for the kidneys in the urinary tract of C57BL/6J mice. Infect Immun 73:2461–2468. https://doi.org/10.1128/IAI.73.4.2461-2468.2005.
33. Lu Y-J, White SW, Rock CO. 2005. Domain swapping between *Enterococcus faecalis* FabN and FabZ proteins localizes the structural determinants for isomerase activity. J Biol Chem 280:30342–30348. https://doi.org/10.1074/jbc.M504637200.
34. Osterman A, Overbeek R. 2003. Missing genes in metabolic pathways: a comparative genomics approach. Curr Opin Chem Biol 7:238–251. https://doi.org/10.1016/s1367-5931(03)00027-9.
35. Galán B, Kolb A, Sanz JM, García JL, Prieto MA. 2003. Molecular determinants of the *hpa* regulatory system of *Escherichia coli*: the HpaR repressor. Nucleic Acids Res 31:6598–6609. https://doi.org/10.1093/nar/gkg851.
36. Yao J, Rock CO. 2017. Exogenous fatty acid metabolism in bacteria. Biochimie 141:30–39. https://doi.org/10.1016/j.biochi.2017.06.015.
37. Saito HE, Harp JR, Fozo EM. 2017. *Enterococcus faecalis* responds to individual exogenous fatty acids independently of their degree of saturation or chain length. Appl Environ Microbiol 84:e01633-17.
38. Cunnane SC, McAdoo KR, Prohaska JR. 1986. Lipid and fatty acid composition of organs from copper-deficient mice. J Nutr 116:1248–1256. https://doi.org/10.1093/jn/116.7.1248.
39. Gentry-Weeks C, Estay M, Loui C, Baker D. 2003. Intravenous mouse infection model for studying the pathology of *Enterococcus faecalis* infections. Infect Immun 71:1434–1441. https://doi.org/10.1128/IAI.71.3.1434-1441.2003.
40. To TMH, Grandvalet C, Tourdot-Marechal R. 2011. Cyclopropanation of membrane unsaturated fatty acids is not essential to the acid stress response of *Lactococcus lactis subsp. cremoris*. Appl Environ Microbiol 77:3327–3334. https://doi.org/10.1128/AEM.02518-10.
41. Paulsen IT, Banerjei L, Myers GSA, Nelson KE, Seshadri R, Read TD, Fouts DE, Eisen JA, Gill SR, Heidelberg JF, Tettelin H, Dodson RJ, Umayam L, Brinkac L, Beanan M, Daugherty S, DeBoy RT, Durkin S, Kolonay J, Madupu R, Nelson W, Vamathevan J, Tran B, Upton J, Hansen T, Shetty J, Khouri H, Utterback T, Radune D, Ketchum KA, Dougherty BA, Fraser CM. 2003. Role of mobile DNA in the evolution of vancomycin-resistant *Enterococcus faecalis*. Science 299:2071–2074. https://doi.org/10.1126/science.1080613.
42. Rigottier-Gois L, Alberti A, Houel A, Taly J-F, Palcy P, Manson J, Pinto D, Matos RC, Carrilero L, Montero N, Tariq M, Karsens H, Repp C, Kropec A, Budin-Verneuil A, Benachour A, Sauvageot N, Bizzini A, Gilmore MS, Bessières P, Kok J, Huebner J, Lopes F, Gonzalez-Zorn B, Hartke A, Serror P. 2011. Large-scale screening of a targeted *Enterococcus faecalis* mutant library identifies envelope fitness factors. PLoS One 6:e29023. https://doi.org/10.1371/journal.pone.0029023.
43. Danne C, Dubrac S, Trieu-Cuot P, Dramsi S. 2014. Single cell stochastic regulation of pilus phase variation by an attenuation-like mechanism. PLoS Pathog 10:e1003860. https://doi.org/10.1371/journal.ppat.1003860.
44. Biswas I, Gruss A, Ehrlich SD, Maguin E. 1993. High-efficiency gene inactivation and replacement system for Gram-positive bacteria. J Bacteriol 175:3628–3635. https://doi.org/10.1128/jb.175.11.3628-3635.1993.
45. Cruz-Rodz AL, Gilmore MS. 1990. High efficiency introduction of plasmid DNA into glycine treated *Enterococcus faecalis* by electroporation. Mol Gen Genet 224:152–154. https://doi.org/10.1007/BF00259462.
46. Lamy M-C, Zouine M, Fert J, Vergassola M, Couve E, Pellegrini E, Glaser P, Kunst F, Msadek T, Trieu-Cuot P, Poyart C. 2004. CovS/CovR of group B *Streptococcus*: a two-component global regulatory system involved in virulence: the CovS/CovR regulatory system of *Streptococcus agalactiae*. Mol Microbiol 54:1250–1268. https://doi.org/10.1111/j.1365-2958.2004.04365.x.
47. Livak KJ, Schmittgen TD. 2001. Analysis of relative gene expression data using real-time quantitative PCR and the 2^{2DDCT} method. Methods 25:402–408. https://doi.org/10.1006/meth.2001.1262.

Downloaded from https://journals.asm.org/journal/jb on 27 September 2021 by 193.52.79.218.

A novel CovS variant harbored by a colonization strain reduces *Streptococcus pyogenes* virulence

Céline Plainvert[a,b], Isabelle Rosinski-Chupin[c], Antonin Weckel[a*] , Clara Lambert[a], Gérald Touak[b*], Elisabeth Sauvage[c], Claire Poyart[a,b], Philippe Glaser[c], Agnès Fouet[a,b,#].

[a] Université Paris Cité, Institut Cochin, INSERM, U1016, CNRS, UMR8104, F-75014 Paris, France ;
[b] Assistance Publique Hôpitaux de Paris, Service de Bactériologie, Centre National de Référence des Streptocoques, Groupe Hospitalier Paris Centre Cochin-Hôtel Dieu-Broca, Paris, France ;
[c] Institut Pasteur, Ecologie et Evolution de la Résistance aux Antibiotiques, UMR3525, Paris, France.

Running Title: A colonization-favoring CovS mutation in *S. pyogenes.*

[#]Address correspondence to Agnes Fouet agnes.fouet@inserm.fr

ABSTRACT

Streptococcus pyogenes, also known as group A *Streptococcus*, causes a wide variety of diseases ranging from mild non-invasive to severe invasive infections. To identify possible causes of colonization to invasive switches, we determined the genomic sequence of ten isolates from five pairs each composed of an invasive and a carriage strain originating from five infectious clusters. Among them, one pair displayed a single nucleotide difference in *covS*, encoding the sensor histidine kinase of the two-component CovRS system that controls the expression of 15% of the genome. In contrast with already described cases where the invasive strains harbor non-functional CovS proteins, the carriage strain possessed the mutation in *covS*. The tyrosine in position 39 was replaced by a histidine. The *covS* mutation affected the expression of the genes from the CovR regulon in a unique fashion. Genes usually over-expressed in *covS* mutant strains were under-expressed and *vice versa*. Furthermore, the *covS* mutant strain barely responded to the addition of the CovS-signaling compounds Mg^{2+} and LL-37. The variations in the accumulation of two virulence factors paralleled the transcription modifications. In addition, the *covS* strain survived less than its wild-type counterpart in murine macrophages. Finally, in two murine models of infection the *covS* strain was less virulent than the wild-type strain. Our study suggests that the CovSY39H protein remains under a kinase active or phosphatase inactive conformation and this yields a non-invasive strain.

IMPORTANCE

Streptococcus pyogenes, also known as group A *Streptococcus*, causes a wide variety of diseases, leading to 517,000 deaths yearly. The two-component CovRS system, that responds to $MgCl_2$ and the antimicrobial peptide LL-37, controls the expression of 15% of the genome. Invasive strains may harbor non-functional CovS sensor proteins that lead to derepression of most virulence genes. We isolated a colonization strain that harbors a *covS* mutation. This mutant strain harbored a transcriptome profile opposite to that of other *covS* mutant strains, barely responded to environmental signals and was less virulent than the wild-type strain. This supports the importance of the derepression of most virulence gene expression, via mutations impacting the regulator CovR phosphorylation, to favor *S. pyogenes* invasive infections.

INTRODUCTION

Streptococcus pyogenes (group A *Streptococcus*, GAS) is an important human pathogen responsible for a large variety of clinical manifestations ranging from mild superficial infections to more life-threatening invasive infections including necrotizing fasciitis (NF) or streptococcal toxic shock syndrome (STSS) (1). Increased frequency of invasive GAS infections has been reported since the last 1980s resulting in a reinforcement of epidemiological surveillance (2). Sequencing of the variable extremity of the *emm* gene is at the basis of epidemiological surveys of GAS infections and more than 225 different *emm* genotypes have been described with variable distribution worldwide; *emm1* and *emm3* genotypes are considered responsible for the most severe clinical forms (3-6). The molecular mechanisms that enable GAS to cause the large range of diseases are unknown although both bacterial and host-specific components are considered to be involved (7, 8). No specific GAS attribute has been associated with a type of infection although a link between genetic background and tissue tropism has been demonstrated (9, 10). In fact, it is rather how GAS can regulate the expression of a variety of gene products involved in GAS adaptation and survival in the human host that will influence the degree of infection severity (11).

The CovRS system (control of virulence, initially termed CsrRS (12)) is the best-studied system among the 13 two-component signal transduction systems (TCS) identified in the GAS genome. The CovRS system is responsible for regulating directly or indirectly approximately

10 to 15% of the GAS genome, mainly as a repressor (13-16). Comparison with TCSs in other species, genetic evidences and *in vitro* studies have indicated that CovS is a member of the bifunctional HisKA family of histidine kinases (17) and CovR is a transcriptional regulator whose activity on promotors is controlled by its phosphorylation state (18-21). CovR is phosphorylated, most probably directly, by CovS and can be phosphorylated by the *S. pyogenes* SP-STK serine/threonine kinase and exogenous acetyl-phosphate (18-23). CovR can be phosphorylated on two sites, aspartate 53, a CovS-dependent reaction that leads to CovR homodimerization and its repressor activity, or threonine 65, catalyzed by STK and abolishing the aspartate 53 phosphorylation (23). CovR can be dephosphorylated by CovS, which also has a phosphatase activity and by the SP-STP phosphatase whose gene is co-transcribed with that of SP-STK (24-27). CovS phosphorylation state is influenced by environmental signals including extracellular Mg^{2+}, LL-37, elevated temperature, acidic pH and high osmolarity (24, 28-31). Mg^{2+} and LL-37 have opposite effects on the expression of the CovRS-controlled genes; Mg^{2+} enhances the repression of CovRS-repressed genes and LL-37 has the paradoxical effect of stimulating their expression (24, 28-31). Mechanistically, a high concentration of magnesium increases the level of phosphorylated CovR in a CovS-dependent manner (25); Mg^{2+} effect is mediated mainly by an impairment of CovS phosphatase activity and not by an enhanced kinase activity (25). Conversely, LL-37 signaling increases CovS phosphatase activity (26). In addition, loss of CovS phosphatase activity impairs *S. pyogenes* pathogenicity (26). An orphan regulator, RocA is a positive regulator of CovRS (32). RocA binds in the membrane to CovS and enhances its autokinase activity or inhibits its phosphatase activity (33). RocA is truncated in *emm3* isolates leading to lower CovR-P level (34, 35). Finally, *in vivo* selection of *covRS* mutants leads to strains with enhanced virulence both in humans and in animal models highlighting the major impact of the CovRS system on GAS virulence (16, 28, 36-41). The mutations all correspond to a loss or a diminution of phosphorylated CovR, either by the absence of CovR or mutation affecting CovS capacity to phosphorylate CovR.

Various groups among the genes controlled by CovRS have been identified (26, 42). A group of CovRS-repressed genes includes, among others, *slo*, that encodes the Streptolysin O, a pore forming toxin that also facilitates the entry of the NAD-glycohydrolase into eukaryotic cells and together these toxins contribute to cell lysis and to GAS pathogenesis (43-45), *speA*, that encodes a superantigen, and the *has* operon, encoding the biosynthetic enzymes of the antiphagocytic poly-saccharide capsule, that is involved in *in vitro* binding to the receptor

CD44, preventing GAS invasion in pharyngeal epithelial cells, and with increased virulence in a mice model (12). In both *covS* and *covR* deleted strains, these genes are over-expressed (14). Another group of genes, sometimes described as activated by CovRS, includes *speB*, encoding the extracellular cysteine protease SpeB, a major virulence factor of *S. pyogenes*, involved in several stages of GAS infections including dissemination, modulation of immune response and inflammation (45-52), and *grab* an α2-macroglobulin binding protein (16, 42, 53-55). These genes are under-expressed in *covS* mutant strains and in defined *covR* mutant strains, but over-expressed in a *covR* deleted strain (16, 42, 53-55). CovR represses their expression more efficiently than CovR phosphorylated on the aspartate 53 (56). Also, *speB* expression is up-regulated at high bacterial cell density. This is the consequence of the modulation of the activity of the *speB* transcriptional activator, RopB, by the cell-to-cell signaling SIP peptide (57).

In France, the epidemiology of GAS invasive infections is performed by the French national reference center for streptococci (CNR-Strep, www.cnr-strep.fr) that collects and analyses invasive GAS strains sent on voluntary basis by laboratories located throughout national territory. The GAS colonization strains isolated as part of the investigations conducted around clusters are also sent to and appraised by the CNR-Strep.

In order to identify factors responsible for the non-invasive to invasive switch, we sought genetic differences between invasive and colonization GAS strains. Ten isolates from five pairs of GAS strains, belonging to five independent clusters and each constituted by an invasive and an asymptomatic colonization GAS strain, have been sequenced. Here, we report the characterization of the strains from one *emm1* pair in which, in contrast to cases described up to now, the carriage strain harbored a mutation in *covS*. The transcription profiles, virulence factor production, cell interaction and *in vivo* virulence for these strains have been assessed and differences between the wild-type (wt) and the paired *covS* mutant strains were observed. The mutation was transferred to an *emm3* clinical isolate and the expression of genes encoding virulence factors and the production of two virulence factors were also assessed and differences again observed.

MATERIALS AND METHODS

Bacterial strains and culture conditions. All clinical GAS strains listed in Table 1 were sent on a voluntary basis to the CNR-Strep by laboratories located throughout the national territory. Clinical characteristics were obtained from questionnaires sent with the isolates. Data collected included sex and date of birth of the patient, date and origin of the sample, geographical area and clinical manifestations. Strains were stored in 2% glycerol Todd Hewitt broth (TH) at -80°C. GAS strains were cultured in static TH broth supplemented with 0.2% yeast extract (THY) at 37°C without agitation. When necessary, 15 mM $MgCl_2$ or 100 nM LL-37 was added to THY.

GAS strains sequencing and sequence analyses. Complete genome sequencing was carried out using the Illumina technology, with read length of 51 nt and a more than 200-fold-coverage on six pairs of GAS strains. Libraries were constructed by using the Illumina TrueSeq kit following the manufacturer's instructions. Illumina short reads were assembled by using the Velvet software (58). In each pair, one assembly was chosen as a reference sequence to align the reads of both strains by using the Burrows-Wheeler Aligner (BWA) (59). SNP calling was made using SAMtools MPILEUP and varFilter. All putative SNP were visually verified by using Tablet (60). Alignment of the reference genome reads allowed the identification of errors in the Velvet assembly. In pairs where SNP were identified, the search for the directionality of the mutation was carried out using NCBI Blastp against the non-redundant protein sequence database and specifying *Streptococcus pyogenes* (Taxid:1314) as described in Almeida *et al* (61). The two strains from pair 1 were found to be of the *emm1* type and differ by a unique SNP in *covS* CDS at codon 39 (TAT versus CAT) leading to either a tyrosine or a histidine. The sequence of the WT strain (isolated from blood) was further completed as described (GenBank LR031521) (62) and used as a reference sequence to confirm SNP uniqueness in the strain isolated from the throat by using breseq (63).

RNA isolation and Illumina RNA-seq sequencing. *S. pyogenes* M1-CovS-WT and M1-CovS-Y39H strains were cultured at 37°C in THY broth supplemented or not with $MgCl_2$ or LL-37, and cells were harvested at late exponential growth phase (OD_{600} 0.7-0.8) as described in (31). Total RNA was extracted as described (64) from three independent cultures for each condition. Residual DNA was removed using DNase (Turbo DNA-free kit Ambion). RNA integrity was analyzed using an Agilent Bioanalyzer (Agilent Biotechnologies). Strand specific RNA-seq libraries ranging in size from 100 to 200 bp (insert size 30-130 bp) were prepared as

previously described (62). Multiplexed libraries (6 samples per lane) were sequenced on the Hi-Seq 2000 platform (Illumina) generating 6,300,000 to 40,000,000 50-bp-long reads per sample.

RNA-Seq data analysis. The M1-CovS-WT sequence (LR031521) was used as a reference sequence to map sequencing reads. RNA-seq data were analysed using bowtie-0.12.7, Rsamtools (version 1.26.2), Genomic-Alignments (version 1.10.1), Genomic Features (version 1.26.2) in R 3.3.1 as previously described (62, 65). For differential expression analysis, normalization and statistical analyses were performed by using the SARTools package and DESeq2 (66, 67). *p* values were calculated and adjusted for multiple testing using the false discovery rate controlling procedure (68).

First-strand cDNA synthesis and quantitative PCR (qPCR). 0.5 µg of total RNA was used for first-strand cDNA synthesis using SuperScript™ II reverse transcriptase and random primers according to the manufacturer's instructions (Invitrogen, Life technologies). Quantitative PCR was carried out with SYBR Green PCR kits (Applied Biosystems, Life technologies) using six pairs of primers (Table S1). Relative quantification of specific gene expression was calculated with the $2^{-\Delta\Delta Ct}$ method using *gyrA* as the housekeeping reference gene and expressed in Log_2-fold change. Each assay was performed on independent biological triplicates and the statistical significance of the differences was inferred by using a two-tailed unequal variances t-test (Welch's test) on the ΔCq values.

SpeB and SLO accumulation assay. Overnight cultures in static THY medium, supplemented or not with $MgCl_2$ or LL-37, were diluted 1:30 in the appropriate growth medium and incubated at 37°C and OD_{600} was followed. Since SpeB, but not SLO, was assayed at a growth phase during which its accumulation becomes consequent, the medium was supplemented with the cysteine protease inhibitor E-64 (mg/mL) for the SpeB assays. Supernatant proteins were precipitated in presence of 0.6 N TCA (2,2,2-trichloroacetic acid) for one hour at 0°C. After centrifugation, pellets were resuspended with 50 mM Tris pH 8.0 and total proteins were quantified using the BCA assay kit (Thermo-Fisher). Defined amounts of total proteins were loaded on a nitrocellulose membrane. Detection of SpeB or SLO was performed using an over-night 4°C incubation with specific anti-SpeB or anti-SLO rabbit antibodies (Abcam). Horseradish peroxidase (HRP)-coupled goat anti-rabbit secondary antibody (Zymed) was added and detection was performed with enhanced chimioluminescence (ECL Reagent, GE

healthcare). Immunoblot assays were analyzed using the ImageJ software. The Kruskal-Wallis or one-way ANOVA tests were used (Prism 9).

Macrophage survival assay. Murine macrophage cell-line RAW264.7 was used to perform phagocytosis and survival assays. Twenty-four well plates were seeded with 5 x 10^5 RAW264.7 per well, in DMEM medium (high glucose) supplemented with 10% fetal calf serum at 37°C under a 5% CO_2 enriched atmosphere. After 24 hours, mid-logarithmic phase bacterial cultures, resuspended in DMEM medium (high glucose) supplemented with 2 mM L-glutamine, were added at a multiplicity of infection (MOI) of 10. The survival assay was carried out as previously described (8). The plates were centrifuged at 6600 RPM for 10 min. The infected cells were then incubated for 45 minutes at 37°C, then washed three times with PBS and treated with penicillin-streptomycin for 30 min. At time 0 (T0 corresponding to 30 min after addition of antibiotics) and at specific time points thereafter, intracellular GAS were recovered and serial dilutions were plated. Results were expressed as the percentage of intracellular GAS relative to T0. For all experiments, 7 independent assays in triplicate were carried out. The 2way ANOVA with a Bonferonni post-test was used (Prism 9).

Animal experiments. The procedures were in agreement with the guidelines of the European Commission for the handling of laboratory animals, directive 86/609/EEC (http://ec.europa.eu/environment/chemicals/lab_animals/home_en.htm) and were approved by the Université Paris Descartes ethic committee. Female CD1 mice (6 weeks old, Charles River laboratories, France) were either injected intravenously in the tail with 4 to 5 x 10^7 cfus from exponentially growing bacteria or infected intranasally with 5 x 10^8 to 1.2 x 10^9 cfus from exponentially growing bacteria, in a volume of 5 µl per nostril. Animal survival was followed for ten days or 15 days. The logrank (Mantel-Cox) and Gehan-Breslow-Wilcoxon tests were used to analyze the data (Prism 9).

RESULTS

A carriage pharyngeal strain harbors a mutation in covS. To identify factors responsible for the shift from non-invasive to invasive strains, we selected five pairs of GAS strains. These were isolated during five independent clustered cases, with an invasive infection, yielding the "invasive strain", and a swab from a family member with no or a non-invasive infection, yielding the "colonization strain" (Table 1). Sequencing these strains identified two pairs (1 and 2) where the *covS* genes differed between the strains, two pairs (3 and 4) where mutations were in the carriage strains in *sfbX* or immediately upstream the *sof-sfbX* operon and one pair (5) in which a *com* gene was lost. In pair 2, composed of *emm11* strains, the invasive strain displayed a single mutation in the *covS* gene leading to a frameshift and a stop codon at the 26th position, whereas the colonization strain harbored a wild-type *covS* gene (Table 1). The presence of such mutations in invasive strains has already been described for GAS strains from different *emm*-types (16, 37, 38, 40, 41).

Table 1 Selected pairs of clinical group A *Streptococcus* strains

Pairs	Strain	Sex	Age	Sample origin	Clinical symptoms	*emm* genotype[a]	PFGE pattern[b]	Mutation
Pair 1	M1-CovS-WT	M	36	Blood culture	NF + STSS	*emm1*	1-A	
	M1-CovS-Y39H	M	7	Throat swab	Pharyngeal carriage	*emm1*	1-A	Point mutation in *covS*
Pair 2	M11CovS	F	56	Blood culture	Peritonitis + STSS	*emm11*	11-A3	Frameshift in *covS*
	M11WT	M	54	Throat swab	Pharyngeal carriage	*emm11*	11-A3	
Pair 3	2003-223	M	72	Pus	Ethmoiditis	*emm77*	77-A	
	2003-223	F	43	Cutaneous	Soft skin infection	*emm77*	77-A	Frameshift in *sfbX*
Pair 4	2009-126	M	75	Blood culture	Bacteremia	*emm77*		
	2009-125	M	80	Cutaneous	Impetigo	*emm77*		upstream *sof*
Pair 5	2007-635	M	47	Blood culture	Bacteremia	*emm94*		
	2007-949	F	85	Cutaneous	Cellulitis	*emm94*		gene

[a], *emm* genotype was obtained as previously described (82). [b], pulse field gel electrophoresis (PFGE) patterns were determined as previously described (83).

The sequences of the pair 1 strains that are of the *emm1* genotype were compared to published complete genome sequences of *emm1* strains and found to be very similar to the

genome sequence of the epidemic strain MGAS5005 (NC_007297.2) and A20 (CP003901.1) isolated from a patient with necrotizing fasciitis, with 60 to 65 SNPs and up to 14 indels of 1 to 21 nucleotides (nt) (62, 69, 70). A single nucleotide difference was observed between the strains from pair 1; it is located in the *covS* gene, *covST115C*. The *covS* gene from one strain was identical to that of the wild-type *covS* gene (70); this strain was named M1-CovS-WT. The single nucleotide difference in *covS* from the other strain led to the substitution of the tyrosine residue at position 39 by a histidine residue (Y39H). This replacement did not appear in the sequences obtained when blasting the first 100 amino-acid residues of CovS against the non-redundant protein sequences from *S. pyogenes* (NCBI database, August 2021). In fact, the tyrosine 39, which is located at the end of the first membrane-spanning domain, is highly conserved within CovS sequences (Fig. 1) (71). Altogether, this suggests that the Y39H modification is not a polymorphism, but may be a mutation; we named the strain M1-CovS-Y39H. In contrast to what has been described up to now and was found in the strains from the *emm11*-strain pair, the mutant M1-CovS-Y39H strain is the carriage strain, while the invasive strain harbors a wild-type *covS* allele (Table 1). To our knowledge, it is the first description of this *covS* mutation and the first report of a carriage strain harboring a *covS* mutation (41, 72). We consequently decided to study this strain further.

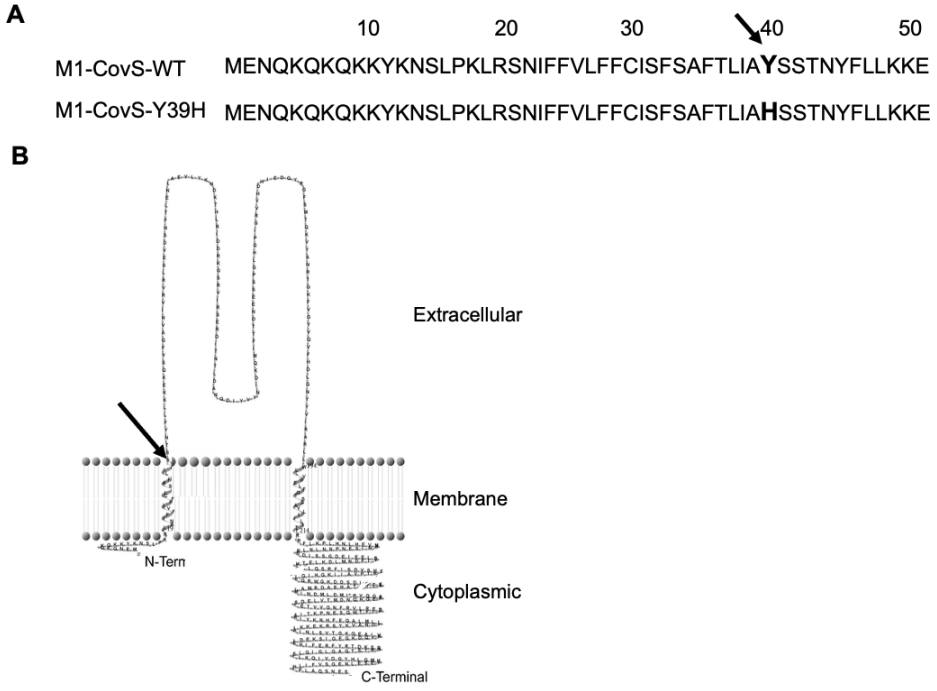

Figure 1. Localization of the Y39H mutation. A) Amino-acid sequence of the 50 first amino-acid residues in the M1-CovS-WT and M1-CovS-Y39H strains; in bold the 39th amino-acid residue. B) Localization of the mutation on a schematic representation of CovS, modified from (71); black arrow, the 39th residue.

The CovSY39H mutation yields unique transcriptomic profiles. Mutations in *covS* have been described to yield growth defects. In contrast, the growth of the M1-CovS-Y39H strain was identical to that of the M1-CovS-WT strain in THY (data not shown). This result indicates that the mutation Y39H did not alter the growth of the M1-CovS-Y39H strain *in vitro*. To characterize the consequences of the CovSY39H mutation further, we compared the transcriptomic profile, determined by RNAseq, of M1-CovS-WT and M1-CovS-Y39H strains grown in THY and harvested at the entry into stationary phase (OD_{600} = 0.7) (Fig. 2A).

Statistical analyses of RNAseq data showed that 81 genes were differentially expressed, with a statistically significant difference and a minimum fold change of 2. In particular, the expression of the genes encoding streptolysin O (*slo*), streptokinase (*ska*), C5A-peptidase *(scpA),* secreted inhibitor of complement (sicC3-like ADP-ribosyltransferase (*spyA*)), fibronectin-binding protein (*fbaA*), all known virulence factors (73, 74), was lower in the M1-CovS-Y39H than in the M1-CovS-WT strain (Fig. 2A). In contrast, expression of the genes encoding exotoxin B (*speB*), immunoglobulin G-binding protein G (*grab*) and genes from the pilus locus, or FCT, was higher in the M1-CovS-Y39H than in the M1-CovS-WT strain. The *has* genes were expressed at very low levels and their expression was not significantly different between both strains. In addition to variations in the expression of genes involved in virulence, the two strains also differed in the expression of metabolic genes, such as genes involved in pyrimidine (including the *pyrR* regulatory gene) and sugar metabolisms. To confirm the RNAseq results, we performed a quantitative RT-PCR analysis, on independent RNA samples, on several virulence genes (Fig. S1A). The *speB* and, to a lesser extent, the *grab* genes were over-expressed in the M1-CovS-Y39H strain compared to the M1-CovS-WT strain, while *ska* was slightly under-expressed and the transcription of *hasA* was not affected. Overall, these results confirmed the RNAseq data although the transcription differences were somewhat weaker in the qRT-PCR experiments. These data indicate that the variations in gene expression between M1-CovS-Y39H and M1-CovS-WT are opposite to those classically described between *covS* and wild-type strains (28-31).

To further explore the phenotype of both strains, we tested the influence of Mg^{2+} on their transcriptomic profiles Fig. 2B, 2C, S1B, Table S1) (28, 29, 31). The addition of 15 mM Mg^{2+} to the growth medium did not impact the growth of these strains (data not shown). Important changes in gene expression were observed for the M1-CovS-WT strain in response to Mg^{2+}, with at least 202 genes being differentially expressed.

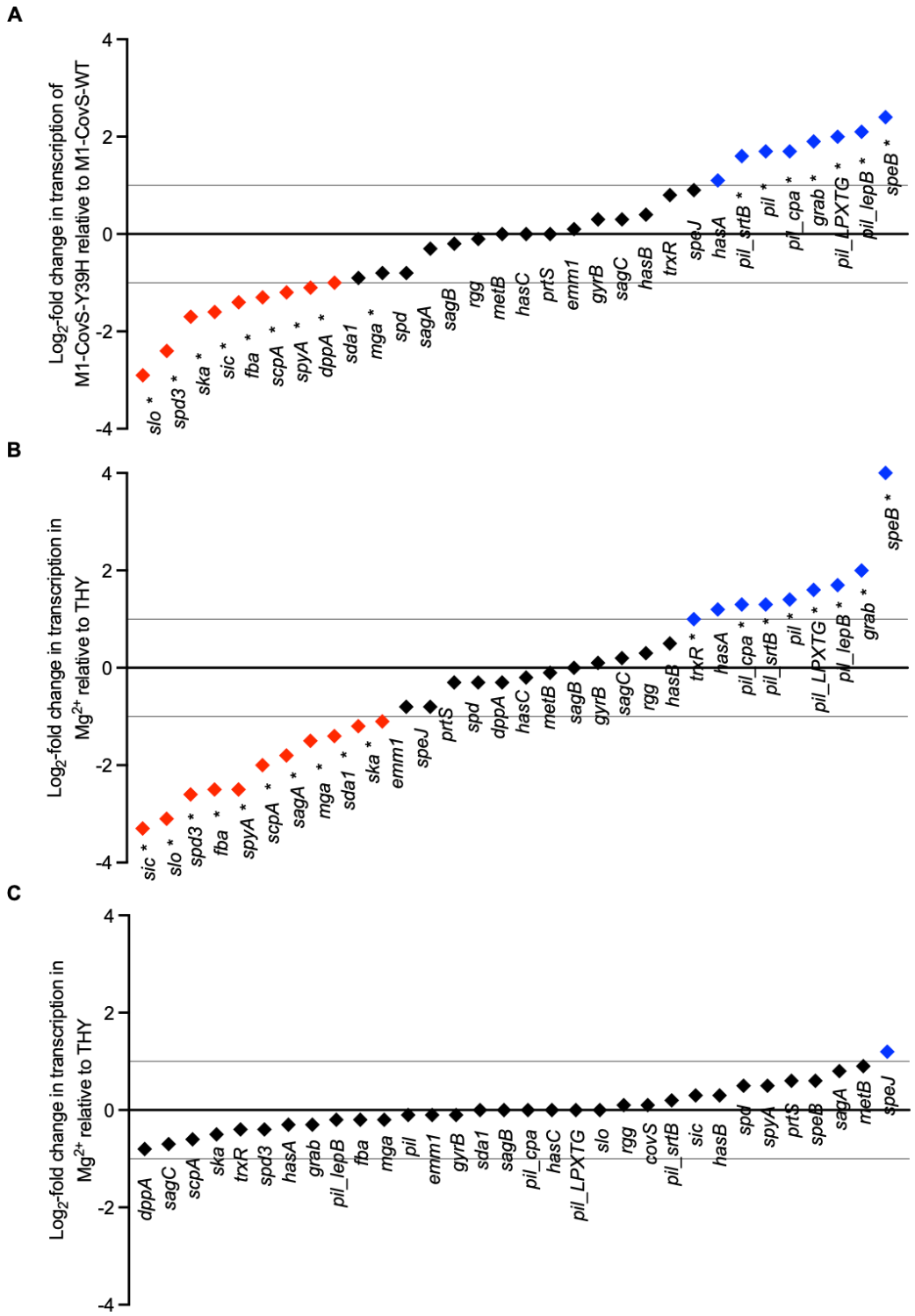

Figure 2. The M1-CovS-Y39H strain displays an atypical transcriptomic profile and responds poorly to an environmental cue. Log_2-fold transcript differences between A) M1-CovS-Y39H and M1-CovS-WT strains grown in THY; B) M1-CovS-WT grown in THY supplemented with $MgCL_2$ and in THY C) M1-CovS-Y39H grown in THY supplemented with $MgCL_2$ and in THY, for selected virulence genes determined by RNAseq analysis. Genes in black; highlighted with a blue diamond above the 0 bar and highlighted with a red diamond below the 0 bar are those that are over-expressed and under-expressed, respectively in A) the M1-CovS-Y39H strain compared to the M1-CovS-WT strain, B) in the M1-CovS-WT strain, in the presence of $MgCL_2$ compared to THY; C) in the M1-CovS-Y39H strain, in the presence of $MgCL_2$ compared to THY. * statistically significant after multiple testing adjustment procedure.

Regarding virulence genes, *speB*, *grab*, genes of the pilus locus and one *has* gene were over-expressed in the presence of Mg^{2+}. In contrast, *sci*, *slo*, *spyA*, *spd3*, among others, were under-expressed (Fig. 2B). qRT-PCR confirmed the RNAseq results and showed that addition of Mg^{2+} results in an over-expression of *speB* and *grab* and an under-expression of *speA, ska, slo* and, a trend to an under expression of *hasA* (Fig. S1B). These results indicate that addition of Mg^{2+} elicited the same effects, as those already described, on the expression of GAS virulence genes in wild-type strains (28, 29, 31). No genes displayed a significantly modified transcription in response to Mg^{2+} in the M1CovS strain (Table S2, Fig. 2C, S1B). These results were confirmed by qRT-PCR (Fig. S1B) This suggests that the $MgCl_2$ effect was strongly attenuated in the M1-CovS-Y39H strain compared to the M1-CovS-WT strain.

To further analyze the functionality of the CovSY39H protein, we tested the consequences of adding the anti-microbial peptide LL-37, that shifts the equilibrium towards CovS phosphatase activity, to the growth medium, on the expression of chosen genes (24, 28-31). The addition of 100 nM LL-37 to the growth medium did not impact the growth of these strains (data not shown). Only the *speB* gene expression was modified for the M1-CovS-WT in response to LL-37 (Fig. 3). However, this change was lost with the M1-CovS-Y39H strain. This suggests that the LL-37 effect was attenuated in the M1-CovS-Y39H strain compared to the M1-CovS-WT strain.

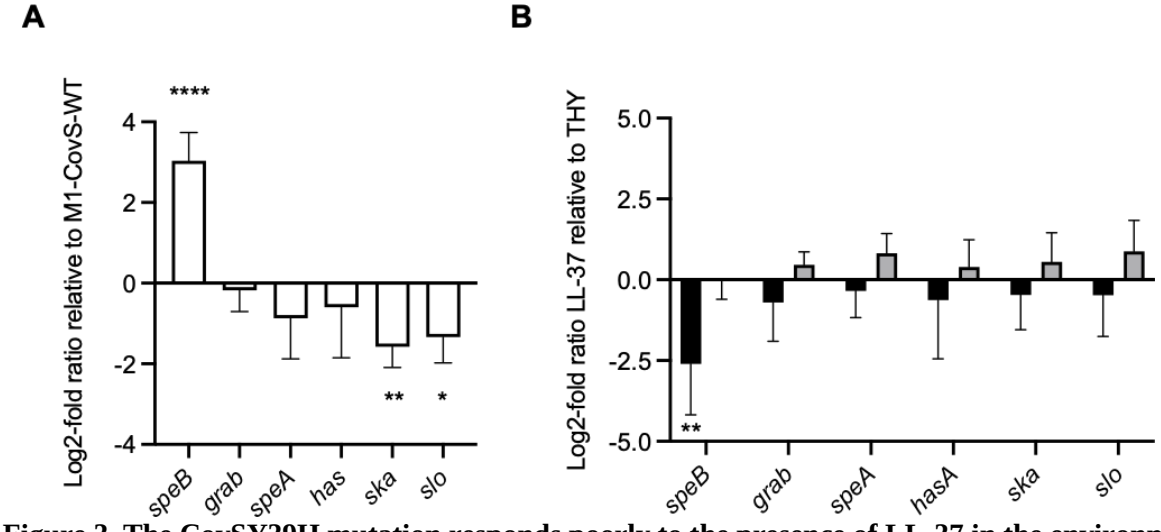

Figure 3. The CovSY39H mutation responds poorly to the presence of LL-37 in the environment. Log_2-fold transcript differences of selected genes were determined by quantitative RT-PCR between A) M1-CovS-Y39H and M1-CovS-WT strains grown in THY; B) M1-CovS-WT and M1-CovS-Y39H strains grown in THY supplemented or not with LL-37. Genes above or under the 0 bar are those that are over-expressed or under-expressed, respectively; A) the M1-CovS-Y39H strain compared to the M1-CovS-WT strain; B) M1-CovS-WT, black rectangles, or M1-CovS-Y39H, grey rectangles, grown in the presence *versus* the absence of added LL-37. N=4. Mean values and SD are indicated; p (unequal variances t-test on ΔCt, *p<0.05;**p<0.01;****p<0.001).

The CovSY39H mutation limits Mg^{2+} and LL-37 influence on SpeB and SLO accumulation. To determine phenotypic consequences of the transcription variations, we assayed SpeB and SLO accumulation produced by the M1-CovS-WT and M1-CovS-Y39H strains cultured in THY, THY+$MgCl_2$ and THY+LL-37, at late (OD_{600} 0.6-0.7) and early (OD_{600} 0.3-0.4) exponential phases for SpeB and SLO, respectively (Fig. 4). Proteins from the supernatants were precipitated and immunoblot analyses was performed with specific anti-SpeB (Fig. 4A, 4C) or anti-SLO (Fig. 4B, 4D) antibodies.

SpeB was more abundant in the supernatant of M1-CovS-Y39H than in that of M1-CovS-WT when strains were grown in THY (Fig. 4A, 4C). SpeB was more abundant in the M1-CovS-WT supernatant when bacteria were grown in the presence of added $MgCl_2$ than in its absence (Fig. 4A). However, this $MgCl_2$ effect was lost in the mutant strain, supporting the transcription results (Fig. 3, S1B). Furthermore, the supernatants of M1-CovS-WT and M1-CovS-Y39H grown in the presence of $MgCL_2$ contained similar amounts of SpeB.

SLO was more abundant in the M1-CovS-WT than in the M1-CovS-Y39H strain supernatants when grown in THY (Fig. 4B). Whereas SLO was more abundant in the supernatant of M1-CovS-WT grown in the absence than in the presence of added $MgCl_2$, such was not the case for the M1-CovS-Y39H strain, where there were no differences (Fig. 4B). Finally in the presence of MgCl2, both strains accumulated the same amount of SLO.

This fully supports the transcription data and strengthens the conclusion that the CovSY39H protein has a reduced capacity to respond to the $MgCl_2$ signal.

We also compared the production of SpeB and SLO by both strains when they were grown in the absence or the presence of LL-37. Addition of LL-37 barely modified the production of SpeB, whose concentration was higher in the M1-CovS-H39Y strain in both conditions. Addition of LL-37 increased SLO relative abundance in the supernatant of M1-CovS-WT. In contrast, it had no effect on the SLO relative abundance in the M1-CovS-Y39H. These results indicate that CovSY39H does not respond to LL-37.

Altogether these results suggest that CovSY39H does not responds to any of the environmental signals.

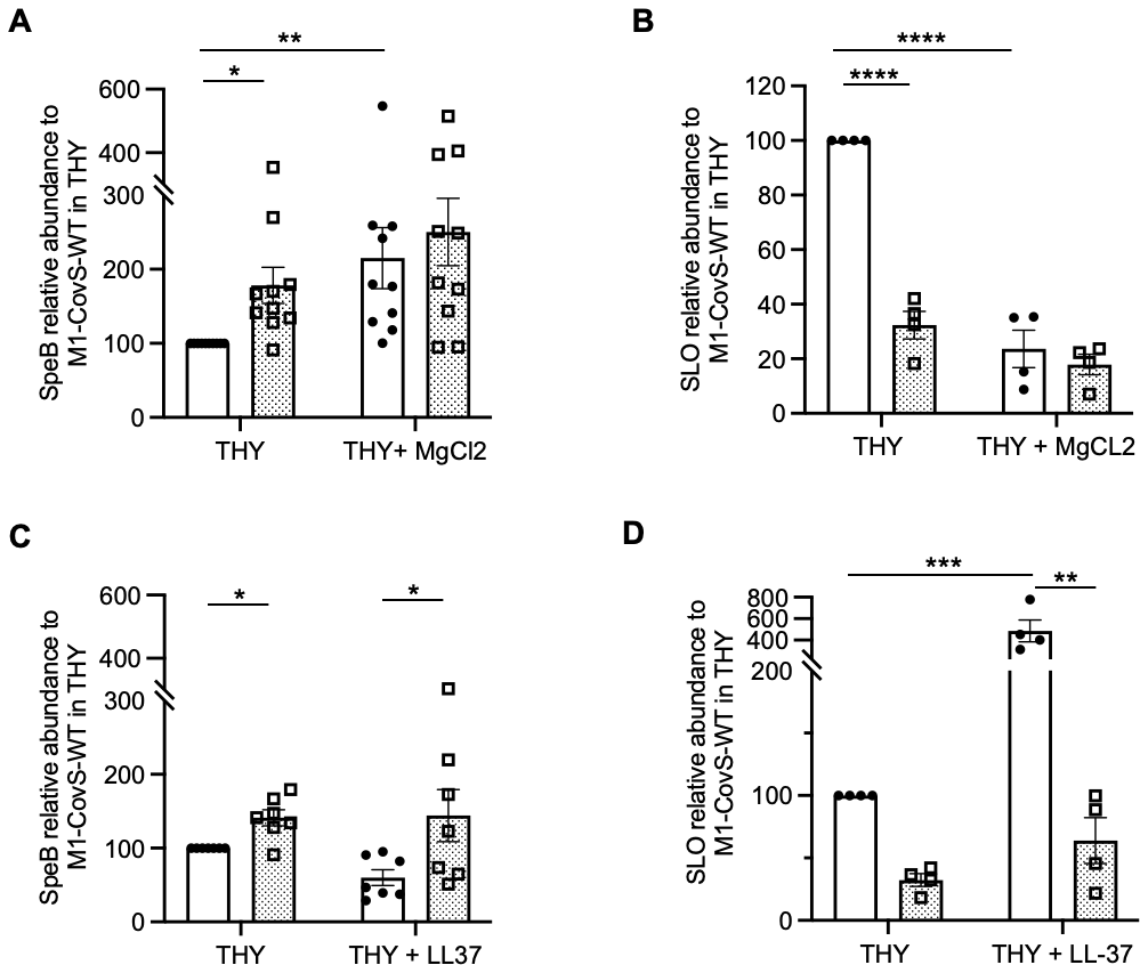

Figure 4. Effect of the CovSY39H mutation on SpeB and SLO production. Ratio of the accumulation of, A, C) SpeB or B, D) SLO, in the supernatants of M1-CovS-WT and M1-CovS-Y39H grown in, A, B) THY or THY+MgCl2; C, D) THY or THY+LL-37 to that in the supernatant of the wild-type strain grown in THY; white rectangles, M1-CovS-WT; grey rectangles, M1-CovS-Y39H. A, N = 10; B N= 4; C, N = 5, D, N=4. Statistical analysis, Kruskal-Wallis, Dunn post-test and One-way anova, Bonferonni post-test for SpeB and SLO, analysis, respectively (Prism 9). *p<0.05, **p<0.01, *** p<0.001 **** p<0.0001.

The M1-CovS-Y39H strain is impaired in macrophage survival capacity. The role of macrophages in the early steps of GAS infection remains unclear; they can kill GAS or the bacteria can survive and even multiply in the macrophage (75-77). They may constitute a reservoir for GAS dissemination as macrophage intracellular persistence and multiplication have been described in an *emm1* GAS strain (77). A phagocytosis assay was performed with murine RAW macrophages using an MOI of 10 bacteria per macrophage (Fig. 5). After a 45 minute-infection period, M1-CovS-WT and M1-CovS-Y39H strains were both phagocytosed at similar levels (not shown). The macrophage survival assay indicated that two hours post-infection the M1-CovS-WT strain survived significantly better than the M1-CovS-Y39H strain

(*p*=0.0062). No significant differences were observed at other time points. This suggests that the CovSY39H mutation weakens GAS survival in macrophages.

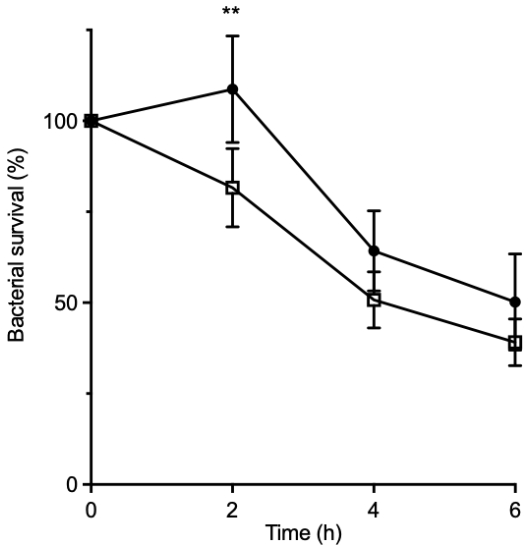

Figure 5. The M1-CovS-WT strain survives better than the M1-CovS-Y39H mutant strain inside macrophages. Macrophage survival assay was performed with mouse RAW246.7 macrophages infected with M1-CovS-WT, close circles, and M1-CovS-Y39H, open squares, at an MOI of 10. GAS Survival is expressed as the percentage of intracellular bacteria at T2, T4, and T6 relative to that at T0. Results are representative of 7 independent experiments performed in triplicate. Error bars represent the mean and standard error of the mean (**p<0.01).

The M1-CovS-Y39H strain is less virulent than the M1-CovS-WT strain. The classical *covS* mutant strains being more virulent in models of invasive infections (36, 38, 71, 78) and the M1-CovS-Y39H strain displaying an atypical phenotype, we assessed whether the virulence of this strain would be modified. Mice were infected intravenously with the M1-CovS-WT and M1-CovS-Y39H strains and survival was followed (Fig. 6A). The M1-CovS-Y39H strain was less virulent (p = 0.0051). To mimic the natural infection and correspond to the location where the M1-CovS-Y39H strain was swabbed, mice were also infected intranasally with the same strains (Fig. 6B). We confirmed the following days that both bacterial strains were found intranasally and in the throat (Fig. S2). Again, the M1-CovS-WT strain tended to be more virulent than the M1-CovS-Y39H mutant strain (p = 0.057). This indicates that with both infection models, the CovSY39H mutation impairs GAS virulence.

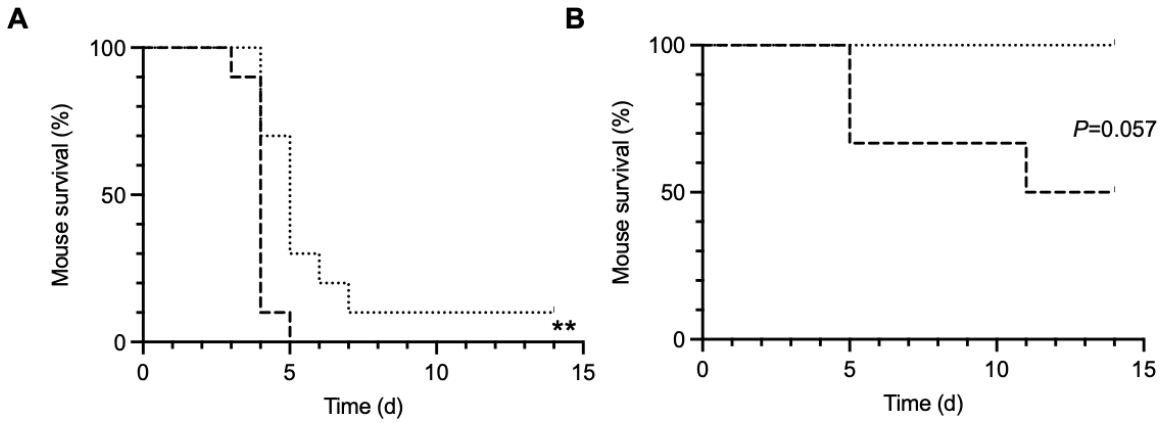

Figure 6. The M1-CovS-WT strain is more virulent than the M1-CovS-Y39H mutant strain. Mice were infected with M1-CovS-WT and M1-CovS-Y39H strains A) intravenously (n = 10) with 4 x 10^7 and 5 x 10^7 cfus, respectively; B) intranasally (n = 6) with 5 x 10^8 and 1.2 x 10^9 cfus, respectively. The survival of the animals was scored for a period of 14 days. M1-CovS-WT, dashed lines; M1-CovS-Y39H, dotted lines. ** p<0.001, Log-rank and Gehan-Breslow-Wilcoxon test.

DISCUSSION

To identify factors involved in the switch from colonization to invasive strains, we isolated, from infectious clusters, pairs of colonization and invasive strains and sequenced their genomes. Two pairs displayed mutations in *covS*. One followed an already described schema, where the *covS* mutant strain is the invasive strain (16, 36-41).

The other pair was atypical with the colonization strain harboring a *covS* mutation. Whether the *covS* mutant strain (M1-CovS-Y39H) is less virulent than its WT counterpart (M1-CovS-WT) was assessed using two murine infection models. In the first one, bacteria were injected intravenously, enabling the evaluation of GAS survival in the blood. The second one, an intranasal infection, takes into account that the oropharyngeal is regarded as the most common site of colonization by GAS and mimics a relevant natural portal of entry (79). In both models, the M1-CovS-Y39H strain was less virulent than the M1-CovS-WT strain. These results strongly support that the resultant mutation in the CovS sensor protein yields, in contrast to all spontaneous CovS mutations isolated thus far, a less virulent strain (16, 36-41). The immune pressure selects *in vivo covR* or *covS* mutations that enable the switch from colonization to invasive phenotype and, among the immune system components, macrophages play an important role, either killing or being a reservoir to GAS (75-77). Our data indicate that whereas the M1-CovS-WT strain multiplied during the first hours after phagocytosis, the elimination of the M1-CovS-Y39H strain was already underway, suggesting

a weaker surviving capacity for this strain. These results account for this mutant clinical isolate being less invasive than the WT isolate and consequently the non-invasive strain of the pair.

The mutation replaces the tyrosine in position 39 by a histidine (CovSY39H). The amino acid residue in position 39 is the first, starting from the N-terminus of the protein, residue of the extracellular domain (71). Most spontaneous mutations in *covS* lead to a stop codon and hence a deleted CovS protein or are in the cytoplasmic domain of CovS that starts at position 215 (41). Two notable exceptions are a triple mutation in the first membrane-spanning α helix and one in the small cytoplasmic domain preceding this helix; yet, both strains, like the other characterized spontaneous mutant isolates, overexpress SLO (41).

Comparing the gene expression profile of the strain harboring the CovSY39H mutation to its wild-type indicated that this mutation yielded an effect opposite to that induced by other natural CovS mutations on the expression of genes belonging to the CovR regulon (16, 42). Genes that are usually over-expressed, such as *slo* or *ska,* in *covS* mutant strains were under-expressed in M1-CovS-Y39H and, conversely, those that are under-expressed in *covS* mutant invasive strains, such as *speB* or *grab*, were over-expressed in M1-CovS-Y39H. Furthermore, this was confirmed at the protein level. SpeB was more abundant in the supernatant of M1-CovS-Y39H than the M1-CovS-WT and SLO was more abundant in that of M1-CovS-WT. Since *speB* and *slo* are repressed by unphosphorylated and phosphorylated CovR, respectively (56, 80), the CovSY39H protein could yield an excess of phosphorylated CovR. That would contrast with classical spontaneous mutations in *covS* recovered from GAS invasive isolates which lead to CovS proteins that have lost the capacity to phosphorylate CovR.

Mg^{2+} and LL-37 are antagonist environmental signals that favor CovR phosphorylated and dephosphorylated states, respectively (25, 26). CovSY39H could be unable to further phosphorylate CovR when Mg^{2+} is added and to dephosphorylate it when LL-37 is added; M1-CovS-Y39H would consequently not respond to the addition of Mg^{2+} or LL-37. The transcriptomic profiles and SpeB and SLO accumulation were therefore compared after cultivating both strains mutant strains in the absence or presence of $MgCl_2$ or of LL-37. The environmental signal effect was weakened in M1-CovS-Y39H. This supports that the transcription modification of genes from the CovR regulon, as exemplified by the higher and lower expressions of *speB* and *slo*, respectively, are consequences of higher phosphorylation of CovR in M1-CovS-Y39H. Altogether, these data indicate that the CovSY39H protein has lost its capacity to respond to an environmental signal.

The level of CovR phosphorylation is a resultant of the kinase and phosphatase activities of CovS. This suggests that either the phosphorylation activity of CovSY39H is intensified or its phosphatase activity is impaired. A strain in which a cluster of the three amino acid residues from CovS extracellular domain that interact with environmental signals, D_{148} - ED_{152}, had been replaced by uncharged residues displayed, like M1-CovS-Y39H, a hyporesponsive phenotype to environmental signals. Further mutations indicated an increased autokinase activity for this triple mutant CovS protein (31). Strains deficient in phosphatase activity also display high levels of phosphorylated CovR and similar hyporesponsive phenotypes (25). Hence, there are experimental evidences that modifications in any of these two activities can yield strains in which phosphorylated CovR is more abundant that in wild-type strains and which weakly respond to environmental signals. Also, and in contrast with the observation made with strains deficient in the phosphatase activity or displaying an increased autokinase activity, the transcription variation due to the CovSY39H mutation was not as strong as that due to the addition of Mg^{2+} (80). The originality of the CovSY39H mutation lies in its position. The 39th residue is the first of the extracellular domain. Altogether, these data suggest that the Y39H mutation induces a conformational change that may constrain the CovS protein in a conformation in which the autokinase is overactive or that is phosphatase incompetent; yet it does not yield an extreme effect on CovR phosphorylation. Further experiments are necessary to discriminate between these possibilities.

Many data have been accumulated, either by analyzing *in vivo* GAS selected strains or by comparing *in vivo* properties of constructed *covS* mutants, supporting that all *covS* mutant strains have an invasive phenotype, with two exceptions. The strain with the triple mutation in the extracellular domain is more susceptible than the wild-type strain to opsonophagocytic killing (31) and loss of CovS phosphatase activity impairs GAS pathogenicity (26). Until now no *covS* mutant displaying a colonization phenotype has been isolated. The M1-CovS-Y39H strain, that was isolated from a healthy carrier during an epidemiological survey concerning an invasive case of GAS infection, has all the *in vitro* characteristics of a specialized colonization strain and, furthermore, displayed an *in vivo* virulence defect.

Studies of naturally occurring *covS* mutant invasive strains demonstrated that these isolates were outcompeted in non-invasive infections, that there is a fitness cost in the naso-pharynx for these strains (42, 81). These studies, together with ours, support the requirement for a wild-type *covRS* in GAS to permit the full cycle leading, after colonization, to

dissemination and invasion. Finally, further analysis of the CovSY39H protein, determination of its structure, of its interaction with CovR would broaden our knowledge on GAS CovRS TCS and possibly on other TCS, corroborating the importance of kinase and phosphatase activities in bifunctional histidine kinases.

ACKNOWLEDGMENTS

We thank C. Méhats for her helpful discussions.

This work was supported and by the High Council for Scientific and Technological Cooperation between France-Israel “Complexity in Biology” program and by INSERM, CNRS, Université de Paris, Santé Publique France, Centre National de Référence des Steeptocoques, Assistance Publique Hôpitaux de Paris.

REFERENCES

1. Cunningham MW. 2000. Pathogenesis of group A streptococcal infections. Clin Microbiol Rev 13:470-511.
2. Carapetis JR, Steer AC, Mulholland EK, Weber M. 2005. The global burden of group A streptococcal diseases. Lancet Infect Dis 5:685-94.
3. Bisno AL, Brito MO, Collins CM. 2003. Molecular basis of group A streptococcal virulence. Lancet Infect Dis 3:191-200.
4. Li Z, Sakota V, Jackson D, Franklin AR, Beall B. 2003. Array of M protein gene subtypes in 1064 recent invasive group A *Streptococcus* isolates recovered from the active bacterial core surveillance. J Infect Dis 188:1587-92.
5. Beall B, Facklam R, Thompson T. 1996. Sequencing *emm*-specific PCR products for routine and accurate typing of group A streptococci. J Clin Microbiol 34:953-8.
6. Dinis M, Plainvert C, Longo M, Guignot J, Gabriel C, Poyart C, Fouet A. 2016. Group A *Streptococcus emm3* strains induce early macrophage cell death. Pathog Dis 74.
7. Kotb M, Norrby-Teglund A, McGeer A, El-Sherbini H, Dorak MT, Khurshid A, Green K, Peeples J, Wade J, Thomson G, Schwartz B, Low DE. 2002. An immunogenetic and molecular basis for differences in outcomes of invasive group A streptococcal infections. Nat Med 8:1398-404.
8. Dinis M, Plainvert C, Kovarik P, Longo M, Fouet A, Poyart C. 2014. The innate immune response elicited by Group A *Streptococcus* is highly variable among clinical isolates and correlates with the *emm* type. PLoS One 9:e101464.
9. Bessen DE, Fiorentino TR, Hollingshead SK. 1997. Molecular markers for throat and skin isolates of group A streptococci. Adv Exp Med Biol 418:537-43.
10. Bessen DE, Sotir CM, Readdy TL, Hollingshead SK. 1996. Genetic correlates of throat and skin isolates of group A streptococci. J Infect Dis 173:896-900.
11. Kreikemeyer B, McIver KS, Podbielski A. 2003. Virulence factor regulation and regulatory networks in *Streptococcus pyogenes* and their impact on pathogen-host interactions. Trends Microbiol 11:224-32.
12. Levin JC, Wessels MR. 1998. Identification of *csrR/csrS*, a genetic locus that regulates hyaluronic acid capsule synthesis in group A *Streptococcus*. Mol Microbiol 30:209-19.
13. Graham MR, Smoot LM, Migliaccio CA, Virtaneva K, Sturdevant DE, Porcella SF, Federle MJ, Adams GJ, Scott JR, Musser JM. 2002. Virulence control in group A *Streptococcus* by a two-component gene regulatory system: global expression profiling and in vivo infection modeling. Proc Natl Acad Sci U S A 99:13855-60.
14. Churchward G. 2007. The two faces of Janus: virulence gene regulation by CovR/S in group A streptococci. Mol Microbiol 64:34-41.
15. Dalton TL, Collins JT, Barnett TC, Scott JR. 2006. RscA, a member of the MDR1 family of transporters, is repressed by CovR and required for growth of *Streptococcus pyogenes* under heat stress. J Bacteriol 188:77-85.
16. Sumby P, Whitney AR, Graviss EA, DeLeo FR, Musser JM. 2006. Genome-wide analysis of group a *Streptococci* reveals a mutation that modulates global phenotype and disease specificity. PLoS Pathog 2:e5.
17. Willett JW, Kirby JR. 2012. Genetic and biochemical dissection of a HisKA domain identifies residues required exclusively for kinase and phosphatase activities. PLoS Genet 8:e1003084.

18. Churchward G, Bates C, Gusa AA, Stringer V, Scott JR. 2009. Regulation of streptokinase expression by CovR/S in *Streptococcus pyogenes*: CovR acts through a single high-affinity binding site. Microbiology 155:566-75.
19. Federle MJ, Scott JR. 2002. Identification of binding sites for the group A streptococcal global regulator CovR. Mol Microbiol 43:1161-72.
20. Gao J, Gusa AA, Scott JR, Churchward G. 2005. Binding of the global response regulator protein CovR to the sag promoter of *Streptococcus pyogenes* reveals a new mode of CovR-DNA interaction. J Biol Chem 280:38948-56.
21. Gusa AA, Scott JR. 2005. The CovR response regulator of group A *Streptococcus* (GAS) acts directly to repress its own promoter. Mol Microbiol 56:1195-207.
22. Gusa AA, Gao J, Stringer V, Churchward G, Scott JR. 2006. Phosphorylation of the group A Streptococcal CovR response regulator causes dimerization and promoter-specific recruitment by RNA polymerase. J Bacteriol 188:4620-6.
23. Horstmann N, Saldana M, Sahasrabhojane P, Yao H, Su X, Thompson E, Koller A, Shelburne SA, 3rd. 2014. Dual-site phosphorylation of the control of virulence regulator impacts group a streptococcal global gene expression and pathogenesis. PLoS Pathog 10:e1004088.
24. Dalton TL, Scott JR. 2004. CovS inactivates CovR and is required for growth under conditions of general stress in *Streptococcus pyogenes*. J Bacteriol 186:3928-37.
25. Horstmann N, Sahasrabhojane P, Saldana M, Ajami NJ, Flores AR, Sumby P, Liu CG, Yao H, Su X, Thompson E, Shelburne SA. 2015. Characterization of the effect of the histidine kinase CovS on response regulator phosphorylation in group A *Streptococcus*. Infect Immun 83:1068-77.
26. Horstmann N, Tran CN, Brumlow C, DebRoy S, Yao H, Nogueras Gonzalez G, Makthal N, Kumaraswami M, Shelburne SA. 2018. Phosphatase activity of the control of virulence sensor kinase CovS is critical for the pathogenesis of group A *Streptococcus*. PLoS Pathog 14:e1007354.
27. Agarwal S, Agarwal S, Pancholi P, Pancholi V. 2011. Role of serine/threonine phosphatase (SP-STP) in Streptococcus pyogenes physiology and virulence. J Biol Chem 286:41368-80.
28. Gryllos I, Grifantini R, Colaprico A, Jiang S, Deforce E, Hakansson A, Telford JL, Grandi G, Wessels MR. 2007. Mg(2+) signalling defines the group A streptococcal CsrRS (CovRS) regulon. Mol Microbiol 65:671-83.
29. Gryllos I, Levin JC, Wessels MR. 2003. The CsrR/CsrS two-component system of group A *Streptococcus* responds to environmental Mg2+. Proc Natl Acad Sci U S A 100:4227-32.
30. Gryllos I, Tran-Winkler HJ, Cheng MF, Chung H, Bolcome R, 3rd, Lu W, Lehrer RI, Wessels MR. 2008. Induction of group A *Streptococcus* virulence by a human antimicrobial peptide. Proc Natl Acad Sci U S A 105:16755-60.
31. Tran-Winkler HJ, Love JF, Gryllos I, Wessels MR. 2011. Signal transduction through CsrRS confers an invasive phenotype in group A *Streptococcus*. PLoS Pathog 7:e1002361.
32. Biswas I, Scott JR. 2003. Identification of rocA, a positive regulator of covR expression in the group A *Streptococcus*. J Bacteriol 185:3081-90.
33. Lynskey NN, Velarde JJ, Finn MB, Dove SL, Wessels MR. 2019. RocA Binds CsrS To Modulate CsrRS-Mediated Gene Regulation in Group A *Streptococcus*. mBio 10.
34. Miller EW, Pflughoeft KJ, Sumby P. 2015. Reply to "A truncation in the regulator RocA underlies heightened capsule expression in serotype M3 group A streptococci". Infect Immun 83:1734.

35. Lynskey NN, Turner CE, Heng LS, Sriskandan S. 2015. A truncation in the regulator RocA underlies heightened capsule expression in serotype M3 group A streptococci. Infect Immun 83:1732-3.
36. Engleberg NC, Heath A, Miller A, Rivera C, DiRita VJ. 2001. Spontaneous mutations in the CsrRS two-component regulatory system of *Streptococcus pyogenes* result in enhanced virulence in a murine model of skin and soft tissue infection. J Infect Dis 183:1043-54.
37. Garcia AF, Abe LM, Erdem G, Cortez CL, Kurahara D, Yamaga K. 2010. An insert in the *covS* gene distinguishes a pharyngeal and a blood isolate of *Streptococcus pyogenes* found in the same individual. Microbiology 156:3085-95.
38. Hollands A, Pence MA, Timmer AM, Osvath SR, Turnbull L, Whitchurch CB, Walker MJ, Nizet V. 2010. Genetic switch to hypervirulence reduces colonization phenotypes of the globally disseminated group A *Streptococcus* M1T1 clone. J Infect Dis 202:11-9.
39. Horstmann N, Sahasrabhojane P, Suber B, Kumaraswami M, Olsen RJ, Flores A, Musser JM, Brennan RG, Shelburne SA, 3rd. 2011. Distinct single amino acid replacements in the control of virulence regulator protein differentially impact streptococcal pathogenesis. PLoS Pathog 7:e1002311.
40. Shea PR, Beres SB, Flores AR, Ewbank AL, Gonzalez-Lugo JH, Martagon-Rosado AJ, Martinez-Gutierrez JC, Rehman HA, Serrano-Gonzalez M, Fittipaldi N, Ayers SD, Webb P, Willey BM, Low DE, Musser JM. 2011. Distinct signatures of diversifying selection revealed by genome analysis of respiratory tract and invasive bacterial populations. Proc Natl Acad Sci U S A 108:5039-44.
41. Ikebe T, Ato M, Matsumura T, Hasegawa H, Sata T, Kobayashi K, Watanabe H. 2010. Highly frequent mutations in negative regulators of multiple virulence genes in group A streptococcal toxic shock syndrome isolates. PLoS Pathog 6:e1000832.
42. Trevino J, Perez N, Ramirez-Pena E, Liu Z, Shelburne SA, 3rd, Musser JM, Sumby P. 2009. CovS simultaneously activates and inhibits the CovR-mediated repression of distinct subsets of group A *Streptococcus* virulence factor-encoding genes. Infect Immun 77:3141-9.
43. Madden JC, Ruiz N, Caparon M. 2001. Cytolysin-mediated translocation (CMT): a functional equivalent of type III secretion in gram-positive bacteria. Cell 104:143-52.
44. Zhu L, Olsen RJ, Lee JD, Porter AR, DeLeo FR, Musser JM. 2017. Contribution of Secreted NADase and Streptolysin O to the Pathogenesis of Epidemic Serotype M1 *Streptococcus pyogenes* Infections. Am J Pathol 187:605-613.
45. Weckel A, Guilbert T, Lambert C, Plainvert C, Goffinet F, Poyart C, Mehats C, Fouet A. 2021. *Streptococcus pyogenes* infects human endometrium by limiting the innate immune response. J Clin Invest 131.
46. Berge A, Bjorck L. 1995. Streptococcal cysteine proteinase releases biologically active fragments of streptococcal surface proteins. J Biol Chem 270:9862-7.
47. Collin M, Olsen A. 2001. Effect of SpeB and EndoS from *Streptococcus pyogenes* on human immunoglobulins. Infect Immun 69:7187-9.
48. Eriksson A, Norgren M. 2003. Cleavage of antigen-bound immunoglobulin G by SpeB contributes to streptococcal persistence in opsonizing blood. Infect Immun 71:211-7.
49. Kuo CF, Lin YS, Chuang WJ, Wu JJ, Tsao N. 2008. Degradation of complement 3 by streptococcal pyrogenic exotoxin B inhibits complement activation and neutrophil opsonophagocytosis. Infect Immun 76:1163-9.

50. Nyberg P, Rasmussen M, Von Pawel-Rammingen U, Bjorck L. 2004. SpeB modulates fibronectin-dependent internalization of *Streptococcus pyogenes* by efficient proteolysis of cell-wall-anchored protein F1. Microbiology 150:1559-69.
51. Terao Y, Mori Y, Yamaguchi M, Shimizu Y, Ooe K, Hamada S, Kawabata S. 2008. Group A streptococcal cysteine protease degrades C3 (C3b) and contributes to evasion of innate immunity. J Biol Chem 283:6253-60.
52. Wei L, Pandiripally V, Gregory E, Clymer M, Cue D. 2005. Impact of the SpeB protease on binding of the complement regulatory proteins factor H and factor H-like protein 1 by *Streptococcus pyogenes*. Infect Immun 73:2040-50.
53. Aziz RK, Pabst MJ, Jeng A, Kansal R, Low DE, Nizet V, Kotb M. 2004. Invasive M1T1 group A *Streptococcus* undergoes a phase-shift in vivo to prevent proteolytic degradation of multiple virulence factors by SpeB. Mol Microbiol 51:123-34.
54. Walker MJ, Hollands A, Sanderson-Smith ML, Cole JN, Kirk JK, Henningham A, McArthur JD, Dinkla K, Aziz RK, Kansal RG, Simpson AJ, Buchanan JT, Chhatwal GS, Kotb M, Nizet V. 2007. DNase Sda1 provides selection pressure for a switch to invasive group A streptococcal infection. Nat Med 13:981-5.
55. Heath A, DiRita VJ, Barg NL, Engleberg NC. 1999. A two-component regulatory system, CsrR-CsrS, represses expression of three *Streptococcus pyogenes* virulence factors, hyaluronic acid capsule, streptolysin S, and pyrogenic exotoxin B. Infect Immun 67:5298-305.
56. Chiang-Ni C, Kao CY, Hsu CY, Chiu CH. 2019. Phosphorylation at the D53 but Not the T65 Residue of CovR Determines the Repression of *rgg* and *speB* Transcription in *emm1*- and *emm49*-Type Group A Streptococci. J Bacteriol 201.
57. Do H, Makthal N, VanderWal AR, Rettel M, Savitski MM, Peschek N, Papenfort K, Olsen RJ, Musser JM, Kumaraswami M. 2017. Leaderless secreted peptide signaling molecule alters global gene expression and increases virulence of a human bacterial pathogen. Proc Natl Acad Sci U S A 114:E8498-E8507.
58. Zerbino DR, Birney E. 2008. Velvet: algorithms for de novo short read assembly using de Bruijn graphs. Genome Res 18:821-9.
59. Li H, Durbin R. 2009. Fast and accurate short read alignment with Burrows-Wheeler transform. Bioinformatics 25:1754-60.
60. Milne I, Stephen G, Bayer M, Cock PJ, Pritchard L, Cardle L, Shaw PD, Marshall D. 2013. Using Tablet for visual exploration of second-generation sequencing data. Brief Bioinform 14:193-202.
61. Almeida A, Villain A, Joubrel C, Touak G, Sauvage E, Rosinski-Chupin I, Poyart C, Glaser P. 2015. Whole-Genome Comparison Uncovers Genomic Mutations between Group B Streptococci Sampled from Infected Newborns and Their Mothers. J Bacteriol 197:3354-66.
62. Rosinski-Chupin I, Sauvage E, Fouet A, Poyart C, Glaser P. 2019. Conserved and specific features of *Streptococcus pyogenes* and *Streptococcus agalactiae* transcriptional landscapes. BMC Genomics 20:236.
63. Deatherage DE, Barrick JE. 2014. Identification of mutations in laboratory-evolved microbes from next-generation sequencing data using breseq. Methods Mol Biol 1151:165-88.
64. Lamy MC, Zouine M, Fert J, Vergassola M, Couve E, Pellegrini E, Glaser P, Kunst F, Msadek T, Trieu-Cuot P, Poyart C. 2004. CovS/CovR of group B *Streptococcus*: a two-component global regulatory system involved in virulence. Mol Microbiol 54:1250-68.

65. Langille MG, Hsiao WW, Brinkman FS. 2010. Detecting genomic islands using bioinformatics approaches. Nat Rev Microbiol 8:373-82.
66. Varet H, Brillet-Gueguen L, Coppee JY, Dillies MA. 2016. SARTools: A DESeq2- and EdgeR-Based R Pipeline for Comprehensive Differential Analysis of RNA-Seq Data. PLoS One 11:e0157022.
67. Anders S, McCarthy DJ, Chen Y, Okoniewski M, Smyth GK, Huber W, Robinson MD. 2013. Count-based differential expression analysis of RNA sequencing data using R and Bioconductor. Nat Protoc 8:1765-86.
68. Benjamini Y, Hochberg Y. 1995. Controlling the False Discovery Rate: A Practical and Powerful Approach to Multiple Testing. J Royal Statistical Society Series B 57:289-300.
69. Sumby P, Porcella SF, Madrigal AG, Barbian KD, Virtaneva K, Ricklefs SM, Sturdevant DE, Graham MR, Vuopio-Varkila J, Hoe NP, Musser JM. 2005. Evolutionary origin and emergence of a highly successful clone of serotype M1 group a *Streptococcus* involved multiple horizontal gene transfer events. J Infect Dis 192:771-82.
70. Zheng PX, Chung KT, Chiang-Ni C, Wang SY, Tsai PJ, Chuang WJ, Lin YS, Liu CC, Wu JJ. 2013. Complete Genome Sequence of *emm1 Streptococcus pyogenes* A20, a Strain with an Intact Two-Component System, CovRS, Isolated from a Patient with Necrotizing Fasciitis. Genome Announc 1.
71. Lin JN, Chang LL, Lai CH, Lin HH, Chen YH. 2014. Association between polymorphisms in the *csrRS* two-component regulatory system and invasive group A streptococcal infection. Eur J Clin Microbiol Infect Dis 33:735-43.
72. Beres SB, Carroll RK, Shea PR, Sitkiewicz I, Martinez-Gutierrez JC, Low DE, McGeer A, Willey BM, Green K, Tyrrell GJ, Goldman TD, Feldgarden M, Birren BW, Fofanov Y, Boos J, Wheaton WD, Honisch C, Musser JM. 2010. Molecular complexity of successive bacterial epidemics deconvoluted by comparative pathogenomics. Proc Natl Acad Sci U S A 107:4371-6.
73. Hoff JS, DeWald M, Moseley SL, Collins CM, Voyich JM. 2011. SpyA, a C3-like ADP-ribosyltransferase, contributes to virulence in a mouse subcutaneous model of *Streptococcus pyogenes* infection. Infect Immun 79:2404-11.
74. O'Seaghdha M, Wessels MR. 2013. Streptolysin O and its co-toxin NAD-glycohydrolase protect group A *Streptococcus* from Xenophagic killing. PLoS Pathog 9:e1003394.
75. Goldmann O, Rohde M, Chhatwal GS, Medina E. 2004. Role of macrophages in host resistance to group A streptococci. Infect Immun 72:2956-63.
76. Thulin P, Johansson L, Low DE, Gan BS, Kotb M, McGeer A, Norrby-Teglund A. 2006. Viable group A Streptococci in macrophages during acute soft tissue infection. PLoS Med 3:e53.
77. Hertzen E, Johansson L, Wallin R, Schmidt H, Kroll M, Rehn AP, Kotb M, Morgelin M, Norrby-Teglund A. 2010. M1 protein-dependent intracellular trafficking promotes persistence and replication of *Streptococcus pyogenes i*n macrophages. J Innate Immun 2:534-45.
78. Tatsuno I, Okada R, Zhang Y, Isaka M, Hasegawa T. 2013. Partial loss of CovS function in *Streptococcus pyogenes* causes severe invasive disease. BMC Res Notes 6:126.
79. Gogos A, Federle MJ. 2020. Colonization of the Murine Oropharynx by Streptococcus pyogenes Is Governed by the Rgg2/3 Quorum Sensing System. Infect Immun 88.
80. Finn MB, Ramsey KM, Dove SL, Wessels MR. 2021. Identification of Group A *Streptococcus* Genes Directly Regulated by CsrRS and Novel Intermediate Regulators. mBio 12:e0164221.

81. Alam FM, Turner CE, Smith K, Wiles S, Sriskandan S. 2013. Inactivation of the CovR/S virulence regulator impairs infection in an improved murine model of *Streptococcus pyogenes* naso-pharyngeal infection. PLoS One 8:e61655.
82. Plainvert C, Doloy A, Loubinoux J, Lepoutre A, Collobert G, Touak G, Trieu-Cuot P, Bouvet A, Poyart C. 2012. Invasive group A streptococcal infections in adults, France (2006-2010). Clin Microbiol Infect 18:702-710.
83. Cady A, Plainvert C, Donnio P, Loury P, Huguenet D, Briand A, Revest M, Kayal S, Bouvet A. 2011. Clonal spread of *Streptococcus pyogenes emm44* among homeless persons, Rennes, France. Emerg Infect Dis 17:315-7.

Supplementary figure

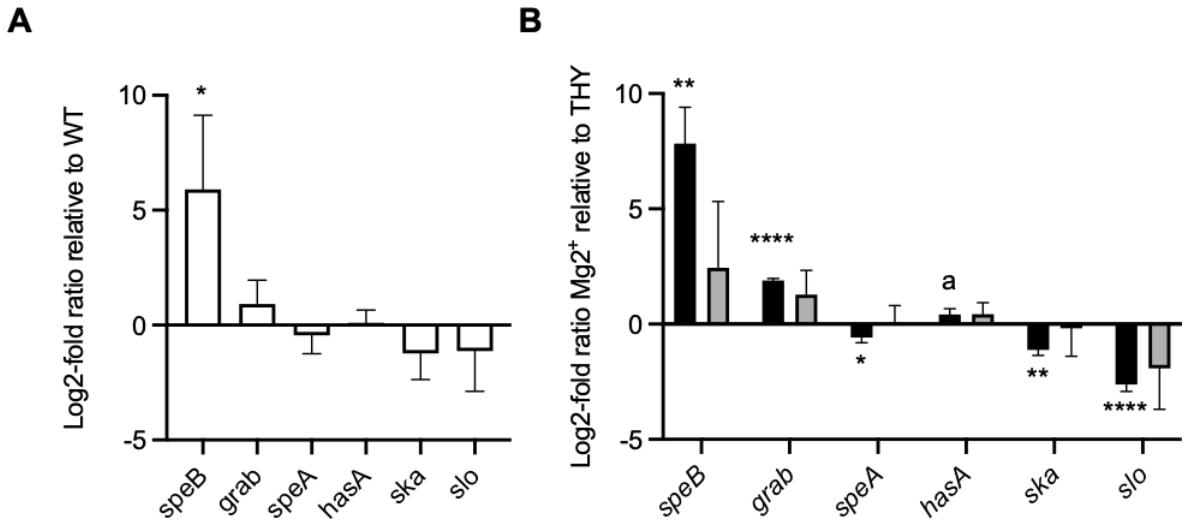

Figure S1. Transcriptomic profile verification by qRT-PCR. Log_2-fold transcript differences of selected genes were determined by quantitative RT-PCR between A) M1CovS and M1WT strains grown in THY; B) M1WT and M1CovS strains grown in THY supplemented or not with $MgCL_2$. Genes above or under the 0 bar are those that are over-expressed or under-expressed, respectively; A) the M1CovS strain compared to the M1WT strain; B) the M1WT, black rectangles, or M1CovS, grey rectangles, grown in the presence *versus* the absence of added $MgCl_2$. The experiments were performed in triplicate. Mean values and SD are indicated; p (unequal variances t-test on ΔCt, *p<0.05;**p<0.01;****p<0.001); a, p = 0.064.

Supplementary table

Table S1. Primer sequences

Oligonucleotides	Sequence (5'→3')	Target gene
gyrA1	GCCATGAGTGTCATTGTGGC	*gyrA*
gyrA2	GGCGATAACTCCACCACTGA	
speA1	CGCAAGAGGTATTTGCTCAA	*speA*
speA2	GCCATCTCTTGGTTCTTAAG	
speB1	CCGCTGGTAGAGTATCCTA	*speB*
speB2	GCTAACCCAGTATTTGCCG	
grab3	GGCCGTAATATTACTTTCGGAG	*grab*
grab4	GCTACAGTTTATAATAGCTTGAAAGAC	
has1	GGAACATCAACTGTAGGAATTTAT	*hasA*
has2	GCATCTGTGTTTGAACTCC	
ska1	GCACTGCTGTTTGCATTAAC	*ska*
ska2	GCAAATGGTTTTGATTTTGGACT	
gasslo_F	ACCGTATCAGCAAACCTTCCT	*slo*
gasslo_R	ACTAAAGGCCGCTTCAACATC	